[redacted]

Westinghouse Atomic Power Division

DISCLAIMER

WCAP-3589-2

PERFORMANCE CHARACTERISTICS OF A LARGE FAST BREEDER REACTOR CORE WITH BUNDLE CONTROLLED EXPANSION (BCEX) FUEL ASSEMBLIES

Topical Report - Task 200

Prepared for

Division of Reactor Development and Technology
U. S. Atomic Energy Commission

Contract No. AT(30-1)-3589
with New York Operations Office, USAEC

May 1966

R. A. Markley
Project Engineer

Approved: _____
P. L. Wyzenbeek, Manager
Advanced Systems Projects

Approved: _____
S. N. Tower, Manager
Advanced Systems Technology

Approved: _____
J. H. Wright, Manager
Advanced Systems Section

WESTINGHOUSE ELECTRIC CORPORATION
Atomic Power Division
P. O. Box 355
Pittsburgh, Pennsylvania 15230

List of Contributors

G. B. Brown
M. J. Brusca
L. F. Cochrun (H)
R. S. Daleas
W. E. Gunson (F)
F. M. Heck (B,K)
L. A. Larsen (G)
R. A. Markley (A,C,L)
J. D. Mottley (I)
W. E. Ray
J. R. Reavis (D)
J. B. Roll
E. E. Smith
J. D. Sutherland (E)
S. N. Tower
J. H. Wright
P. L. Wyzenbeek (J)

A - Project Engineer

B - Responsible engineer, CEX concept and its problem areas

C - Responsible engineer, Thermal and hydraulic analyses

D - Responsible engineer, Mechanical design

E - Responsible engineer, Mechanical bowing analyses

F - Responsible engineer, Transient analyses

G - Responsible engineer, Nuclear design and analyses

H - Responsible engineer, Cermet materials evaluation

I - Responsible engineer, Carbide fuel and structural material evaluation

J - Report review

K - Technical Director

L - Report editor

Westinghouse Distribution List

W. E. Abbott
R. J. Allio
H. N. Andrews
E. F. Beckett
H. E. Braun
G. B. Brown
C. C. Christensen
L. F. Cochrun
P. Cohen
R. J. Creagan
R. S. Daleas
H. M. Ferrari
J. A. George
N. J. Georges
H. W. Graves
W. E. Gunson
F. M. Heck
J. D. Herb
A. R. Jones
I. M. Keyfitz
E. L. Kuno
L. A. Larsen
R. A. Markley
J. D. Mottley
J. F. Patterson
C. C. Randall
W. E. Ray
J. R. Reavis
L. R. Rees
J. C. Rengel
J. B. Roll
D. J. Rop
E. E. Smith
D. C. Spencer
T. Stern
J. D. Sutherland
S. N. Tower
R. L. Witzke
J. H. Wright
P. L. Wyzenbeek

ABSTRACT

The work performed by Westinghouse Electric Corporation under the sponsorship of the USAEC (Contract AT(30-1)-3589) is reported. This work included the identification of the problem areas, and the analyses and evaluation of the performance characteristics of the Bundle Controlled Expansion (BCEX) concept in the Westinghouse Large Fast Breeder Reactor using a modular, carbide-fueled core. The dynamic behavior of a second concept, fuel rod Clad Controlled Expansion (CCEX), was also studied briefly in the carbide-fueled modular core. The dynamic performance of the BCEX and CCEX concepts were also briefly investigated in a gas bonded, oxide-fueled core.

The results of all the transient analyses performed in this investigation demonstrated that utilization of either of the axial thermal expansion concepts, CCEX or BCEX, significantly improved the core transient behavior over that of the non-CEX (zero thermal expansion) core. Both BCEX and CCEX can potentially provide ceramic-fueled fast reactor cores with a predictable, negative, axial expansion, reactivity feedback mechanism that will contribute significantly in terminating a power excursion by supplementing the Doppler coefficient.

If predictable fuel thermal expansion due either to expansion of its clad (CCEX) or expansion of the solid column of fuel can be demonstrated, the BCEX concept appears to offer only marginal improvement over CCEX in terminating various nuclear excursions in either a carbide core or an oxide core. CCEX has a simpler mechanical design, due to elimination of the half core-length fuel bundles and the cermet rod array. For these reasons, the CCEX concept is an attractive alternate to BCEX, and it is recommended that further development work be carried out on the CCEX concept.

If predictable ceramic fuel thermal expansion cannot be demonstrated, then BCEX offers a significant improvement in the dynamic behavior of a non-CEX core. Therefore, both concepts - BCEX and CCEX - should be further investigated in parallel to permit the selection of the more attractive concept for ultimate application to commercial fast breeder reactors.

TABLE OF CONTENTS

Section No.	Title	Page No.
	ABSTRACT	v
	TABLE OF CONTENTS	vi
	LIST OF FIGURES	x
	LIST OF TABLES	xxii
	SUMMARY	xxiv
I.	PROBLEM STATEMENT	I.1
II.	INTRODUCTION	II.1
II.1	Authorization and Scope of Contract	II.1
II.2	Initial Design Bases and Groundrules	II.4
II.3	CEX Concept Background Information	II.8
III.	DISCUSSION AND RESULTS	III.1
III.1	Reference Westinghouse Large Modular Fast Breeder Reactor System Description	III.1
III.1.1	General	III.1
III.1.2	Reference Reactor Design Description	III.1
III.1.3	Description of Performance and Conditions	III.27
III.1.4	Reactor Safety Considerations	III.35
III.1.5	Fuel Cycle Costs	III.40
III.2	BCEX Concept and Its Problem Areas	III.44
III.2.1	Introduction	III.44
III.2.2	General Concept Description	III.44

TABLE OF CONTENTS (Cont'd)

Section No.	Title	Page No.
III.2.3	Problem Areas	III.47
III.3	Thermal and Hydraulic Analyses and Results	III.58
III.3.1	General	III.58
III.3.2	Design Basis and Ground Rules	III.59
III.3.3	Discussion and Results	III.62
III.4	Mechanical Design and Analysis	III.94
III.4.1	Fuel Assembly Description	III.94
III.4.2	Carbide Fuel Rod Description	III.99
III.4.3	Controlled Expansion Feature	III.101
III.4.4	Fuel Clad Stresses and Strains	III.111
III.4.5	Cermet Design	III.116
III.4.6	Fuel Assembly Can Stresses and Strains	III.118
III.4.7	BCEX Fuel Assembly Thermal Bowing	III.122
III.4.8	Recommendations for Future Work	III.131
III.5	Transient Analyses	III.136
III.5.1	Scope of Work	III.136
III.5.2	Computer Code Modifications	III.137
III.5.3	Nuclear, Thermal, and Materials Parameters	III.139
III.5.4	Parameter Study	III.145
III.5.5	Accident Analyses	III.201
III.5.6	Controlled Expansion Quasi-Equilibrium Reactivity Feedback and Alternate Clad Materials	III.228

TABLE OF CONTENTS (Cont'd)

Section No.	Title	Page No.
III.5.7	Summary and Conclusions	III.239
III.6	Nuclear Analyses	III.244
III.6.1	Introduction	III.244
III.6.2	Description and Calculational Method	III.245
III.6.3	Results and Discussion	III.251
III.6.4	Recommendation and Conclusion	III.262
III.7	Material Review and Analyses	III.262
III.7.1	General	III.265
III.7.2	Properties of 316 L Stainless Steel	III.265
III.7.3	Properties of (U,Pu)C Fuel	III.274
III.7.4	Effect of Sodium Environment on 316 L Stainless Steel	III.286
III.7.5	Calculation of Usage Factor for BCEX Elements	III.289
III.7.6	Uranium-Plutonium Dioxide - 316 L Stainless Steel Cermet Fuel	III.289

TABLE OF CONTENTS (Cont'd)

Section No.	Title	Page No.
	APPENDIX A - BCEX FUEL ASSEMBLY DYNAMICS	A-1
	APPENDIX B - BCEX FUEL ASSEMBLY THERMAL BOWING	B-1
	APPENDIX C - FUEL CLAD STRESSES AND STRAINS	C-1
	APPENDIX D - CERMET STRESSES AND STRAINS	D-1
	APPENDIX E - SAMPLE OF WESTINGHOUSE FORE COMPUTER PROGRAM OUTPUT	E-1
	APPENDIX F - NEUTRON ENERGY GROUP STRUCTURE OF STANDARD WAPD 18 GROUP LIBRARY	F-1
	APPENDIX G - CERMET MATERIALS LITERATURE SEARCH	G-1

LIST OF FIGURES

Figure No.	Title	Page No.
III.1-1	Reactor Building Elevation	III.2
III.1-2	Reactor System Schematic	III.3
III.1-3	Modular Core Array	III.4
III.1-4	Fuel Assembly Installation and Removal	III.8
III.1-5	Radial Blanket Assembly	III.10
III.1-6	Module Parameter Top Locating Grid	III.11a
III.1-7	One-Quarter Reactor Core Section	III.12
III.1-8	Reactor Vessel	III.13
III.2-1	CEX (Controlled Expansion) Fuel Assembly	III.45
III.3-1	Cermet Thermal Conductivity	III.63
III.3-2	Cermet Fuel Relationships	III.64
III.3-3	Cermet Fuel Volume Fraction vs. Weight Fraction	III.65
III.3-4	Cermet Fuel Burnup Relationships	III.66
III.3-5	Carbide Fuel Rod Steady State Temperature Profile	III.68
III.3-6	Temperature Drop Through the Cladding of the Carbide Fuel Rods	III.69
III.3-7	Parametric Survey of Cermet Rod Steady State Temperatures	III.70
III.3-8	Cermet Rod Steady State Data	III.71
III.3-9	Cermet Rod Steady State Temperature Profile Q = 0.20	III.72
III.3-10	Cermet Rod Steady State Temperature Profile Q = 0.25	III.73
III.3-11	Cermet Rod Steady State Temperature Profile Q = 0.30	III.74
III.3-12	Cermet Rod Steady State Temperature Profile Q = 0.40	III.75

LIST OF FIGURES (Cont'd)

Figure No.	Title	Page No.
III.3-13	Fat Cermet Rod Steady State Data	III.78
III.3-14	Cermet Rod Steady State Temperature Profile Fat Rod, Q = 0.20	III.79
III.3-15	Cermet Rod Steady State Temperature Profile Fat Rod, Q = 0.25	III.80
III.3-16	Cermet Rod Steady State Temperature Profile Fat Rod, Q = 0.30	III.81
III.3-17	Cermet Steady State Rod Temperature Profile Fat Rod, Q = 0.40	III.82
III.3-18	Exit Coolant Temperature Distribution in Various Zones of Core as a Function of Transverse Position in Zone Beginning-of-Life Power Distribution	III.84
III.3-19	Temperature Difference Can Wall-to-Can Wall in Various Zones of Core for no Transverse Coolant Mixing vs. Axial Position (Beginning-of-Life Power Distribution)	III.85
III.3-20	Exit Coolant Temperature Distribution in Various Zones of Core as a Function of Transverse Position in Zone 33,333 MWD/T Power Distribution	III.87
III.3-21	Temperature Difference Can Wall-to-Can Wall in Various Zones of Core for no Transverse Coolant Mixing vs. Axial Position (33,333 MWD/T Power Distribution)	III.88
III.3-22	Exit Coolant Temperature Distribution in Various Zones of Blanket	III.89
III.3-23	Temperature Difference Can Wall-to-Can Wall in Various Zones of Blanket	III.90
III.3-24	UO_2 - SS Cermet Burnup - Temperature History	III.91

LIST OF FIGURES (Cont'd)

Figure No.	Title	Page No.
III.4-1	Fuel Assembly	III.95
III.4-2	Fuel Bundle Assembly	III.96
III.4-3	Fuel Assembly Cross-Section	III.97
III.4-4	Fuel Rod	III.100
III.4-5	Bundle Displacement vs. Time for Three Terminated Transients	III.103
III.4-6	Post Transient Bundle Vibration Amplitude vs. Characteristic Transient Time (Terminated Transient)	III.104
III.4-7	Number of Cermet Rods vs. Characteristic Transient Time (Terminated Transient, Reference Fuel Assembly Design)	III.105
III.4-8	CEX Assembly Parameters (Terminated Transient)	III.106
III.4-9	Minimum Allowable Transient Time vs. Cermet Mechanical Properties	III.107
III.4-10	CEX Fuel Assembly Parameters (Unterminated Transient	III.108
III.4-11	Correlation of Secondary Creep Rate Data - 316 SST	III.121
III.4-12	Unrestrained Thermal Bowing of Outermost Core Subassembly	III.124
III.4-13	Effect of Restraints on Thermal Bowing of Fuel Assembly Cans	III.125
III.4-14	Thermal Bowing of Reference Fuel Assembly	III.126
III.4-15	Thermal Bowing of Alternate Fuel Assembly	III.127
III.4-16	Effect of Clearances and Transients on Bowing of Reference Fuel Assembly	III.128

LIST OF FIGURES (Cont'd)

Figure No.	Title	Page No.
III.4-17	Effect of Clearances and Transients on Bowing of Alternate Fuel Assembly	III.129
III.4-18	Shear and Moment Distribution in Reference Fuel Assembly Can	III.132
III.4-19	Shear and Moment Distribution in Alternate Fuel Assembly Can	III.133
III.5-1	Total Reactivity Feedback Carbide Fueled Core Ramp Reactivity Insertion 80 Cents in 0.1 Seconds	III.148
III.5-2	Total Reactivity Feedback Carbide Fueled Core Ramp Reactivity Insertion 2$ in 0.1 Seconds	III.149
III.5-3	Total Reactivity Feedback Carbide Fueled Core Ramp Reactivity Insertion 2$ in 1.0 Second	III.150
III.5-4	BCEX Performance in Carbide Fueled Core Ramp Reactivity Insertion 80 Cents in 0.1 Seconds	III.152
III.5-5	BCEX Performance in Carbide Fueled Core Ramp Reactivity Insertion 2$ in 0.1 Seconds	III.153
III.5-6	BCEX Performance in Carbide Fueled Core Ramp Reactivity Insertion 2$ in 1.0 Second	III.154
III.5-7	Axial Expansion Reactivity Feedback Ramp Reactivity Insertion 80 Cents in 0.1 Seconds	III.156
III.5-8	BCEX Fraction of Total Reactivity Feedback Carbide Fueled Core - Ramp Reactivity Insertion 80 Cents in 0.1 Seconds	III.157
III.5-9	Doppler Fraction of Total Reactivity Feedback Carbide Fueled Core - Ramp Reactivity Insertion 80 Cents in 0.1 Seconds	III.158

LIST OF FIGURES (Cont'd)

Figure No.	Title	Page No.
III.5-10	BCEX Fraction of Cermet Worth - Carbide Fueled Core - Ramp Reactivity Insertion 80 Cents in 0.1 Seconds	III.159
III.5-11	BCEX Expansion Performance - Carbide Fueled Core - Ramp Reactivity Insertion 80 Cents in 0.1 Seconds	III.161
III.5-12	Core Average Temperatures - Carbide Fueled Core - Ramp Reactivity Insertion 80 Cents in 0.1 Seconds	III.163
III.5-13	Average and Hot Channels Average Temperatures Carbide Fueled Core - Ramp Reactivity Insertion 2$ in 0.1 Seconds	III.164
III.5-14(a)	Fuel Average Temperatures - Carbide Fueled Core - Ramp Reactivity Insertion 2$ in 1.0 Second	III.165
III.5-14(b)	Average and Hot Channel Average Temperatures Carbide Fueled Core - Ramp Reactivity Insertion 2$ in 1.0 Second	III.166
III.5-15	Hot Channel Fuel Maximum Centerline Temperature Carbide Fueled Core - Ramp Reactivity Insertion 80 Cents in 0.1 Seconds	III.167
III.5-16	Hot Channel Fuel Maximum Centerline Temperature Carbide Fueled Core - Ramp Reactivity Insertion 2$ in 0.1 Seconds	III.168
III.5-17	Hot Channel Fuel and Cermet Temperatures Carbide Fueled Core - Ramp Reactivity Insertion 2$ in 1.0 Seconds	III.169
III.5-18	Hot Channel BCEX Cermet Temperatures - Carbide Fueled Core Axial Section Number 4 (4 of 6) Ramp Reactivity Insertion 80 Cents in 0.1 Seconds	III.170

LIST OF FIGURES (Cont'd)

Figure No.	Title	Page No.
III.5-19	Cermet Temperatures - Carbide Fueled Core Ramp Reactivity Insertion 2$ in 0.1 Seconds	III.171
III.5-20	BCEX Cermet Temperature as a Function of Cermet Rod Diameter - Ramp Reactivity Insertion 80 Cents in 0.1 Seconds - Carbide Fueled Core	III.173
III.5-21	Hot Channel Cermet Temperatures as a Function of Doppler and Sodium Density Coefficients Carbide Fueled Core	III.174
III.5-22	Total Reactivity Feedback - Oxide Fueled Core Ramp Reactivity Insertion 80 Cents in 0.1 Seconds	III.176
III.5-23	Total Reactivity Feedback - Oxide Fueled Core Ramp Reactivity Insertion 2$ in 1.0 Second	III.177
III.5-24	BCEX Performance in Oxide Fueled Core - BCEX Heat Generation 40% of Fuel - Ramp Reactivity Insertion 80 Cents in 0.1 Seconds	III.178
III.5-25	BCEX Performance in Oxide Fueled Core Ramp Reactivity Insertion 2$ in 1.0 Second	III.179
III.5-26	BCEX Expansion Performance Oxide Fueled Core Ramp Reactivity Insertion 80 Cents in 0.1 Seconds	III.180
III.5-27	Average Fuel Temperatures - Oxide Fueled Core Ramp Reactivity Insertion 80 Cents in 0.1 Seconds	III.182
III.5-28	Average Temperatures Oxide Fueled Core Ramp Reactivity Insertion 80 Cents in 0.1 Seconds	III.183
III.5-29	Average Fuel Temperatures - Oxide Fueled Core Ramp Reactivity Insertion 2$ in 1.0 Second	III.184
III.5-30	Hot Channel Fuel Temperatures - Oxide Fueled Core - Ramp Reactivity Insertion 80 Cents in 0.1 Seconds	III.185

LIST OF FIGURES (Cont'd)

Figure No.	Title	Page No.
III.5-31	Hot Channel Fuel Maximum Centerline and Radial Average Temperatures - Oxide Fueled Core - Ramp Reactivity Insertion 2$ in 1.0 Second	III.186
III.5-32	BCEX Cermet Hot Channel Temperatures - Oxide Fueled Core - Ramp Reactivity Insertion 80 Cents in 0.1 Seconds	III.188
III.5-33	BCEX Cermet Hot Channel Temperatures - Oxide Fueled Core - Ramp Reactivity Insertion 2$ in 1.0 Second	III.189
III.5-34	Comparison of BCEX Reactivity Feedback in Carbide and Oxide Cores - Ramp Reactivity Insertion 80 Cents in 0.1 Seconds	III.190
III.5-35	BCEX Fraction of Total Feedback Worth - CEX Rod Diameter Effects - Fuel Material Effects Ramp Reactivity Insertion 80 Cents in 0.1 Seconds	III.192
III.5-36	Doppler Fraction of Total Feedback Worth CEX Rod Diameter Effects - Ramp Reactivity Insertion 80 Cents in 0.1 Seconds	III.193
III.5-37	BCEX Fraction of Cermet Worth - Cermet Rod Diameter Effects - Ramp Reactivity Insertion 80 Cents in 0.1 Second	III.194
III.5-38	Comparison of BCEX Expansion in Carbide and Oxide Fueled Cores - Ramp Reactivity Insertion 80 Cents in 0.1 Seconds	III.196
III.5-39	Change in Core Average Fuel Temperature With Time - Ramp Reactivity Insertion 80 Cents in 0.1 Seconds	III.197
III.5-40	Change in Core Average Cermet Temperature With Time - Ramp Reactivity Insertion 80 Cents in 0.1 Seconds	III.198
III.5-41	Change in Core Average Fuel Clad Temperature With Time - Ramp Reactivity Insertion 80 Cents in 0.1 Seconds	III.199

LIST OF FIGURES (Cont'd)

Figure No.	Title	Page No.
III.5-42	Change in Core Average Coolant Temperature With Time - Ramp Reactivity Insertion 80 Cents in 0.1 Seconds	III.200
III.5-43	Accident Analyses: Dropping Fuel Assembly Reactivity Insertion vs. Time	III.203
III.5-44	Accident Analyses: Dropping Fuel Assembly Change in Core Power With Time (P_o = 2.08 MW)	III.204
III.5-45	Accident Analyses: Dropping Fuel Assembly Change in Core Average Fuel Temperatures 20% Sodium Flow - 0.5% Decay Heat - Coolant Inlet 400°F	III.206
III.5-46	Accident Analyses: Dropping Fuel Assembly Change in Core Average Cermet Temperature 20% Sodium Flow - 0.5% Decay Heat - Coolant Inlet 400°F	III.207
III.5-47	Accident Analyses: Dropping Fuel Assembly Fuel Temperature in Hot Channel - Decay Heat Coolant Inlet 400°F	III.208
III.5-48	Accident Analyses: Dropping Fuel Assembly Cermet Temperatures in Hot Channel - 20% Sodium Flow - 0.5% Decay Heat - Coolant Inlet 400°F	III.209
III.5-49	Accident Analyses: Dropping Fuel Assembly Core Exit Coolant Temperatures - 20% Sodium Flow - 0.5% Decay Heat - Coolant Inlet 400°F	III.210
III.5-50	Accident Analyses: Dropping Fuel Assembly Average Clad Temperatures - 20% Sodium Flow 0.5% Decay Heat - Coolant Inlet 400°F	III.212
III.5-51	Accident Analyses: Control Rod Ejection Reactivity Insertion vs. Time	III.214
III.5-52	Accident Analyses: Control Rod Ejection Change in Core Power With Time (P_o = 415.5 MW)	III.215

LIST OF FIGURES (Cont'd)

Figure No.	Title	Page No.
III.5-53	Accident Analyses: Control Rod Ejection Change in Core Average Fuel Temperatures	III.216
III.5-54	Accident Analyses: Control Rod Ejection Change in Core Average Cermet Temperature	III.217
III.5-55	Accident Analyses: Control Rod Ejection Fuel Temperatures in Hot Channel Axial Section 4 (4 of 6)	III.218
III.5-56	Accident Analyses: Control Rod Ejection Cermet Temperatures in Hot Channel Axial Section 4 (4 of 6)	III.219
III.5-57	Accident Analyses: Control Rod Ejection Average Clad Temperatures Axial Section 5 (5 of 6)	III.221
III.5-58	Accident Analyses: Control Rod Ejection Core Exit Coolant Temperatures	III.222
III.5-59	Accident Analyses: Loss of Pump Power Change in Core Power and Flow From 100% Power and Flow	III.223
III.5-60	Accident Analyses: Loss of Pump Power Cermet Temperatures in Hot Channel Axial Section 4 (4 of 6)	III.225
III.5-61	Accident Analyses: Loss of Pump Power Average Clad Temperatures in Section 5 (5 of 6)	III.226
III.5-62	Accident Analyses: Loss of Pump Power Core Exit Coolant Temperatures	III.227
III.5-63	Reactivity Feedback for Sodium Bonded Carbide Fuel	III.232
III.5-64	Reactivity Feedback for Gas Bonded Oxide Fuel	III.235
III.5-65	Reactivity Feedback Versus Bulk Ceramic Clad Material	III.236

LIST OF FIGURES (Cont'd)

Figure No.	Title	Page No.
III.5-66	Power Coefficients	III.237
III.6-1	Geometric Model for Nuclear Analysis	III.246
III.6-2	Axial Power Distribution Beginning of Life	III.253
III.6-3	k_{eff} vs. Burnup	III.254
III.6-4	Radial Power Distribution Beginning of Life	III.255
III.6-5	Radial Power Distribution 33,333 MWD/MT	III.256
III.6-6	Radial Power Distribution 66,667 MWD/MT	III.257
III.6-7	Axial Blanket Power Distribution (Power Normalized in Core)	III.258
III.6-8	Radial Power Distribution	III.259
III.6-9	$\frac{q''' \text{ cermet}}{q''' \text{ fuel}}$ vs. Burnup	III.261
III.7-1	Variation in Mechanical Properties With Temperature	III.267
III.7-2	Creep Rupture Behavior of Selected Austenitic Stainless Steel	III.268
III.7-3	Modulus of Elasticity of Type 316 Stainless Steel	III.269
III.7-4	Stress Amplitude vs. Cycles to Failure for 316 SS	III.271
III.7-5	Thermal Conductivity and Mean Coefficient of Thermal Expansion of Type 316 Stainless Steel	III.273
III.7-6	Effect of Irradiation on the Ductility of Type 304 Stainless Steel	III.275
III.7-7	The Effect of Plutonium Content on the Thermal Conductivity of Uranium - Plutonium Carbides	III.277
III.7-8	The Influence of Temperature on the Thermal Conductivity of Uranium - Plutonium Carbides	III.278

LIST OF FIGURES (Cont'd)

Figure No.	Title	Page No.
III.7-9	Influence of Carbon Content on the Thermal Conductivity of $(U_{0.85}\ Pu_{0.15})C$	III.280
III.7-10	Specific Heat of Uranium Monocarbide	III.282
III.7-11	Thermal Expansion of Uranium - Plutonium Carbide	III.284
III.7-12	Specific Heat on UO_2 - SS Cermets as a Function of Temperature	III.292
III.7-13	Coefficient of Thermal Expansion of UO_2 - 316 L - SS as a Function of Temperature	III.294
III.7-14	Thermal Conductivity of UO_2 - SS as a Function of Temperature	III.296
III.7-15	Thermal Conductivity of UO_2 - SS as a Function of Ceramic Content	III.297
III.7-16	Ultimate Tensile Strength of UO_2 - SS Cermets as a Function of Temperature	III.300
III.7-17	Ultimate Tensile Strength of UO_2 - SS Cermets as a Function of Cermet Content	III.301
III.7-18	Typical UO_2 - SS Cermet Tensile Curve	III.302
III.7-19	Ratio of Yield to Tensile Strength for UO_2 - SS Cermets	III.304
III.7-20	Fatigue of UO_2 - SS Cermets	III.306
III.7-21	Bend Test Data	III.307
III.7-22	Calculated Effect of Dispersion Fuel Particle Size and Ceramic Content on Selection Criteria	III.311
III.7-23	Irradiation Behavior of UO_2 - SS Cermets - Estimates of Usable Life as a Function of Temperature	III.314
III.7-24	Design Usable Life of UO_2 - SS Cermet as a Function of Centerline Temperature	III.316

LIST OF FIGURES (Cont'd)

Figure No.	Title	Page No.
III.7-25	Fission Gas Pressure in a Particle as a Function of Particle Content and Temperature	III.321
	APPENDICIES	
B-1	Transverse Temperature Gradient as a Function of Axial Position in Outermost Core Subassembly	B-4
B-2	Restrained Thermal Bowing - Assumed Geometry	B-7
B-3	Can to Bundle Forces	B-14

LIST OF TABLES

Table No.	Title	Page No.
II.1	Summary of CEX Concept History	II.9
III.1-1	Refueling Machine Design Parameters	III.23
III.1-2	Reactor Mechanical Design Data	III.26
III.1-3	Summary of Steady State Performance Characteristics for the Westinghouse BCEX Large High Power Density Carbide Core	III.28
III.1-4	List of Primary System Abnormalities Causing Scram and/or Alarm	III.38
III.1-5	Westinghouse Large FBR Modular Core Fuel Cycle Costs Based on Oyster Creek Method[14]	III.41
III.4-1	Summary of Fuel Clad Strains	III.114
III.4-2	Comparison of Fuel Clad Strains and Stresses With Fracture Values	III.115
III.5-1	Core Data Summary	III.140
III.5-2	Material Physical Properties Used in the Transient Analyses	III.142
III.5-3	Time Constants	III.143
III.5-4	Reactivity Coefficients Used in Transient Analyses	III.144
III.5-5	Terminating Limits for Transient Analyses	III.146
III.5-6	Quasi-Equilibrium Reactivity Data	III.231
III.6-1	Volume Fractions	III.245
III.6-2	Nuclear Data	III.252
III.7-1	Chemical Composition of 316 L SS	III.266
III.7-2	Impact Strength and Hardness of Type 316 L	III.270
III.7-3	Major Element Concentration of (U,Pu)C Fuel	III.274

LIST OF TABLES (Cont'd)

Table No.	Title	Page No.
III.7-4	Average Corrosion Rates for Stainless Steel in Sodium	III.287

APPENDICIES

B-1	Rod Bundle Moment of Inertia	B-17

SUMMARY

General

Safety is a key problem area in the development of economical fast breeder reactors. Various design arrangements have been proposed for enhancing the safety of fast reactors. One arrangement is utilizing controlled, structural, thermal expansion to provide a reliable, negative reactivity feedback, which is the principle of operation of the controlled expansion, CEX, concept. Controlled expansion, CEX, can be achieved in various ways. One of these, the Bundle Controlled Expansion, BCEX, fuel assembly concept is the main subject of this investigation.

This study constitutes the first step of a program to develop a controlled expansion, CEX, fuel assembly for fast breeder power reactors that will contribute a reliable, negative power coefficient to supplement the Doppler coefficient for inherent control and safety. The scope of this study includes the identification of the problem areas of the BCEX concept, and the analyses and evaluation of its performance characteristics, in a reference large fast breeder reactor. It also includes a brief study of the dynamic behavior of a second concept, fuel rod Clad Controlled Expansion, CCEX.

The reference reactor design selected for this study is the Westinghouse Large Fast Breeder Reactor using a modular, carbide fueled core. This reactor is the Westinghouse-AEC 1000 MWe Fast Breeder Reactor design with an uprated core power density and lower operating temperatures which provide improved fuel cycle costs. The performance of the BCEX and CCEX concepts are also briefly investigated in a gas-bonded oxide-fueled core.

Summary of Concept Description

The BCEX fuel assembly is a modification of a conventional ceramic fuel assembly. It consists of two half core-length bundles of ceramic fuel rods attached to an array of full core-length cermet rods. Thus, the two

fuel bundles are in series, and are attached only at the ends of the cermet rod array. This entire assembly is hung from the top of the fuel assembly can, with the lower end left free to expand and contract with temperature changes. The fuel content of the cermet ensures that the cermet rods will expand more rapidly with power than the clad around the ceramic fuel. Therefore, an increase in power, which causes the cermet rods to expand, results in pulling the two ceramic fuel bundles apart. This removes fuel having a high worth from the core center and reduces the total reactivity of the core. Controlled bowing of the fuel rods is another advantage of the BCEX concept. Thus, the BCEX concept can introduce a fast-acting negative reactivity coefficient into the reactor core by two means: axial thermal expansion, and radial bowing.

In the clad controlled expansion, CCEX, concept, the clad expansion of compartmented fuel is utilized as a major contributor in terminating a power excursion. In this concept, the stack of active fuel pellets are divided among compartments of appropriate length so that the fuel moves with the cladding. The clad is stainless steel, which has a well known and predictable expansion behavior. With the selection of the appropriate compartment length, the CCEX concept should always provide ceramic fueled cores with a dependable, negative, axial-expansion, reactivity coefficient during a power excursion.

Summary of Problem Areas of BCEX

The BCEX fuel assembly is a complex structure in which the desired effect - a negative power coefficient - is the net result of several, interacting, positive and negative effects, each having a different time response behavior. In BCEX, the controlled axial expansion is achieved by using a cermet fuel rod array which moves the upper and lower fuel bundles apart, thus displacing fuel material from the center of the core. However, this cermet outward expansion reactivity worth is partially counteracted by the positive feedback from the movement of compartmented fuel toward the center of the core due to clad expansion. Detailed transient analyses must deter-

mine the dynamic behavior and effectiveness of these interacting, time-dependent, positive and negative effects.

The cermet-rod cluster functions as a structural member of each fuel assembly and as a small, low power, fuel subassembly within each fuel assembly. These two major functions, to be performed successfully within the reactor core environment, provide a series of design problems which are either unique to the BCEX concept or are significantly more important in BCEX design than in conventional fuel assembly design. Structural integrity of the cermet rods is essential to a successful BCEX fuel assembly design. The effects of many parameters on the structural integrity of cermet fuels must be determined. Important parameters which govern burnup lifetimes of cermet fuels are fuel volume fraction, fuel particle size, percent of theoretical density of the fuel particle, fuel enrichment, neutron flux level and energy spectrum and operating temperature. A thorough understanding of the effects of these parameters is required for BCEX concept adaptation. Unfortunately, the presently available data in the unclassified literature is quite inadequate, thus it does not permit confident design of the cermet structures for BCEX application.

The low melting point of cermet, relative to ceramic fuels, and cermet fuel burnup imposes an inherent limitation to the BCEX concept. Because of this limitation, the allowable volumetric heat generation rate in cermet fuel rods of comparable sizes must be less than 50% of that in the ceramic fuel. This slightly reduces the thermal power rating in the core (2.5 to 4.5%). The heat generation rate in the cermet fuel is an important design parameter in determining BCEX effectiveness. A BCEX element using "cermet" rods with zero volume fraction of fuel would be structurally acceptable, but would not provide sufficient negative reactivity feedback. As the fuel loading in the cermet is increased from zero, the negative feedback which it can contribute increases, but the length of time during which the cermet will perform satisfactorily as a structural member in the reactor decreases.

A BCEX fuel assembly is certainly a more complicated mechanical design than a conventional ceramic fuel assembly. Because of this, some problem areas requiring resolution are: 1) galling, fretting or self-welding due to relative motion of subassemblies, 2) cermet array buckling unless adequate lateral support is provided, 3) fuel and cermet subassembly attachment to each other and to the fuel assembly can to obtain structural integrity while not inhibiting desired subassembly movement, 4) establishment of optimum number, size and relative positioning of the rods of the cermet structure, 5) dynamic and static loading of the cermet structure, 6) selection of the most appropriate cermet clad bond, and, 7) design of fuel assembly to best utilize the advantageous bowing feature.

Balancing of the relative coolant flow rates around the cermet and ceramic fuel rods is an important engineering development problem in the BCEX fuel bundle design, because less heat generation occurs in the cermet rods. Overcooling of the cermet rods will somewhat inhibit BCEX response and increase the amount of ineffective coolant flow in the reactor core.

Summary of Results

Transient Analyses

A parametric study was performed to investigate the transient characteristics of the two controlled axial expansion concepts (BCEX and CCEX) using two different fast reactor cores: the reference sodium-bonded, carbide-fueled core and a gas-bonded, oxide-fueled core. A core having zero axial expansion was selected as the base line from which to evaluate the merits of BCEX and CCEX. The oxide-fueled core was designed to have the same fuel volumetric power density as the carbide-fueled core. This was achieved by adjusting the oxide fuel pellet diameter to ensure tolerable fuel temperatures. As the overall height and diameter of the oxide core are approximately equal to those of the carbide core, the temperature-dependent reactivity coefficients of the carbide core were assumed to be applicable to the oxide core. Thus, the differences in behavior of BCEX and CCEX in the carbide and oxide cores is due solely to the differences in their thermal properties.

Three postulated accidents were also analyzed to study the transient characteristics of BCEX and CCEX in the reference carbide core:

1. Refueling accident - dropping a fuel assembly into a just subcritical core.
2. Expulsion of a control rod at 100 percent core thermal power, and
3. Loss of electrical power to all primary pumps at 100 percent core thermal power.

A cermet rod diameter of 0.360 inches O.D., and a volumetric heat generation rate of 30% of that of the carbide fuel, were used in the accident analyses.

Both BCEX and CCEX were found to provide ceramic fueled fast reactor cores, which possess assumed zero axial expansion, with a predictable, negative, axial expansion, reactivity feedback mechanism that will contribute significantly in terminating a power excursion. In terms of reactivity fractional worth, during the initial stages of an excursion, BCEX is more effective in the oxide core in assisting the other negative reactivity feedbacks to terminate the excursion. In the carbide core, the effectiveness of BCEX is greatly reduced during the initial stages of an excursion by the rapid expansion of the clad on the fuel rod. The carbide fuel rod time constant is 0.47 seconds, compared to 0.79 seconds for the cermet rod, and 2.08 seconds for the oxide fuel rod. Thus, the clad on the oxide fuel rod has the slower response; this prevents a sharp reduction in the fractional worth of BCEX in the oxide fueled core during the initial stage of the excursion.

As new equilibrium thermal conditions are approached in the core after the reactivity input has been terminated, the reactivity feedback fractional worth of BCEX is greater in the carbide core than in the oxide core. The BCEX fractional worth may be 80% greater than the Doppler's fractional worth, depending upon the cermet rod diameter and volumetric heat generation

rate. In the oxide core, the BCEX fractional worth is less than the Doppler worth.

If the compartmented fuel moves in a predictable manner with the clad, the performance characteristics of CCEX in the carbide core are - depending upon the reactivity insertion rate - as good as, or better, during an excursion than those of BCEX. This is especially true in the early stages of an excursion, when the temperature overshoot characteristic of BCEX in a carbide core may become quite large. For example, in the CCEX analysis for a two dollar insertion at a rate of 20$/second in the carbide core, only the CCEX core was not damaged. The response of CCEX decreases with an increasing fuel rod time constant. In an oxide core, CCEX is a less effective accident terminating mechanism than in a carbide core.

The net reactivity worth at equilibrium conditions of BCEX using metallurgically bonded cermet rods ranges from 50% to 65% of the cermet's outward expansion reactivity worth. In other words, the effect of the fuel clad inward-expansion is to downgrade the gross cermet's reactivity worth by 35% to 50%. The BCEX performance characteristics are improved by using a fuel clad material having a lower linear expansion coefficient, or increasing the cermet rod diameter, cermet volumetric heat generation rate, and/or the cermet-to-clad contact resistance (inverse of conductance).

In the study of the expulsion of a control rod (one dollar at an acceleration of 100 ft/sec^2) from a carbide core, BCEX and CCEX are equally effective in terminating the excursion. However, in the refueling accident, when the maximum worth fuel assembly - two dollars - is dropped under one g acceleration into a just subcritical carbide core, BCEX is much less effective than CCEX in controlling the resultant power excursion during the important first few milli-seconds. The assumed initial refueling power level and flow rate used were 0.5 percent and 20 percent of rated conditions, respectively. The transient characteristics in the BCEX core resulted in a temperature overshoot sufficient to exceed the nominal

coolant boiling temperature at the outlet of the hot channel. In the CCEX core, the maximum coolant temperature was well below the boiling temperature at a pressure of 40 psia.

The net reactivity feedback from BCEX during the loss of all electrical power to the primary pumps was found to be always negative for the assumed flow decay characteristic, even though the clad inward expansion slightly exceeded the cermet expansion. Since the sodium temperature coefficient is negative, it prevents BCEX and CCEX from demonstrating their excursion terminating effectiveness in this type of accident.

Mechanical Analyses

The mechanical design of the reference BCEX fuel assembly was investigated. This assembly consists of four main components; the full-length central cermet subassembly, identical upper and lower half-length fuel bundles, and the subassembly can. Each hexagonal fuel bundle consists of 120 (Pu,U)C, compartmented, sodium-bonded, vented fuel rods with 0.01 inch thick clad with a 0.300 inch O.D. arranged on a triangular pitch on 0.426 inch centers. The central cermet subassembly consists of seven rods containing mixed oxide fuel particles dispersed in a stainless steel matrix which is metallurgically bonded to a 10 mil thick stainless steel clad. The hexagonal shaped can, which is approximately 5.1 inches across flats and has a wall thickness of 0.093 inches, encloses each fuel assembly to support the fuel and to provide an autonomous flow channel for efficient orificing.

The dynamic response of the reference BCEX fuel assembly was analyzed to determine its performance characteristics for both terminated and unterminated transients. It was found that for any characteristic times (i.e., transient ramp periods) longer than 0.023 and 0.016 seconds, for the terminated and unterminated transient cases respectively, the stresses in the cermet rods due to inertia forces and the post-transient reactivity fluctuation due to bundle vibration, will be negligible. None of the

characteristic times for any of the terminated or unterminated transients which were analyzed in this study were less than 0.050 seconds. The effects of such BCEX design parameters as number of cermet rods, cermet rod length, cermet sonic velocity, weight of cermet rod bundle, weight of fuel bundle, cermet and fuel density and cross-sectional area, and cermet elastic modulus are also presented. Large variances from any of the values of the reference design parameters are required before any significant inertial forces occur in the cermet assembly.

The cermet rod design was examined for all recognized failure modes. The cermet surface strain due to internal heat generation is between 0.3 and 0.4 percent. Column loading from a buckling standpoint is negligible during any of the transients postulated. Stresses due to vibration, bending due to bowing induced by core radial temperature gradients, bundle flow drag and static weight, and axial temperature gradients were found to be negligible. The lack of cermet ductility and other pertinent data, and the lack of an accurate solution to the fuel swelling and fission gas pressure problem in this as well as in other investigations, presently, makes it difficult to predict definitely the cermet integrity from an analytical point of view. Discussion of the cermet design from an empirical point of view is presented, where it is concluded that the cermet design appears to be adequate for the desired lifetime and operating conditions based upon available data.

Each carbide fuel rod is vented to the sodium coolant. This eliminates clad stresses due to coolant or fission gas pressure. Stresses and strains still arise in the fuel cladding. The following specific causes of stresses and strains in the nuclear reactor core were investigated: (a) restraint to bundle bowing, (b) non-linear radial bundle temperature gradient, (c) clad radial temperature gradient, (d) clad axial temperature gradient, (e) static weight and flow drag, (f) rod vibration in parallel flow and bundle vibration in parallel flow. The resulting stresses and strains were evaluated with appropriate fracture criteria. The largest single component of strain due to any postulated loading was found to be approximately 0.001 inches per inch, caused by the radial temperature drop

across the clad wall. The maximum calculated superimposed strain was 0.00134 inches per inch. Cumulative usage factors of .0016 or less and minimum times to long-time stress rupture of greater than 100,000 hours were found.

The mechanical design of the hexagonal shaped can which encloses each fuel assembly was investigated. Raised bosses are provided on the can outer surface to contact similar bosses on adjacent cans. From a check of the static internal pressure loading against the Fermi design and conditions, a comparable can wall thickness is obtained. Creep deflections of less than 0.001 inches were also calculated. Negligible strains are developed due to can internal heat generation.

Various modes of fuel assembly bowing were analyzed. The effect of such parameters as number and location of restraints, effect of a clearance, and operating level changes (0 to 100% power and 100% to 200% power) were investigated for the reference core incorporating the BCEX fuel assembly design for anticipated operating conditions. An alternate method of restraint was also investigated. On the basis of the bowing analyses performed in this study:

a) Two judiciously located upper can restraints appear adequate to provide the most realistic method for controlling thermal bowing of the BCEX fuel assemblies.
b) Both the reference and alternate designs for conditions between zero and 200 percent power were found to have a net reactivity effect due to thermal bowing between zero and minus 10 cents, and
c) The maximum bending moment and shear forces required for acceptable bowing restraint induced in the fuel assembly can to restrain "free bowing" in the reference and alternate designs are -25,000 and -17,000 inch-pounds and 7,000 and 3,000 pounds respectively. These loads are considered acceptable.

Thermal and Hydraulic, Nuclear and Materials Analyses

Supporting work was performed in the areas of Thermal and Hydraulic, Nuclear, and Materials analyses to provide the required input data for the two main areas of analysis performed in this study: transient and mechanical.

The burnup temperature history of the UO_2 - 316 stainless steel cermet was compared to ORNL empirical estimates. Using a burnup criterion based upon average cermet temperatures, for an anticipated 100,000 MWD/MT average burnup of fuel, the volumetric heating ratio of the cermet to ceramic fuel is limited to 0.30 and 0.25 for 0.300 and 0.368 inch O.D. cermet rods, respectively. Sufficient data is not presently available to substantiate such a criterion, but it is a logical approach to conservative data.

The magnitude of the transverse coolant temperature gradients within the reference fuel assembly design was investigated as a function of coolant mixing and as a function of the axial and radial position of the assembly in the core and blanket. For the worst time in life for zero transverse coolant mixing, the maximum can-wall to can-wall exit coolant temperature differences in the core was 77°F in the outer radial ring of fuel assemblies. Much larger transverse temperature differences were calculated for the innermost zone of the radial blanket.

The nuclear characteristics of the reference BCEX core pertaining to the BCEX concept and related safety features were calculated using standard Westinghouse Atomic Power Division fast reactor calculational procedures. The following reactivity coefficients were utilized in the transient analyses (at beginning of equilibrium fuel cycle, 33,000 MWD/MT for the reference core. The Doppler coefficient, $T \frac{dk}{dT}$, = -0.00335, the total core sodium coefficient, $\rho \frac{dk}{d\rho}$, = +0.0164, the BCEX cermet expansion coefficient, $L \frac{dk}{dL}$, = -0.762, the BCEX fuel rod clad back expansion coefficient L dk/dL, = +0.368, the CCEX fuel rod clad expansion coefficient, $L \frac{dk}{dL}$ = -0.394; and the bowing coefficient, R dk/dR, = -0.5255.

For the reference core design, the fuel clad and core structure material is 316 L stainless steel and the fuel material is uranium-plutonium monocarbide. The properties of these materials and sodium environment effects on 316 L stainless steel are reviewed and tabulated.

Cermet fuel, consisting of $(U,Pu)O_2$ in a 316 L stainless steel matrix with 316 L stainless steel cladding, has been selected for the control element in the BCEX assembly. Generally, the properties of cermets are linear functions of matrix content; therefore, they are strongly governed by the volume fraction of ceramic particles present. For a given composition, the method of fabrication exerts far more control over properties than any other factor. There is little information available on long term properties such as creep and stress rupture, and even less on post-irradiation properties of the cermet matrix material.

An evaluation of cermet selection characteristics shows that particle size, particle density, and volume percent ceramic are important factors. The reference design particle size was selected as 250-350 μ. Smaller particles will give thinner matrix ligaments for restraint of strain. Even larger sizes would be desirable; however, data for larger particle sizes were not reported. The reference particle density was selected as 85 percent because a) a low density is desired to obtain more space to accommodate fuel swelling and fission gas, and b) 85 percent is the lowest density which the literature indicated any confidence of achieving. The design limit for the volume percent ceramic was selected as 35 percent due mainly to lack of data at higher percentages.

Empirical burnup limits are defined as a function of operating temperature. Design considerations show the primary mode of failure to be fuel swelling augmented by pressure from fission gas buildup.

Conclusions and Recommendations

In determining whether the cost of developing CEX, and the higher fuel cycle cost with CEX, are justifiable, the crucial question is: what is the degree of effectiveness, or worth, of CEX in controlling the dynamic behavior of the reactor. This investigation quantified some of the information required to judge the effectiveness of two CEX concepts, BCEX and CCEX.

In all transient analyses performed in this investigation, utilization of either the BCEX or the CCEX concepts (axial thermal expansion) significantly improved the core transient behavior over the non-CEX (zero expansion) core. Both BCEX and CCEX will provide ceramic fueled fast reactor cores, which possess assumed zero axial expansion, with a predictable, negative, axial expansion, reactivity feedback mechanism that will contribute significantly in terminating a power excursion.

The relative value of the component time constant is a good indicator of early dynamic response. The relative values of the time constants of the carbide fuel rod, cermet rod, and oxide fuel rod are 0.47, 0.79 and 2.08 seconds, respectively. Thus, the clad on the oxide fuel has the slower response. This fact makes a) BCEX relatively more effective in an oxide core than in a carbide core, and b) CCEX more effective in a carbide core than in an oxide core during the initial stages of a power excursion. However, in case (a), the dynamic response is considerably different for quasi-steady state conditions, where the reactivity feedback fractional worth of BCEX is greater in the carbide core than in the oxide core.

The simplest way to obtain effective negative control in the dynamic behavior of fast reactors through the use of axial thermal expansion is expansion of the solid column of fuel, itself. However, it has not been demonstrated that operating fuel behaves in a predictable manner (hence the assumption of zero expansion in the analysis). It was found in this study, that the behavior of the fuel can alter significantly both the absolute and relative values of CCEX and BCEX. Fuel and clad properties

which enhance BCEX will adversely effect CCEX, and vice versa. Further work is recommended to establish the optimum compartment size and the resulting performance of CCEX and BCEX. This work should include experimental determination of the range of fuel expansion properties and emphasize design parameters which potentially offer improved safety performance.

If predictable fuel thermal expansion due either to expansion of its clad (CCEX) or expansion of the solid column of fuel can be demonstrated, the BCEX concept appears to offer only marginal improvement over CCEX in terminating various nuclear excursions in either a carbide core or an oxide core. CCEX has a simpler mechanical design, due to elimination of the half core-length fuel bundles and the cermet rod array. For these reasons, the CCEX concept is an attractive alternate to BCEX, and it is recommended that further development work be carried out on the CCEX concept.

If the technical and commercial feasibility of predictable fuel thermal expansion cannot be demonstrated, then BCEX offers a significant improvement in the dynamic behavior of a non-CEX core. Therefore, both concepts BCEX and CCEX - should be further investigated in parallel to permit the selection of the more attractive concept for ultimate application to commercial fast breeder reactors.

The further development tasks for BCEX should include the evaluation of alternates to the reference BCEX design concept. Alternates which may significantly improve BCEX performance characteristics are 1) using fuel rod clad material having a linear expansion coefficient lower than that of 316 L stainless steel, 2) changing cermet-to-clad contact resistance, 3) designing the BCEX fuel assembly so that the cermet and fuel clad expansions are additive, and 4) using an alternate cermet matrix material. Investigation of these alternates were not within the scope of this study, but are warranted in the future.

An important requirement for further investigation of a cermet fuel for a particular application is the establishment of a reference process and product design including development of optimum size fuel particles. Substantial effort is required in this area of development. For this reference process and product design, typical non-irradiated thermal and mechanical properties must be determined. Long term mechanical properties such as creep, stress rupture, and fatigue must be well established. Cermet irradiation studies, both analytical and experimental, must receive major emphasis, as cermet irradiation properties must be extensively investigated to obtain more positive assurance of cermet structural integrity. Present data do not provide the required assurance to permit design of a fuel element with a specific lifetime for specific nuclear, thermal, and mechanical conditions.

Inertial stresses in the reference cermet rods due to any of the transients postulated in this study are negligible. Large variations from any of the values of the reference design parameters are required before any significant inertial forces in the cermet assembly would be obtained. It can be concluded that all stresses and strains for the reference fuel clad and assembly can designs for the reference reactor conditions are well within allowable limits. The can wall thickness of 0.096 inches is sufficient for the reference operating conditions for a 25,000 hour lifetime. Thus, the reference BCEX fuel assembly design is considered quite adequate from a transient as well as all other mechanical design viewpoints for all conditions postulated in this study based upon the limited available data.

Friction, galling and wear between moving parts of the fuel assembly must be fully evaluated in a sodium environment at design conditions.

A prototype BCEX fuel assembly should be built and tested in-pile to study the feasibility of the fabrication and operation of the bundle controlled expansion assembly design.

Thermal bowing of the reference core incorporating BCEX fuel assemblies can be controlled so as to have a net reactivity effect between zero and minus 10 cents. Fuel bowing for the range of actual reactor design conditions must be further investigated. Further analyses are required to determine the optimum method of supporting (location and number of restraints) the fuel bundles within the can so as to minimize bundle restraining forces and not impede BCEX response capabilities. As the choice of location and number of support points greatly affect the net movement of fuel, bowing analyses should be closely correlated with physics calculations to obtain a zero-to-negative bowing reactivity coefficient. The bowing analyses illustrated the importance of minimizing initial clearances between fuel assemblies. Bowing analyses should be extended to cover the full range of power levels anticipated. This is important as, until sufficient bowing of the fuel has occurred to take up initial clearances and reach a stable geometry, unusual effects may be observed.

Coolant mixing schemes must be devised to obtain adequate coolant mixing between ceramic fuel rods and cermet fuel rods. Schemes which will enhance transverse mixing of the coolant across the fuel assembly thereby reducing fuel bundle bowing are also required.

Continued improvement of calculations for Doppler and sodium void effects will be necessary to accurately evaluate the need and relative benefits of fast breeder reactor safety features such as the CEX concepts. The measurement of the reactivity effects of either the bundle controlled expansion, BCEX, or the clad controlled expansion, CCEX, using existing critical facilities (ZPR-III, ZPR-VI) is an obvious early step in pinning down the coefficients and evaluating the analysis techniques.

In the CEX concept, fissile material is removed from high importance regions of the core (e.g., the core center) and placed in low importance regions (e.g., the core-blanket interface). When this is recognized, it becomes clear that the reactivity worth of various fissile materials, as a function of position in the core, is a key quantity. In numerous

experiments, notably with ZPR-III, this quantity has been measured and reported in the literature. An extensive comparison between calculations and experimental determinations of reactivity worths would either increase confidence in present calculational methods or indicate that these methods need improvements. This may well be the next logical step before designing a critical experiment test on the CEX concept.

This study was limited to the Westinghouse Large Fast Breeder Modular Reactor. Analysis of the reactivity effects in reactor cores with other geometries, i.e. pancake, right circular cylinder cores ($L/D \gtrsim 1$), etc., may prove that the CEX concept is the automatic control device that changes a marginal reactor into a safe reactor. This would allow the use of reactors with superior economic advantages but with otherwise marginal safety characteristics.

I. PROBLEM STATEMENT

Safety is one of the key problem areas in the development of fast breeder reactors.

One of the methods which has been proposed to assist in the solution of this problem is to provide a negative power coefficient to supplement the Doppler coefficient by utilizing structural, thermal expansion in a controlled and predictable manner. This is the Controlled Expansion (CEX) Concept. One of the CEX concepts is the Bundle Controlled Expansion (BCEX) concept. The use of the BCEX concept has been proposed in references 1 through 9* as a means of obtaining a distinct, in-core, thermal expansion characteristic. This characteristic provides a supplementary, inherent, safety and control mechanism for fast breeder reactors.

The potential merit of the BCEX concept was recognized in 1964 by the AEC evaluation of the four design studies of a 1000 MWe FBR[10] which included the following summary statement about the BCEX concept:

> "the feasibility of devices such as the controlled expansion fuel element which substitutes mechanical motion for materials properties to achieve a negative temperature coefficient of reactivity should be studied. This fuel element may offer an alternate to enhancing the Doppler effect by BeO addition."

This study is addressed to the problem of determining the feasibility of controlled expansion fuel elements, as recommended by the AEC.

This study constitutes the first step of a program to develop a fuel assembly for fast breeder power reactors which will contribute a negative power coefficient to supplement the Doppler coefficient for control and safety. Specifically, this first step should 1) identify the problem areas of the BCEX concept and 2) determine and evaluate the performance characteristics of the BCEX concept for a large FBR

---

*References appear at the end of the section.

core. The overall problem then, of which this study is the first step, is 1) the determination of the feasibility of the use of the controlled expansion concept for Large Fast Breeder Reactor application, and 2) the development of a practical controlled expansion fuel assembly design which can be utilized in a commercial fast breeder power reactor.

Section I - References

1. "Westinghouse Proposal for Fast Breeder Reactor Development Program to U. S. Atomic Energy Commission",submitted by WAPD, February 1963.

2. Heck, F. M., "Westinghouse Fuel Assembly for Fast Breeder Reactor Application", WCAP-2237, March 1963.

3. Heck, F. M., "Westinghouse Fuel Assembly for Fast Breeder Reactor Application", WCAP-2237 (Rev.), March 1963.

4. Heck, F. M., "Neutron Controlled Expansion Fuel for Fast Breeder Reactors", Proceedings of the Conference on Breeding, Economics, and Safety in Large Fast Power Reactors, ANL 6792, October 7-10, 1963.

5. Heck, F. M., et al, "Liquid Metal Fast Breeder Reactor Design Study", WCAP-3251-1, January 1964.

6. Gunson, W. E., et al, "The Liquid Metal Fast Breeder Reactor Design Studies", WCAP-2635, July 1964.

7. Gunson, W. E., et al, "High Power Density, Stainless Steel Reference FBR Core Design", WCAP-2638, July 1964.

8. Keyfitz, I. M., et al, "200 MWe Sodium Fast Reactor Prototype (SFRP) Design Study", WCAP-2628, September 1964.

9. Westinghouse Proposal for Modifications of the Hallam Nuclear Plant Facility, presented to the U. S. Atomic Energy Commission in March 1965.

10. "An Evaluation of Four Design Studies of a 1000 MWe Ceramic Fueled Fast Breeder Reactor" prepared by Reactor Engineering Division, COO-279, USAEC, December 1, 1964.

II. INTRODUCTION

II.1 Authorization and Scope of Contract

II.1.1 Authorization and Objectives

This study was authorized under United States Atomic Energy Commission (AEC) contract AT(30-1)-3589. It is being administered by the New York Operations Office of the AEC. The contract initiation date was August 2, 1965. This study constitutes the first phase of a program to develop a controlled expansion (CEX) fuel assembly for fast breeder power reactors that will contribute a negative power coefficient to supplement the Doppler coefficient for control and safety.

This study consists of: a) analyses and evaluation of the performance characteristics of a bundle controlled expansion (BCEX) fuel element in a large fast breeder reactor (FBR) core; b) the preliminary design of a bundle controlled expansion (BCEX) fuel element assembly for testing in EBR-II, and c) recommendations of development requirements for the BCEX concept. The results of a) are reported in this topical report.

This study has the following objectives:

1. To identify the problem areas of the BCEX concept.
2. To determine and evaluate the performance characteristics of the BCEX fuel element for a large FBR core. (In the work program for this study, the reference core was designated as either the Westinghouse-AEC 1000 MWE FBR modular core or an uprated version of this core.)
3. To prepare a preliminary design of a BCEX fuel element assembly for testing in EBR-II.
4. To evaluate projected results for BCEX fuel element test assembly operation in EBR-II.
5. To recommend future development of BCEX fuel elements.

This study constitutes an important first step in determining the behavior of a CEX fuel element in a fast reactor, thus contributing to the ultimate development of this concept as a supplementary fast reactor safety and control mechanism.

II.1.2 Scope

In the contract, the scope of the technical work for this study is worded as follows:

> "The contractor shall perform the work generally in accordance with the technical details described on pages 4 through 11 (phase I) of the contractor's proposal for "Controlled Expansion Fuel Development Program" dated May 1963[1]* and revised December 1964[2] and further revised by the letter from the contractor to the Commission (Rees to Shaw) dated March 2, 1965[3]. The work shall include:
>
> (1) Analytical studies of (a) the parameters describing the operational characteristics of the controlled expansion fuel element, and (b) the physical properties, including the effects of irradiation, of materials suitable for use in the controlled expansion fuel element to obtain design information and establish design criteria for a fast breeder nuclear power reactor controlled expansion fuel element assembly.
>
> (2) Preliminary design of a controlled expansion fuel element assembly for demonstration and performance testing in a nuclear reactor to be designated by the Commission, and a design report for the CEX test assembly will be furnished; and
>
> (3) Development of a program presenting the scope of work for detailed design, fabrication, demonstration testing and performance testing of the designed assembly, and the estimated cost and schedule for the program.

*References appear at the end of the section.

The aforesaid parametric studies of operational characteristics, studies of materials properties, and preliminary design of the controlled expansion fuel element assembly shall include considerations of mechanical, thermal, hydraulic and nuclear design. The fuel element assembly design shall have as a prime objective the demonstration and performance testing of the criteria established to describe the fast breeder nuclear power reactor controlled expansion fuel element assembly."

II.2 Initial Design Bases and Groundrules

The Westinghouse Large Fast Breeder Modular Reactor (WLFBMR) was selected as the reference reactor design for the analysis of the performance characteristics of the bundle controlled expansion (BCEX) fuel assembly concept. This was the most significant ground rule established for the study. The Westinghouse Large Fast Breeder Modular Reactor Core is the Westinghouse-AEC 1000 MWe Fast Breeder Reactor modular core design developed under AEC contract AT(30-1)-3251 and reported in WCAP-3251-1[4] with an uprated power density and lower operating temperature as outlined in WCAP-2638[5]. The WLFBMR core was selected as the reference design because, as a result of reduced fuel inventory, its fuel cycle cost is more than 20 percent lower than that for the original Westinghouse-AEC 1000 MWe FBR core.

The basis for the design of the reference Westinghouse Large Fast Breeder Modular Reactor core is outlined in the "Liquid Metal Fast Breeder Reactor Design Study"[4], and in the "High Power Density, Stainless Steel Reference FBR Core Design"[5]. A summary of this basis follows:

1. The design philosophy for the Westinghouse-AEC 1000 MWe FBR Study[4] was predicated upon the following considerations which are also applicable to the WLFBMR:
   a. Maximum utilization of existing technology.
   b. Adoption of advanced concepts that offer significant technological and economic gains and reasonable probability of achievement.
   c. Recognition of calculational uncertainties and observance of a prudent course with respect to safety; and
   d. Exploitation of the economic potential of the large fast breeder power plant to the maximum, consistent with the above considerations.

2. The objective of the Westinghouse-AEC 1000 MWe FBR Study[4] was to develop a conceptual design for the nuclear portion of a 1000 MWe fast breeder power reactor such that a prototype plant could be under construction before 1975. These targets are still pertinent.
3. The reactor is a fast spectrum-breeder which provides safe and stable operation. Inherent reactor dynamic stability is required. A seven modular core was selected to provide a safe, economic design. The reactor is sodium cooled and has a high breeding ratio and short doubling time.
4. The reactor thermal energy output is based on an average carbide fuel linear power rating of 15.6 kw/ft, which was determined to be acceptable in previous Westinghouse investigations (reported in references 5 and 6). The thermal and hydraulic imposed limitations used to determine the acceptability of this core are defined later in this section. This power rating specified a module (excluding blanket and cermet rods) power output of 404 MWt.
5. The core and fuel assembly mechanical design from the Westinghouse-AEC 1000 MWe Study[4] is adopted for this study. The reference core design is described in Section III-1. The mechanical design emphasizes design simplicity, ease of fabrication and maintainability; it provides inherent and controlled safety, and does not unduly limit or compromise the reactor performance.
6. Plutonium-uranium carbide fuel, thermally bonded by sodium to the clad and vented to the coolant, is utilized.
7. The core coolant mixed mean outlet temperature is 1100°F, and the coolant inlet temperature is 850°F. The reactor operating conditions are further described in Section III-1.

8. The average carbide fuel burnup is 100,000 MWD/MT.
9. Fuel clad material is stainless steel, type 316 L.
10. The cermet fuel material is $(Pu\text{-}U)O_2$ fuel in a 316 stainless steel matrix material.
11. Both upper and lower axial blankets are 12 inches thick, and fueled with depleted UC.
12. A one-year refueling period is assumed.

Certain thermal and hydraulic imposed limitations which established the reference reactor core design used in this study are:

1. The steady state fuel clad surface hot spot temperature is limited to approximately 1300°F at 100% power.
2. The steady state fuel surface hot spot temperatures should be less than 1500°F at 100% power. This is more than 100°F below the boiling point of sodium at one atmosphere pressure.
3. The carbide fuel hot spot temperature is limited to 2450°F.
4. Core pressure loss is limited to 90 psi so that the total primary system pressure drop will be less than the available head from a single-stage impeller pump.
5. An adequate DNB ratio is required to prevent the occurrence of burnout.

Some initial ground rules which were established for this study are:

1. The materials effort will consist of a literature review and updating of past work on 316 stainless steel clad, cermet and carbide fuel, to provide estimates of materials engineering properties for design purposes in this study. This materials effort should be limited to obtaining the information readily available and to the broad requirements of the contract scope of work.

2. The nuclear analyses will be performed on the "Hybrid" or "average" module whose neutron flux boundary conditions represent a weighted value between a completely reflected module, i.e. the center module of seven modules, and the partially reflected modules, i.e., the outer six modules.

II.3 CEX Concept Background Information

II.3.1 Summary

Table II.1 summarizes the history of the CEX concept.

II.3.2 Conception

The controlled expansion (CEX) fuel assembly concept, which provides a supplementary, inherent, safety and control mechanism for fast breeder reactors, was conceived in January 1963 by F. M. Heck of Westinghouse Atomic Power Division[7]. A bundle controlled expansion (BCEX) fuel assembly design for a fast reactor core application was developed by H. Keller and H. N. Andrews of Westinghouse Atomic Power Division in January 1963[8]. Westinghouse patents on these two inventions are presently pending.

II.3.3 Fermi Proposal

In February 1963, the first application of the CEX fuel assembly concept was proposed in the "Westinghouse Proposal for Fast Reactor Development Program to the U.S. AEC,"[9]. In this document, the development of the CEX fuel assembly for fast breeder application (Enrico Fermi reactor) was proposed, and the following four principal safety features of the BCEX assembly concept were suggested:

a. Axial expansion of fuel out of the center of the reactor.
b. Radial bowing of rods away from the center of the reactor core.
c. Provision of sufficient volume of U-238 to produce a negative Doppler coefficient of reactivity.
d. This increased amount of U-238 will also provide additional delayed neutrons from fast fission and will permit an in-core breeding component.

Table II.1

Summary of CEX Concept History

Note: Dates only approximate

CEX Concept Conception	January 1963
CEX Fuel Assembly Design Conception	January 1963
W Fermi Proposal (incorporated BCEX fuel assembly design)	February 1963
Initial CEX Development Program Proposal	March 1963
W Funded BCEX Mechanical Design Studies	March-December 1963
Second (three-phase fuel development) BCEX Program Proposal	May 1963
W-AEC 1000 MWe FBR Study, Contract AT(30-1)-3251	June-December 1963
W Evaluation of Four AEC 1000 MWe FBR Studies	April-July 1964
W 1000 MWe FBR Upgrading (to high power density core)	May-July 1964
W 200 MWe SFR Prototype Design Study	May 1964-March 1965
Revised CEX Development Program Proposal	December 1964
W "SAFER" Design Study	November 1964-May 1965
Hallam Proposal	March 1965
W FBR Right Circular Cylinder Core Design Study	May 1965-January 1966
W AEC CEX Fuel Element Development Program (Phase I) Contract AT(30-1)-3589	August 3, 1965-present

The proposal describes a "conceptual" BCEX fuel assembly to be inserted in the Enrico Fermi Reactor, its special features, and its mechanical design problems. A recommended testing program to develop this concept was also described. Preliminary thermal and hydraulic, nuclear, and transient performance analyses, and some materials properties aspects were also discussed.

II.3.4 First Published Reports on CEX

In March 1963, the BCEX concept design features and description were published in "Westinghouse Fuel Assembly for Fast Breeder Reactor Application"[10] and "Westinghouse Fuel Assembly for Fast Breeder Reactor Application (Rev.)"[11]. These two reports are an introduction to the CEX concept and discuss many of its features. They describe the "conceptual" BCEX fuel assembly designed for "Fermi"; discuss cermet fuel design considerations, and the results of preliminary investigations of controlled axial expansion and bowing of the BCEX fuel assembly; they also present a very preliminary discussion of stability analyses and of development requirements for the CEX concept.

II.3.5 Westinghouse-AEC 1000 MWe FBR Study (AEC Contract AT(30-1)-3251)

In this investigation, which is well documented in the "Liquid Metal Fast Breeder Reactor Design Study",[4] the BCEX fuel assembly was selected as the reference design to provide an inherent negative reactivity coefficient by fuel axial motion for a mixed Pu-U carbide fueled, 1000 MWe, fast breeder reactor utilizing a modular core. This investigation included a study of some of the nuclear, thermal and hydraulic, transient, and mechanical characteristics and features of the reference 1000 MWe FBR core with BCEX fuel assemblies.

Nuclear reactivity coefficients were obtained for a 1/2 inch and for a 1 inch center gap in the fuel assembly from one-dimensional multigroup analyses in the axial direction for the reference 1000 MWe reactor core design. The reference BCEX assembly consisted of seven centrally

located cermet rods (full core length) with volumetric heat generation rates of 20 percent of that of the carbide fuel, and 120 carbide fuel rods, all of 0.300 inch diameter, on 0.426 inch pitch. The carbide fuel rods were half-core lengths of about 51 inches spaced to provide for the "BCEX" operation. The rods were vented to the coolant with a sodium bond between the fuel pellet and clad. All structurals were 316 L stainless steel. Round ferrules were utilized for spacing and were brazed with the fuel and cermet rods into a single stable structure.

Some transient analyses were performed on the 1000 MWe reactor "CEX" core. In particular, the effects were studied of such variables as the cermet volumetric heat generation rates, reactivity feedback worths per unit of temperature rise, cermet rod diameters, and coolant inlet temperatures. The use of cermet rods to provide a strong, negative, mechanical (expansion) temperature coefficient in a ceramic-fueled core was found to enhance core stability and response to reactivity changes. The physical and mechanical properties of cermet fuel were reviewed very briefly during this study.

II.3.6 Westinghouse Funded CEX Mechanical Design

A mechanical design study was conducted during 1963 based upon the original Westinghouse 1000 MWe FBR fuel assembly design. This work was reported in references 12 and 13, and at the 1963 ANL Fast Power Reactor Conference[14]. Some nuclear parameters were generated at this time as required by this study.

During this study, a "BCEX" fuel assembly design was developed. Several problem areas associated with the design were explored, including: "BCEX" fuel assembly hold down device concept; BCEX fuel assembly can wall stresses; fuel assembly - can lateral support; fuel assembly thermal bowing; clad thermal stresses; and, cermet fuel assembly dynamics. In this latter area of investigation, a simple analytical model was set up to describe "BCEX" fuel assembly performance following a sudden step insertion of excess reactivity.

Some additional, unpublished, mechanical design analyses, which are pertinent to the development of the CEX fuel assembly, were performed during the first half of 1965 in the following areas:

a. Bowing of fuel assemblies under radial thermal gradients.
b. Fuel assembly hold down latch.
c. Vibration of fast reactor fuel rods in parallel flow.
d. Pressure stresses in reactor fuel assembly cans.
e. Fuel assembly spring grid design.

Some of these analyses extended the work performed in 1963.

II.3.7 Recent, Westinghouse Funded, FBR Design Studies Which Investigated or Utilized BCEX

Since completing the Westinghouse-AEC 1000 MWe Fast Breeder Reactor study, Westinghouse has performed numerous fast breeder reactor design studies which utilized and investigated BCEX fuel assemblies.

In 1964, Westinghouse evaluated the four AEC 1000 MWe FBR studies. The results and conclusions of the Westinghouse evaluation are summarized in WCAP-2635[15]. One conclusion was that "the CEX fuel assembly gave the Westinghouse design a distinct, superior, thermal expansion characteristic". The AEC evaluation of the four design studies of a 1000 MWe FBR[16] included the following summary statement about the CEX concept:

> "the feasibility of devices such as the controlled expansion fuel element which substitutes mechanical motion for materials properties to achieve a negative temperature coefficient of reactivity should be studied. This fuel element may offer an alternate to enhancing the Doppler effect by BeO addition."

In a subsequent company funded study, the Westinghouse-AEC 1000 MWe FBR core was upgraded to a "high power density" FBR design, which

became the reference Westinghouse Large Fast Breeder Modular Reactor core. The results of this study are presented in WCAP-2638[5]. The core size and configuration (including BCEX fuel assemblies) were identical to that of the Westinghouse-AEC 1000 MWe FBR study; however, specific power density, kw/kg metal, was optimized by parametric thermal and hydraulic analyses for private ownership of the fuel material. In summary, the following significant results were achieved:

a. Fuel rod linear power outputs were increased from 12 to 15.6 kw/ft.
b. Coolant inlet and mixed mean outlet temperatures were selected as 850° and 1100°F, respectively.
c. Fuel costs (private ownership) became 0.57 m/kwh, a 20% improvement over the Westinghouse-AEC study results.

The BCEX fuel assembly design was also incorporated into the Westinghouse 200 MWe Sodium Fast Reactor Prototype (SFRP) Design Study[17]. This study entailed the design, analyses, and fuel cost investigation of a 200 MWe SFRP as a "hook-on" plant with turbine inlet steam conditions of 1800 psig/1000°F. The core, blanket, and reflector design of this reactor approximated one module of the Westinghouse-AEC 1000 MWe FBR core design; the operating conditions approximated the Westinghouse "high power density" FBR. During this study, the original one-dimensional calculation of the reactivity worth of the BCEX mechanism was checked by a two-dimensional calculation. In the Westinghouse-AEC 1000 MWe FBR study[4], original calculations by one-dimensional analyses indicated a negative insertion of 0.75% Δk for a 600°F temperature rise. The two-dimensional analyses predicted a 40% reduction in the original 0.75% Δk value. If realizable, this is still an appreciable contribution to FBR safety.

The clad controlled expansion (CCEX) concept is not new. Westinghouse first reported the results of transient studies on the use of the clad controlled axial expansion (CCEX) concept for fast reactor

application in "Conceptual Design and Preliminary Accident Analysis of a Sodium Cooled, Carbide-Fueled, Large Modular Fast Reactor",[6] presented at the Fast Reactor Conference, Argonne National Laboratory, in October 1965. In this study, compartmentation - where the fuel moves with the clad - was adopted to obtain fuel axial expansion. Compartmented nuclear fuel was originally utilized by Westinghouse in Yankee Core 1[18] as a precautionary measure to minimize fuel slumping.

Throughout these aforementioned studies, the reactivity effects of BCEX and CCEX were found to be geometry dependent, being a maximum for a tall "skinny" core or for other designs featuring high radial leakage. It has also been established that the fabrication cost of a core utilizing a CEX fuel elements will be somewhat higher than a ceramic fueled core with no compartmentation or separated fuel bundles.

Listed below are additional, recent, Westinghouse-funded studies, which incorporated the CEX principle, and which included nuclear, thermal and hydraulic, mechanical, and transient analyses:

1. The Westinghouse FBR right circular cylinder core design study.
2. 30 MWt Sodium Advanced Fast Experimental Reactor (SAFER) Plant Design and Program[19].
3. Proposal to USAEC to design a fast reactor core for the Hallam plant[20].

II.3.8 Westinghouse CEX Concept Proposals

Based upon the preliminary work described in references 10 and 11, Westinghouse proposed a "Study Program on Controlled Expansion Fuel Assembly for Fast Breeder Reactor Application"[21] to further investigate the desirability of the CEX concept, identify the problems to be solved, and advance the development to where CEX fuel could be used with a high probability of success. This proposal was presented informally to the AEC in March 1963.

A more comprehensive, three-phase, program to develop and demonstrate the CEX concept for fast breeder power reactor fuel, "The Controlled Expansion Fuel Development Program"[1], was presented to the AEC in May 1963. Appendix 2 of this proposal contained WCAP-2237 Rev. - "Westinghouse Fuel Assembly for Fast Breeder Reactor Application"[11].

In December 1964, the proposal was revised at the request of the AEC[2]. The concept feasibility part of the program was deleted and the proposed program became a fuel assembly design demonstration effort. Phase I of the proposed program consisted of the preliminary design of a suitable test element for insertion in the FARET reactor. Phase II consisted of the detailed design, fabrication, testing and interpretation of the results of the CEX test assembly. Minor changes were submitted to reference (2) in March 2, 1965 by letter[3] to M. Shaw, AEC Headquarters. These changes involved the introduction and description of Task 2, model analysis, in reference 2.

Section II - References

1. Westinghouse Proposal to U. S. Atomic Energy Commission for "Controlled Expansion Fuel Development Program", May 1963.

2. Westinghouse Proposal to U. S. Atomic Energy Commission for "Controlled Expansion Fuel Development Program", May 1963, Revised December 1964.

3. Letter of March 2, 1965 to M. Shaw, U. S. Atomic Energy Commission from L. Rees, WAPD, "Controlled Expansion Fuel Development Program".

4. Heck, F. M., et al, "Liquid Metal Fast Breeder Reactor Design Study", WCAP-3251-1, January 1964.

5. Gunson, W. E., et al, "High Power Density, Stainless Steel Reference FBR Core Design", WCAP-2638, July 1964.

6. Wright, J. H., et al, "Conceptual Design and Preliminary Accident Analysis of a Sodium Cooled, Carbide Fueled, Large Modular Post Reactor", presented in Panel discussion on Safety of Large Fast Power Reactors, Fast Reactor Conference, Argonne National Laboratory, Argonne, Ill., October 11-14, 1965 (to be published).

7. Heck, F. M., "Fuel Assemblies for a Neutronic Reactor", Westinghouse Patent Application, Case No. 35408, Filed June 21, 1963, based on "Controlled Expansion Nuclear Fuel Assembly", January 16, 1963, Westinghouse Patent Disclosure Book No. 7192, page 1, W D-57633.

8. Keller, H. W. and Andrews, H. N., "Fuel Assembly for a Neutronic Reactor", Westinghouse Patent Application, Case No. 35428, Filed June 21, 1963, Westinghouse Disclosure Book No. D-57954, January 1963.

9. "Westinghouse Proposal for Fast Breeder Reactor Development Program to U. S. Atomic Energy Commission", submitted by WAPD, February 1963.

10. Heck, F. M., "Westinghouse Fuel Assembly for Fast Breeder Reactor Application", WCAP-2237, March 1963.

11. Heck, F. M., "Westinghouse Fuel Assembly for Fast Breeder Reactor Application", WCAP-2237 (Rev.), March 1963.

12. "Westinghouse Quarterly Progress Report, Division General Research Programs by Reactor Development", WCAP-2353, April 1 to June 30, 1963, issued July 1963.

13. "Westinghouse Quarterly Progress Report, Division General Research Programs by Reactor Development", WCAP-2561, October 1 to December 31, 1963, issued April 1964.

14. Heck, F. M., "Neutron controlled Expansion Fuel for Fast Breeder Reactors", Proceedings of the Conference on Breeding, Economics, and Safety in Large Fast Power Reactors, ANL 6792, October 7-10, 1963.

15. Gunson, W. E., et al, "The Liquid Metal Fast Breeder Reactor Design Studies", WCAP-2635, July 1964.

16. "An Evaluation of Four Design Studies of a 1000 MWe Ceramic Fueled Fast Breeder Reactor", prepared by Reactor Engineering Division, COO-279, USAEC, December 1, 1964.

17. Keyfitz, I. M., et al, "200 MWe Sodium Fast Reactor Prototype (SFRP) Design Study", WCAP-2628, September 1964.

18. "Design of Yankee Core I Fuel Assembly", YAEC-154, January 1960.

19. Markley, R. A., et al, "30 MWt Sodium Advanced Fast Experimental Reactor (SAFER) Plant Design and Program", WCAP-2745, February 1965.

20. Westinghouse Proposal for Modifications of the Hallam Nuclear Plant Facility, presented to the U. S. Atomic Energy Commission in March 1965.

21. "Study Program on Controlled Expansion Fuel Assembly for Fast Breeder Reactor Applications", March 26, 1963.

III. DISCUSSION AND RESULTS

III.1 Reference Westinghouse Large Modular Fast Breeder Reactor System Description

III.1.1 General

This section summarizes the design and performance highlights of the Westinghouse Large Modular Fast Breeder Reactor. This reactor concept is the product of numerous Westinghouse studies of fast breeder reactor systems and components. Detailed descriptions of the Westinghouse Large Modular Fast Breeder Reactor are reported in references (1)* through (7).

The 1000 MWe Fast Breeder Reactor which utilized a modular core and bundle controlled expansion (BCEX) fuel assembly design, prepared by Westinghouse under AEC sponsorship and reported in WCAP-3251-1[1], with an uprated power density and lower operating temperatures as outlined in WCAP-2638[2], was employed as the reference reactor design for the analytical studies on the BCEX concept. This higher power density core has a substantially lower fuel cycle cost than the Westinghouse-AEC 1000 MWe Fast Breeder Reactor core design. The basis and limitations for the design of this uprated, high power density Large Modular Fast Breeder Reactor core are summarized in Section II.2.

III.1.2 Reference Reactor Design Description

Reactor System

The Westinghouse Large Fast Breeder Reactor primary system consists of three identical loops to transfer heat from the reactor core to the intermediate sodium system. The general arrangement of a loop is presented in Figures III.1-1 and III.1-2. Each of these loops consists of a circulating pump, the single intermediate heat exchanger, connecting double walled piping, hot and cold traps for impurity control and removal of fission products, and instrumentation for operational control of the system. The pump suction is connected to the inter-

*References appear at the end of the section.

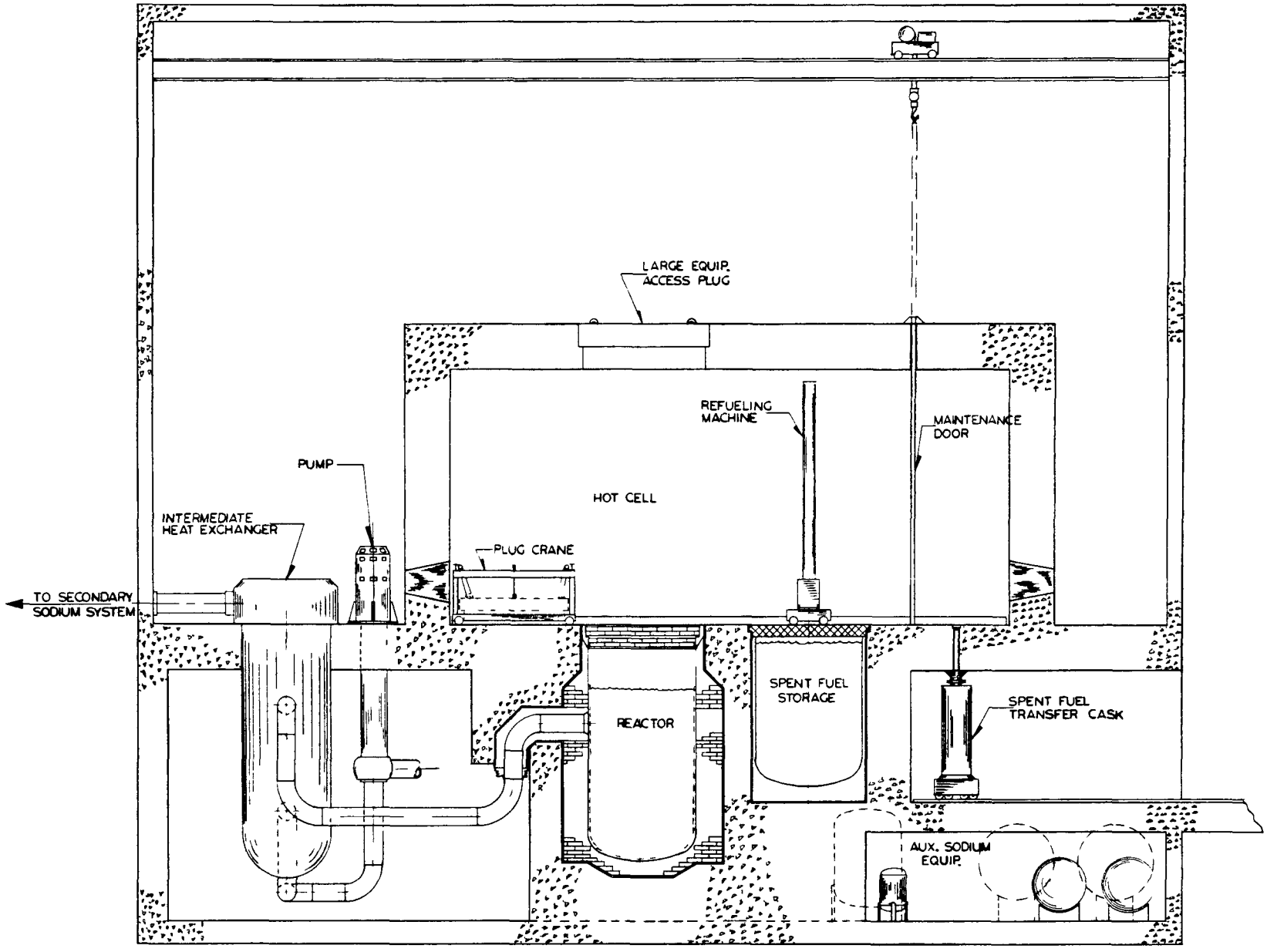

REACTOR BUILDING ELEVATION

Figure III.1-1

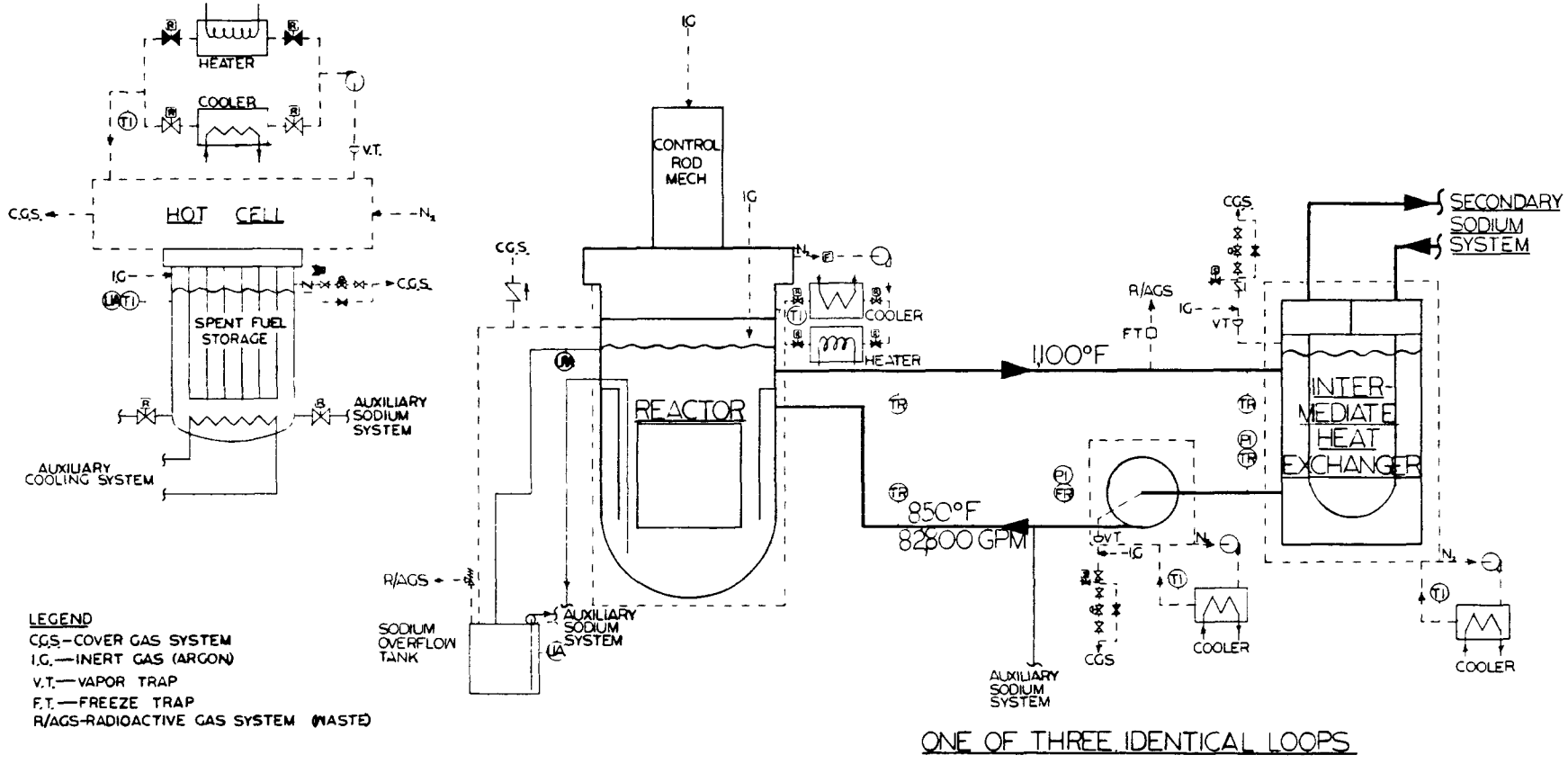

Figure III.1-2

MODULAR CORE ARRAY

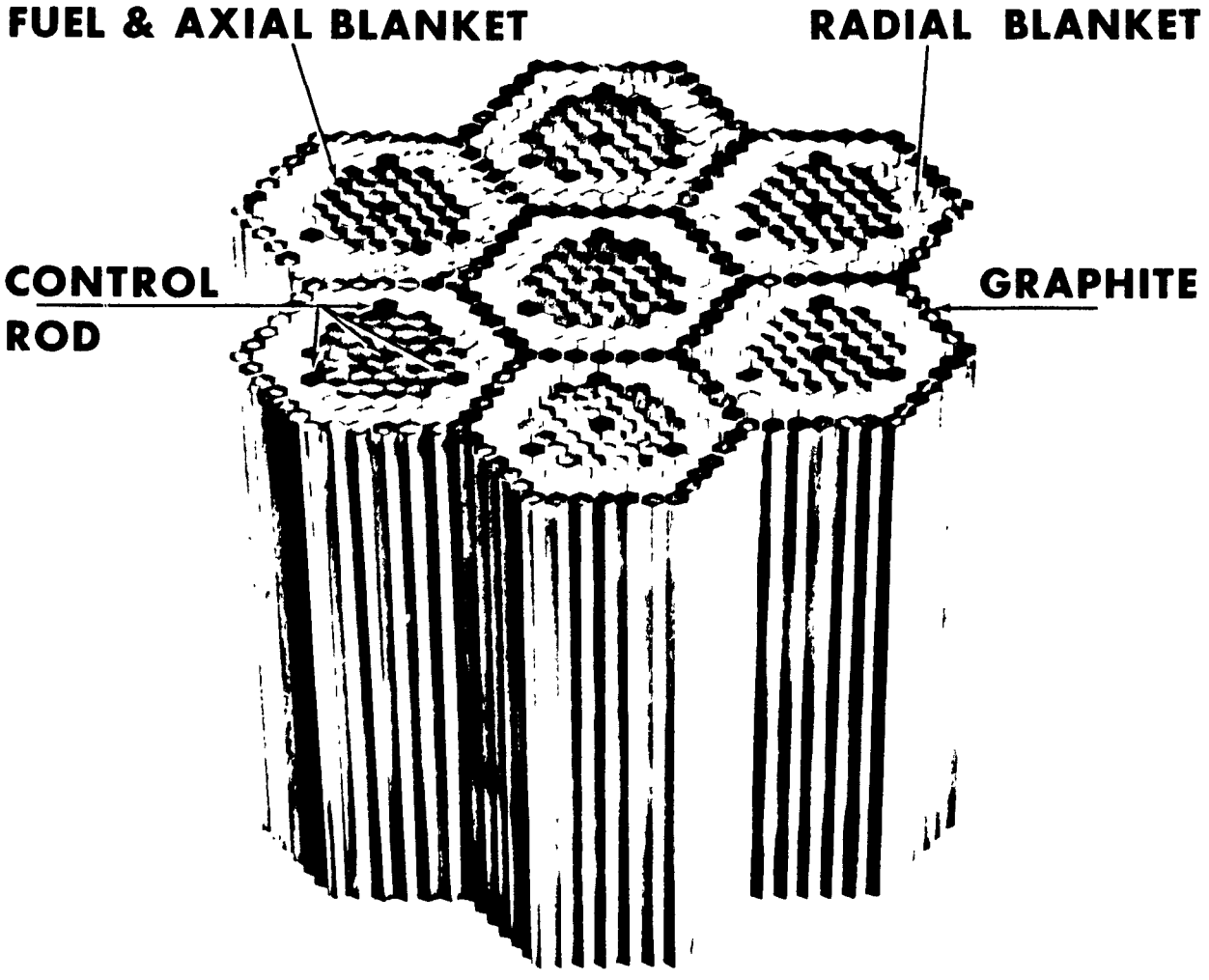

Figure III.1-3

mediate heat exchanger shell, while the pump discharge is connected to the reactor vessel top inlet. The top discharge from the reactor vessel is connected to the intermediate heat exchanger. All system equipment that contains sodium is heat-traced. All primary system equipment is located inside the primary reactor containment. The entire primary system is doubly contained in an inert gas atmosphere to minimize the consequences of a primary leak.

The reactor system layout stresses accessibility and ease of maintenance. These two factors contribute significantly to long-term plant safety. High accessibility permits thorough routine inspection and increases the probability of locating small or incipient problems before they become major problems or incidents. Ease of maintenance permits more routine maintenance to be accomplished, and increases the probability that maintenance or repair work will be successful.

Modern steam conditions can be produced by the plant powered by this reactor system.

Reactor Core

The Westinghouse Large Modular Fast Breeder Reactor concept design used in this study is based on plutonium-uranium carbide fuel, contained in bundle controlled expansion (BCEX) fuel assemblies, and incorporated into a modular core array as shown in Figure III.1-3. The modular core geometry was selected because it enhances the breeding by exposing most of the radial blanket assemblies, with their high fertile material density, to core leakage flux from two sides. A graphite barrier also provides local blanket moderation which enhances the competition of fertile material for neutrons without softening the spectrum of the core region. Another advantage of the modular concept is that by the addition of modules the thermal power rating can be extended, in units of a module, to a wide range of desired powered levels. This flexibility in the concept removes all apparent size restrictions confronting fast

reactor cores. The modular concept can easily be prototyped through the use of a single module for a demonstration plant. A further advantage is that the safety coefficients, particularly the sodium temperature and voiding, can be adjusted to any desired value by changing the dimensions, height and diameter, of the individual modules to obtain the necessary neutron leakage. In addition, the neutron coupling between modules can be controlled, within limits, by adjusting the radial blanket thickness between modules.

The complete reactor core for the Westinghouse Large Fast Breeder Reactor consists of seven distinct, identical-sized, hexagonal cells or modules arranged in a hexagonal pattern separated by an annular graphite reflecting region and coupled by the neutron flux. The module is approximately 8.5 feet tall by 4.5 feet (across the flats). Each module contains a central core region approximately 34 inches in diameter and 72 inches tall. Surrounding the cores are fertile, axial and radial blankets. The fuel and blanket assemblies are replaced on the usual refueling schedules.

Each reactor core module consists of 37 fuel assembly positions, one (the center position) is occupied by a safety rod. Each of the 36 hexagonal fuel assemblies contain 120 ceramic and 7 cermet fuel rods with a 0.300 inch O.D. arranged on a triangular pitch on 0.426 inch center. The ceramic fuel rods are compartmented. Each compartment consists of stacks of stabilized (U-Pu)C pellets contained in 10 mil thick stainless steel clad. The stabilization provides compatibility with the clad by chemically tying up the offending free element. The axial blankets, consisting of depleted uranium carbide pellets, are integral with the fuel rods.

The carbide fuel pellets are sodium bonded to the clad. The carbide rods are vented to the sodium coolant. These two features (sodium bonding and vented fuel) along with long fuel cycle lifetimes, 100 MWD/kg, are necessitated by economic considerations. The sodium bonding,

plus the high thermal conductivity of the carbides, permits low fuel temperatures. The low fuel temperatures reduce fuel swelling and thus allow longer fuel life. The sodium bond allows the use of unground pellets, and permits fuel swelling to be accommodated, with associated cost reductions in fabrication, loss of fissionable materials and allowable lifetime. Vented fuel eliminates fission product gas pressure buildup, hence does not require the neutron embrittled clad to accept large strain at the end of fuel life. The presence of some fission products in the primary sodium adds only a small increment to the cost of maintaining a sodium system, which is already highly radioactive, on a time schedule consistent with large fast breeder reactor downtime costs.

The cermet fuel consists of mixed oxide fuel particles dispersed in a 316 L stainless steel matrix. The matrix is metallurgically bonded to a 10 mil thick stainless steel clad. The fuel rods are brazed into hexagonal bundles measuring about 5 inches across the flats. These bundles are then fabricated into BCEX (bundle controlled expansion) fuel assemblies (see Figure III.1-4) to provide a supplementary negative power coefficient.

A variable flow orifice is provided at the upper end of each fuel assembly. Each fuel assembly is contained in a hexagonal can which is approximately eleven feet long (including end fittings). Each can latches into the lower core plate by a mechanical gripper which functions in a manner analogous to certain ball point pens. Operation of the gripper is illustrated in Figure III.1-4. As the fuel assembly is inserted into the core plate, the 3 gripper fingers bend inwards. The assembly is pushed downwards against spring force until the grippers emerge from the bottom side of the core plate. At this point, the gripper fingers are released, permitting them to snap back to their original position, thus locking the fuel assembly in place. Latching is tested by an upward pull. To remove an assembly the assembly is pushed downwards

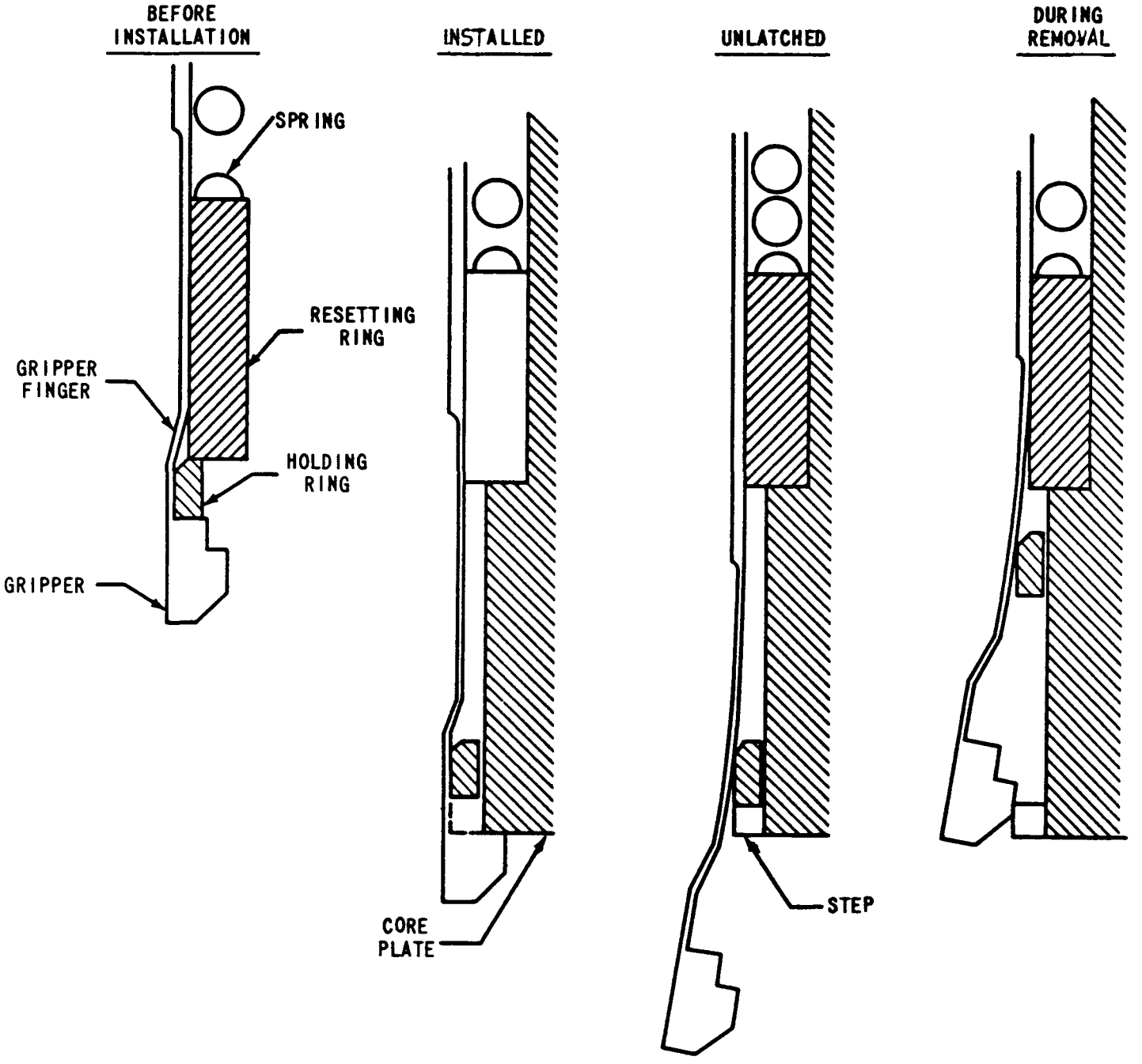

Figure III.1-4 - FUEL ASSEMBLY INSTALLATION & REMOVAL

approximately 1 inch past its installed position. This pushes a holding ring over ramps in the gripper fingers, deflecting the grippers inward. With the grippers in, the fuel assembly may be pulled upwards and free of the core plate. As the fuel element is being withdrawn, the spring acting through a resetting ring pushes the holding ring to its initial position. The installation-removal sequence may then be repeated with no further adjustment.

A detailed description of the BCEX fuel assembly and carbide and cermet fuel rod designs are given in Section III.4.

Surrounding the fuel assemblies are 54 radial blanket assembly positions, of which six are occupied by control rods. The radial blanket assembly shown in Figure III.1-5 consists of 91 rods of 0.420 inch O.D., depleted uranium oxide, pressed and sintered, pellets clad in 0.020 inches of 316 L stainless steel, having an outside diameter of 0.464 inches. These rods are spaced on a regular triangular pitch pattern by wire wrap and fabricated into assemblies. The blanket rods are full core length. The tubing or clad is dry-gas filled and hermetically sealed. The radial space between pellet and clad, and particularly the end chambers, are used to accommodate fission gas storage. The radial blanket assemblies are externally identical with fuel assembly cans with smaller diameter latches to prevent insertion of fuel assembly cans into blanket positions. Oxide fuel is specified in the radial blanket because carbide properties are not required there and the oxide is cheaper to fabricate.

Moderation between modules improves the nuclear as well as the heat transfer conditions (by flattening the blanket power distribution). Thus, each module is surrounded along the entire vertical side by 36 moderator-reflector assemblies, each of which is shared by an adjacent module except on the outer periphery of the reactor. The reflector assembly cans are dimensionally similar to fuel assembly cans. The reflector cans contain short lengths of graphite logs. These cans do

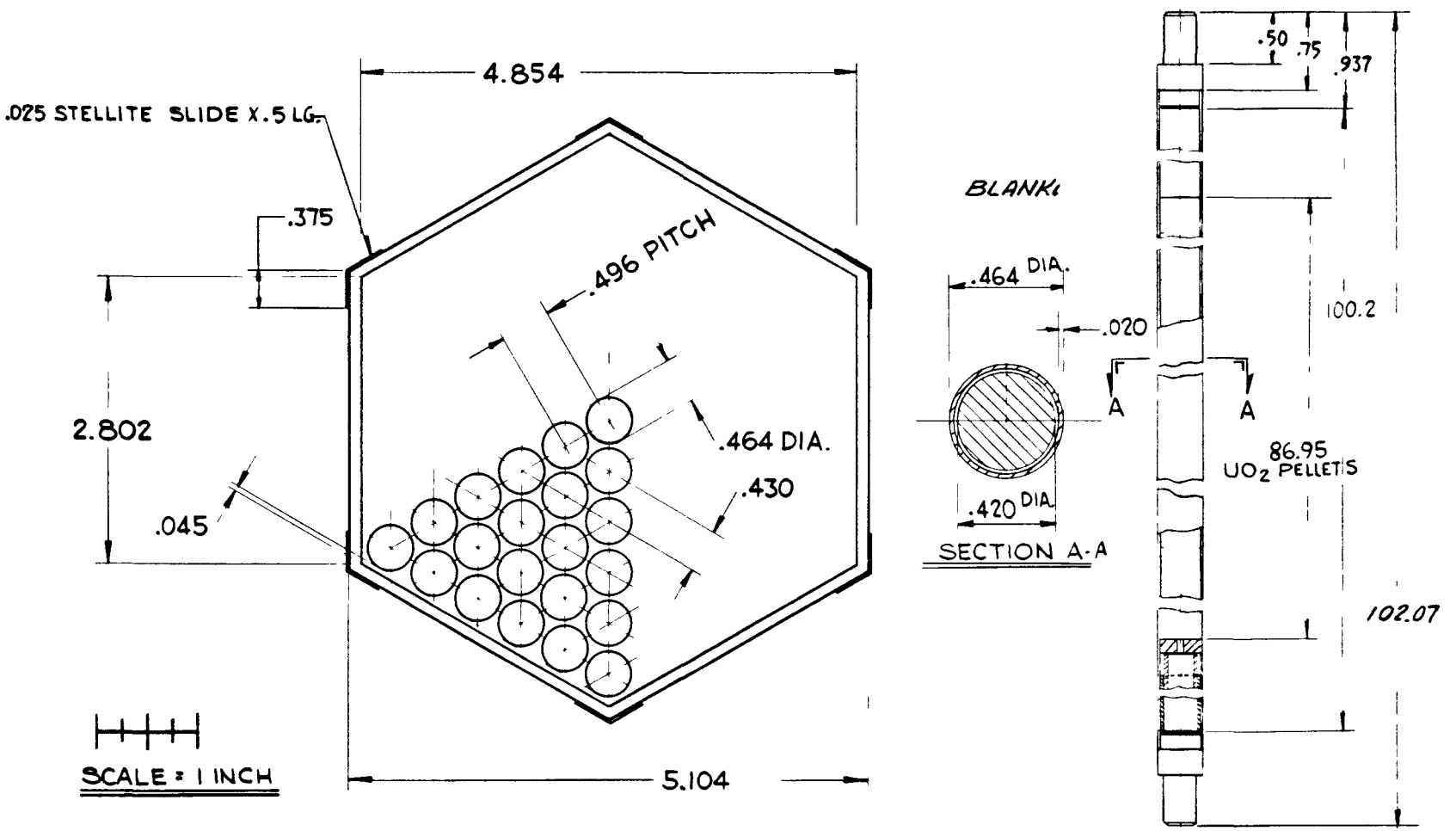

Radial Blanket Assembly

Figure III.1-5

not depend upon the graphite for support. They are helium back filled and welded shut. The reflector cans have end fittings which socket into the core support structure at the bottom and into the reflector support grid at the top. The reflector support grid positions the reflector around each module as shown in Figure III.1-6 and limits the lateral movement of fuel and blanket cans. The perimeter moderator-reflector assemblies are permanent and not ordinarily replaced. In its location the reflector can does not interfere with refueling.

A one-quarter reactor core layout illustrating the core, blanket and reflector arrangement is shown in Figure III.1-7.

There are a total of 49 control rods, 7 rods per module, in the reactor core. The central rod in each module is a safety rod and the six peripheral rods, located in the first row of radial blanket assemblies, are used for power regulating and shim control. The total worth of the 49 rods is 6.9% k against an estimated reactivity requirement of 6.3% k. The control rod assembly consists of a hexagonal array of tubes occupying the center section of the modified fuel assembly. The absorber, B_4C powder, bearing tubes are segmented, with a horizontal grid at about one foot intervals making a unit assembly of the tube array. The top grid from which all rods hang is provided with a vertical connecting member to the control rod drive coupling. The radial spacer grids permit differential linear expansion of the inidivdual rods to eliminate any bowing which might otherwise develop due to flux gradients around the control rod perimeter. Strips attached at the spacer grids provide running surfaces against the control rod guide tube.

Reactor Vessel

The reactor vessel shown in Figure III.1-8 is of double walled construction, consisting of a primary vessel and a secondary vessel, and is fabricated entirely from type 304 stainless steel. The primary vessel provides containment for the reactor core and serves as the support

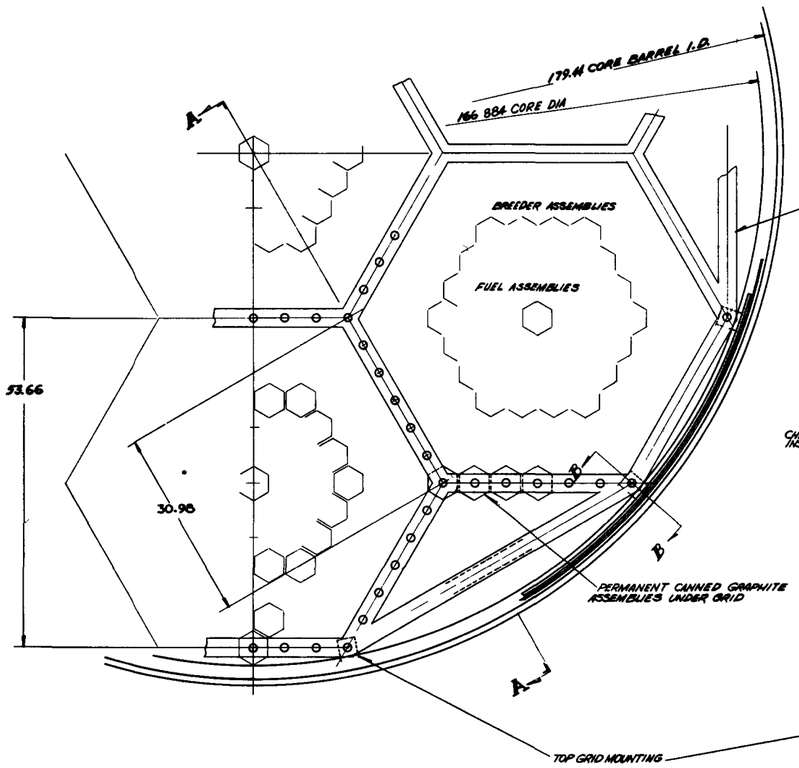

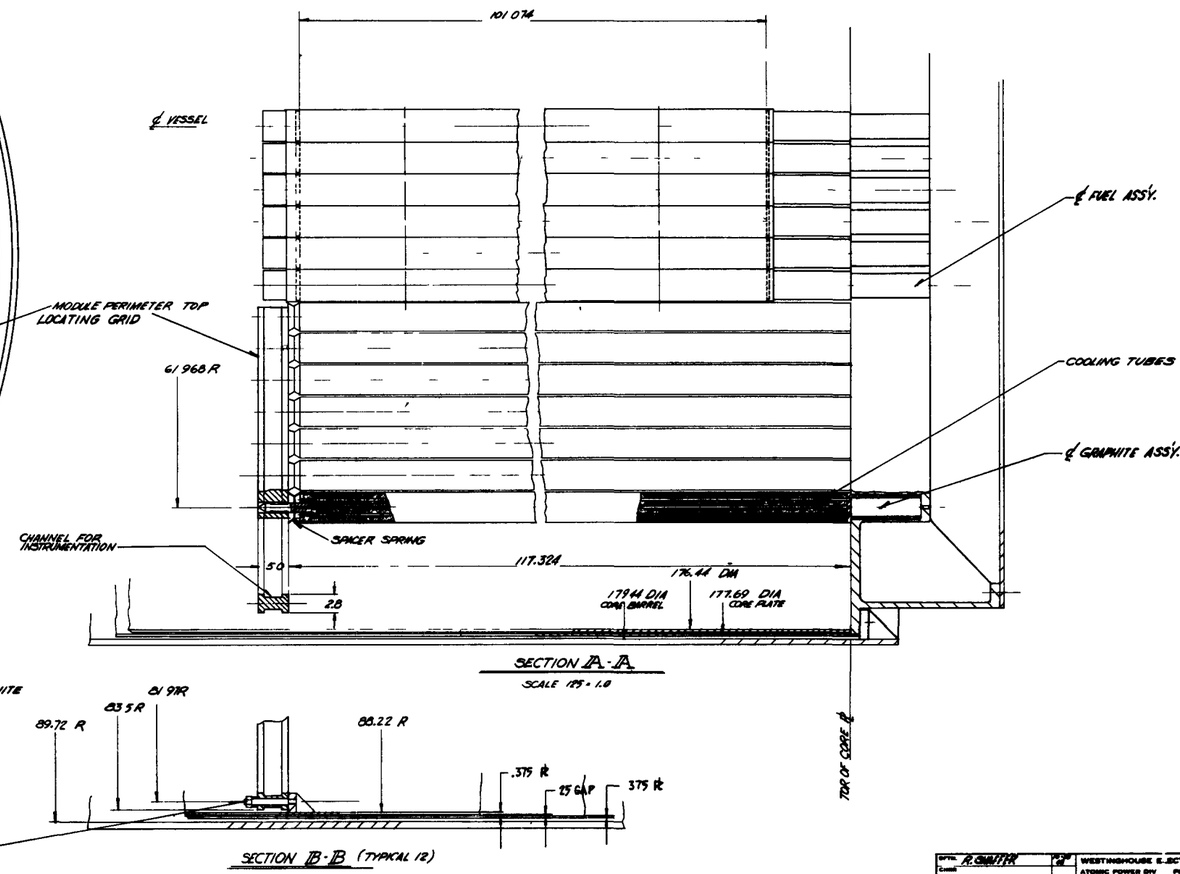

DRWN. R. SMITH	10-29-62	WESTINGHOUSE ELECTRIC CORPORATION	
CHKD.		ATOMIC POWER DIV. PITTSBURGH PA. U.S.A.	
ENGR.	10-30-62	TITLE 1000 MW CRBR BREEDER REACTOR MODULE PERIMETER TOP LOCATING GRID	
APPD.	10-30-62	SCALE 1:2	SK 282250 J
APPD.		DIMENSIONS IN INCHES DO NOT SCALE	SHT 1 SHTS REV
APPD.	11-1-62		

ER SK 282250-J
SECT 2.2.1

ONE QUARTER REACTOR CORE SECTION

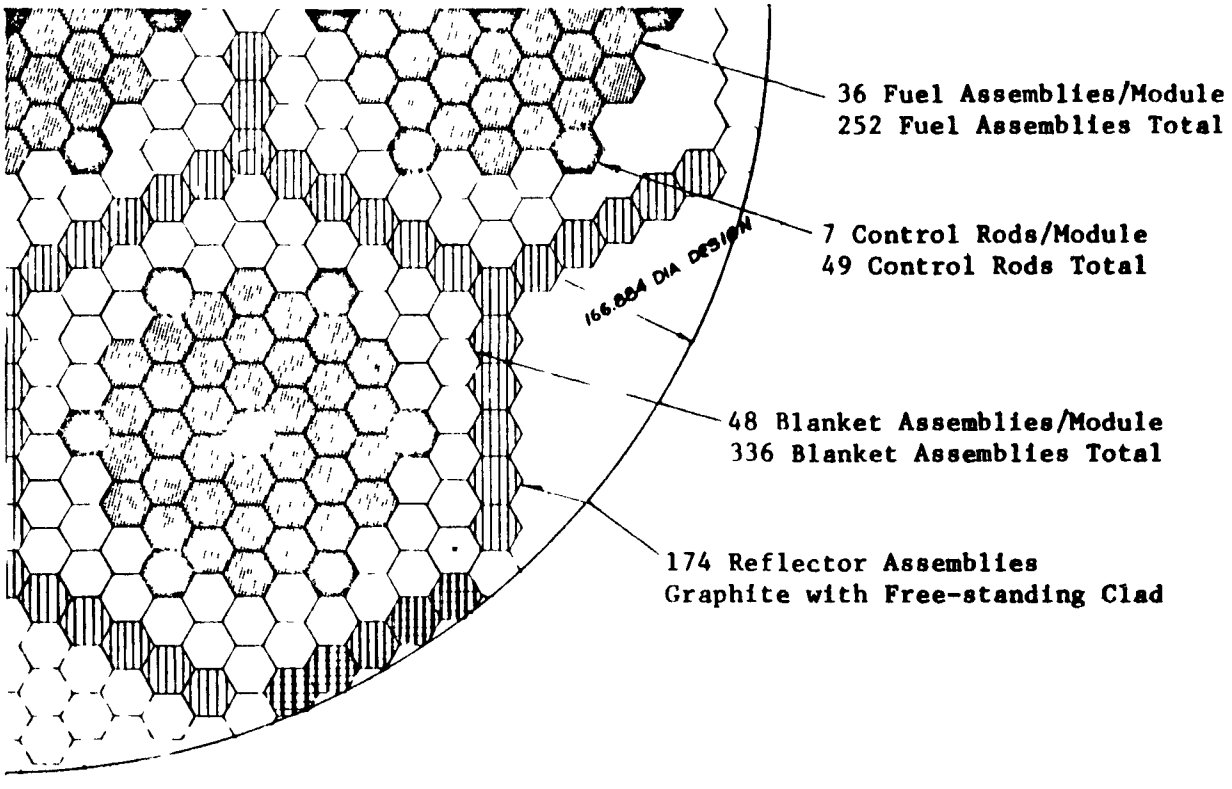

Figure III.1-7

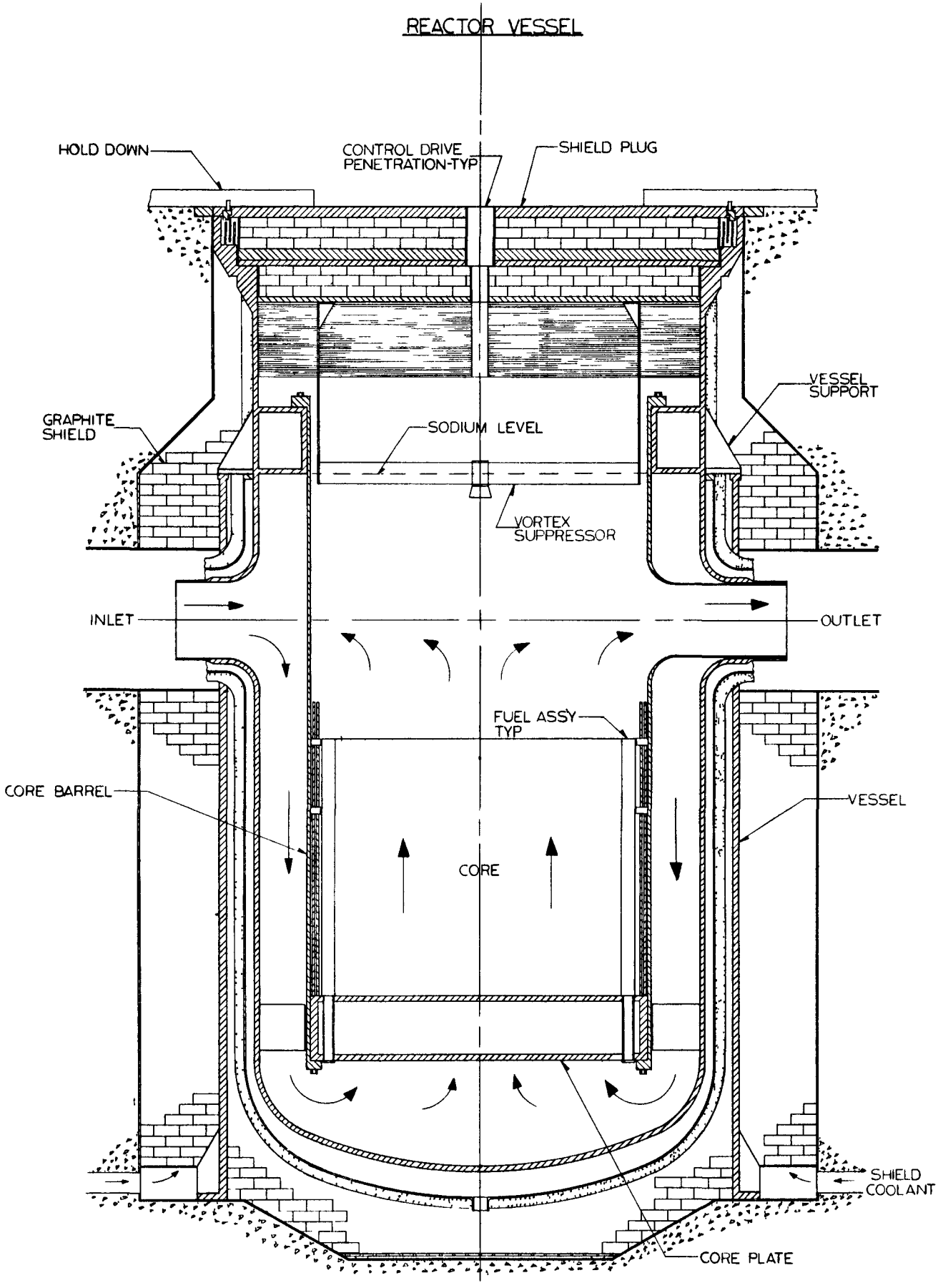

Figure III.1-8

member for the core and core barrel. The upper end of the primary vessel is welded to the vessel support ring. The secondary vessel provides sodium containment in the unlikely event of a failure of the primary vessel. Three inches of stainless steel reflective insulation covers the outside of the secondary vessel.

A radial gap between the primary and secondary vessels is provided so that if drainage of sodium from the primary to the secondary vessel occurs, the core will remain submerged in sodium. During power operation this gap is filled with stagnant nitrogen. At shutdown, the sodium within the vessel is heated by circulating hot nitrogen between two vessels.

The sodium coolant enters the reactor vessel above the top of the core, and flows down an annulus within the vessel to maintain the outer vessel wall at the lowest possible temperature. From the annular downcomer, the sodium flows through variable orifices into two plenum regions in the bottom of the vessel. One plenum feeds the core regions; the other feeds the blanket regions.

The core support structure is attached to a core barrel suspended from the upper part of the inner reactor vessel. The reactor vessel head is a composite plug comprised of blast absorbing material on the bottom and radiation absorbing material above. Control rod drives mechanisms are located on top of the plug. Access to the reactor for refueling or maintenance is obtained by uncoupling the control rod drive lines, unlatching the plug from the vessel, hoisting the plug by means of a traveling hoist, and rolling it to one side.

Shield Plug

The shield plug shown in Figure III.1-8 has three major functions:

1. Provide a full diameter opening at the top of the vessel capable of containing the full design pressure.

2. Provide shielding to attenuate neutron flux and gamma radiation.
3. Provide support and alignment for control rod drive mechanisms.

The total plug shield thickness is five feet and consists of the following materials listed from top to bottom: 4 inches of carbon steel, 12 inches of stacked 3 w/o boronated graphite block; a layer of carbon steel shielding (not a structural or pressure containing component); a type 304 stainless steel structural member; 12 inches of boronated graphite block; a type 304 stainless steel structural and pressure containing member; and 24 inches of blast absorbing crushable material. The total minimum thickness of the four steel plates is 11-1/2 inches.

The two lower stainless steel plates, above the crushable material, provide the structural support for the plug assembly and the design pressure loading. The space between these two plates contains ribs or similar stiffening members to enhance the load carrying capability of the assembly.

Reflective stainless steel insulation is attached to the bottom of the plug assembly as required to reduce the rate of heat transfer through the plug and to promote satisfactory temperature distributions throughout the upper region of the vessel and support structure.

Nitrogen is provided for plug cooling in order to maintain the upper plug surface and seal at temperatures below 130°F.

Shield Plug Closure

The vessel closure is sealed and secured in place during normal operating conditions (15 psig) by a low-melting point metal alloy. Cerroben, a lead-cadmium-tin-bismuth alloy, is typical of several possible seal materials. It has a density of 0.339 lb/in^3, and a melting point of 158°F. A shear strength of around 3500 psi makes it adequate for

closure hold down at many times the normal operating pressure of 15 psig.

A rotating shear block closure, provides a backup hold down and is capable of securing the plug at pressures of at least 150 psig. This mechanical closure is simple in design and will have the capability of being operated remotely by pneumatic cylinders mounted to the refueling cell floor. Additional beams across the plug hold the plug in place in the event a large explosive energy release occurs. Human access to the closure mechanism during plug removal is contemplated only under unusual conditions.

Axial Thermal Shield and Meltdown Pan

An axial thermal shield and meltdown pan assembly is supported at the bottom of the vessel below the core support structure. It consists of a 304 stainless steel dished head with a conical piece welded to it. One inch in diameter by 6 inch in length 1.0 w/o natural boron type 304 stainless steel rods are welded to the assembly.

Control Rod Drive System

The control rod drives, rack and pinion type, are located on the top of the upper plug and are completely enclosed by gas tight shell. Power, control and gas supply lines form helical coils which are suspended from the ceiling of the refueling cell. This arrangement makes it possible to remove the top plug from the reactor and hoist it up and move the plug to its storage position without disconnecting any cables or gas supply lines.

A positive pressure of inert gas is maintained in the containment shell around the drives to prevent contamination of the mechanisms by the cell atmosphere. Bellow seals similar to those used on Fermi and EBR-II isolate the control rod drive components from the reactor cover gas.

An inert gas pressure higher than the reactor cover gas pressure is maintained in the mechanism housing as further insurance against contamination.

The rack, which is attached to the control rod, is driven up and down by a pinion. As the rack moves up a spring is compressed.

The motor torque is transmitted through a gear reduction unit and an electromagnet clutch to the pinion. Provision is made in the drive train for continuous control rod position indication.

A scram is initiated by cutting the power to the electromagnetic clutch which allows the rack and control rod to fall freely. The spring in the rack housing provides an initial force to accelerate the control rod more rapidly at the beginning of a scram. A spring or pneumatically operated dash pot within the rack housing decelerates the control rod train at the end of its fall.

The lower end of the rack assembly is attached to the control rod with a latch.

Pumps

The three primary, sodium, variable speed, circulating pumps are double suction, vertical, centrifugal units of the free surface type consisting of:

1. A pump drive motor mounted on a shield deck.
2. A pump volute located in the primary sodium system piping below the shield deck.
3. A pump impeller located in the volute and connected to the motor by a shaft.
4. A vertical column between the shield deck and the volute to contain the shaft.

The vertical column contains a sodium pool, argon cover gas chamber, gas shaft seal and other necessary pump components.

All parts of the pumps in contact with sodium are stainless steel except the bearings and other special parts. Each pump is equipped with a smaller auxiliary motor connected to a separate power supply to insure adequate minimum sodium flow in the event of loss of power.

Intermediate Heat Exchangers

The intermediate (Na to Na) heat exchangers are of the vertical shell and tube type with the primary sodium on the shell side of the heat exchanger, entering and leaving through two diametrically opposed horizontal nozzles. Intermediate sodium flows through the tubes. The shell side contains a free sodium surface covered by argon gas to prevent oxidation and minimize tube sheet thermal stresses. The argon space contains a sodium overflow line to accommodate volume surges.

The thermal center of the heat exchanger is located above the center of the core to provide coolant natural circulation after a complete loss of power accident. The tube sheets and tube bundle may be removed from the shell for inspection or maintenance.

Valves

No loop isolation or pump check valves are provided. Loop isolation valves are omitted as power operation is not contemplated if one pump becomes inoperative. In this event, the plant would be shut down for the necessary repairs. By eliminating shut-off valves, system complexity is reduced and plant economics are improved.

Piping

The primary piping is fabricated of ASTM A-358 Type 304 stainless steel. A wall thickness of 3/8 inch was selected for structural stability even

though the piping code requires less than 1/4 inch. All primary piping is enclosed by secondary containment. The purpose of the secondary containment pipe is to limit the loss of coolant in the event of a leak. Without a secondary shell surrounding the primary piping, a leak in the piping could drain the pumps and other sections of the primary system preventing circulation of sodium to remove decay heat. The secondary containment material in the reactor plenum is stainless steel and the rest is 1-1/4 Cr, 1/2 Mo. Leak detectors are located at the low points of the containment.

Insulation and Heat Tracing

All equipment that contains sodium is heat-traced to prevent sodium solidification. Selection of an ultimate heating system will be based on detailed engineering and economic analysis. The sodium piping and equipment are covered with insulation to minimize heat losses.

Temperatures

Temperature detectors in the hot and cold leg of each loop provide signals for primary sodium system control during startup, shutdown, and normal operation. The temperature signals are used by the reactor control and protection system for control of system temperature and are recorded in the main control room.

Sodium Level

The reactor vessel is equipped with a sodium level detector. A low or high sodium level alarm is sent to the reactor control and protection system to scram the reactor. Sodium level is recorded and alarm indicators are located in the main control room.

Primary Sodium Flow

Flow rates are measured in each primary sodium loop cold leg. A loop flow signal in any loop actuates an alarm in the main control room.

The low flow alarm is sent to the reactor control and protection system, which initiates a low flow scram if flow falls below a predetermined value.

Cell Structures

The primary system hot cell is a gas-tight structure enclosed by 6 ft. thick concrete shield walls lined with stainless steel. The floor and ceiling are also lined with stainless steel. Periscopes and lead glass windows are provided in the walls and ceiling for viewing critical operations. Provisions are made to heat the cell walss during refueling operations to prevent sodium vapor condensation.

A shield door closes off one end of the cell, providing a maintenance area for the refueling machine. With the door closed, air may be admitted to the maintenance area. Air leakage to the rest of the cell is prevented by introducing inert gas between two sets of door seals at a pressure slightly higher than that in either cell area. Normally, this maintenance area will be used only when the reactor spent fuel storage pool plugs and the reactor top plug are in the place in order to protect the sodium from possible air leakage. Maintenance inside the hot cell will be performed by personnel wearing breathing apparatus and protective clothing. The cell will not be supplied with air except for major maintenance when the sodium in the reactor vessel and storage pool must be covered or removed.

Reactor Plug Crane

The reactor plug crane is a remotely controlled bridge crane designed to lift the top plug from the reactor, move it aside for refueling, and replace it after refueling. Four separate hoists are provided to lift the plug; and a bridge drive is provided to move to move the crane along the rails.

The control rod drives are lifted integrally with the plug after remote disconnection of the drive shafts. Electric cables connected to the drives have enough slack to allow the plug to be lifted and moved without disconnecting the cables.

The crane hoists are permanently connected to the plug top. During reactor operation, the crane is parked directly over the reactor. The lifting cables are rigged through sheaves over to the hoist mechanisms located on the end of the bridge in the equipment tunnel. The four separate hoists are driven by variable speed DC motors, with speed adjustment circuits in the control system that allow the motors to be driven individually or balanced to function together. Each hoist drum has two separate drive units connected to the drum by electric clutches. Power is carried to the hoist and bridge drive through a feed rail in the ventilation corridor. Circuits are provided for each motor so that a complete dual drive system is available for the hoists, bridge drive and clutches.

When replacing the plug, the reactor plug crane is positioned over the reactor, by driving against fixed stops. Level indicating instruments are located directly on the plug top and readings can be checked through a wall periscope. Corrections to level the plug are made by driving the hoists individually.

Fuel Handling

The reactor is refueled by a remotely controlled refueling machine operating in the shielded, inert atmosphere cell. The refueling machine accomplishes all the fuel handling operations, from the introduction of new fuel assemblies into the cell, to the final loading of the spent fuel into the transfer cask. In addition to handling fuel, the refueling machine also removes and replaces reflector elements and control rods. All core components except control rods have lifting fixtures identical to the fuel.

The refueling machine is a remotely controlled rectilinear crane that carries a verticay telescoping mast. Fuel assemblies and control assemblies are transported between the reactor, storage pool, entry and discharge ports with this machine. Inert gas cooling with backup is provided for spent fuel elements during transfer.

The bridge and trolley are driven by variable speed drive units powered and controlled from supply lines and control leads hung in festoons along the cell wall. The mast of the machine is made in telescoping sections with provision to prevent rotation. A gripper for engaging and lifting core components is attached to the bottom of the mast. In addition to the lifting function, the mast must be capable of exerting a downward force of at least 200 lbs. in order to unlatch the fuel assembly from the support structure. The gripper mechanism is actuated with a pneumatic (nitrogen) cylinder located well above the sodium level. The gripper is designed so that it remains closed (latched) unless the pneumatic system is pressurized; even then it is not possible to open it if a weight exceeding 200 pounds is hanging from it.

The method of powering all refueling machine motions is through use of pneumatic (nitrogen) piston type motors and pneumatic cylinders. All control systems and valves are located outside the cell. Reliability, simplicity and environment were the major factors in selecting this type of power unit. Electric motors would require complex cooling systems to operate in the cell atmosphere.

Cables or auxiliary power drives are provided to move the refueling machine and unload the fuel into the storage pool in the event of a failure of the normal motive equipment. Spent core assemblies are cooled during transfer by nitrogen gas flow through the mast assembly supplied from a hose trailed behind the machine.

Two cooling systems are provided with separate gas supplies. Automatic controls switch from one system to the other in the event of a

system failure. The forced cooling system must operate continuously during a spent core assembly transfer. The design provides a method of checking the cooling system immediately after a fuel element is withdrawn from the sodium. If cooling gas is lost during a transfer, a fuel element could reach the boiling point of sodium in five minutes.

The refueling machine is positioned at the desired location by aligning position markers attached to the machine with markers on the crane and trolley rails by means of optical equipment. An alternate system would use an electronic positioning system. Proper location is determined with an electrical position repeat-back system on both bridge and trolley which indicates the position of the vertical mast in relation to a fixed grid pattern. The electronic position indication system would be backed up with the visual system described. The design parameters for the refueling machine are presented in Table III.1-1.

Table III.1-1

Refueling Machine Design Parameters

Minimum lift capacity	1000 lb.
Nitrogen cooling flow	3000 #/hr at 200°F
Decay heat of hottest fuel assembly	54 kw
Maximum bridge travel speed	20
Maximum trolley travel speed	5 ft/min
Maximum vertical mast speed	20 ft/min
Positioning accuracy, linear	± 1/32 in. (mast extended)

Spent Fuel Storage

Spent fuel assemblies and control rods are stored in a sodium-filled tank located below the cell floor. Ports extend through a top cover plate and shield down into a tank in which sodium coolant is circulated. This provides storage space for more than a full core load of fuel and

blanket assemblies. Because sodium is used as the coolant, the storage pit can also be utilized for storing partially spent fuel during maintenance operations. The heat rejection system and heat capacity of the spent fuel storage pit are also used to remove decay heat from the reactor.

The shield plate and the height of sodium above the fuel provides sufficient gamma shielding in case the hot cell must be entered for maintenance. The storage pool sodium is isolated from the cell atmosphere by seal plugs placed by the manipulator or refueling machine into the top guide sleeves of each storage position. An inert cover gas blanket is maintained under the top plate at a pressure slightly below that in the refueling cell. This helps prevent contamination of the cell by fission gases released by the stored fuel. Decay heat is removed by circulating the sodium through an intermediate sodium-NaK heat exchange to maintain a temperature of 300°F.

Cover Gas System

The cover gas systems serve the general function of providing a protective inert atmosphere for the sodium coolant. In addition, the cover gas is used as a collection mechanism for fission product gases (released from the vented fuel), for pressure control, and for continuous purging of the control rod drive mechanisms. There are two argon cover gas systems used to carry out these functions. One of these is the cover gas supply system and the other is the cover gas purification system.

The cover gas supply system maintains an inert gas blanket in the reactor and in all piping, vessels, or equipment where a free surface of sodium exists. The system is designed to maintain the constant gas pressures required in the reactor, primary system, and the primary drain tank. Argon is also utilized as the displacement gas during draining, filling and transferring sodium.

The cover gas purification system serves to remove gaseous fission products (released from vented fuel) from the argon cover gas from primary system components. The gaseous fission products released to the cover gas are assumed to be xenon and krypton isotopes as existing data indicates that the halogen fission gases released from the fuel react chemically with the coolant. The system is designed to handle the full flow of the reactor and the fuel storage cover gas volumes (where the fission gases are expected to concentrate) and also bleed flow from other primary system component cover gas volumes where fission gases that become entrained in the sodium coolant may be released.

Nitrogen System

The purpose of the nitrogen system is to maintain an inert atmosphere in the hot cell, primary pump and pipe cells, heat exchanger cell, and maintenance cell to minimize the possibility of a fire with radioactive sodium. The system is also used to blanket areas where an inert atmosphere is desirable, such as the sodium melt stations and cyclone separators connected to the rupture disc from the steam generators. It also backs up compressed air systems for pneumatic tools and instruments. In addition to its use for an inert atmosphere, the nitrogen is also used for cooling purposes.

Summary

A brief summary of the reactor mechanical design data is presented in Table III.1-2.

Table III.1-2

Reactor Mechanical Design Data

Reactor Size	
Diameter	14 ft
Active Core Height	6.25 ft
Assembly Length	11 ft
Module Size	
Height	8.5 ft
Diameter (across flats)	4.5 ft
Core Modules	
Number of modules	7
Number of fuel assemblies/module	36
Number of blanket assemblies/module	48
Number of reflector assemblies/module	18
Number of control assemblies/module	7
Ceramic Fuel Rods	
Total fuel height, inches	72.0
Pellet diameter, inches	0.268
Clad thickness, inches	0.010
Clad outside diameter, inches	0.300
Fuel material	(U,PU) C (mod.)
Thermal bond material	Na
Clad material	316 L S.S.
Axial Blanket Rods (Integral with Fuel Rods)	
Blanket length each end, inches	12.0
Blanket material	UC
Fuel Assemblies	
Type of rod array	triangular
Fuel rod pitch, inches	0.426
Type of can	hexagonal
Can width across flats, inches	5.104
Carbide fuel rods per assembly	120
Cermet fuel rods per assembly	7
Fuel assembly length (approximate) inches	132

III.1.3 Description of Performance and Conditions

The thermal design of the Westinghouse-AEC 1000 MWe FBR Modular core has been revised to increase the power density to more nearly optimize the fuel cycle cost for private ownership of fuel, 10% annual charge, and commercial acceptability (see fuel cycle costs in Section III.1.5). The power density was increased by reducing the sodium outlet temperature from 1200°F[1] to 1100°F which is still high enough to obtain steam temperatures between 950 and 1000°F. The increased power density raised the total thermal power rating of the seven modules from 2500 MWt[1] to 3255 MWt; 465 MWt output per module for an equilibrium core including cermet fuel and blanket. This increase in total power reduced the fuel inventory per unit of power. The lower sodium temperature reduces the requirements of the IHX and steam generator materials. Concurrently, the pump size is reduced, the cost of heat exchange apparatus is decreased, and the reliability of the fuel cladding is increased. The resultant Large Fast Breeder Reactor plant rating would be approximately 1250 MWe.

The reduction in coolant outlet temperature, while permitting a 30% increase in the specific power density, kw/kg of fissile material, allows a reduction in the clad surface hot spot temperature from approximately 1400°F to 1310°F, with a simultaneous increase in the reactor coolant temperature rise from 220°F to 250°F. The fuel rod average and maximum linear powers are 15.6 kw/ft and 33.6 kw/ft, respectively. The core average fuel temperature is approximately 1300°F, whereas the maximum fuel centerline temperature is 2230°F. The thermal calculations are based upon an average carbide fuel thermal conductivity at operating conditions of 10.0 Btu/hr-ft-°F. The core pressure drop is approximately 80 psi.

A summary of the steady state thermal and hydraulic characteristics for the reference Westinghouse Large Fast Breeder Reactor Modular core incorporating the bundle controlled expansion (BCEX) concept is presented

in Table III.1-3. Data for cermet rods with a 0.360 inch diameter and with a volumetric heating ratio of 0.30 are used in this summary.

Table III.1-3

Summary of Steady State Performance Characteristics for the Westinghouse BCEX Large High Power Density Carbide Core

I. Rating	
A. Reactor	
Total thermal power (equilibrium core)	3255 MWt
Estimated electrical output	1250 MWt
Total primary system flow rate	148.0×10^6 lb/hr
B. Total Thermal Power per Module (Equilibrium Core), MWt	465.0
1. After refueling	
a) Carbide fuel rods	404
b) Cermet rods (Q=0.30, O.D.=0.360 in.)	12
c) Blanket	49
2. Before refueling	
a) Carbide fuel rods	374
b) Cermet rods (Q=0.30, O.D.=0.360 in.)	11
c) Blanket	80
Power density (core after refueling), kw/liter	396
Specific power (after refueling), kw/kg metal	∿ 115
Average fuel linear power (after refueling), kw/ft	15.6
Maximum fuel linear power (after refueling), kw/ft	33.6
Refueling period	one year
Average carbide fuel burnup	100,000 MWD/T
Peak carbide fuel burnup	120,000 MWD/T

II. Conditions (after refueling)

A. Temperatures at rated power

Core and blanket coolant inlet	850°F
Mixed mean outlet	1100°F
Average channel outlet	1113°F
Hot channel outlet	1277°F
Carbide fuel rod (100% mixing with cermet coolant)	
a) Maximum clad surface	1310°F
b) Maximum fuel centerline	2230°F
Cermet rod (Q=0.30, O.D.=0.360 in.)	
a) Maximum clad surface	1235°F
b) Maximum fuel centerline	1785°F
c) Maximum fuel average	1490°F

B. Hydraulics (per module) at rated power

Total core flow rate (per module)	18.9×10^6
Bypass flow	5%
Effective core flow rate (per module)	18.0×10^6
Flow area in core of module	2.99 ft^2
Core average mass velocity	6.02×10^6 $lb/hr\text{-}ft^2$
Core orificing (held constant through life)	
a) Zone 1	1.14
b) Zone 2	1.00
c) Zone 3	0.9533
Core zone average mass velocity (held constant (throughout life)	
a) Zone 1	6.85×10^6 $lb/hr\text{-}ft^2$
b) Zone 2	6.02×10^6 $lb/hr\text{-}ft^2$
c) Zone 3	5.73×10^6 $lb/hr\text{-}ft^2$

Core coolant pressure drop - 80 psia

Core coolant velocities - normal channel average

a) Zone 1	37.3 ft/sec.
b) Zone 2	32.7 ft/sec.
c) Zone 3	31.1 ft/sec.
Loss coefficient per grid	0.3
Core flow channel equivalent diameter	0.02914 ft
Total blanket flow per module average	2.23×10^6 lb/hr

Blanket orificing (held constant through life)

a) Inner row	1.25
b) Outer row	0.825

III. Hot Channel Factors

A. Engineering

Heat flux F_q^E	1.04
Enthalpy rise $F_{\Delta H}^E$	1.15
Heat transfer $F_{\Delta T}^E$	2.00

B. Power peaking factor

Core	1.14
Radial blanket	1.00

C. Nuclear (max. to ave.)

Time	Core		Radial Blanket	
	Radial	Axial	Radial	Axial
Beginning-of-life	1.33	1.36	2.83	1.36
33,333 MWD/T	1.27	1.345	1.8	1.345
66,667 MWD/T	1.215	1.33	1.52	1.33

IV. Design

A. Module

Number of modules per core	7
Number of fuel assemblies per module	36
Number of blanket assemblies per module	51
Number of control rod assemblies per module	7
Equivalent module core radius	16.5 inches (41.89 cm)
Active core height	75.5 inches

B. Fuel assembly

Shape	hexagonal
Carbide fuel rods per fuel assembly	120
Cermet rods per fuel assembly	7
Fuel rod array	triangular
Axial distance between grids	9.0 inches
Number of core grids	8

C. Carbide fuel rod

Type	vented
Active fuel length	72.0 inches
Fuel pellet diameter	0.268"
Fuel clad I.D.	0.280"
Fuel clad O.D.	0.300"
Fuel material	(Pu-U)C
Clad material	316 L S.S.
Type of fuel-clad bond	sodium
Fuel rod pitch/diameter ratio	1.42
Total number of rods per module	4320
Percent of theoretical density of fuel	92

D. Cermet rod

Active length	75.55 in.
Cermet material	$(Pu\text{-}U)O_2$ - 316 SS
Total cermet rods/module	252

Percent of theoretical density $(Pu-U)O_2$	85
Theoretical density of 316 SS	8.0 g/cc
Theoretical density of $(Pu-U)O_2$	11.05 g/cc
Cermet rod size	
Rod O.D.	0.360 in.
Cermet rod diameter	0.340 in.
Cermet clad I.D.	0.340 in.
Clad thickness	0.010 in.

E. Volume percents in core

1. v/o based on cross-section area of a fuel assembly

Fuel	29.84%
Steel	13.34%
Sodium	56.82%

2. v/o based on cross-sectional area of a fuel assembly and corrected for axial gaps (steel and sodium) in fuel stack

Fuel	28.46%
Steel	13.96%
Sodium	57.58%

3. v/o based on cross-sectional area of a fuel assembly and corrected for axial gaps in fuel stock and the one control rod assembly (steel and sodium)

Fuel	27.69%
Steel	13.78%
Sodium	58.53%

F. Radial blanket assembly

Shape of fuel assembly	hexagonal
Number of fuel assemblies	357
Rods per fuel assembly	91
Fuel rod array	triangle
Fuel material	UO_2 (depleted)
Clad material	316 L SS

Active blanket length	87.6 inch
Fuel pellet diameter	0.420 inch
Type of fuel-clad bond	gas
Clad	
a) I.D.	0.424 inch
b) Thickness	0.020 inch
c) O.D.	0.464 inch
Fuel rod pitch, inch	0.496 inch
Fuel rod pitch/diameter ratio	1.07
Total heat transfer area	27,650 ft^2

G. Volume percents in radial blanket (where radial blanket is defined as encompassing a length of 87.6 inches)

1. v/o based on cross-sectional area of a blanket assembly

Fuel	54.59%
Steel	17.98%
Gas bond	1.05%
Sodium	26.38%

2. v/o based on cross-sectional area of a blanket assembly and homogenizing 3 control rod assemblies over the 2 rows of blanket

Fuel	51.56%
Steel	16.98%
Gas bond	0.99%
Sodium	30.47%

H. Volume percents in axial blankets - v/o based on cross-sectional area of a blanket assembly and corrected for axial gaps (steel and sodium in blanket stack)

Fuel	29.84%
Sodium	58.82%
Structure and clad	13.34%

I.	Heat transfer data	
	Total core heat transfer area per module	2036 ft^2
	Core maximum heat flux	1.46×10^6 Btu/hr-ft^2
	Core average heat flux	0.677×10^6 Btu/hr-ft^2
	Thermal conductivity of clad	11.0 Btu/hr-ft-°F
	Thermal conductivity of core fuel	10.0 Btu/hr-ft-°F
	Thermal conductivity of blanket fuel	1.6 Btu/hr-ft-°F
	Fuel-clad heat transfer coefficient in core assembly	72,000 Btu/hr-ft^2-°F
	Fuel-clad heat transfer coefficient in blanket assembly	1,000 Btu/hr-ft^2-°F
	Cermet-clad interface heat transfer coefficient	100,000 Btu/hr-ft^2-°F
J.	Axial blanket (upper and lower)	
	Thickness (upper and lower)	12.0 inches
	Number of grids in lower blanket	1
	Fuel material	UC (depleted)
	Rods per assembly	120
	Clad O.D.	0.300 inches
	Clad I.D.	0.280 inches
K.	Fuel	
	Material	(Pu-U)C
	Maximum atom fraction burnup - 0.12 atoms fissioned/atoms heavy metal	
	Average atom fraction burnup - 0.10 atoms fissioned/atoms heavy metal	
	New fuel enrichment	16.26 a/o Pu-239 + Pu-241

III.1.4 Reactor Safety Considerations

A prime objective of the design efforts on the Westinghouse Large Modular Fast Breeder Reactor system is that "it must be safe". This reactor system incorporates many design and safety features that enhance safe operation. The following summary of some of the inherent safety features of the Westinghouse-AEC 1000 MWe core which are also applicable to the Westinghouse Large FBR Modular core was given in reference (1): "Safety considerations motivated a) a modular core, which provides neutronics similar to a small reactor in a reactor of large size, b) a negative Doppler coefficient, c) a controlled expansion fuel assembly which provides an inherent negative reactivity coefficient by fuel motion, d) fuel rod separation into multiple compartments to minimize the effect of fuel movement, e) sodium bonding to maintain low fuel temperature and thus inhibit fuel motion by preferential diffusion, f) a loss of reactivity upon complete loss of sodium and a sodium void reactivity effect of less than a dollar under the worst possible conditions, g) a design to encourage the fast fission of U-238 so as to increase the overall delayed neutron fraction, h) a coupling between modules which will decrease the positive effect of reactivity added inadvertently to a single module and thus partially compensate for the small delayed neutron fraction and the short fast neutron lifetime, and i) moderation of radial blanket neutrons which provide increased low energy fissions, and some of the benefits of the slow-fast reactor concept."

An additional inherent safety feature, which has not been incorporated into any of the transient analyses, is a negative feedback contribution to the power coefficient from the radial structural thermal expansion of the core. A brief summary of some of the many additional design features which have been incorporated into the Westinghouse Large Fast Breeder Reactor system to meet the safety objective follows.

Each of the seven module has a safety rod in the center. The seven of these together are worth 2% of the total reactor. Each module also has six identical peripheral control rods - three of which are used as safety rods and three as regulating rods. All 21 peripheral safety rods from the seven modules together are worth 2.45% to the total reactor, and all 21 peripheral control rods together are worth 2.45% to the total reactor. This provides a total shutdown margin in excess of 3% cold, and sufficient operating reactivity to permit annual refueling. One rod drive power supply is provided for each module, which is capable of activating only one rod at a time. Thus the maximum number of rods, one rod in each module, which can be simultaneously actuated is seven. All rods can be scrammed simultaneously with a release time of 200 milliseconds (similar to Fermi and EBR-II).

Positive reactivity due to partial voiding of sodium, although highly unlikely in the modular core concept, can be controlled by rod scram action. The time between initiation of a power excursion and the beginning of sodium boiling is sufficient to permit the insertion of fast acting control rods. Further investigations on core voiding must be made to fully understand the interaction and time dependency of not only Doppler and sodium temperature coefficients, but also the dynamic behavior of sodium under abnormal conditions of boiling, two-phase flow, expulsion and voiding.

The reactor vessel is doubled-walled so that leaks in the reactor vessel cannot drain the core and leave it without natural cirulcation cooling. The inlet and outlet nozzles to the reactor vessel are located above the core, so that leaks anywhere in the primary system cannot siphon the core dry. The primary piping is of double wall construction with sodium leak detectors located at the low points of the containment.

Blanket assemblies have smaller lower nozzles than fuel assemblies, so that fuel assemblies cannot inadvertently be inserted into blanket positions.

The shield plug is equipped with two feet of energy absorbing material on the lower face to partially absorb the high energy release in the event of the core meltdown accident. In addition, strong hold down latches are located at the top of the plug to prevent the plug from becoming a missile.

The reactor protection system is designed to detect potentially unsafe trends and conditions and initiate corrective action. The reactor will scram automatically when an unsafe condition develops. The functions connected with the primary system which will automatically scram the reactor are listed in Table III.1-4. Shutdown capability is provided by control rods that are spring assisted into the core. The reactivity shutdown margin is greater than 3.0% for the core with sodium.

A safety margin is provided by placing the reactor and its entire primary coolant system in reinforced concrete cells, which are backed-up by a low-leakage steel containment shell. The two containment barriers will be designed to withstand conditions more severe than any that are expected to occur. The structural integrity of both containment barriers, reactor vessel and piping will be provided by conforming to all applicable design and structural codes, laws and regulations of the appropriate regulating bodies.

The primary system coolant pumps are equipped with flywheels attached to the rotor shaft of the drive motor. This provides inertia to the system to obtain a pump coastdown characteristic giving 60% of full flow after five seconds.

A coolant loss due to primary system rupture would, by itself, cause no increase in pressure within the containment barriers as the reactor operates near atmospheric pressure, 15 psig, with temperatures at least 500°F below the boiling temperature of sodium at atmospheric pressures. Mechanisms that could increase the temperatures and pressures within the containment barriers are: (1) a nuclear power excursion giving a

Table III.1-4

List of Primary System Abnormalities Causing Scram and/or Alarm

1. Source flux level low, (A)
2. Log count-rate level high
3. Log count-rate period short or detector voltage low, (B)
4. Log N - period short or detector voltage low, (B)
5. Power range above fixed level or detector voltage low, (B)
6. Any control rod unlatched
7. Any control rod not "Full Down" (A)
8. Reactor inlet coolant flow low or rate of flow change high
9. Reactor outlet coolant temperature high or rate of change high
10. Primary pump power interruption
11. Primary system coolant level low
12. Reactor cover gas pressure high
13. Cell isolation trip (access open)
14. Manual scram
15. Reactor "noise" due to boiling or voiding in a single fuel subassembly
16. Mismatched sodium outlet temperature from the various assemblies

Notes:

(A) Effective only prior to reactor operation; bypass when control power is available.

(B) During startup, any two out of three channels will cause scram and alarm.

rapid release of energy, and (2) a chemical reaction of sodium with air or water vapor. The effect of a chemical reaction between sodium and air within the concrete cells is minimized by maintaining an inert atmosphere, nitrogen, within these cells. The mechanical design of the concrete cells provide protection in the improbable event of a nuclear power excursion.

Many potential accidents have been studied for this reactor system. The results of all these accident analyses have indicated that a fast breeder reactor designed with mixed uranium-plutonium carbide fuel in a multiple modular geometric array possesses inherently safe operating characteristics.

Reference 7 reports the results of investigations on an isolated module of several postulated accidents representative of the more severe disturbances to which the reactor system could be subjected. Reference 8 reports the results of the transient behavior of two modules neutronically coupled. The results of all these investigations indicated inherent stability of the reference reactor core. For the most severe accidents postulated in reference 7, the results indicated that the behavior of the reactor would not imperil the public or the operating staff, nor even result in economically severe damage to the plant. The most severe accident analyzed was flow blockage to one fuel assembly. This is severe becuase of the difficulty in detecting such a small perturbation in the coolant flow until severe damage has been done to that one assembly. Even this case would not result in damage to the remainder of the core unless a large fraction of the safety rods refused to move in response to reactor over-power, over-temperature, neutron level and neutron period scram signals; a very improbable event.

Reference 7 concluded for this Large Modular Fast Breeder Reactor system that "It would appear from the results of these analyses ..... that the particular core concept chosen may be overly conservative.

Future cores could be considered having less strongly pronounced safety advantages; liberalized in terms of higher specific powers and internal breeding ratios and lower neutron leakage, inventory requirements, doubling times, and overall fuel cycle costs."

III.1.5 Fuel Cycle Costs

As previously mentioned, the Westinghouse-AEC 1000 MWE FBR core[1] conditions were revised as described in reference (2) because of economic considerations.

The fuel cycle analyses on the Westinghouse Large Fast Breeder Reactor modular core have been placed on a more realistic basis than was directed by the USAEC during the four conceptual design studies[1,9,10,11]. For example, a 10% annual charge was assumed to apply on all working capital and inventory charges rather than the 4-3/4% directed by the Commission in 1963. Further, estimates on the plutonium value have been carefully developed as a function of the commercial and technical status of the industry[12].

The fuel cycle costs for the Westinghouse Large Fast Breeder Reactor using private ownership of fuel and commercial utility practice are given in Table III.1-5. The fuel cycle cost for the design reported in reference (1) and normalized by the Argonne National Laboratory[13] is given in the first column. The fuel cycle cost for this same design using typical commercial utility practice[14] is given in the second column. The fuel cycle costs for the reference Westinghouse Large Fast Breeder Reactor modular core design are given in the third column. The reduction in the plutonium credit, which was found to decrease by about 20%, reflects a reassessment of the breeding gain using more sophisticated analytical tools.

This shifting to commercial utility groundrules places strong emphasis upon obtaining higher specific power and results in the technical changes to the thermal design noted in reference (2). The more realistic

Table III.1-5

Westinghouse Large FBR Modular Core Fuel Cycle Costs
Based on Oyster Creek Method[14]

	1000 MWe W-AEC Design[1]		Westinghouse Large Modular FBR Design (Updated Physics)
	ANL[13] Normalization (AEC Fuel Ownership)	Using Typical Utility practice[14]	
Working Capital	0.39[d,g]	0.88[c,d,f]	0.53-0.63[c,d,f]
Fabrication	0.40	0.31	0.2-0.3
Processing	0.21	0.27[e]	0.25-0.28[e]
Pu Credit[d]	(0.39)	(0.60)[a]	(0.45-0.5)[b]
	0.61	0.86	0.53-0.71

a. Based on a breeding ratio of 1.57 as reported in WCAP-3251-1.

b. Latest revised physics calculations.

c. Fuel, including bred material, fabrication and processing @ 10.4%/yr.

d. Pu @ $10/gm (fissile) as nitrate.

e. Includes processing @ $21,150/day and NFS processing rates, shipping and reprocessing losses @ 1%.

f. Capacity factor @ 88%, typical of first fifteen years operation in Oyster Creek Plant analysis[14].

g. Use charge of 4.75%/yr.

appraisal under commercial ground rules has led to a factor of 2 or 3 increase in the fuel cycle cost, for the same design, over that reported in reference (1) using AEC ground rules.

Section III.1 - References

1. Heck, F. M., et al, "Liquid Metal Fast Breeder Reactor Design Study", WCAP-3251-1, January 1964.

2. Gunson, W. E., et al, "High Power Density Stainless Steel Reference FBR Core Design", WCAP-2638, July 1964.

3. Heck, F. M., "Neutron Controlled Expansion Fuel for Fast Breeder Reactor", Proceedings of the Conference on Breeding, Economics and Safety in Large Fast Power Reactors, October 7-10, 1963.

4. Gunson, W. E., et al, "The Liquid Metal Fast Breeder Reactor Design Studies", WCAP-2635, July 1964.

5. Keyfitz, I. M., et al, "200 MWe Sodium Fast Reactor Prototype (SFRP) Design Study", WCAP-2628, September 1964.

6. Markley, R. A., et al, "30 MWt Sodium Advanced Fast Experimental Reactor (SAFER) Plant Design and Program", WCAP-2745, February 1965.

7. Wright, J. H., et al, "Conceptual Design and Preliminary Accident Analysis of a Sodium Cooled, Carbide Fueled, Large Modular Power Reactor", presented in panel discussion on Safety of Large Fast Power Reactors, Fast Reactor Conference, Argonne National Laboratory, Argonne, Ill., October 11-14, 1965 (to be published).

8. Gunson, W. E., Heck, F. M., and Daleas, R. S., "Transient Response of Coupled Fast Reactor Cores", presented at Fast Reactor Conference, Argonne National Laboratory, Argonne, Illinois, October 11-14, 1965 (to be published).

9. Klotz, C., et al, "Large Fast Reactor Design Study", ANCP-64503, January 1964.

10. McNelly, M. J., et al, "Liquid Metal Fast Breeder Reactor Design Study, (1000 MWe UO_2-PuO_2 Fueled Plant)", GEAP-4418, January 1964.

11. Visner, S., et al, "Liquid Metal Fast Breeder Reactor Design Study", CEND-200, January 1964.

12. Smith, E. E. and Wright, J. H., "Future Energy Needs and Nuclear Fuel Use", Atomics, Vol. 18, No. 3, pages 22-26, May-June 1965.

13. "An Evaluation of Four Design Studies of a 1000 MWe Ceramic Fueled Fast Breeder Reactor", COO-279, December 1964.

14. "Report on Economic Analysis for Oyster Creek Nuclear Electric Generating Station", Jersey Center Power and Light Company, February 17, 1964.

III.2 BCEX Concept and Its Problem Areas

III.2.1 Introduction

This section describes the BCEX concept and discusses the many aspects of the BCEX concept, with emphasis on the possible problem areas relevant to its application in a fast reactor core.

A general description of the BCEX concept and problem areas follows. The more specific details of this concept and its problem areas are discussed and investigated in subsequent sections of this report.

III.2.2 General Concept Description

A predictable structural expansion characteristic of a nuclear reactor core, which will provide a rapid, inherent, negative temperature coefficient, is highly desirable to enhance safe reactor operation. Such an expansion capability could contribute significantly in terminating power excursions. Although core structural expansion can be accomplished in several different ways, unfortunately, most of them are presently either quite unpredictable and/or extremely complicated.

Recently, two controlled structural expansion concepts, which will provide a predictable, core axial, structural expansion behavior, have received attention in reactor design. The first of these, the bundle controlled expansion (BCEX) fuel assembly, is the subject of the investigation described in this report. A brief study of the dynamic performance characteristics of a second concept, fuel rod clad controlled expansion (CCEX), is also performed.

The BCEX concept, which is illustrated in Figure III.2-1, takes advantage of the rapid, predictable, coefficient of thermal expansion of a central cermet fuel structure to obtain a rapid and significant separation of the half-length fuel bundles which are attached to the ends of this central cermet fuel structure. This significant separation or response is achieved because the cermet structure will operate at a higher temperature level (with resultant greater ΔT's during power excursions) than a non-fueled structural material (i.e., stainless steel) because of

CEX (CONTROLLED EXPANSION) FUEL ASSEMBLY

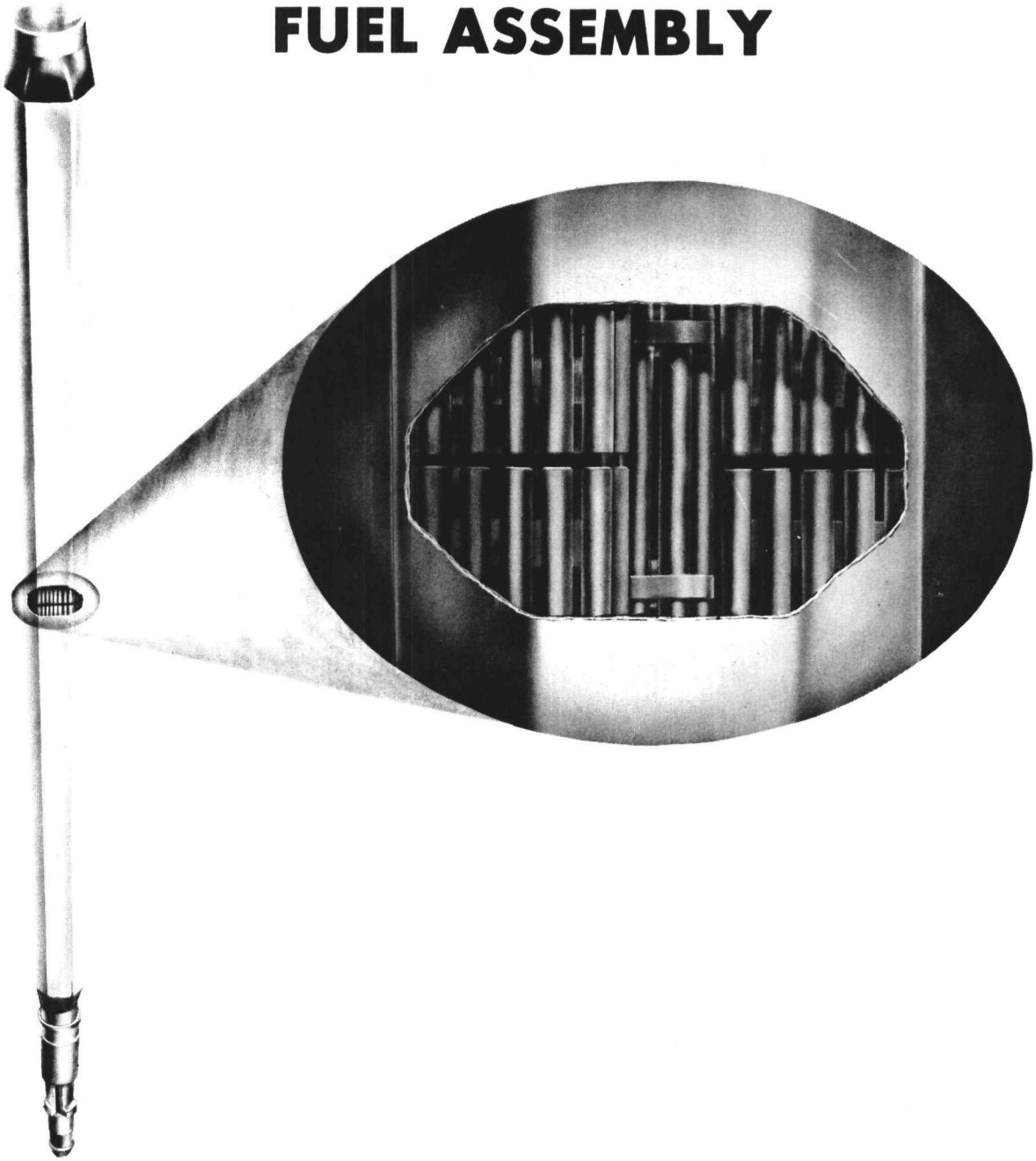

CEX (Controlled Expansion) Fuel Assembly

Figure III.2-1

the much greater internal heat generation rate of the cermet fuel structure. Rapid response is also achieved because of the instantaneous internal, fission heat generation in the cermet rods. Controlled bowing of the fuel assembly, which can result in a decrease in reactivity for increases in temperatures, is another possible advantage of the BCEX concept.

In the second concept, CCEX, the fuel assembly would be designed so that the fuel would move axially with its clad due to compartmentation, thus providing an inherent negative reactivity effect. In both concept investigations, no account is taken of fuel material thermal expansion.

The BCEX assembly is a modification of a ceramic fuel assembly. Each fuel rod is manufactured as two separate half rods, rather than as one single full-core length rod. The upper half rods are assembled by brazing into an upper bundle, and the lower half rods into a lower bundle. Rods are missing from the center of each bundle. An array of full-length cermet rods is inserted through the two fuel bundles. The two fuel bundles are then attached to the outer ends of the cermet rods by end fittings.

Thus, the two fuel bundles are in series, and are attached only at the ends of the cermet array. This entire assembly is then hung from the top of the assembly can with the lower end left free to expand and contract. Thus, during reactor power operation, the cermet rods are always in compression because the drag forces due to coolant up-flow exceed the gravity forces on the bundle. Resilient stabilizers center the bundle in the can.

The cermet rods expand and contract with power or temperature changes. The fuel content of the cermet ensures that the cermet rods will expand more rapidly with power than the clad around the ceramic fuel. Therefore, an increase in power, which causes the cermet rods to expand, results in

pulling the two ceramic fuel bundles apart at the center. This reduces the total reactivity of the core in the same way that pulling apart both halves of a split-table critical reduces reactivity. By this principle, the BCEX assembly introduces a fast-acting negative reactivity coefficient into the core.

The brazed fuel bundles of the BCEX fuel assembly are restrained to be parallel to the can at the core top and bottom (i.e., they act as cantilever beams). When the bundles bow due to a power gradient across the bundle, the bowing moves the center ends of the half-length bundles away from the hot spot. This action results in a negative bowing coefficient. This is the reverse of the behavior of the middle of a bundle of end-attached, full-length rods, which move toward the hot spot or the core center.

III.2.3 Problem Areas

III.2.3.1 General

The bundle controlled expansion, BCEX, fuel assembly is an extremely sophisticated structure, in which the desired effect - a negative power coefficient - is the net result of several, complex, interacting, positive and negative effects, each having a different time response behavior.

It is tempting to point to the cermet structure in the BCEX concept and say that its structural integrity is the paramount problem. Unfortunately, the BCEX problems cannot be simplified to this degree. A BCEX element using "cermet" rods with zero volume fraction of fuel would be structurally acceptable, but would not provide sufficient negative reactivity feedback. As the fuel loading in the cermet is increased from zero, the length of time during which the cermet will perform satisfactorily as a structural member in the reactor decreases. Simultaneously, the negative feedback which it can contribute increases. Ideally then, it is only necessary to plot allowable cermet life versus fuel loading; then, from the required life to find the maximum allowable fuel loading. By this procedure, it

can be determined whether the loading allowed by cermet life provides sufficient negative feedback. However, the problem cannot be handled this easily.

There is considerable data on the performance of uranium oxide-stainless steel cermets, but the interpretation of this data, especially for mixed oxide-stainless steel cermet rods, is not clear. Furthermore, the available data is usually correlated by plotting total fissions/cm^3 versus the cermet surface temperature. Whether these are the two most pertinent variables is questionable. If surface temperature, or any other cermet temperature, is used, the results are very sensitive to the overall reactor design and plant operating temperature levels. For example, using the common correlation, a cermet fuel loading giving adequate life for a 1050°F reactor outlet temperature may fail when used with a 1150°F outlet temperature. Similarly, the difference between a uniformly loaded core and a zone loaded core might dictate success or failure. In addition, it is not clear that the 300 series stainless steels are the best matrix materials. Still further, a large portion of the available irradiation data was obtained using plate geometries, and the thermal and structural behavior of plate fuel elements is quite different from rod type elements.

The net negative reactivity feedback of the BCEX concept is a function of the differences between the physical and mechanical properties of the ceramic fuel, its clad, and its bond, and the physical and mechanical properties of the cermet, its clad, and its bond. The net, negative, instantaneous feedback is also a function of the reactivity insertion rate and magnitude, the core geometry, the other power coefficients, the coolant flow rates, and the initial power and temperature levels. As previously mentioned, the net negative feedback depends on the ceramic fuel material and the clad materials. For example, niobium clad on the ceramic fuel provides a significant ($\sim$ 30 percent) increase in the net negative effect.

The specific problems requiring investigation are described below under the following headings: Alternates, Cermet Design and Properties, Fuel Design and Properties, and BCEX Effectiveness.

III.2.3.2 Alternates

The expansion of the clad on the cermamic fuel pins of a BCEX fuel assembly tends to move fuel material toward the axial center of the core and thereby contribute a positive reactivity. Because this partially counteracts the negative effect of the cermet rod expansion, it would be desirable to minimize or eliminate this effect. The reference design tends to maximize this effect because the 300 series stainless steel used as a clad is estimated to have a 10% higher thermal expansion coefficient than the same material used as the matrix for a cermet. The use of alternate clad material could help to solve this specific problem. For example, the use of niobium as a clad for the cermaic fuel is a potentially attractive alternate because its coefficient of thermal expansion is about one-half that of the 300 series stainless steels, and its thermal conductivity is appreciably higher. Therefore, it would not only expand less per degree of temperature, but it would experience a smaller temperature rise for a given increase in reactor power. Preliminary estimates place the gain in the net negative reactivity effect at about 30 percent. Detail studies would be required to assess the over-all gain, as some reduction in Doppler effect and sodium coefficients would result from the use of niobium clad. The amount of the change would depend upon the thickness of the niobium clad.

A second clad alternate is the use of either martensitic or ferritic stainless steels. These exhibit about 20 percent higher thermal conductivity and less than two-thirds the thermal expansion of the austenitic stainless steels. With these materials as clad on the ceramic rods, the net negative feedback might be increased by 15 to 25 percent. The fabricability of martensitic or ferritic stainless steels would certainly be an important consideration in assessing the feasibility of such an alternate clad material.

A different fuel bundle design is possible which would more than double the net negative feedback by making the ceramic clad expansion a negative effect rather than a positive one. This can be accomplished by moving the half-length fuel bundle support webs or spiders from the extremities of the core to the core center. The support spiders would then be connected to the extremities of the cermet rods by a two-piece sheath around the cermet rods. While this increases the complexity of the assembly somewhat, it provides two other advantages in addition to doubling the negative feedback. This structure moves the upper fuel bundle support spider from the region of maximum coolant temperature (at the subassembly outlet) to the region of mean coolant temperature at the center of the core. The presence of the sheath also permits better control of the coolant flow around the cermet rods because orificing could then be more easily accomplished.

Elimination of the clad on the cermet might improve the cermet dynamic response. However, this was not adopted in this study because of the possibility of exposing ceramic particles thereby contaminating the coolant or forming a corrosion cell. Detailed analyses of these various alternates are not within the scope of this study.

III.2.3.3 Cermet Design and Properties

The cermet rod cluster functions both as a structural member of each fuel assembly and as a small, low power, fuel subassembly within each fuel assembly. To perform these two major functions successfully in the reactor core environment, several design problems must be solved. These problems are either unique to the BCEX concept, or have significantly greater importance in BCEX design than in conventional fuel assembly design.

Cermet Structural Integrity

Structural integrity of the cermet rods is essential to a successful BCEX fuel assembly design. The production of a successful fuel bearing cermet is still an art, and interpretation of the limited available performance data is correspondingly difficult. There is some evidence to indicate that a simple correlation of accumulated fissions per unit volume versus surface temperature can predict success or failure. This would appear to be a gross over-simplification even though it seems to correlate existing data. One expects that low density ceramic particles surrounded with a high fraction of steel matrix which is undamaged by recoil fission products would not fail at the same temperature and fissions per unit volume as high density particles and a low fraction of undamaged steel matrix. For example, one would also expect that a high temperature rise from surface to center would be more adverse than a low rise. In addition, rod fuel geometries have significantly different structural capabilities than plates, annuli, etc. None of these effects can be seen in the existing data, possibly because the variations of these factors have been small between samples from which data is reported. Furthermore, most of the existing data was acquired from relatively short time exposures, typically around 2500 hours or less, where a different failure mechanism may apply. Cermet fuel data for BCEX design for commercial reactor application must be taken over time periods of the order of 20,000 hours to ensure that creep effects are investigated and understood. In addition, data for BCEX design requires that the cermet rods be mechanically loaded during irradiation. In short, the presently available data in the unclassified literature is quite inadequate; thus, it does not permit confident design of the cermet structures for BCEX application.

The following kinds of data are needed as functions of time, temperature, and neutron irradiation level:

Short time yield and ultimate strengths;
Short time elongation to failure (ductility);
Low cycle fatigue strength;
Static and dynamic modulus of elasticity;
Creep rupture strength;
Primary and secondary creep rates;
Elongation at rupture by creep;
Impact strengths;
Extent of blistering, cracking, swelling or distortion.

Coolant Flow Balancing

Useful values for the linear heat generation rate in the cermet rods seem to lie in the range between 1/5 and 1/2 that of the associated ceramic rods, depending on such factors as reactivity feedback requirements, temperature limitations, cermet rod fuel content limitations, relative diameters of the rods, type of ceramic material, etc. Therefore, less coolant is required for the cermet rods than for the ceramic rods of the same diameter. Overcooling of the cermet rods will somewhat inhibit their response by holding down the total temperature rise seen by the cermet in response to a power change. (The ΔT in the rod is not affected, but the coolant temperature change will be less.) Balancing of the relative flow rates around cermet and ceramic rods is an important engineering problem.

Several alternates have been suggested. Flow guide vanes or fingers might be provided which would insure rapid and essentially complete mixing across the entire fuel assembly. This has the disadvantage of increasing the pressure drop through the assembly.

Special grid assemblies might be designed to increase the pressure drop along the cermet rods so that the flow along the cermet rods is inhibited and the temperature rise kept in balance with that around the ceramic rods.

The pitch of the cermet rods can be reduced, and a flow baffle provided around the cermet subassembly. In principle, by combining this with appropriate cermet rod spacers, both the pressure drop and the temperature rise can be matched to that of the ceramic rods.

The diameter of the cermet pins can be increased, and the pitch adjusted so that the coolant pressure drop and temperature rise are matched to that around the ceramic rods. This alters the cermet response (see discussion in Section III.5).

Heat Generation Rate Versus Diameter

An important design parameter is the average temperature rise in the cermet. This is discussed under Cermet Effectiveness. A given average linear heat generation rate in the cermet fuel defines the average cermet temperature rise. The necessary volumetric heat generation rate must then be determined. The product of volumetric heat generation rate and rod diameter squared is directly proportional to linear heat generation rate. Thus, a trade-off is possible between volumetric heat generation rate and cermet rod diameter. The volumetric heat generation rate establishes the volume fraction of ceramic in the cermet for a given enrichment and also sets the integrated fissions per unit volume which the cermet will undergo for a given lifetime.

It is desirable to minimize both the volume fraction of ceramic in the cermet and the integrated fission dose in order to maximize the reliability of the cermet structure. This would lead to low volumetric heat rates and large rod diameters. However, large cermet rod diameters have an adverse effect on the kinetic response of the structure, as the large rod has a large thermal time constant and, therefore, tends to respond more slowly to a change in power levels. The large rod also has a lower natural frequency for axial vibration. Hence, it has a greater tendency to lag and then overshoot mechanically than does a small diameter rod.

The previous discussion points out that some compromise diameter and heat generation rate for the cermet rods must be determined for each given ceramic fuel design, due to their different thermal properties.

Cermet Internal Time Constant

The time delay between generation of heat in the ceramic particles and dispersion of the heat through the steel matrix is important. For ceramic particle sizes of interest in this study, the time constants for the particles are of the order of a millisecond. Therefore, the effective time delay will be negligible with respect to realistic insertions of reactivity, which require hundreds of milliseconds or more.

Enrichment

The preferred design for the cermet uses an enrichment level and isotope(s) identical with that in the associated bulk ceramic fuel. This maintains the relative values of cermet and bulk ceramic fuel properties constant with time. Fabrication or structural property considerations might suggest a higher enrichment to achieve a lower volumetric fraction of ceramic phase in the cermet. Therefore, it would be desirable to have some freedom in this respect.

From the practical design standpoint, considerable deviation in enrichment is permissible with a relatively small effect on performance. It is estimated that an increase of 50 percent in enrichment could cause the relative power in the cermet to decline about 10 percent by end of life. Taking into account that in a typical fuel equilibrium cycle only a fraction of the assemblies are at the end of life simultaneously, with the resultant lowered worth at that time, the effect of the 50 percent increase in cermet enrichment on core reactivity response is probably of the order of 10 to 15 percent.

Substitution of a different fissile material might be attractive from the fabrication standpoint. For example, enrichment with U-235 instead

of plutonium could eliminate the need for shielding during fabrication. This does not appear to be an attractive alternate from the performance standpoint, because it requires almost one-third more ceramic phase volume to achieve the same power generation rate.

Cermet-Clad Bond

In the reference design, the cermet rods have metallurgically bonded clad. An unbonded or gas bonded clad might be used. This has the advantage of reducing the degree of restraint which the clad imposes on the axial thermal expansion of the cermet. Unbonded or gas bonded clad raises the cermet temperature for a given power generation rate and, therefore, increases the expansion. There may be a suitable compromise between bonding, volumetric heat generation rate, and cermet temperature which would improve performance without shortening the life of the cermet.

A sodium bond could provide the advantage of reducing restraint without increasing cermet temperature. It is currently judged that the increased fabrication cost and design complexity would out weight this advantage.

Cermet Lateral Support

As the cermet rod subassembly is a long slender column, it could buckle under relatively small compressive axial loads unless it has lateral support along its length. During steady state full power operation, this could be a problem as the lower bundle, which is free to move, is lifted by the coolant flow, putting the cermet structure in compression. However, any compressive loads will be small and only a minimum of lateral support will be required. During low flow operation and during power excursions, gravity forces may exceed the drag forces and the cermet structure may then be loaded in tension.

It is not practical to support the cermet structure from the assembly can wall. Therefore, it is necessary to depend upon the ceramic fuel bundles, which in turn are supported by the can wall, for lateral support

of the cermet structure in the reference design. This will require investigation of the performance of rubbing straps under reactor conditions to insure that sufficient lateral support can be achieved without galling, fretting, or welding.

Cermet Structure Geometry

The geometry of the cermet structure must be investigated to establish the optimum number of rods, size of rods, and their relative position with respect to each other and to the ceramic fuel rods.

III.2.3.4 Fuel Design and Properties

In subsequent sections, the performance behavior of an oxide and carbide fueled core utilizing the controlled expansion concept will be investigated and compared. The greater time constant of the oxide fuel is significant. Because of this, it is presumed that the clad on the oxide fuel rod will have a slower response, and its inward expansion will be slower, thereby increasing the BCEX effectiveness during the early stages of an excursion.

In this study, the ceramic fuel is assumed to be divided into compartments so that the fuel will move with the cladding. Clad such as 316 stainless steel, whose expansion behavior is well known and predictable, should provide ceramic fueled cores with a dependable axial expansion characteristic during transient conditions. Thus, the controlled clad expansion, CCEX, feature is obtained. This clad expansion of the ceramic fuel becomes an inward expansion and thereby offsets some of the negative reactivity obtained from outward axial expansion of the fuel bundles in the BCEX concept.

III.2.3.5 BCEX Effectiveness

The crucial question to answer in determining whether the cost of development of BCEX and the fuel cycle cost penalty are justifiable is the degree of effectiveness or the worth of BCEX in controlling the dynamic behavior of the reactor.

The desirability of negative power coefficients is well recognized from the control, stability, and incident termination standpoints. There is no standard of value nor even a clear definition of the magnitude of power or temperature coefficient which is acceptable. In addition, there is an uncertainty of plus or minus 25 to 50 percent on the magnitude of the major inherent reactivity coefficient (Doppler). Thus, there appears to be no definite standard by which BCEX effectiveness can be evaluated.

In lieu of a standard, certain other questions related to effectiveness may be asked. From best estimates, based on the available data of the properties of the cermet, what heat generation rates in the cermet can be achieved with respect to the heat generation rates in bulk ceramic fuel? What negative power or temperature coefficients could be achieved? How much negative reactivity can be generated during a transient? How much might limitations on reactivity for control be increased with the use of BCEX? How much might the positive reactivity which could be inserted in an incident be increased? How much does BCEX increase the margin of safety from gross core damage. What is the relative performance of BCEX with different bulk ceramic fuels?

The investigation reported in subsequent sections of this report is an attempt to quantify some of the information required to judge the effectiveness of the controlled expansion concept.

III.3 Thermal & Hydraulic Analyses and Results

III.3.1 General

The Westinghouse - AEC 1000 MWe Fast Breeder Reactor modular core design, prepared under AEC contract AT (30-1)-3251 and reported in WCAP-3251-1[1], with an uprated power density and lower operating temperatures as outlined in WCAP-2638[2], was selected as the reference design for the bundle controlled expansion (BCEX) fuel assembly performance analyses performed under this contract. The thermal and hydraulic analyses were performed on one module of this seven module FBR core. The module equivalent diameter and active fuel height are 2.8 ft. and 6 ft., respectively. Each of the 36 fuel assemblies contain 127 rods: 120 fuel rods (lower and upper) and 7 full length cermet rods. All carbide fuel rods are 0.300 inch O.D. with a triangular pitch on 0.426 inch centers.

The thermal and hydraulic analyses were performed with the Westinghouse Liquid Metal Cooled Thermal & Hydraulic Design (LMCTHD) Computer Program, a steady state thermal and hydraulic design code for sodium cooled reactors. This code divides the entire length of each coolant channel into finite increments, and progressively solves for the conditions for each increment of the entire channel. The code can subdivide the core (module in this case) into as many as 5 radial zones and 10 axial increments. The fuel assemblies can be regular (all fuel rods) or non-regular (part fuel rods and part control rods or crement fuel rods as in BCEX). Either the actual or a chopped cosine axial power distribution can be used.

The coolant, clad, and fuel temperatures are calculated for the average fuel rod. Then, using the specified hot channel factors, axial power profile, zone to core average radial power ratio ($\bar{P}_{\text{zone, j}}/\bar{P}_{\text{core}}$), and the maximum to normal radial power ratio within

each radial zone ($P_{max.\ j}/\overline{P}_{zone,\ j}$), the coolant, clad, and fuel temperatures in the normal and hot channel are calculated for each zone at as many as eleven axial locations. The effects of flow orificing can be analyzed for each zone. If the fuel rods are unvented, the fission gas volume is calculated for the hot channel in each zone. The pressure drop through the fuel bundle in each zone is calculated. The fuel bundle consists of the lower and upper axial blankets, active core, and the fission gas reservoir length. The number of grids or brazed ferrule rows is calculated from a given spacing. The effect of the grids or brazed ferrules is incorporated into the core pressure drop calculations.

The thermodynamic and transport properties of sodium used in the thermal and hydraulic analyses were taken from the liquid metal survey[3,4,5] conducted by the Southwest Research Institute.

III.3.2 Design Basis and Ground Rules

The basis for the results presented in Section III.3.3 is outlined below.

As previously mentioned, the Westinghouse Large Fast Breeder Reactor modular core was selected as the reference design in which to analyze the performance characteristics of BCEX. The initial design bases and ground rules for this study are listed in Section II-2. The reference reactor design and operating conditions are described in Section III-1.

Listed below are some of the design bases that were selected during this study and employed in the thermal and hydraulic analyses:

1. Hot channel factors
   - A. Engineering
     1. Heat flux, $F_q^E = 1.04$
     2. Enthalpy rise, $F_{\Delta H}^E = 1.15$
     3. Heat transfer, $F_{\Delta T}^E = 2.00$

B. Power Peaking

1. Core 1.14
2. Radial Blanket 1.00

C. Nuclear (overall maximum to average)

	Core		Core	
	Radial	Axial*	Radial	Axial
Beginning of life	1.33	1.36	2.83	1.36
33,000 MWD/T	1.27	1.345	1.80	1.345
67,000 MWD/T	1.22	1.33	1.52	1.33

*Control rods fully withdrawn

D. Nuclear (by radial zone, beginning of life)

1. Fuel and cermet

Zone average to core average, Zone 1 = 1.27
" " " " " Zone 2 = 1.10
" " " " " Zone 3 = 0.844

2. Fuel

Maximum to average in Zone 1 = 1.05
" " " " Zone 2 = 1.10
" " " " Zone 3 = 1.17

3. Cermet

Maximum to average in Zone 1 = 1.01
" " " " Zone 2 = 1.02
" " " " Zone 3 = 1.03

2. Core orificing factors:

Zone 1 = 114% flow
Zone 2 = 100% flow
Zone 3 = 0.953% flow

3. The carbide fuel was assumed to be 92% of theoretical density.

4. The average thermal conductivity of the 316L stainless steel clad is 11.0 Btu/hr. ft °F. The clad is 0.010 inches thick which is sufficient for corrosion, fission fragment recoil damage, etc.

5. The average thermal conductivity of the carbide fuel is 10.0 Btu/hr. ft °F. The carbide fuel pellets are thermally bonded to the clad with sodium. The equivalent heat transfer coefficient at the fuel clad interface is 72,000 Btu/hr-ft^2 °F.

6. The clad-cermet fuel interface heat transfer coefficient is 100,000 Btu/hr ft^2 °F. This assumes a) a good metallurgical bond between the cermet and its clad, and b) that defective areas that would greatly increase temperatures at the clad-cermet interface are highly improbable.

7. The pressure loss coefficient for grids is 0.3.

8. The coolant by-pass flow (between fuel assemblies, control rod cooling, etc) is 5% of the total core flow.

9. The value of the thermal conductivity of the cermet fuel as a function of volume percent fuel, used in the T&H calculation for this study, is shown in Figure III.3-1.

10. The cermet rods will be clad with 316L stainless steel.

11. The fuel content in the cermet rods is limited to 35 volume percent. A change in enrichment is required, if more fuel is required. The cermet fuel will consist of mixed oxide, so that matched burnup of cermet fuel and ceramic fuel will be preserved.

12. Compartmentation of the fuel rods is assumed. Thus, the fuel moves with the clad as the clad expands and contracts.

The convective heat transfer coefficient was calculated by using the Dwyer-Tu heat transfer correlation for triangular-spaced rod arrays.

This Dwyer-Tu correlation is:

$$Nu = 0.93 + 10.81\left(\frac{P}{D}\right) - 2.01\ \left(\frac{P}{D}\right)^{2.0} + 0.0252\ \left(\frac{P}{D}\right)^{0.27}\ \left(\overline{\Psi}\ P_e\right)^{0.8}$$

where:

P	Rod pitch
D	Rod diameter
P_e	Peclet number
N_u	Nusselt number
$\overline{\Psi}$	Dwyer's eddy transport correction

The DNB ratio was checked by using the forced convection burnout heat flux correlations of Lowdermilk[7] and Noyes[8] and liquid metal pool boiling correlations of Caswell and Balzhiser[9] and Noyes[5].

III.3.3 Discussion & Results

The results of the thermal & hydraulic analyses are strongly influenced by the selection of an average linear power of 15.6 KW/ft. as the basis for the design of the carbide fuel rods. Flow orificing by zones in the core is assumed.

In this study, an important parameter used in investigating the cermet fuel performance is its volumetric heating ratio, Q. This is defined as the ratio of the volumetric heat rate in the cermet fuel to the volumetric heat rate in the ceramic fuel, or:

$$Q = \frac{q'''_{\text{cermet fuel}}}{q'''_{\text{ceramic fuel}}}$$

Figures III.3.2 and III.3.3 show the relationships between the volume fraction, weight fraction, percent of theoretical density, and the volumetric heating ratio in the cermet fuel. The cermet fuel burnup relationships are illustrated in Figure III.3-4. The basis for these relationships are presented in the curves.

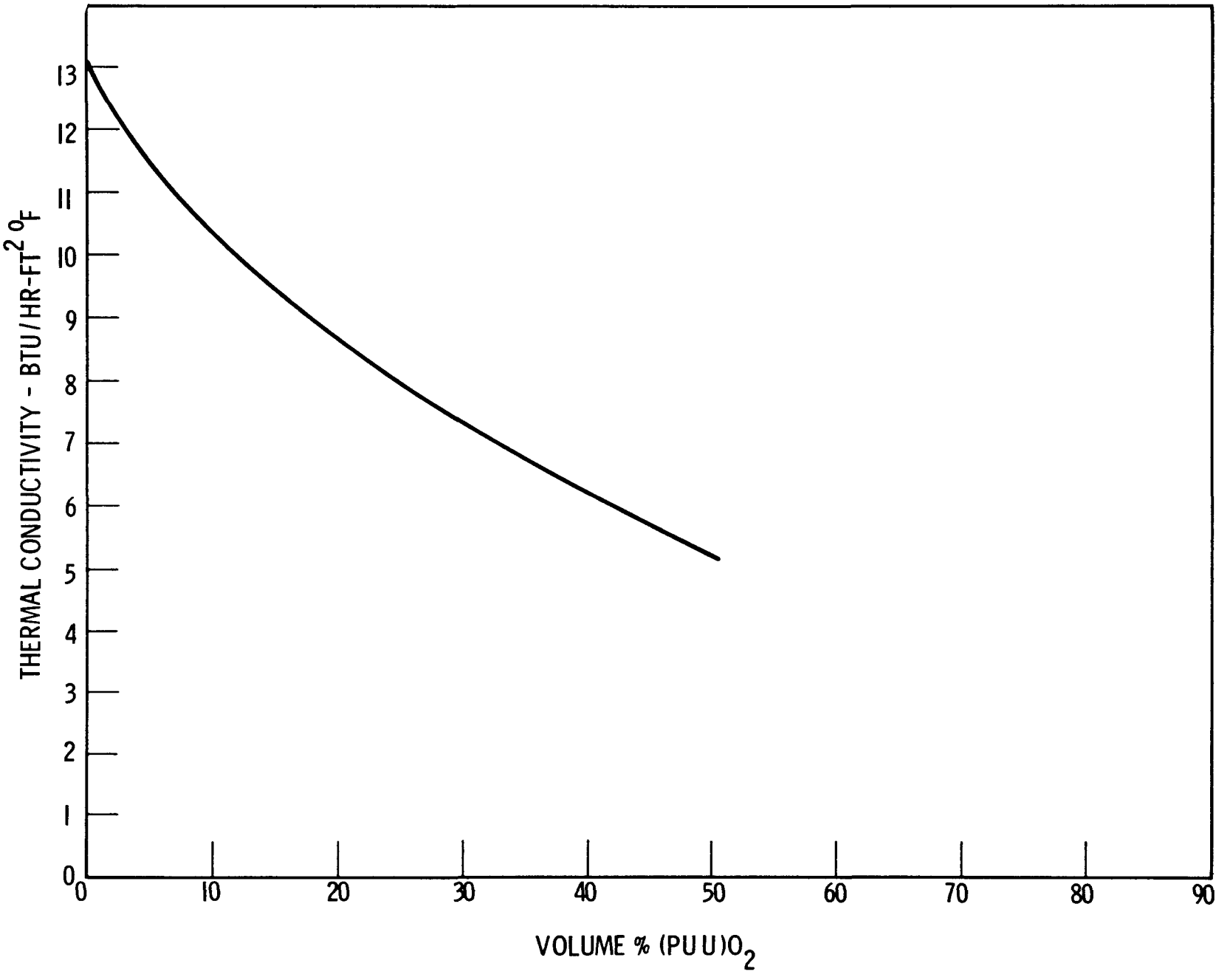

CERMET THERMAL CONDUCTIVITY

Figure III.3-1

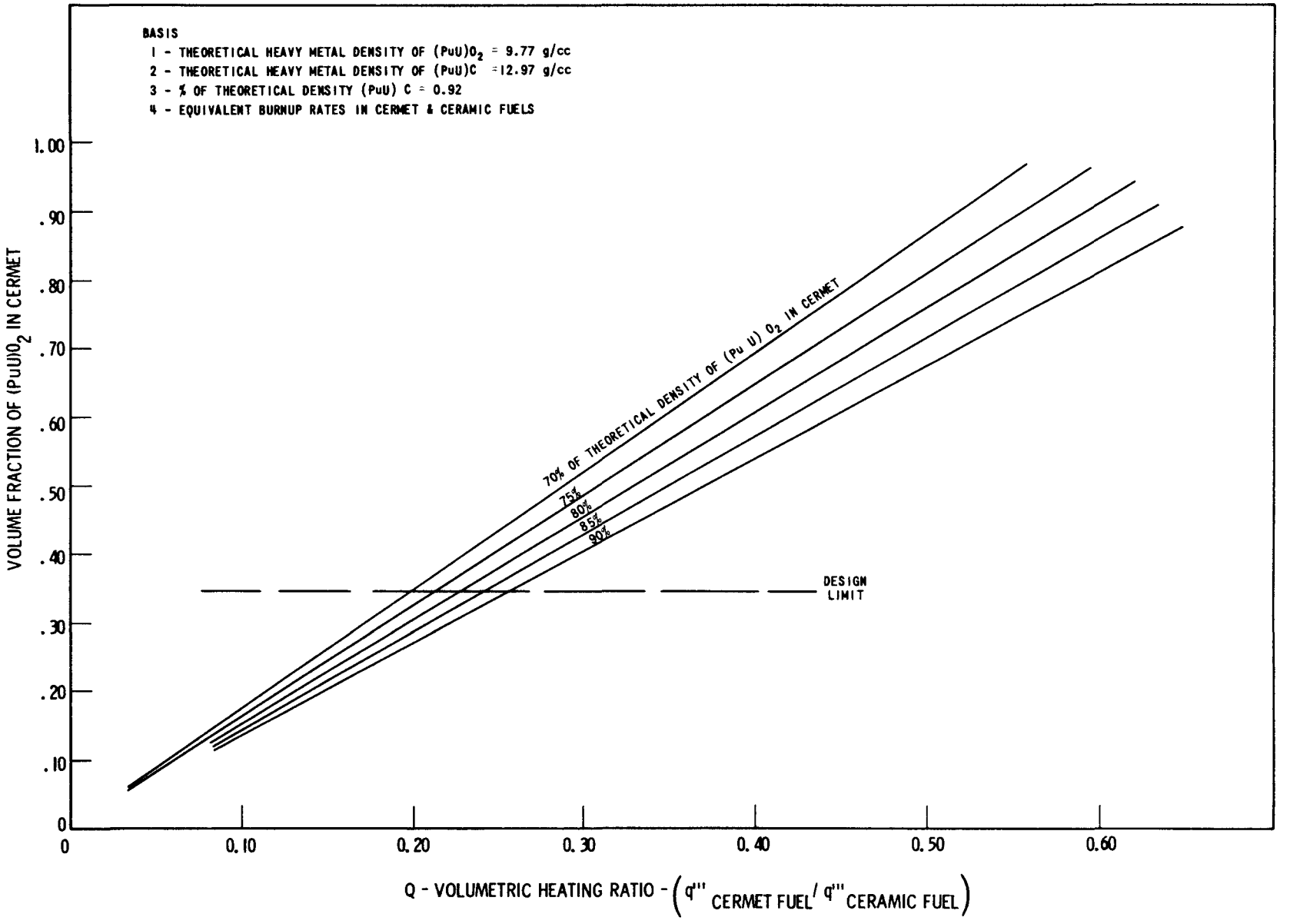

CERMET FUEL RELATIONSHIPS

Figure III.3-2

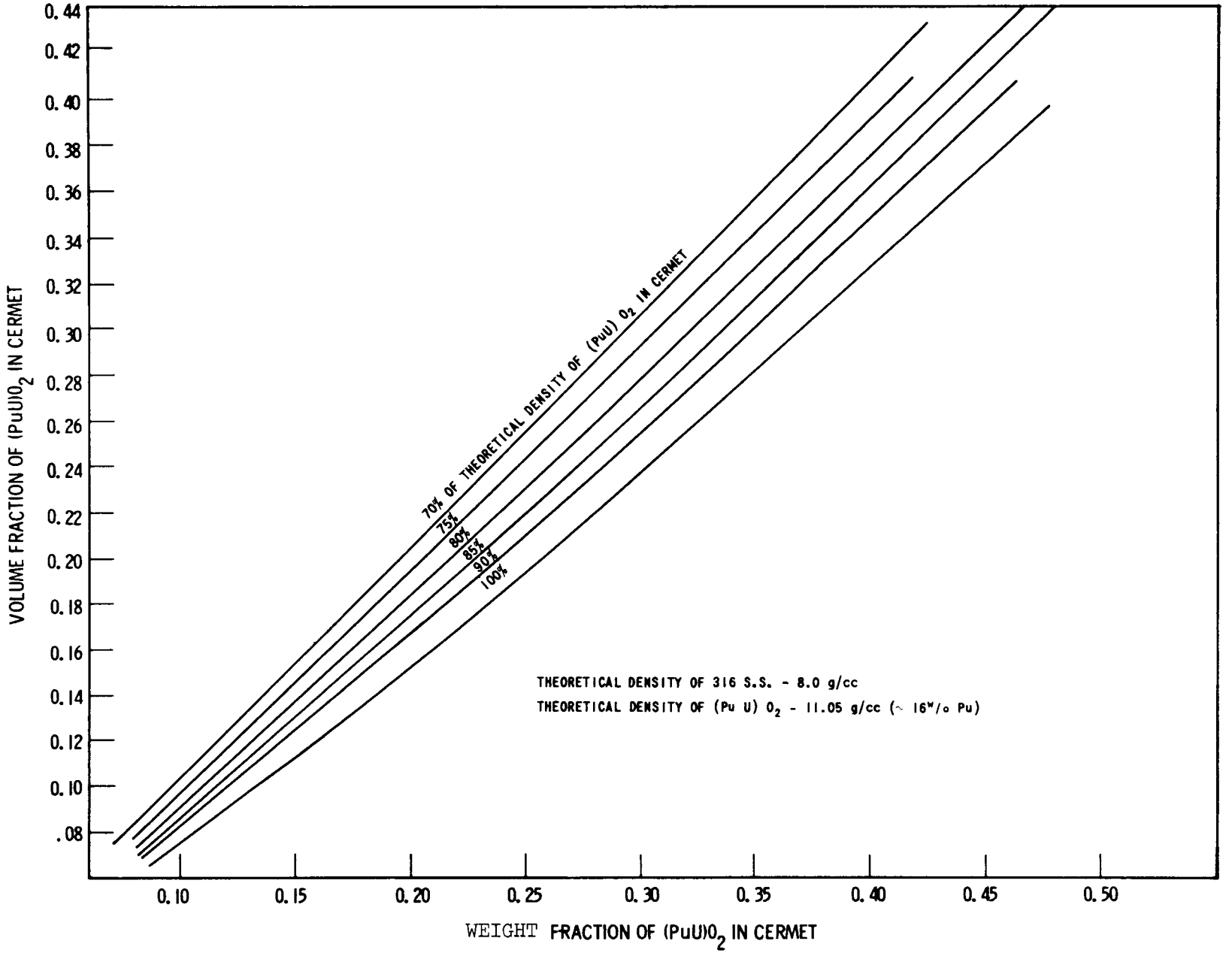

CERMET FUEL VOLUME FRACTION VS WEIGHT FRACTION

Figure III.3-3

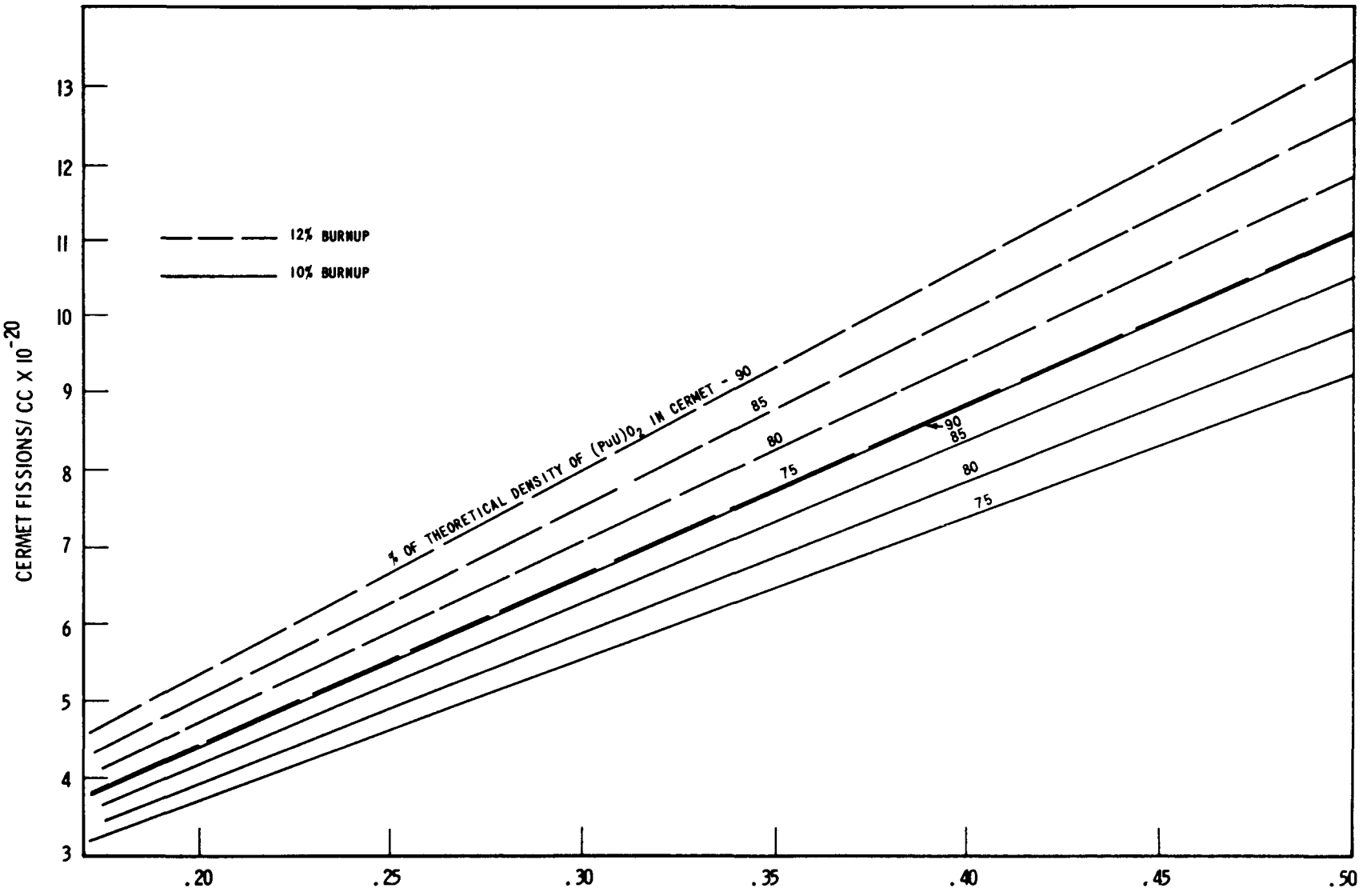

CERMET FUEL BURNUP RELATIONSHIPS

Figure III.3-4

Figure III.3-5 presents the steady state temperature profile for the carbide fuel rods, based on the actual core heat flux distribution at 100% power. These conditions also assume 100% coolant mixing between the coolant heated by the fuel and the coolant heated by the cermet rod within an assembly. This does not assume mixing between the fuel across an assembly. Figure III.3-6 presents the temperature drops through the cladding of the carbide fuel at 100% power for the three radial core zones. Both the hot and average channel temperatures are shown on these curves.

A summary of the steady state thermal and hydraulic data for the reference Westinghouse Large Fast Breeder Reactor Modular Core incorporating the bundle controlled expansion (BCEX) concept was presented in Table III.1.3 in section III.1.3.

The variations in the circumferential steady state temperature of the 0.300 inch O.D. carbide fuel rods, with a 0.426 inch pitch were checked with the AXTHRM[10] code. Negligible, 3-6°F, temperature variations were calculated around the periphery of a fuel rod.

Thermal and hydraulic analyses were performed on the cermet rods to establish their steady state temperatures. Figures III.3-7 thru III.3-12 presents the results of the analyses of the 0.300 inch O.D. cermet fuel pins at beginning of life conditions and at 100 percent power. A chopped cosine power profile was used in these calculations. Figure III.3-7 illustrates the effect of (1) the fuel coolant mixing fraction into the cermet channel and (2) Q, the volumetric heating ratio,* on the maximum cermet centerline, hot channel coolant outlet, and average coolant outlet temperatures. Figure III.3-8 shows the effect of Q only on various parameters at 100 percent mixing. Figures III.3-9, III.3-10, III.3-11, and III.3-12 present the steady state hot and average channel temperature profiles for Q = 0.20, 0.25, 0.30 and 0.40

*Which is defined as the ratio of the volumetric heating rate in the cermet fuel to the volumetric heating rate in the ceramic fuel.

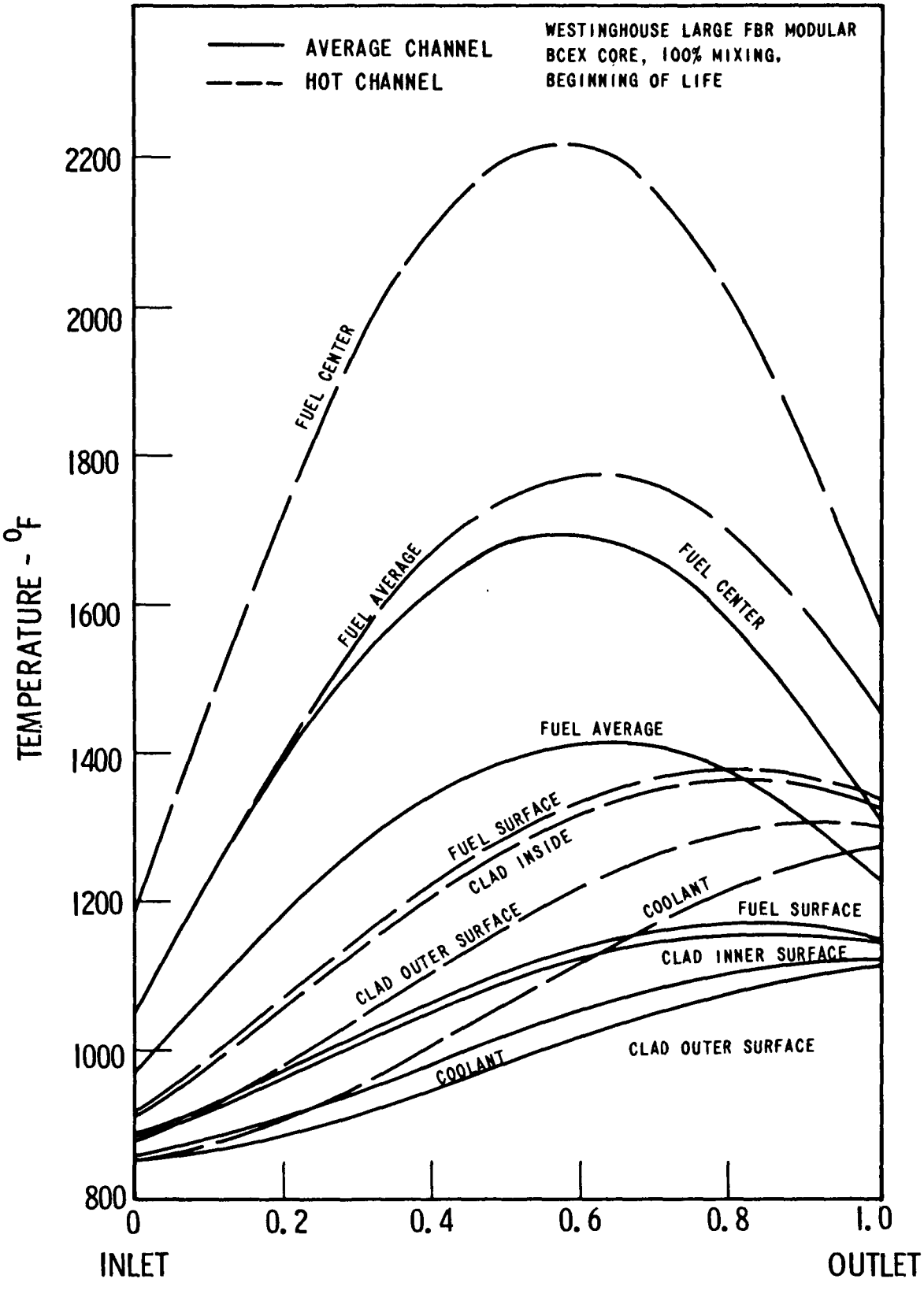

CARBIDE FUEL ROD STEADY STATE TEMPERATURE PROFILE

Figure III.3-5

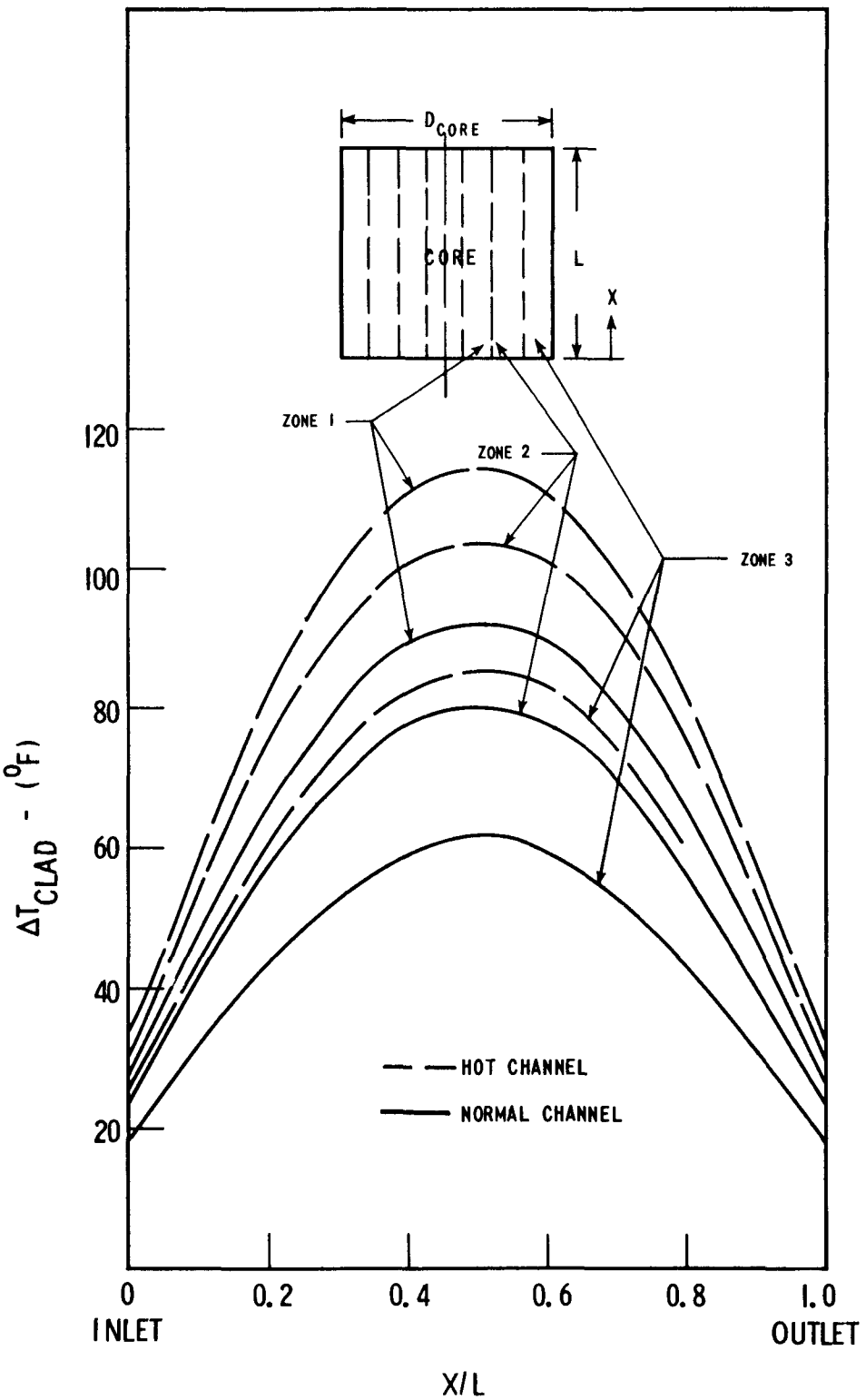

TEMPERATURE DROP THROUGH THE CLADDING OF THE CARBIDE FUEL RODS

Figure III.3-6

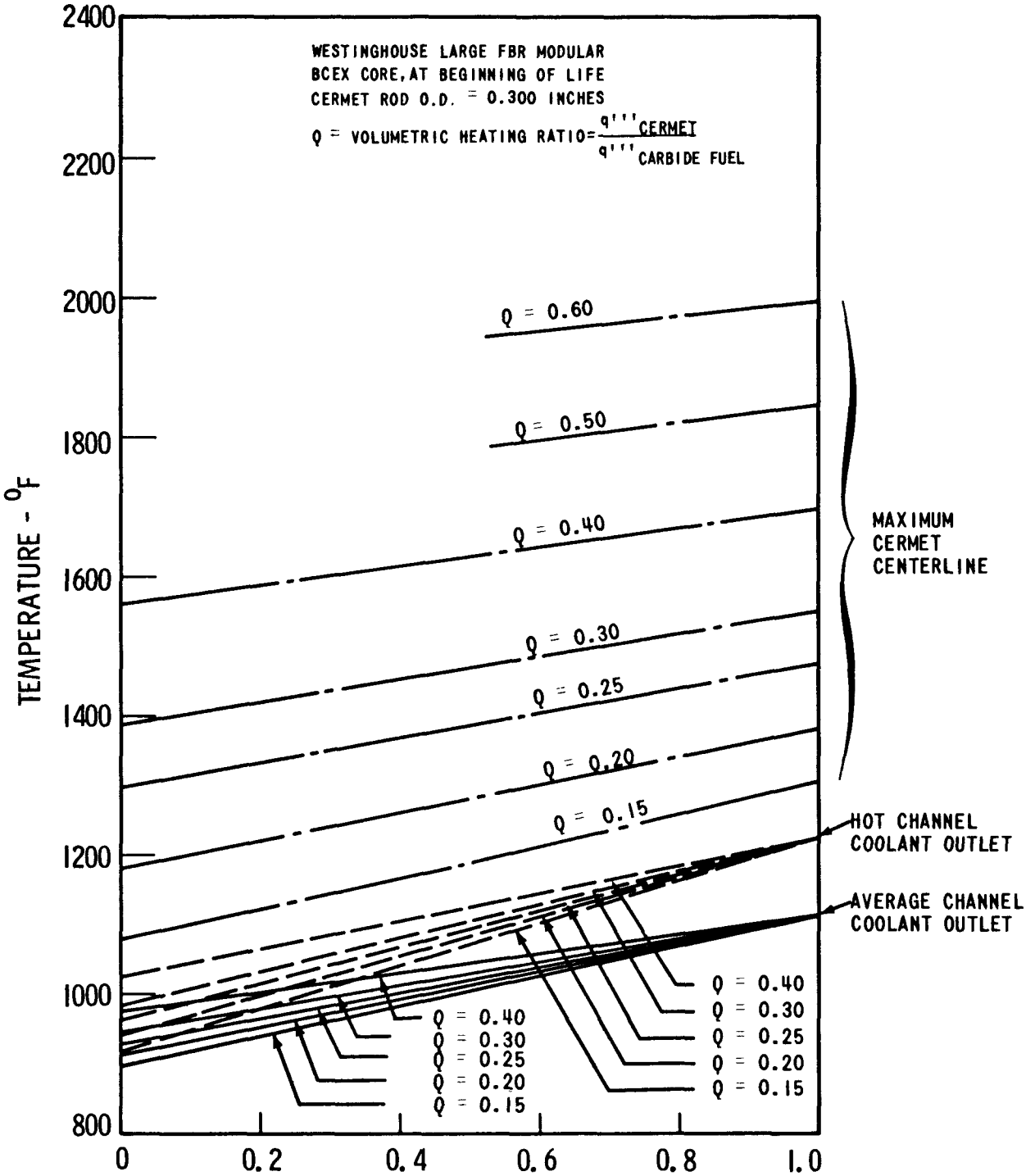

PARAMETRIC SURVEY OF CERMET ROD

STEADY STATE TEMPERATURES

Figure III.3-7

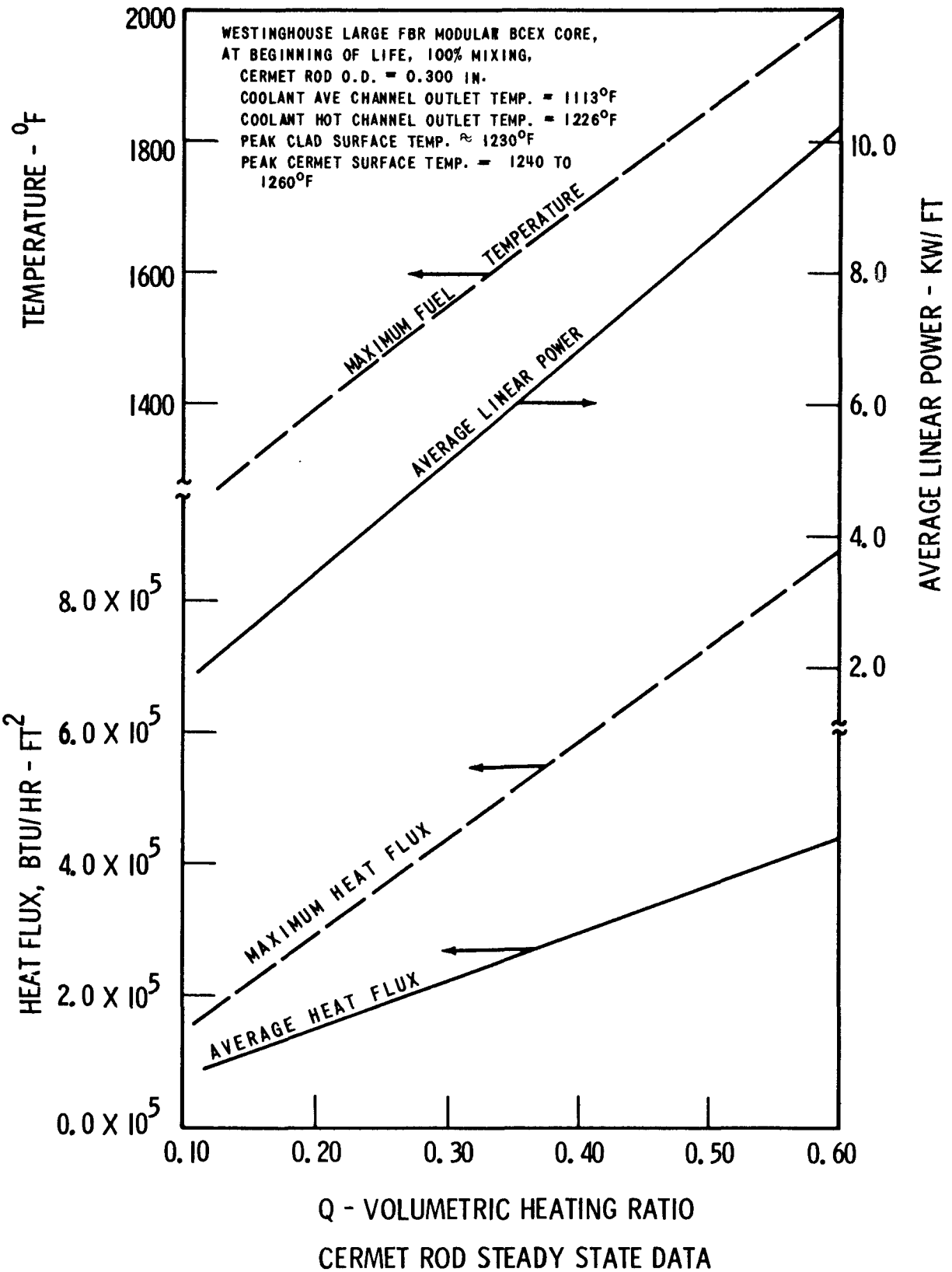

Figure III.3-8

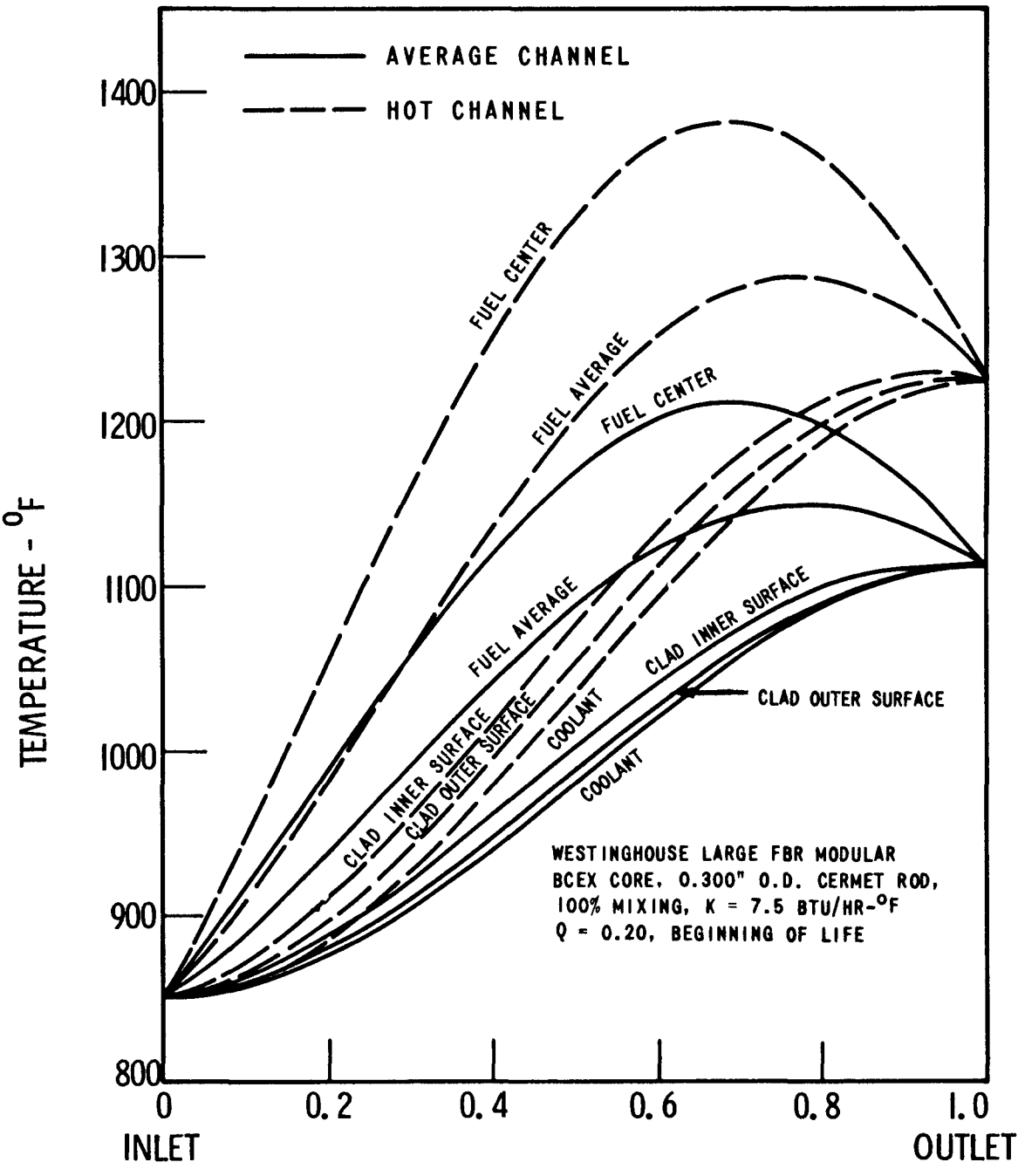

CERMET ROD STEADY STATE TEMPERATURE PROFILE, Q = 0.20

Figure III.3-9

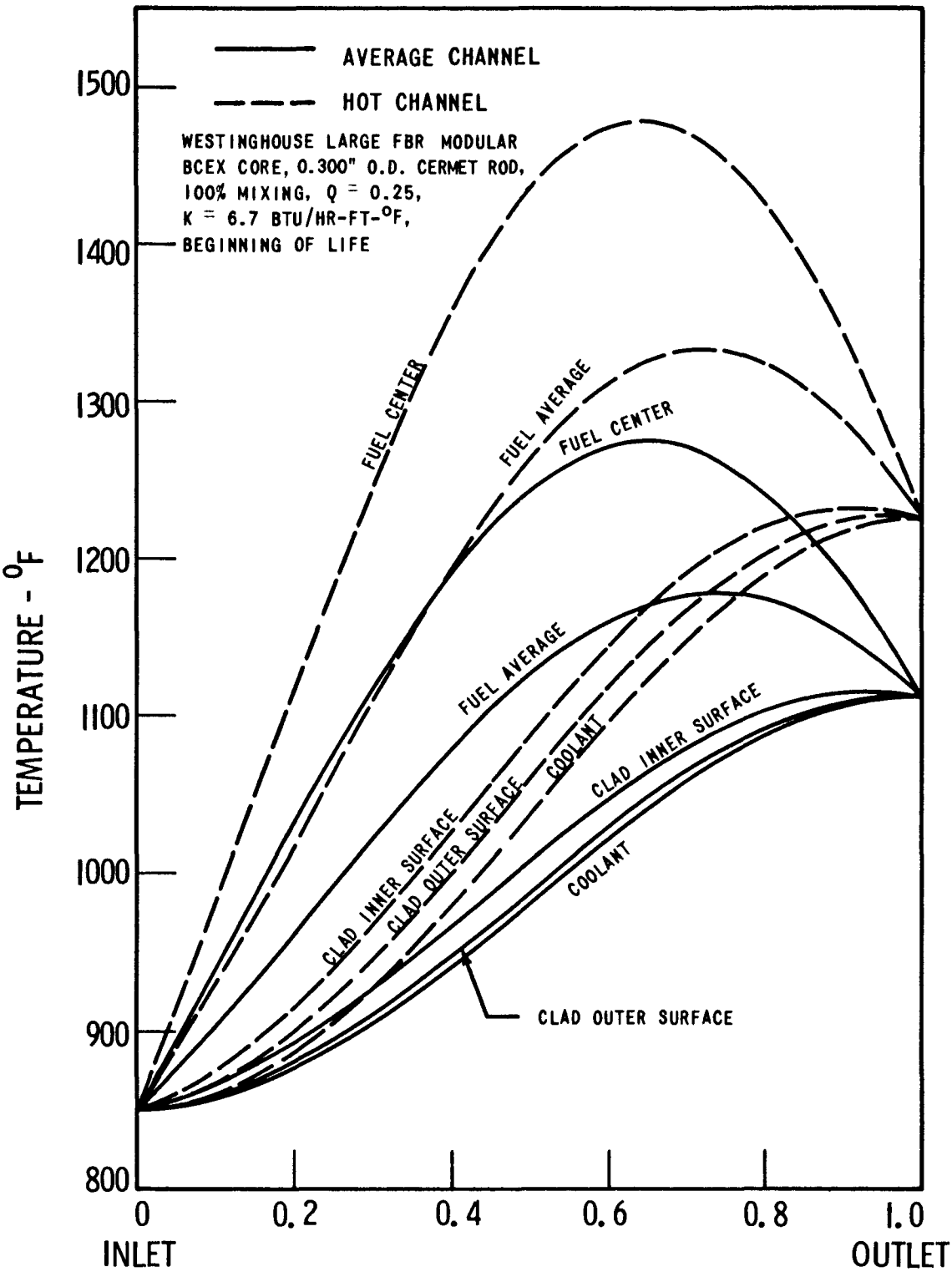

CERMET ROD STEADY STATE TEMPERATURE PROFILE, Q = 0.25

Figure III.3-10

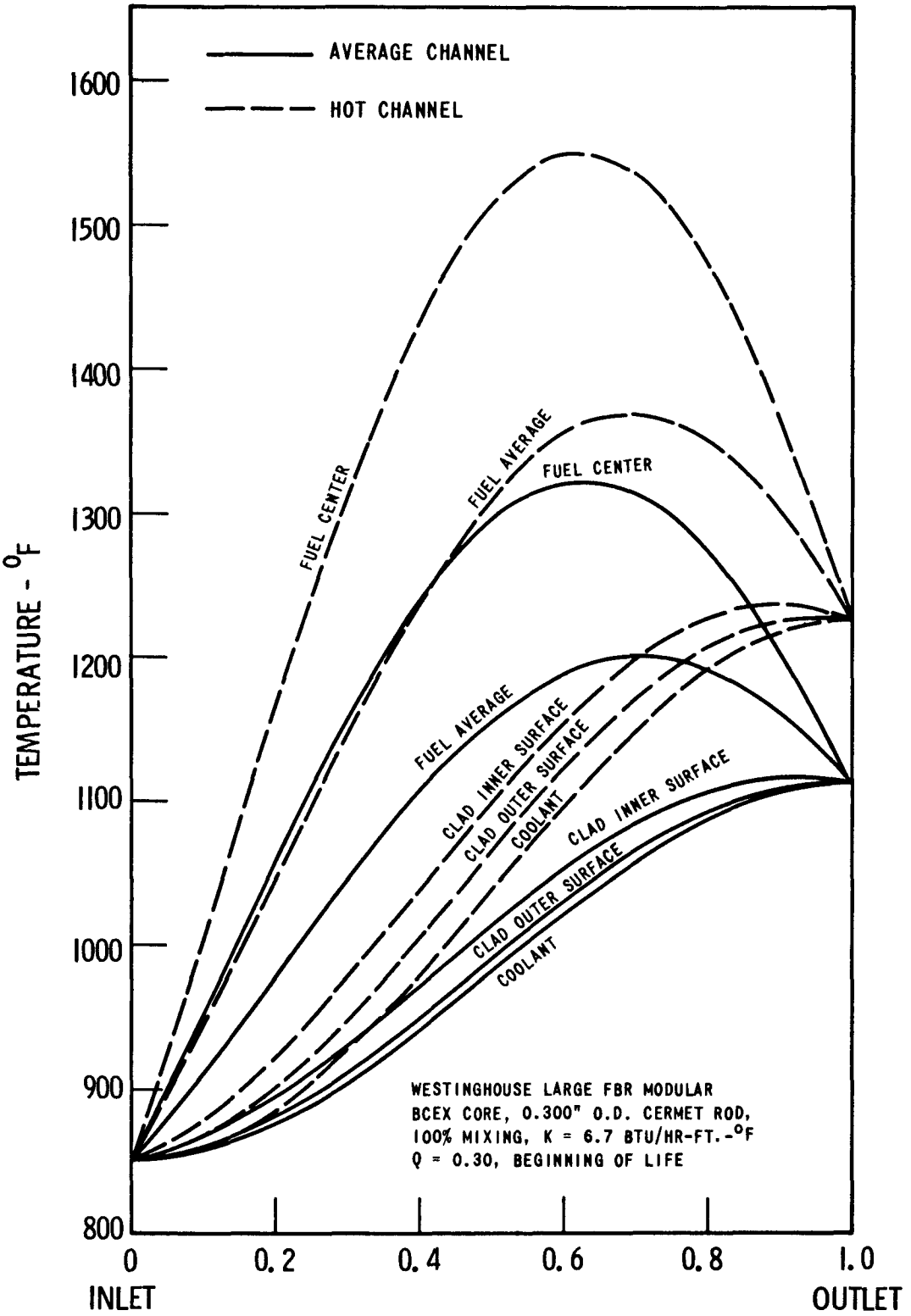

CERMET ROD STEADY STATE TEMPERATURE PROFILE, Q = 0.30

Figure III.3-11

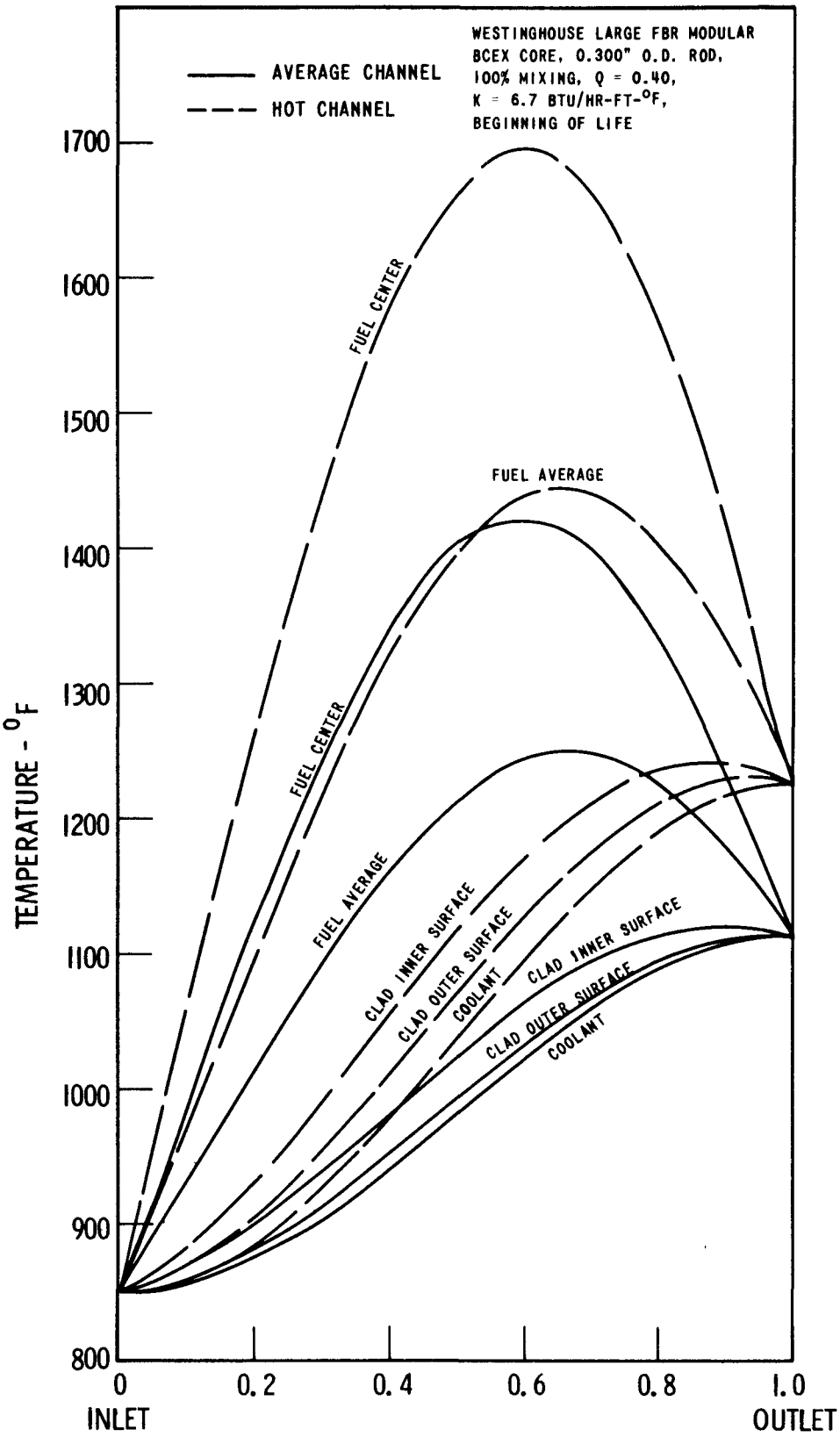

CERMET ROD STEADY STATE TEMPERATURE PROFILE, Q = 0.40

Figure III.3-12

respectively; these profiles assume 100 percent mixing of the coolant heated by the cermet rods with the coolant heated by the ceramic fuel rods. The thermal conductivity which was used for the cermet rod in these analyses is presented in Figure III.3-1. Since 35 volume percent fuel in the current material was established as a design limit, the thermal conductivity at this value was used for values of Q which require a greater volume percent when equal enrichments in cermet and ceramic fuels are assumed. For example, for the case of Q = 0.30 (assuming 85 percent of theoretical density for the UO_2 particles), 43 volume percent cermet would be required if equal enrichments were assumed in the cermet and ceramic fuel. Thus, in order to remain below the design limit of 35 volume percent, the enrichment in the cermet particles must be increased to approximately 123 percent of the ceramic fuel enrichment. (The effect of this difference in enrichments on burnout is studied in Section III.6.) Thus, because of the design limit at 35 volume percent, the thermal conductivity at this value was used for the cermet rods for values of Q which require a greater volume percent (when equal enrichments in cermet and ceramic fuel are assumed). For the cases when the required volume fraction would be greater than 35 volume percent for the equal enrichment assumption, it was assumed that cermet fuel enrichment would be increased as required and the fuel content limited to 35 volume percent, to obtain the required amount of heating in the cermet rod. A design value of 85 percent of theoretical density for the ceramic fuel in the cermet was assumed for these analyses.

In the previous discussion, the cermet rods have the same diameter and pitch as the fuel rods. Unless there is substantial intercoolant mixing, different heat generation rates in the cermet and fuel rods will cause the coolant temperature around a fuel rod to differ sharply from the coolant temperature around a cermet rod. This situation can be relieved by changing the cermet rod diameter and pitch to adjust the coolant flow rate around the cermet rods so that each pound of coolant picks up as much enthalpy around the cermet rods as around the fuel rods.

Calculations were performed to determine whether the seven central cermet rods could be arranged to satisfy the above criterion within the existing fuel assembly design, that is, for a fuel rod diameter of 0.300 inch and a pitch of 0.426 inch. It was found that each pound of coolant would pick up the same amount of enthalpy around all the elements in a fuel assembly with the following approximate cermet dimensions:

Volumetric heating ratio, Q	0.25	0.30	0.40
Cermet rod O.D., in.	0.368	0.360	0.345
pitch of center cermet rod to other six cermet rods, in.	0.427	0.427	0.427
pitch of six cermet rods to first ring of fuel rods	0.425	0.425	0.425

Figure III.3-13 gives the calculated cermet rod diameters required to obtain equal enthalpy pickup for a Q between 0.15 and 0.60. These analytical results will certainly have to be substantiated by experimental flow tests.

Figures III.3-13 thru III.3-17 presents the results of the steady state thermal and hydraulic analyses for the "fat"* cermet fuel pins for the actual core heat flux distribution at beginning of life conditions and 100 percent power.

Figure III.3-13 shows the effect of Q on the average and peak heat flux, the average linear power, and the peak cermet center temperature. For the range of volumetric heating ratios presented, the peak clad outer surface temperatures range from 1230°F to 1245°F, and the peak cermet surface temperatures range from 1245°F to 1265°F.

Figures III.3-14, III.3-15, III.3-16 and III.3-17 present the "fat" cermet rod steady state temperature profile for Q = 0.20, 0.25, 0.30 and 0.40, respectively.

---

*"Fat" will be the term used to identify the cermet rods with outside diameters greater than 0.300 inches.

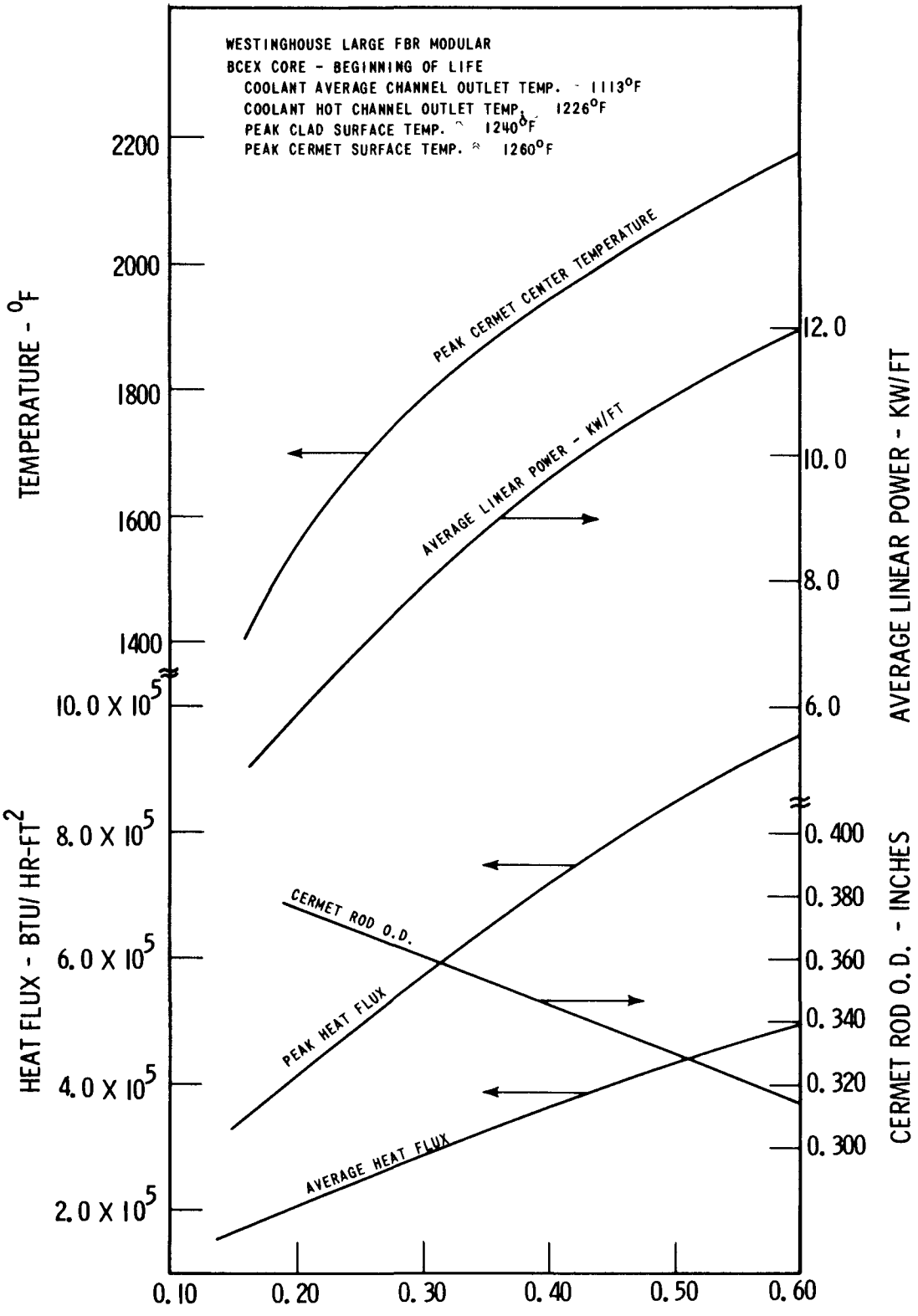

FAT CERMET ROD STEADY STATE DATA

Figure III.3-13

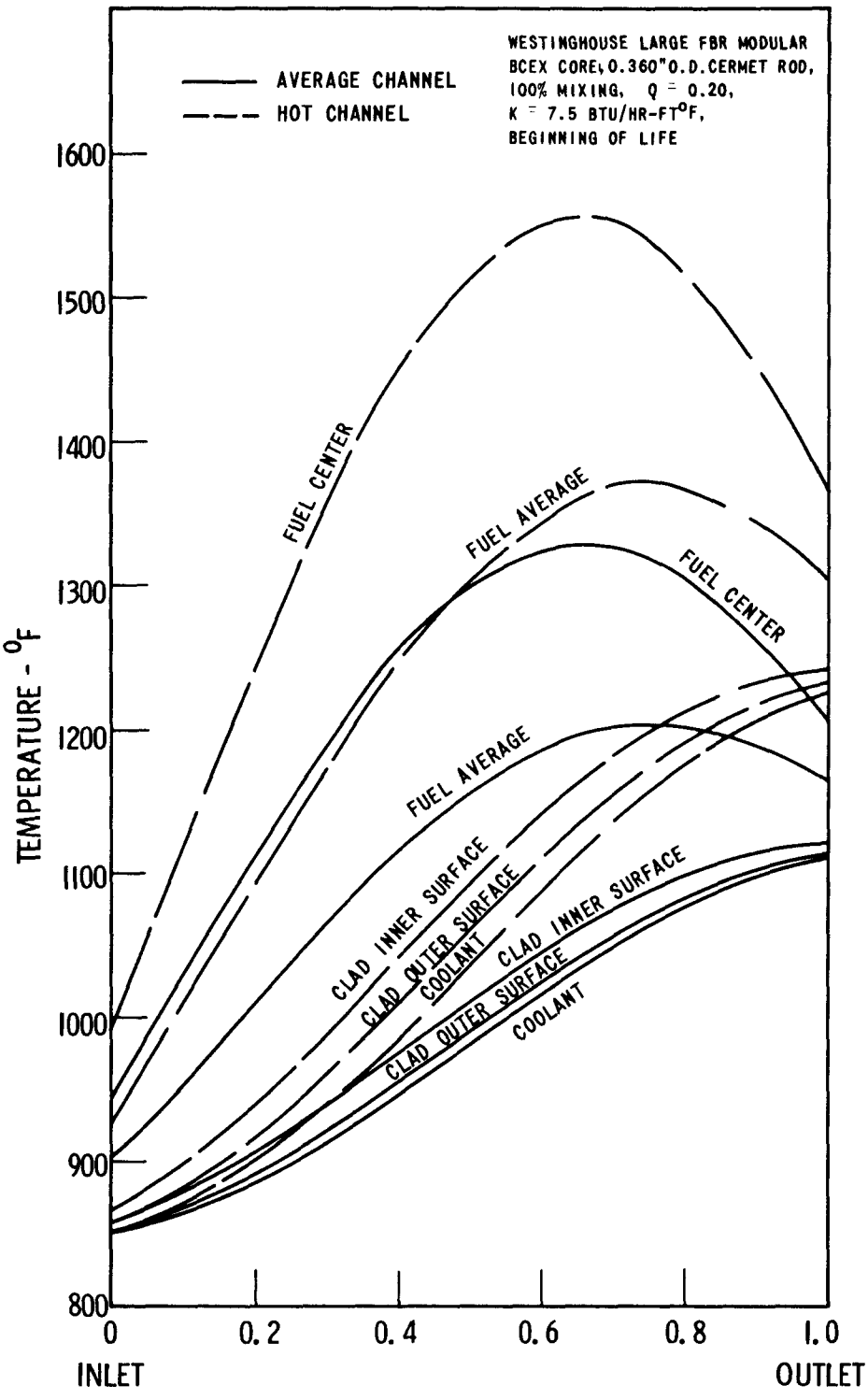

CERMET ROD STEADY STATE TEMPERATURE PROFILE
FAT ROD, Q = 0.20

Figure III.3-14

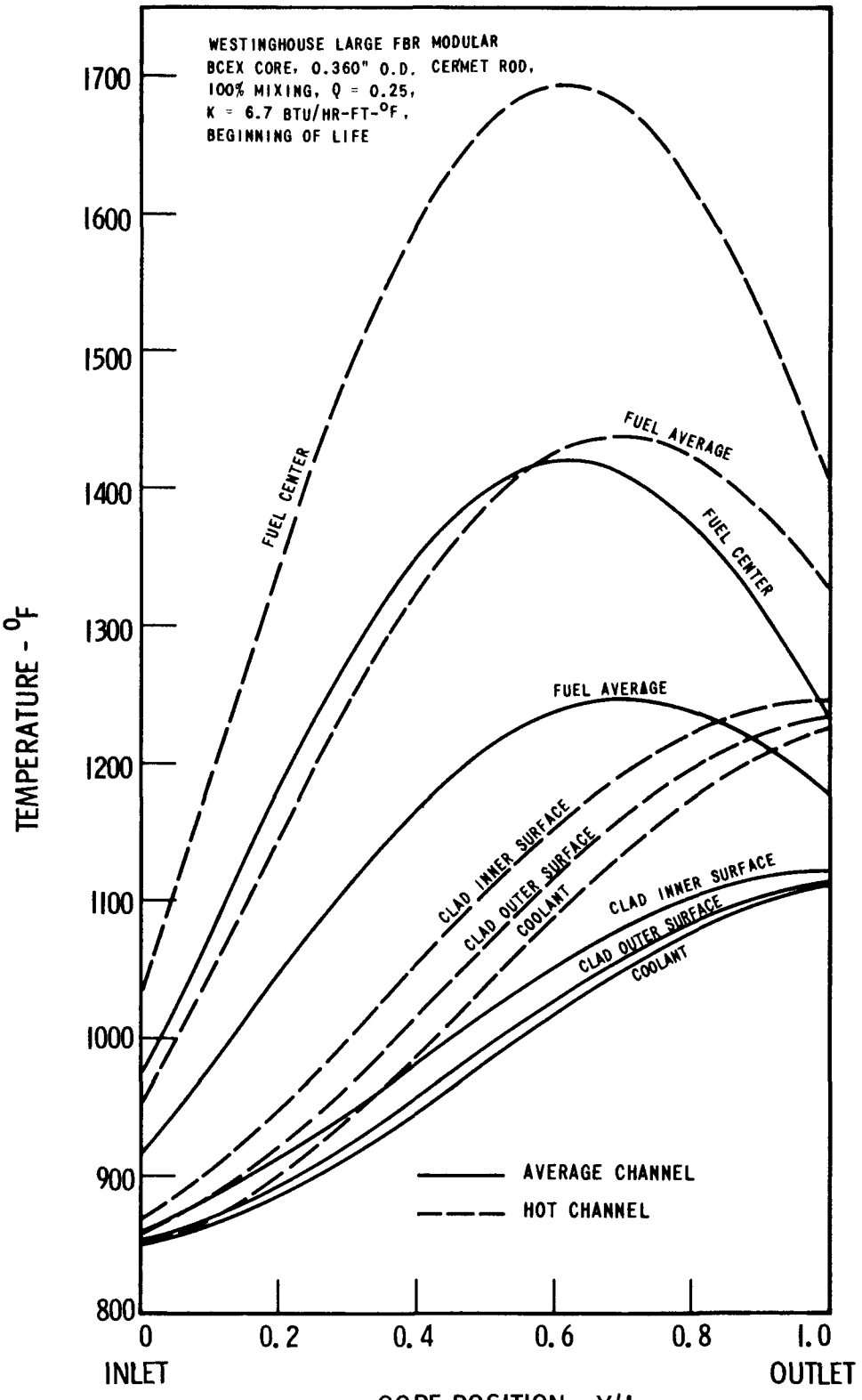

CERMET ROD STEADY STATE TEMPERATURE PROFILE
FAT ROD, Q = 0.25

Figure III.3-15

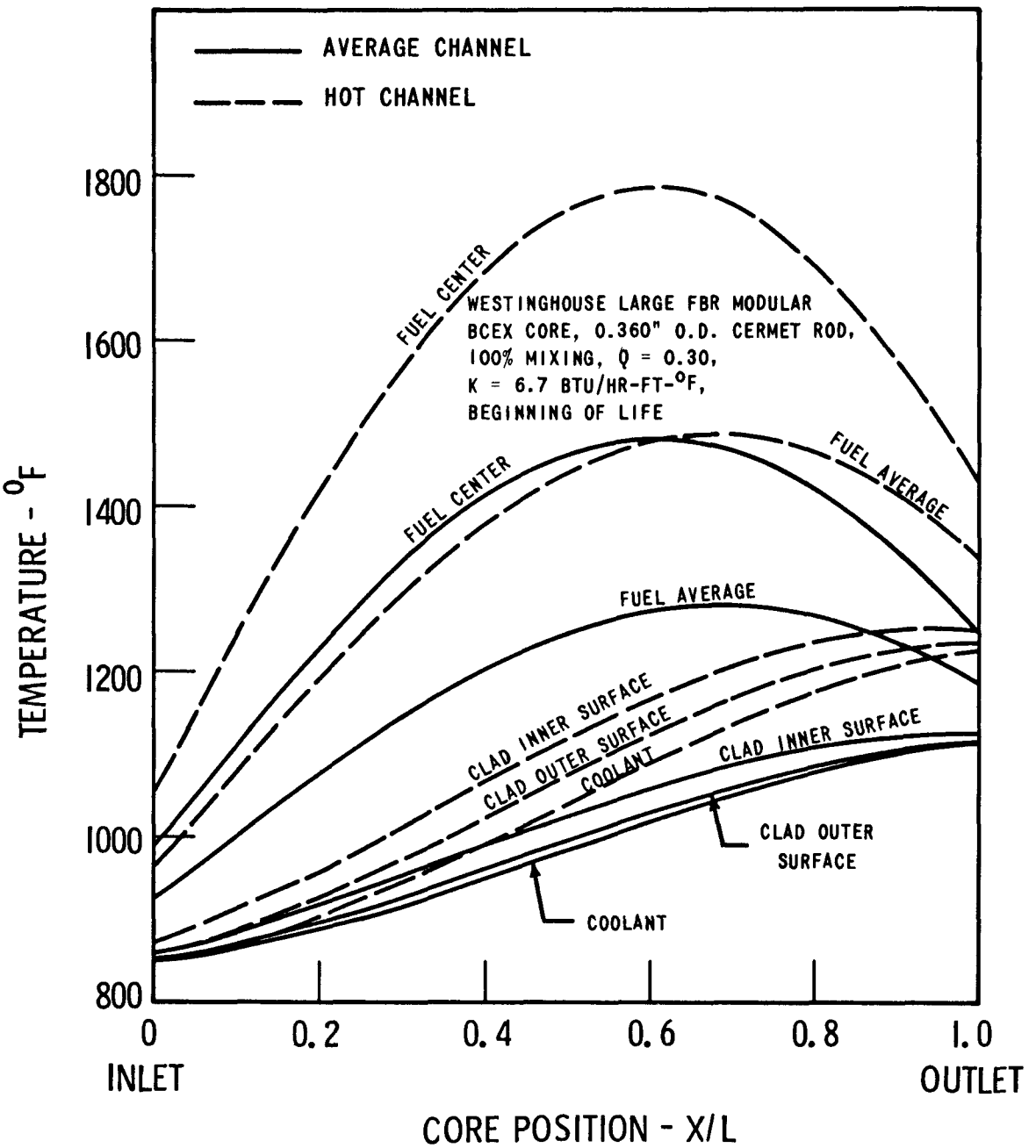

CERMET ROD STEADY STATE TEMPERATURE PROFILE
FAT ROD, Q = 0.30

Figure III.3-16

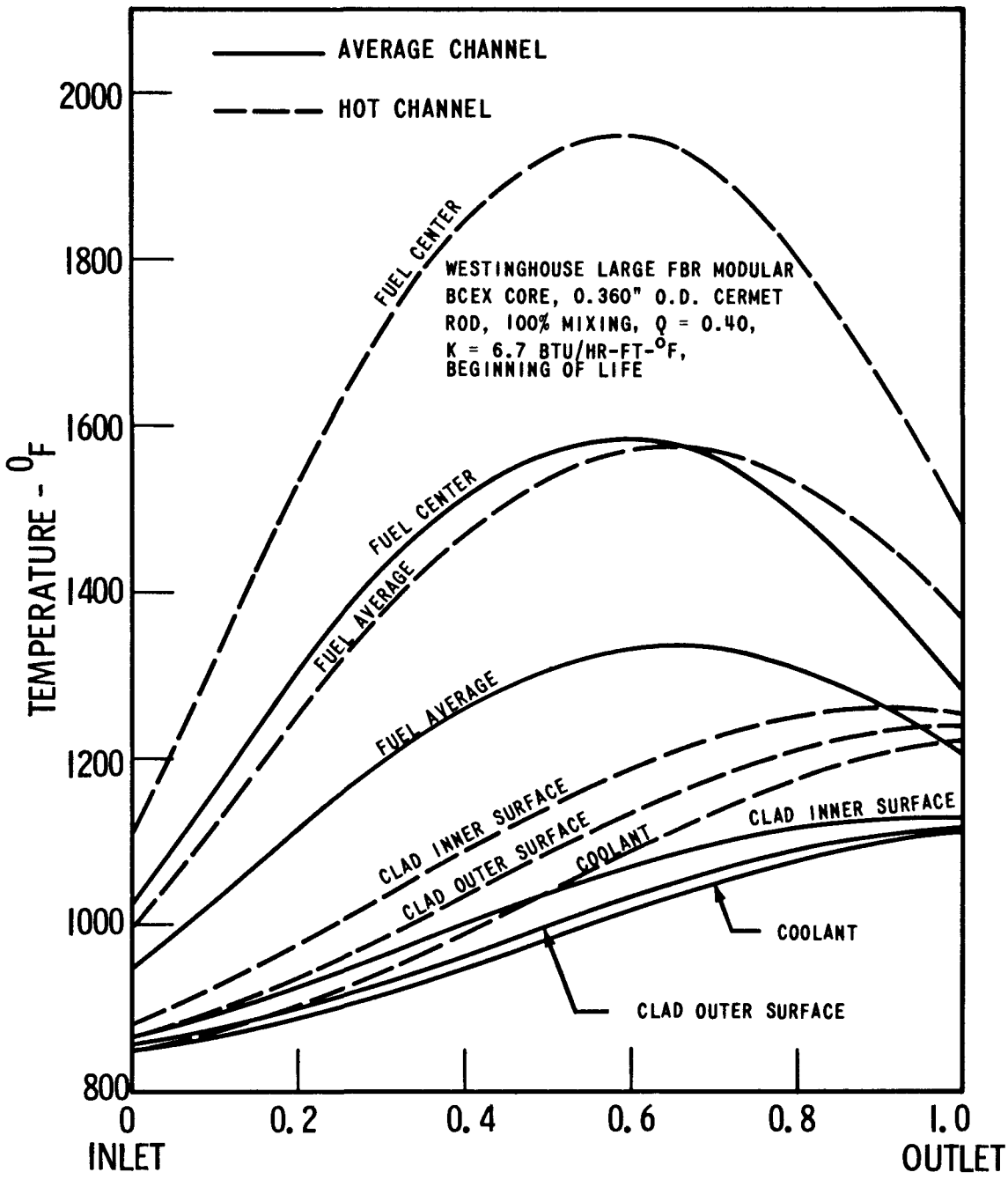

CERMET STEADY STATE ROD TEMPERATURE PROFILE
FAT ROD, Q = 0.40

Figure III.3-17

The total pressure drop across the core module, including the 12 inch thick axial blankets, is 80 psi at 100 percent power conditions. This pressure drop includes orificing to obtain 114 percent rated flow in the inner six fuel assemblies.

The critical heat flux was checked for the reference core conditions by using various existing correlations. Using the Noyes[8] correlation for forced convection critical heat flux for sodium, and the Lowdermilk[7] correlation for forced convection critical heat flux for water, the minimum DNB ratio-based upon a local system pressure of one atmosphere is greater than 2.0.

Using Noyes[5] critical heat flux correlations at a local system pressure of one atmosphere, the DNB ratio for sodium pool boiling is approximately 1.3. Using Caswell and Balzhiser[9] pool boiling correlation for alkali metal burnout, the DNB ratio is approximately 1.1 at a local system pressure of one atmosphere.

The magnitude of the transverse coolant temperature gradients within a fuel assembly were calculated for use in the analysis of the thermal bowing phenomenon. To generate the required information, it was assumed that there would be no transverse coolant mixing within a fuel assembly. This condition will give the maximum temperature gradient across an assembly, and hence produce the maximum possible thermal bowing of the assembly can.

Two types of curves were generated. The first type of curve, e.g. Figure III.3-18, is a plot of the temperature of the coolant leaving a fuel assembly as a function of transverse position (from one can wall to the other) at the assembly outlet. The second type of curve, e.g. Figure III.3-19, is a plot of the difference in coolant temperature across an assembly (can wall-to-can wall) as a function of axial position along the assembly (from assembly inlet to assembly outlet). The two types of curves were generated for an assembly in

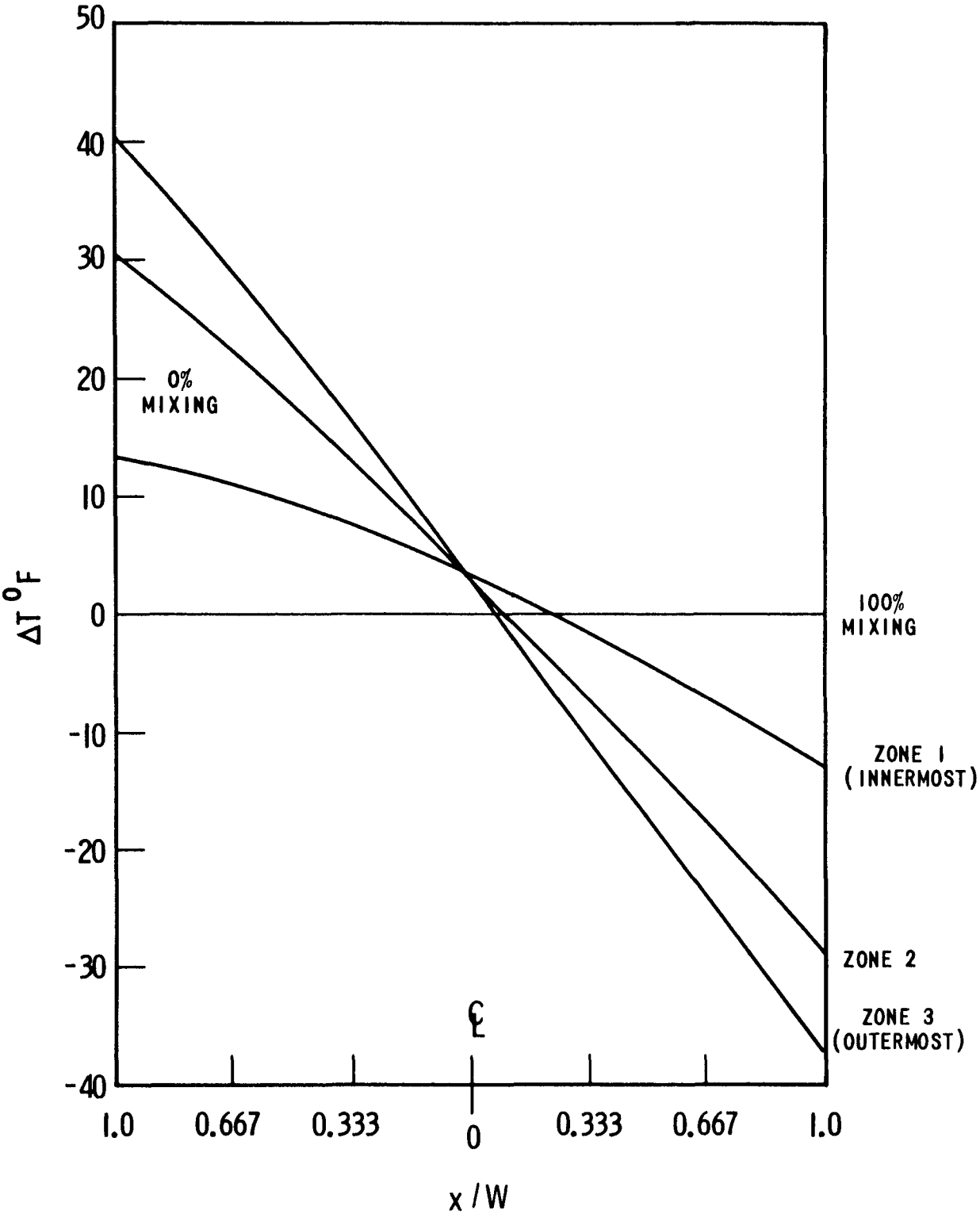

EXIT COOLANT TEMPERATURE DISTRIBUTION IN VARIOUS ZONES OF CORE AS A FUNCTION OF TRANSVERSE POSITION IN ZONE BEGINNING-OF-LIFE POWER DISTRIBUTION

Figure III.3-18

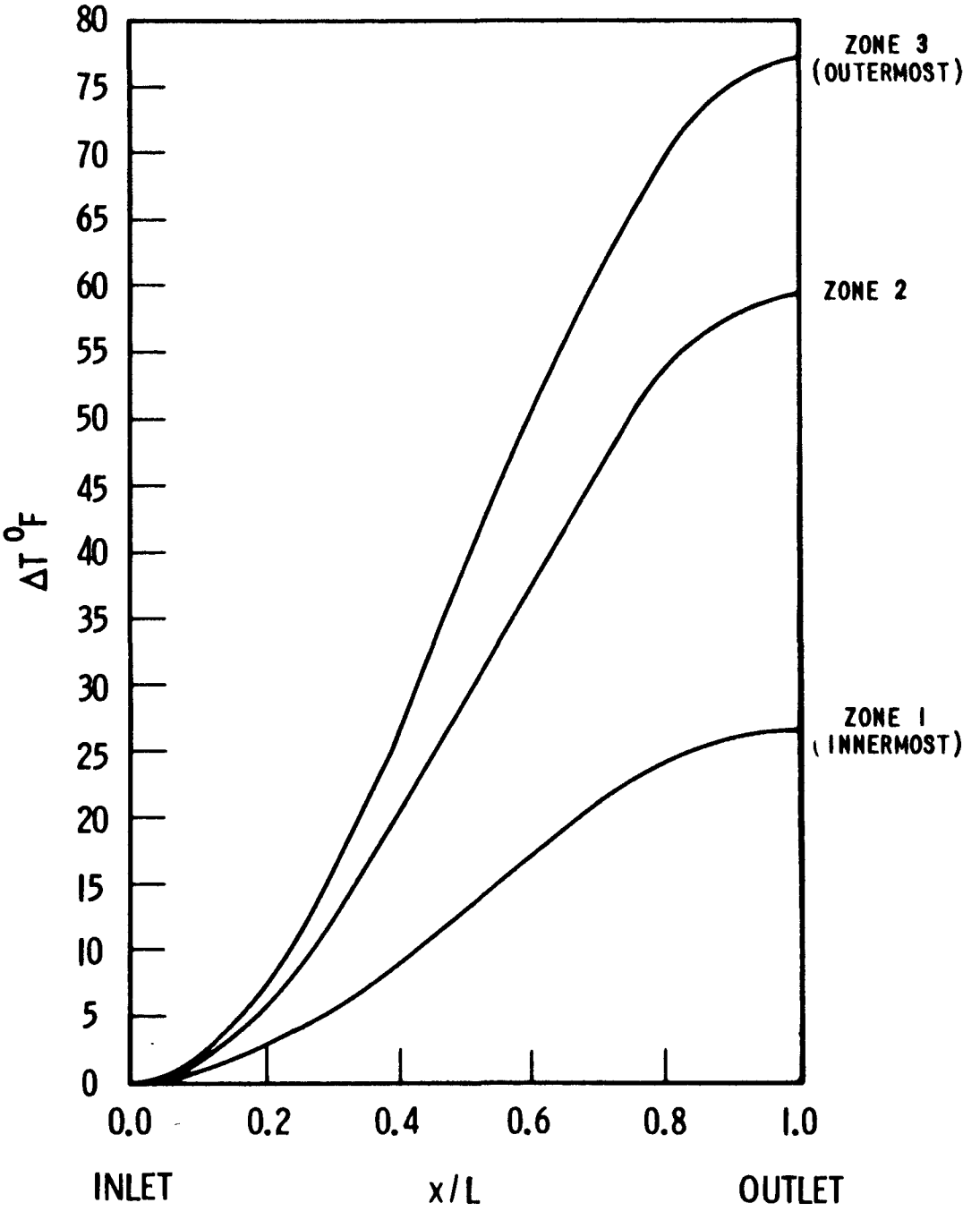

TEMPERATURE DIFFERENCE CAN WALL-TO-CAN WALL IN VARIOUS ZONES OF CORE FOR NO TRANSVERSE COOLANT MIXING vs. AXIAL POSITION (BEGINNING-OF-LIFE POWER DISTRIBUTION)

Figure III.3-19

each of the three core rings (or zones) and for two conditions: beginning-of-reactor life, and equilibrium loading (33,333 MWD/T) power distribution (see Figures III.3-18 thru III.3-23). The curves generated for an assembly in each of the two blanket zones are only for the 33,333 MWD/T power distribution, because the first core loading would require a special blanket design. No curves were generated for an equilibrium discharge (66,666 MWD/T) power distribution because the coolant temperature gradients would be less at this time in life due to the flattening of the power profile as the fuel burns down.

For an assembly in the third zone with a beginning-of-reactor life power distribution, the maximum temperature difference across a core assembly is 77°F. For a 33,333 MWD/T power distribution, the maximum temperature difference across the first row of blanket assemblies is 202°F. The maximum can wall-to-can wall temperature difference across the second ring of blanket assemblies is 57°F, but due to the power distribution across this ring, the maximum temperature gradient in the can wall occurs over only part of the assembly (see Figures III.3-22 and III.3-23).

The burnup-temperature history of the UO_2 -316 stainless steel cermet is plotted in Figure III.3-24. Two carbide fuel burnups are considered. These correspond to the anticipated core average and peak burnups of 100,000 and 120,000 MWD/T, respectively. A burnup criterion based on 1964 ORNL[11] estimates, extrapolated to cermet rod <u>average</u> temperatures, is superimposed on Figure III.3-24. This was done by adding 50°F to the ORNL data, which is basically for plates, to translate the abscissa from peak fuel surface temperature to peak fuel average temperature. Sufficient data is not presently available to substantiate such a criterion, but is is a logical approach to what is felt to be conservative data. Justification by theory, and ultimately by experiments, is certainly required in this area.

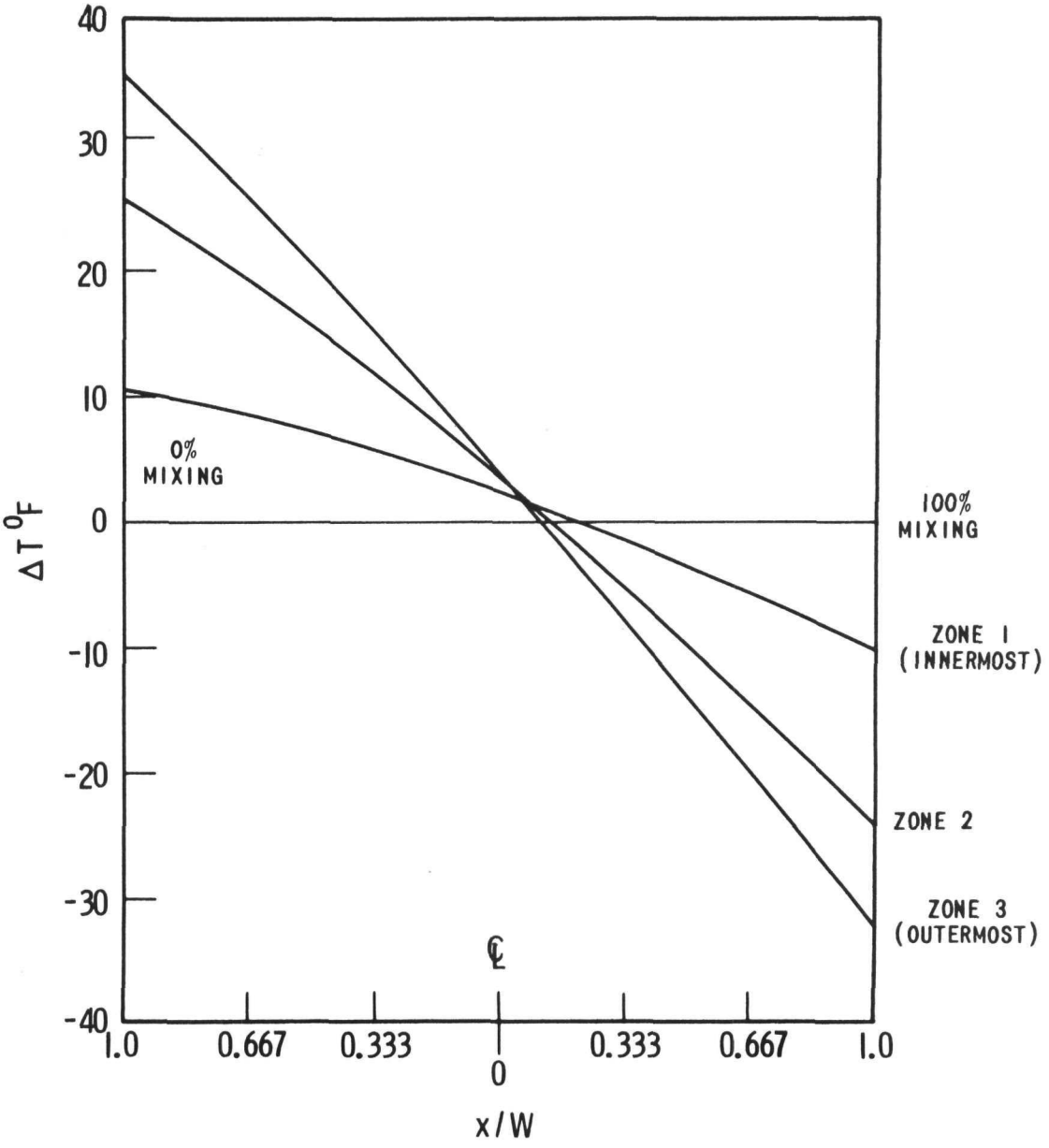

EXIT COOLANT TEMPERATURE DISTRIBUTION IN VARIOUS ZONES OF CORE AS A FUNCTION OF TRANSVERSE POSITION IN ZONE 33,333 MWD/T POWER DISTRIBUTION

Figure III.3-20

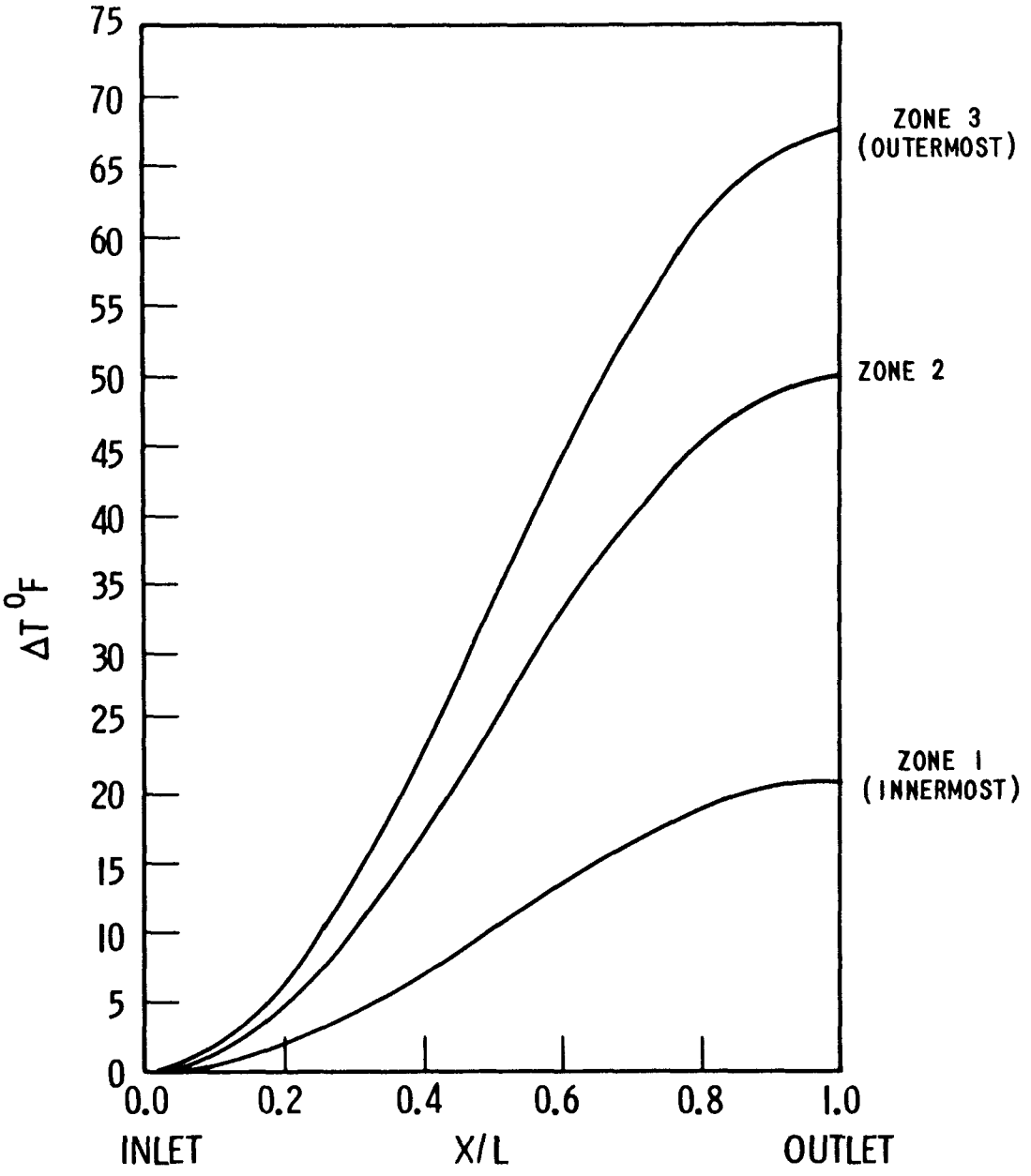

TEMPERATURE DIFFERENCE CAN WALL-TO-CAN WALL IN VARIOUS ZONES OF CORE FOR NO TRANSVERSE COOLANT MIXING vs. AXIAL POSITION (33,333 MWD/T POWER DISTRIBUTION.)

Figure III.3-21

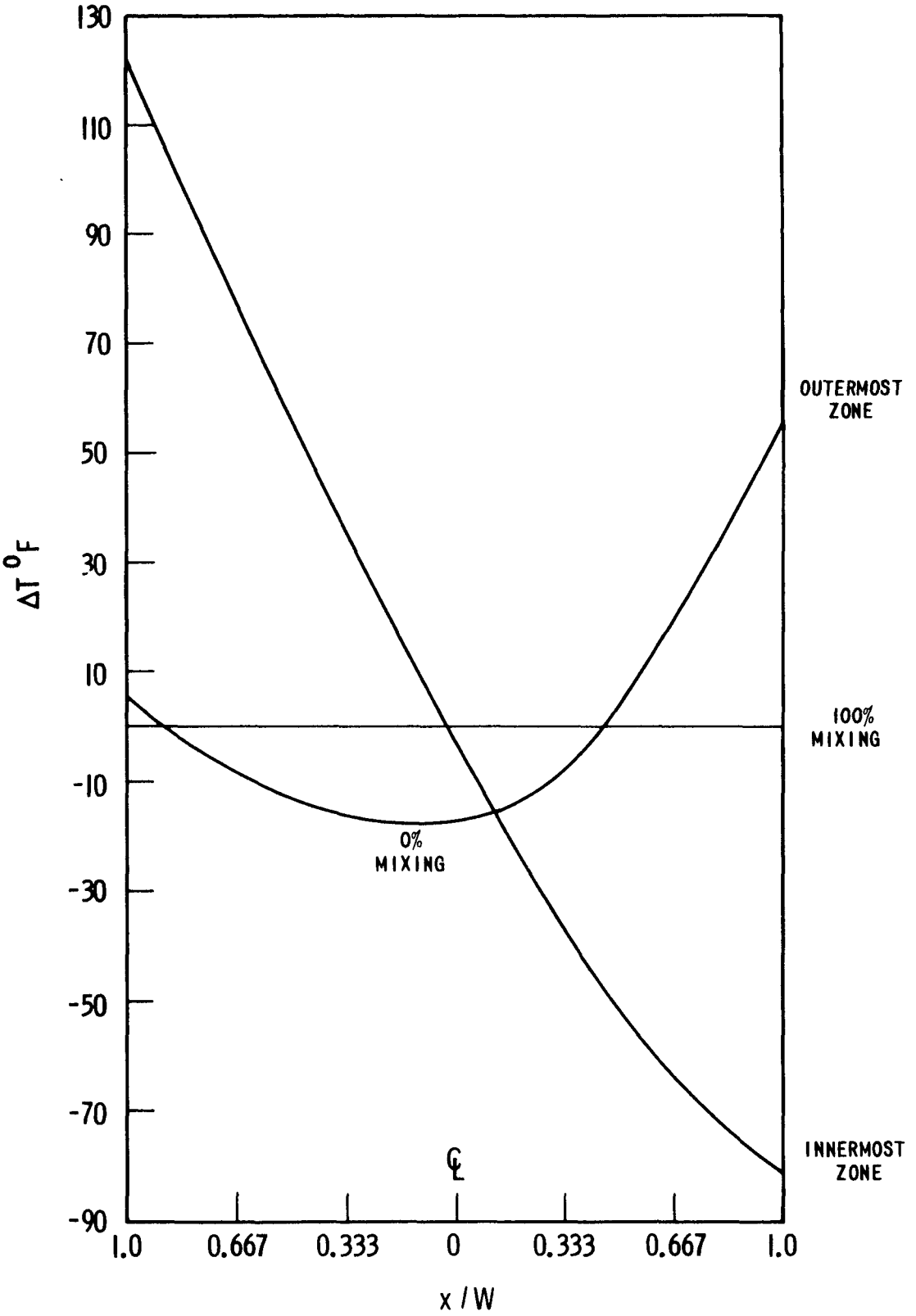

EXIT COOLANT TEMPERATURE DISTRIBUTION IN VARIOUS ZONES OF BLANKET AS A FUNCTION OF TRANSVERSE POSITION IN ZONE 33,333 MWD / T POWER DISTRIBUTION

Figure III.3-22

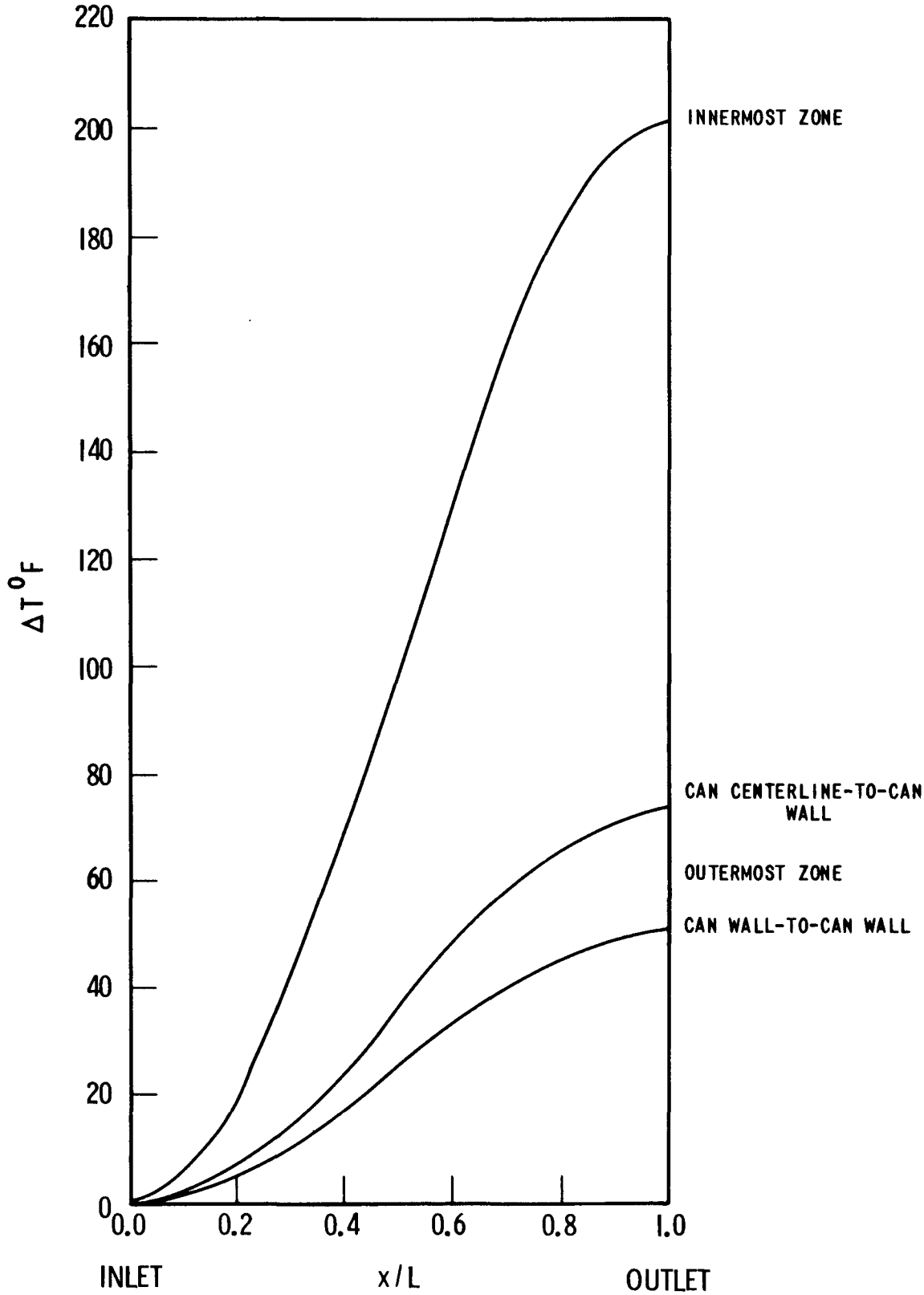

TEMPERATURE DIFFERENCE CAN WALL-TO-CAN WALL IN VARIOUS ZONES OF BLANKET FOR NO TRANSVERSE COOLANT MIXING vs. AXIAL POSITION (33,333 MWD/T POWER DISTRIBUTION)

Figure III.3-23

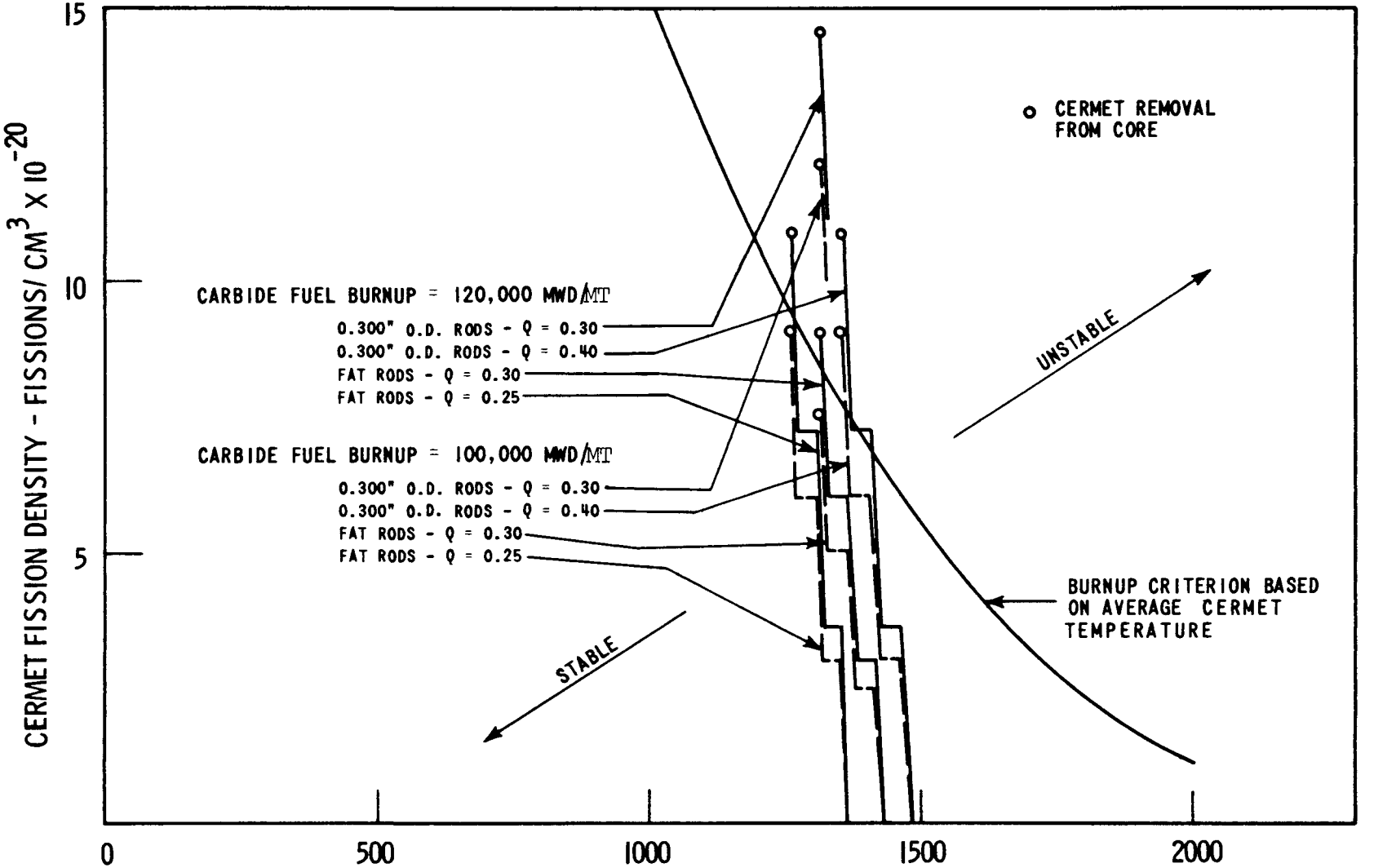

UO_2 - SS CERMET BURNUP - TEMPERATURE HISTORY

Figure III.3-24

Using the aforementioned design burnup criterion, only the 0.300 inches O.D. cermet rod with Q = 0.30, and the "fat" rod with Q = 0.25 for 100,000 MWD/MT burnup, remain stable. The other cases investigated exceeded this criterion.

References Section III.3

(1) "Liquid Metal Fast Breeder Reactor Design Study", WCAP-3251-1, January 1964.

(2) Gunson, W. E., "High Power Density, Stainless Steel Reference FBR Core Design", WCAP-2638, July 1964.

(3) Weatherford, W. D., Taylor, J. C., and Ku, P. M., "Properties Inorganic Energy Conversion and Heat Transfer Fluids for Space Application", Southwest Research Institute, WADD-TR-61-96, November 1961.

(4) Efferding, L. E., and Bishop, A. A., "Liquid Metal Heat Transfer and Pressure Drop", WCAP-4402, October 1963.

(5) Burdi, G. F., "SNAP Technology Handbook, Vol. I, Liquid Metals", NAA-SR-8617, August 1964.

(6) Dwyer, O. E., "Eddy Current Transport in Liquid Metal Heat Transfer", AICHE Journal, March 1963, pp 261-268.

(7) Lowdermilk, W. H., Lanzo, C. D., and Siegel, B. L., "Investigation of Boiling, Burnout and Flow Stability for Water Flowing in Tubes", NACA TN-4382..

(8) Lurie, H. and R. C. Noyes, "Boiling Studies for Sodium Reactor Safety Part II", NAA-SR-9477, October 15, 1964.

(9) Caswell, B. F., and Balzhiser, R. E., "The Critical Heat Flux for Boiling Liquid Metal Systems", AICHE Preprint 22, August 1965.

(10) Axford, R. A., "Multi Region Analyses of Temperature Fields and Heat Fluxes in Tube Bundles with Internal, Solid, Nuclear Heat Sources", LA-3167, February 25, 1965.

(11) Thurber, W. F., et. al., "Irradiation Testing of Fuel for Core B of the Enrico Ferni Fast Breeder Reactor, ORNL 3709, November 1964.

III.4 Mechanical Design and Analysis

III.4.1 Fuel Assembly Description

The entire fuel assembly, shown on Figure III.4-1, consists of three main subassemblies: (Part 1) the 7-rod central "cermet" sub-assembly; (Part 2) identical upper (Part 3) and lower half-length, 120-rod, fuel bundles or sub-assemblies. The central 7-rod cermet sub-assembly extends through the entire length, from top to bottom rod support grids, and holds the two half-length fuel bundles or sub-assemblies together. The fuel sub-assemblies (top and bottom halves) are separated in the center of the assembly to provide for bundle controlled expansion (BCEX).

Each half-length, 120-rod, fuel sub-assembly (Figures III.4-2 and III.4-3) consists of an array of compartmented fuel-filled rods spaced by round ferrules and brazed into a single stable structure. Forty-eight of the fuel rod end plugs (the rods on the outer row and under the three spokes) extend and are fastened into the end grid. This is most easily accomplished by plug-welding from the end after the basic cluster is completely assembled and tested. The fuel rod bundles or clusters are made in processes similar to those employed for Yankee Cores 1, 2, and 3. The cluster consists of an array of fuel rods and spacer ferrules brazed into a unit structure. When installed, the brazed ferrule system supports the inner rods that are not directly supported from the end grids.

The entire fuel assembly is suspended from the top grid (Part 4) which is attached to the side walls of the can. A heavy rigid fitting at the top of the can provides a coolant outlet and a fuel handling grip. The fuel assembly hangs straight down in the can (Part 5). At zero or partial flow, the weight of the lower fuel sub-assembly is supported by the cluster of seven central cermet rods. At full flow, the hydraulic drag forces are greater than the weight of the assembly. Thus, the fuel assembly is under compressed loading. Figure III.4-1

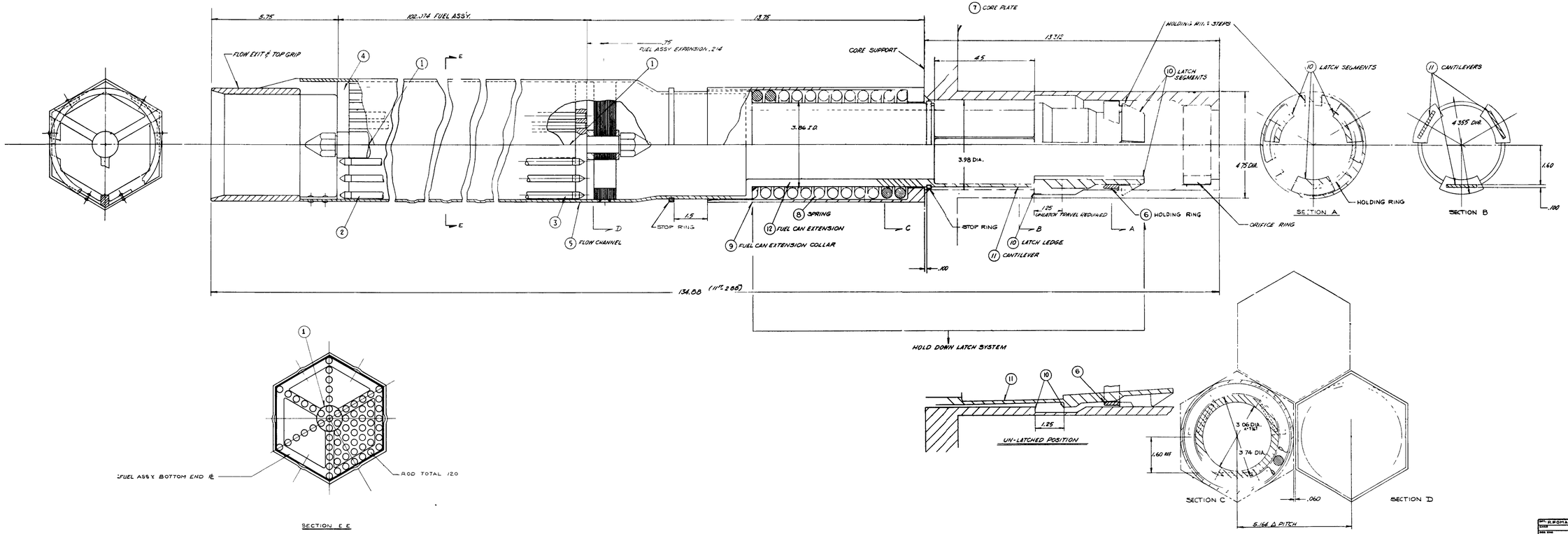

ED 9K 28244G-J
SUB SHT 2 of 2

APP'D. R.ROMAIRO	SAP	WESTINGHOUSE ELECTRIC CORPORATION
DRWN		ATOMIC POWER DIVISION PITTSBURGH, PA.
DES. ENG.		SHIP 1000 MW TAS REACTOR
APPD. ENG.		REACTOR CORE
APP		ASSEMBLY
SUP		SIZE D DWG. NO. 28244G-J
DATE RLSD.		DO NOT SCALE SHT 1 OF 2 REV. A

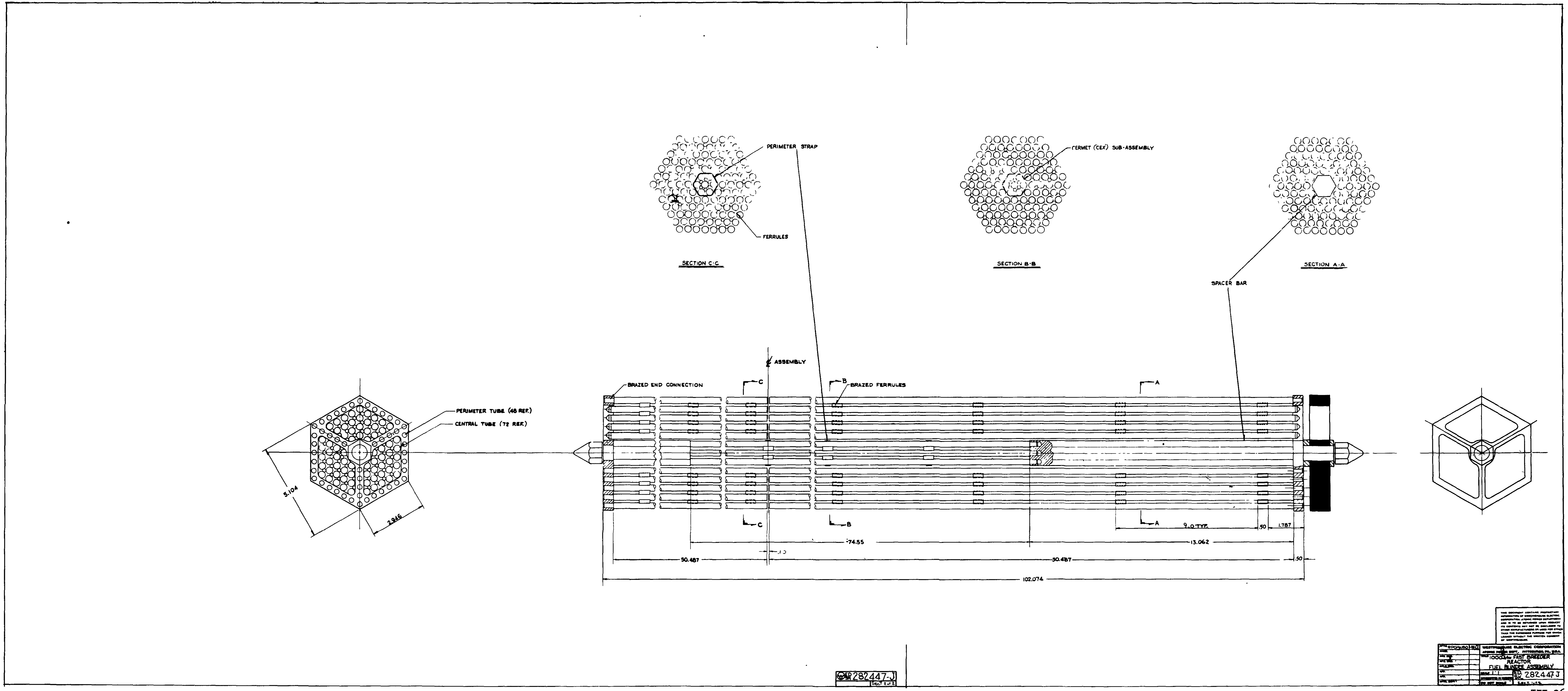

PERIMETER STRAP
FERRULES
SECTION C-C
CERMET (CEX) SUB-ASSEMBLY
SECTION B-B
SECTION A-A
SPACER BAR
PERIMETER TUBE (48 REF.)
CENTRAL TUBE (72 REF.)
5.104
2.946
℄ ASSEMBLY
BRAZED END CONNECTION
BRAZED FERRULES
9.0 TYP.
.50
1.787
74.55
13.062
50.487
50.487
.50
102.074
282447-J
THIS DOCUMENT CONTAINS PROPRIETARY INFORMATION OF WESTINGHOUSE ELECTRIC CORPORATION (ATOMIC POWER DEPARTMENT AND IS TO BE RETURNED UPON REQUEST ITS CONTENTS MAY NOT BE DISCLOSED TO OTHER MANUFACTURERS OR USED FOR OTHER THAN THE EXPRESSED PURPOSE FOR WHICH LOANED WITHOUT THE WRITTEN CONSENT OF WESTINGHOUSE.
WESTINGHOUSE ELECTRIC CORPORATION
ATOMIC POWER DEPT., PITTSBURGH, PA. U.S.A.
1000 Mw FAST BREEDER REACTOR
FUEL BUNDLE ASSEMBLY
SCALE 1:1
DO NOT SCALE
ED. SK. 282447 J

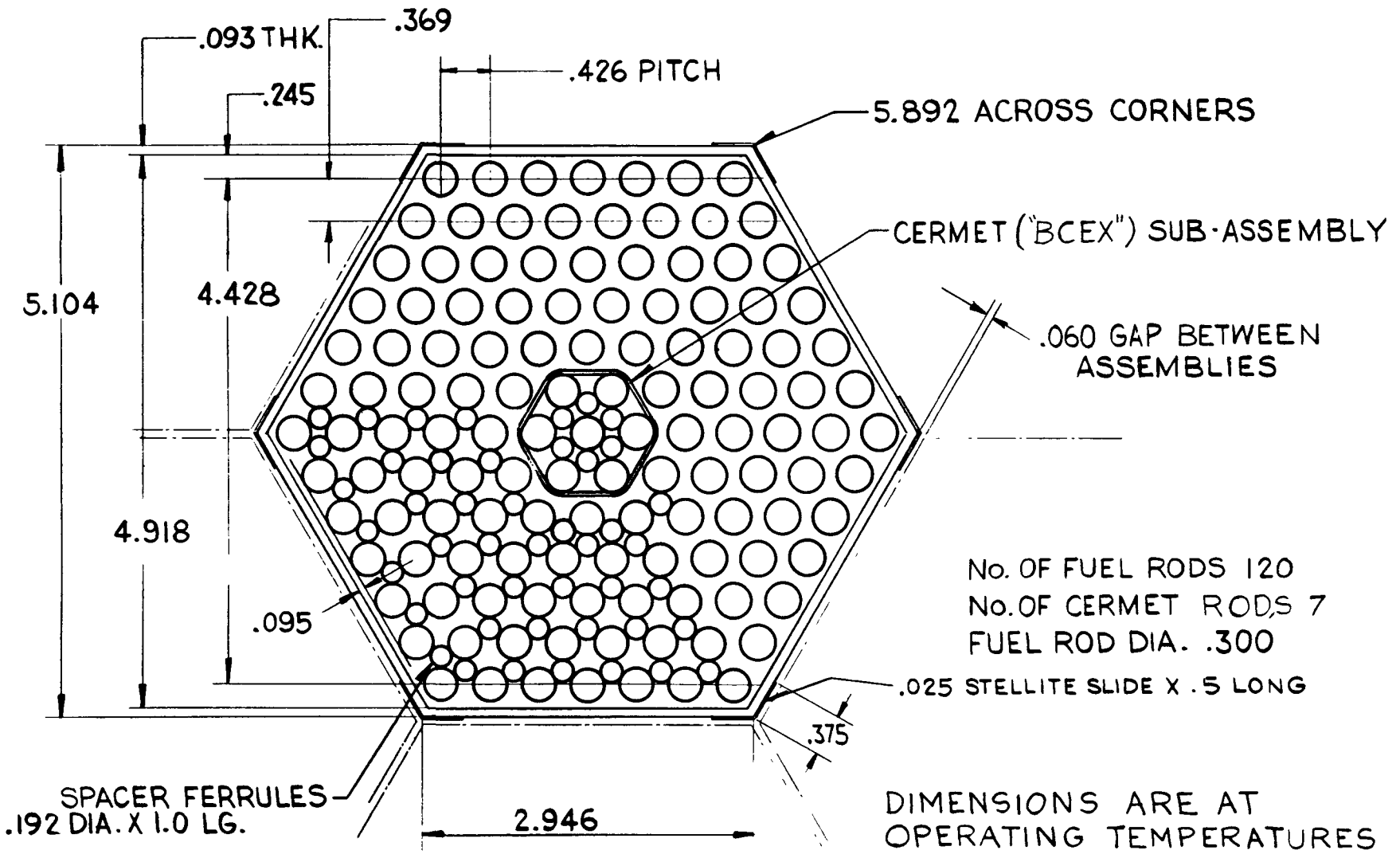

Figure III.4-3
Fuel Assembly Cross Section

depicts a scheme for fastening the lower end of the fuel assembly to the can. A stack of leaf springs center the lower end of the cermet rod structure in the can, yet offer relatively little resistance to cermet axial movement. For an axial movement of 0.20 inches, approximately 120 lb. axial force is required; 23,000 psi bending and tensile stress is induced in the springs, and 12,500 psi in the can. Lateral support by leaf springs minimizes the possibility of bundle-to-can rubbing with subsequent welding of the fuel bundle to the can, which would inhibit proper BCEX performance.

The hexagonal shaped can encloses each fuel assembly to support the fuel and to provide an autonomous flow channel for efficient orificing. Minimum distortion of the can is desired to maintain adequate clearances to assure free movement of the lower fuel bundle during power transients and adequate clearance between assemblies for ease of refueling. Core pressure drop creates a pressure gradient across the can, tending to bulge the can panels into contact with adjacent fuel assembly cans. The maximum pressure difference occurs at the lower core plate, and decreases lenearly with distance above the lower core plate. The maximum can wall deflection is less than 0.009 inches. Can internal heat generation creates negligible strains of around 0.01%, in the outer fibers of the can.

Figure III.4-1 shows the lower end (Part 6) of the fuel assembly can inserted into its orificed position in the core support structure. The core plate (Part 7) is shown to be about 13-1/3 inches thick. The fuel assembly is inserted and latched into it. The fuel assembly is located by its position in the core plate and held securely by latches. Neither top-of-core hold-down nor positioning is required.

III.4.2 Carbide Fuel Rod Description

Each fuel bundle consists of 120, (Pu U) C fuel rods. The carbide fuel rods (Figure III.4.4) are half-core lengths of about 51 inches, and are spaced to provide for the "BCEX" (bundle controlled expansion) operation. The rods are vented to the coolant. Consequently, there is a sodium bond between the fuel pellet and clad. The stack of active fuel pellets in the fuel rod are divided among compartment so that the fuel will move with the tube wall.

Three 12-inch columns of fuel (Plutonium-Uranium Carbide) pellets occupy the center of the core chambers of each half-length fuel rod. At one end of each half-length rod (top and bottom of core), there is a 12-inch column of depleted UC which acts as the axial breeder blanket. The chambers are separated by hollow tube discs, with a 0.40 inch average axial pellet expansion space provided in each chamber. Tube discs are locked into the tube wall as shown in the drawing and by brazing. The discs are brazed at the same time as the fuel assembly spacer ferrules. This process is similar to that used for Yankee Reactor Cores 1, 2, and 3.

The tube wall is 0.01-inch thick, Type 316L stainless steel. The mass transfer of nickel in this clad is discussed in detail in the Materials Review Section of this report. In this design, the clad provides for mechanical location of the fuel pellet columns in a stable core array. Because of the vented rod design, there is no internal hoop stress on the clad due to fission gas release. Fission gas released from the fuel will evolve upward through the sodium filled tube, through the hollow tube disc locks, then out of the fuel rod through the vent hole in the top end plug. In each half rod, only one vent is provided in the top end plug. Therefore, no coolant flows through the fuel rod due to either pressure or thermal gradients.

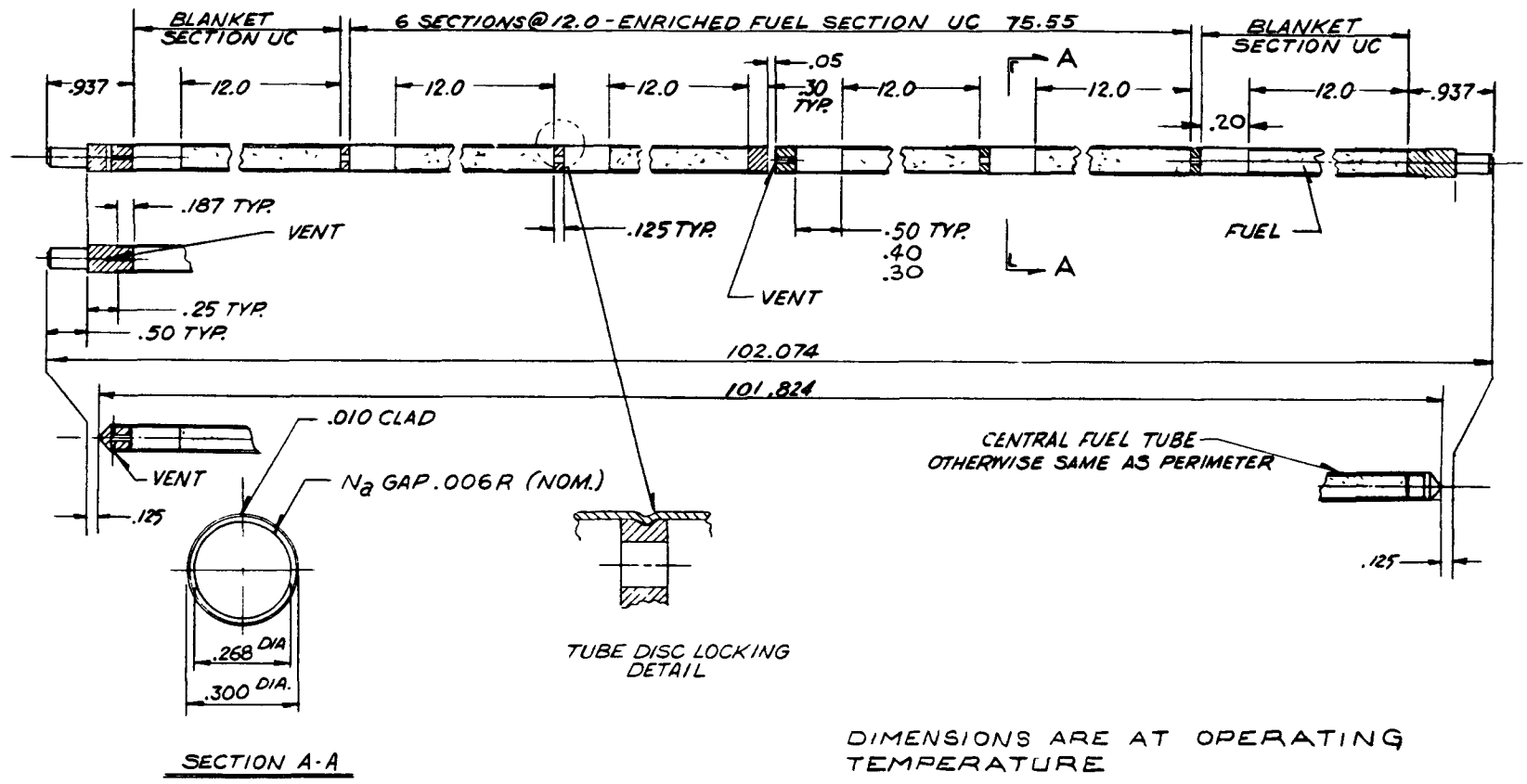

Figure III.4-4 Fuel Rod

The fuel pellet is pressed and sintered to 92% of theoretical density to a nominal size of 0.268 inch diameter. The following allowances are provided in pellet-to-clad clearance. Pellet swelling at 2% Δ V/V per atom % burnup is equal to approximately 20% for 100,000 MWD/ton burnup. One-half of the 20% Δ V/V is absorbed into the pellet porosity; or 8% Δ V/V clearance is already provided within the fuel for swelling. An additional allowance of ± 0.0025-inch is made for idameter deviation of pressed and sintered unground pellets. There is also a ± 0.0005-inch allowance for the inner diameter of the tube. No additional clearance is needed for differential pellet-to-clad thermal expansion since they are of equal magnitude.

Each fuel rod consists of three compartments separated by tube disc locks, installed progressively as each fuel rod is loaded. The compartments are mechanically locked in position by rolling the tube wall into the circumferential groove in each disc lock. The disc lock is plated with a brazing material, so that when the assembly is furnace brazed, the disc locks are brazed at the same time, thereby re-inforcing the mechanical crimp. No insulation disc is needed between these lock discs and pellet stack as there is internal sodium bonding to the 1400°F (peak) wall, and because of the relatively cool (2000°F) pellet center temperature.

III.4.3 Controlled Expansion Feature

The Bundle Controlled Expansion fuel assembly (BCEX) consists of upper and lower half-length bundles of fuel rods which are attached to a central structure of full-length cermet rods. During a rapid increase in core power level, the cermet rods heat up and separate the two bundles axially due to differential thermal expansion.

Because of its inertia, the bundle tends to resist this axial movement. This resistance to movement causes compressive stresses in the cermet rods. These stresses are proportional to the difference in the unrestrained thermal displacement and the actual or restrained thermal displacement of the fuel bundle. This situation is analogous to a mass (bundle) on a spring (cermet rods), where the spring end opposite to the mass is given a displacement which varies with time.

The detailed analyses, which are presented in Appendix A, of fuel assembly response to changes in cermet temperature are divided into four sections. In the first section the cermet rods are considered to be representative of an isotropic, elastic continuum with zero body forces. The assumptions inherent to this model are pointed out. Further simplifying assumptions are introduced and discussed. The second section applies appropriate boundary conditions to the continuum, including the reaction forces in the bundle-to-cermet connection. The resulting equation is that of the undamped harmonic oscillator. The third section discusses two types of cermet temperature programs, and the fourth section derives the response of the fuel assembly to these programs.

Analyses were performed on the BCEX fuel assembly to determine its performance characteristics for both terminated and unterminated transients. Figures III.4-5 thru III.4-10 present the results of the mechanical dynamic analysis of the BCEX fuel assembly. Equations (A-11)* and (A-12)*, solved for the bundle displacement, X, are plotted in Figure III.4-5 for three values of characteristic transient time, $\omega\tau$. ω is the natural frequency of the fuel bundle-cermet assembly, and τ is the characteristic response time to achieve terminal or total free cermet rod expansion, Y_τ. The instantaneous, free, cermet thermal expansion is designated as Y. The amplitude, A, of the BCEX fuel bundle vibration is shown in dimensionless form. For $\omega\tau=\pi/2$,

* See Appendix A

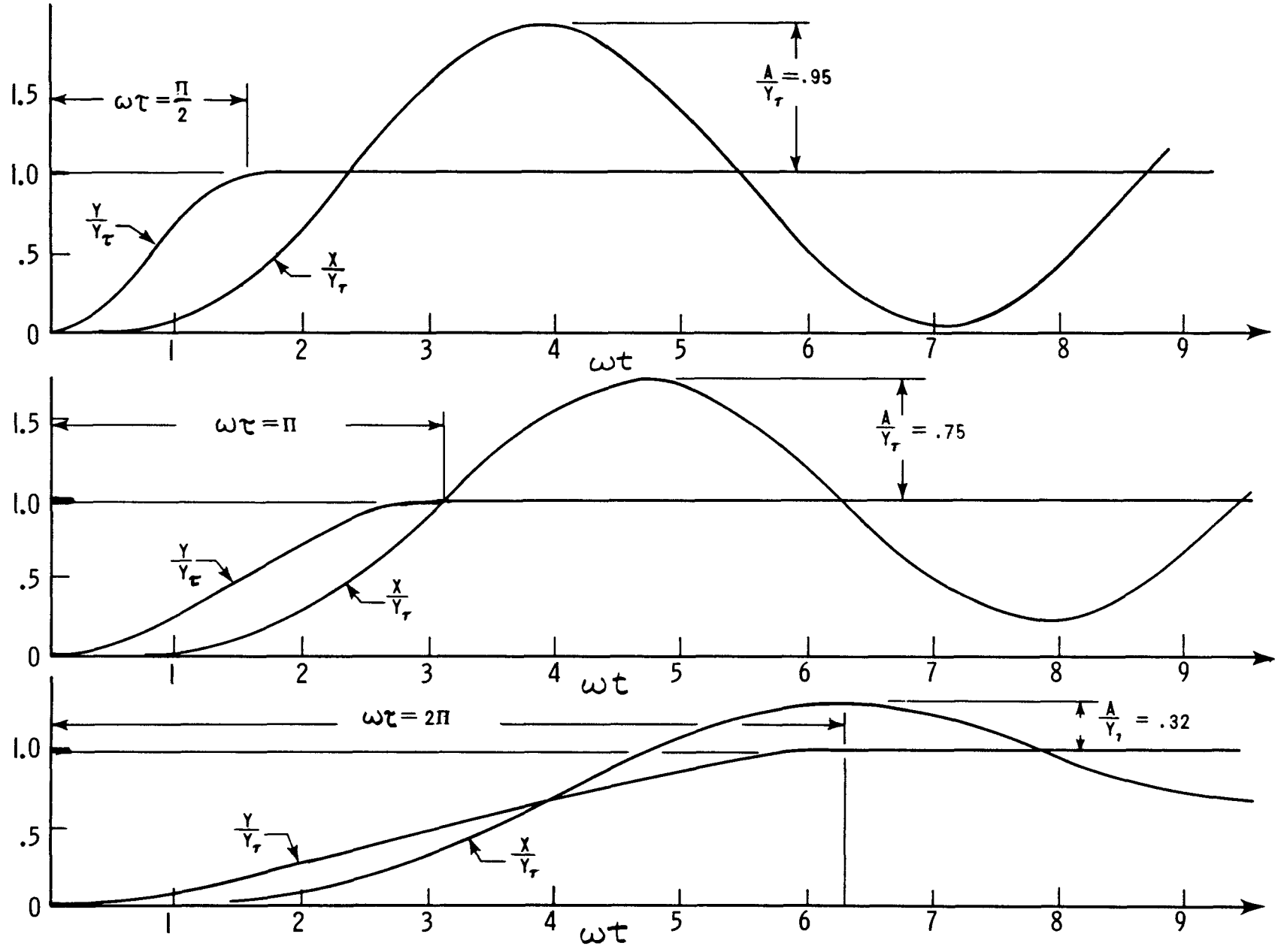

BUNDLE DISPLACEMENT vs. TIME FOR THREE TERMINATED TRANSIENTS

Figure III.4-5

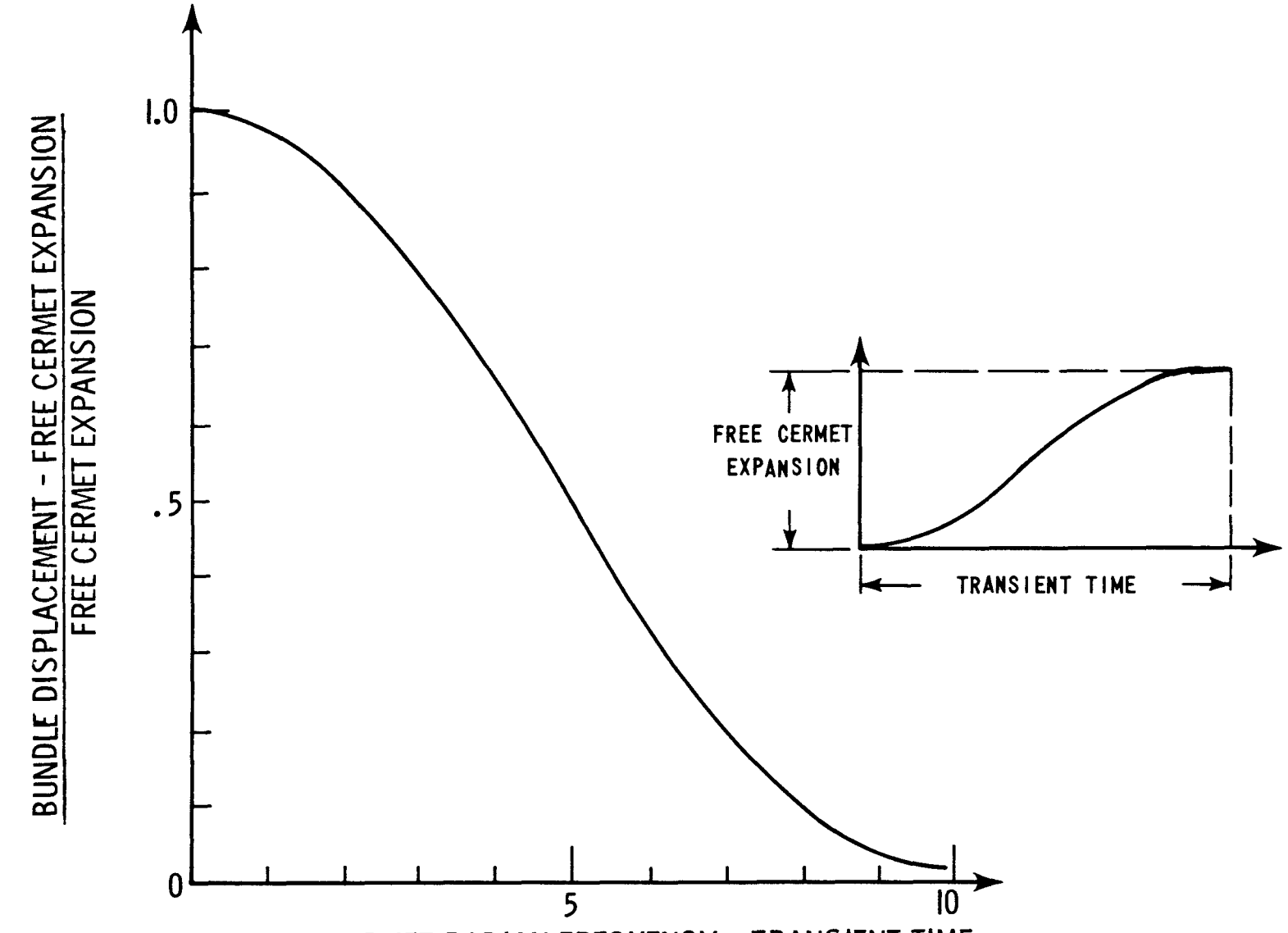

POST TRANSIENT BUNDLE VIBRATION AMPLITUDE vs. CHARACTERISTIC TRANSIENT TIME
(Terminated Transient)

Figure III.4-6

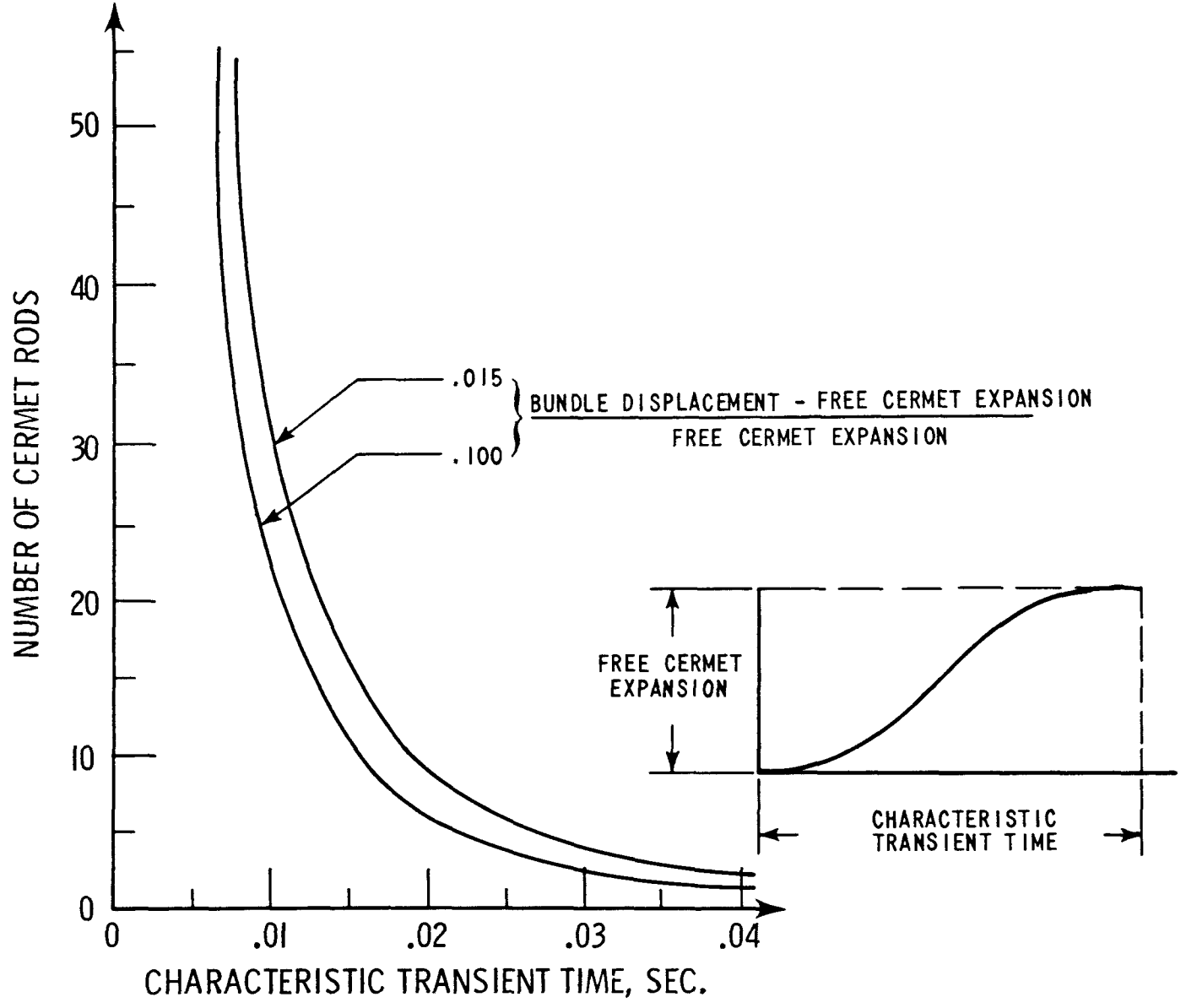

NUMBER OF CERMET RODS vs. CHARACTERISTIC TRANSIENT TIME
(Terminated Transient, Reference Fuel Ass'y Design)

Figure III.4-7

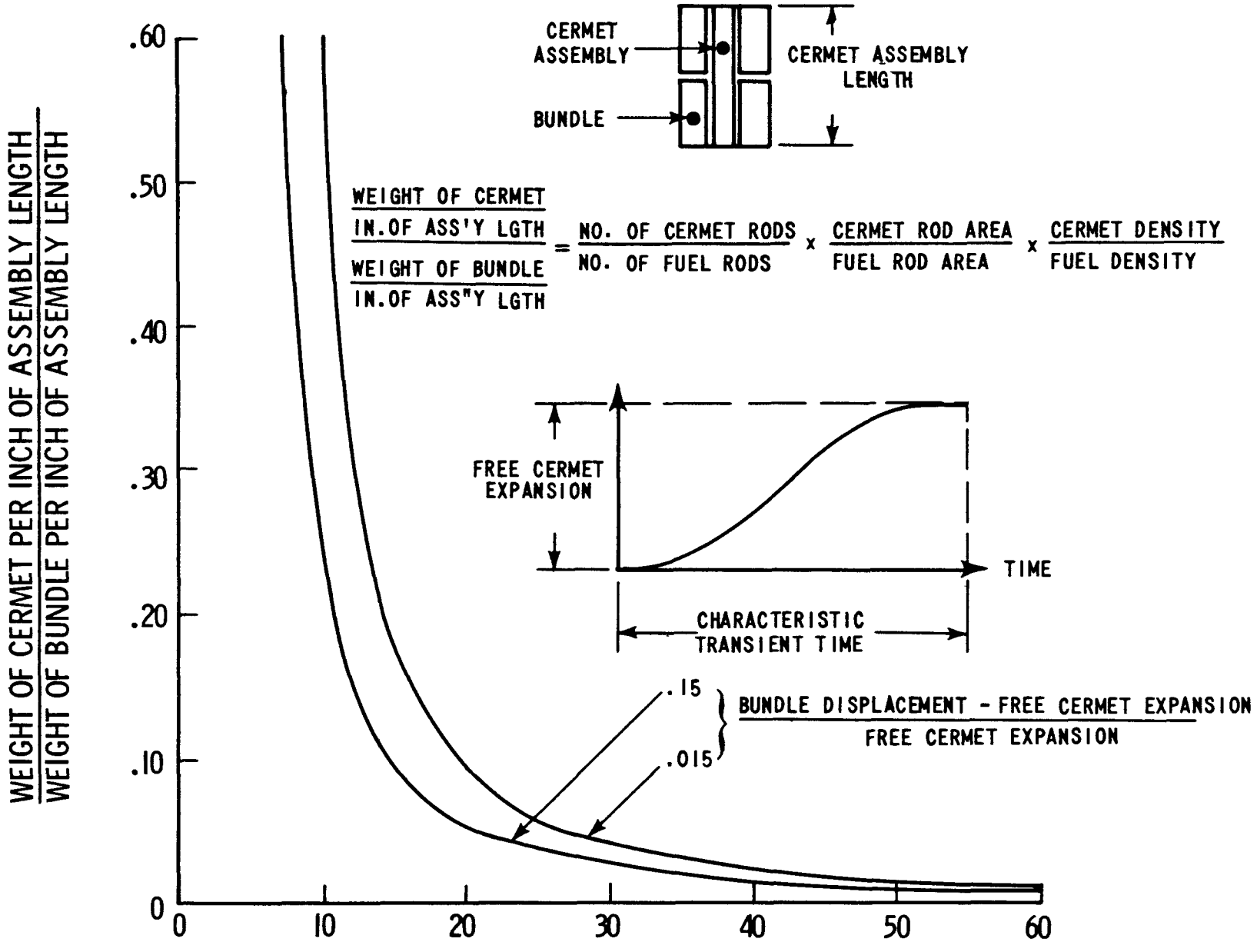

CEX FUEL ASSEMBLY PARAMETERS (TERMINATED TRANSIENT)

Figure III.4-8

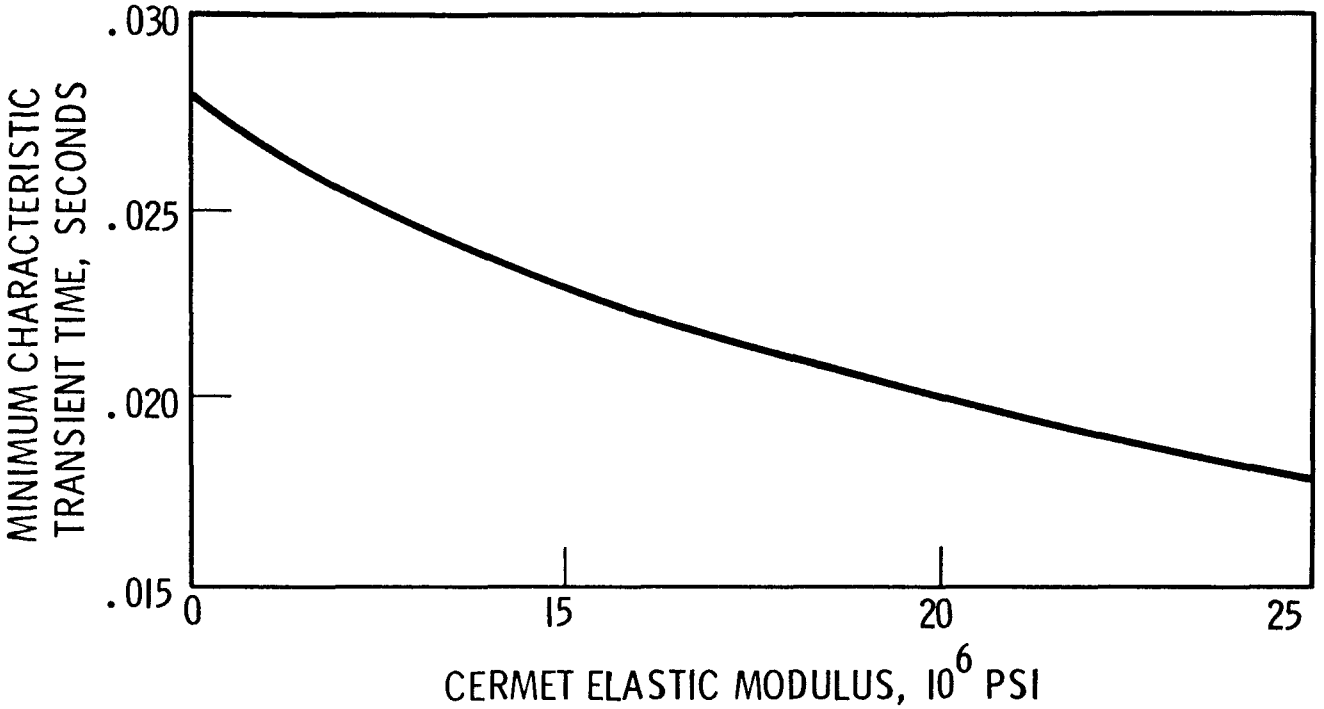

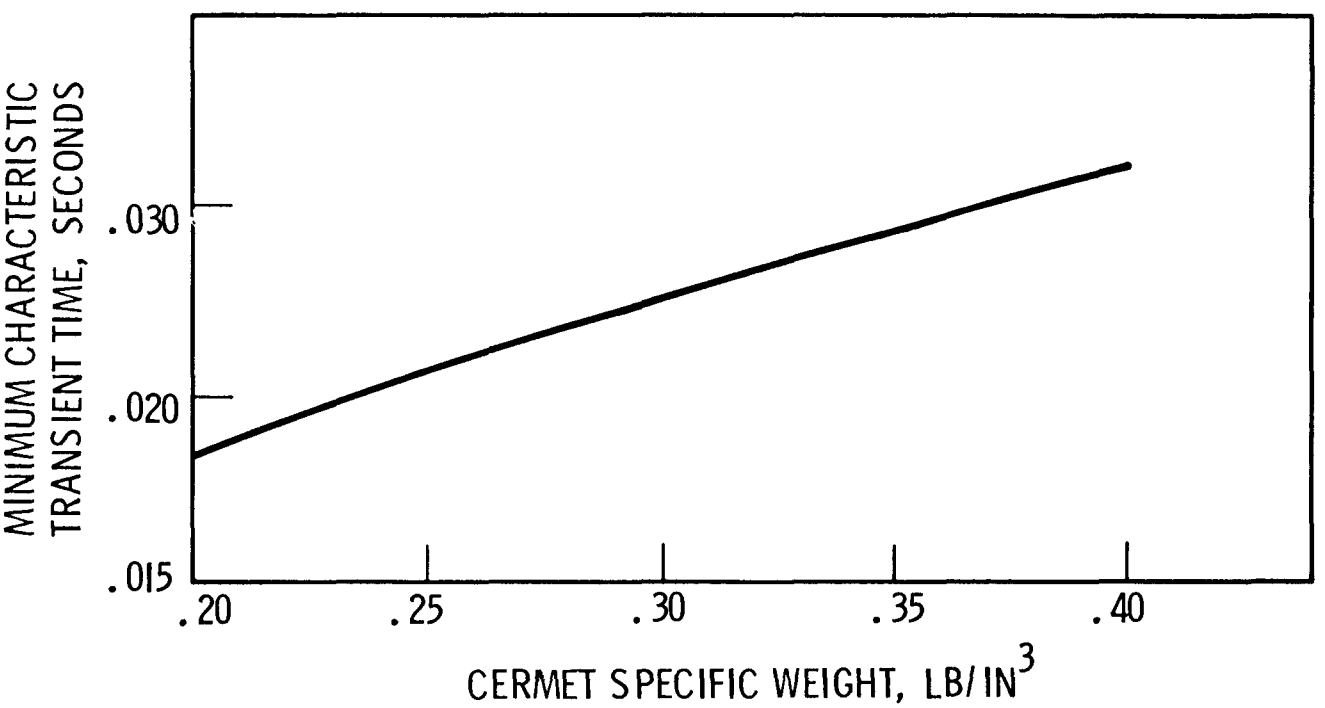

MINIMUM ALLOWABLE TRANSIENT TIME
VERSUS
CERMET MECHANICAL PROPERTIES

Figure III.4-9

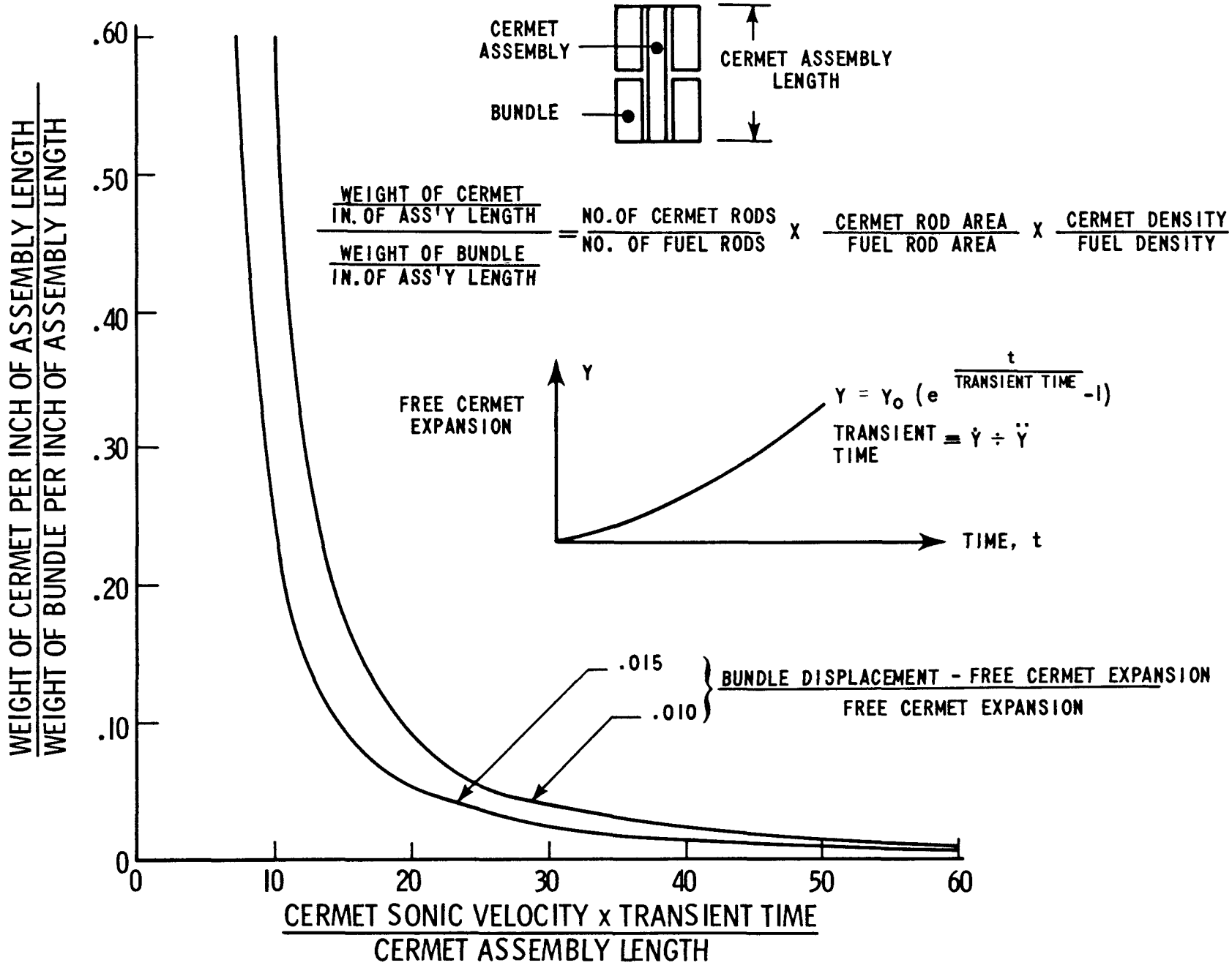

CEX FUEL ASSEMBLY PARAMETERS (UNTERMINATED TRANSIENT)

Figure III.4-10

the bundle does not follow or "track" the free cermet expansion nearly as well as for $\omega\tau = 2$. This reduces the effective, anticipated, negative reactivity cnntribution of the cermet; increases the transient stress in the cermet rod ($\alpha_{max} = E\, Z_{max}/L$)**; and, could introduce some undesirable fluctuations in reactivity, at times greater than τ.

Equation (A-15)* is plotted in Figure III.4-6 for A/Y_τ versus $\omega\tau$ for a terminated transient. For $\omega\tau$ greater than 10, the amplitude of post transient bundle oscillation is less than 2% of Y_τ, and the bundle essentially tracks free cermet expansion; the cermet transient stress is negligible for Y_τ less than 3/4 inches, and post transient reactivity fluctuations due to bundle vibration are small. For $\omega = 430$ radians per second and $\omega\tau = 10$, $\tau = 0.023$ seconds. Thus, for characteristics times, τ (i.e. transient ramp times) greater than 0.023 seconds, the stresses in the cermet rods due to inertia forces, and the post transient reactivity fluctuations due to bundle vibration, will be negligible. Since none of the ramp times resulting from the transient analyses in section III.5 were less than 0.050 seconds, it can be concluded that inertial stresses in the cermet rods, due to any of the terminated transients investigated, are negligible.

For the terminated transient case, Figure III.4-7 shows the effect of the number of cermet rods on the characteristic transient time for the reference fuel assembly design. This is shown for two values of A/Y_τ, the ratio of the bundle displacement minus the free cermet expansion to the free cermet expansion. A reduction in the number of cermet rods per fuel assembly would increase the characteristic transient time. Figure III.4-7 reveals no great reduction in the characteristic transient time for significant increases in the number of cermet rods. Furthermore, when the number of cermet rods is reduced to as few as three per assembly, the characteristic transient times are well below .050 seconds. Thus, stresses due to inertia

** See nomenclature in Appendix A

* See Appendix A

forces are still insignificant in the cermet rods for any of the transients studied in this investigation, for cermet rod assemblies having three or more rods.

Figure III.4-8 is a more generalized plot of BCEX fuel assembly parameters for the terminated transient case. This figure illustrates the effect on the cermet inertial forces of such parameters as cermet length, cermet sonic velocity, characteristic transient times, weight of cermet rod bundle, and weight of fuel rod bundle. The effect of cermet and fuel density and crossectional area can be determined from this curve.

Figure III.4-9 shows the effect of the Elastic Modulus and the specific weight (density) of the cermet fuel material on the minimum characteristic transient time for the terminated transient case.

From equation (A-16)*, the disparity between bundle displacement and free cermet expansion is approximately 2% for $\omega\tau_o = 7$ in an unterminated transient. τ_o is the characteristic time for the unterminated transient. Thus, for a bundle natural frequency of 430 radians per second, the characteristic time equals 0.016 seconds for the unterminated transient. In other words, cermet rod stresses due to inertia forces will be insignificant for any ramp involving a time of greater than 0.016 seconds. None of the unterminated transients studied in section III.5 were this low in value.

System parameters were substituted for ω in equation (A-16)*, and the resulting Figure III.4-10 is a general parameter plot of the BCEX fuel assembly characteristics for the unterminated transient case. These curves illustrate the interrelated effect of such parameters as cermet length, cermet sonic velocity, transient time, weight of fuel rod bundle and cermet and fuel density and rod size.

---

*See Appendix A

The effect of restraining forces on bundle controlled expansion (BCEX) response is also investigated in Appendix A. The fuel rod bundles are considerably less rigid than the can. If close clearances are maintained at many points between the can and the bundles, the bundles will bend to match the can contour. Can to bundle forces will be generated in the process. The effect of these forces on the response of the lower bundle to transients was calculated. It was concluded that the magnitude of these forces must be minimized. This can be accomplished by supporting the lower rod bundle at only two places. The bundles are then free to assume their unrestrained curvature, and no restraining forces are generated. In the reference design, the lower bundle is supported at its lower end from the fuel assembly can, and at an upper point from the cermet bundle. The upper rod bundle is completely restrained by the can. An alternate design was investigated where both upper and lower bundles are supported at only two points from the can.

In conclusion, in none of the terminated or unterminated transients studied in section III.5 does the characteristic transient time approach a value as small as 0.025 seconds. Thus, the reference fuel assembly design is considered quite adequate from a transient mechanical design viewpoint for all transients investigated in this study. In addition, large variances in the values of the cermet elastic modulus or density will not increase this minimum characteristic transient time (point at which there is still insignificant stresses in the cermet rods) to a value as large as any transient investigated in this study.

III.4.4 Fuel Clad Stresses and Strains

Each carbide fuel rod is vented to the sodium coolant. This eliminates clad stresses due to coolant or fission gas pressure. Stresses and strains still arise in the fuel cladding due to:

a) temperature gradients,

b) static weight,

c) flow drag, and

d) flow induced vibration.

Appendix C discusses and itemizes the stresses and strains due to these loadings, and relates them to appropriate failure criteria. The specific areas which cause stresses and strains in the nuclear reactor core are investigated in Appendix C.

Restraint to Bundle Bowing

The brazed fuel bundle is subjected to a core radial variation in coolant temperature. The temperature gradient in the lower bundle is small, and the bundle is allowed to bow freely. The upper bundle gradient is much greater, and this bundle must be constrained by the fuel assembly can to remain straight. This constraint results in bending strains in the bundle. Near the bundle ends, the bending strain is zero and the ferrules are subjected to shear stresses. Since the ferrule shear area is 4 to 5 times the clad wall area, the fuel cladding sees the higher shear stresses.

Non-Linear Radial Bundle Temperature Gradient

The core radial coolant temperature gradient across a bundle is not linear, but has a quadratic component. This quadratic term in the temperature profile generates stresses and strains equivalent to those in a beam with uniform internal heat generation.

Clad Radial Temperature Gradient

Large temperature gradients exist across the clad of the carbide fuel rods because of the high heat fluxes inherent to reactor cores. These large temperature gradients cause clad strains due to internal restraint.

Clad Axial Temperature Gradient

Within a reactor core, the clad temperature varies non-linearly with axial distance. Stresses and strains arise from the non-linear terms in the axial temperature profile due to internal restraint.

Static Weight and Flow Drag

Each BCEX fuel bundle is supported at its extremities by 48 of the 120 total fuel rods. The static weight of the bundle on the fuel rod cladding causes slight stresses and strain. In addition, forces are imposed on the fuel bundles due to coolant flow drag.

Rod Vibration in Parallel Flow

Flow induced fuel rod vibration between spacer ferrules results in an oscillating component of clad strain at the natural frequency of the span.

Bundle Vibration in Parallel Flow

Because of flow excitation, the fuel rod vibrates between spacer ferrules, and so does the entire bundle, causing clad strain.

Table III.4-1 summarizes the fuel clad strains investigated in Appendix C. The largest single component of strain is approximately 0.001 inch per inch, caused by the radial temperature drop across the clad wall of the carbide fuel rod. In the table, region 1 refers to the second ring consisting of six fuel assemblies in the core, region 2 to the third ring consisting of twelve fuel assemblies, and region 3 to the fourth ring consisting of eighteen fuel assemblies. These three regions or rings comprise the entire core of one module, because the first ring is a control rod location.

Table III.4-2 compares the fuel clad strains and stresses with fracture values. The stresses and strains from Table III.4-1 are superimposed. The resulting total strains and stresses are compared with the following three fracture criteria:

TABLE III.4.1

SUMMARY OF FUEL CLAD STRAINS

Strain Units - in/in x 100%

	Region I				Region II				Region III			
	Top Bundle		Lower Bundle		Top Bundle		Lower Bundle		Top Bundle		Lower Bundle	
	Max.	Min.	Max.	Min.	Max.	Min.	Max.	Min.	Max.	Min.	Max.	Min.
Restraint to Bundle Bow	±.012	0	0	0	±.028	0	0	0	±.038	0	0	0
Non-Linear Rad. Bundle Temp. Gradient	+.002	0	+.001	0	+.002	0	+.001	0	+.002	0	+.001	0
Clad Radial Temp. Gradient	±.107	±.061	±.104	±.060	±.097	±.053	±.094	±.051	±.079	±.040	±.077	±.040
Clad Axial Temp. Gradient	0	0	0	0	0	0	0	0	0	0	0	0
Static Weight	+.003	+.002	-.003	-.002	+.003	+.002	-.003	-.002	+.003	+.002	-.003	-.002
Flow Drag Less Static Weight	-.003	-.002	+.002	+.002	-.002	-.001	+.001	+.001	-.001	-.001	+.001	+.001
Rod Vibration in Parallel Flow	±.006	±.012	±.006	±.009	±.003	±.009	±.003	±.006	±.003	±.006	±.003	±.006

TABLE III.4-2

COMPARISON OF FUEL CLAD STRAINS AND STRESSES WITH FRACTURE VALUES

	Region 1				Region II				Region III			
	Top Bundle		Lower Bundle		Top Bundle		Lower Bundle		Top Bundle		Lower Bundle	
	Max.	Min.	Max.	Min.	Max.	Min.	Max.	Min.	Max.	Min.	Max.	Min.
Max. Operating Strain - %	+.130	+.065	+.116	+.068	+.134	+.055	+.102	+.055	+.124	+.042	+.086	+.044
*Min. Fracture Strain - %	25	25	57	57	23	23	65	65	34	34	68	68
Start-up/Shut-down Strain Range - %	0 to .115	0 to .057	0 to .110	0 to .064	0 to .122	0 to .050	0 to .099	0 to .054	0 to .115	0 to .037	0 to .085	0 to .043
*Usage Factor = No. of actual cycles / cycles to failure	← LESS THAN 10^{-4} →											
Operating Strain Range - %	0 ±.012	0 ±.006	0 ±.009	0 ±.006	0 ±.009	0 ±.003	0 ±.006	0 ±.003	0 ±.006	0 ±.003	0 ±.006	0 ±.003
*Usage Factor	.0016	.	← LESS THAN .0016 →									
*Cumulative Usage Factor	.0016		← LESS THAN .0016 →									
Primary Stress, psi	-515	-310	+485	+290	-295	-180	+275	+165	-225	-135	+205	+125
*Time to Rupture (minimum)	← GREATER THAN 100,000 HRS. →											

*Based on Operating Temperature of 1300°F.

a) Short time tensile test elongation at rupture

b) Fatigue failure

c) Failure due to long-time stress rupture

Details of the fatigue analysis are presented in section III-7.

It can be concluded from Tables III.4-1 and III.4-2 that all clad stresses and strains are well within allowable limits.

III.4.5 Cermet Design

The central, 7-rod, cermet sub-assembly is built-up from single rods brazed together by spacer ferrules. The fuel bundle/cermet rod spacing and mutual positioning is accomplished at the interface between cermet bonding straps and bundle ferrules.

The cermet rod design was examined for possible failure modes. Failure may occur either from excessive distortion that would alter the cermet performance characteristics, or from formation of cracks. Distortion may arise from asymmetric thermal gradients or forces. Cracks may develop from excessive static, dynamic, or creep strains. The results of the analyses of the cermet rod stresses and strains due to a variety of causes are summarized in the following paragraphs.

An analytical model was derived which relates secondary creep strain in the stainless steel matrix to fuel swelling and fission gas pressure. As the resulting, first order, non-linear, differential equation was not solved, the analysis is not complete. The analysis is included in Appendix D as a reference for possible future work.

Internal heat generation within the cermet rod results in a parabolic radial temperature gradient and attendant thermal strains. The axial and tangential strain values at the outer rod surface are given by:[1]

$$\frac{0.5\ \alpha}{1 - \mu} \times \text{(rod center temperature-rod surface temperature)}$$

For a 30% volumetric heating ratio in the cermet fuel, the maximum, hot channel, temperature difference in the 0.300 inch O.D. cermet fuel rod is approximately 500°F. The cermet fuel linear coefficient of expansion, α, may range from 8.5 to 11 x 10^{-6} per °F. Thus, the cermet surface strain due to internal heat generation is between 0.3 and 0.4 percent.

Column loading of the cermet rods from a buckling standpoint during a BCEX transient is negligible. Bundle support of the cermet rod complex further reduces the possibility of buckling as a failure mode.

The moment of inertia of the cermet complex is much greater than that of a single fuel rod. Therefore, vibration amplitude and attendant stress is negligible for the cermet rods.

Cermet axial temperature gradients are comparable to those in the fuel clad. Fuel clad strains due to axial temperature gradients were shown to be negligible. The same conclusion applies to the cermet rod.

Coolant mixing will be induced within the cermet complex thereby minimizing core radial temperature gradients. Therefore, there is little tendency for the cermet rods to bow. The fuel bundles are partially constrained by the can to remain straight. Therefore, there is some small amount of bow induced in the cermet complex from external causes which will induce only small bending stresses.

Transient loads during the worst transient considered are negligible. This was fully discussed in section III.4.3.

The cross-sectional area of the cermet rods which supports the fuel bundle is about the same as the total fuel clad area. Fuel clad stresses and strains due to bundle flow drag and static weight were negligible. The same conclusion applies to the cermet rod.

Lack of cermet ductility data and lack of a solution to the fission gas pressure problem makes discussion of cermet mechanical design difficult from an analytical point of view. The value of 0.3 to 0.4 percent strain due to internal heat generation seems high when compared to probable ductility values of approximately 1 percent. Discussion of the cermet design from an empirical point of view is presented in the materials review and analyses section, where it is concluded that the cermet design appears to be adequate.

III.4.6 Fuel Assembly Can Stresses and Strains

A hexagonal shaped can, which encloses each fuel bundle, supports the fuel and provides an autonomous flow channel for efficient orificing. Can distortion is of primary interest in maintaining adequate envelope clearance for the free movement of the lower bundle during power transients and assuring adequate clearance between assemblies for ease of refueling.

Raised bosses are provided on the can outer surface to contact similar bosses on adjacent cans. Bundle and can bowing is thus restricted, and the resulting reaction forces are eventually transmitted to the reflector assemblies. These are supported by the module perimeter top locating grid, located around the perimeter of each core module. The close fit between the bosses is of a local nature requiring but a relatively small axial motion of the assembly during refueling to break free of this close fit.

Can distortion due to can internal pressure was investigated. Core pressure drop results in a pressure gradient across the can tending to bulge can panels into contact with adjacent fuel assembly cans. The maximum pressure difference occurs at the lower core plate and decreases linearly with distance above the lower core plate.

Removing a unit strip from a can panel and treating it as a built-in beam with end tensile loads appears as follows:

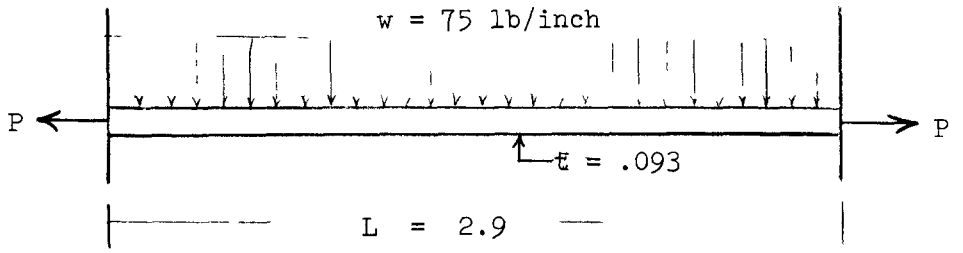

From Table VI of reference (2) the maximum bending moment:

$$M = wj^2\left(1 - \frac{U/2}{\sinh U/2}\right)$$

The maximum deflection:

$$y = \frac{wj^2}{8P}\left[\frac{4U(1 - \cosh U/2)}{\text{Sinh } U/2} + U^2\right] = .0083 \text{ inches}$$

Where:

$$U = L/j; \quad j^2 = EI/P; \quad EI = \text{flexural rigidity}$$

Since

$$P = wL \cos 30^\circ = 188 \text{ lb.}$$

and

$$E = 24 \times 10^6 \text{ psi} = \text{Young's Modulus for 316 SST @ } 850^\circ F$$

The bending stress (max) = $6M/t^2$ = 35,700 psi, and the tensile stress = 188/.093 = 2,000 psi

Thus, the maximum total stress = + 37,700 psi at the can corners

Checking the BCEX can wall thickness against the Fermi can thickness (reference 3) by dimensional analyses with the following expression:

$$\left(\frac{t}{t_f}\right) = \left(\frac{b}{b_f}\right)\left(\frac{P}{P_f}\right)^{1/2}\left(\frac{s}{s_f}\right)^{-1/2}$$

where

t = BCEX fuel assembly wall thickness

t_f = Fermi fuel assembly wall thickness = 0.096 inches

b = BCEX fuel assembly panel span = 2.9 inches

b_f = Fermi fuel assembly panel span = 2.45 inches

P = BCEX fuel assembly pressure gradient = 75 psi

P_f = Fermi fuel assembly pressure gradient = 97 psi

s = ASME Boiler Code VIII allowable stress at operating temperature for 316 SST = 16,500 psi at 850°F

s_f = ASME Boiler Code VIII allowable stress at Fermi operating temperature for 316 SST = 17,150 psi at 550°F

The comparable BCEX fuel assembly wall thickness is 0.101 inches

The can wall was checked for creep deflection. From Figure 6 of reference (4), and from the creep data for 316 stainless steel in Figure III.4-11, the following table can be constructed for a clamped/clamped beam:

Beam Temp., °F	n	$y_c \left[\frac{wL^2}{2t^2}\right]^n \frac{L^2}{t}\tau$
800	11.60	5.4×10^{-69}
900	10.75	2.5×10^{-62}
1000	10.00	1.7×10^{-56}
1100	9.37	1.4×10^{-51}
1200	8.81	3.2×10^{-47}
1300	8.31	2.5×10^{-43}
1400	7.86	8.0×10^{-40}
1500	7.46	1.1×10^{-36}
1600	7.10	7.0×10^{-34}

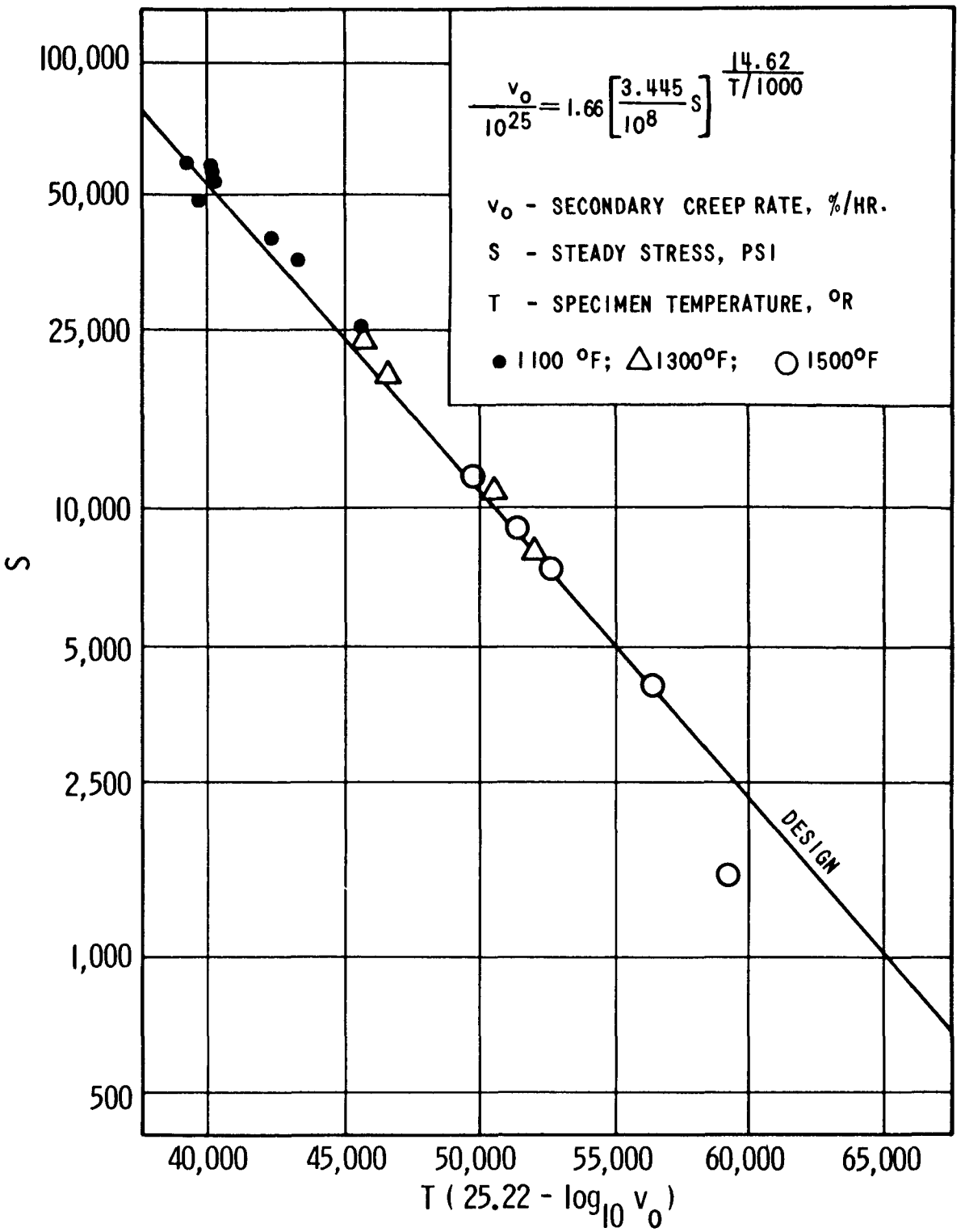

CORRELATION OF SECONDARY CREEP RATE DATA - 316 SST.
(Pg. 86, ASTM-ASME STP No. 124)

Figure III.4-11

y_c is the mid-span deflection (inches) at time τ (hours) due to creep. The other symbols have been defined previously. In the bottom half of the core, the can temperature is less than 1000°F, the pressure difference is less than 75 psi, and y_c is less than .001 inches. In the top half of the core, the can temperature is less than 1100°F, the pressure is less than 41 psi, and y_c is less than .0001 inches. Thus, it can be concluded that the can wall thickness is sufficient to withstand the imposed pressure gradients for τ = 25,000 hours.

Can internal heat generation causes a thermal gradient across the can wall that results in can outer fiber strains of $2\ \alpha\ \Delta T/3\ (1-\mu)$[1]. Where α, the thermal expansion coefficient, equals 10^{-5} per °F, the maximum can wall temperature difference, ΔT, is less than 10°F, and μ, the Poisson's Ratio equals 0.3, a surface strain on the order of 0.01 percent is developed. This strain is considered negligible.

III.4.7 BCEX Fuel Assembly Thermal Bowing

During operation of the EBR-I reactor, an instability was experienced that resulted in a partial meltdown of the Mark II core[5,6]. This instability was caused by a prompt positive power coefficient followed by a larger negative one. The initial prompt power coefficient has been attributed to inward bowing of the reactor fuel rods under the influence of a radial temperature gradient. Since then, reactor core designers have expended considerable effort to insure that thermal bowing of fuel rods and assemblies move fuel away from the core center line[7,8,9,10].

A bundle controlled expansion (BCEX) fuel assembly can is shown in Figure III.4-1. It is assumed to be rigidly attached to the reactor-core plate at its lower end. If the upper end of the can is unrestrained, it will bow outward under the effect of the core radial temperature gradient. The unrestrained bowing curve is plotted in

Figure II.4-12, assuming no transverse coolant mixing occurs in the fuel assembly. The outward bowing is desirable from a reactivity standpoint, but the configuration is prone to flow induced vibrations. It becomes necessary, therefore, to add restraints at the upper end of the fuel assembly can.

The effects of several alternate systems of restraint are illustrated in Figure III.4-13. Initially, calculations were made (details of the bowing calculations are given in Appendix B) assuming that no net movement of the can occurs at the points of restraint. One upper restraint is unacceptable as it results in a large inward movement of the can. Either two or three upper can restraints appear to provide a workable solution. At 100 percent power, the deflections of the cans and fuel bundles for two and three restraints are shown in Figures III.4-14 and III.4-15. There is a net movement of fuel away from the core centerline in both the reference design (three upper restraints) and an alternate design (two restraints). As shown in figures III.4-14 and III.4-15, the latter case (two restraints) results in a somewhat greater net outward movement.

Analysis to this point has assumed that there was no net movement at the points of restraint. In reality, manufacturing tolerances will exist and clearances will be necessary to permit installation of core assemblies. Experience with EBR-II[8] suggests that a net movement of 0.010 in. at each support point is realistic. With this assumption, the bowing curves were re-calculated (see appendix B). The results appear in Figures III.4-16 and III.4-17. The effect of clearances is to considerably reduce the net outward movement of fuel in both the reference and alternate designs. In the reference design, the reduction is sufficient to completely remove the need for the lowest restraint. Hence, only two upper restraints are effective for this case.

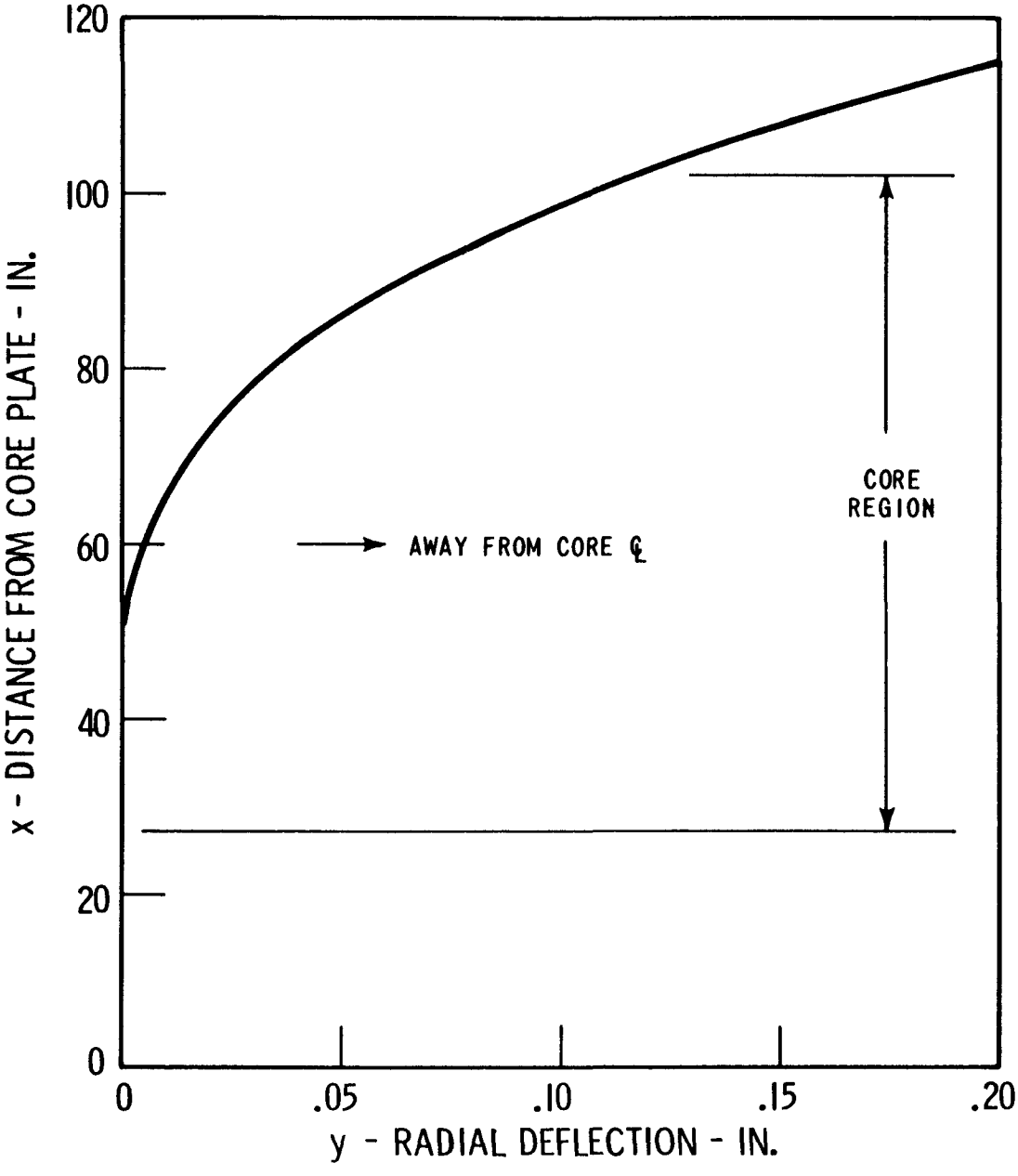

UNRESTRAINED THERMAL BOWING OF OUTERMOST CORE SUBASSEMBLY

Figure III.4-12

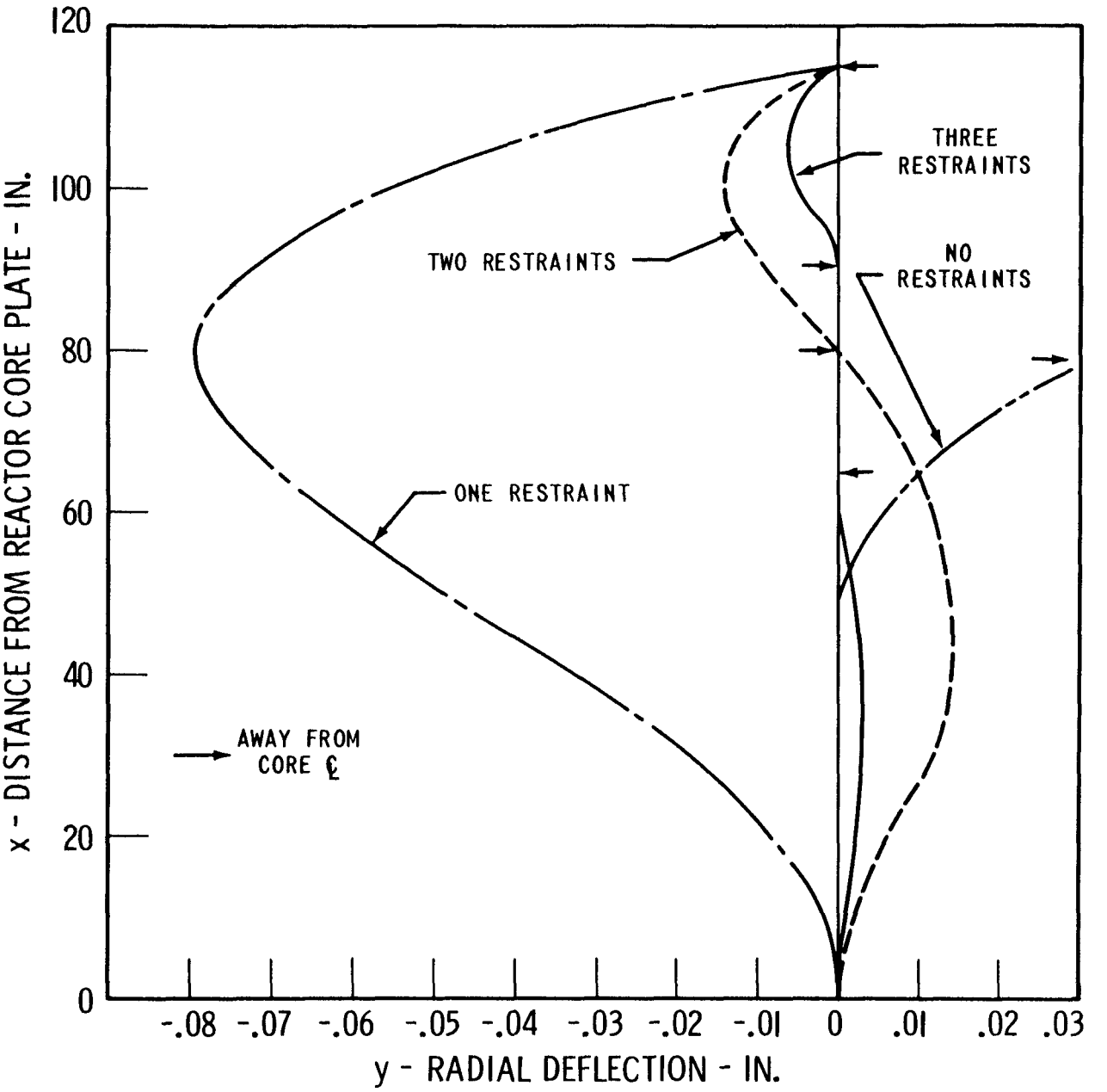

EFFECT OF RESTRAINTS ON THERMAL BOWING OF FUEL ASSEMBLY CANS

Figure III.4-13

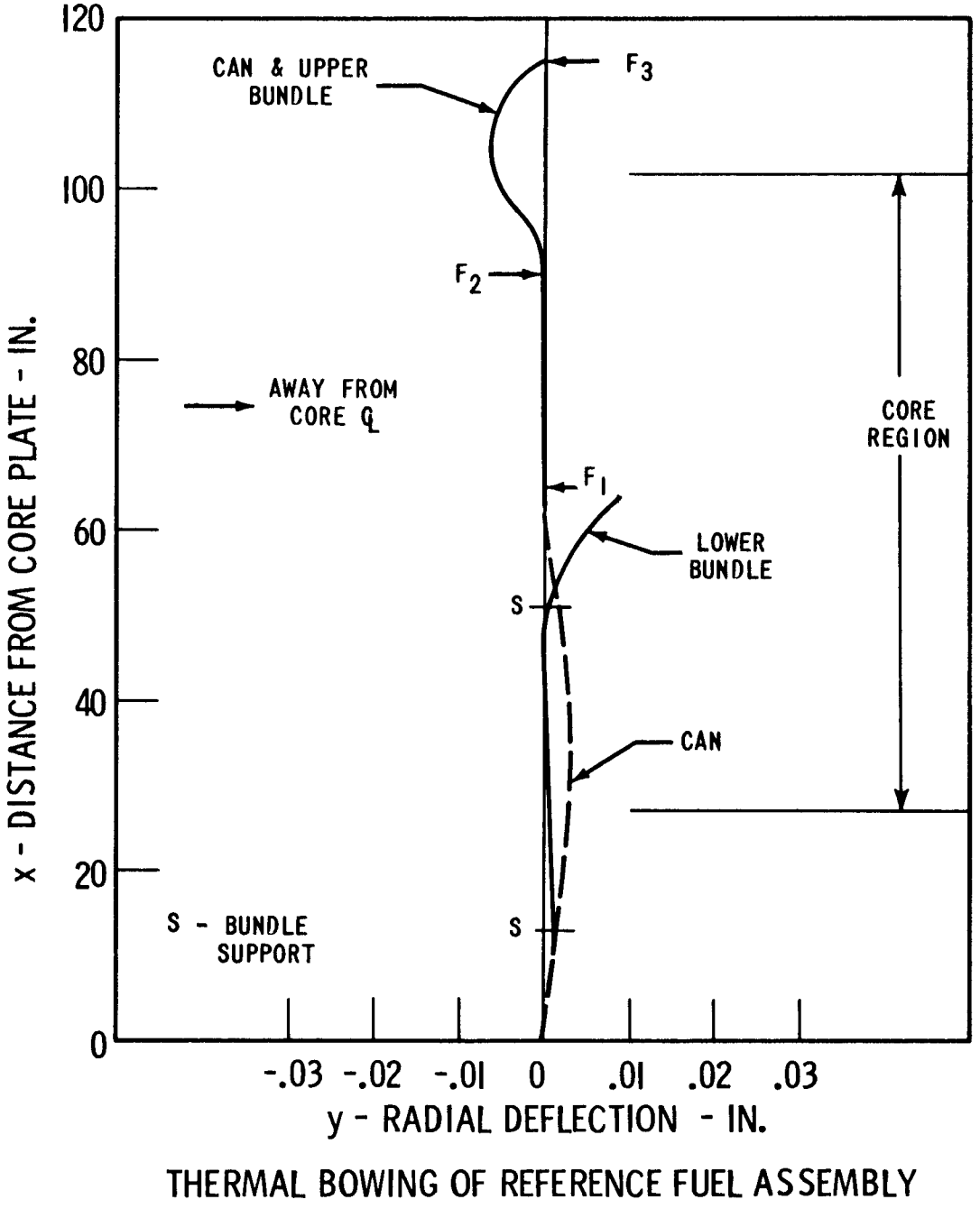

Figure III.4-14

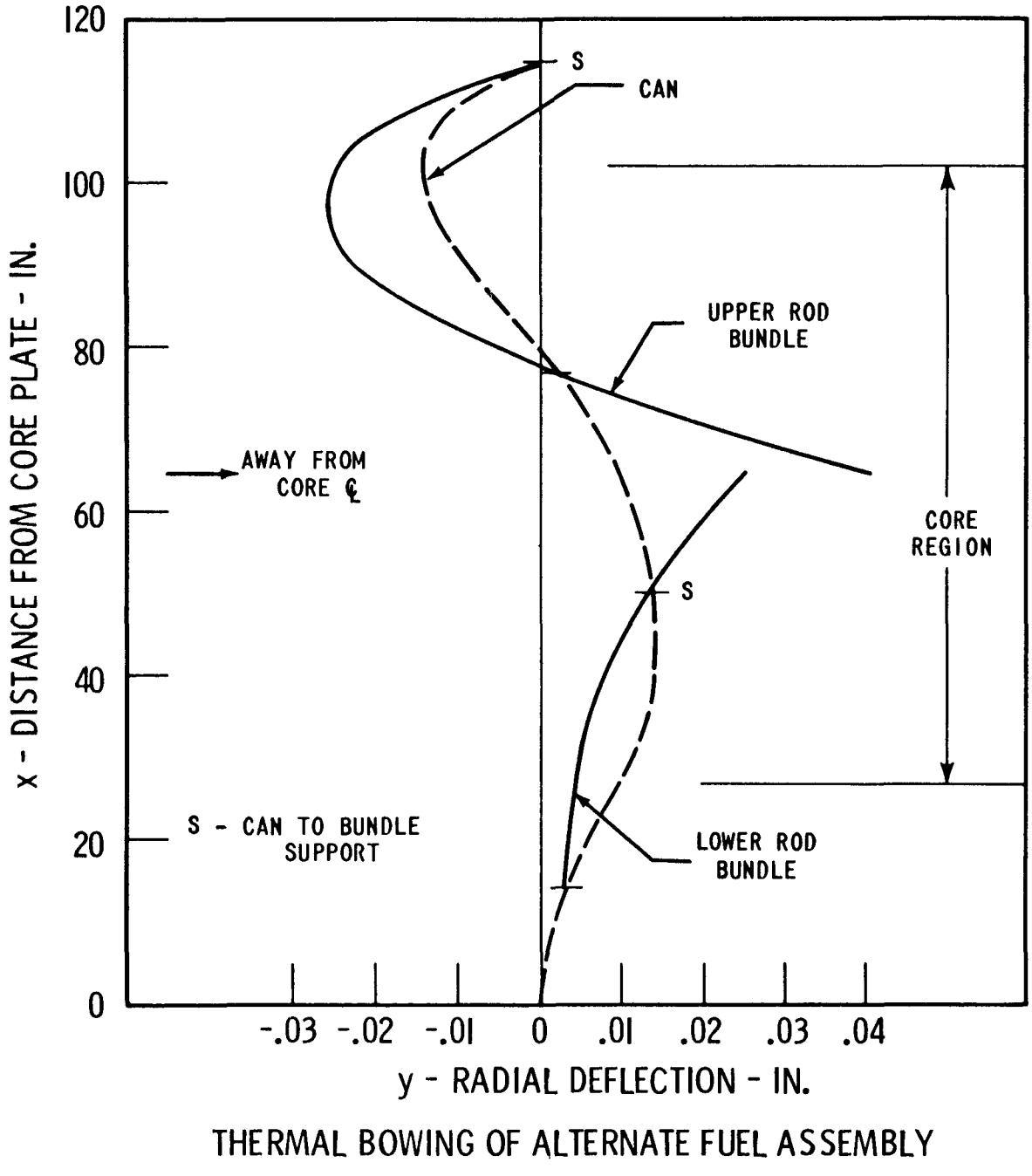

Figure III.4-15

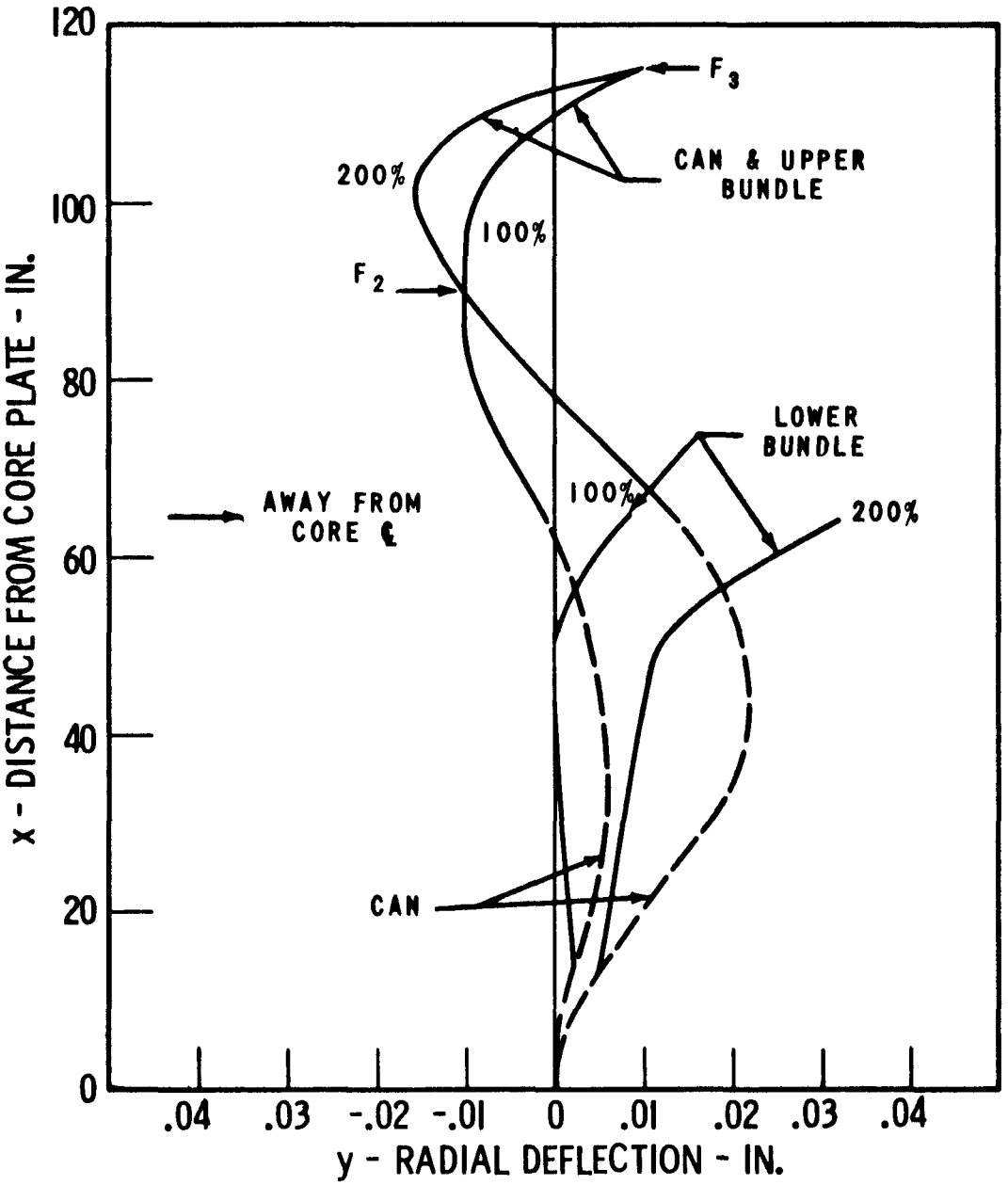

EFFECT OF CLEARANCES AND TRANSIENTS ON BOWING OF REFERENCE FUEL ASSEMBLY

Figure III.4-16

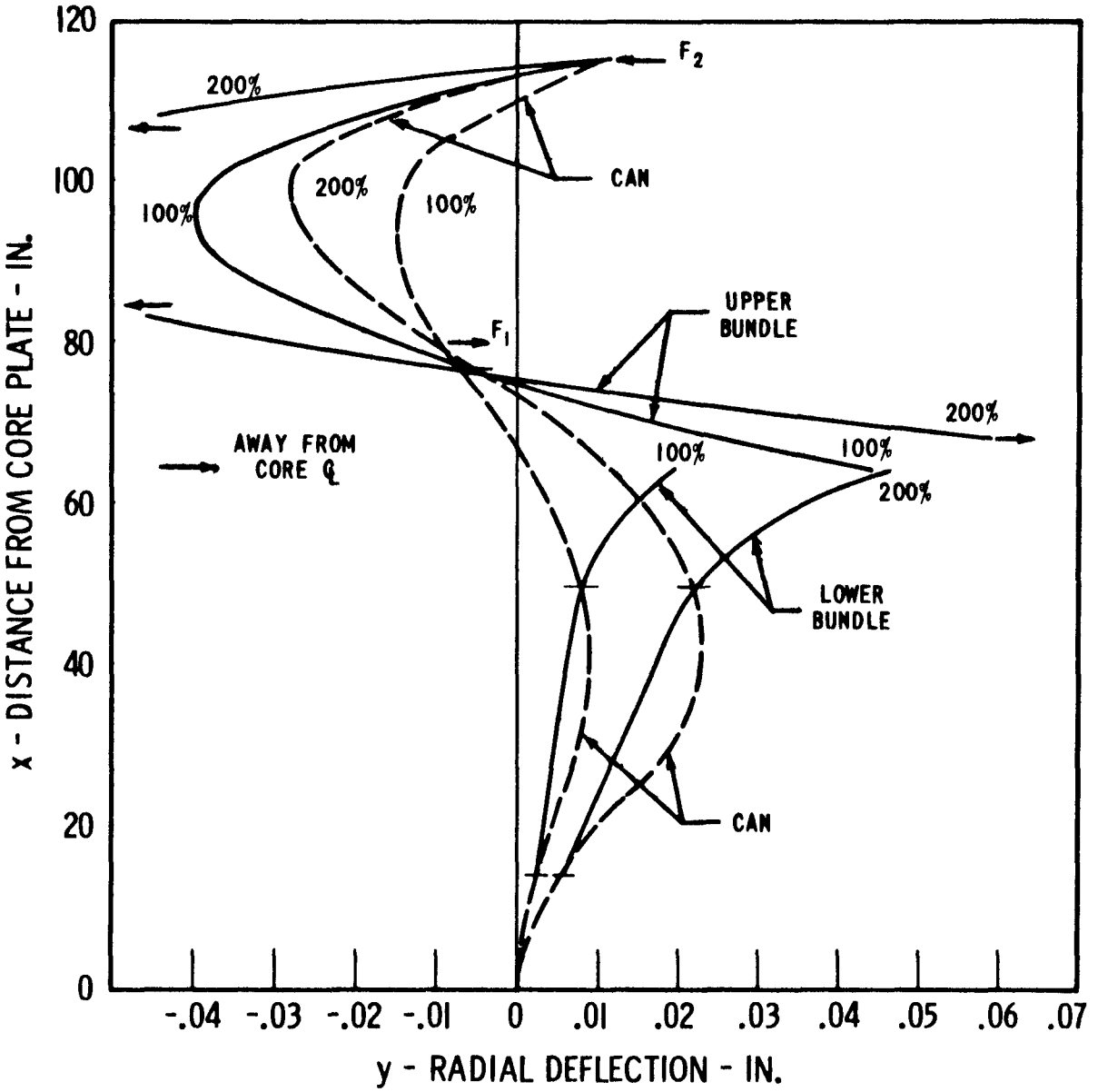

EFFECT OF CLEARANCES AND TRANSIENTS ON BOWING OF ALTERNATE FUEL ASSEMBLY

Figure III.4-17

To minimize restraining forces on the fuel assembly (so that BCEX response is not adversely affected), both upper and lower bundles are supported at only two points from the can, for the alternate design. In the reference design, the lower bundle is supported at its lower end from the fuel assembly can, and at an upper point from the cermet bundle. The upper rod bundle is closely restrained by the can.

Bowing behavior during an accident or transient condition is an important consideration. Bowing was analyzed at 200 percent power, which corresponds to a reactivity insertion of approximately 80 cents in 0.10 sec. The resulting bowing appears in Figures III.4-16 and III.4-17. It is seen that for both the reference and alternate designs, there is a net outward movement of fuel in going from 100 percent to 200 percent power.

On the basis of the bowing analysis performed in this study, the following conclusions and recommendations can be made:

1. Two judiciously located upper can restraints appear to provide the most realistic method for controlling thermal bowing of BCEX fuel assemblies.
2. Effort should be made to minimize initial gaps between adjacent fuel assemblies.
3. Further work is required to determine the optimum points or axial locations for can restraints.
4. Further analysis is required to determine the optimum method of supporting the fuel bundles within the can so as to minimized bundle restraining forces and so as not to impede BCEX response capabilities. Since the choice of location and number of support points greatly affects the net movement of fuel, bowing analysis should also be correlated closely with physics calculations.

5. Bowing analysis should be extended to cover a wide range of power levels. This is important as, until sufficient bowing of the fuel can has occurred to take up initial clearances and reach a stable geometry, unusual effects may be observed.

6. Based upon the results of the bowing analyses performed in this study, the reference and alternate designs would have a net reactivity effect between zero and 200 percent power due to thermal bowing between zero and minus 10 cents.

7. The bending moment and shear stresses induced in the fuel assembly can to restrain "free-bowing" in the reference design case is greater than for the alternate design case as shown in Figures III.4-18 and III.4-19.

III.4.8 Recommendations for Future Work

More positive assurance of cermet structural integrity is required. Analytical work such as that begun during this project relating steel matrix creep to gas pressure should be continued. Reliable structural and mechanical properties data of irradiated rod specimens is required for the development of the BCEX concept.

Friction, galling, and wear between moving parts of the fuel assembly must be evaluated in a sodium environment at design conditions.

A prototype assembly should be built and tested in-pile to study the feasibility of fabrication and operation of the bundle controlled expansion design.

A preliminary bowing investigation was performed during this study. Further investigations of fuel bowing for the range of actual reactor design conditions must be pursued. Further effort is required in the areas of design and location of fuel assembly restraints so as to minimize bundle restraining forces while not impeding BCEX response capability.

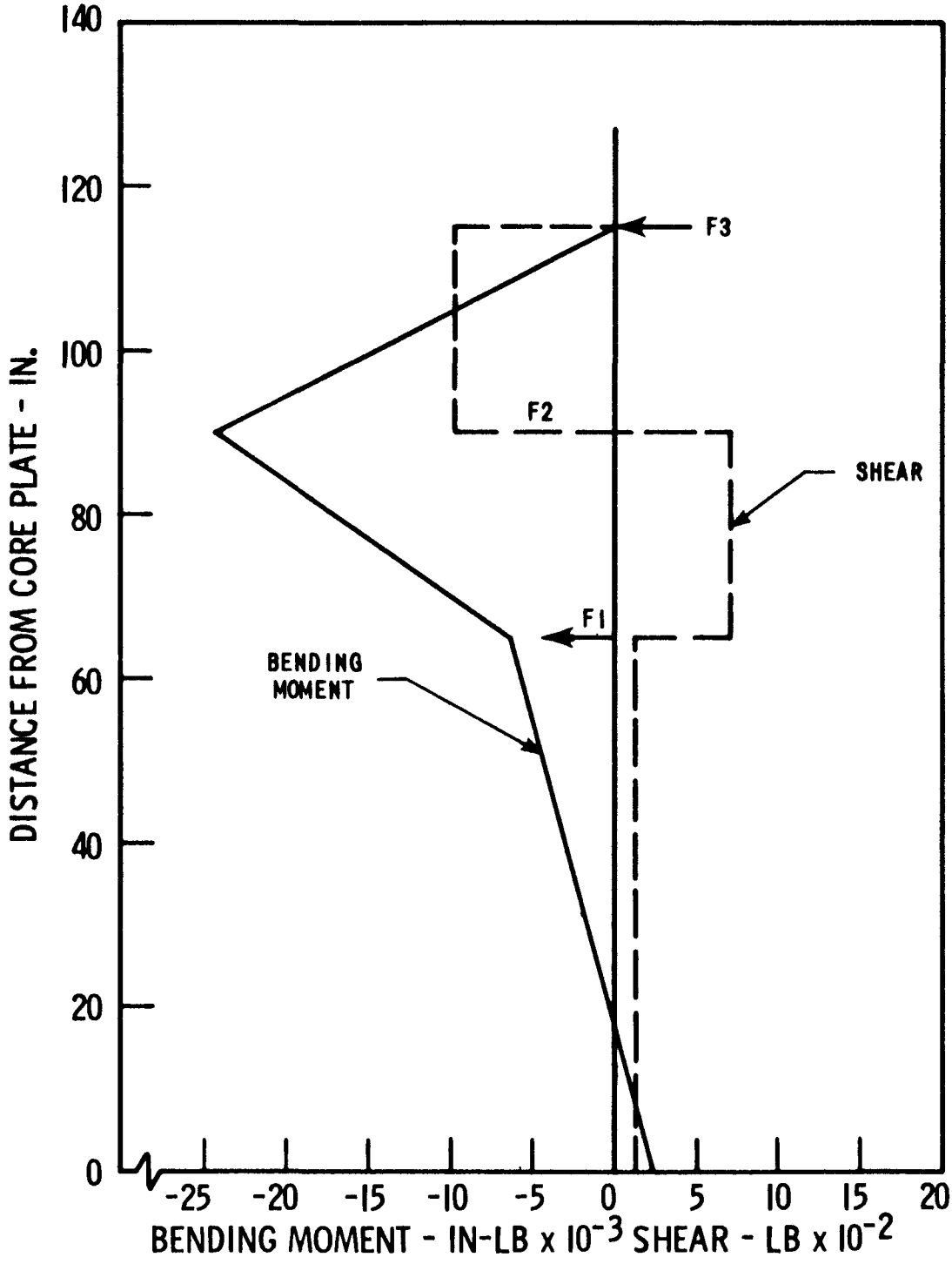

SHEAR AND MOMENT DISTRIBUTION
IN REFERENCE FUEL ASSEMBLY CAN

Figure III.4-18

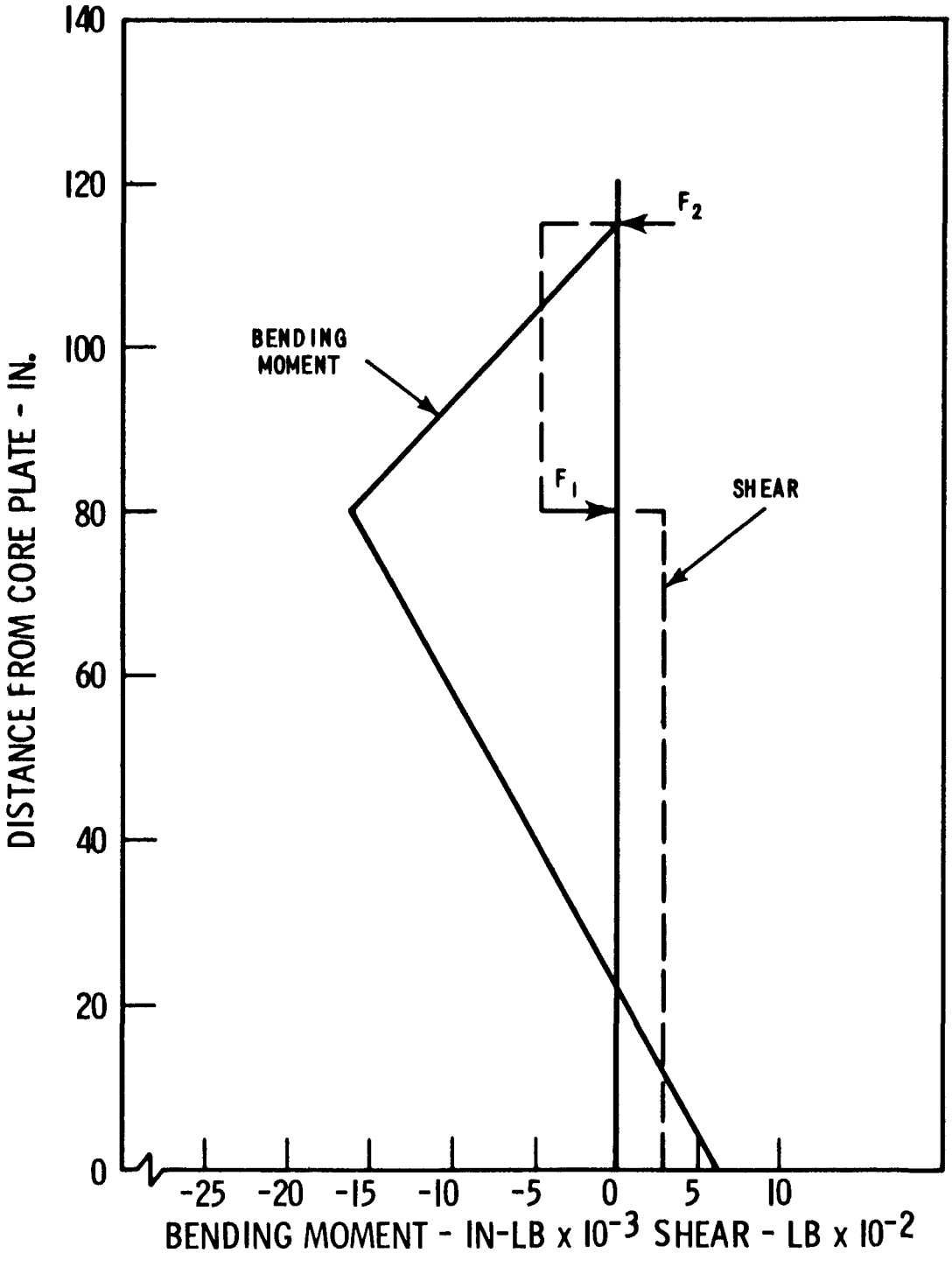

SHEAR AND MOMENT DISTRIBUTION IN ALTERNATE FUEL ASSEMBLY CAN

Figure III.4-19

Coolant mixing schemes must be devised to obtain adequate coolant mixing between ceramic fuel rods and cermet fuel rods. Schemes which will enhance transverse mixing of the coolant across the fuel assembly, thereby reducing fuel bundle bowing, are also required.

References Section III.4

1. Hankel, "Stress and Temperature Distributions", Nucleonics, Vol. 18, No. 11, Nov. 1960, p. 168.

2. Roark, "Formulas for Stress and Strain", Third Edition, McGraw-Hill Book Co., New York, 1954, p. 138.

3. APDA-124. "Enrico Fermi Atomic Power Plant", January 1959.

4. Meck, "An Approximate Analysis of Beam Deflection in Creep Bending", ASME 64-WA/MET-9.

5. ANL-5577, "Some Problems in the Safety of Fast Reactors", R. O. Brittan.

6. ANL-6266, "Instability Studies with EBR-I, Mark II", R. R. Smith, et al.

7. APDA-128, "Thermal Bowing of Core Subassemblies", A. de Stordeur.

8. ANL-5719, "Hazard Summary Report Experimental Breeder Reactor II (EBR-II)", E. J. Koch, et al.

9. "Thermal Bowing of Fuel Rods During Transients", W. K. Ergen, Journal of Nuclear Energy, Parts AIB, Vol. 18, pp. 537-545.

10. TRG Report 863(S), "The Problem of the Restrained Bowing of a Nuclear Fuel Element", W. N. Miller.

III.5 Transient Analyses

III.5.1 Scope of Work

The scope of work of the transient analyses consisted of performing analytical, parametric studies to determine and to evaluate the transient performance characteristics of a controlled expansion fuel element (CEX) in a large fast breeder reactor. The Westinghouse AEC-1000 MWe FBR Study[1] core and CEX fuel assembly design with an uprated power density and lower operating temperatures as outlined in WCAP-2638[2] (see Section III.1), were adopted as the reference design for these analytical studies. The analyses also included simulating several postulated accidents that might occur in the reference reactor[1,2]. These studies were performed using the Westinghouse version of the FORE[3] digital computer program, which was modified to investigate the controlled expansion fuel assembly dynamic performance. The transient analyses did not include full reactor systems transient studies.

In order to properly perform this evaluation of the CEX concepts, the parameter study in the above scope of work included a study of the effect of the cermet rod diameter on the transient behavior of the CEX assembly, the behavior of a controlled expansion fuel assembly in a gas bonded oxide fueled core, and the behavior of clad expansion in a sodium bonded carbide fueled compartmented core. In the ceramic fuel rod design, the stack of active fuel pellets are divided among compartments so that the fuel will move with the cladding. The clad is stainless steel, whose expansion behavior is well known and predictable and should provide ceramic fueled cores with a dependable axial expansion characteristic during transient conditions. In the carbide core, the sodium bonding increases the carbide fuel-clad conductance sufficiently to give a time constant less than 0.5 seconds for the heat being generated in the fuel to reach the clad. The clad thus has a response fast enough to be a major contributor in terminating a power excursion.

For clarity in latter discussions, the controlled expansion using cermet rods to move the fuel bundles is designated BCEX, and the controlled expansion using clad expansion of compartmented fuel is designated CCEX.

III.5.2 Computer Code Modifications

The Westinghouse version of the digital computer program FORE[3] was modified, as part of this study, to investigate the dynamic behavior during a power excursion of the controlled expansion assembly utilizing cermet rods to obtain predictable axial expansion. The Westinghouse program was checked with the available errata and addenda sheets[4,5,6] to insure that all recommended corrections and modifications existed in the Westinghouse program. Other program corrections were also made. For example, the error in the calculation of the radial node point temperatures in the fuel rod at zero time was corrected.

To incorporate the fuel assembly controlled expansion feature into the program, extensive modifications were made to the major subroutines. All heat transfer and coolant heat balance equations were changed from the basis of a single rod to a mixed multi-rod, fuel and cermet, array as would exist in the reference CEX fuel assembly[1]. The new equations were derived assuming that the fuel rods and the cermet rods in an assembly see the same coolant temperature, that is, 100% mixing of the coolant exists between the ceramic fuel and cermet rods. The maximum number of axial core sections employed in calculating temperatures was increased to six. The temperature within the fuel and the cermet are calculated for the same number of radial node points (a maximum of nine and a minimum of five) as described in reference (3). The code programming was simplified to save computer drum storage, and to reduce computer running time.

The reactivity feedback for the BCEX fuel assembly accounts for the negative outward axial effects due to the cermet expansion pushing the

two core halves (bundles) apart, as well as for the positive effect from the inward fuel movement due to thermal expansion. By an input option, this fuel* movement due to thermal expansion is calculated by using either changes in the fuel average temperature or the clad average temperature for the case of compartmented fuel. The change in length of the fuel and cermet rods are calculated and printed out to allow a study of the gap clearance between fuel bundles as a function of time. The utilization of the other reactivity feedbacks, Doppler, coolant density, and so forth, remain unchanged from that given in references 3, 4, 5, and 6. The reactivity effects from the thermal bowing of the fuel rods and fuel cans and the clad restraint on the cermet expansion are not included in the computer program.

The input, termination, and output subroutines were simplified and modified as required for the cermet rod. Any number of problems can be run, one after the other, through the use of overlay cards which modify the full data deck read in with the first problem.

The capability of the Westinghouse version of the FORE[3] code is markedly increased by these modifications. The code can now consider an all-fuel rod or an all-cermet rod assembly, as well as a mixed multi-rod assembly with its combinations of negative and positive reactivity effects. An additional feature of this code provides for a programmed reactor scram** based on an input reactor power setting with a scram control circuit delay time.

---

* In the subsequent discussion in this section, "fuel" refers to the ceramic fuel, i.e., either carbide or oxide whichever is being considered.

** This reactor scram modification was completed prior to the beginning of the modifications for the controlled expansion assembly and prior to the CEX project initiation.

The program calculates the reactor power and the fuel, cermet, clad and structure temperatures as a function of time in response to a programmed reactivity insertion. Lumped radial temperature profiles are computed in specific axial sections, (maximum of 6) for the average and peak power fuel and cermet rods. Constant axial-wise volumetric heat generation is assumed in each axial section. The heat of fusion which accompanies melting is taken into account for the fuel rods only. A sample problem with its computer output is described in Appendix E.

III.5.3 Nuclear, Thermal, and Materials Parameters

The core geometry data used in the transient analyses is given in Table III.5-1. The fuel rod linear power, kw/ft, in the oxide-fueled core was one-half of that in the carbide fueled core. The fuel pellet diameter in the oxide core was selected to make the fuel volumetric heat generation rate, kw/ft^3 of fuel, identical to that in the carbide core. Thus the volumes of fuel and cermet in each core are identical.

The nominal cermet rod diameter in the BCEX analyses was made identical to the respective fuel rod diameter, or 0.300 inches in the carbide fueled core and 0.215 inches in the oxide fueled core. In addition, in BCEX, the cell flow area around the cermet rods was adjusted to obtain the same coolant temperature rise along the cermet rod as along the fuel rod even if zero coolant mixing occurs within the assembly. To accomplish this, the cermet rod outer diameter, for a cermet volumetric heat generation rate of 30% of that of the fuel, was increased to 0.360 inches in the carbide core and to 0.260 inches in the oxide core. For additional studies, the cermet rod diameter in the oxide core was further increased to 0.300 inches, the maximum diameter which will fit within the rod array.

In the BCEX parametric investigations, the cermet volumetric heat generation rates studied were 20%, 30%, and 40% of that of the fuel pellet value. From these analyses, a 30% relative heat generation rate was selected for the BCEX cermet rod for the accident analyses.

Table III.5-1

Core Data Summary

	Carbide	Oxide
Core active height, inches	72	72
Fuel rod O.D., inches	0.300	0.215
Clad thickness, mils	10	10
Fuel pellet diameter, inches	0.268	0.190
Total fuel volume, ft^3	10.2	10.2
Fuel rod linear power, kw/ft	15.6	7.8
Heat generation rate, kw/ft^3 of fuel	39,800	39,800
Type of fuel clad bond	sodium	gas
Fuel-clad conductance, $Btu/hr\text{-}ft^2\text{-}°F$	72,000	2,000
Clad-coolant heat transfer coefficient, $Btu/hr\text{-}ft^2\text{-}°F$	15,000	15,000
Coolant temperature, 100% power		
Inlet	850	850
Outlet (mixed-mean)	1100	1100
BCEX cermet rod O.D., inches	0.300-0.360	0.215-0.260-0.300
BCEX cermet rod clad thickness, mils	10	10
Cermet diameter, inches	0.280-0.340	0.195-0.240-0.280
Total cermet volume, ft^3	0.65-0.95	0.65-0.95-1.29
Cermet-clad conductance, $Btu/hr\text{-}ft^2\text{-}°F$		
Metallurgical bond	100,000	100,000
Gas bond	1,000	---

The physical properties of the core materials, fuel, cermet, cladding, and coolant, are given in Table III.5-2. The temperature limits used in the analyses for computer problem terminations are assumed to be indicative of onset of core damage, and were thus set higher than either the melting or boiling point temperatures listed in Table III.5-2.

Using the material properties given in Table III.5-2, and the fuel rod diameters, clad thickness, and heat transfer coefficient given in Table III.5-1, the time constants associated with transient heat transfer are given in Table III.5-3. The time constant is defined as the ratio of heat capacitance to heat conductance. The carbide fuel rod time constant is approximately two-thirds of the cermet rod value, whereas the oxide fuel rod is nearly 2.6 times greater. Within the cermet rod, the time constant associated with the transient heat conduction between fuel particles with average diameter of 6 mils and the stainless steel matrix is approximately 1 millisecond, which is small relative to the time increments studied in this investigation.

The values used in this study for the temperature dependent reactivity coefficients for the reference FBR core at the start of an equilibrium fuel cycle (33,300 MWD/T) are given in Table III.5-4. An axial distribution was applied to the sodium density coefficient as given in the footnote of Table III.5-4. The oxide core overall dimensions, diameter and height, are essentially identical to the carbide core. The same reactivity coefficients were used in the oxide core analyses in order to have a common basis for comparing its transient characteristics to those of the carbide fueled core. For the fuel clad axial expansion CCEX analyses, the fuel is assumed to be in compartments and move with the clad. The CCEX coefficient, $Hdk/dH = -0.394$, is an overall expansion coefficient based on total change in core height and the corresponding change in material densities. Distributing the CCEX's axial expansion coefficient according to the axial fuel compartment was not considered in the analyses. For the reference core, the neutron life time is

Table III.5-2

Material Physical Properties Used in the Transient Analyses

	Density lbs/ft^3	Specific Heat Btu/lb	Thermal Conductivity Btu/hr-ft-°F	Linear Expansion 10^{-6}/°F	Melting or Boiling Point °F
a. Fuel					
1. Carbide, (Pu-U)C	785.1	0.0733(A)	11.43(A)	8.0(E)	4200(G)
2. Oxide, (PU-U)O_2	630.1	0.080(C)	1.49(B)	---	5000(G)
b. Clad, Fuel and Cermet	494.4	0.16	12.1	11.0	2400
c. Cermet, UO_2-SS	517.6	0.1149(B)	7.6(B)	10.0	2400
d. Coolant, Sodium	51.2	0.30	38.3(D)	57.3	1800(F)

(A) Value at 1400°F. In analyses is a function of temperature.

(B) Value at 1200°F. In analyses is a function of temperature.

(C) Value at 2000°F. In analyses is a function of temperature.

(D) Value at 900°F.

(E) Not used in calculating axial thermal expansion in the transient analyses.

(F) Value at approximately two atmospheres pressure.

(G) Average value in range of (Pu,U) composition of interest.

Table III.5-3

Time Constants

Defining the time constant as:

$$\frac{\rho\, c_p\, V}{U\, A_{surface}} = \frac{\text{Heat capacitance}}{\text{Heat conductance}}$$

	From Location of Average Fuel Temperature (at r/R_o = 0.7) to Clad Midpoint	From Location of Average Fuel Temperature (at r/R_o = 0.7) to Coolant
Carbide pellet (0.268 inches)	0.47 sec.	0.57 sec.
Oxide pellet (0.190 inches)	2.08 sec.	2.15 sec.
Cermet (0.300 inch O.D.)	0.79 sec.	0.91 sec.

Table III.5-4

Reactivity Coefficients Used in Transient Analyses

Beginning of equilibrium fuel cycle in carbide core, 33,333 MWD/T

Doppler, T dk/dT	-0.00335
Sodium, $\rho dk/d\rho$*	+0.0164
Expansion, H dk/dH	
A. BCEX	
1. Cermet	-0.762
2. Clad, fuel rod	+0.368
B. CCEX	
1. Clad, fuel rod	-0.394

*In the analyses, the sodium density coefficient was given an axial distribution for the core's 6 axial sections as follows:

	$\rho dk/d\rho$
First one-sixth (inlet)	+0.003448
Second one-sixth	+0.002720
Third one-sixth	+0.001994
Fourth one-sixth	+0.001981
Fifth one-sixth	+0.002720
Sixth one-sixth (outlet)	+0.003541
Total	+0.0164

3.5×10^{-7} seconds, and the effective delay neutron fraction, β, is 0.00364. In the analyses, six groups of delayed neutrons were used.

III.5.4 Parameter Study

The results of the parameter study on both the oxide and carbide fueled cores will be discussed first, followed by a comparison of the performance of BCEX and CCEX in the carbide and oxide cores. The reference reactor used to measure the improvement in the transient behavior of a core due to BCEX or CCEX is one with zero axial expansion reactivity coefficients that is, a core containing only Doppler and sodium density reactivity feedbacks.

In the parameter study, the material physical properties and the axial expansion coefficients for BCEX or CCEX were not varied. In the BCEX analyses for the carbide core, the Doppler and sodium density coefficients were varied to better understand the worth of BCEX in terminating an excursion.

In the parameter study, finite ramp reactivity insertions of eighty cents and two dollars were used. The ramps were terminated either at 0.1 second or at 1.0 second, after which the inserted reactivity was held constant at the above values. The selected amounts of inserted reactivity represent the approximate worth of some core components such as a control rod or fuel assembly. In addition, the two insertions allow the BCEX and CCEX performance characteristics to be studied above and below prompt criticality. Finally, the insertion times are characteristic of the time period associated with an incident involving a core component.

The computer runs for the parameter analyses were set to terminate either at seven seconds in real time, or after exceeding one of the temperature or power upper limits given in Table III.5-5. The temperature limits were checked in axial section number 5 (5 of 6) in the hot

Table III.5-5

Terminating Limits for Transient Analyses[a]

Name	Carbide Fuel	Oxide Fuel
1. Thermal power, 10^8 Mw	1.0	1.0
2. Fuel center temperature, °F	6000	8000
3. Fuel average temperature, °F	5500	7500
4. Fuel surface temperature, °F	5000	7000
5. Coolant temperature, °F	2000	2000
6. Cermet center temperature, °F	2400	2400
7. Cermet average temperature, °F	2400[b]	2400[b]
8. Cermet surface temperature, °F	2400[b]	2400[b]

Notes:

(a) The temperature values selected for problem termination are above the melting point of the respective fuel and are above the published values for fuel rod failure; for example 6500°F for $(Pu,U)O_2$. The selected values permit the center portion of the fuel pellet to become molten. The computer code considers the heat of fusion during melting.

(b) Lower temperature values, if desired, may be specified in input data.

channel. The limits were selected as being somewhat in excess of the conditions at which core damage would occur.

III.5.4.1 Carbide Fueled Core

Analyses were performed on the reference reactor core using the stated reactivity insertions for the three BCEX cermet volumetric heat generation rates and for the CCEX-clad axial expansion case. In the 80 cents in 0.1 second analyses, the BCEX cermet rod diameter was increased from 0.300 inches to 0.360 inches which, as noted previously, is the suggested cermet rod diameter along with a BCEX cermet heat generation rate of 30% of the fuel. In addition, to study the performance of gas-bonded cermet, the cermet-clad interface conductance was decreased from the value for a metallurgical bond, 100,000 Btu/hr-ft^2-°F, to the value for a gas bond, 1000 Btu/hr-ft^2-°F. This latter analysis was performed on a cermet rod with a 40% heat generation rate and a 0.300 inch diameter.

The total reactivity feedback, Δk, from all temperature dependent mechanisms is shown in Figure III.5-1 for the 80 cents in 0.1 second reactivity ramp, in Figure III.5-2 for the 2 dollars in 0.1 second ramp, and in Figure III.5-3 for the 2 dollars in 1.0 second ramp. Figure III.5-1 shows that after 1 second, the total reactivity feedback is increased, as expected, from the reference core (no BCEX - no CCEX) by increasing the BCEX volumetric heat generation rate, by increasing the cermet rod diameter, and by decreasing the BCEX cermet-clad interface conductance. In Figure III.5-2, the total reactivity feedback for all BCEX heat rates from the end of the ramp insertion, 0.1 seconds, to approximately 0.4 seconds, falls below both the no-CEX reactor core as well as the CCEX reactor core. In the following discussion, this phenomenon will be shown to result from the feedback characteristics of BCEX. The large feedback in the no BCEX - no CCEX core is due simply to the much higher temperatures which were obtained in this reactor relative to the other cores. The total feedback characteristics for the 2 dollars in 1.0 second ramp, Figure III.5-3, were not clearly established as the analyses

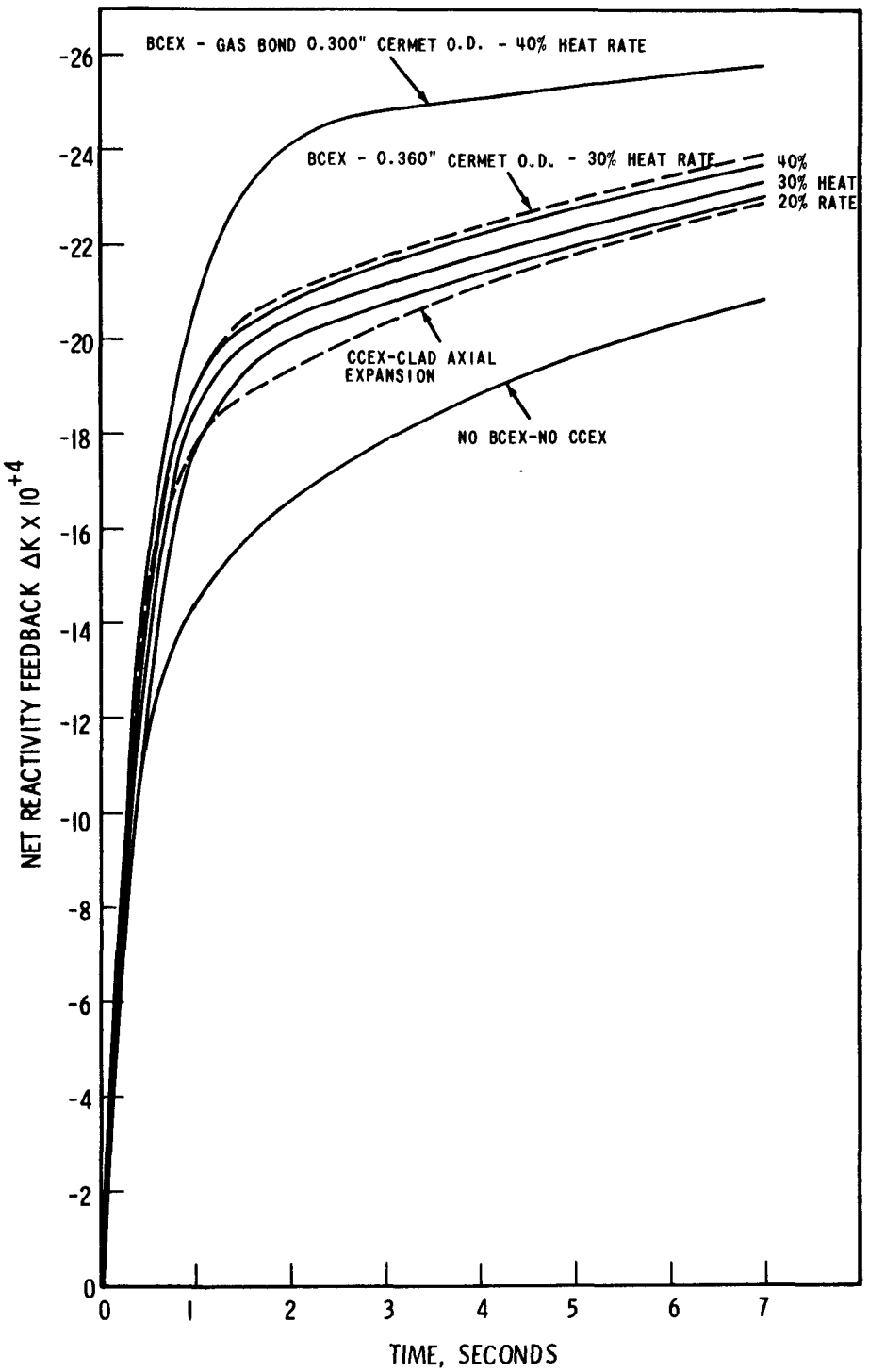

TOTAL REACTIVITY FEEDBACK
CARBIDE FUELED CORE
RAMP REACTIVITY INSERTION 80 CENTS IN 0.1 SECONDS
CARBIDE FUEL ROD DIAMETER 0.300 INCHES
BCEX CERMET ROD DIAMETER 0.300 INCHES

Figure III.5-1

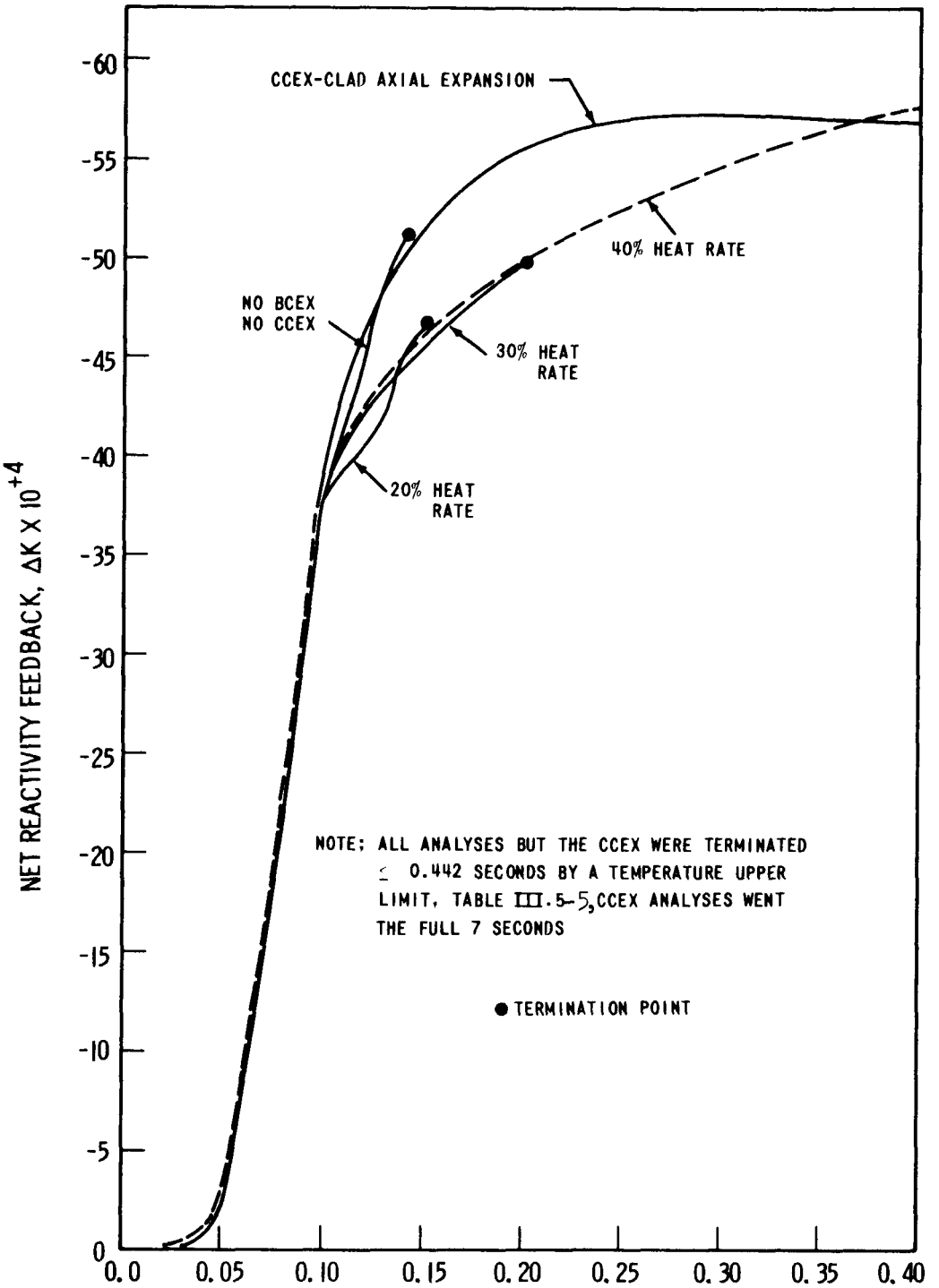

TOTAL REACTIVITY FEEDBACK
CARBIDE FUELED CORE
RAMP REACTIVITY INSERTION 2$ IN 0.1 SECONDS
CARBIDE FUEL ROD DIAMETER 0.300 INCHES
BCEX CERMET ROD DIAMETER 0.300 INCHES

Figure III.5-2

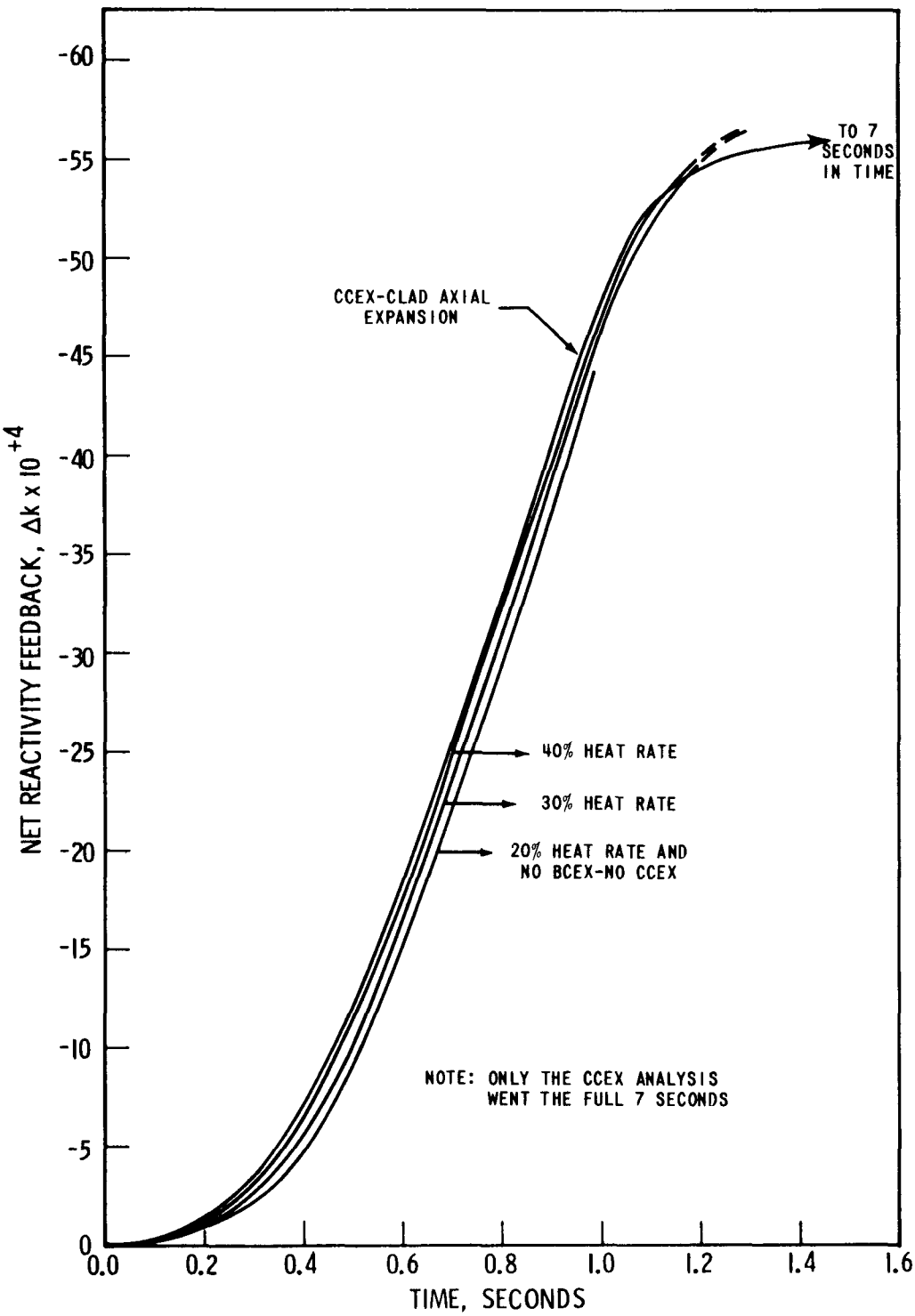

TOTAL REACTIVITY FEEDBACK-CARBIDE FUELED CORE
RAMP REACTIVITY INSERTION 2$ IN. 1.0 SECOND
CARBIDE FUEL ROD DIAMETER 0.300 INCHES
BCEX CERMET ROD DIAMETER 0.300 INCHES

Figure III.5-3

encountered various terminating temperature limits. However, the trend appears to be quite similar to that encountered with the 80 cents in 0.1 second insertion, Figure III.5-1.

In Figure III.5-1 below 0.6 seconds, and in Figure III.5-3 below 1.1 seconds, the CCEX total reactivity feedback exceeds the metallurgically bonded BCEX total feedback, for all heat generation rates and rod diameters studied. The gas bonded BCEX at 40% relative heat rate is the only case studied which exceeds the CCEX feedback during these times, (see Figure III.5-1).

As can be seen in Figure III.5-1 after 1 second, the CCEX reactivity feedback falls slightly below that obtained with the 20% cermet heat rate (for the 0.300 inch BCEX cermet rod). This trend is indicated in Figure III.5-3 for the 2 dollars in 1.0 second insertion. Thus, the BCEX may give a significant negative reactivity feedback gain, depending on the reactivity insertion rate, to a core having no axial expansion feedback, and, at most, only a marginal negative reactivity feedback gain to a core having a predictable clad axial expansion feedback (CCEX).

The cermet outward expansion and the fuel clad inward expansion, the two components which comprise the BCEX reactivity feedback, are shown in Figures III.5-4, III.5-5, and III.5-6, for the three reactivity insertions studied. In all the analyses performed, in the first 0.1 second, as best illustrated in Figure III.5-5, the BCEX net reactivity feedback is more negative than that of the CCEX. This is due to the relatively instantaneous response of the cermet with respect to that of the clad. During the time period between 0.1 and 1.0 seconds in all the analyses, the fuel clad expands more rapidly than the cermet, thus causing the BCEX net reactivity feedback to be less negative than that of the CCEX. This latter time period is the important time period for excursion termination. In fact, for the 2 dollars insertion in 0.1 seconds, shown in Figure III.5-5, the fuel clad expands at a rapid enough rate to hold the BCEX net reactivity essentially constant

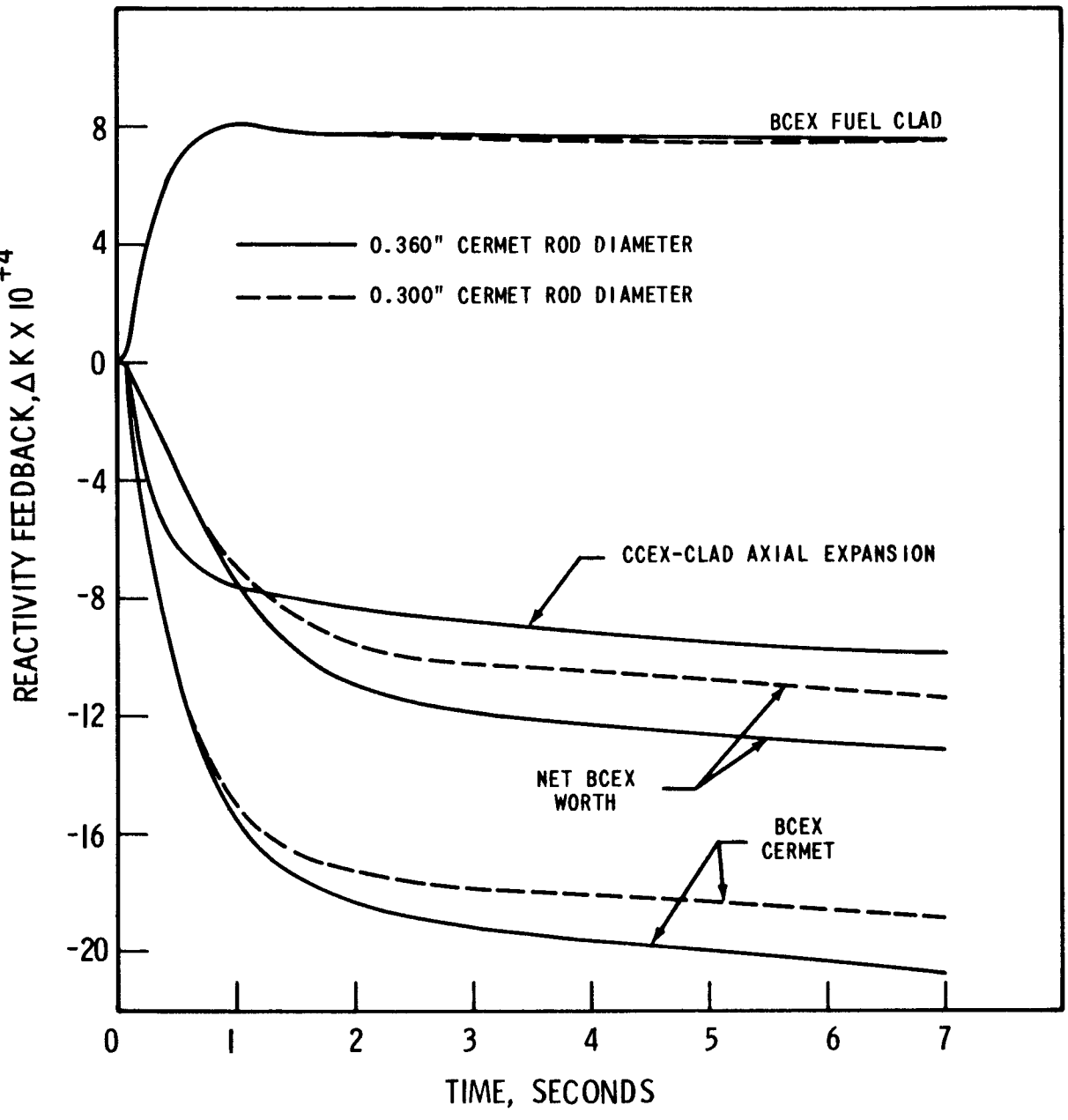

BCEX PERFORMANCE IN CARBIDE FUELED CORE-BCEX ROD DIAMETER EFFECT-BCEX HEAT GENERATION RATE 30% OF THE FUEL-RAMP REACTIVITY INSERTION 80 CENTS IN 0.1 SECONDS-CARBIDE FUEL ROD DIAMETER 0.300 INCHES

Figure III.5-4

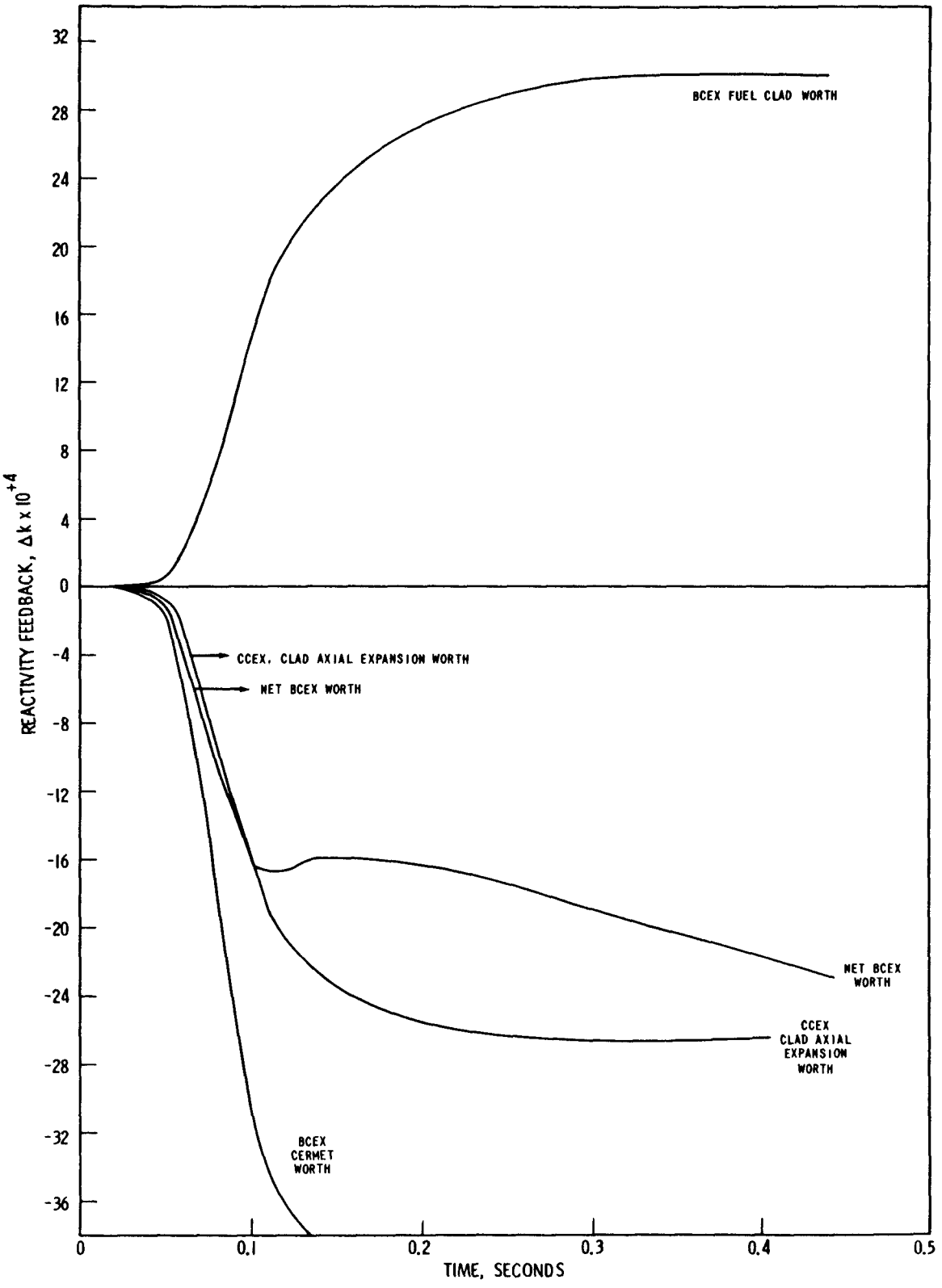

BCEX PERFORMANCE IN CARBIDE FUELLED CORE - BCEX HEAT GENERATION 40% OF FUEL
RAMP REACTIVITY INSERTION 2$ IN 0.1 SECONDS - BCEX CERMET ROD DIAMETER 0.300 INCHES
CARBIDE FUEL ROD DIAMETER 0.300 INCHES

Figure III.5-5

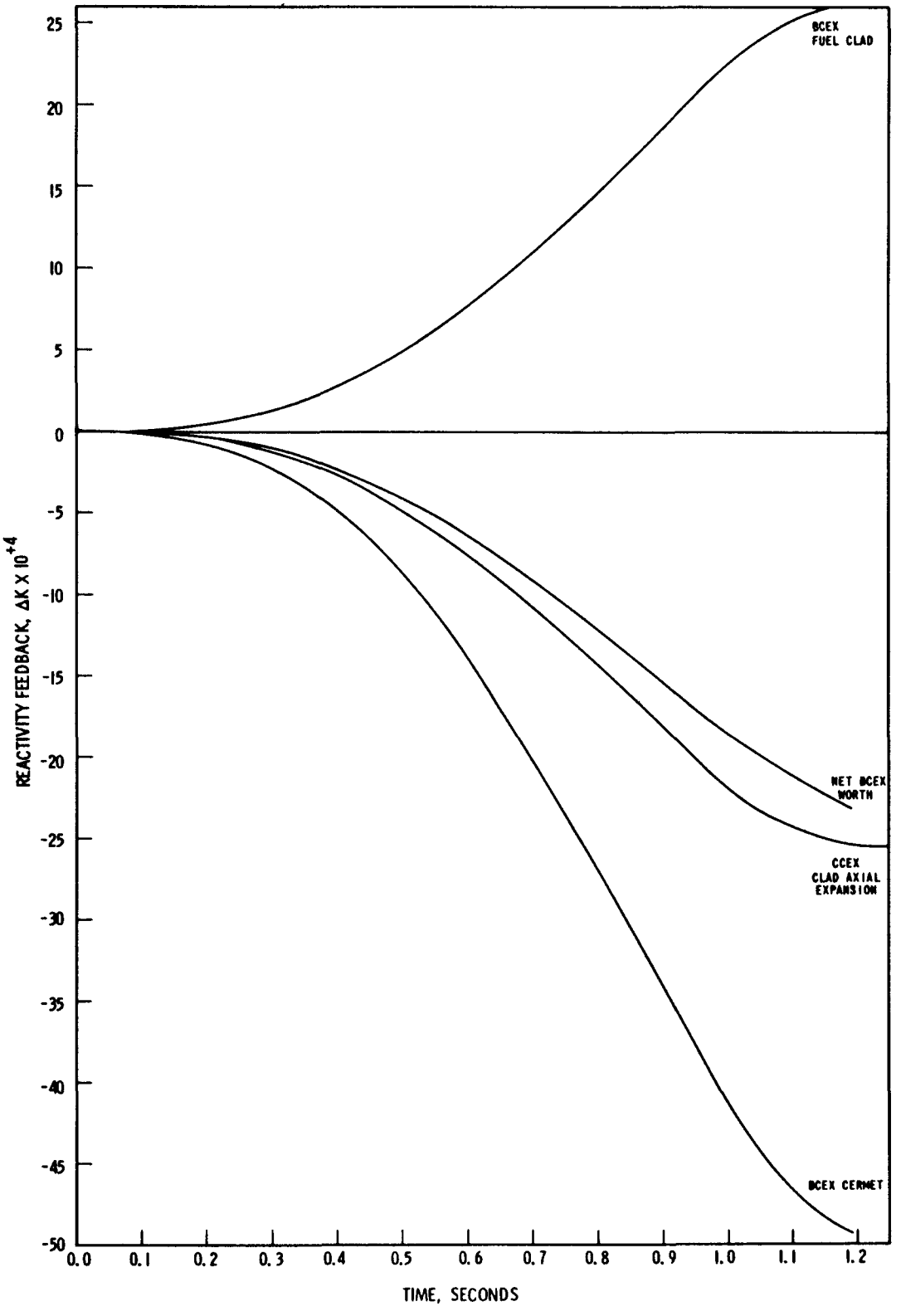

BCEX PERFORMANCE IN CARBIDE FUELED CORE
BCEX CERMET HEAT GENERATION RATE 40% OF FUEL
RAMP REACTIVITY INSERTION 2$ IN 1.0 SECOND
CARBIDE FUEL ROD DIAMETER 0.300 INCHES

Figure III.5-6

for approximately 0.150 seconds. The shorter time constant, Table III.5-3, between the carbide pellet and clad, 0.47 seconds compared to 0.79 seconds for the cermet to clad, is the reason why the fuel clad expands faster than the cermet. This same trend holds true for all the carbide core BCEX analyses, regardless of the reactivity insertion or the relative heat generation rate - as can be seen in Figure III.5-7 for an 80 cents in 0.1 second insertion. Figure III.5-7 shows the CCEX relative to BCEX behavior for a range of heat generation rates and cermet rod sizes, as well as BCEX performance with gas bonding.

The fractions of the total reactivity feedback attributed to BCEX and to Doppler for the 80 cents in 0.1 second insertion, and the effect of cermet heat generation rate, rod diameter and rod bonding, are shown in Figures III.5-8 and III.5-9. The effect of the fuel clad inward expansion, which downgrades the BCEX performance during the first second of the excursion, is clearly illustrated in Figure III.5-8. This downgrading of the BCEX fractional worth is, of course, undesirable from the standpoint of terminating the excursion. Figure III.5-9 shows Doppler to be the dominant feedback mechanism in the crucial period of the excursion. As equilibrium conditions are approached in the core, the BCEX fraction of the total feedback, for all metallurgical bonded rod diameters and cermet heat generation rates studied, increases to and remains between 0.4 and 0.55. The Doppler fraction correspondingly decreases to between 0.3 and 0.4. Thus, after the excursion has been terminated, the reactivity feedback from BCEX can be 80% greater than the Doppler feedback.

The ratio of the net BCEX reactivity to the reactivity associated with the outward expansion of the cermet rod is shown in Figure III.5-10 for the 80 cents in 0.1 second insertion. The effect of the BCEX fuel clad expansion is again clearly illustrated, as it is the difference between 1.0 and any point on a curve. Increasing the BCEX cermet rod diameter, for a given heat generation rate, decreases the clad expansion downgrading effect as the core approaches an equilibrium condition.

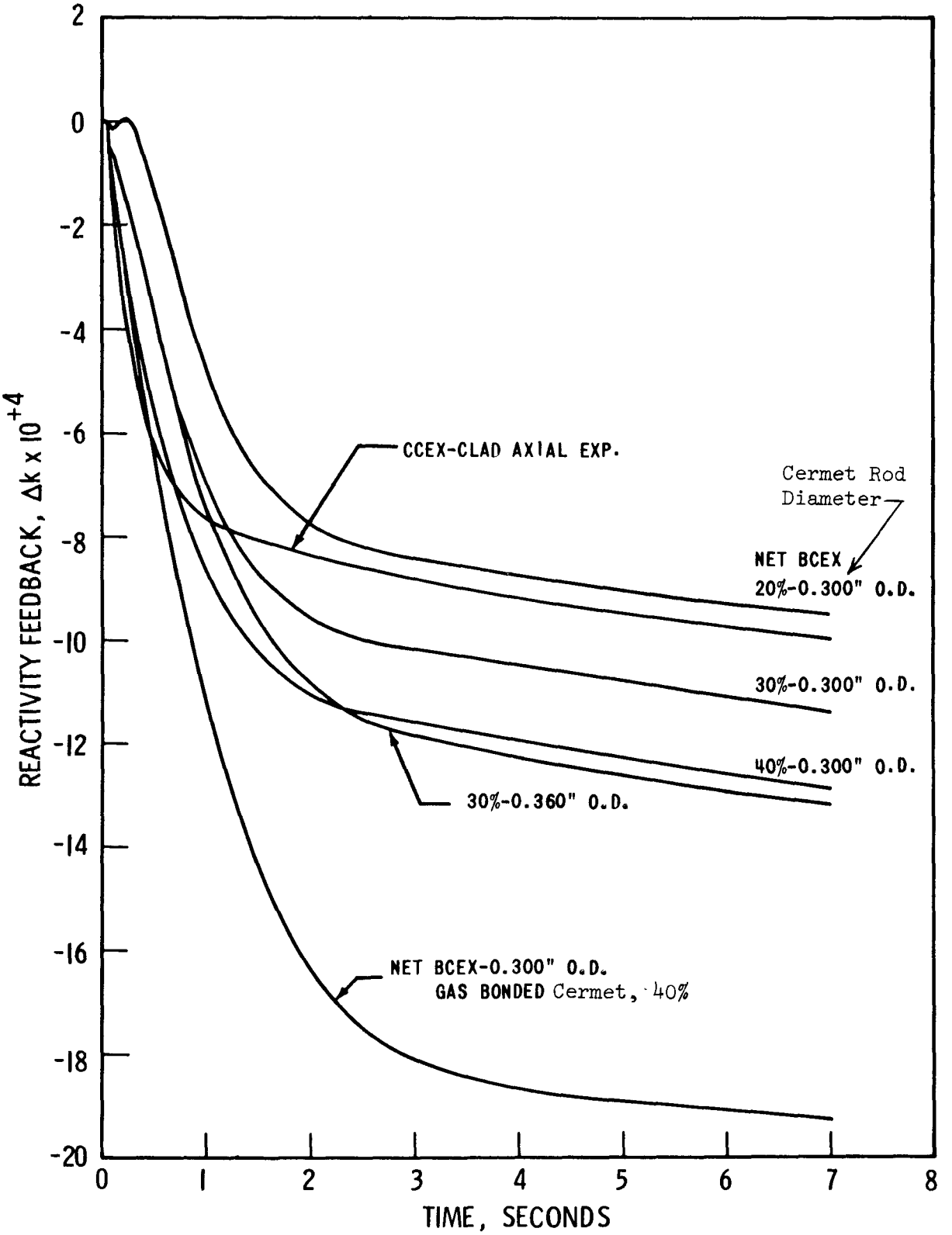

AXIAL EXPANSION REACTIVITY FEEDBACK-CARBIDE FUELED CORE
RAMP REACTIVITY INSERTION 80 CENTS IN 0.1 SECONDS
CARBIDE FUEL ROD DIAMETER 0.300 INCHES

Figure III.5-7

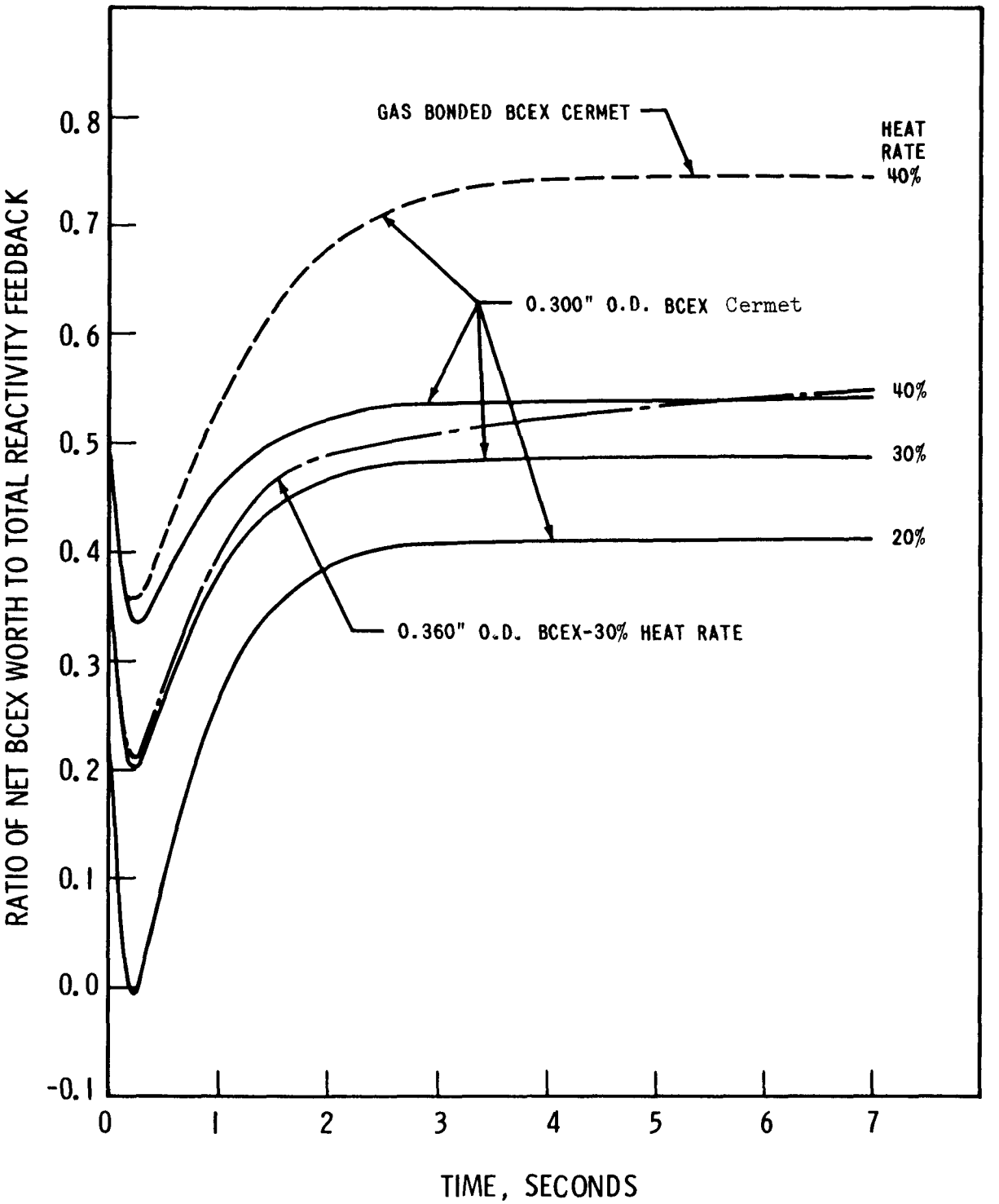

BCEX FRACTION OF TOTAL REACTIVITY FEEDBACK - CARBIDE FUELED CORE - EFFECT OF BCEX HEAT GENERATION RATE, CERMET ROD DIAMETER, AND CERMET - CLAD BONDING RAMP REACTIVITY INSERTION 80 CENTS IN 0.1 SECONDS CARBIDE FUEL ROD DIAMETER 0.300 INCHES

Figure III.5-8

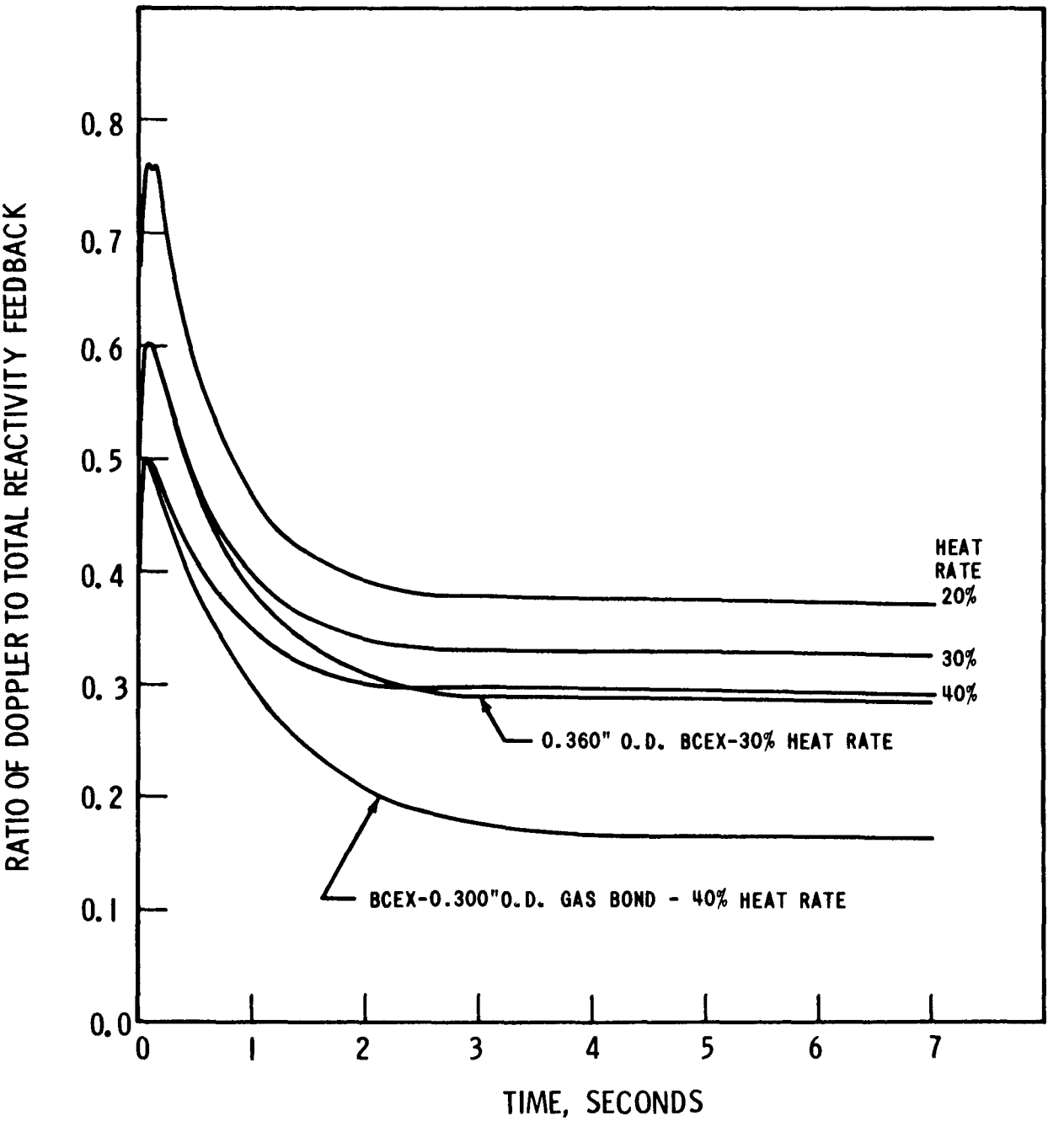

DOPPLER FRACTION OF TOTAL REACTIVITY FEEDBACK
CARBIDE FUELED CORE-RAMP REACTIVITY INSERTION
80 CENTS IN 0.1 SECONDS - CARBIDE FUEL ROD AND
BCEX ROD DIAMETERS 0.300 INCHES

Figure III.5-9

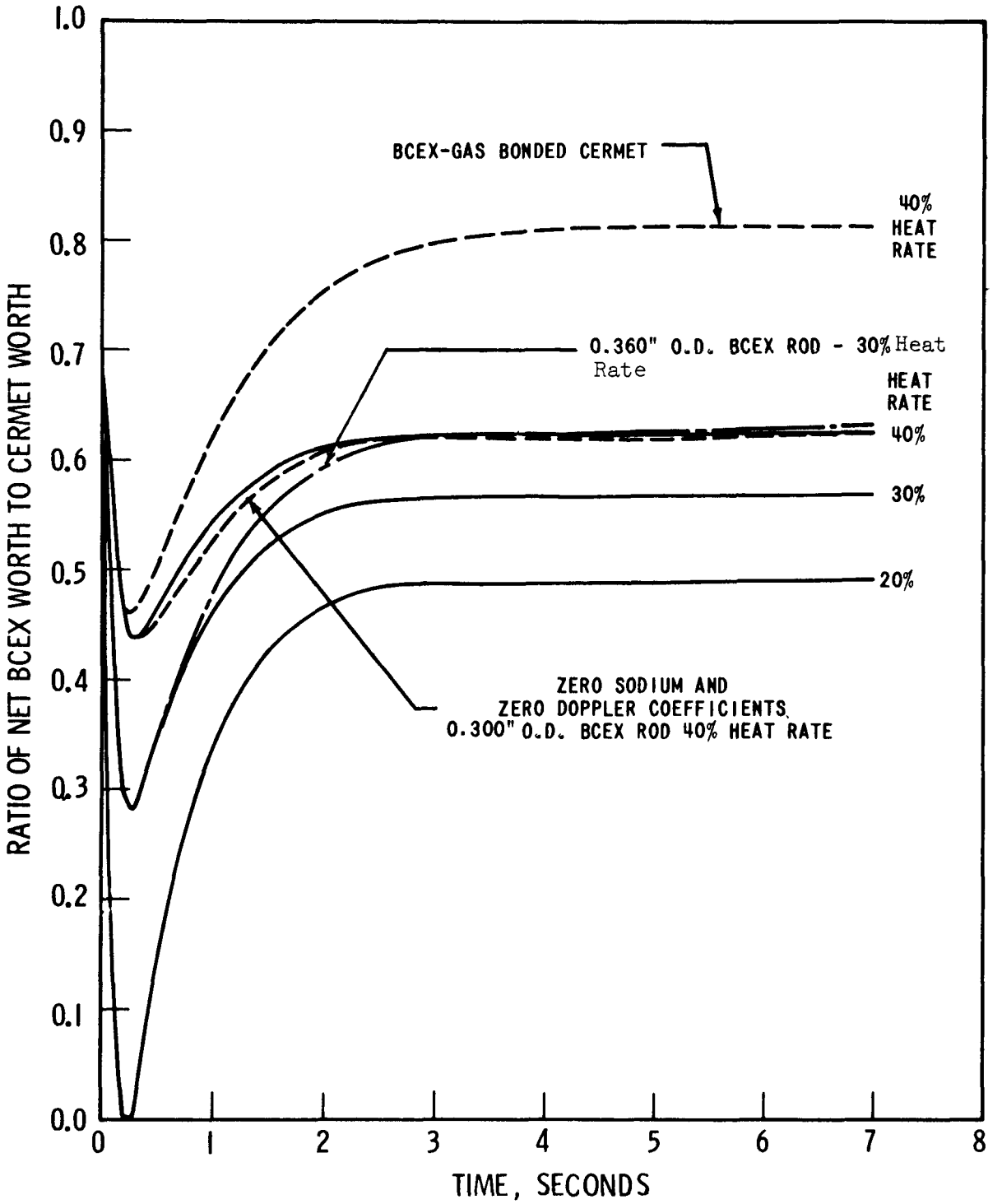

BCEX FRACTION OF CERMET WORTH-CARBIDE FUELED CORE
EFFECT OF BCEX HEAT GENERATION RATE, CERMET ROD DIAMETER,
CERMET-CLAD BONDING AND DOPPLER AND SODIUM REACTIVITY
COEFFICIENTS-RAMP REACTIVITY INSERTION 80 CENTS IN 0.1 SECONDS
0.300" O. D. CARBIDE FUEL ROD
0.300" O. D. BCEX CERMET ROD

Figure III.5-10

In all analyses performed for metallurgically bonded BCEX rods, the clad expansion downgrades the cermet expansion from 35% to 50% near the core's equilibrium conditions. Reducing the BCEX cermet-clad contact conductance to a gas bonded value (1000 Btu/hr-ft^2-°F) reduces significantly this downgrading phenomenon. For example, at a 40% heat generation rate in a 0.300 inch BCEX cermet rod, the downgrading was reduced by 50 percent (see Figure III.5-10). The improvement in the gas bonded BCEX is due to the increased temperature rise in the cermet for a given change in power resulting from the increased contact resistance between the cermet and its clad.

The net BCEX to cermet expansion reactivity ratio was found to be essentially independent of the other temperature dependent reactivity feedbacks. In the analyses, the BCEX to cermet ratio was only slightly affected when the Doppler and sodium density coefficients were set to zero (see Figure III.5-10).

The ratio of the cermet to fuel clad linear expansion is shown in Figure III.5-11. A ratio greater than unity means that the gap between the lower and upper fuel bundles has increased in width from its initial value. During an excursion in a BCEX core, it is desirable to have the gap width increase with time to maximize the reactivity worth of the core axial expansion. From Figure III.5-11, all the analyses performed show the gap width initially decreasing to a minimum value before increasing to a new equilibrium width. For the equilibrium gap width to be larger than the initial value, a relative heat generation rate in the cermet greater than 25% is required. For example, in the reference BCEX core[1], the analyses on a 0.300 inch diameter cermet rod having a 30% relative heat generation rate and an 80 cents in 0.1 second insertion show the gap width to be reduced by 27 mils at the minimum point, Figure III.5-11, while at the core's new equilibrium condition the gap width was increased by 21 mils.

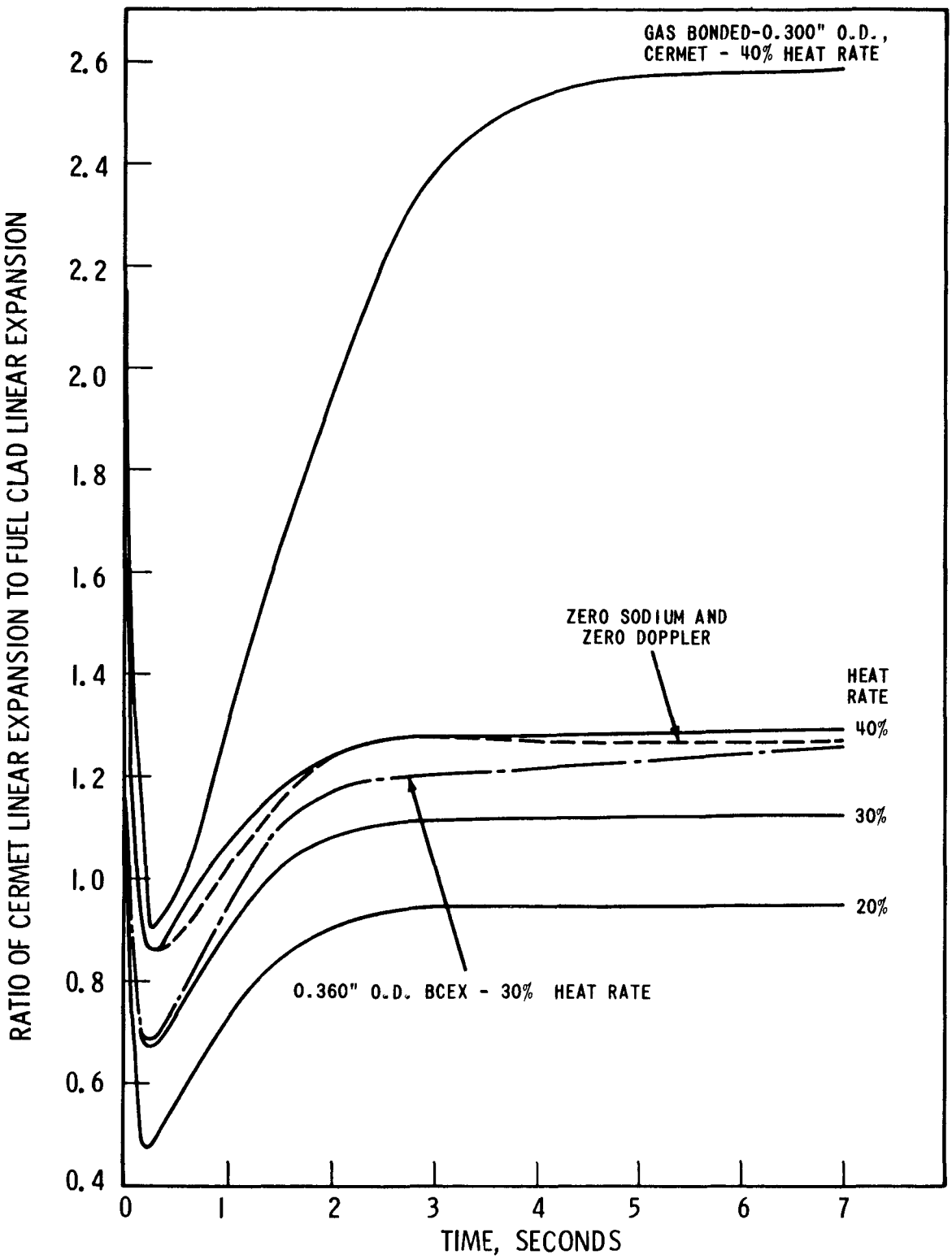

BCEX EXPANSION PERFORMANCE - CARBIDE FUELED CORE
RAMP REACTIVITY INSERTION 80 CENTS IN 0.1 SECONDS
BCEX CERMET ROD DIAMETER 0.300 INCHES - CARBIDE FUEL
ROD DIAMETER 0.300 INCHES

Figure III.5-11

The carbide fuel, cermet, fuel clad, and coolant average (integrated total length-wise) temperatures, as a function of time, are shown in Figure III.5-12 for the BCEX cermet relative heat generation rate of 30% for an 80 cents insertion in 0.1 seconds. The results for the 40% relative heat rate and the two dollar reactivity insertion are presented in Figure III.5-13 for the 0.1 second insertion time, and in Figures III.5-14(a) and III.5-14(b) for the 1.0 second insertion time. The maximum centerline temperatures of hot channel fuel for the above cases are shown in Figures III.5-15, III.5-16, and III.5-17. The introduction of axial expansion feedback reduces all the temperatures significantly. For the 80 cents in 0.1 second insertion, Figure III.5-12, the reduction in the average channel fuel maximum centerline temperature from the no BCEX - no CCEX core is 510°F for the CCEX clad axial expansion case, 570°F for the 0.300 inch O.D. BCEX rod case (30% relative heat rate), and 610°F for the 0.360 O.D. BCEX rod case (30% relative heat rate). Similarly, the average channel coolant outlet temperature drops by 210°F for CCEX case, 220°F for the 0.300 inch O.D. BCEX rod case, and 250°F for the 0.360 inch O.D. BCEX rod case.

For both two dollar insertions, only the CCEX analyses, Figures III.5-13, III.5-14(a), III.5-16, and III.5-17, were not terminated by one of the temperature upper limits given in Table III.5-5. The fuel center and coolant temperatures were the usual cause for problem termination. Thus, for reactivity insertions into the reference sodium bonded carbide fueled core[1] resulting in prompt criticality, clad axial expansion, CCEX, is more effective than BCEX in terminating the excursion. The downgrading of the cermet outward expansion by the fuel clad inward expansion, Figures III.5-5 and III.5-6, during large rapid insertions, essentially makes BCEX an ineffective excursion terminating mechanism.

The BCEX hot channel cermet maximum centerline and average temperature in axial section number 4 (4 of 6) for the three reactivity insertions are shown in Figures III.5-17, III.5-18, and III.5-19. The average

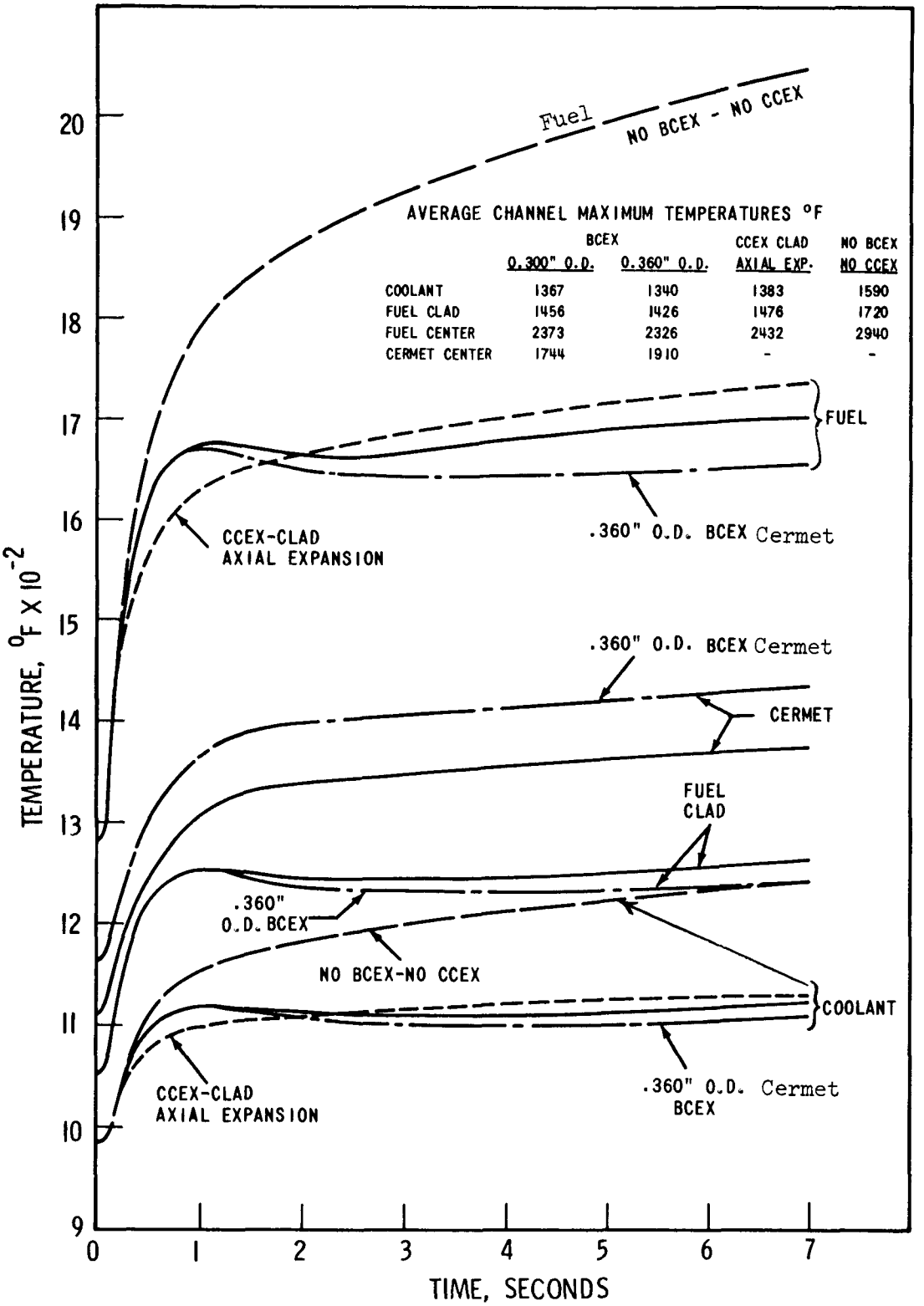

CORE AVERAGE TEMPERATURES
CARBIDE FUELED CORE
RAMP REACTIVITY INSERTION 80 CENTS IN 0.1 SECONDS
BCEX HEAT GENERATION 30% OF FUEL
BCEX CERMET AND CARBIDE FUEL ROD DIAMETERS 0.300 INCHES

Figure III.5-12

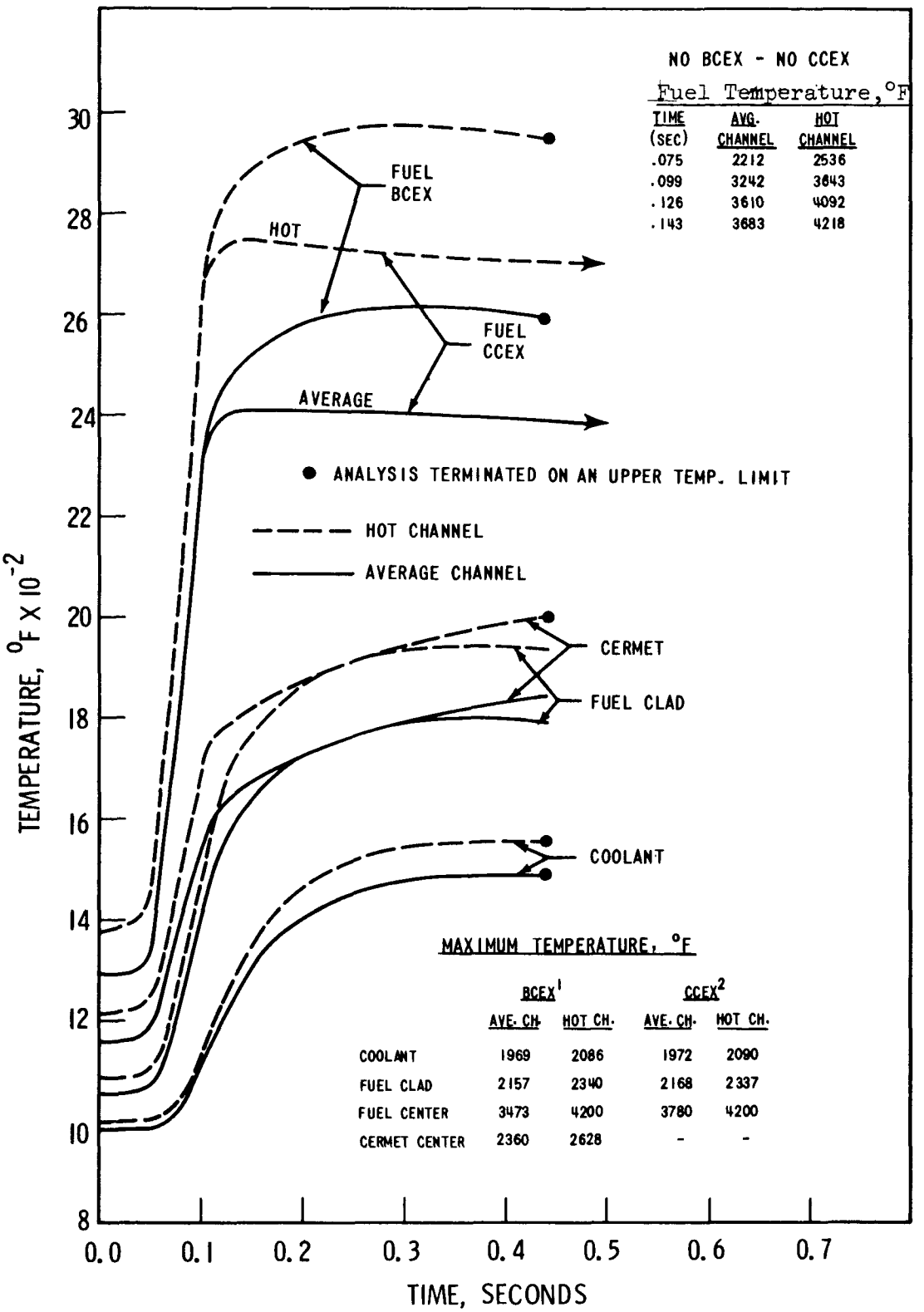

1 - TERMINATED ON CERMET TEMPERATURE LIMIT AT 0.442 SECONDS
2 - TERMINATED ON PROBLEM TIME AT 7 SECONDS

AVERAGE AND HOT CHANNELS AVERAGE TEMPERATURES CARBIDE FUELLED CORE - BCEX HEAT GENERATION 40% OF FUEL - RAMP REACTIVITY INSERTION 2$ IN 0.1 SECONDS - CARBIDE FUEL ROD AND BCEX CERMET ROD DIAMETERS 0.300 INCHES

Figure III.5-13

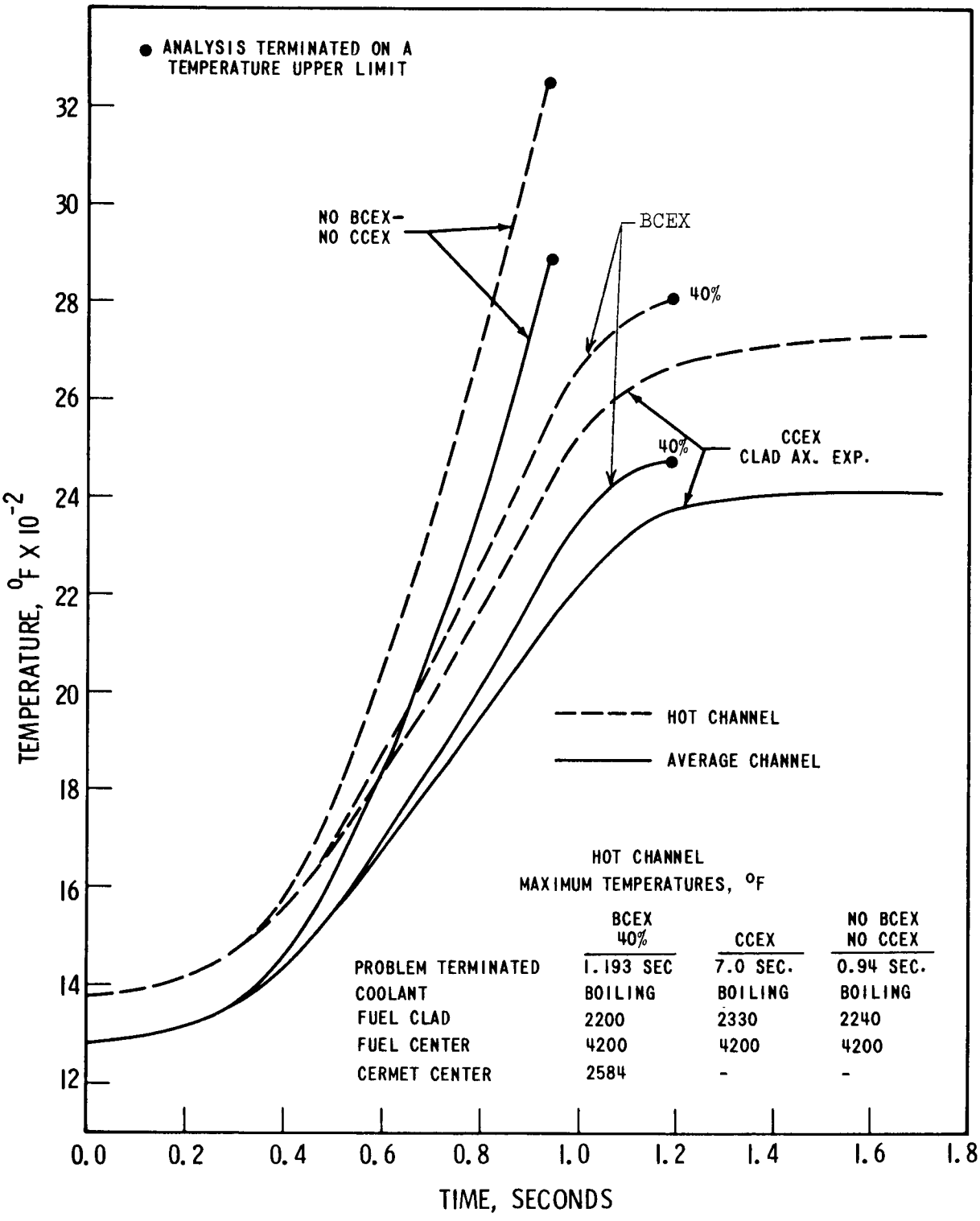

HOT CHANNEL
MAXIMUM TEMPERATURES, °F

	BCEX 40%	CCEX	NO BCEX NO CCEX
PROBLEM TERMINATED	1.193 SEC	7.0 SEC.	0.94 SEC.
COOLANT	BOILING	BOILING	BOILING
FUEL CLAD	2200	2330	2240
FUEL CENTER	4200	4200	4200
CERMET CENTER	2584	-	-

FUEL AVERAGE TEMPERATURES
CARBIDE FUELED CORE-BCEX CERMET HEAT GENERATION
40% OF FUEL - RAMP REACTIVITY INSERTION 2$ IN 1.0
SECOND-CARBIDE FUEL ROD DIAMETER 0.300 INCHES
BCEX CERMET ROD DIAMETER 0.300 INCHES

Figure III.5-14(a)

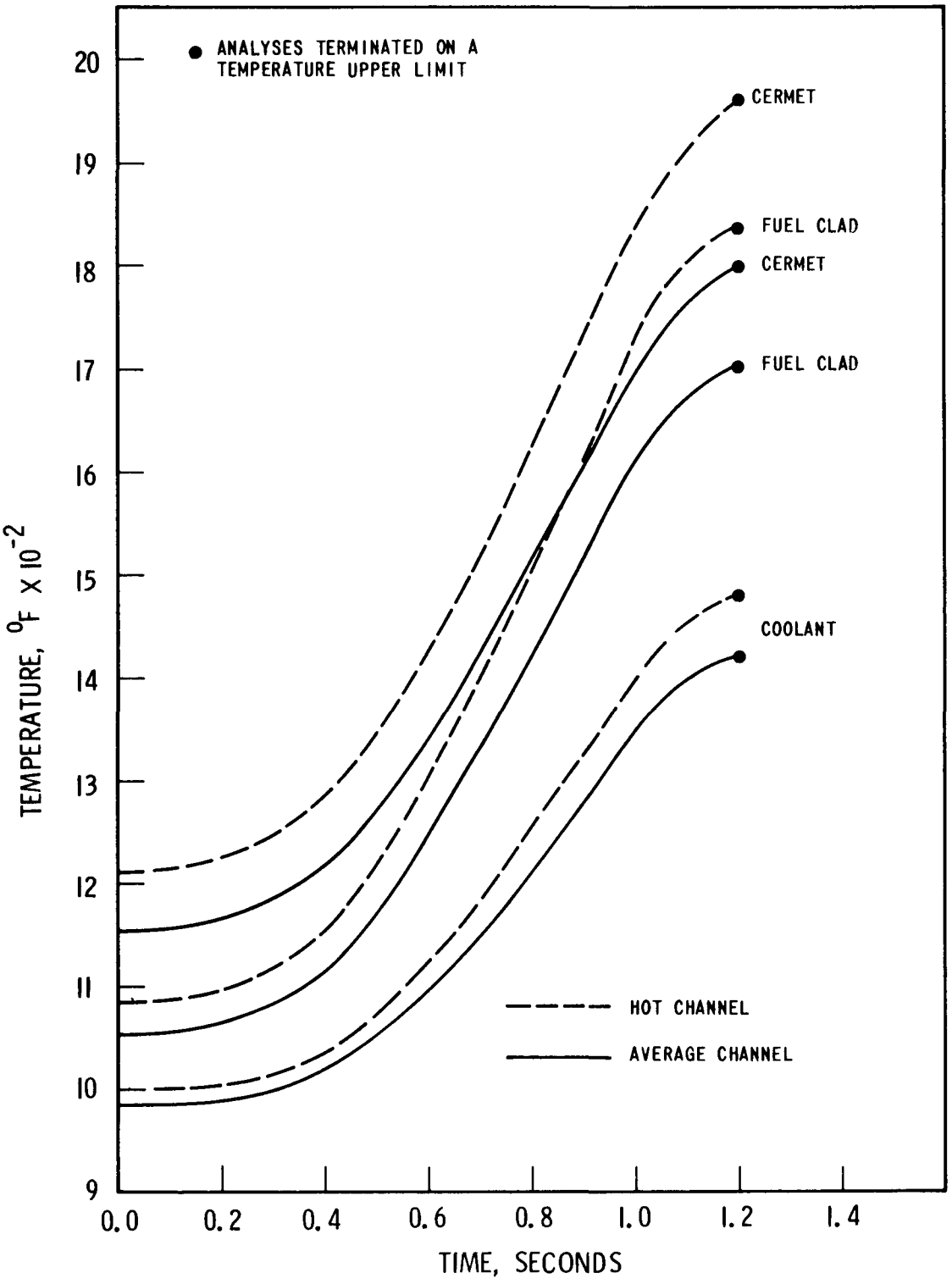

AVERAGE AND HOT CHANNEL AVERAGE TEMPERATURES
CARBIDE FUELED CORE - BCEX CERMET HEAT GENERATION
40% OF FUEL - RAMP REACTIVITY INSERTION $2 IN 1.0 SECOND
CARBIDE FUEL ROD DIAMETER 0.300 INCHES
BCEX CERMET ROD DIAMETER 0.300 INCHES

Figure III.5-14(b)

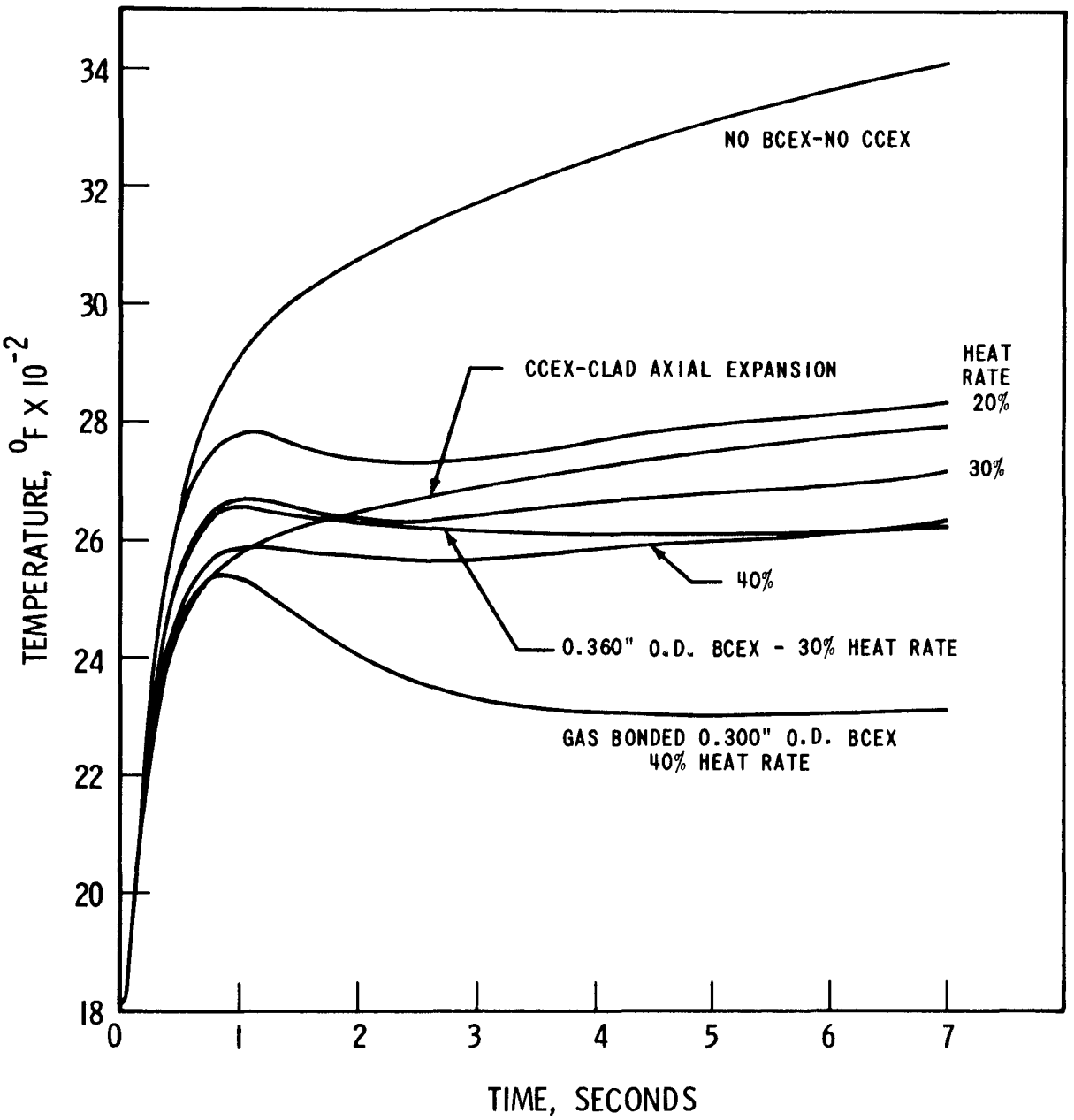

HOT CHANNEL FUEL MAXIMUM CENTERLINE TEMPERATURE CARBIDE FUELED CORE-EFFECTS OF CERMET HEAT GENERATION RATE, CERMET ROD DIAMETER, CERMET-CLAD BONDING AND CCEX CLAD AXIAL EXPANSION-AXIAL SECTION NUMBER 4 (4 OF 6)-RAMP REACTIVITY INSERTION 80 CENTS IN 0.1 SECONDS - BCEX CERMET ROD DIAMETER 0.300 INCHES - CARBIDE FUEL ROD DIAMETER 0.300 INCHES

Figure III.5-15

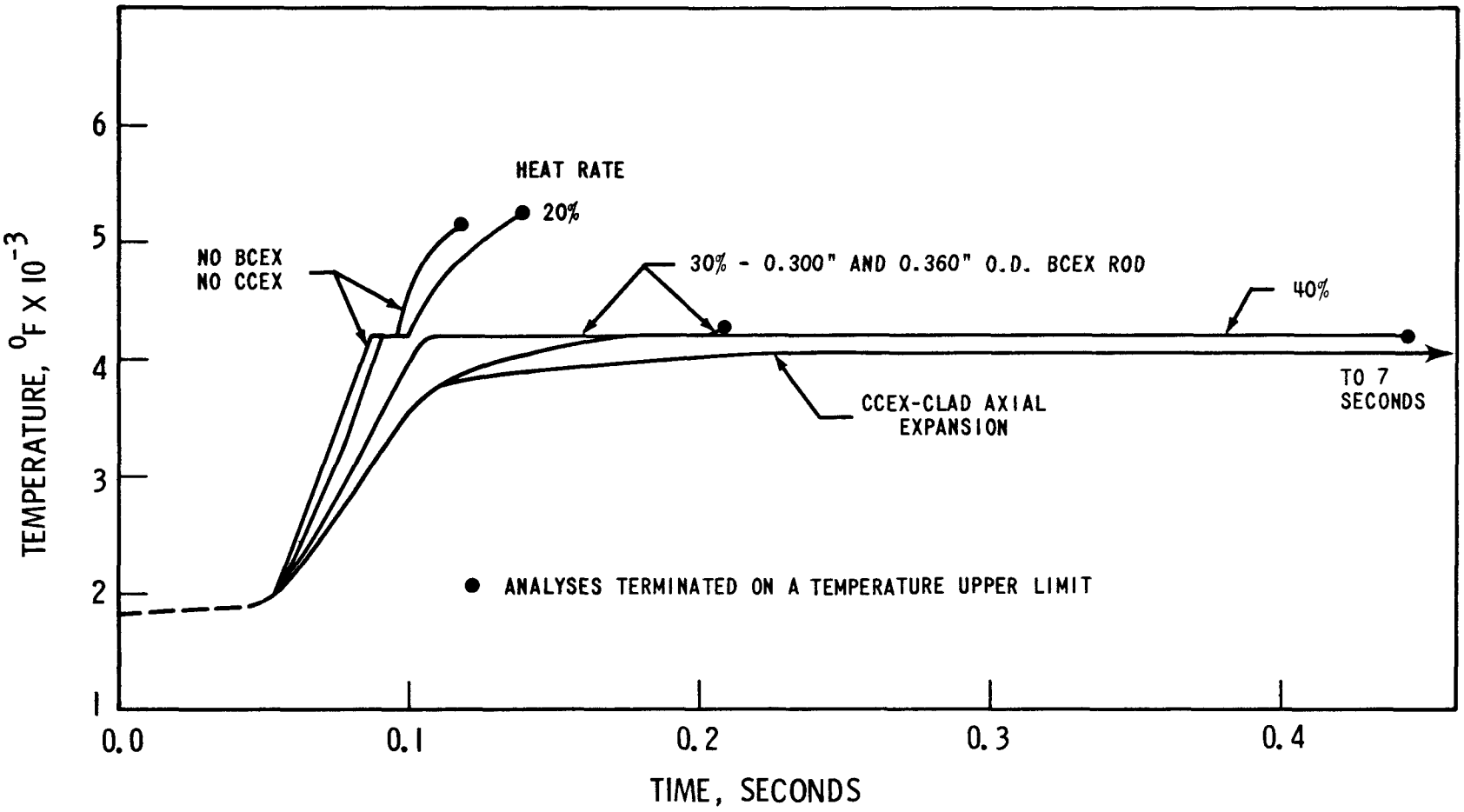

HOT CHANNEL FUEL MAXIMUM CENTER LINE TEMPERATURE - CARBIDE FUELED CORE - AXIAL SECTION NUMBER 4 (4 OF 6) - EFFECT OF CERMET HEAT GENERATION RATE - RAMP REACTIVITY INSERTION 2$ IN 0.1 SECONDS - CARBIDE FUEL AND BCEX CERMET ROD DIAMETERS 0.300 INCHES - FUEL MELTING TEMP. 4200^{o}F

Figure III.5-16

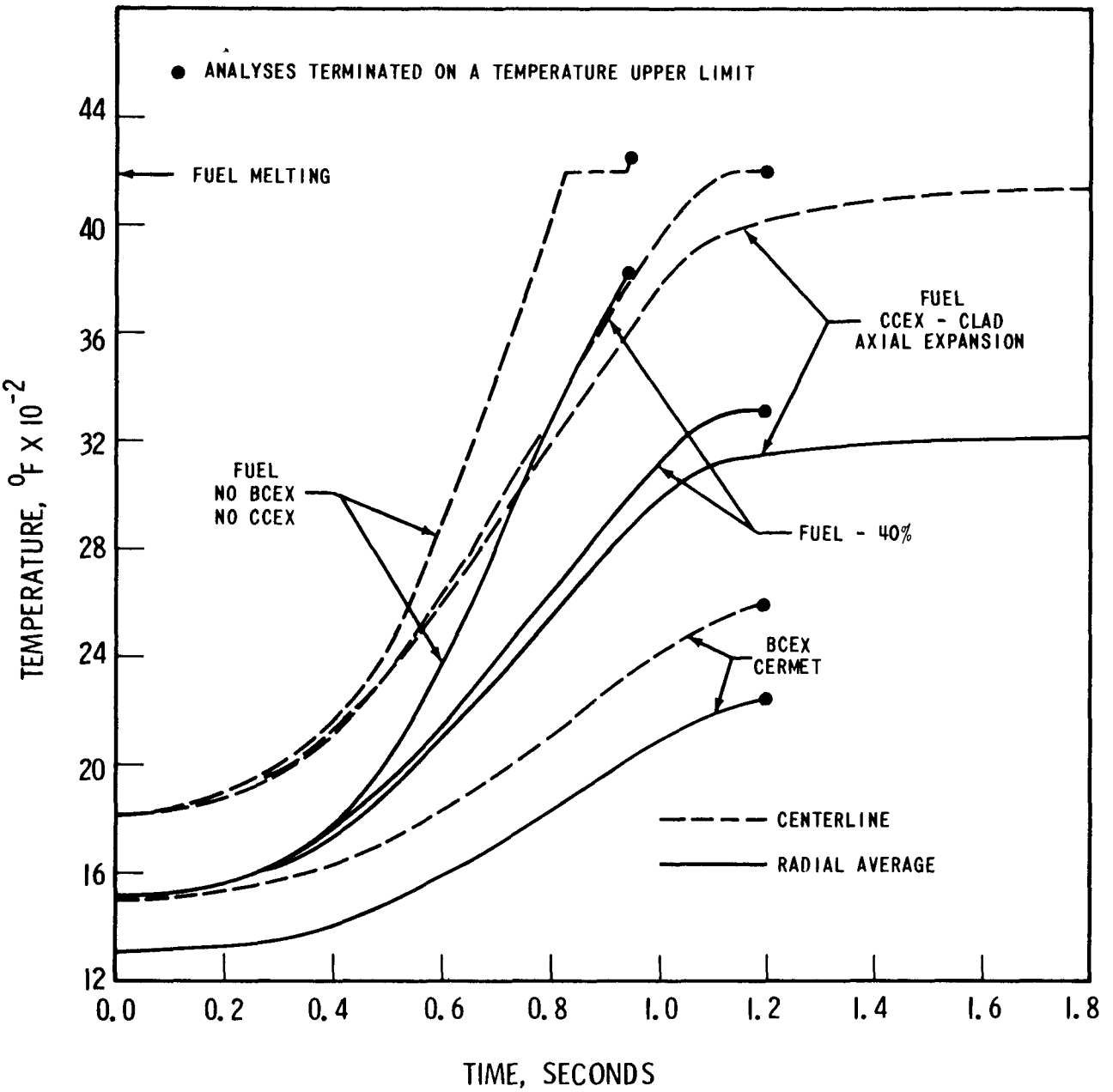

HOT CHANNEL FUEL AND CERMET TEMPERATURES-CARBIDE FUELED CORE-CERMET HEAT GENERATION 40% OF FUEL-AXIAL SECTION NUMBER 4 (4 OF 6)-RAMP REACTIVITY INSERTION 2$ IN 1.0 SECOND- CARBIDE FUEL AND BCEX CERMET ROD DIAMETERS 0.300 INCHES

Figure III.5-17

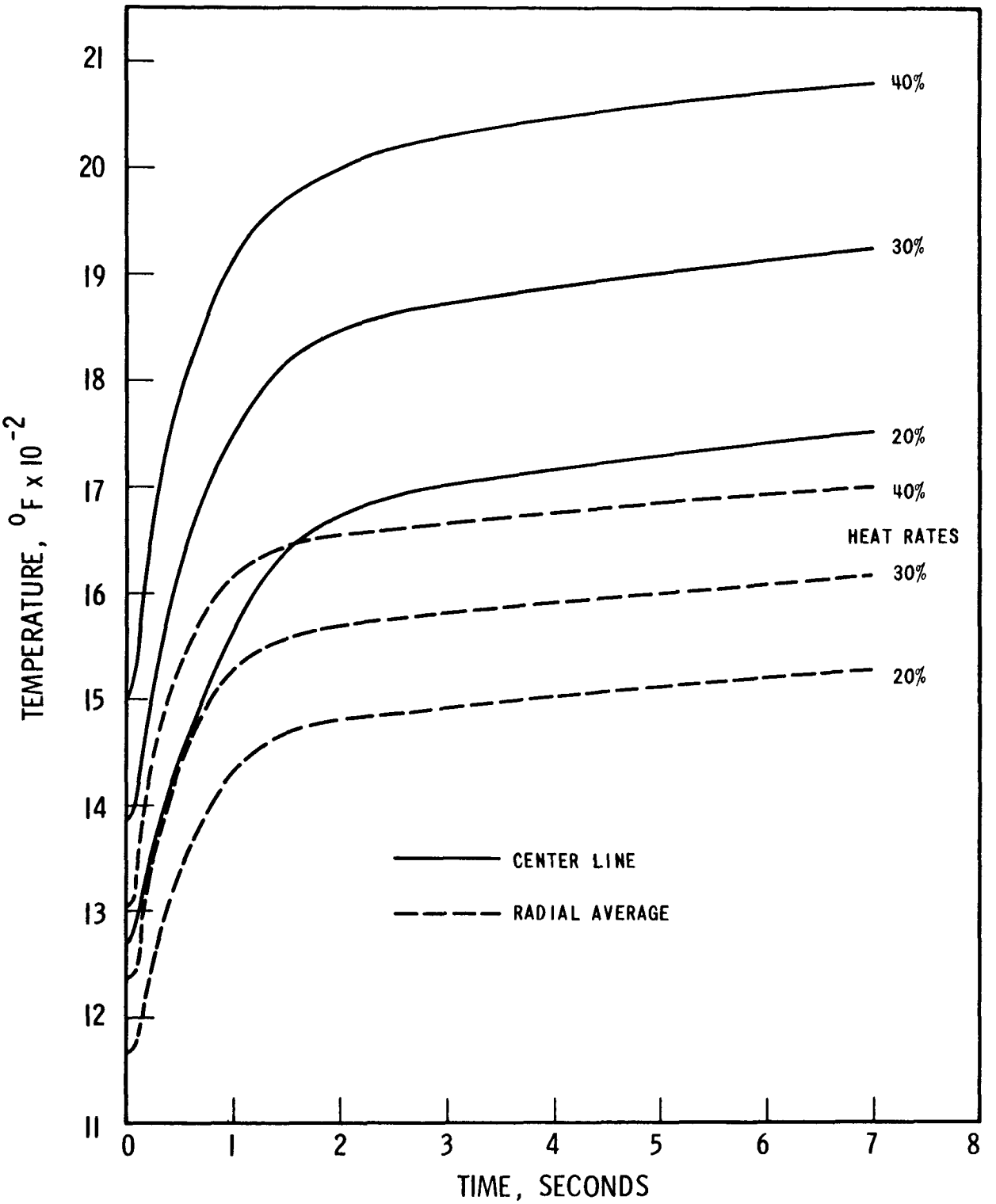

HOT CHANNEL BCEX CERMET TEMPERATURES-CARBIDE FUELED CORE AXIAL SECTION NUMBER 4 (4 OF 6)-EFFECT OF CERMET HEAT GENERATION RATE RAMP REACTIVITY INSERTION 80 CENTS IN 0.1 SECONDS-CARBIDE FUEL AND BCEX CERMET ROD DIAMETER 0.300 INCHES

Figure III.5-18

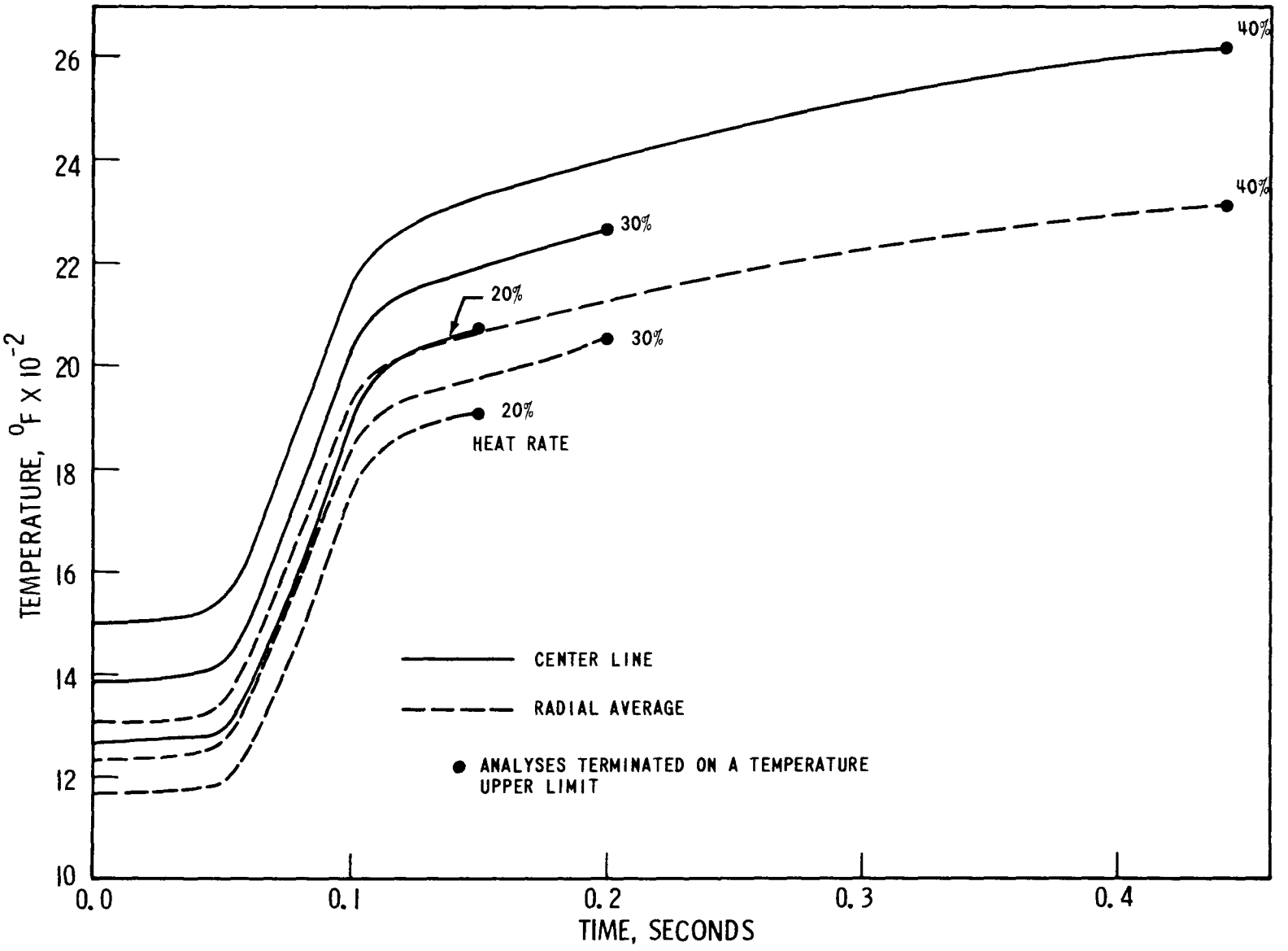

Figure III.5-19 - CERMET TEMPERATURES - CARBIDE FUELED CORE - AXIAL SECTION NUMBER 4(4 OF 6) - EFFECT OF CERMET HEAT GENERATION RATE - RAMP REACTIVITY INSERTION 2$ IN 0.1 SECONDS - CARBIDE FUEL AND BCEX CERMET ROD DIAMETERS 0.300 INCHES

temperature in an integrated average temperature over the cermet radius. The rise in temperature from zero time was found to be proportional to the ratio of the heat generation rate to the 0.24 power. Likewise when increasing the cermet rod diameter, Figure III.5-20, the temperature rise at a fixed heat rate was found to be proportional to the 0.53 power of the ratio of diameters.

The effect of changes in the Doppler and sodium density coefficients on the cermet temperatures, at a 40% relative heat rate and with the 80 cents in 0.1 second reactivity insertion, is illustrated in Figure III.5-21. As the coefficients for the other temperature dependent feedback mechanisms become more positive, BCEX, of course, contributes more in terminating the excursion. Figure III.5-21 is a plot of cermet temperatures, centerline and radial average in section 3 (3 of 6), as a function of the reactivity coefficients. In a reactor having BCEX as the only negative feedback mechanism, the reactivity worth of all core components would have to be limited to a value that would not produce an excursion sufficient to substantially melt the cermet in the event of an accident. For example, if the reference core[1] had only BCEX to introduce negative reactivity, the recommended maximum worth of any core component would be 80 cents or less.

In conclusion, the application of BCEX in a sodium bonded carbide fueled core would require imposing a limit between that for a no BCEX-no CCEX core upon the reactivity worth of any single core component, in order to limit the effects of the downgrading of BCEX by the fuel clad inward expansion and/or the melting of the cermet. In large rapid excursions, such as from a two dollar reactivity insertion in one second, the short time constant between the carbide and clad makes clad axial expansion, CCEX, a more effective terminating mechanism than BCEX.

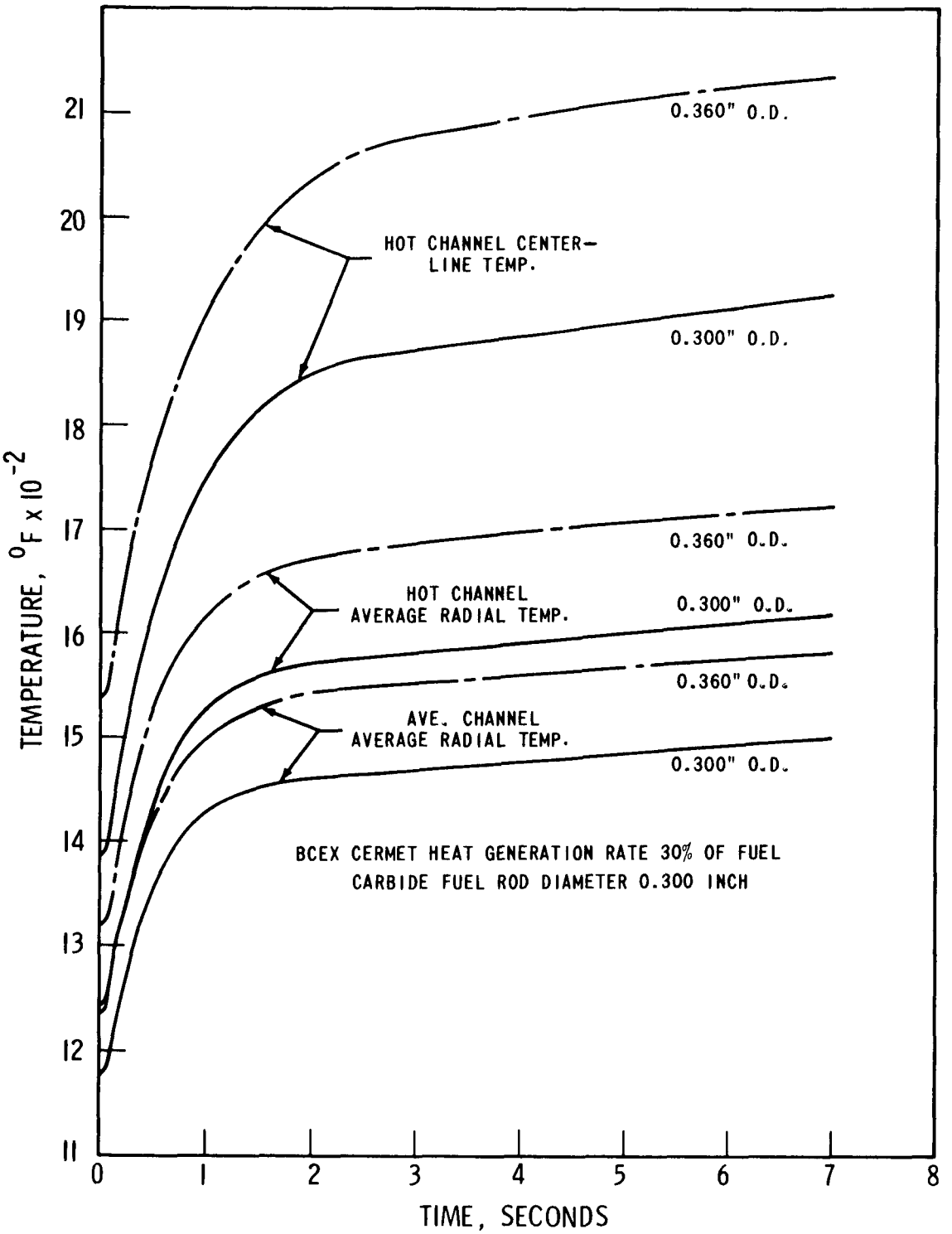

BCEX CERMET TEMPERATURE AS A FUNCTION OF CERMET ROD DIAMETER
AXIAL SECTION NUMBER 4 (4 OF 6)
RAMP REACTIVITY INSERTION 80 CENTS IN 0.1 SECONDS
CARBIDE FUELED CORE

Figure III.5-20

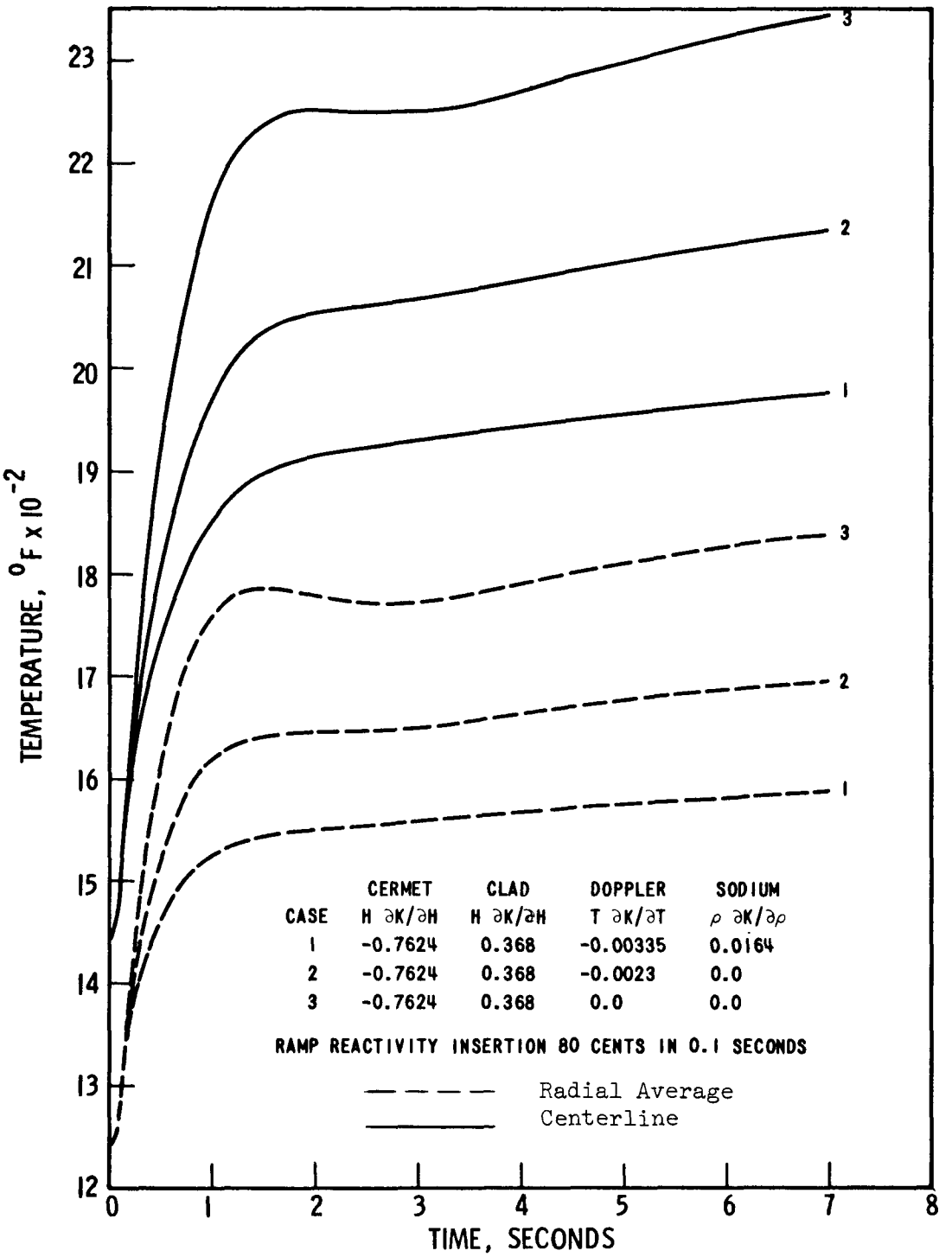

HOT CHANNEL CERMET TEMPERATURES AS A FUNCTION
OF DOPPLER AND SODIUM DENSITY COEFFICIENTS
CARBIDE FUELED CORE
CERMET HEAT GENERATION 40% OF FUEL
AXIAL SECTION NUMBER 3 (3 OF 6)
CARBIDE FUEL AND BCEX CERMET ROD DIAMETERS 0.300 INCHES

Figure III.5-21

III.5.4.2 Oxide Fueled Core

Analyses were performed on the oxide fueled core, Table III.5-1, for two reactivity insertions: 80 cents in 0.1 second, and 2 dollars in 1.0 second. For the 80 cents in 0.1 second insertion, three BCEX cermet rod diameters, 0.215 inches, 0.260 inches and 0.300 inches, were studied using each of the three cermet relative volumetric heat generation rates: 20%, 30%, and 40%. The 2 dollars in 1.0 second insertion analysis was limited to be 0.300 inch O.D. BCEX cermet rod. The oxide fuel rod diameter, 0.215 inches, was held constant for all analyses. The oxide core analyses were naturally limited in scope because the reference BCEX reactor[1] in the study is a carbide fueled core.

The characteristics of the total reactivity feedback in the oxide core for both insertions are shown in Figures III.5-22 and III.5-23. The longer oxide pellet-to-clad time constant, Table III.5-3, improves the BCEX performance characteristics over those noted for the carbide core during the initial stages of the excursion (less than 0.8 seconds). During this time period in all analyses, the BCEX feedback exceeds the CCEX feedback, see Figures III.5-24 and III.5-25. For this same time period in the carbide core analyses, Figure III.5-7, the CCEX feedback was greater than the net BCEX feedback. Thus, in the initial stages of an excursion, BCEX is a more important excursion terminating mechanism in a gas bonded oxide core than in a sodium bonded carbide core.

In the oxide core, the gap between the lower and upper fuel bundles in the 30% and 40% relative heat rate BCEX analyses for the 80 cents in 0.1 second insertion was found to be always equal to or larger than the zero time gap value, Figure III.5-26. Depending upon the cermet rod diameter and heat rate, the gap width continues to increase, increases to a maximum value and then remains at an essentially constant value, or increases to a maximum value and thereafter decreases toward the zero time gap width. For example, in the 30% relative heat rate analyses, the gap increases with time for the 0.300 inch cermet rod. For the

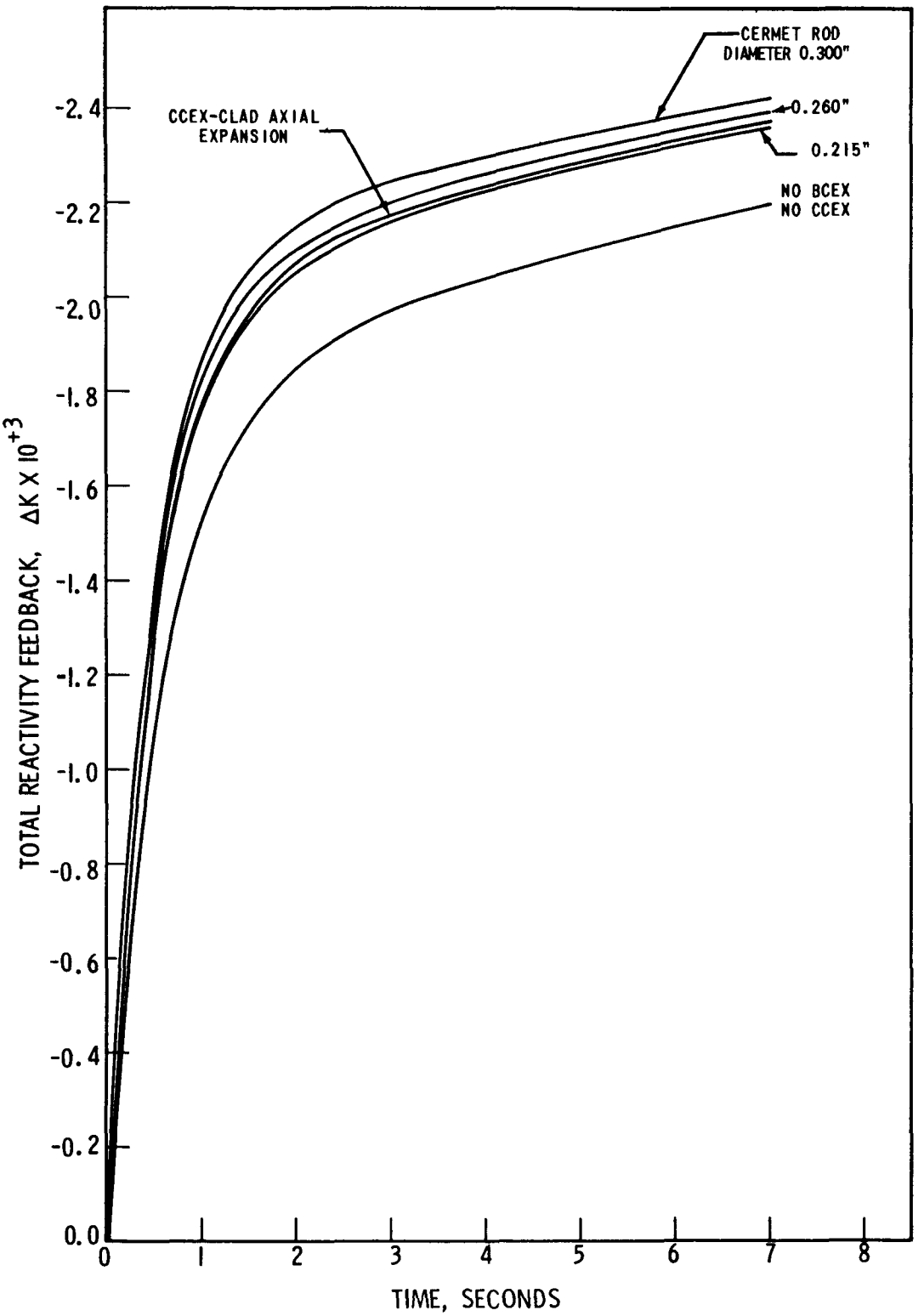

TOTAL REACTIVITY FEEDBACK
OXIDE FUELED CORE
RAMP REACTIVITY INSERTION 80 CENTS IN
0.1 SECONDS
BCEX HEAT GENERATION 30% OF FUEL
OXIDE FUEL ROD DIAMETER 0.215 INCHES

Figure III.5-22

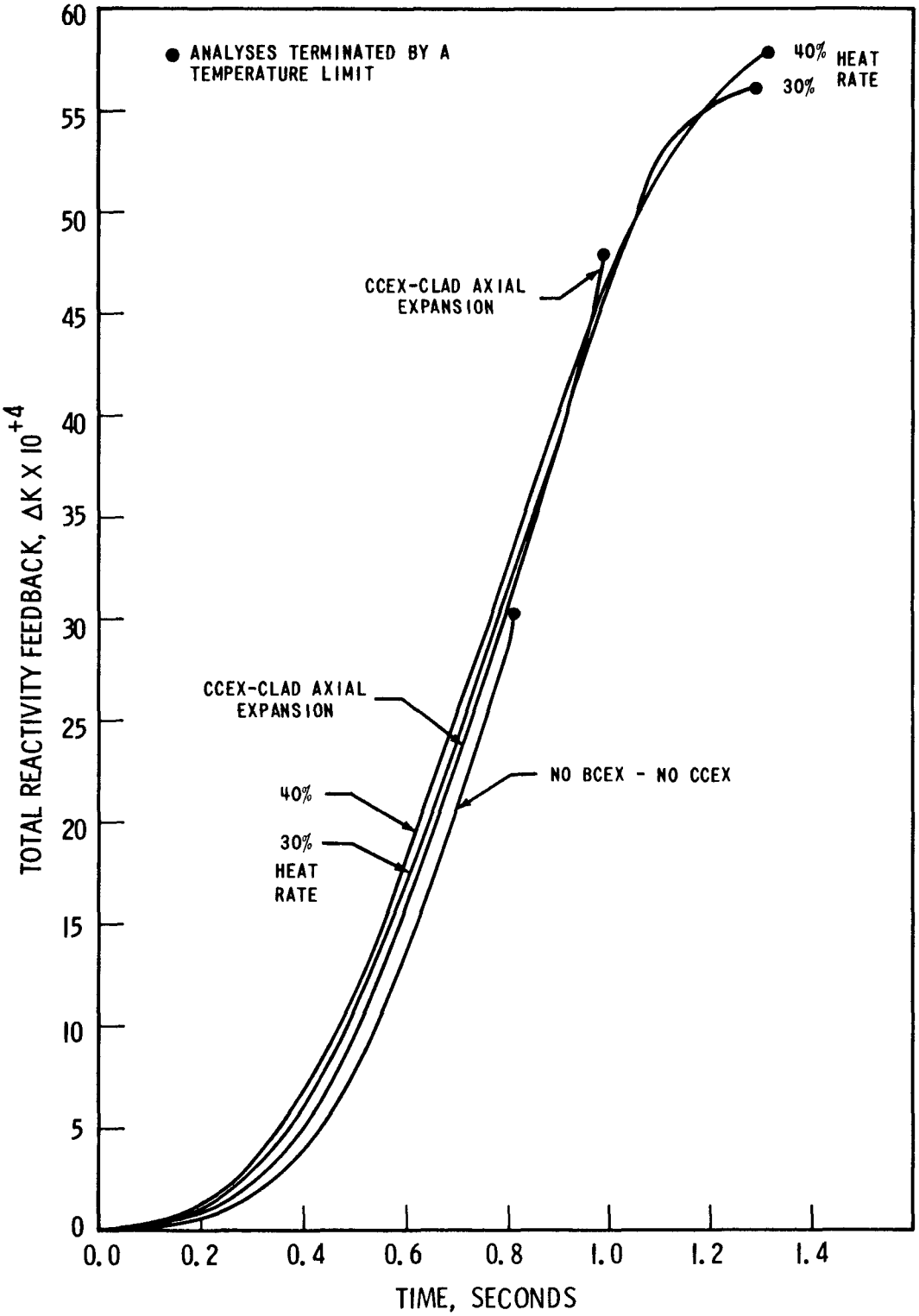

TOTAL REACTIVITY FEEDBACK-OXIDE FUELED CORE
RAMP REACTIVITY INSERTION 2$ IN 1.0 SECOND
BCEX CERMET ROD DIAMETER 0.300 INCHES
OXIDE FUEL ROD DIAMETER 0.215 INCHES

Figure III.5-23

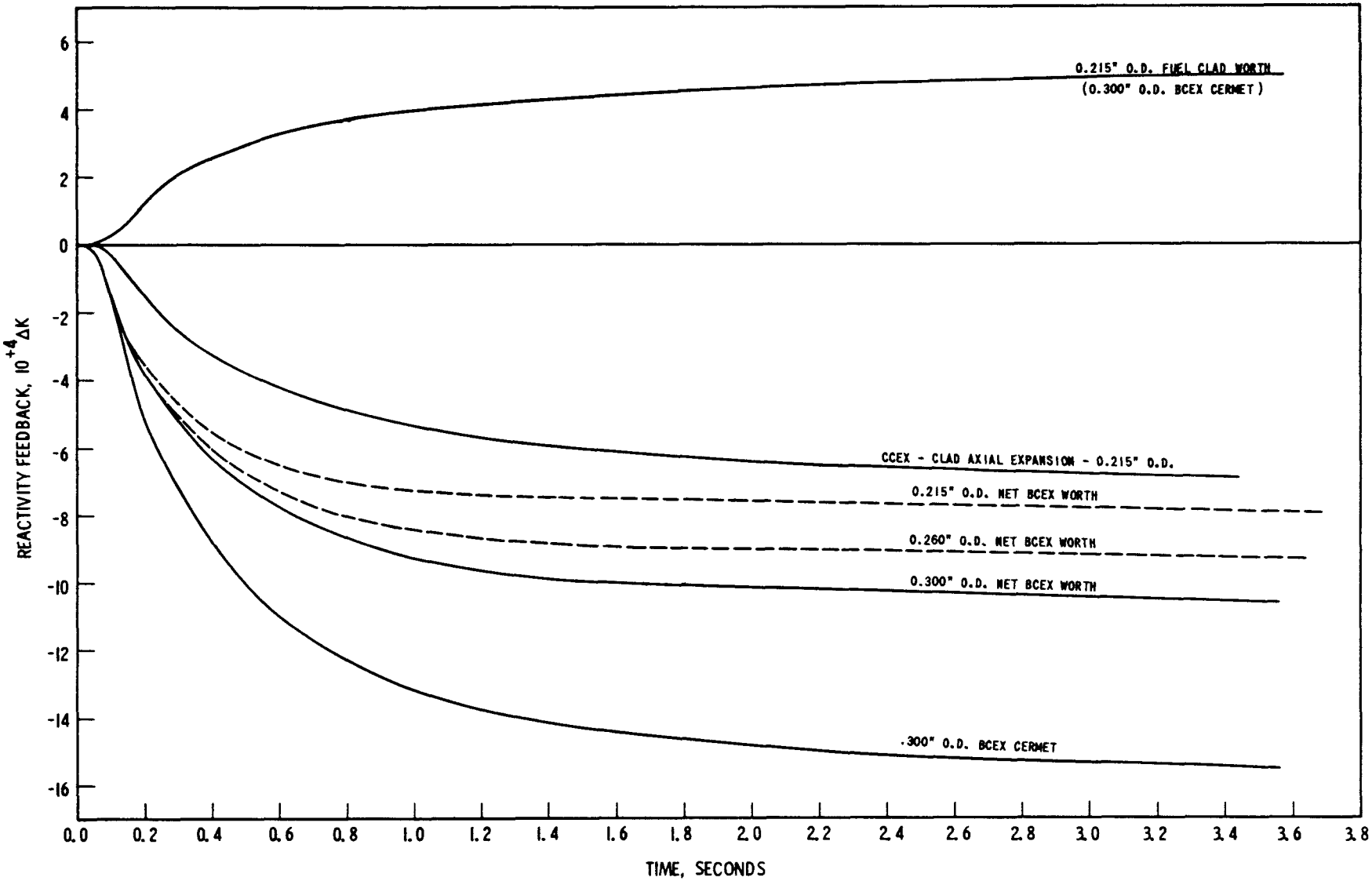

BCEX PERFORMANCE IN OXIDE FUELED CORE
BCEX HEAT GENERATION 40% OF FUEL
EFFECT OF CERMET ROD DIAMETER
RAMP REACTIVITY INSERTION 80 CENTS IN 0.1 SECONDS
OXIDE FUEL ROD DIAMETER 0.215 INCHES

Figure III.5-24

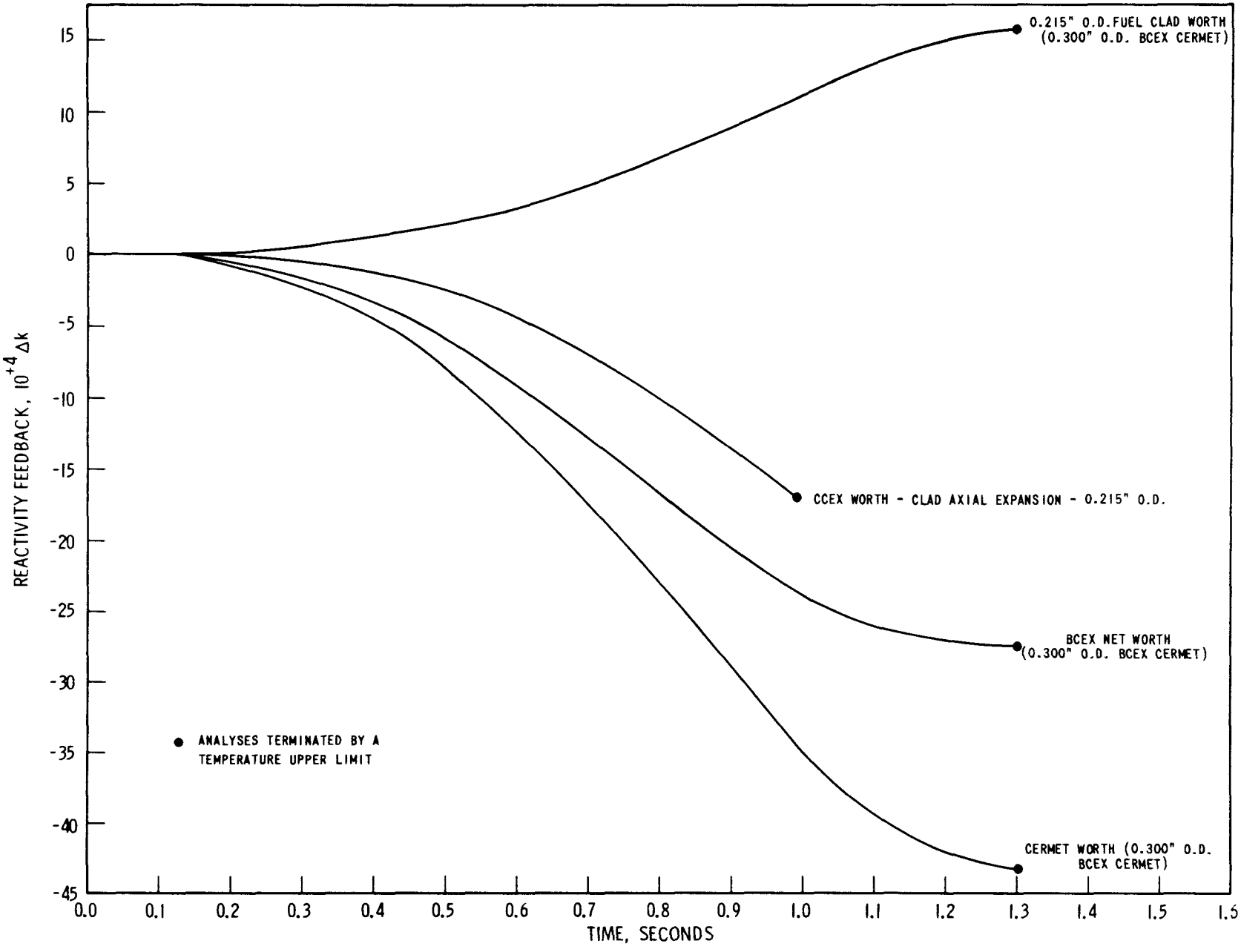

BCEX PERFORMANCE IN OXIDE FUELLED CORE - BCEX HEAT GENERATION 40% OF FUEL
RAMP REACTIVITY INSERTION 2¢ IN 1.0 SECOND - OXIDE FUEL ROD DIAMETER 0.215 INCHES

Figure III.5-25

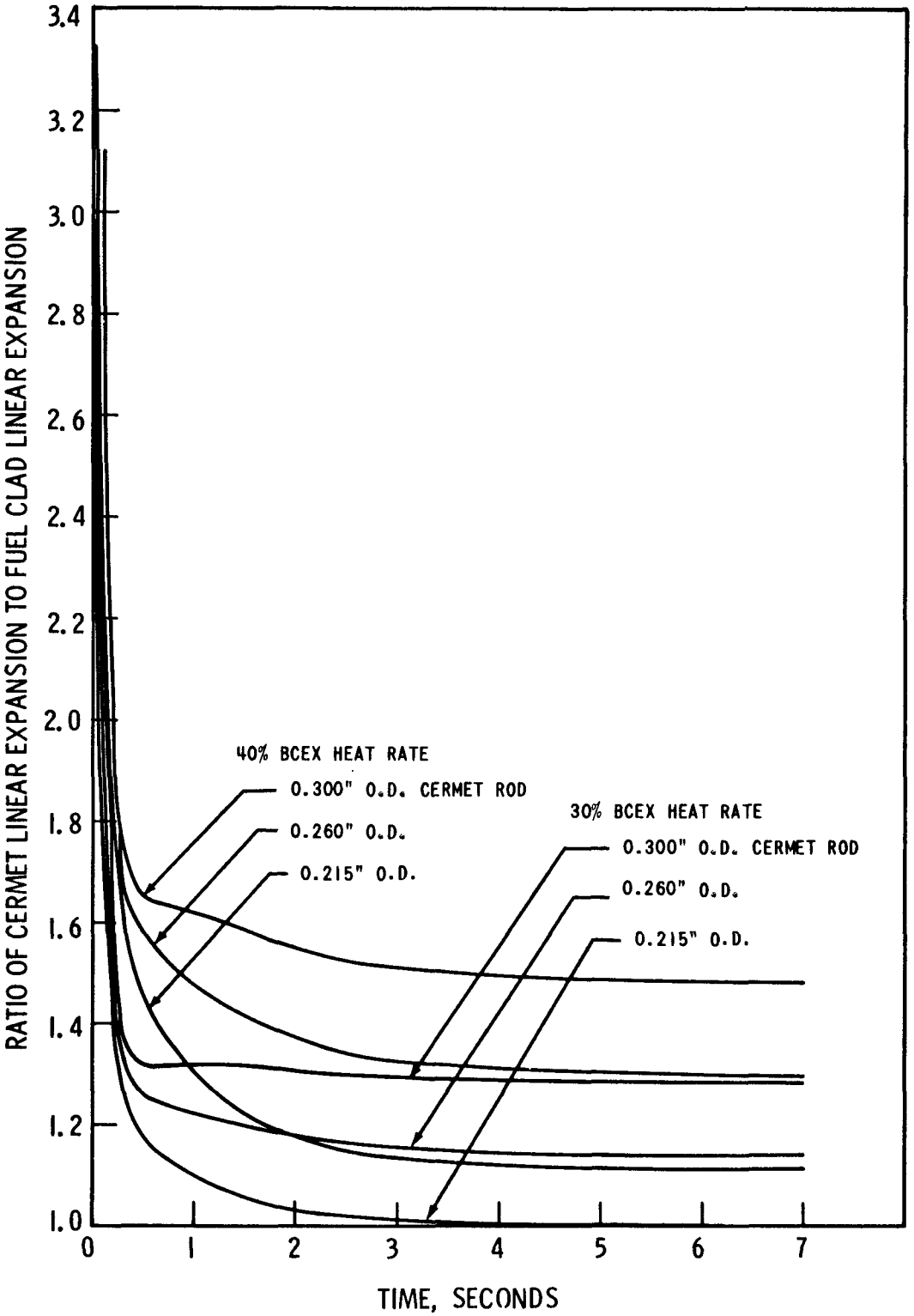

BCEX EXPANSION PERFORMANCE
OXIDE FUELED CORE
RAMP REACTIVITY INSERTION 80 CENTS
IN 0.1 SECONDS
OXIDE FUEL ROD DIAMETER 0.215 INCHES

Figure III.5.26

0.260 inch cermet rod, the gap increases in width by 20 mils during the first second, and remains essentially at this new width for the duration of the analyses. However, for the 0.215 inch cermet rod, the gap width increases by 11 mils at 1.5 seconds, and then decreases back to essentially the zero time width.

The average and hot channel temperatures for the 0.260 inch BCEX cermet rod analyses for the insertion of 80 cents in 0.1 seconds are shown in Figure III.5-27 and III.5-28 for the fuel, cermet, fuel clad, and coolant. The oxide core temperatures continue to rise with time, whereas in the carbide core, Figure III.5-12, the temperatures go through a maximum point followed by a minimum point before increasing gradually as the new equilibrium core conditions are approached. The rate of temperature rise in the 0.260 inch diameter cermet rod in the average channel, after the initial delay due to the cermet time constant, is 275°, 375°, and 475°F/sec. for the 20%, 30%, and 40% relative heat rates, respectively (see Figure III.5-28). The 20% BCEX cermet relative heat rate case and the CCEX case lowers by 410°F the reference core (no BCEX-no CCEX) average fuel temperatures. Increasing the BCEX cermet relative heat rate to 40% lowers the fuel average temperature by another 140°F. The average fuel temperatures, average and hot channels, for the 0.300 inch diameter BCEX cermet rod core with the 2 dollars in 1.0 second insertion are shown in Figure III.5-29. Fuel melting of more than 50% of the fuel pellet diameter occurred in several of 6 axial segments in both the average and hot channels by the time all the analyses were terminated.

The hot channel fuel maximum centerline and radial average temperatures, which occur in axial section number 4 (4 of 6), are shown in Figures III.5-30 and III.5-31 for the insertion of 80 cents in 0.1 seconds into the 0.260 inch cermet diameter BCEX core, and the insertion of 2 dollars in 1.0 second into the 0.300 inch cermet diameter BCEX core, respectively. In both analyses, melting at the fuel centerline occurs, but only in the 2 dollar insertion did the average fuel temperature in this axial section

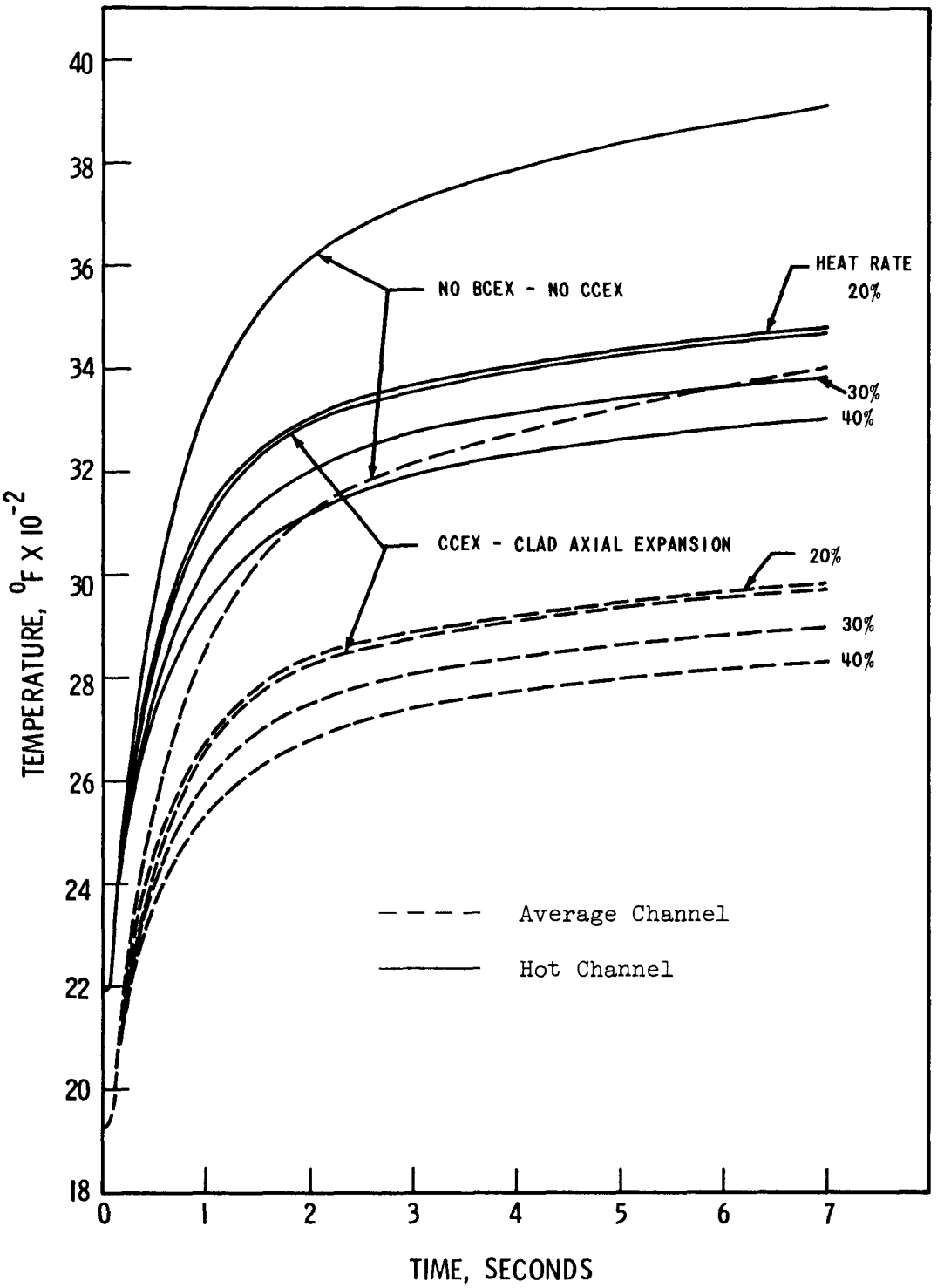

AVERAGE FUEL TEMPERATURES - OXIDE FUELED CORE - BCEX CERMET ROD DIAMETER 0.260 INCHES - EFFECTS OF CERMET HEAT GENERATION AND CLAD AXIAL EXPANSION - RAMP REACTIVITY INSERTION 80 CENTS IN 0.1 SEC. - OXIDE FUEL ROD DIAMETER 0.215 INCHES

Figure III.5-27

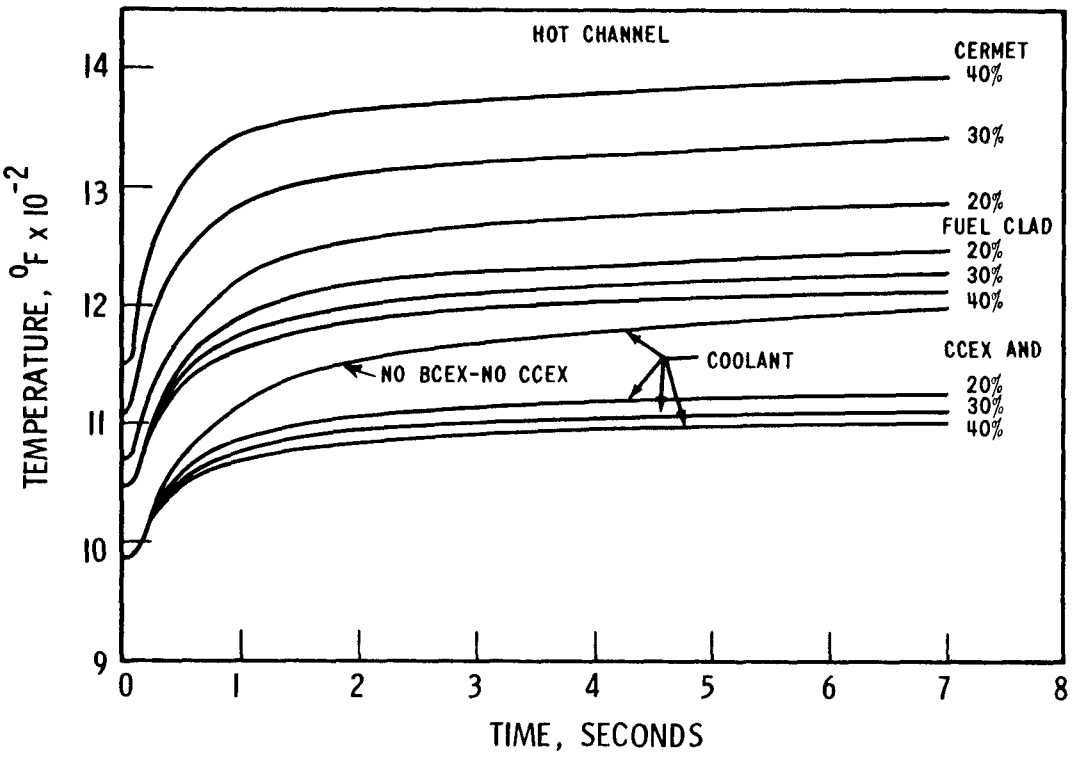

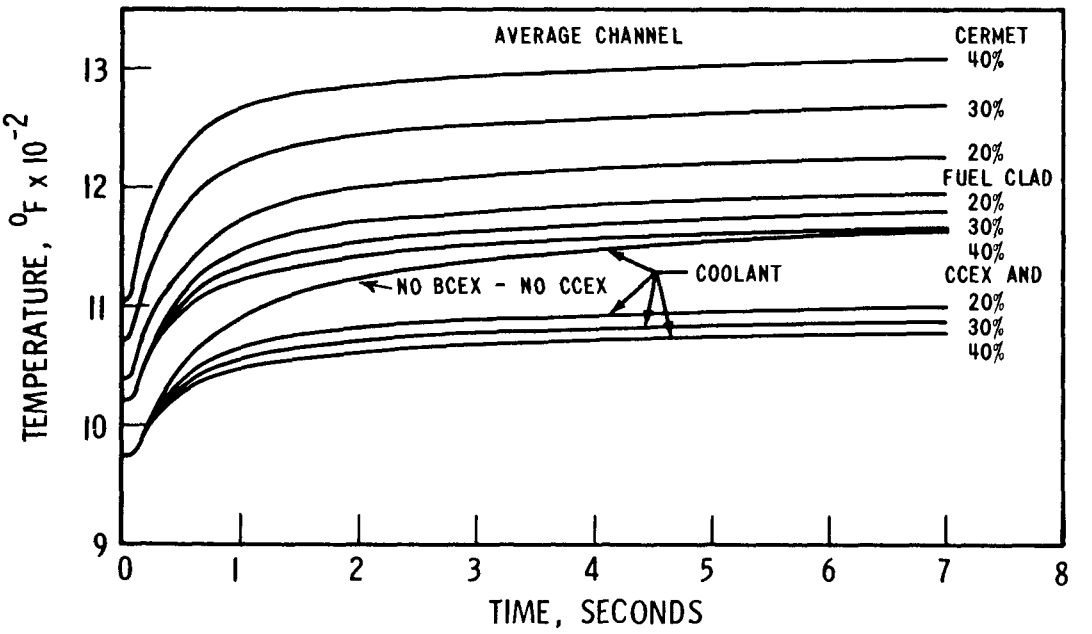

AVERAGE TEMPERATURES OXIDE FUELED CORE
CERMET ROD DIAMETER 0.260 INCHES
EFFECTS OF CERMET HEAT GENERATION AND CLAD AXIAL EXPANSION
RAMP REACTIVITY INSERTION 80 CENTS IN 0.1 SECONDS
OXIDE FUEL ROD DIAMETER 0.215 INCHES

Figure III.5-28

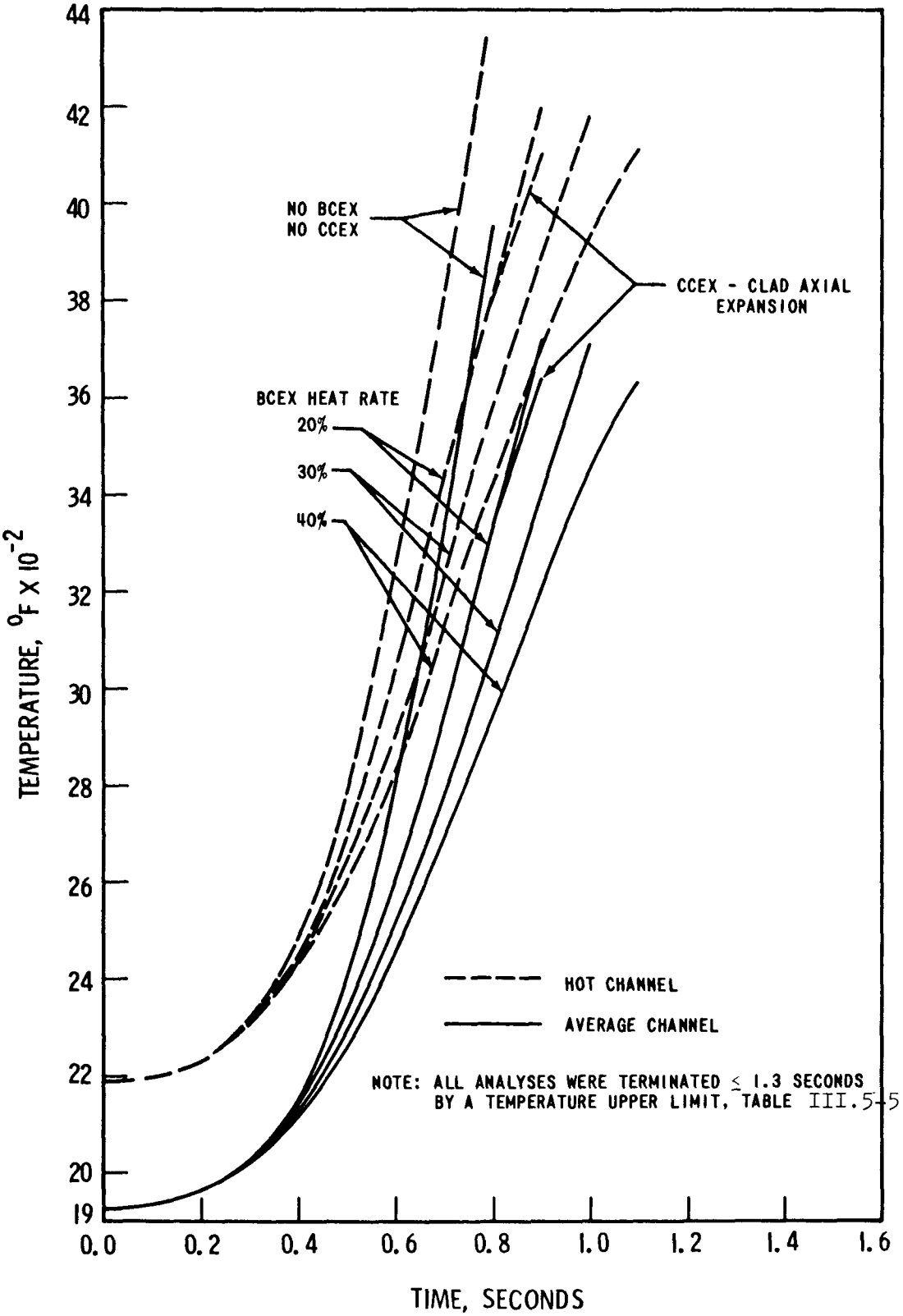

AVERAGE FUEL TEMPERATURES - AVERAGE AND HOT CHANNELS - OXIDE FUELED CORE - BCEX CERMET ROD DIAMETER 0.300 INCHES - OXIDE FUEL ROD DIAMETER 0.215 INCHES - RAMP REACTIVITY INSERTION 2$ IN 1.0 SECOND

Figure III.5-29

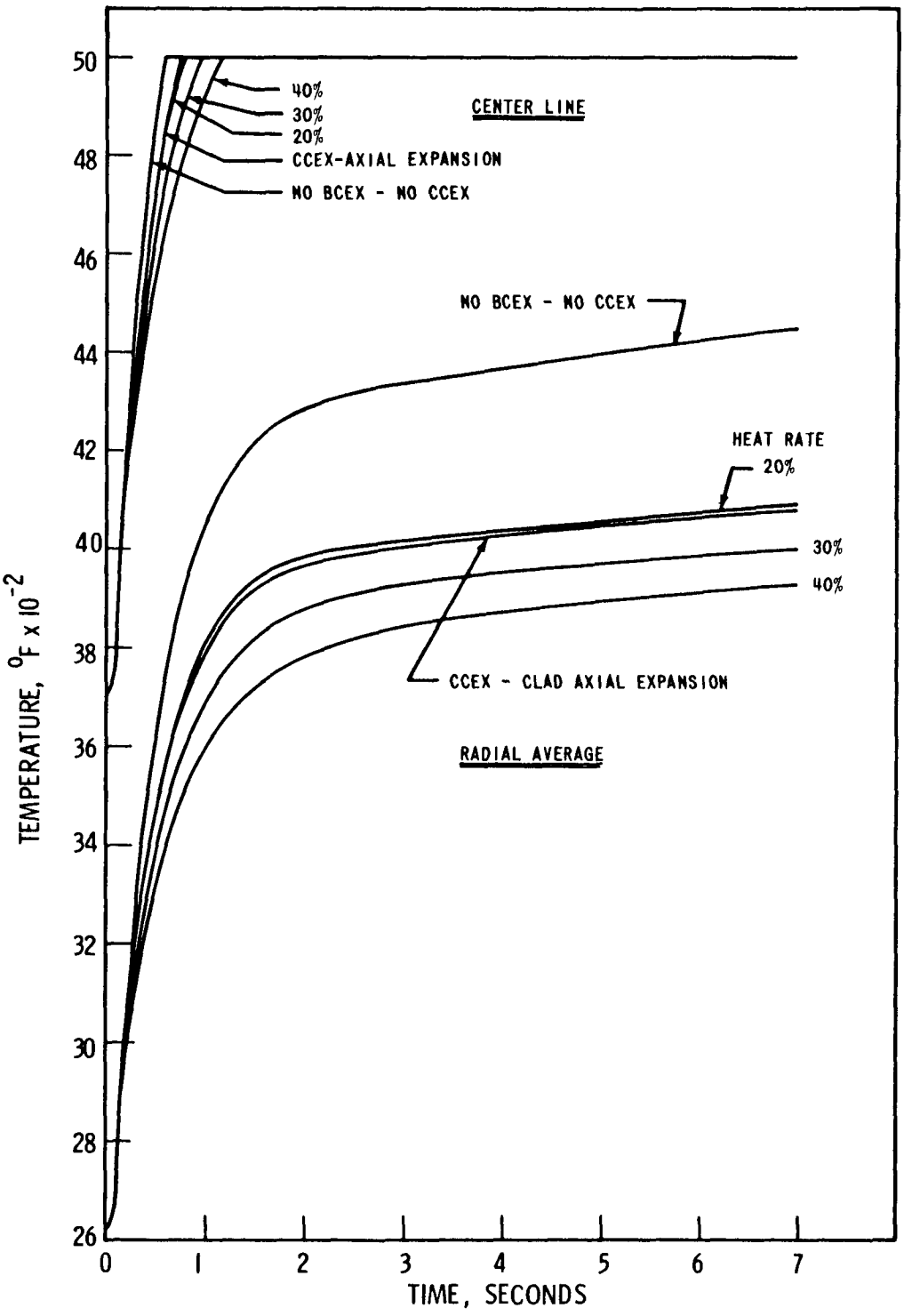

HOT CHANNEL FUEL TEMPERATURES - AXIAL SECTION NUMBER 4 (4 OF 6) CERMET ROD DIAMETER 0.260 INCHES - OXIDE FUELED CORE - EFFECTS OF CERMET HEAT GENERATION AND CLAD AXIAL EXPANSION - RAMP REACTIVITY INSERTION 80 CENTS IN 0.1 SECONDS - OXIDE FUEL ROD DIAMETER 0.215 INCHES

Figure III.5-30

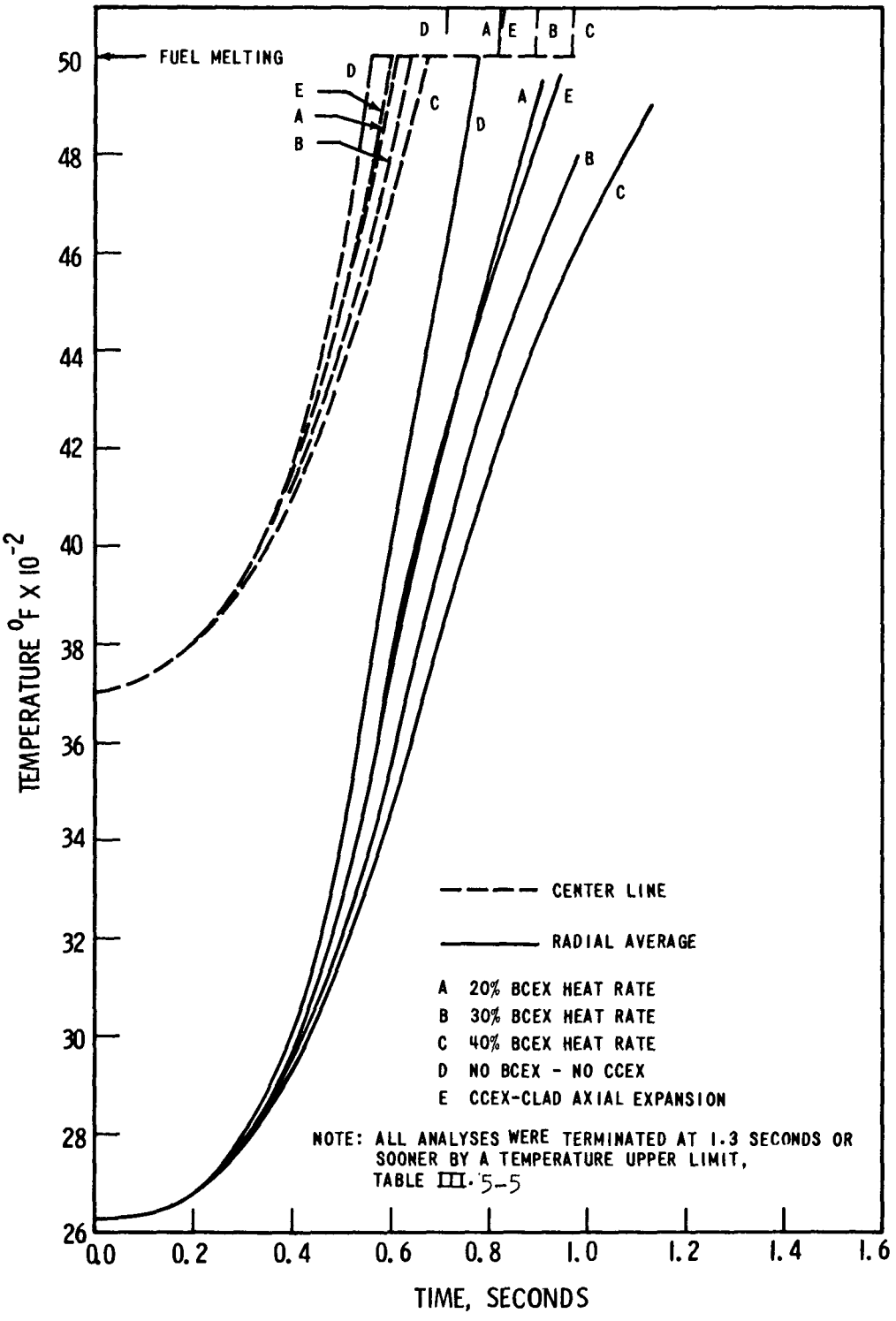

HOT CHANNEL FUEL MAXIMUM CENTERLINE AND RADIAL AVERAGE TEMPERATURES - AXIAL SECTION NUMBER 4 (4 OF 6) - OXIDE FUELED CORE-BCEX CERMET ROD DIAMETER 0.300 INCHES - OXIDE FUEL ROD DIAMETER 0.215 INCHES-RAMP REACTIVITY INSERTION 2$ IN 1.0 SECOND

Figure III.5-31

reach the melting point, 5000°F. The average temperature in a section is an integrated average over the radius of the fuel pellet.

The hot channel cermet maximum centerline and radial average temperatures for these two sets of analyses are shown in Figures III.5-32 and III.5-33. The rise in the cermet temperature follows the same pattern as was noticed for the carbide core, Figures III.5-18 and III.5-19.

In conclusion, because of the longer time constant in an oxide fuel rod, BCEX is a more important excursion termination mechanism in an oxide core than in a carbide core. The longer time constant delays the fuel clad inward expansion, and thus the cermet negative reactivity feedback is not downgraded as severely during the initial stages of the excursion as in a sodium bonded carbide core. This delay in clad expansion, however, is detrimental with respect to the BCEX in an oxide core in which CCEX is employed. A core incorporating CCEX has significantly improved dynamic behavior over a no BCEX-no CCEX core.

III.5.4.3 BCEX Performance Comparison in the Carbide and Oxide Cores

The performance characteristics of BCEX in the carbide and oxide fueled cores is compared below for the 80 cents in 0.1 second ramp reactivity insertion and a heating rate of 30% of the fuel, which is the recommended BCEX cermet relative volumetric heat generation rate. The comparison includes all the cermet rod diameters analyzed at this heat rate for both oxide and carbide fuel materials.

Figure III.5-34 shows the BCEX net reactivity feedback, Δk, for each cermet diameter analyzed in both cores. The comparison clearly shows that during the first second of the excursion, the BCEX's feedback is greater in the oxide core for all the cermet diameters studied. The longer time constant for the oxide fuel rods, 2.1 seconds versus 0.47 seconds for the carbide fuel rods, delays the downgrading of the oxide core BCEX outward expansion by the fuel clad inward expansion. However,

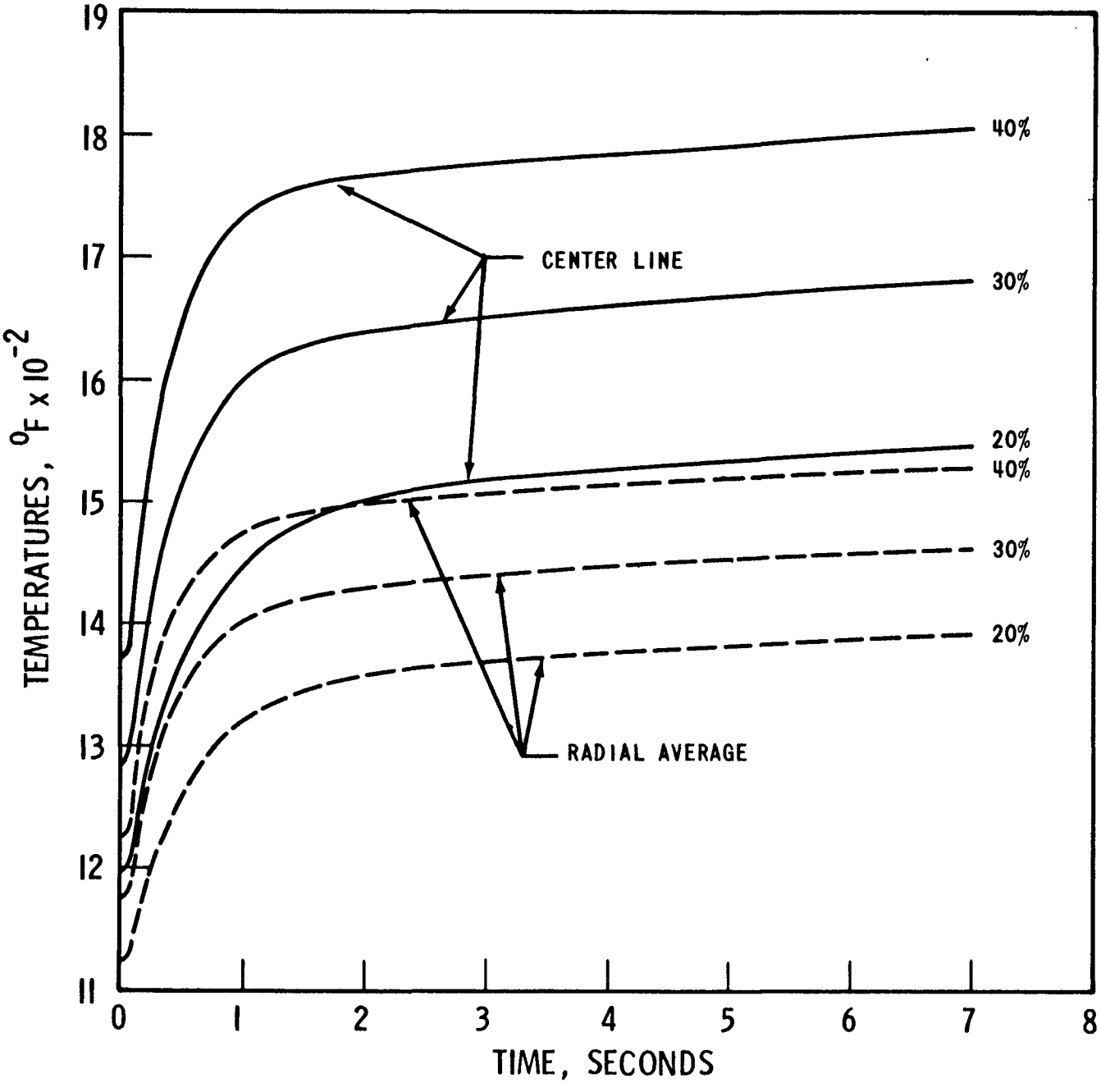

BCEX CERMET HOT CHANNEL TEMPERATURES-AXIAL SECTION NUMBER 4
(4 OF 6)-BCEX CERMET ROD DIAMETER 0.260 INCHES-OXIDE FUELED CORE
EFFECTS OF CERMET HEAT GENERATION
RAMP REACTIVITY INSERTION 80 CENTS IN 0.1 SECONDS
OXIDE FUEL ROD DIAMETER 0.215 INCHES

Figure III.5-32

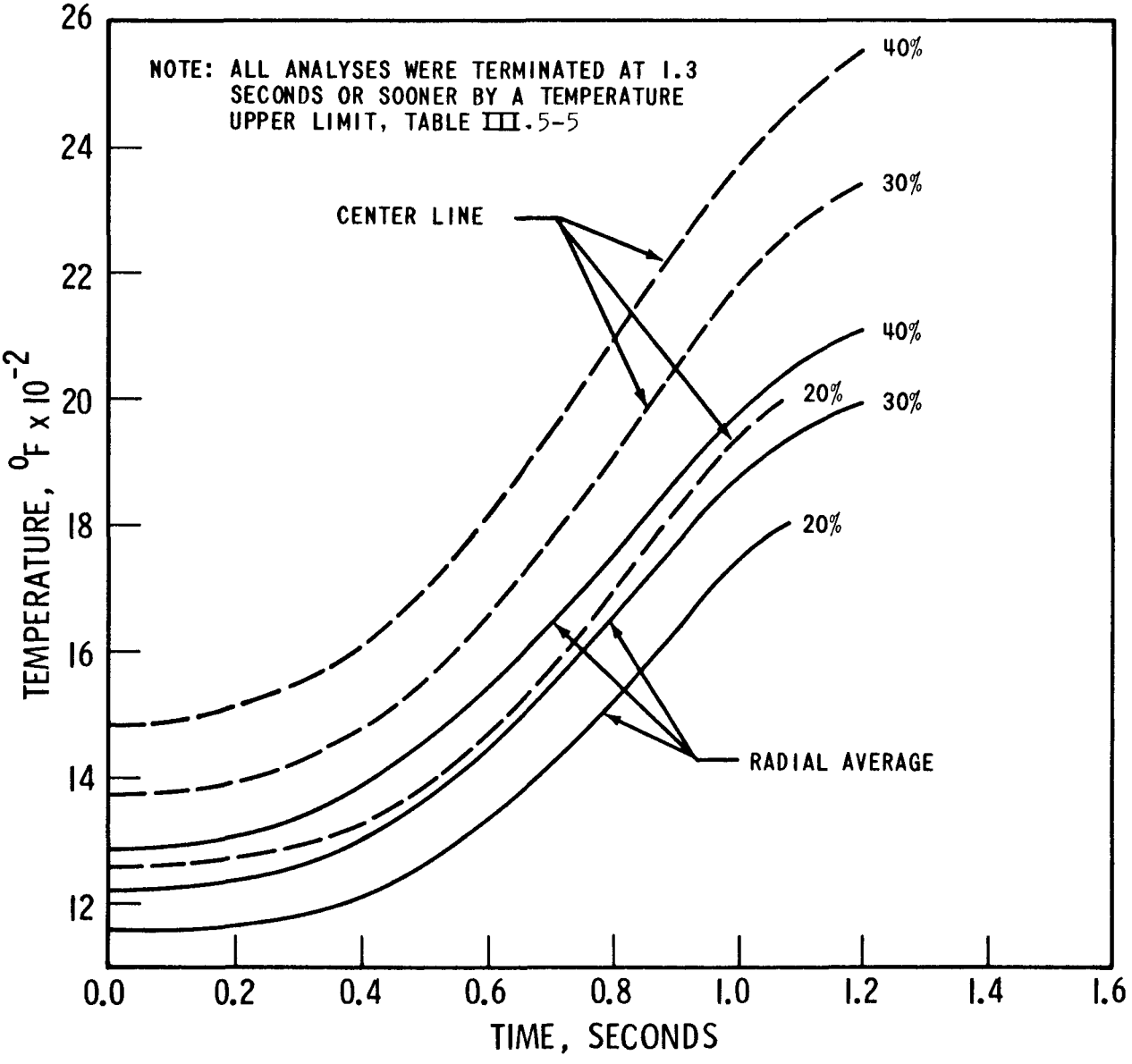

BCEX CERMET HOT CHANNEL TEMPERATURES - AXIAL SECTION NUMBER 4 (4 OF 6) - BCEX CERMET ROD DIAMETER 0.300 INCHES - OXIDE FUELED CORE OXIDE FUEL ROD DIAMETER 0.215 INCHES - RAMP REACTIVITY INSERTION 2¢ IN 1.0 SECOND

Figure III.5-33

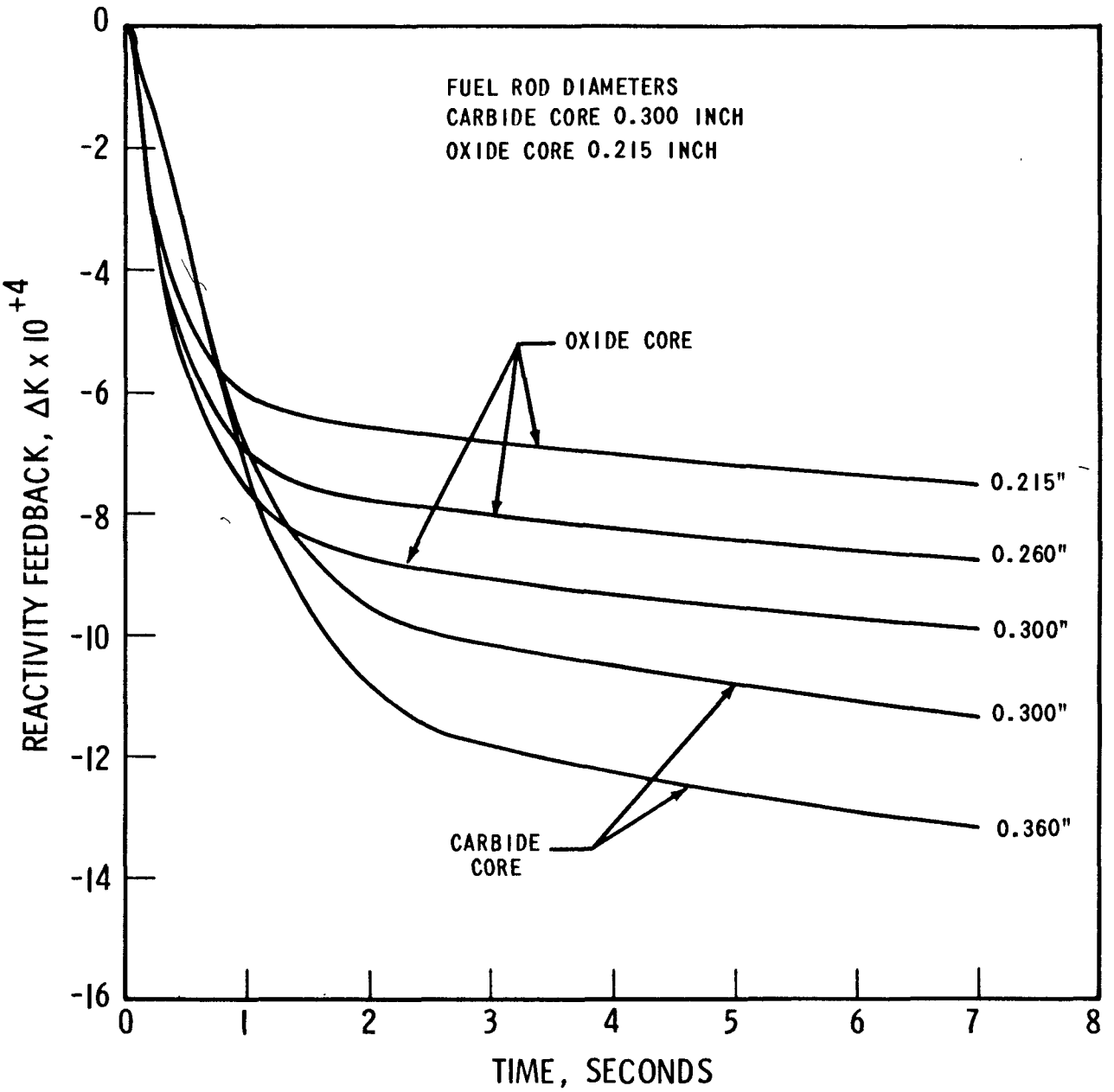

COMPARISON OF BCEX REACTIVITY FEEDBACK IN CARBIDE AND OXIDE CORES
BCEX CERMET HEAT GENERATION 30% OF FUEL-RAMP REACTIVITY INSERTION
80 CENTS IN 0.1 SECONDS

Figure III.5-34

after the first second, the BCEX feedback is greater in the carbide core. Thus, during the initial period of an excursion, BCEX is a more important excursion termination mechanism in an oxide core than in a carbide core. However, as new equilibrium conditions are approached, BCEX performs better in the carbide core as a mechanism for inserting negative reactivity feedback. In both cores, the BCEX feedback after the initial rise is found to be proportional to the 0.835 power of the ratio of cermet rod diameters.

Figures III.5-35 and III.5-36 compare the ratios of the net BCEX reactivity feedback to the total feedback, and the Doppler feedback to the total feedback, respectively. During the first second of the excursion, BCEX in the oxide core is seen to be nearly as important as Doppler in terminating the excursion, whereas, in the carbide core, Doppler is the major reactivity feedback for excursion termination. During this initial period, the BCEX feedback in the carbide core is greatly reduced by the positive feedback from the inward expansion of the fuel rod cladding.

After the first second of the excursion, the fractions of the total feedback in the oxide core due to BCEX and to Doppler remain essentially at a constant value, Figures III.5-35 and III.5-36, with Doppler being somewhat greater than BCEX. However, in the carbide core, BCEX's fractional worth of the total feedback increases from a minimum value to a value considerably greater than the Doppler fractional worth. For example, as new equilibrium thermal conditions are approached in the carbide core, the 0.360 inch diameter BCEX's fractional worth is 80 percent greater than the Doppler fractional worth. Thus BCEX's importance as a mechanism for negative reactivity feedback is greater for the oxide fueled core during the early stages of an excursion and for the carbide fueled core during the later stages of an excursion.

Figure III.5-37 compares the ratio of the net BCEX reactivity feedback to the cermet feedback. The cermet feedback is the negative reactivity

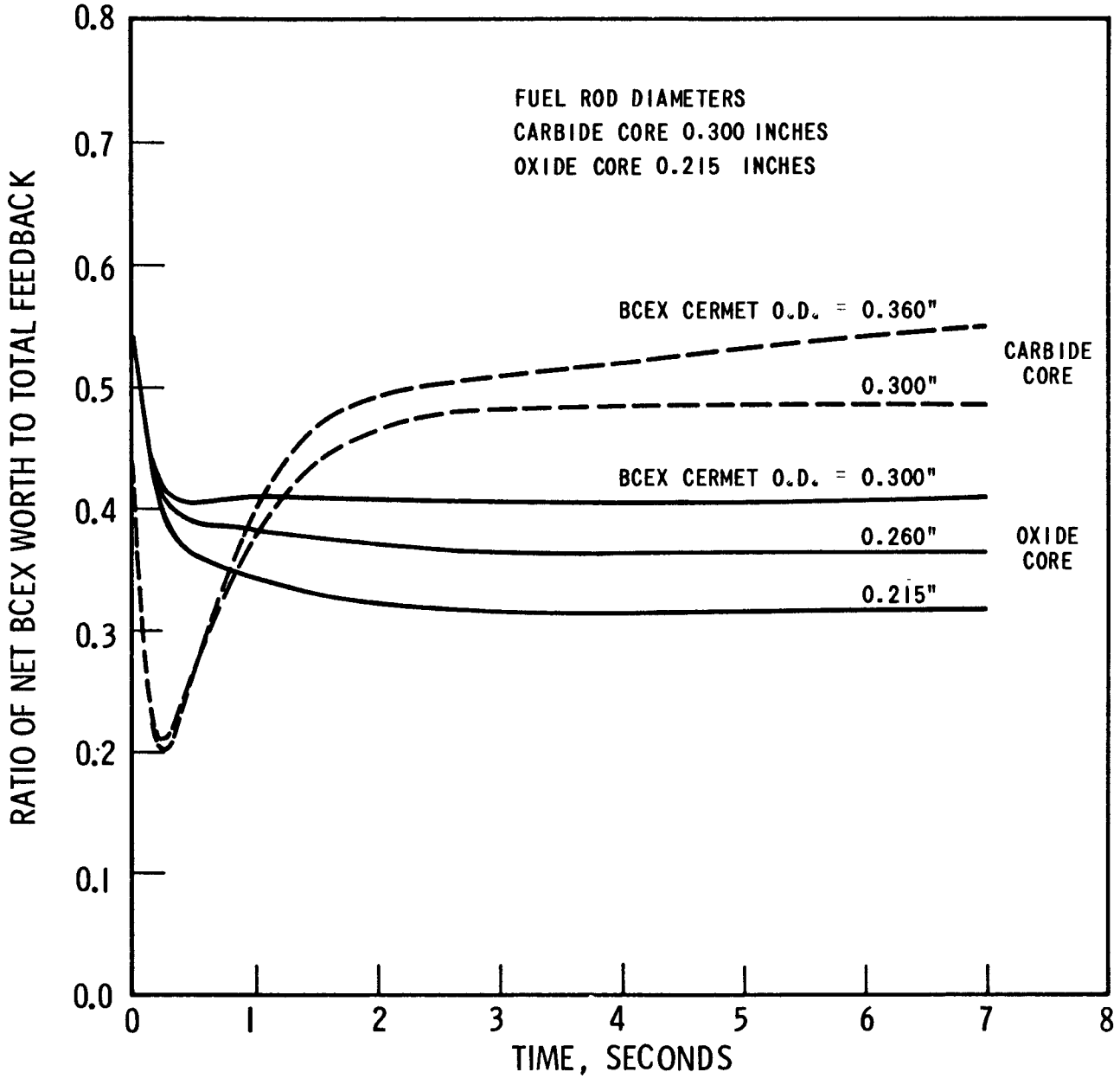

BCEX FRACTION OF TOTAL FEEDBACK WORTH
CEX ROD DIAMETER EFFECTS-FUEL MATERIAL EFFECTS
BCEX CERMET HEAT GENERATION 30% OF FUEL
RAMP REACTIVITY INSERTION 80 CENTS IN 0.1 SECONDS

Figure III.5-35

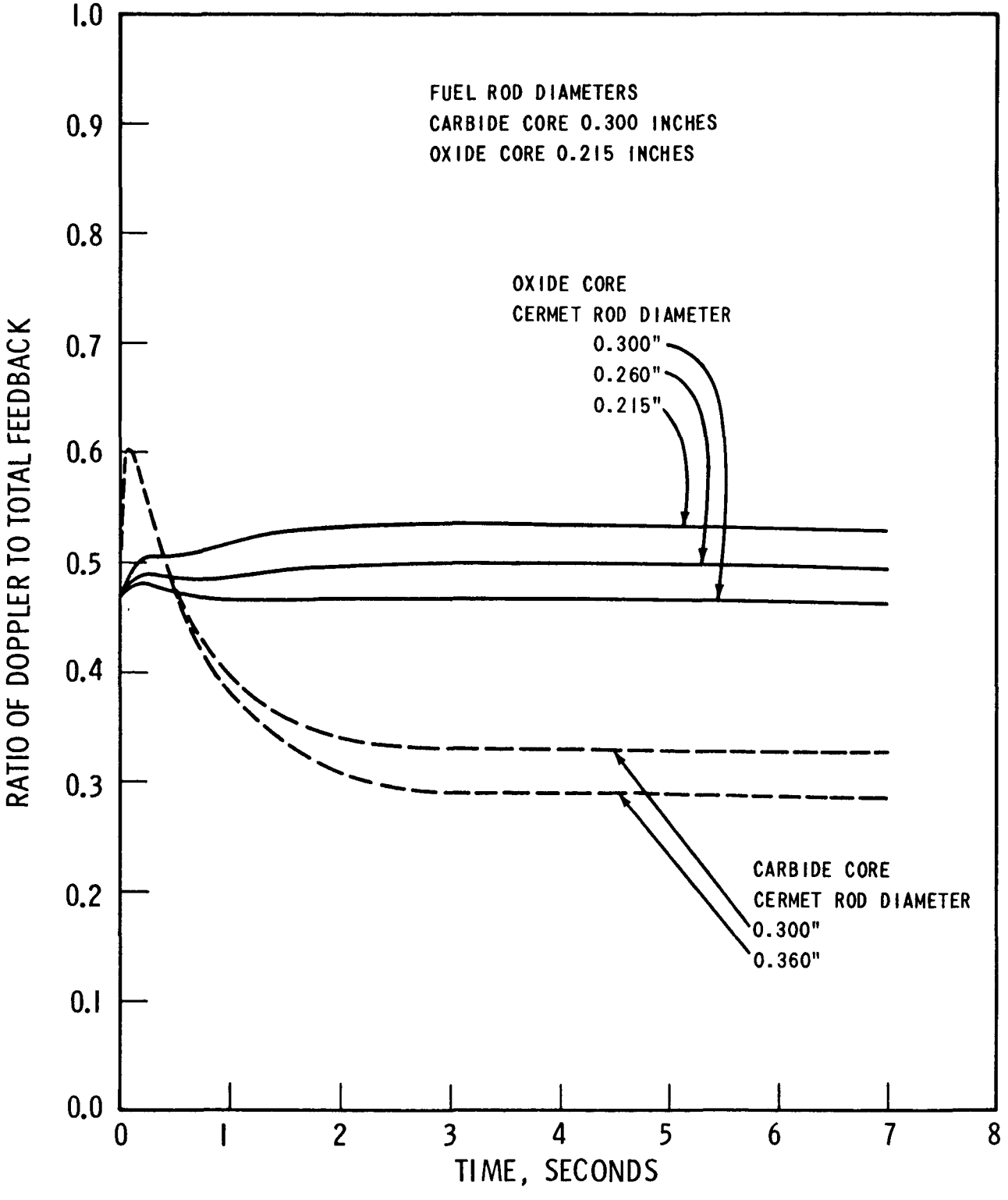

DOPPLER FRACTION OF TOTAL FEEDBACK WORTH-CEX ROD DIAMETER EFFECTS
BCEX CERMET HEAT GENERATION 30% OF FUEL
RAMP REACTIVITY INSERTION 80 CENTS IN 0.1 SECONDS

Figure III.5-36

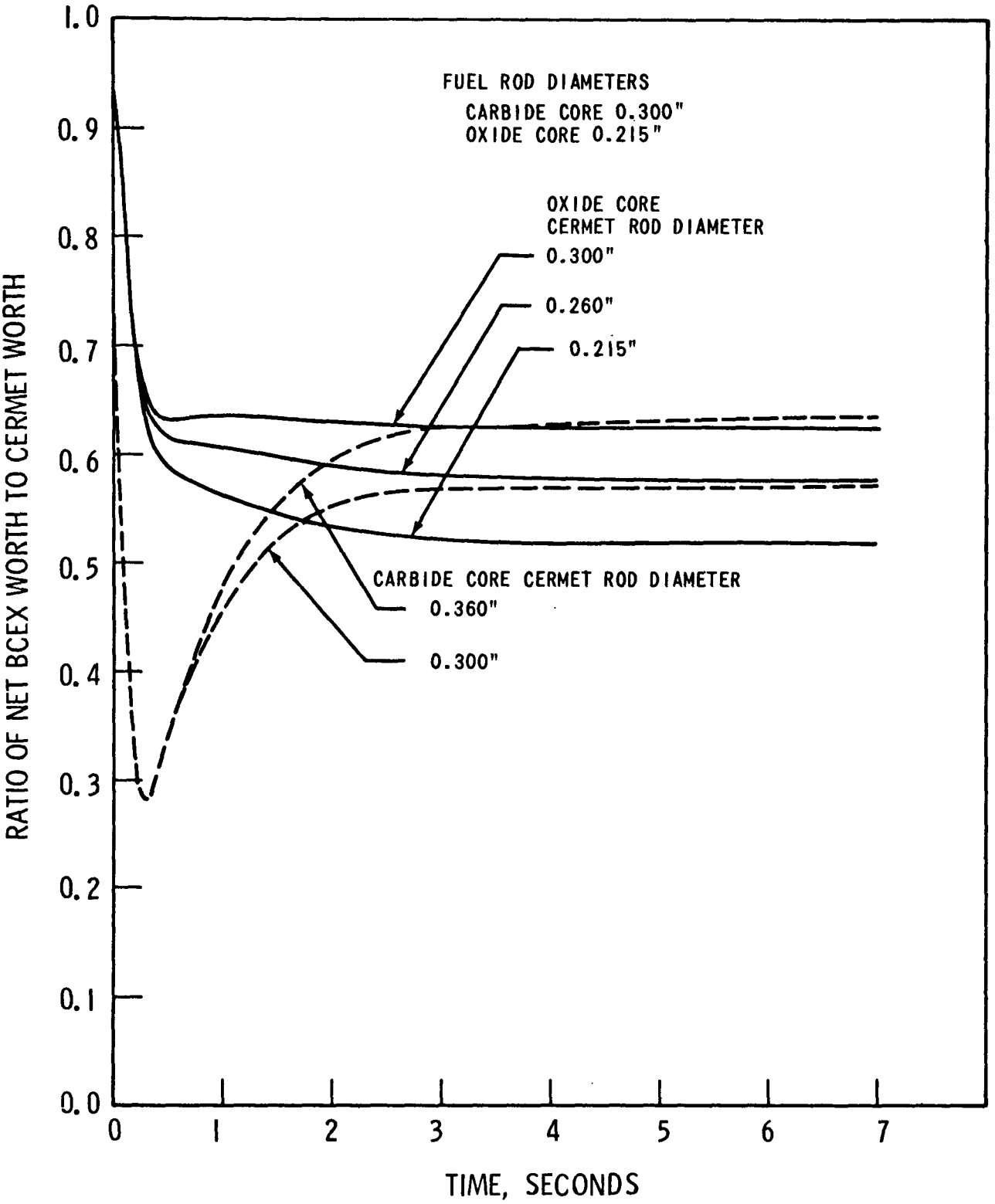

BCEX FRACTION OF CERMET WORTH - CERMET ROD DIAMETER EFFECTS - BCEX CERMET HEAT GENERATION 30% OF FUEL - RAMP REACTIVITY INSERTION 80 CENTS 0.1 SEC.

Figure III.5-37

feedback due only to the outward expansion of the cermet rod. As new equilibrium thermal conditions are approached in either core, BCEX's net fractional worth of the cermet expansion ranges from 0.52 to 0.64, depending upon the cermet rod diameter. The positive effect from fuel clad inward expansion is the difference between 1.0 and any of the curves shown in Figure III.5-37. The large reduction or downgrading of the effectiveness of BCEX in the carbide core as an excursion terminating mechanism is clearly illustrated.

The gap width between the lower and upper fuel bundles of the oxide core, at a BCEX 30% relative volumetric heat generation rate, is never less than the gap width at time zero, Figure III.5-38. However, in the carbide core, the rapid inward expansion of the fuel clad initially reduces the gap width to less than the zero time value. Thus, the application of BCEX in a sodium bonded carbide fueled core would require that the zero time gap width be large enough to insure that the upper fuel bundle does not hit the lower fuel bundle during an excursion.

The rise in the core fuel, cermet, fuel clad and coolant average temperatures from time zero for both the carbide and oxide cores, are compared in Figures III.5-39, III.5-40, III.5-41, and III.5-42, respectively. The behavior characteristics of BCEX noted in the reactivity feedback curves are reflected in the shape of the temperature curves. The smaller magnitude of the slope of the carbide core temperature curves after the initial rise results from the overshoot in temperature and the shorter time constants than those in the oxide core. The percentage reduction at 7 seconds in the no BCEX-no CCEX core fuel temperatures with the addition of axial expansion is 40% in the carbide core compared to 29% in the oxide core.

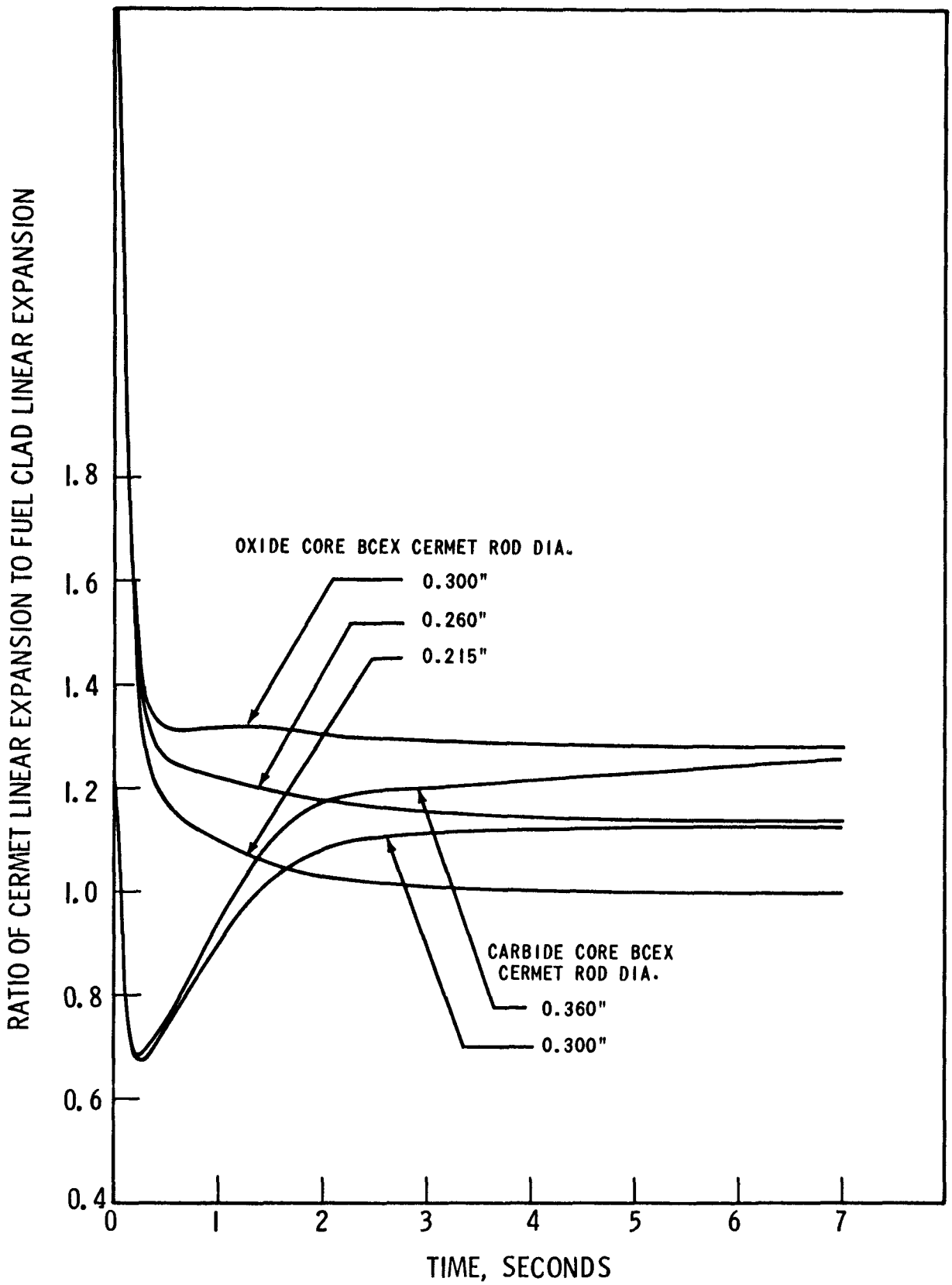

COMPARISON OF BCEX EXPANSION IN CARBIDE AND OXIDE FUELED CORES - BCEX CERMET HEAT GENERATION 30% of FUEL - RAMP REACTIVITY INSERTION 80 CENTS IN 0.1 SECONDS

Figure III.5-38

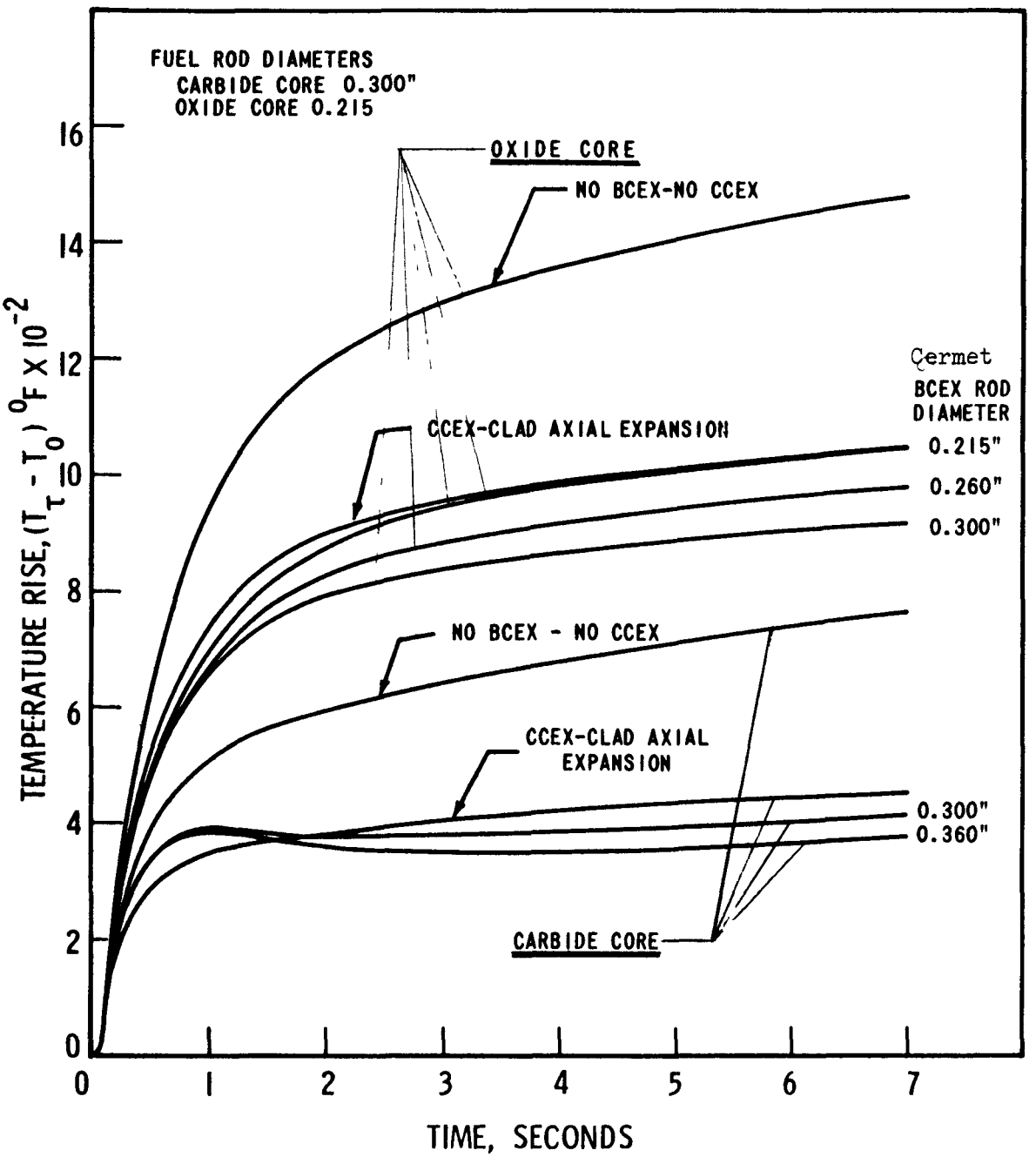

CHANGE IN CORE AVERAGE FUEL TEMPERATURE WITH TIME - BCEX CERMET HEAT GENERATION 30% OF FUEL - RAMP REACTIVITY INSERTION 80 CENTS IN 0.1 SECONDS

Figure III.5-39

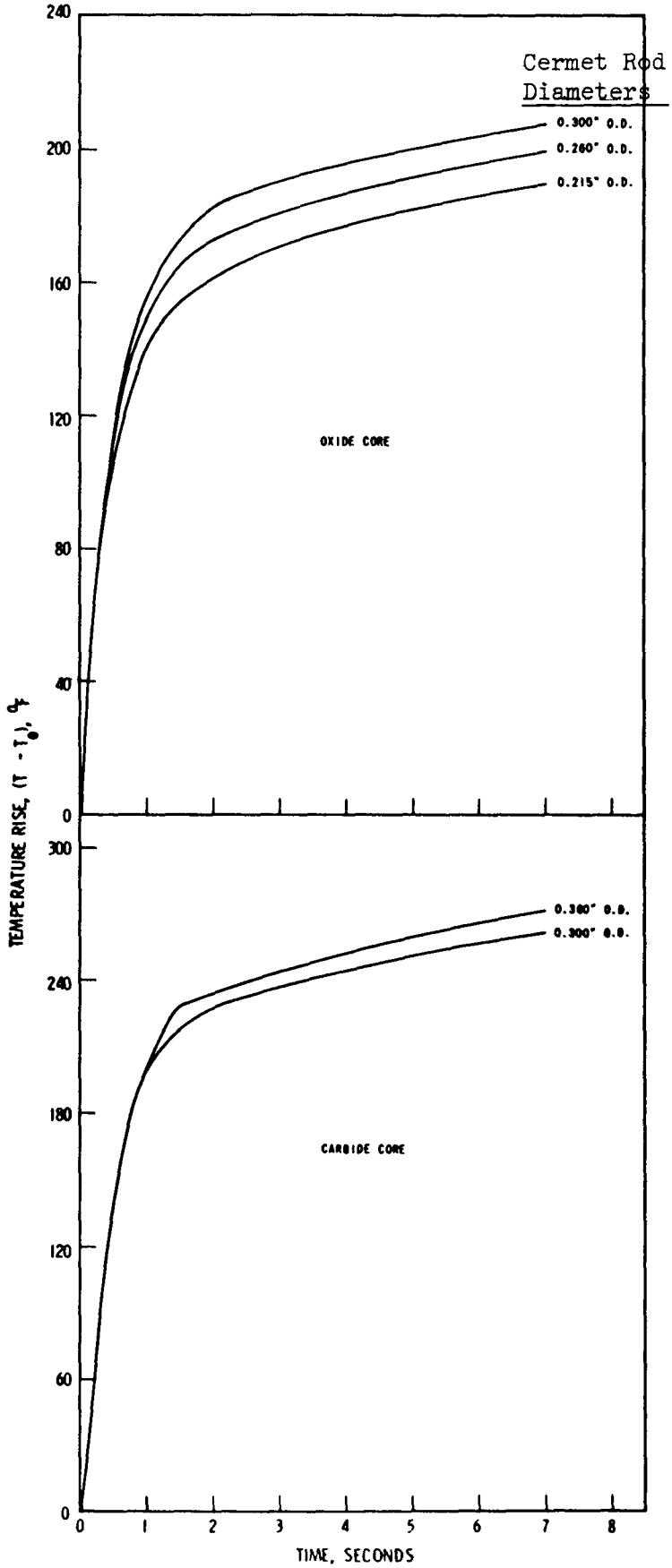

CHANGE IN CORE AVERAGE CERMET TEMPERATURE WITH TIME
BCEX CERMET HEAT GENERATION 30% OF FUEL
RAMP REACTIVITY INSERTION 80 CENTS IN 0.1 SECONDS
CARBIDE FUEL ROD DIAMETER 0.300 INCHES
OXIDE FUEL ROD DIAMETER 0.215 INCHES

Figure III.5-40

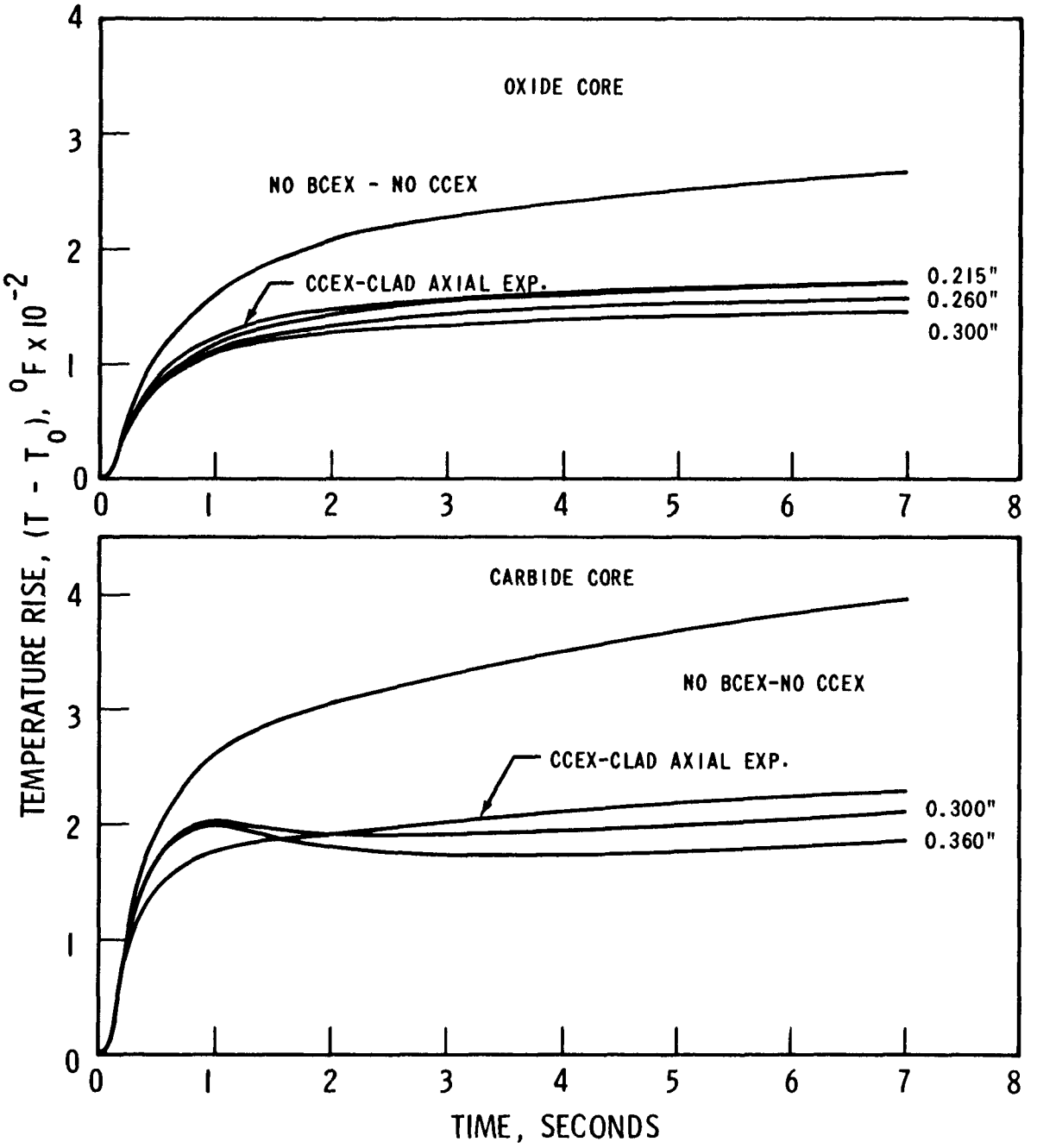

CHANGE IN CORE AVERAGE FUEL CLAD TEMPERATURE WITH TIME
BCEX CERMET HEAT GENERATION 30% OF FUEL
RAMP REACTIVITY INSERTION 80 CENTS IN 0.1 SECONDS

Figure III.5-41

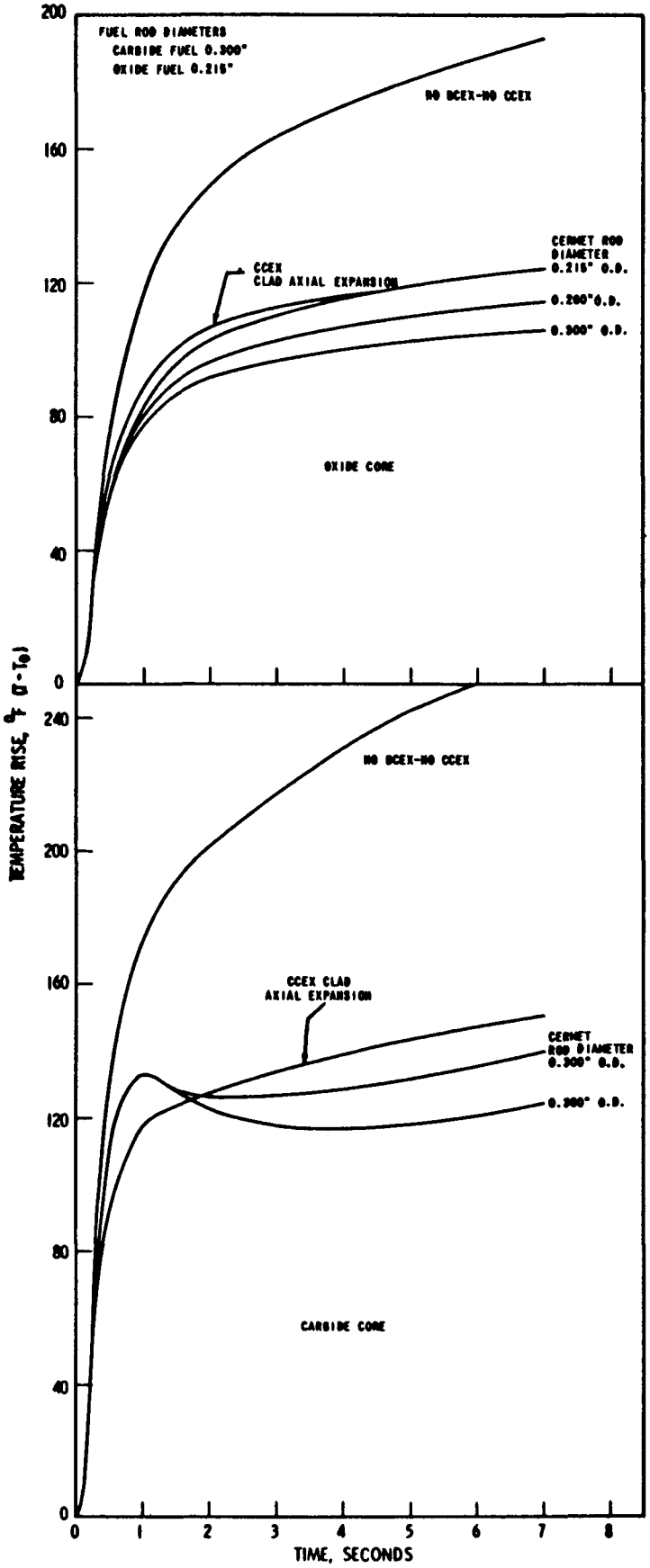

CHANGE IN CORE AVERAGE COOLANT TEMPERATURE WITH TIME
BCEX CERMET HEAT GENERATION 30% OF FUEL
RAMP REACTIVITY INSERTION 80 CENTS IN 0.1 SECONDS

Figure III.5-42

III.5.5 Accident Analyses

From a review of the reactor designs in references 1 and 7, the following three reactor accidents considered most likely to occur were selected for study and for comparison of the BCEX and the CCEX cores' characteristics to those of the no BCEX-no CCEX core.

1. Refueling accident - dropping a fuel assembly into a just subcritical core.
2. Expulsion of a control rod at 100% core thermal power.
3. Loss of electrical power to all primary pumps at 100% core thermal power.

The analyses for these three accidents were performed on an isolated carbide fueled core representing one module of a multi-module system[1]. The BCEX analyses were performed using the recommended cermet rod diameter, 0.360 inch O.D., and volumetric heat generation rate of 30% of that of the fuel. As noted previously, the fuel rods are divided into compartments containing twelve inch stacks of active fuel pellets. The fuel is assumed to move with the clad. In the BCEX analysis, the fuel clad expansion is inward, that is, towards the mid-plane of the core; in the CCEX analyses, it is outward, that is, it increases the core height.

The temperature dependent reactivity coefficients which were used are given in Table III.5-4. The fuel assembly and control rod reactivity worths selected for the first two accidents are the maximum worth of the components to the entire seven modular core system[1,7]. In the loss of all electrical power accident, each primary pump is assumed to be equipped with a high inertia flywheel attached to the rotor of the drive motor to obtain the desired flow decay characteristic.

III.5.5.1 Refueling Accident - Dropping Fuel Assembly into a Just Subcritical Core

This accident assumes a loss of administrative control followed by a mechanical failure. Loss of administrative control means that the reactor has been allowed to become just subcritical with a center fuel assembly missing. Then as the center fuel assembly is being lowered into the core, a mechanical failure causes the latch mechanism to release the fuel assembly allowing it to fall freely into the core.

The maximum worth of a fuel assembly in the seven modular system[7] is two dollars. The fuel assembly is assumed to free fall into the core unimpeded by the flowing sodium. Under this assumption, 0.615 seconds are required for complete insertion into a six foot core. The reactivity addition is taken to be proportional to distance travelled instead of the usual "S" shape distribution, Figure III.5-43.

The core is assumed to be at a decay heat power level of 0.5% of full power (2.08 megawatts), sodium flow at 20% full flow, and the core inlet temperature to be 400°F. The 0.5% decay heat corresponds to the residual heat generation in a thermal reactor (PWR) seven days after shutdown.

The normalized power, P/P_o, as a function of time is shown in Figure III.5-44 for this postulated dropped-fuel assembly accident. The peak powers are 7250 megawatts in the no BCEX-no CCEX core, 5920 megawatts in the BCEX core, and 5550 megawatts in the CCEX core. Only after two seconds has elapsed does the BCEX core power level fall below the CCEX core power level. Thus, the trends noted in the parameter study concerning BCEX's initial lower feedback performance hold true in this postulated accident. Only after the degrading of the cermet outward expansion by the clad inward expansion stops in the BCEX case does the crossover of the two power curves occur. The no BCEX-no CCEX analyses terminated at 1.33 seconds on an upper coolant temperature limit, Table III.5-5.

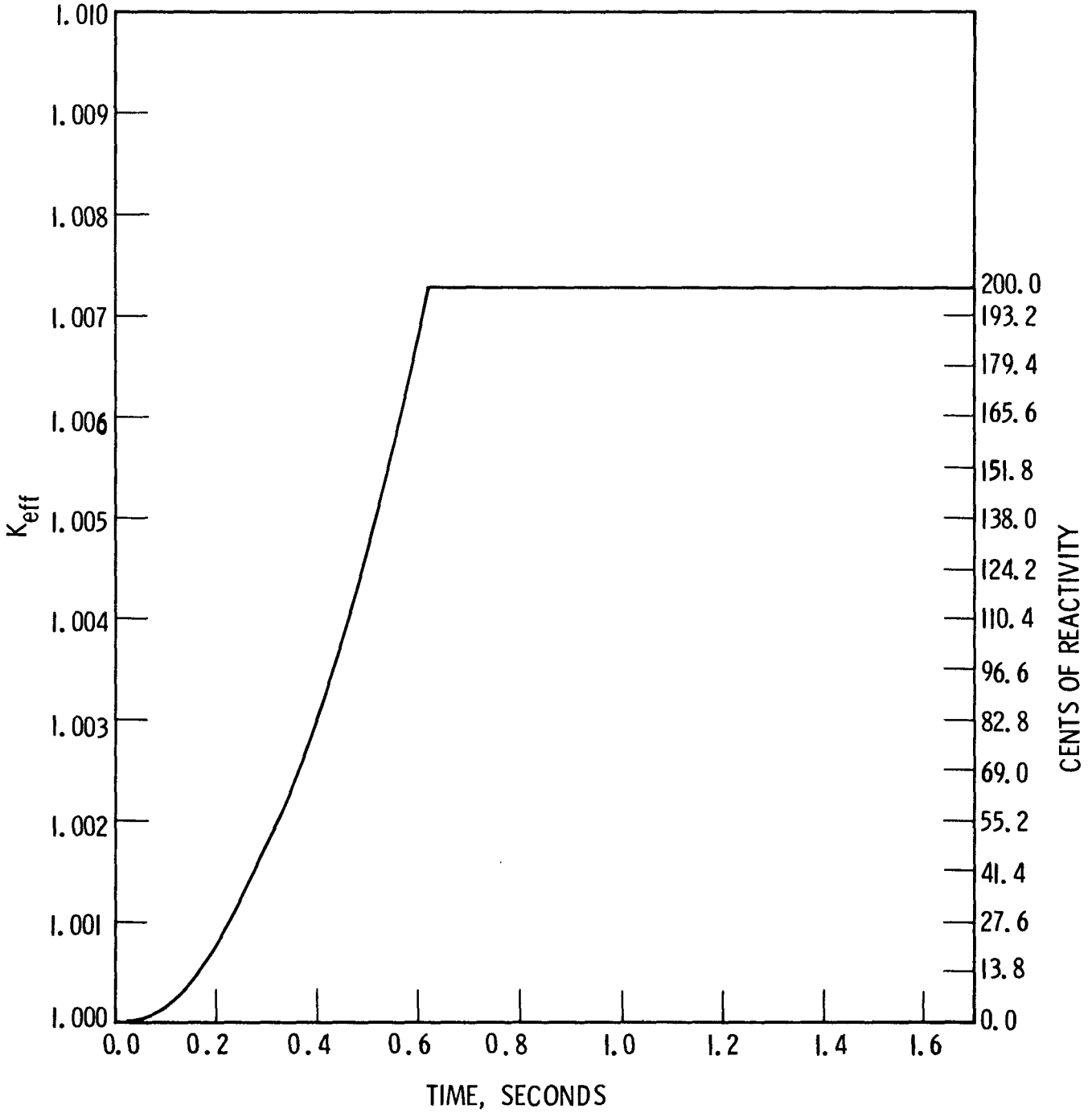

ACCIDENT ANALYSES: DROPPING FUEL ASSEMBLY
REACTIVITY INSERTION VS TIME

Figure III.5-43

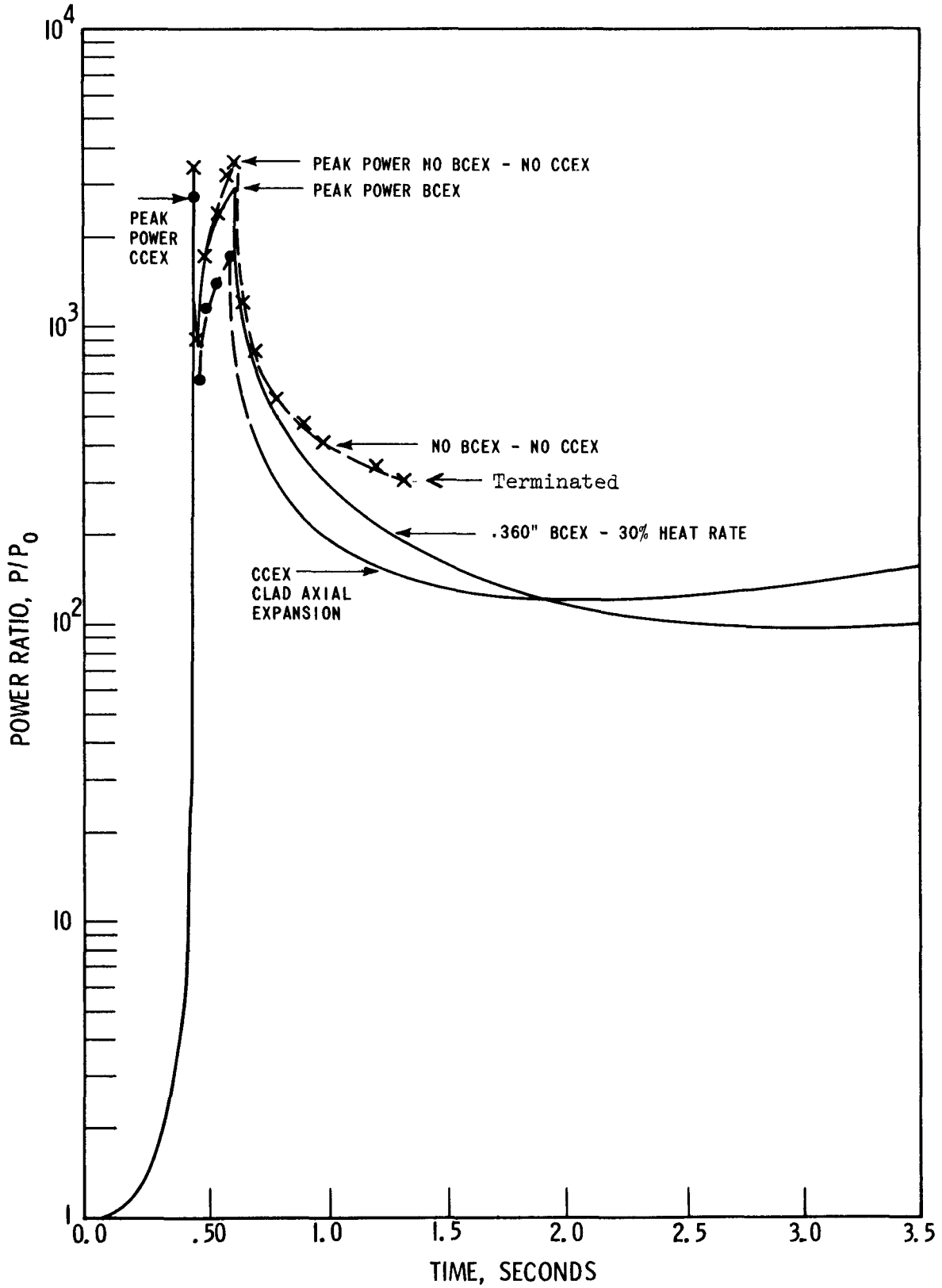

ACCIDENT ANALYSIS: DROPPING FUEL ASSEMBLY-CHANGE IN CORE POWER WITH TIME (P_0 = 2.08 MW)

Figure III.5-44

The fuel temperature rise in the average and hot channels, and the BCEX cermet temperature rise in the average channel are shown in Figures III.5-45 and III.5-46. The no BCEX-no CCEX case was terminated after 1-1/3 seconds. The BCEX core fuel peak temperature rise occurs at one second and is approximately 50% higher than the peak in the CCEX core. The BCEX equilibrium temperature rise at 10 seconds is 20°F below the CCEX core's rise. The BCEX core's peak cermet average temperature rise is 815°F at 2.3 seconds, which then reduces to 675°F at 10 seconds, Figure III.5-46.

The hot channel fuel maximum temperature occurs in axial section number 4 (4 of 6). Figure III.5-47 shows the centerline and radial average temperatures for this axial section. The maximum fuel centerline temperatures are 3000°F (when terminated) in the no BCEX-no CCEX core, 2700°F in the BCEX core, and 2000°F in the CCEX core. The no BCEX-no CCEX exceeded one of the temperature limits listed in Table III.5-5, the other cases did not exceed any of these limits.

The BCEX hot channel cermet maximum temperature occurs in axial section number 5 (5 of 6). The hot channel centerline and radial average temperatures for the cermet rod and for axial section number 5 is shown in Figure III.5-48. It is interesting to note that from 0.8 seconds to 0.3 seconds the cermet centerline temperature falls below the radial average temperature. This occurs because the coolant is hotter and thus gives up heat to the cermet rod (see insert in Figure III.5-48). After the coolant temperature drops below its peak value (see Figure III.5-49), the cermet then gives up heat to the coolant and the centerline temperature rises above the radial average.

In this accident, coolant boiling, Figure III.5-49, was encountered in both the no BCEX-no CCEX and the BCEX cores. The assumed boiling temperature of 1830°F corresponds to a pressure of 40 psia and does not include any liquid superheat effect. In the no BCEX-no CCEX core, boiling occurs in the average channel as well as in the hot channel.

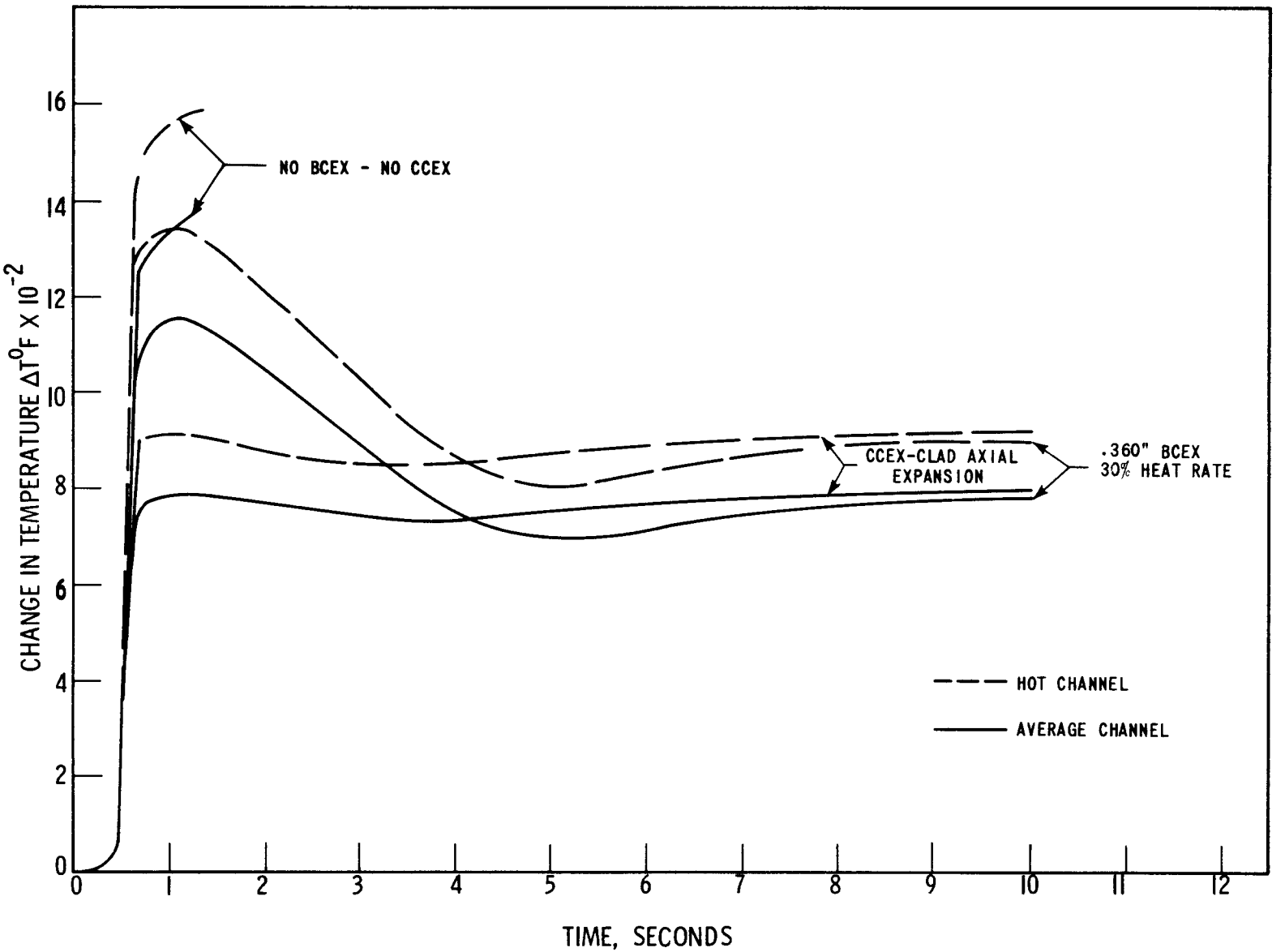

ACCIDENT ANALYSES: DROPPING FUEL ASSEMBLY-CHANGE IN CORE AVERAGE FUEL TEMPERATURES-20% SODIUM FLOW - 0.5% DECAY HEAT - COOLANT INLET 400°F

Figure III.5-45

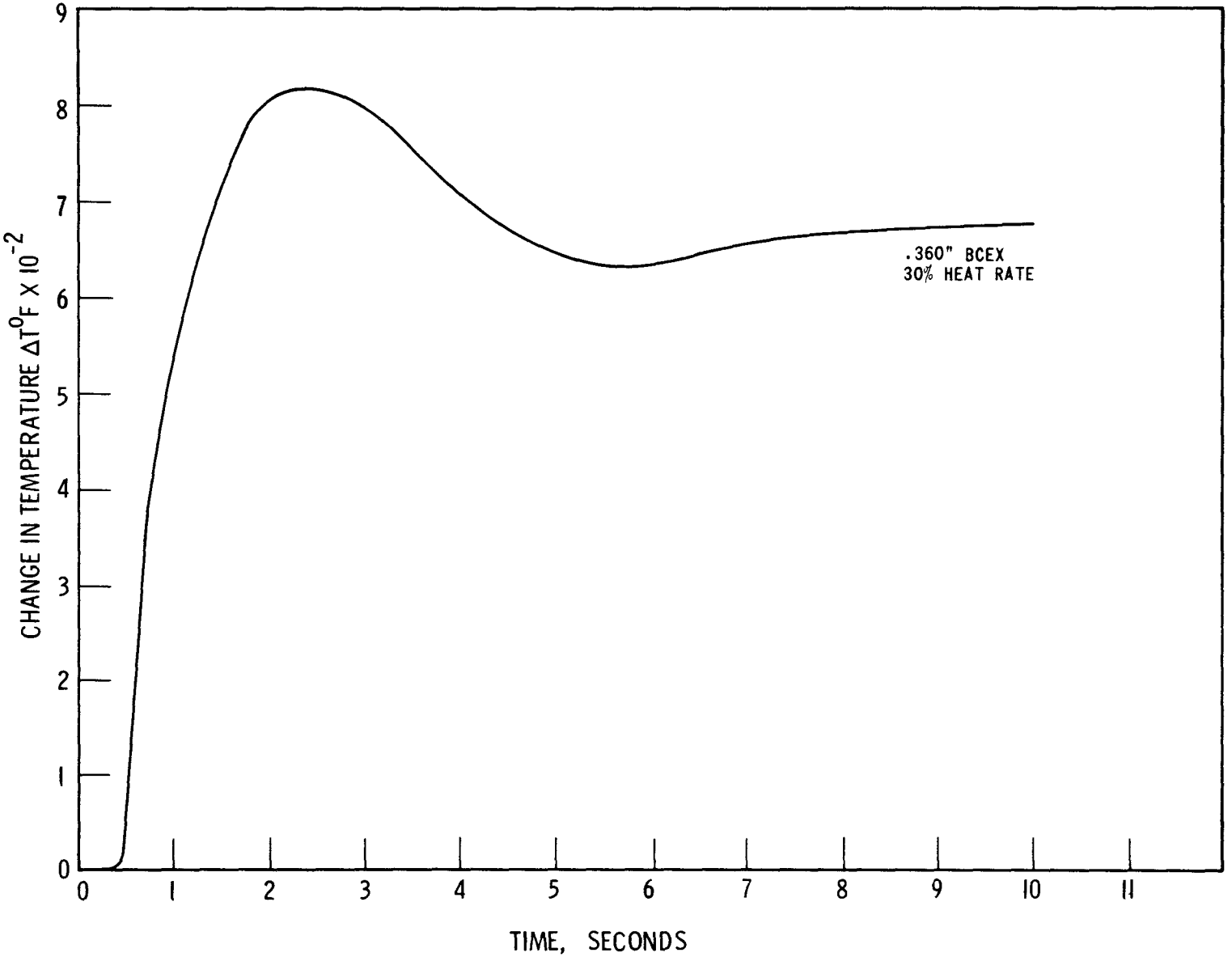

Figure III.5-46 - ACCIDENT ANALYSES: DROPPING FUEL ASSEMBLY - CHANGE IN CORE AVERAGE CERMET TEMPERATURE - 20% SODIUM FLOW - 0.5% DECAY HEAT - COOLANT INLET 400°F

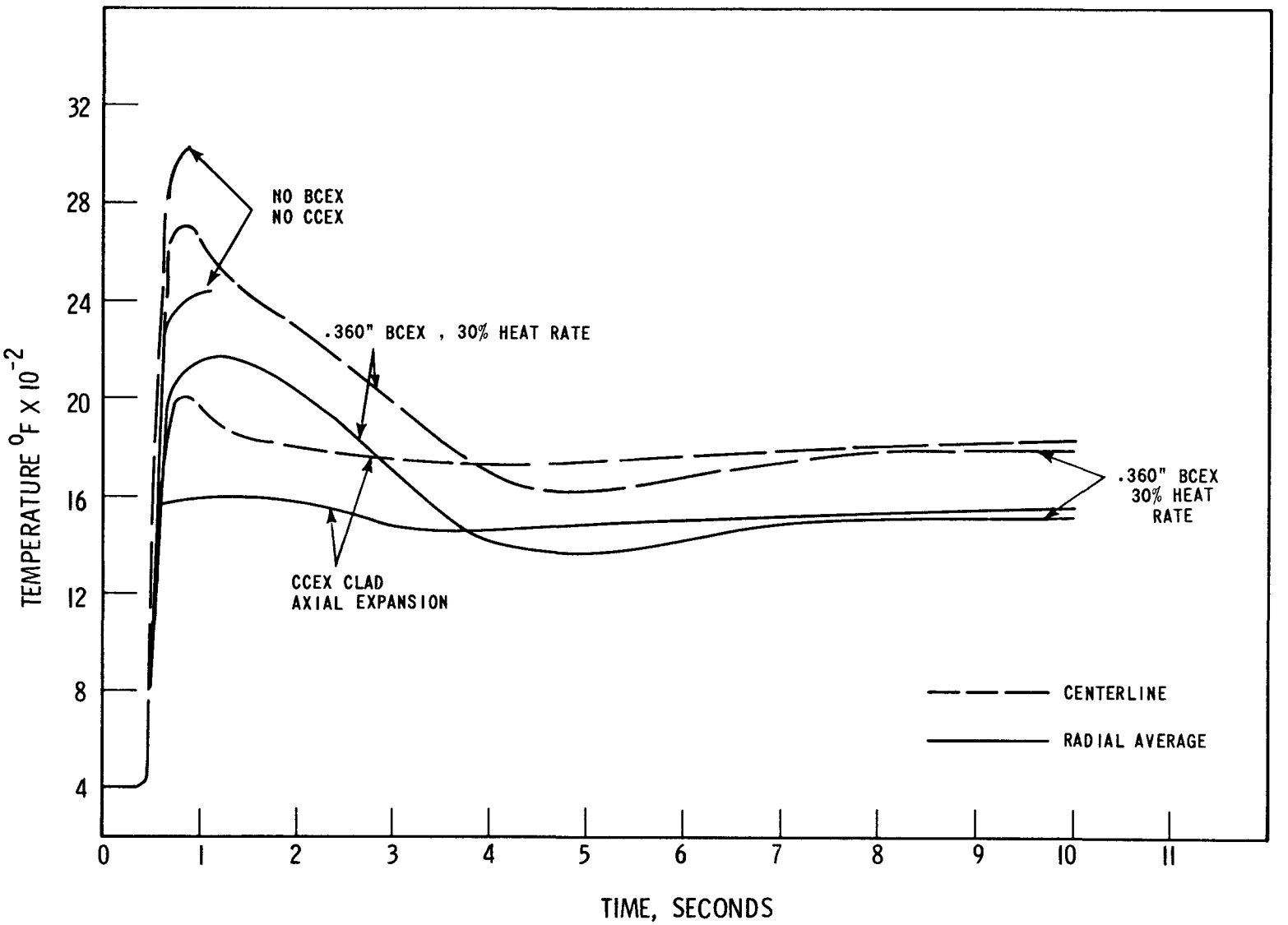

ACCIDENT ANALYSES: DROPPING FUEL ASSEMBLY-FUEL TEMPERATURE IN HOT CHANNEL AXIAL SECTION 4 (4 OF 6)-20% SODIUM FLOW - 0.5% DECAY HEAT - COOLANT INLET 400°F

Figure III.5-47

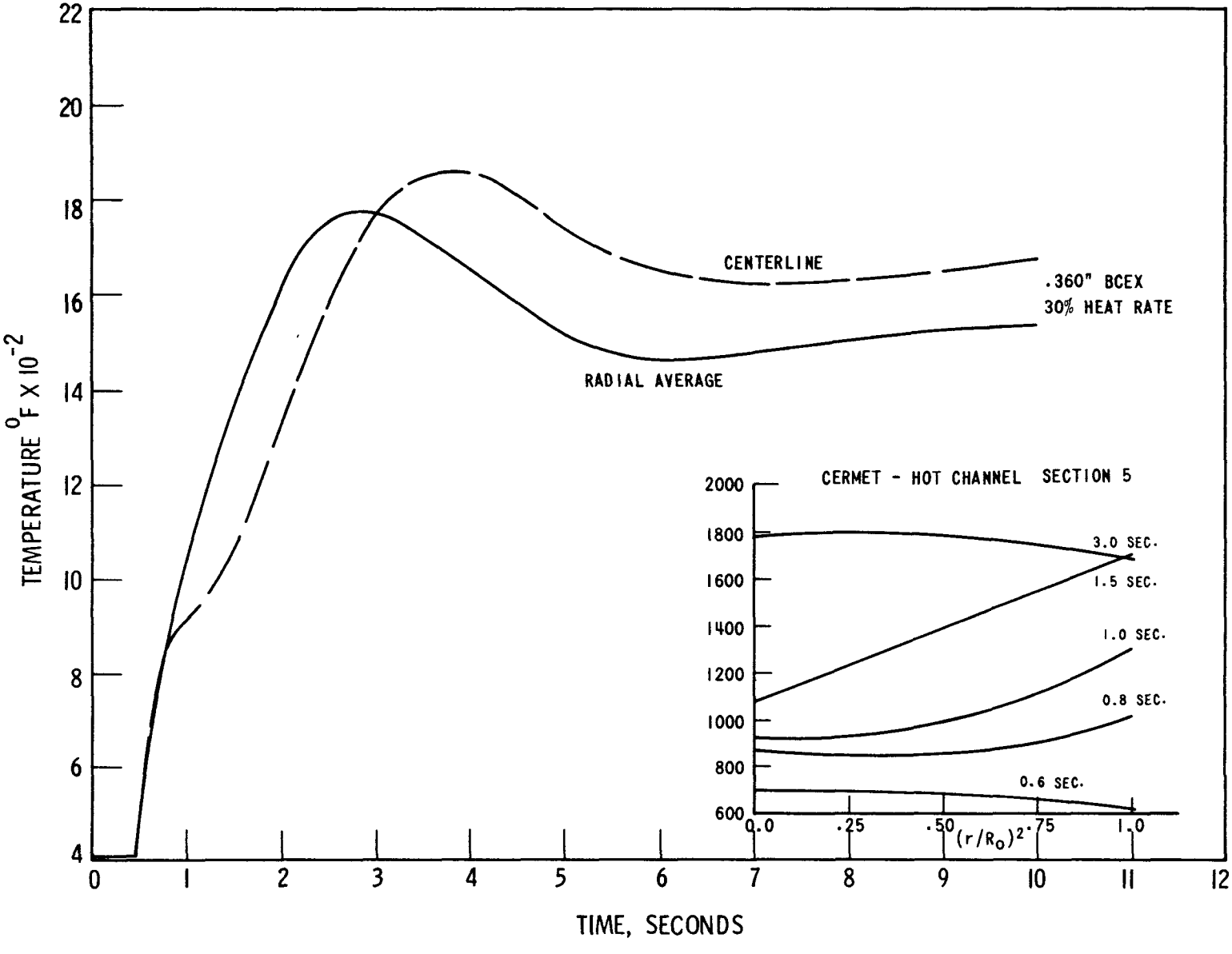

Figure III.5-48 - ACCIDENT ANALYSES: DROPPING FUEL ASSEMBLY-CERMET TEMPERATURES IN HOT CHANNEL, AXIAL SECTION 5 (5 OF 6)-20% SODIUM FLOW - 0.5% DECAY HEAT - COOLANT INLET 400°F

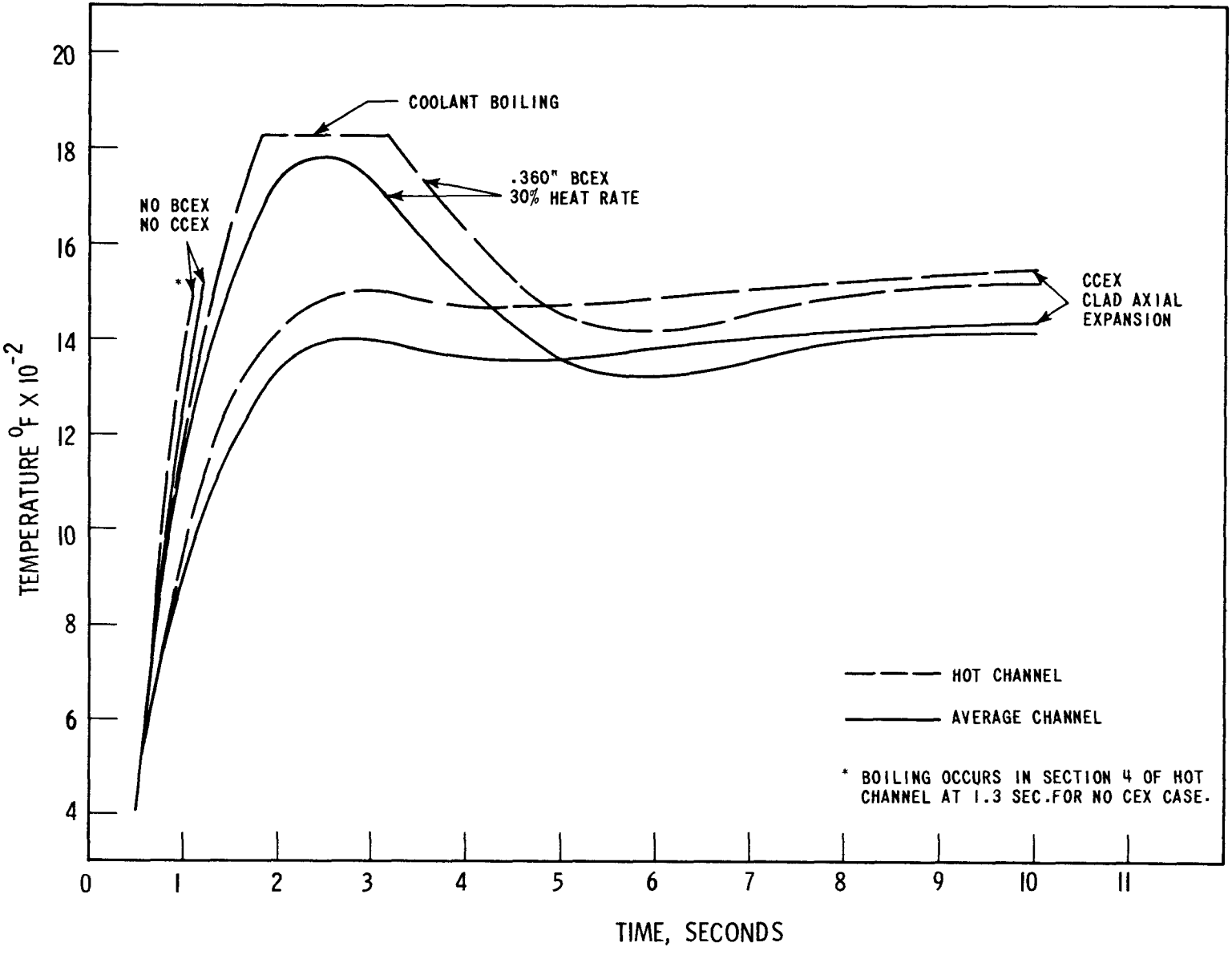

ACCIDENT ANALYSES: DROPPING FUEL ASSEMBLY-CORE EXIT COOLANT TEMPERATURES-20% SODIUM FLOW - 0.5% DECAY HEAT - COOLANT INLET 400°F

Figure III.5-49

In the BCEX core, coolant boiling occurs only in the outlet of the hot channel. The rate of core voiding, once coolant boiling begins, was not studied, as the modifications to the Westinghouse version of the FORE computer code[2] did not include two phase flow and coolant pressure drop considerations. The maximum coolant temperature occurring in the CCEX core is 1550°F, 280°F below the assumed boiling point.

The fuel clad maximum temperatures in the average and hot channels occur in axial section number 5 (5 of 6) and are shown in Figure III.5-50. The BCEX core's hotspot clad temperature is 1940°F versus 1480°F in the CCEX core. At 10 seconds, the fuel clad maximum temperatures in the two cores differ by 20°F, 1450°F in the CCEX core and 1430°F in the BCEX core. The no BCEX core calculation was terminated around 1.3 seconds.

In summary, the rapid negative reactivity feedback response obtained from the fuel clad axial expansion, CCEX, prevented coolant boiling and, thus, any damage associated with core voiding during this postulated refueling accident. In the BCEX core, the fuel clad axial expansion is a positive reactivity feedback which reduces the excursion termination effectiveness of BCEX in the initial stages of the accident. The temperature overshoot, which was noted in all the studies, is exaggerated in this case due to the large amount of reactivity that was inserted. This temperature overshoot would be serious in this incident, since it results in coolant boiling and possible core voiding in the outlet of the hot channel and, thus, possible core damage. Nevertheless, both the CCEX and BCEX core performance demonstrated substantial improvement over the no CEX core.

III.5.5.2 Expulsion of a Control Rod at 100% Core Thermal Power

In the seven modular core array[7], there is a total of 49 control rods, seven rods per module. The maximum worth of a control is one dollar. This analysis assumes that the maximum worth control rod is in the fully

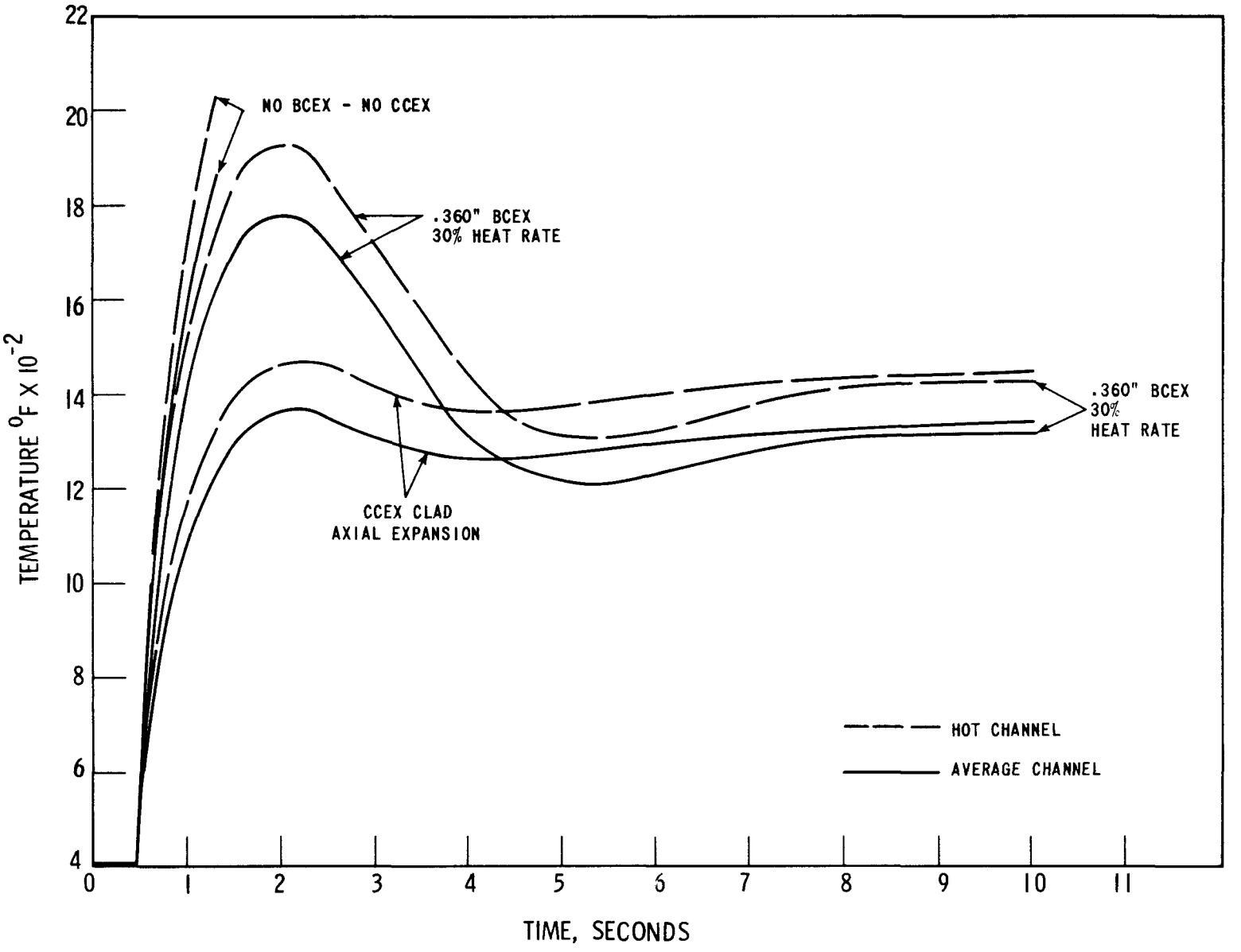

ACCIDENT ANALYSES: DROPPING FUEL ASSEMBLY - AVERAGE CLAD TEMPERATURES IN AXIAL SECTION 5 (5 OF 6) - 20% SODIUM FLOW - 0.5% DECAY HEAT - COOLANT INLET 400°F

Figure III.5-50

inserted position when expelled from the core. In expelling the control rod, it was assumed that either the control rod drivr mechanism or the control rod extension shaft breaks and, subsequently, the full core pressure drop of 100 psi acts on the control rod. Under these conditions, the control rod would be expelled at an acceleration of 100 ft/sec.^{2} (approximately 3 g's), neglecting fluid drag forces. In this analysis, the initial acceleration was held constant for the full core height, six feet. The rod would then be fully out of the core in 0.35 seconds. The control rod ejection effect on k_{eff} is shown in Figure III.5-51. The initial core conditions were assumed to be 100% power and full coolant flow.

The core power ratio, P/P_o, as a function of time is shown in Figure III.5-52. As noted in the previous analyses, the lowest peak power, 5.9 times full power, occurs in the CCEX core, whereas the lowest new equilibrium power, 2.2 times full power at six seconds, occurs in the BCEX core. The peak powers in the no BCEX-no CCEX and the BCEX cores are 8.35 and 6.85 times full power, respectively. The new equilibrium powers in the no BCEX-no CCEX core and the CCEX core are 3.7 and 2.5 times full power, respectively.

The temperature rise in the fuel, average and hot channels, and in the BCEX cermet, core average, are shown in Figures III.5-53 and III.5-54. In this accident, the fuel temperatures in either of the axial expansion cores, BCEX or CCEX, are lower by 25% or more (215°F at one second to 665°F at seven seconds) than in the no BCEX-no CCEX core. Up to 1.7 seconds, the CCEX core has a lower average fuel temperature than the BCEX core, but after this time, the BCEX core fuel temperatures are approximately 100°F lower at seven seconds. After seven seconds, the rise in the BCEX cermet average temperature is 350°F, Figure III.5-54.

The maximum hot channel fuel and cermet temperatures, centerline and radial average, occur in axial section number 4 (4 of 6), Figure III.5-55 and III.5-56. In the no BCEX-no CCEX core, the hotspot fuel centerline

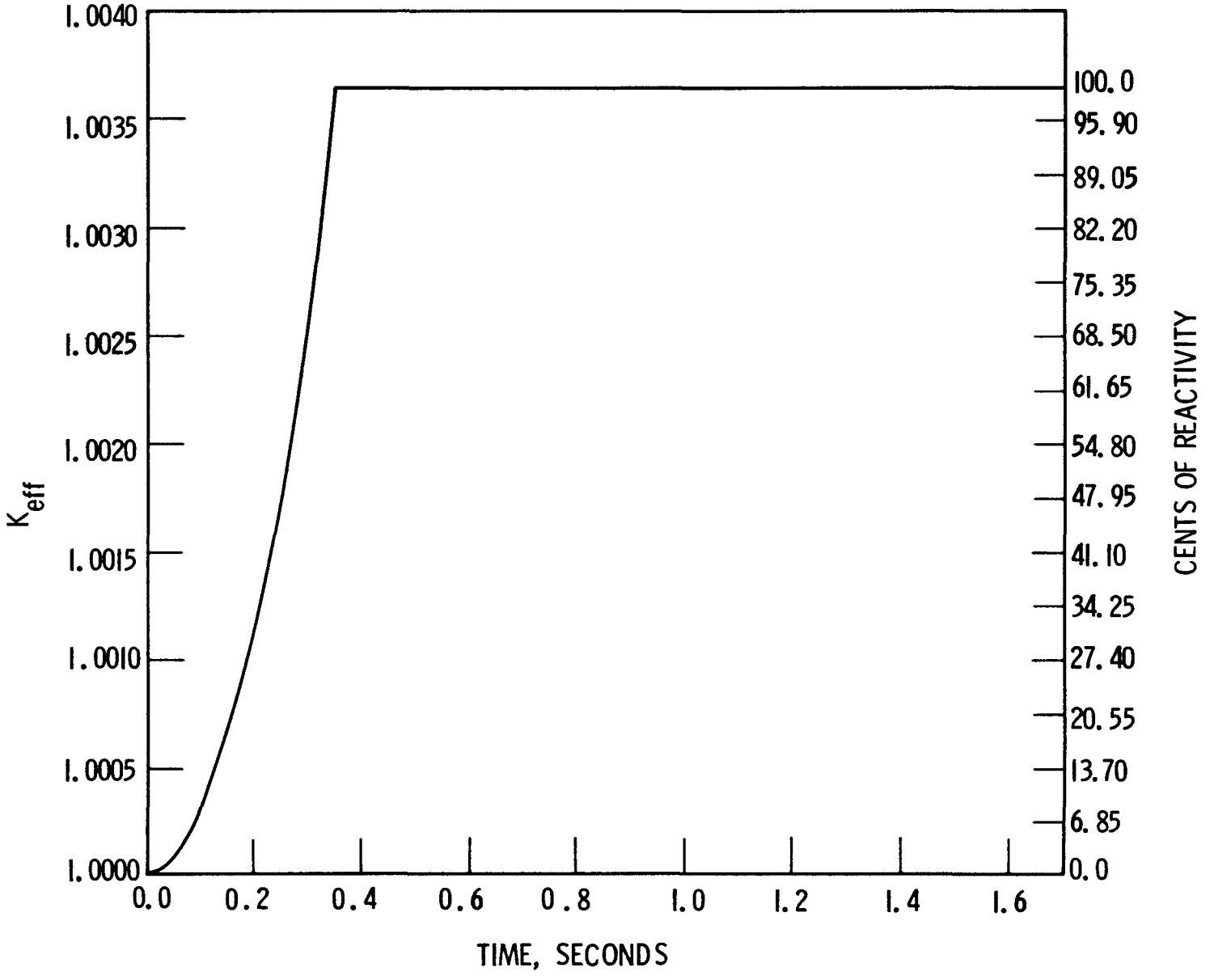

ACCIDENT ANALYSES: CONTROL ROD EJECTION
REACTIVITY INSERTION VS TIME

Figure III.5-51

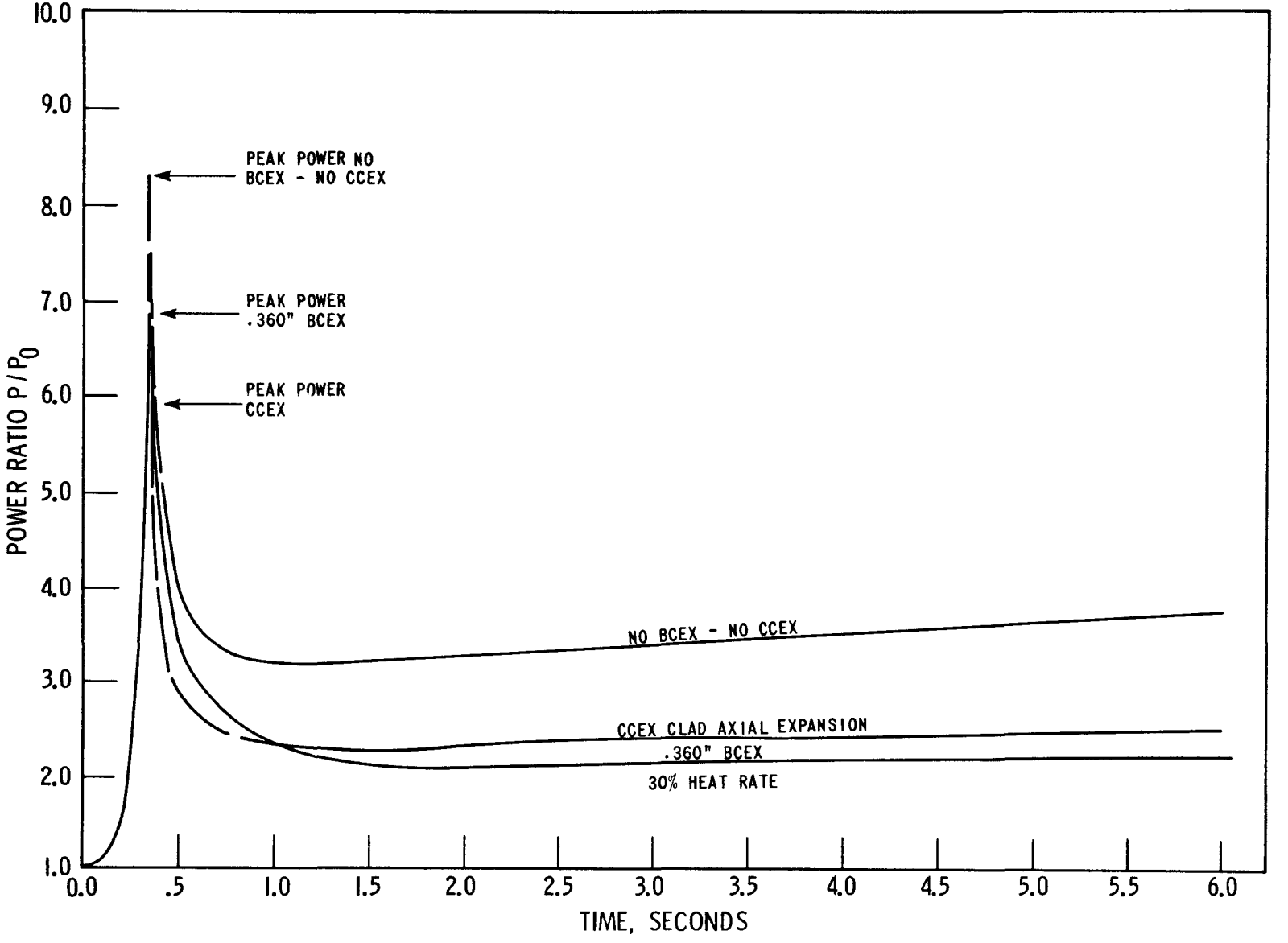

ACCIDENT ANALYSES: CONTROL ROD EJECTION-CHANGE IN CORE POWER WITH TIME (P_0 = 415.5 MW)

Figure III.5-52

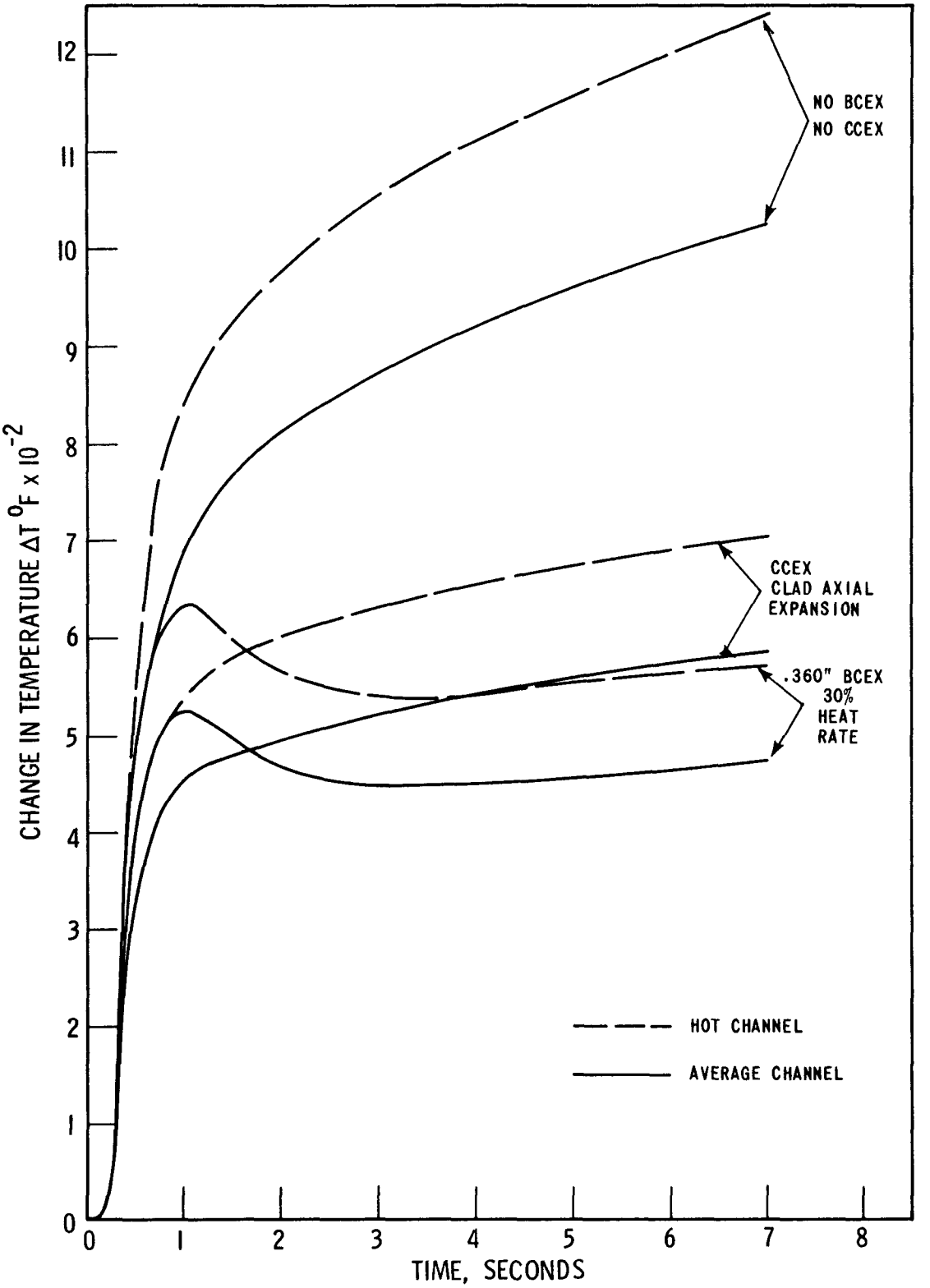

ACCIDENT ANALYSES: CONTROL ROD EJECTION-CHANGE IN CORE AVERAGE FUEL TEMPERATURES

Figure III.5-53

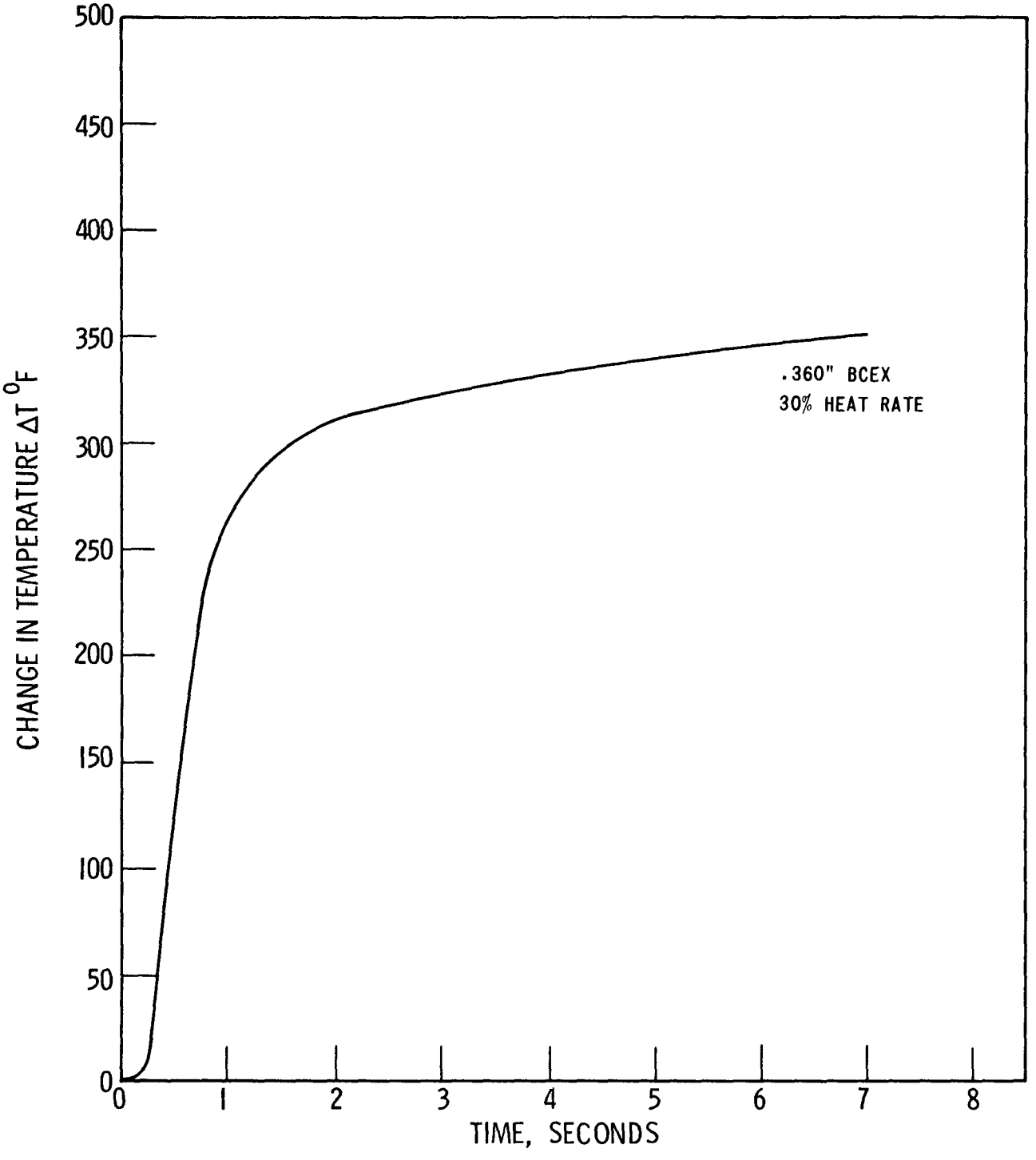

ACCIDENT ANALYSES: CONTROL ROD EJECTION-CHANGE IN CORE AVERAGE CERMET TEMPERATURE

Figure III.5-54

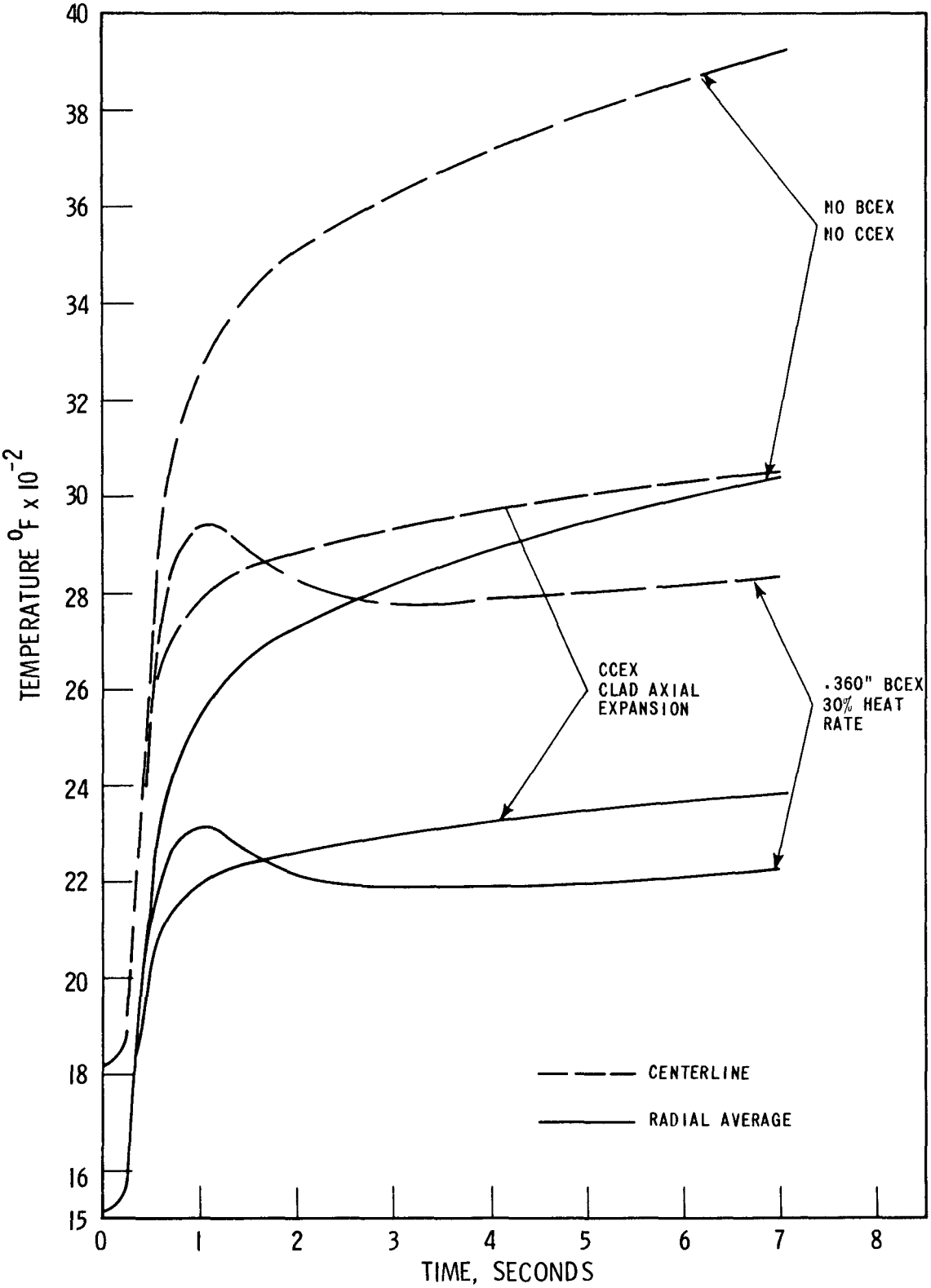

ACCIDENT ANALYSES: CONTROL ROD EJECTION-FUEL TEMPERATURES IN HOT CHANNEL AXIAL SECTION 4 (4 of 6)

Figure III.5-55

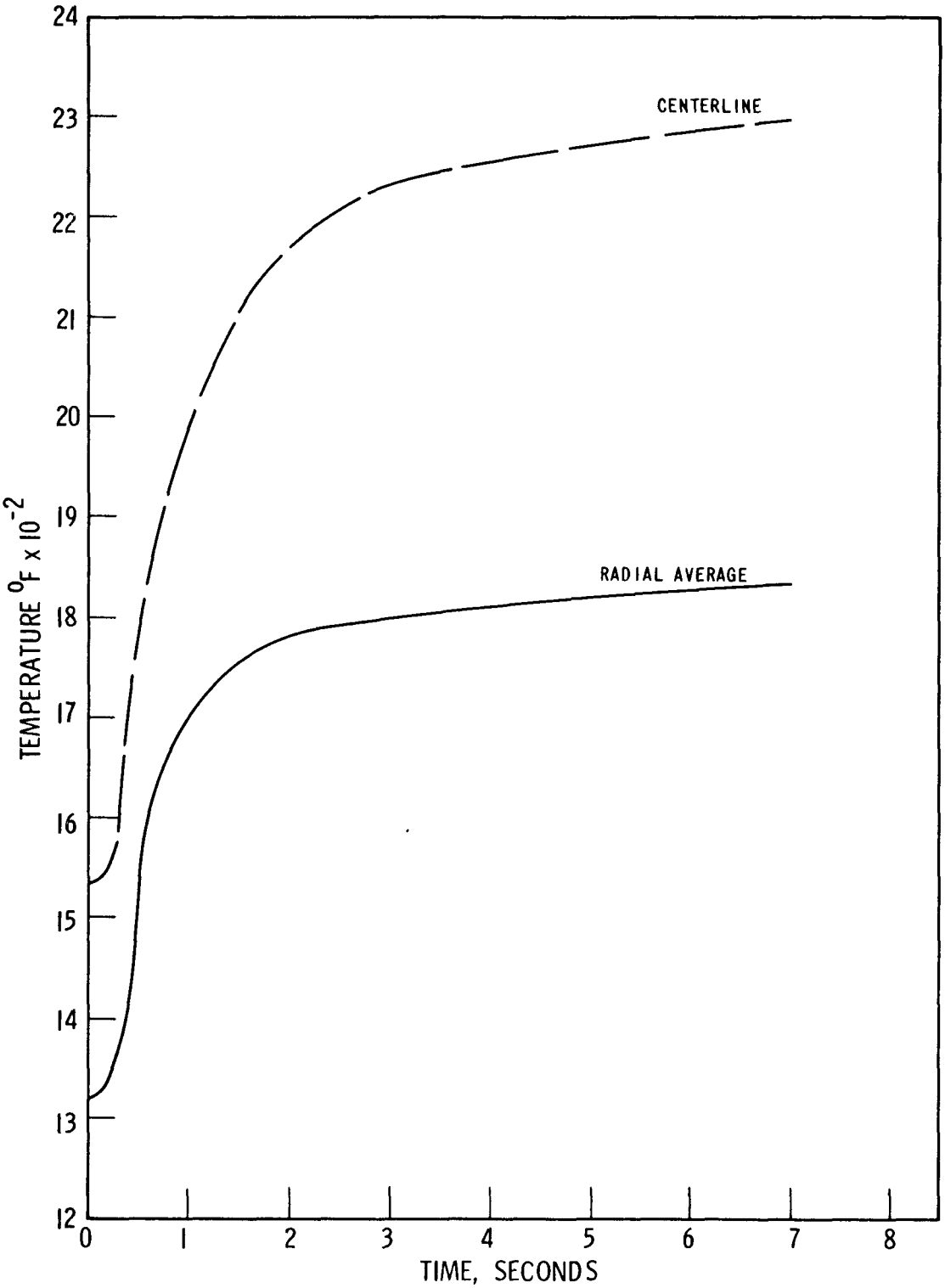

ACCIDENT ANALYSES: CONTROL ROD EJECTION-CERMET TEMPERATURES IN HOT CHANNEL AXIAL SECTION 4 (4 of 6)

Figure III.5-56

temperature is 3920°F and still rising after seven seconds. In the two axial expansion cores, BCEX and CCEX, the fuel hotspot centerline temperatures are less than 3100°F, Figure III.5-55. In the BCEX cermet, the cermet hotspot centerline temperature is 2300°F and still rising after seven seconds, Figure III.5-56. The fuel clad hotspot temperatures, hot and average channels, are shown in Figure III.5-57. In the no BCEX-no CCEX core, the hot channel clad hotspot is 2060°F and still rising after seven seconds, whereas in the BCEX and CCEX cores, the clad hotspot temperature is less than 1700°F for the entire excursion period.

Figure III.5-58 shows the core exit coolant temperatures, average and hot channels, as a function of time. Boiling of the coolant occurs at the outlet of the no BCEX-no CCEX core hot channel, whereas the coolant temperatures in the two axial expansion cores, BCEX and CCEX, are less than 1550°F during the entire time period of the incident.

In summary, the postulated control rod ejection accident yields approximately equal maximum temperatures in the two axial expansion cores, BCEX and CCEX. Either axial expansion mechanism prevented coolant boiling and resulting core damage in this postulated accident.

III.5.5.3 Loss of Electrical Power to All Primary Pumps at 100% Core Thermal Power

The loss of primary pump power is a credible accident for all nuclear reactors. The safety and integrity of the core during this accident strongly depends on the flow decay characteristics of the primary system pumps. Because of their importance, each primary pump is assumed to be equipped with a high inertia flywheel attached to the rotor of the drive motor to obtain the flow decay characteristic curve shown in Figure III.5-59.

At the time of loss of electrical power to all primary pumps, the core conditions are 100% power and 100% flow. As all the temperature dependent reactivity coefficients introduce negative reactivity with increas-

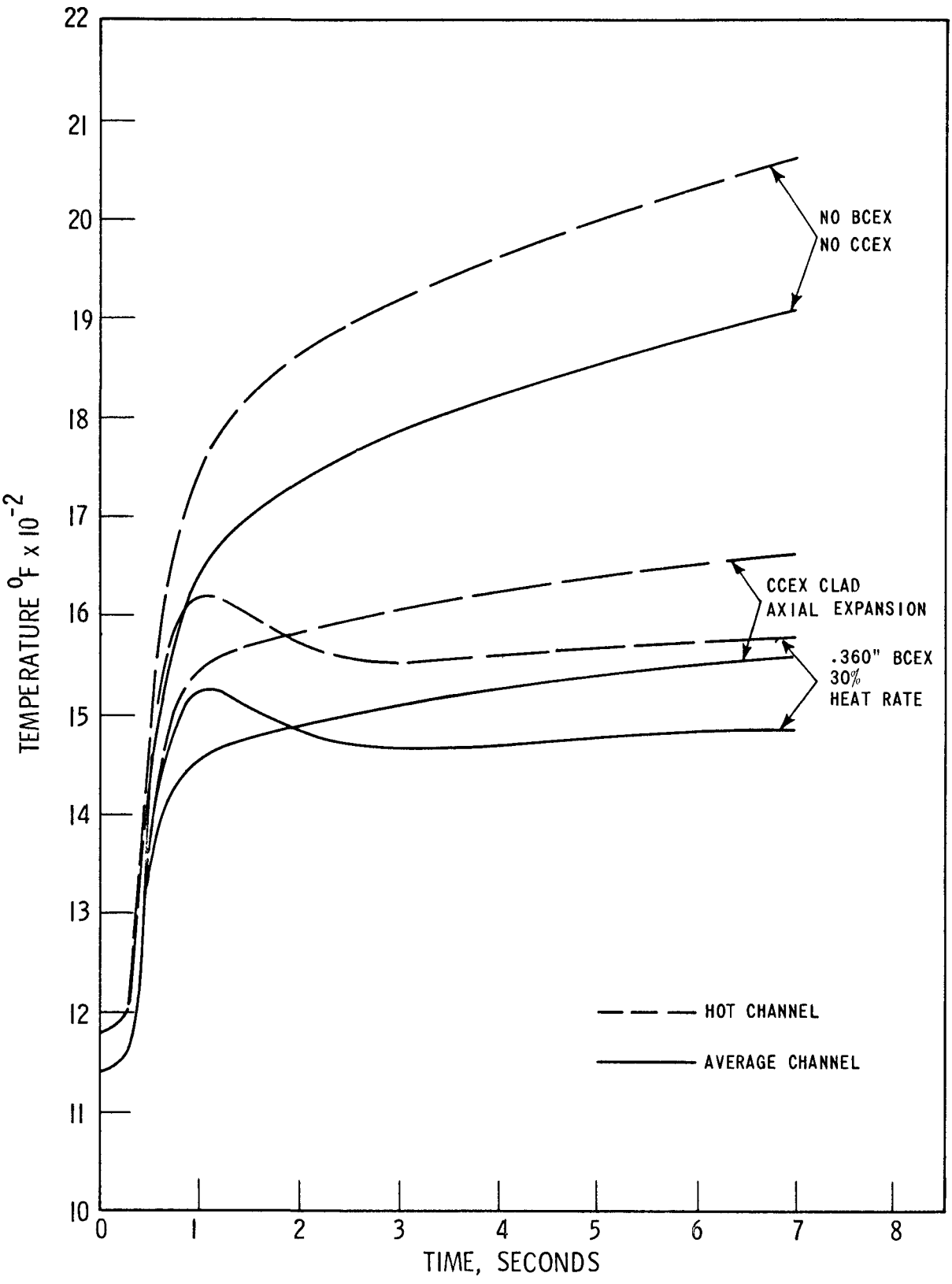

ACCIDENT ANALYSES: CONTROL ROD EJECTION-AVERAGE CLAD TEMPERATURES
AXIAL SECTION 5 (5 of 6)

Figure III.5-57

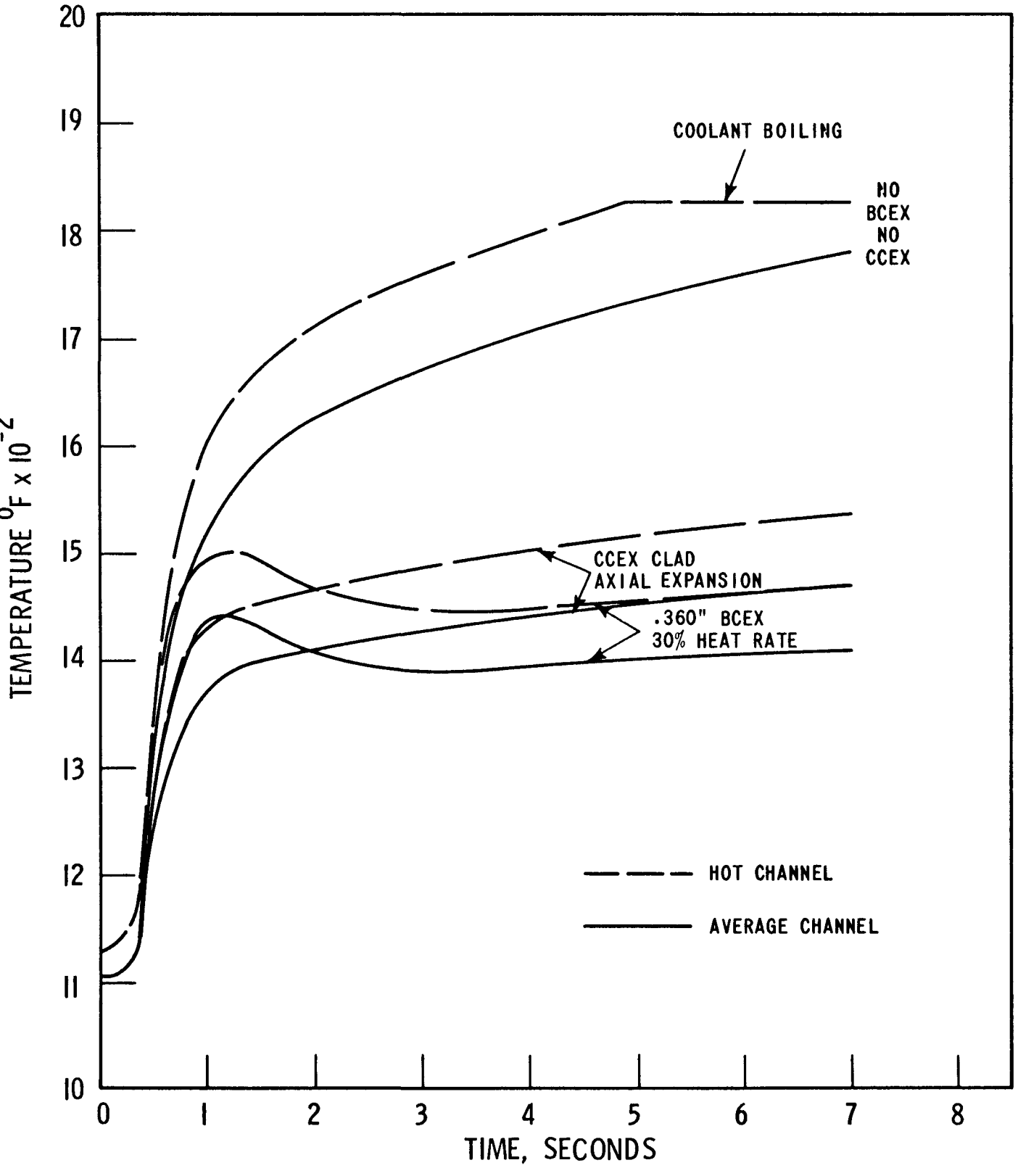

ACCIDENT ANALYSES: CONTROL ROD EJECTION - CORE EXIT COOLANT TEMPERATURES

Figure III.5-58

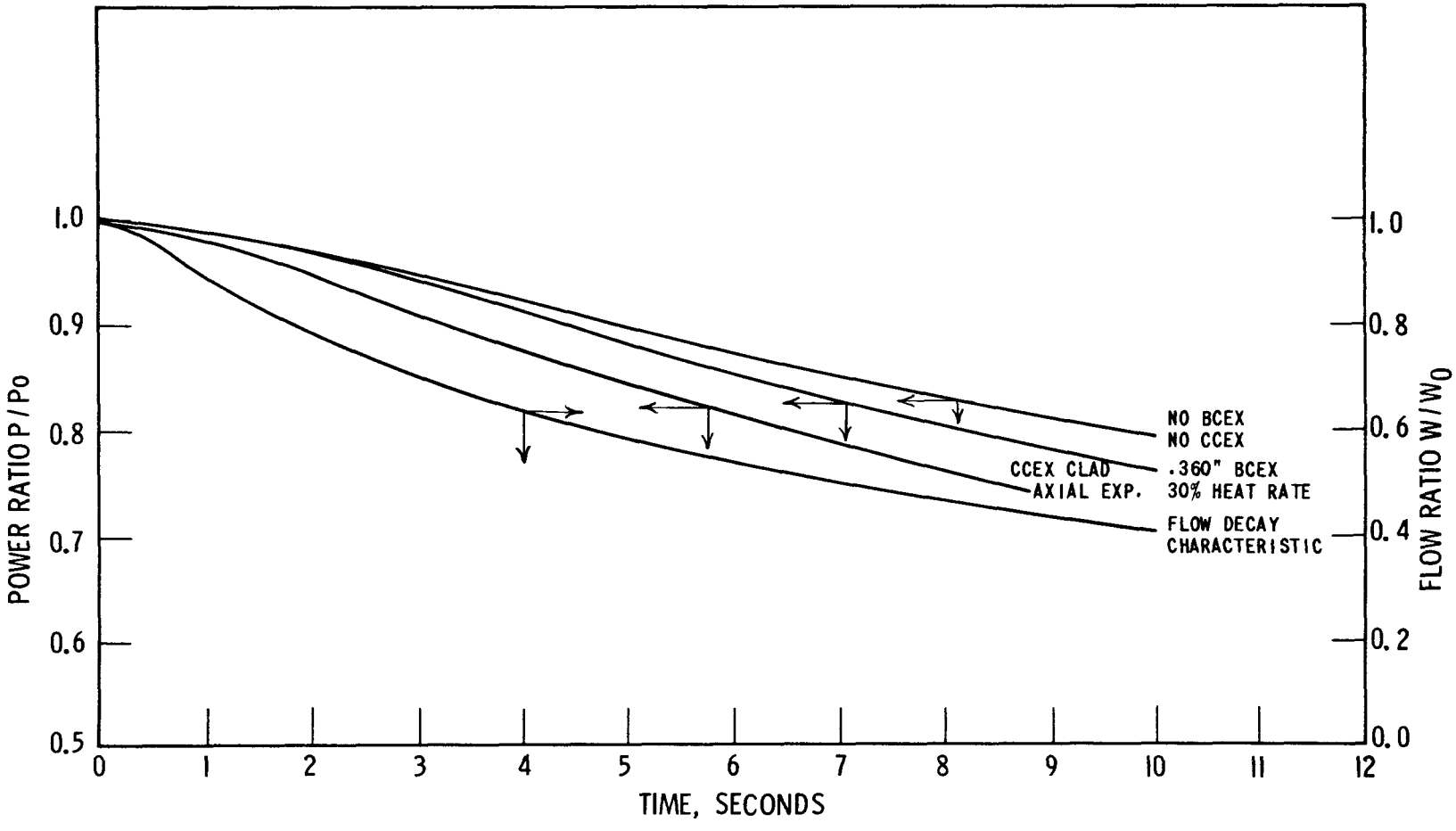

ACCIDENT ANALYSES: LOSS OF PUMP POWER-CHANGE IN CORE POWER AND FLOW FROM 100% POWER AND FLOW

Figure III.5-59

ing system temperature, the decay in the reactor power follows the pump flow, but with a time delay (see Figure III.5-59). The BCEX core power is between the values for the no BCEX-no CCEX core and the CCEX cores. The BCEX net reactivity worth was negative during the time period that the assumed pump flow decay rate was studied, even though the fuel rod clad linear expansion exceeded the cermet linear expansion. The rate of temperature rise, °F/sec., in the fuel clad is approximately twice the rate for the BCEX cermet, Figures III.5-60 and III.5-61. The gap between the lower and the upper BCEX fuel bundles in the average channel was 18 mils, 24 mils, and 29 mils less than the zero time gap after 5, 7.8, and 10 seconds, respectively. The core exit coolant temperatures, average and hot channels, are less than 1400°F during the time period this accident was studied, Figure III.5-62.

In summary, the BCEX net reactivity feedback was always negative during this postulated loss of pumping power accident. The excursion termination capability of BCEX or CCEX is not fully demonstrated by this analysis, as the sodium temperature coefficient is negative. Even the no BCEX-no CCEX core temperatures are below the threshold values for core damage.

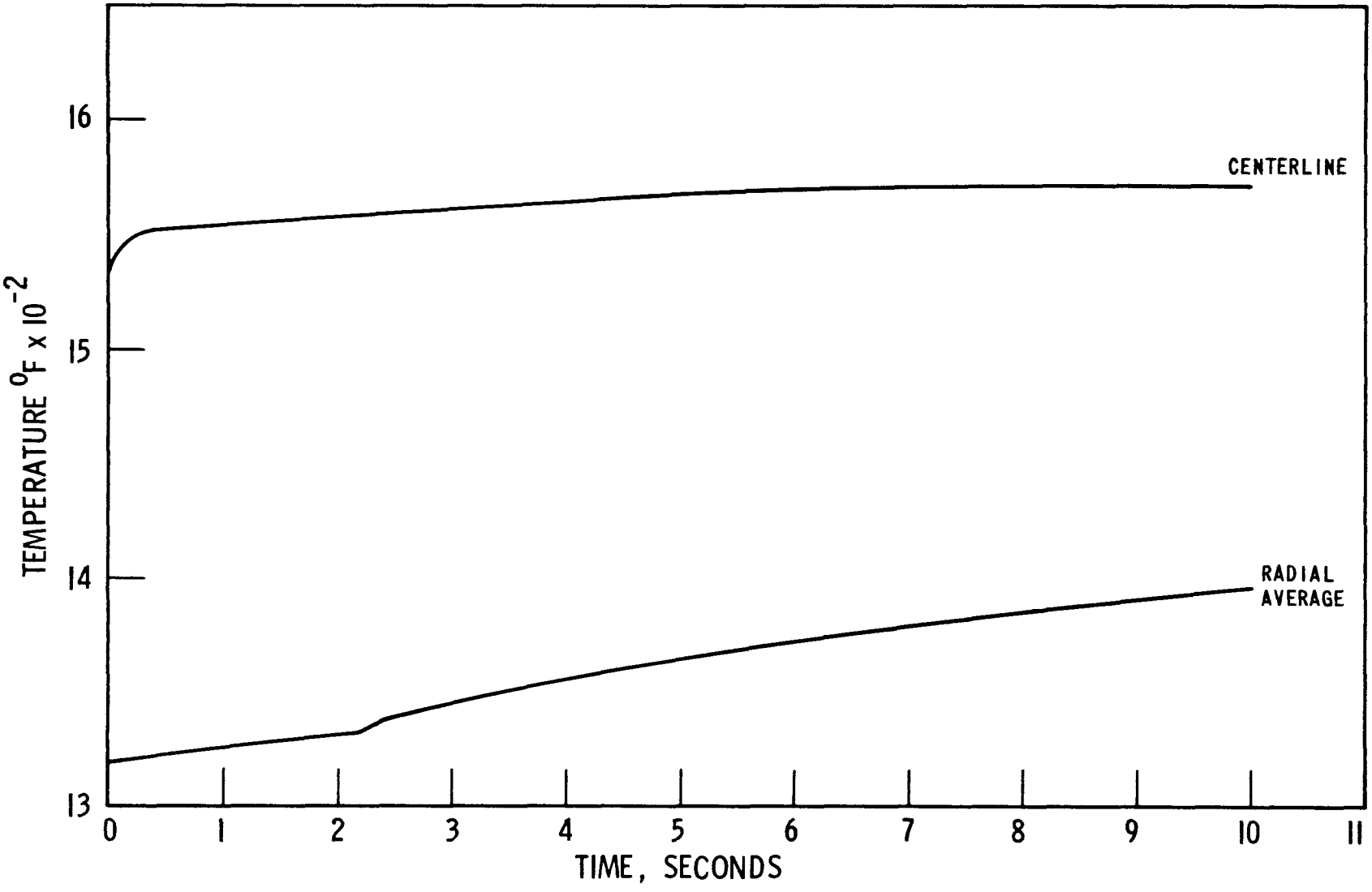

ACCIDENT ANALYSES: LOSS OF PUMP POWER-CERMET TEMPERATURES
IN HOT CHANNEL AXIAL SECTION 4 (4 of 6)

Figure III.5-60

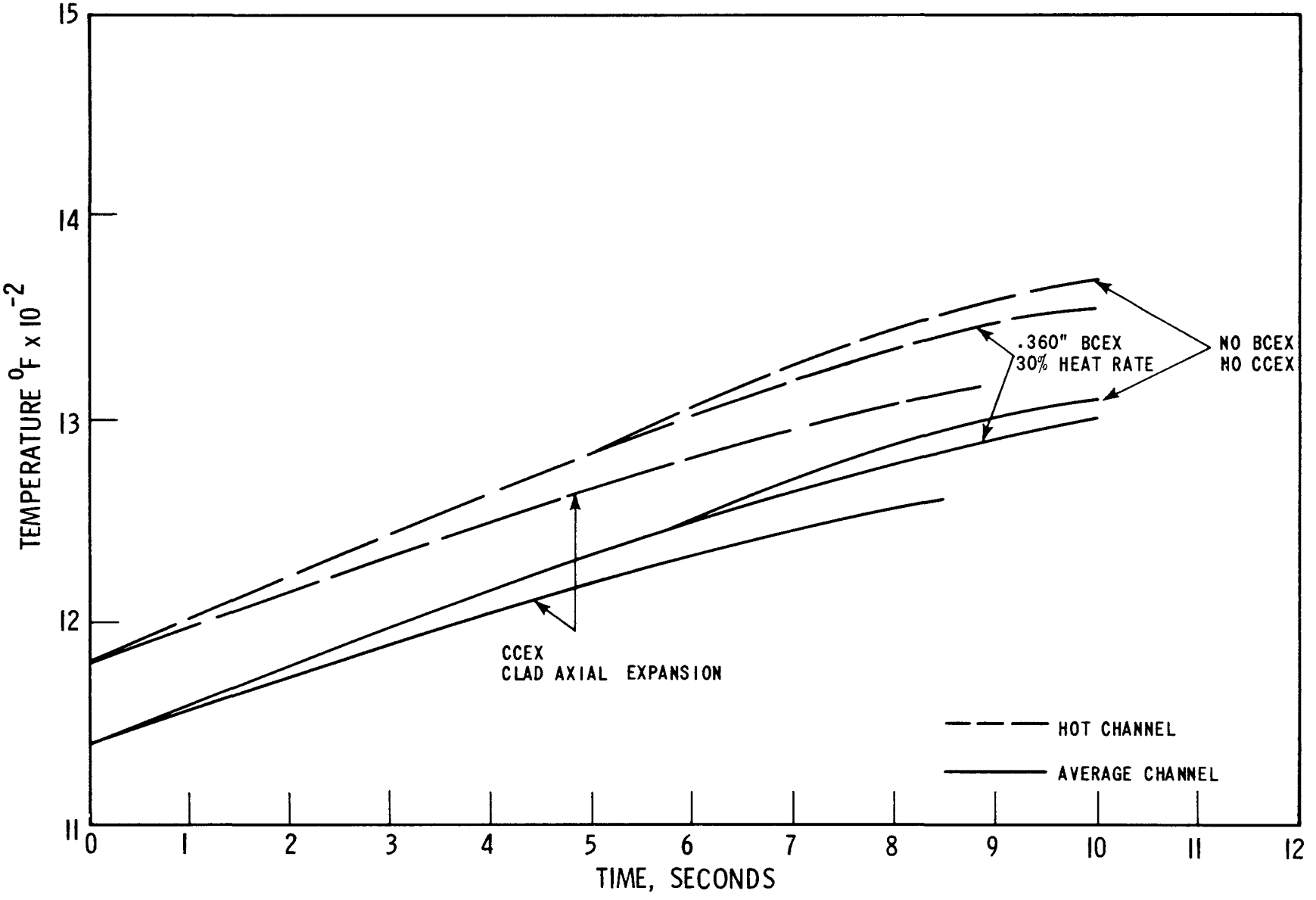

ACCIDENT ANALYSES: LOSS OF PUMP POWER - AVERAGE CLAD TEMPERATURES IN SECTION 5 (5 of 6)

Figure III.5-61

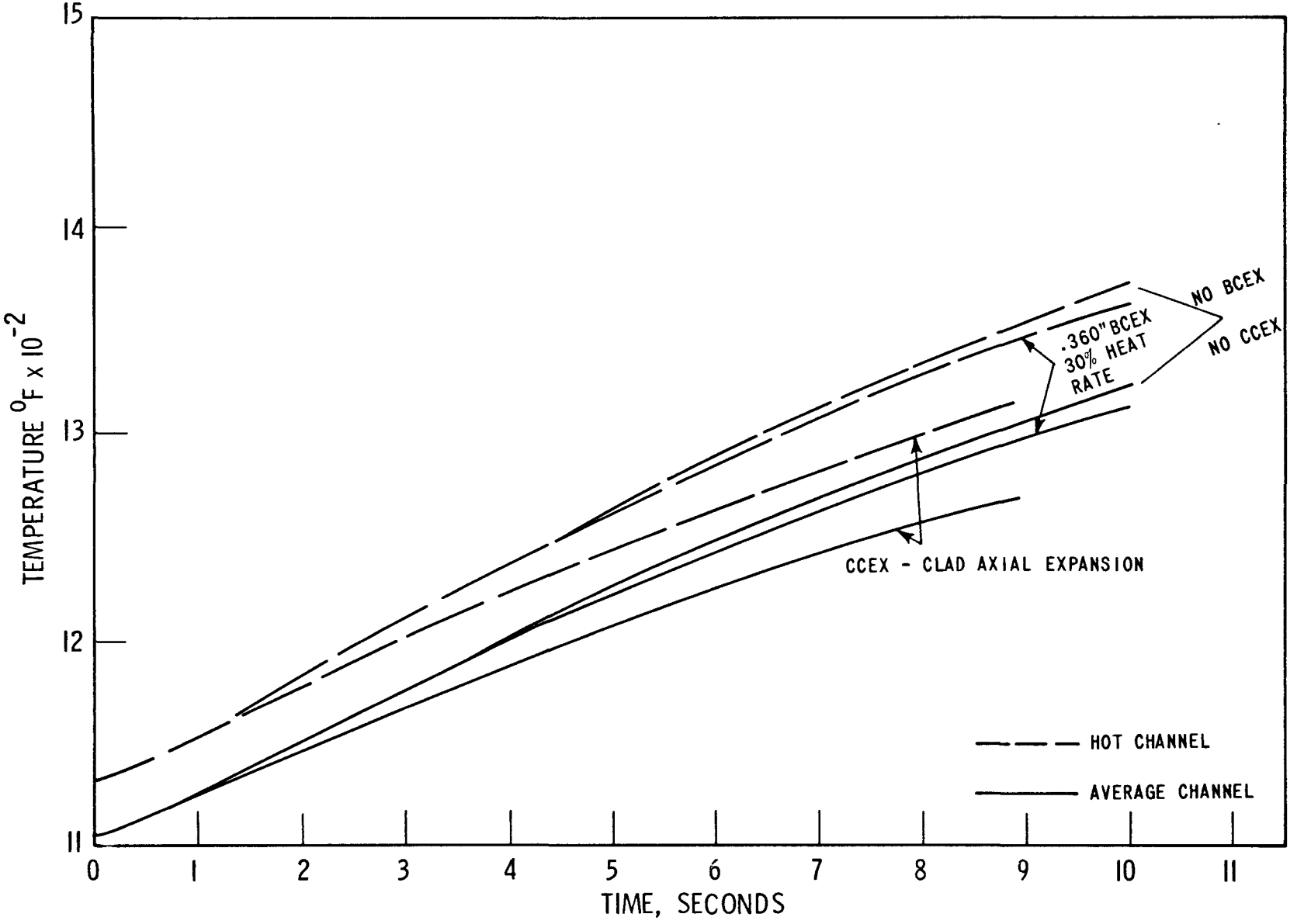

ACCIDENT ANALYSES: LOSS OF PUMP POWER-CORE EXIT COOLANT TEMPERATURES

Figure III.5-62

III.5.6 Controlled Expansion Quasi-Equilibrium Reactivity Feedback and Alternate Clad Materials

The ultimate, net, reactivity feedback of the controlled expansion element can be determined from an analytical study of its contribution to the overall power coefficient. As this type of analysis assumes constant material properties and equilibrium reactor conditions, the time dependency between the various feedbacks can be neglected. During a rapid transient, the initial rate of power and temperature rise, and the resulting feedbacks, are controlled by the positive reactivity insertion rate. Immediately after a positive reactivity insertion ceases, the core temperatures and feedbacks are functions of the integrated energy to that point and of the remaining excess reactivity. The preceding transient analyses showed that there is no simple way to present the relationship between feedback and power in the transient mode.

However, it is of interest to explore the relationship between steady-state power and feedback. Because of the complex thermal delays present in the reactor, the rapid transient behavior cannot be deduced directly from the steady-state relationship between power and reactivity. The steady state relationship, however, will indicate the maximum potential for feedback, and approximately describe a pseudo steady-state condition. The steady-state relationships can also give some insight into the relative merits of design alternates not considered in the transient studies.

The relationship between power and the BCEX reactivity expansion feedback generated by power is the partial derivative of reactivity with respect to power, neglecting everything except expansion. The resultant expression is:

$$\frac{\partial k}{\partial P} = \frac{\partial k}{\partial L_1} \cdot \frac{\partial L_i}{\partial \bar{T}_1} \cdot \frac{\partial \bar{T}_1}{\partial P} + \frac{\partial k}{\partial L_2} \cdot \frac{\partial L_2}{\partial \bar{T}_2} \cdot \frac{\partial \bar{T}_2}{\partial P}$$

where L_1 and $\overline{T}_1$ are the length and average temperature of the bulk ceramic clad, and L_2 and $\overline{T}_2$ are length and average temperature of the cermet.

Rewriting the relationship gives:

$$\frac{\partial k}{\partial P} = \sum_i \left(L_i \frac{\partial k}{\partial L_i}\right) \left(\frac{1}{L_i} \frac{\partial L_i}{\partial \overline{T}_i}\right) \left(\frac{\partial \overline{T}_i}{\partial P}\right)$$

where the summation is over the two components of the reference BCEX assembly. The first term, $\left(L_i \frac{\partial k}{\partial L_i}\right)$, represents the reactivity expansion coefficients, γ_i, which are constants. The second term, $\left(\frac{1}{L_i} \frac{\partial L_i}{\partial \overline{T}_i}\right)$, represents the ordinary thermal expansion coefficients, α_i, which are also constants (to a reasonable approximation). Hence,

$$\frac{\partial k}{\partial P} = \sum_i \gamma_i \alpha_i \frac{\partial \overline{T}_i}{\partial P}$$

The average metal (clad or cermet) temperature is a function of the inlet temperature, the average coolant temperature rise, the average bulk coolant to surface temperature rise, and the average metal temperature rise. In the most common case of fixed coolant flow rate during a transient, the average temperature rise values are proportional to total power. This assumes constant radial and axial neutron flux shape, a good approximation in fast reactor systems. Thus, the metal average temperature can be written as:

$$\overline{T} = T_{in} + CP, \text{ where C is a constant.}$$

Then $\frac{\partial \overline{T}}{\partial P} = C$

and $\frac{\partial k}{\partial P} = \sum_i \gamma_i \alpha_i C_i = \text{cons.}$

Thus, the δk feedback from thermal expansion is a constant times the change in the reactor power.

The values of the γ_i have been computed for clad and cermet, the values of the α_i are known (approximately), and the values for the C_i can be computed. The values for the C_i can be obtained from the steady-state thermal-hydraulic calculations directly, as

$$\overline{T}_i = T_{in} + C_i P$$

$$\text{or} \quad C_i = \frac{T_i - T_{in}}{P}$$

and $\overline{T}_i$, T_{in}, and P are known. These values are tabulated in Table III.5-6 for the reference carbide and oxide cases. Note that the total assembly, isothermal expansion, temperature coefficient, $\frac{\partial k}{\partial T_{iso}}$, cannot be used to predict $\frac{\partial k}{\partial P}$.

The data plotted in Figure III.5-63 are the values of partial and total reactivity feedback versus power for the reference carbide design. The spread in the data, shown by the shaded bands, is an indication of the minimum uncertainty. The least negative total feedbacks are those used in the preceding transient studies. The values leading to the most negative total feedback result from data used in the steady state studies to yield conservative estimates of allowable burnup. The CCEX values are essentially the same as those which would be achieved with an all cermet core. In fact, as the nuclear calcualtions neglected fuel expansion on the basis that this would be adequate for compartment size, the CCEX expansion effect was calculated exactly as if it were a cermet with an average temperature equal to the average clad temperature. As can be seen in Figure III.5-63, the total, net, steady-state reactivity effect for the reference case is approximately twice that of CCEX.

Table III.5-6

Quasi-Equilibrium Reactivity Data

		γ	α	$\frac{\partial k}{\partial T_{iso}}$	C	$\partial k/\partial P$
BCEX Carbide:	Clad	+0.368	11×10^{-6}	$+4.05 \times 10^{-6}$	0.489	$+1.98 \times 10^{-6}$
(w/0.360" cermet	Cermet	-0.762	10×10^{-6}	-7.62×10^{-6}	0.754	-5.74×10^{-6}
@ 30%)	Total	-	-	-3.57×10^{-6}	-	-3.76×10^{-6}
BCEX Oxide:	Clad	+0.368	11×10^{-6}	$+4.05 \times 10^{-6}$	0.412	$+1.67 \times 10^{-6}$
(w/0.260" cermet	Cermet	-0.762	10×10^{-6}	-7.62×10^{-6}	0.531	-4.05×10^{-6}
@ 30%)	Total	-	-	-3.57×10^{-6}	-	-2.38×10^{-6}

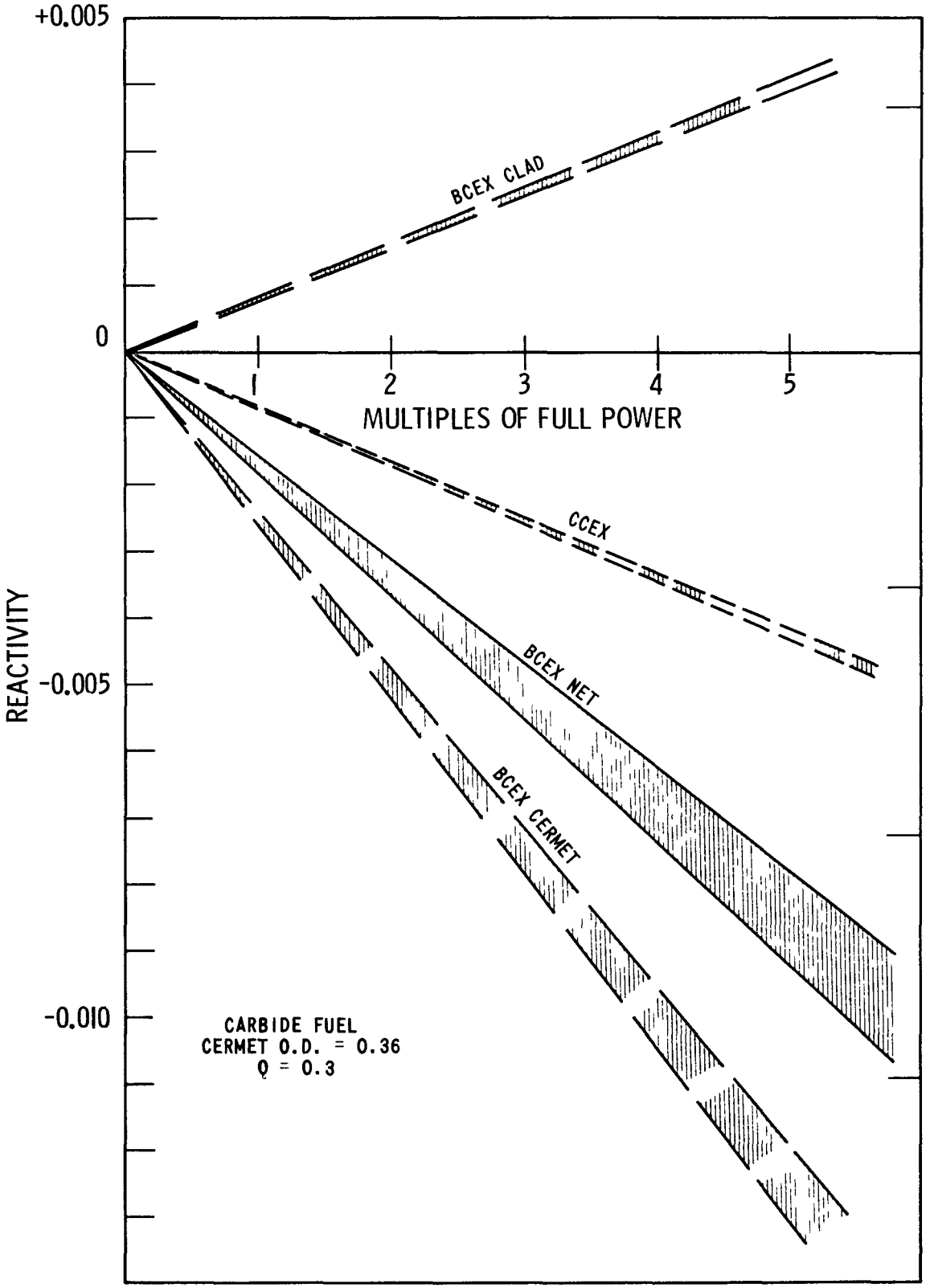

REACTIVITY FEEDBACK

For Sodium Bonded Carbide Fuel

Figure III.5-63

The data plotted in Figure III.5-64 are the values of partial and total feedback versus power rise between two equilibrium conditions for the reference oxide design. The cermet negative reactivity shown in Figure III.5-64 is less than in Figure III.5-63. This is due to the smaller cermet diameter, as equal cermet volumetric heat generation rates, BTU/hr-ft^3, were specified in both cores.

The potential advantage of using a clad on the bulk ceramic with a lower coefficient of thermal expansion was investigated. The two representative examples selected for this analyses are the ferritic (400 series) stainless steels and the niobium alloys. These alloys have higher thermal conductivity than the austenitic (300 series) stainless steels used in the reference design, but this is a minor improvement compared to the improved thermal expansion characteristics. The advantage can be estimated by adjusting the thermal coefficient of expansion for the bulk ceramic clad. For this analyses of steady-stage conditions, Figure III.5-65 illustrates the relative BCEX performance with alternate clad for carbide and oxide fuel. Ferritic clad would increase the negative response of the reference carbide by 20%, and of the oxide by 25%. Niobium would increase the negative response of the reference carbide by 25%, and of the oxide by 35%.

The effect of ferritic or niobium clad is shown more clearly by plotting the reactivity coefficient for power versus the relative power generation rate in the cermet (relative to the power generation rate in the bulk ceramic). Figure III.5-66 illustrates this for the carbide and oxide reference designs. It can be seen that the improvement in the power coefficient obtainable by using a low thermal expansion clad is a fixed magnitude not a percentage change. The magnitude of the improvement, dk/dP, ranges between 0.6×10^{-6} and 1.0×10^{-6}. Alternatively, the same power coefficient can be achieved at a relative power generation rate which is lower by 4 to 5 percentage points. The difference in slope between the carbide and oxide power coefficient curves arises from the larger cermet pin diameter in the carbide reference design.

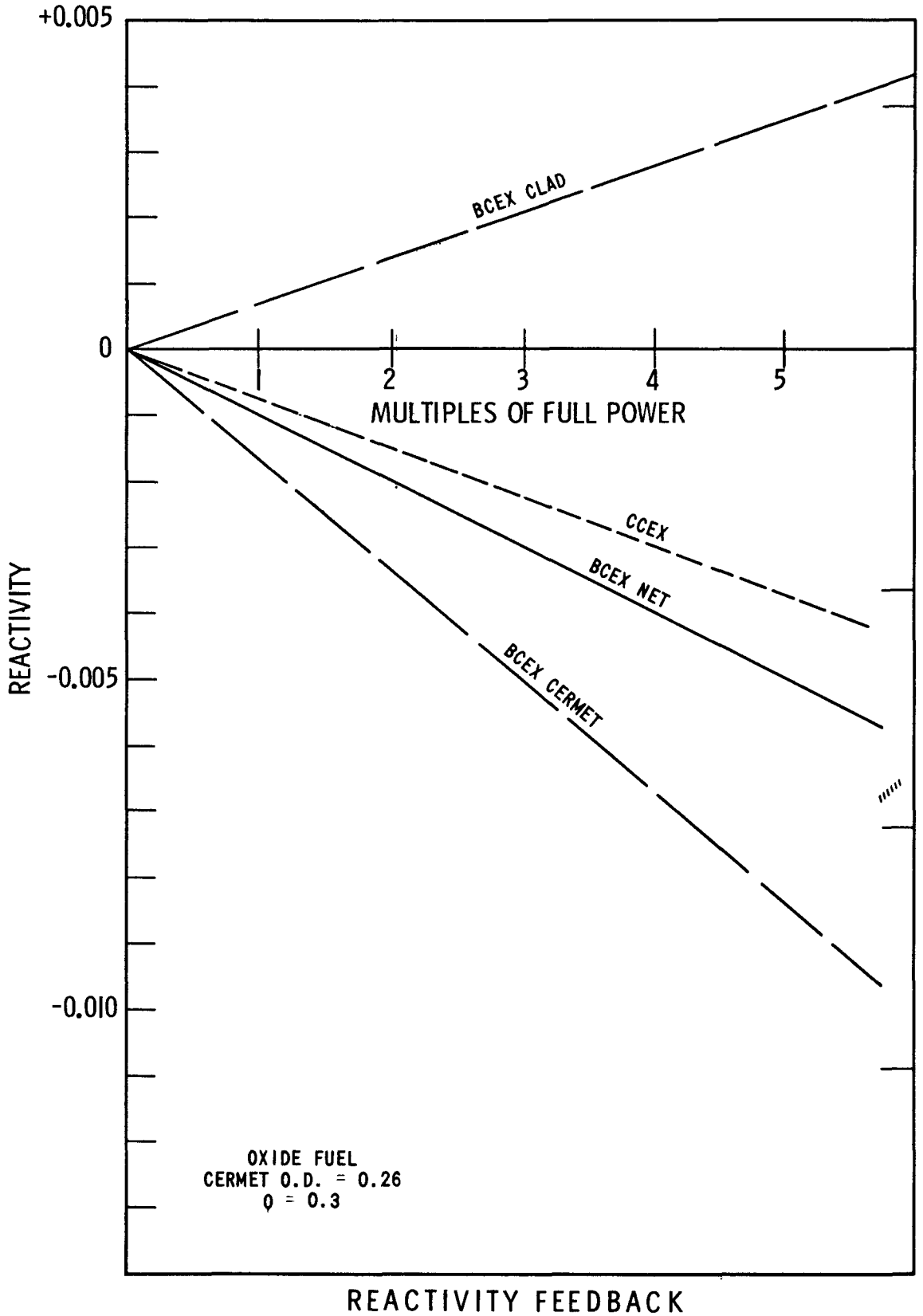

For Gas Bonded Oxide Fuel

Figure III.5-64

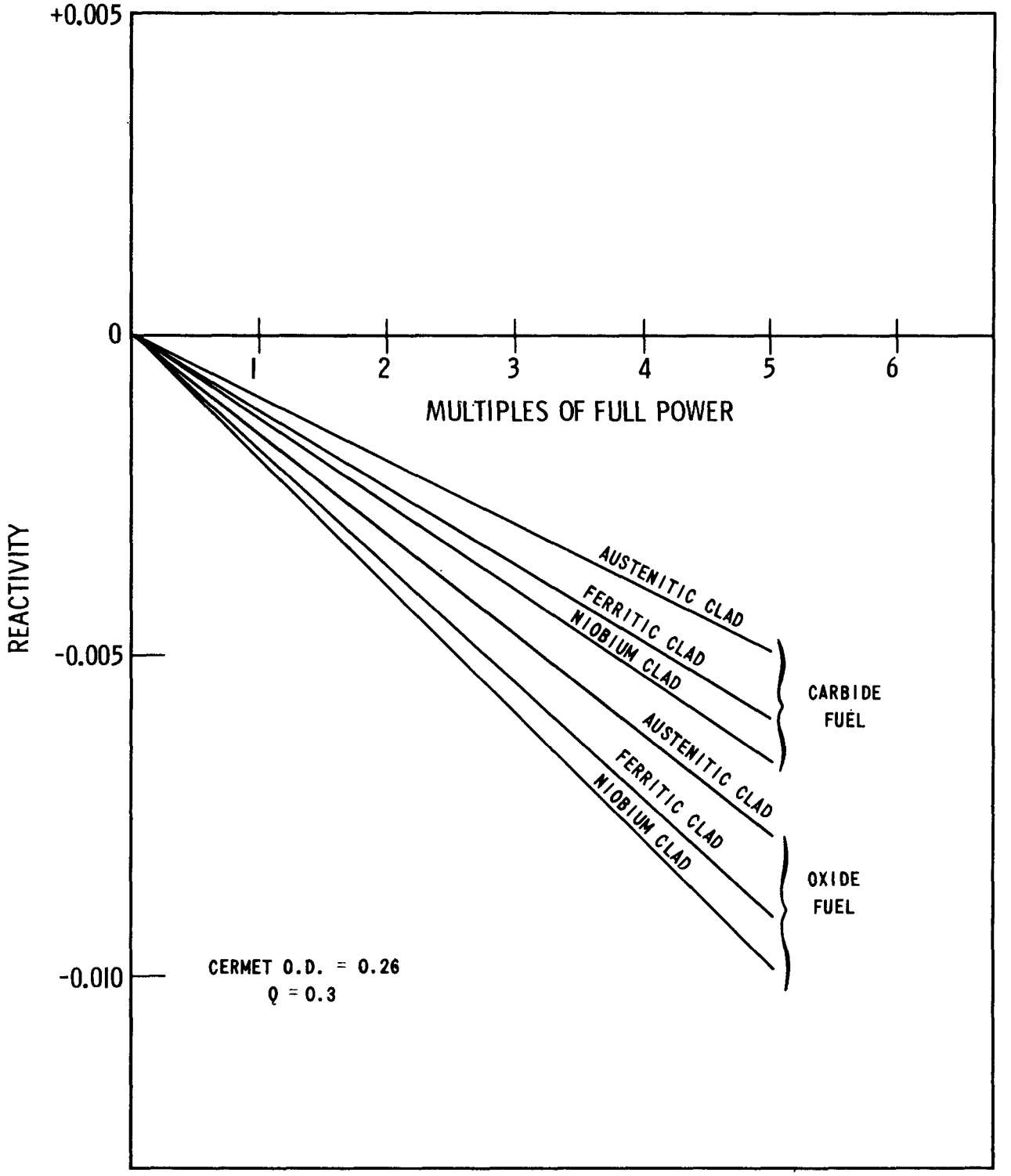

REACTIVITY FEEDBACK

Versus Bulk Ceramic Clad Material

Figure III.5-65

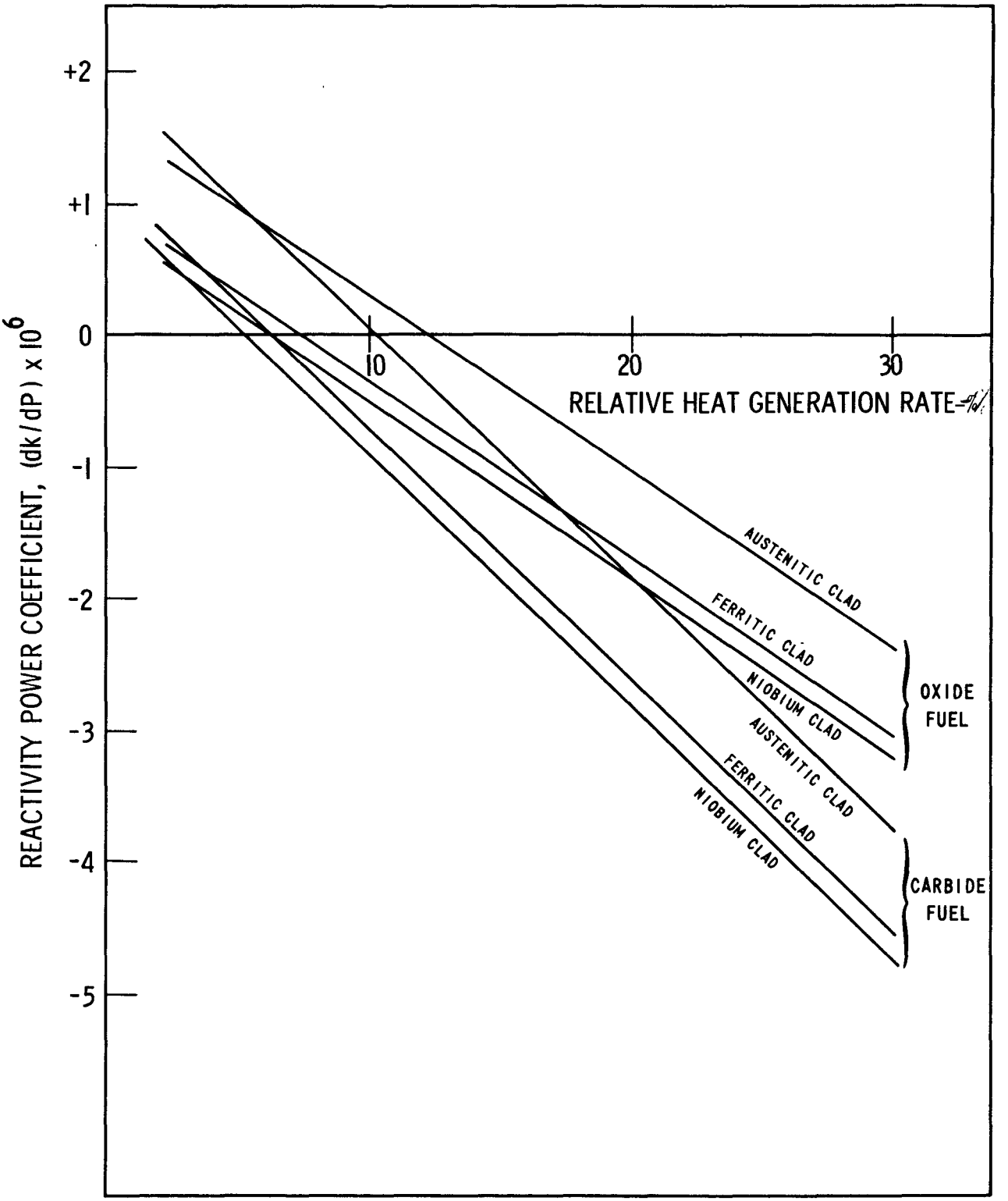

POWER COEFFICIENTS

Figure III.5-66

In summary, this analysis shows the possible obtainable final net reactivity worth between two steady state power conditions of the two proposed methods of achieving a controlled axial expansion. The time dependency and interactions of the various reactivity feedbacks occurring during a power excursion, shown by the preceding transient analyses, were neglected. Thus, the results of this analytical analyses is mainly applicable to the study of power excursions which are sufficiently slow that the core is always at a steady state condition; for example, the powered withdrawal of a control rod at a slow reactivity insertion rate.

III.5.7 Summary and Conclusions

Two methods of controlled axial expansion, bundle controlled expansion (BCEX) and clad controlled expansion (CCEX), were studied using two different fast reactor cores: the reference sodium bonded carbide fueled core[1,2,7] and an extrapolated design of a gas bonded oxide fueled core. In BCEX, the controlled axial expansion is achieved through the use of cermet rods located in the center of each fuel assembly which move the upper and lower fuel bundles apart, thus displacing fuel material from the center of the core. However, the cermet outward expansion reactivity worth is reduced by the positive feedback from the movement of the fuel towards the center of the core due to clad expansion. The BCEX analyses assumes that the fuel in both the upper and lower bundles is compartmented and, moves with the clad. Likewise, in CCEX, the fuel pellets are placed in compartments in the fuel rods and, again, the fuel is assumed to move with the stainless steel clad. In both analyses, for BCEX and for CCEX, the feedback for axial expansion is based on changes in the core's overall height.

A parameter study and analyses of three postulated accidents were performed to study the transient characteristics of the two controlled axial expansion concepts. A core having zero axial expansion was selected as the base line from which to evaluate the merits of BCEX and CCEX. The oxide fueled core was designed to have the same total volume of fuel, and thus the same fuel volumetric heat generation rate, BTU/ft^3, as the carbide fueled core. This was achieved by adjusting the oxide fuel pellet diameter to ensure tolerable fuel temperatures. The oxide core's overall height and diameter are approximately equal to those of the carbide core, and thus, the carbide core's temperature dependent reactivity coefficients were assumed to be applicable to the oxide core. Thus, the differences in behavior of BCEX and CCEX in the carbide and oxide cores is due solely to the differences in their thermal properties.

BCEX and CCEX are methods for providing ceramic fueled fast reactor cores, which possess assumed zero axial expansion, with a predictable, negative, axial expansion, reactivity feedback mechanism that will contribute significantly in terminating a power excursion. The merits of BCEX and CCEX were shown in the results presented for the parameter study and the accident analyses. In terms of reactivity fractional worth, during the initial stages of an excursion, BCEX is more effective in the oxide core in assisting the other negative reactivity feedbacks to terminate the excursion. In the carbide core, the effectiveness of BCEX is greatly reduced during the initial stages of an excursion by the rapid expansion of the clad on the fuel rod. The carbide fuel rod time constant is 0.47 seconds, compared to 0.79 seconds for the cermet rod, and 2.08 seconds for the oxide fuel rod. The clad on the oxide fuel rod has the slower response, thus preventing a sharp reduction in the fractional worth of BCEX in the oxide fueled core during the initial stage of the excursion. The downgrading of the carbide core's BCEX reactivity fractional worth causes a temperature overshoot; the temperature overshoot becoming larger and thus there is a greater possibility of fuel damage in the case of large rapid reactivity insertions (such as dropping a fuel assembly).

As new equilibrium thermal conditions are approached in the core after the reactivity input has been terminated, the reactivity feedback fractional worth of BCEX is greater in the carbide core than in the oxide core. The BCEX fractional worth may be 80% greater than the Doppler's fractional worth depending upon the cermet rod diameter and volumetric heat generation rate. In the oxide core, the BCEX fractional worth is less than the Doppler worth.

If the compartmented fuel moves in a predictable manner with the clad, the performance characteristics of CCEX in the carbide core are - depending upon the reactivity insertion rate - as good as or better during an excursion than those of BCEX. This is especially true in the early stages

of an excursion, when the temperature overshoot characteristic of BCEX in a carbide core may become quite severe. For example, the carbide core's CCEX analysis for a two dollar insertion at a rate of 20$/sec. was the only analysis not terminated by a temperature upper limit. It should be understood that cermet rod overheating caused some of the terminations of the BCEX analyses. The upper temperature limits were selected to indicate the onset of damage to the core. The response of CCEX decreases with an increasing fuel rod time constant. In an oxide core, CCEX is a less effective accident terminating mechanism than in a carbide core. Thus, at best, BCEX offers a marginal improvement over CCEX in increasing the negative reactivity feedback for terminating certain excursions in either a carbide or oxide core.

The net reactivity worth at equilibrium conditions of BCEX using metallurgically bonded cermet rods ranges from 50% to 65% of the cermet's outward expansion reactivity worth. In other words, the effect of the fuel clad inward expansion is to downgrade the gross cermet's reactivity worth by 35% to 50%. Using a fuel clad material having a lower linear expansion coefficient, or increasing the cermet rod diameter, cermet volumetric heat generation rate, and/or the cermet-to-clad contact resistance (inverse of conductance) improves the BCEX performance characteristics.

In the study of the expulsion of a control rod (one dollar at an acceleration of 100 ft/sec^2) from a carbide core, BCEX is as effective as CCEX in terminating the excursion. However, in the refueling accident when the maximum worth fuel assembly, two dollars, is dropped under one g acceleration into a just subcritical carbide core, BCEX is much less effective than CCEX in controlling the resultant power excursion during the important first few seconds. The assumed initial refueling power level and flow rate used were 0.5% and 20% of rated conditions, respectively. The transient characteristics in the BCEX core resulted in a temperature overshoot sufficient to produce coolant boiling at the outlet of the hot channel. In the CCEX core, the maximum coolant temperature was 200°F, or more, below the boiling temperature. The assumed coolant boiling

temperature is 1830°F, which corresponds to a pressure of 40 psia, neglecting the liquid superheat effect.

The net reactivity feedback from BCEX during the loss of all electrical power to the primary pumps was found to be always negative for the assumed flow decay characteristic, even though the clad inward expansion exceeds the cermet expansion by 29 mils after 10 seconds. Since the sodium temperature coefficient is negative, it prevents BCEX and CCEX from demonstrating their excursion terminating effectiveness.

In all analyses performed in this investigation, utilization of the BCEX and CCEX features (axial expansion) significantly improved the core transient behavior over the non-CEX (zero expansion) core.

Section III.5 - References

1. Heck, F. M., et al, "Liquid Metal Fast Breeder Reactor Design Study", WCAP-3251-1, January 1964.

2. Gunson, W. E., et al, "High Power Density Stainless Steel Reference FBR Core Design", WCAP-2638, July 1964.

3. Greebler, P., Sherer, D. B., and Walton, N. H., "FORE - A Computational Program for the Analysis of Fast Reactor Excursion", GEAP-4090, October 1962.

4. Errata and Addenda Sheet, EA-1, October 1963.

5. Errata and Addenda Sheet, EA-2, February 1965.

6. Errata and Addenda Sheet, EA-3, June 1965.

7. Wright, J. H., Gunson, W. E., Daleas, R. S., Heck, F. M., "Conceptional Design and Preliminary Accident Analysis of a Sodium Cooled, Carbide Fueled, Large Modular Fast Reactor", to be published in the proceeding of the ANL FBR Conference, October 1965.

III.6 Nuclear Analyses

III.6.1 Introduction

The nuclear characteristics of the reference CEX fuel assemblies were calculated using standard Westinghouse Atomic Power Division fast reactor calculation procedures. Specifically, the characteristics of the CEX fuel assembly, as installed in the reference Westinghouse sodium cooled large fast breeder reactor modular design were investigated. In particular, those properties of the reactor pertaining to the CEX concept and related safety features were analyzed in detail. The nuclear analysis of this concept assumed a supporting role in this study, and was used mainly to supply information for use in the transient analyses. There was relatively little effort on obtaining data required for such things as economic analysis. Burnup calculations were performed to obtain parameters needed to calculate reactivity coefficients at various stages in the life of the reactor core. In this way, conservative values of the various coefficients could be used in the safety analysis of the CEX concept. The following principal coefficient were calculated:

(a) Coolant temperature coefficient
(b) Doppler coefficient
(c) Cermet expansion coefficient
(d) Clad expansion coefficient

The Westinghouse modular reactor consists of seven identical hexagonal modules, six of which surround the seventh. Of the forty-two sides of the seven modules, twenty-four border on another module, while the remaining eighteen border on the peripheral radial reflector; or, equivalently, four-sevenths of the modules are "reflected" modules, and three-sevenths are isolated modules. The analysis was performed on a "hybrid" or "average" module whose neutron flux boundary conditions represent a compromise between the reflected and isolated modules. This was the best way to obtain the properties of the entire seven module reactor.

III.6.2 Description and Calculational Method

III.6.2.1 Description of Model Used in the Nuclear Analysis

A module of the Westinghouse 1000 MWe design[1] consists of a tall cylindrical core ($L/D \simeq 2.3$) with one foot thick, top and bottom, axial blankets. Each module is radially surrounded by a blanket, a row of graphite three-fourth as thick as the normal graphite row, and a six inch reflector consisting of sodium and steel. As the isolated module has a full row of graphite surrounding the radial blanket, while the reflected module has only one-half row thickness because it shares the graphite with the adjacent module, an approximate value of three-fourth of the normal graphite row thickness was used. The enrichment, breeding ratio, and spectrum of the hybrid module fall approximately midway between those of the isolated and reflected modules, and hence should adequately represent the "average" module of the reactor. Figure III.6-1 shows a vertical section through the "average" module; all parameters are homogenized in each of the regions shown. Table III.6-1 gives the volume fractions for the regions indicated.

Table III.6-1

Volume Fractions

Region	Fuel	Coolant	Structure and Clad	Graphite	Void
Core	.2846	.5758	.1396		
Axial Blanket	.2984	.5682	.1334		
Radial Blanket	.5156	.3047	.1698		.0099
Graphite Reflector		.0500	.0500	.9000	
SS + Na Reflector		.7500	.2500		
Center Rod Hole		1.00			

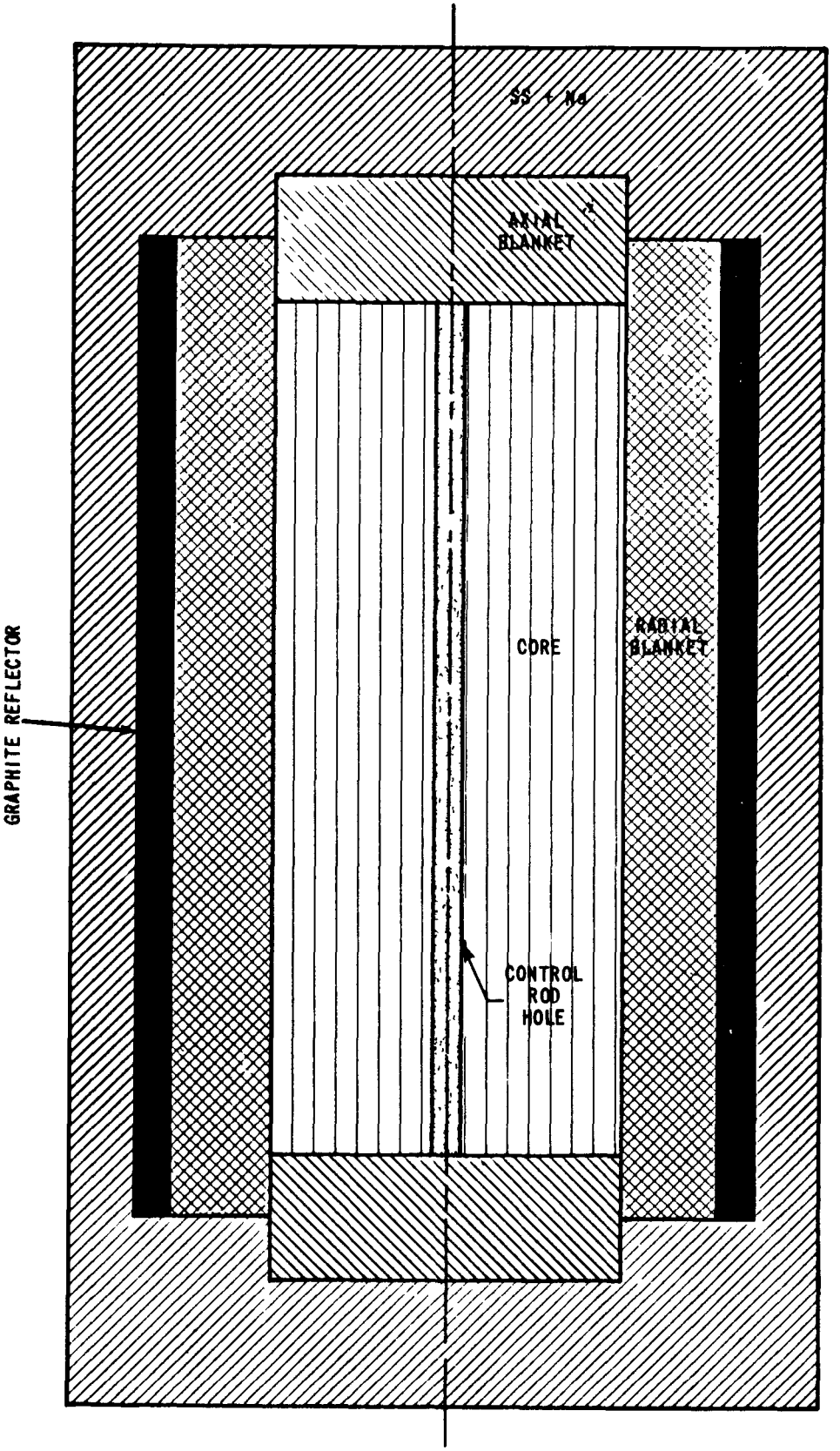

GEOMETRIC MODEL FOR NUCLEAR ANALYSIS

Figure III.6-1

The radial blanket volume fractions include three, full assembly size, control rod holes.

For certain calculations it was necessary to homogenize the central control rod hole into the core. The core volume fractions for this case are:

Fuel	.2769
Coolant	.5853
Structure and Clad	.1378

The core consists of 37 hexagonal assemblies, each with a 23.094 $in.^2$ cross sectional area. This yields an equivalent core radius of 41.889 cm. The equivalent radius of the central control rod is 6.292 cm. The equivalent outer radius of the radial blanket is 65.695 cm., yielding a blanket thickness of 23,805 cm. The thickness of a full row of graphite is 11.914 cm., giving a three-fourth thickness of 8.936 cm. As mentioned previously, the graphite is surrounded by 15.24 cm. of steel and sodium reflector. The boundary condition used at the outer edge of this reflecter is $d\phi/dr = 0$.

III.6.2.2 Calculation Method

The one-dimensional, 18 group, multiregion, W-MOBI diffusion theory code (based on the FAIM[2] code) was used in most of the calculations. SIZZLE, a one-dimensional, 6 group, multiregion diffusion theory, depletion code was used for burnup calculations. These burnup calculations formed the basis for the parameters used to evaluate later-in-life reactivity coefficients.

Generally, for radial calculations, the module was divided into five regions: the central control rod hole, the core, the radial blanket, the graphite reflector, and the sodium-stainless steel reflector.

Two kinds of axial calculations were made: those with a center gap between the upper and lower half bundles of the fuel rods, and those without this center gap, i.e., with the center gap homogenized into the core. The former were used to calculate the cermet expansion coefficient and the clad expansion coefficient; the latter were used to calculate Doppler and sodium temperature coefficients. The coefficients were calculated for a burnup of 0, 33,333 MWD/MT and 66,667 MWD/MT, which represent the average core burnup for beginning of life, equilibrium loading, and equilibrium discharge, respectively, for a three-cycle Roundelay refueling scheme.

The average temperatures of the fuel, structure, and sodium coolant were assumed to be 1250°F, 1000°F, and 1000°F respectively. At these temperatures, the basic number densities are:

Fuel (PuC-UC)	$.029466 \times 10^{+24}$ atom/cm.^{3} (at 92% of theoretical density)
Structure (SS-304)	$.08565 \times 10^{+24}$ atom/cm.^{3}
Coolant (Sodium)	$.021584 \times 10^{+24}$ atom/cm.^{3}

The depleted UO_2 in the radial blanket is 90% of theoretical density, and at 1400°F yields a basic number density of $.21471 \times 10^{24}$ molecules/cm.^{3} The basic number densities of stainless steel and sodium in the blankets are assumed to be the same as in the core. The plutonium composition is 0.659, 0.290, 0.041, and 0.010 for Pu-239, 240, 241, and 242, respectively.

The ARES-II resonance integral code was used to calculate absorption cross sections at three fuel temperatures for the isotopes U-238, Pu-239, and Pu-240, and fission cross sections for Pu-239 in the lower 8 groups, i.e., below 40.7 kev. The remaining cross sections employed were from standard Westinghouse Atomic Power Division 18 group library (See Appendix F). The Doppler coefficient was calculated at the three burnup stages by using the temperature-dependent cross-sections in W-MOBI.

The sodium temperature coefficient was calculated from the change in k_{eff} obtained by reducing the sodium number density ten percent. This coefficient is very sensitive to the neutron energy spectrum and to core leakage, so that for non-spherical cores, a one-dimensional calculational scheme is not generally adequate. A pseudo, two-dimensional method (essentially an 18 group buckling iteration) was used, which takes into account the changes in the transverse leakage in each of the 18 lethargy groups. This method has been used very successfully at Westinghouse Atomic Power Division in calculating the spectra of various ZPR-III and ZPR-VI critical experiments.

To provide a reactivity coefficient for the mechanical bowing of fuel assemblies, a calculation was performed in which the core radius was increased by one centimeter and the fuel and structure (stainless steel) number densities were reduced in such a manner that the total amount of fuel and structure in the core remained constant.

To obtain the cermet expansion coefficient and the clad expansion coefficient, axial W-MOBI calculations were performed at three burnup conditions, and a two-dimensional PDQ-04 calculation was performed at beginning of life. The W-MOBI results were normalized to the PDQ values, so that they agreed at beginning of life. The calculation of these coefficients was done in such a manner as to duplicate the actual phenomenon as closely as possible. Three axial cases were considered:

1. Reference Case: Center Gap = 0.1 inch, Fuel # Density = A
   Clad # Density = B
   Na # Density = C
   Core Length = L (incl. gap)
   Reference $k_{eff} = k_1$

2. Cermet Expanded: Center Gap = 0.6 inch, Fuel # Density= A
   Clad # Density= B
   Na # Density = C
   Core Length = L+0.5 inch (incl. gap)
   $k_{eff} = k_2$

3. Cermet and Fuel Clad Expanded: Center Gap = 0.1 inch

Fuel # Density = $A(\frac{L}{L + 0.5})$

Clad # Density = $B(\frac{L}{L + 0.5})$

Na # Density = C

$k_{eff} = k_3$ Core Length = L+0.5 inch (incl. gap)

The coefficients are then:

A. Cermet Expansion, $L(\frac{dk}{dL})_{cermet} = L(\frac{k_2 - k_1}{0.5})$ L in inches

B. Fuel Clad Expansion, $L(\frac{dk}{dL})_{clad} = L(\frac{k_3 - k_2}{0.5})$ L in inches

As $k_2 < k_1$, $L(\frac{dk}{dL})_{cermet} < 0$, and as $k_3 > k_2$, $L(\frac{dk}{dL})_{clad} > 0$. The cermet expansions serve to move fuel from the high worth center region to the low worth core boundary region, while the clad expansion pushes fuel back into the center region. The reactivity coefficient for the clad controlled expansion (CCEX) concept is obtained from cases 1 and 3 above. Neglecting the effects of the small, constant, center gap, we get:

$$L(\frac{dk}{dL})_{CCEX} = L(\frac{k_3 - k_1}{0.5}).$$

Burnup calculations were performed with the SIZZLE, one-dimensional, diffusion theory, depletion code in radial geometry. The calculation was carried to 100,000 Megawatt days per metric ton of heavy metal in the core (MWD/MT) in nine time steps. It was assumed that at 33,333 MWD/MT one-third of the core would be replaced and again 33,333 MWD/MT later another third would be replaced, etc. In the equilibrium cycle, the average burnup in the core would always be between 33,333 and 66,667 MWD/MT. The calculation of the various coefficients (Doppler, coolant temperature, etc.) were performed at 0, 33,333 and 66,667 MWD/MT using number densities generated in the SIZZLE burnup analysis.

When fresh fuel is placed next to burned fuel, a power peak occurs in the fresh fuel. The magnitude of this peak is given by:

$$P = \frac{\sum_{i=1}^{18} \Sigma_{\text{fiss. i}} \phi_i(r_{\text{fresh}})}{\sum_{j=1}^{18} \Sigma_{\text{fiss. j}} \phi_j(r_{\text{burned}})}$$

To simplify the calculation, it was assumed that $\phi_k(r_{\text{fresh}}) = \phi_k(r_{\text{burned}})$; this is a valid assumption for neighboring fuel elements in a fast reactor.

In all previous calculation, identical enrichments were assumed in the carbide and cermet fuel so that equivalent burnups would be obtained. A knowledge of the effects of cermet enrichments greater than the fuel enrichment was desired. Radial burnup calculations were performed on a single fuel assembly for various cermet enrichments. In the SIZZLE calculation, the stainless steel, sodium and UO_2-PuO_2 (cermet fuel) were homogenized into a central region with 1.492 centimeter radius and the remaining part of the assembly formed a ring from 1.492 to 6.886 centimeters radius. The enrichment of the central region was varied, the enrichment for the annular section was held constant in these calculations.

III.6.3 Results and Discussion

Table III.6-2 and Figures III.6-2 thru III.6-8 present the results of the nuclear analyses. The calculational methods used to obtain these results are described in the previous section.

Figures III.6-2 thru III.6-8 require little further explanation. The axial power distribution at beginning of life for the reference core is presented in Figure III.6-2. A core peak to average axial power of 1.36 was obtained. The core effective multiplication factor is shown in Figure III.6-3 as a function of burnup for a 3 cycle

Table III.6-2

Nuclear Data

Module Total Power (Equilibrium Core)	465 MWt	
Module Core Power (average at fuel discharge)	385 MWt	
Module Blanket Power (average fuel discharge)	80 MWt	
Fuel Enrichment (beginning of life)	16.26	a/o Pu-239 + Pu-241
Cermet Enrichment (beginning of life), E	16.26	a/o Pu-239 + Pu-241
Alternate Cermet Enrichments: (1.5E)	24.39	a/o Pu-239 + Pu-241
(1.9E)	30.89	a/o Pu-239 + Pu-241
Local Power Peaking	1.10	

	Beginning of Life	33,333 MWD/MT	66,667 MWD/MT
Effective Multiplication Factor, k eff	1.0568	1.0235	1.0025
Doppler Coefficient: T dk/dT	- .00370	- .00335	- .00300
Sodium Removal: ρ dk/dρ			
(Starting at Top of Core)			
First 1/6 of Core	.00333	.00345	.00307
Second 1/6 of Core	.00252	.00272	.00194
Third 1/6 of Core	.00172	.00199	.00093
Fourth 1/6 of Core	.00170	.00198	.00092
Fifth 1/6 of Core	.00252	.00272	.00194
Sixth 1/6 of Core	.00342	.00354	.00315
Total Core	0.01521	0.01640	0.01195
Cermet Expansion L dk/dL	-0.7890	-0.7624	-0.7181
Clad Back Expansion L dk/dL	+0.3808	+0.3680	+0.3466
Clad CEX Expansion L dk/dL	-0.4082	-0.3944	-0.3715
Radial Maximum-to-Average Power (core)	1.325	1.268	1.212
Axial Maximum-to-Average Power (core)	1.358	1.345	1.333
Central Control Rod Worth	.0553	.0522	.0483
Bowing Coefficient R dk/dR	-0.5255		

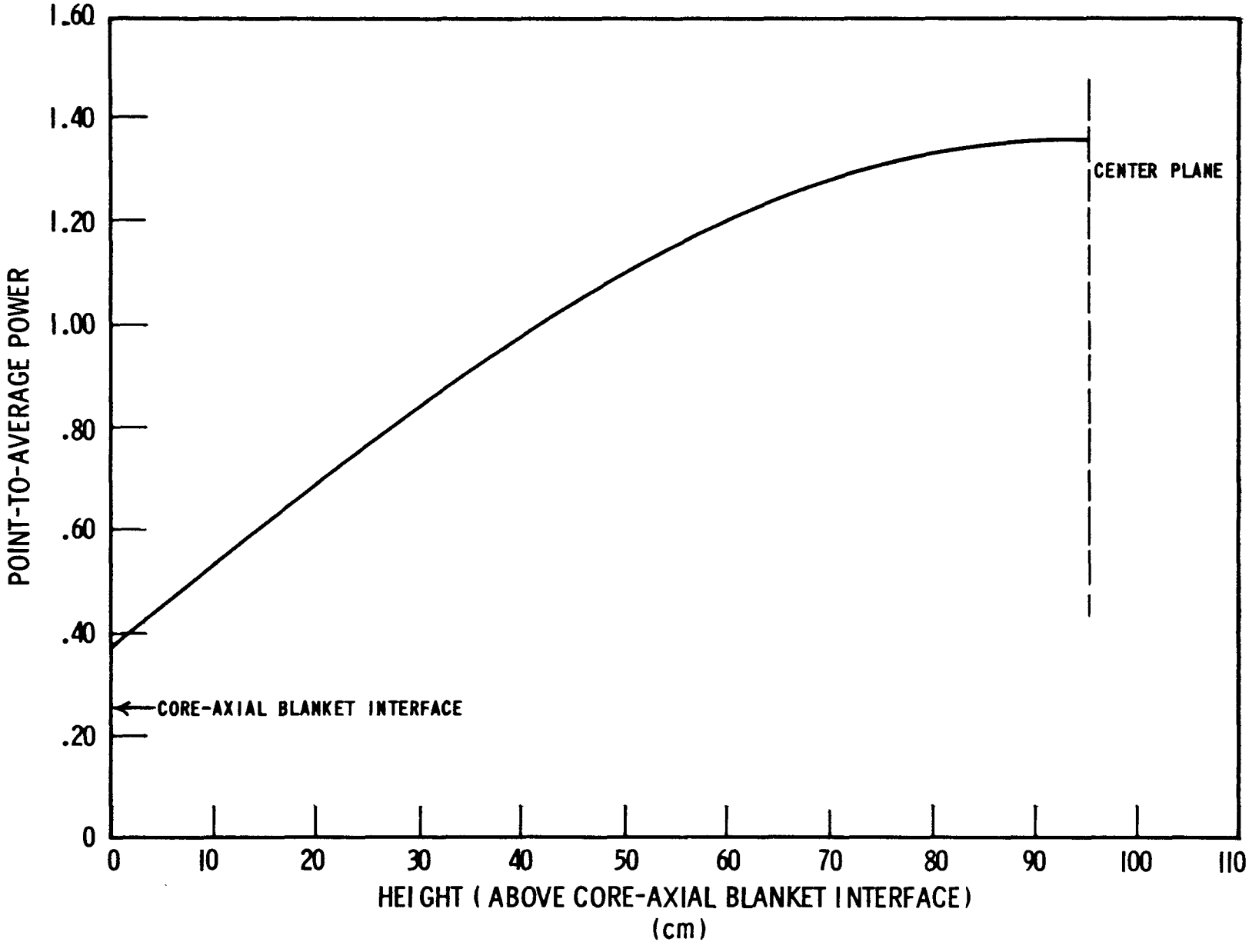

AXIAL POWER DISTRIBUTION BEGINNING OF LIFE

Figure III.6-2

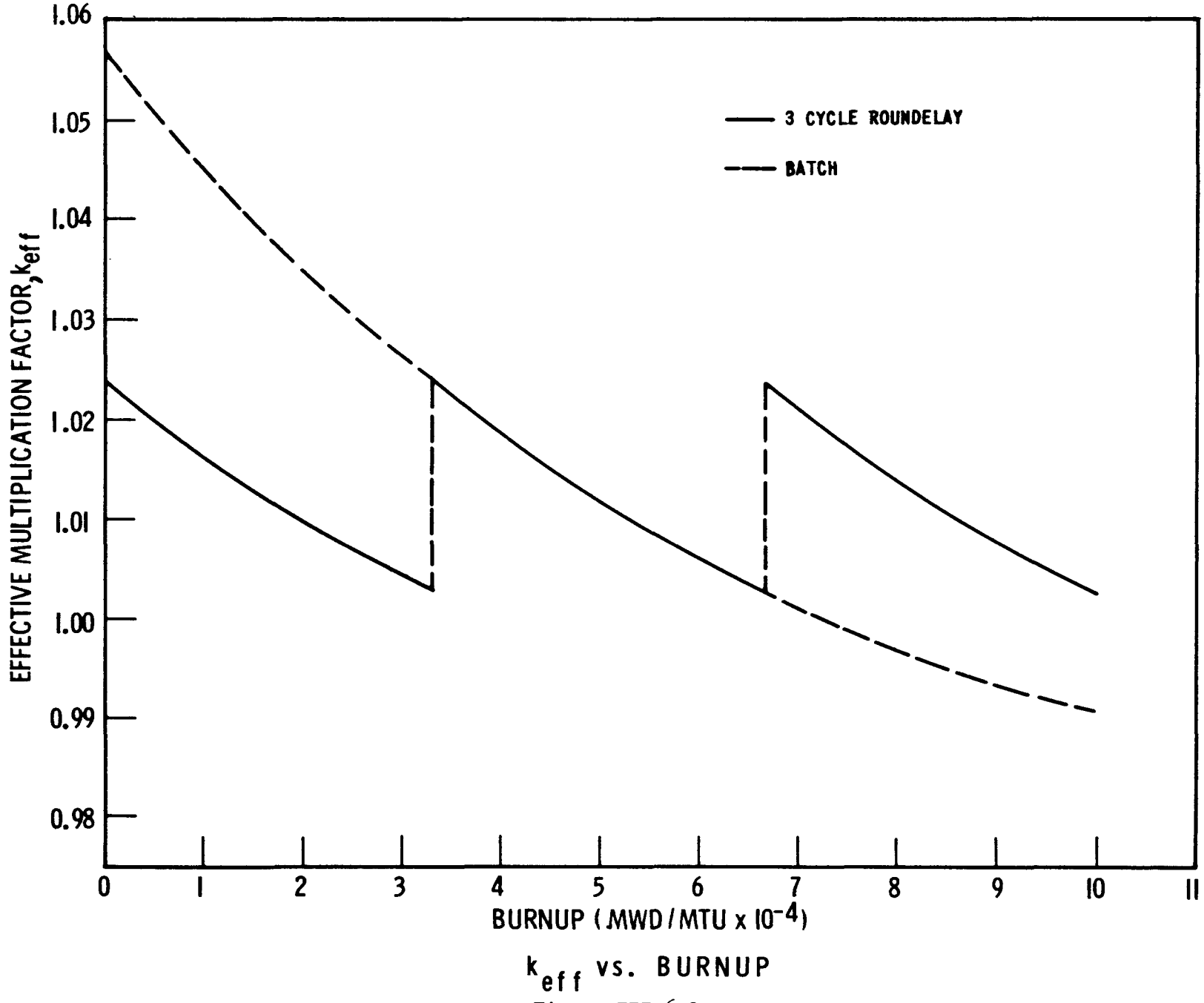

k_{eff} vs. BURNUP

Figure III.6-3

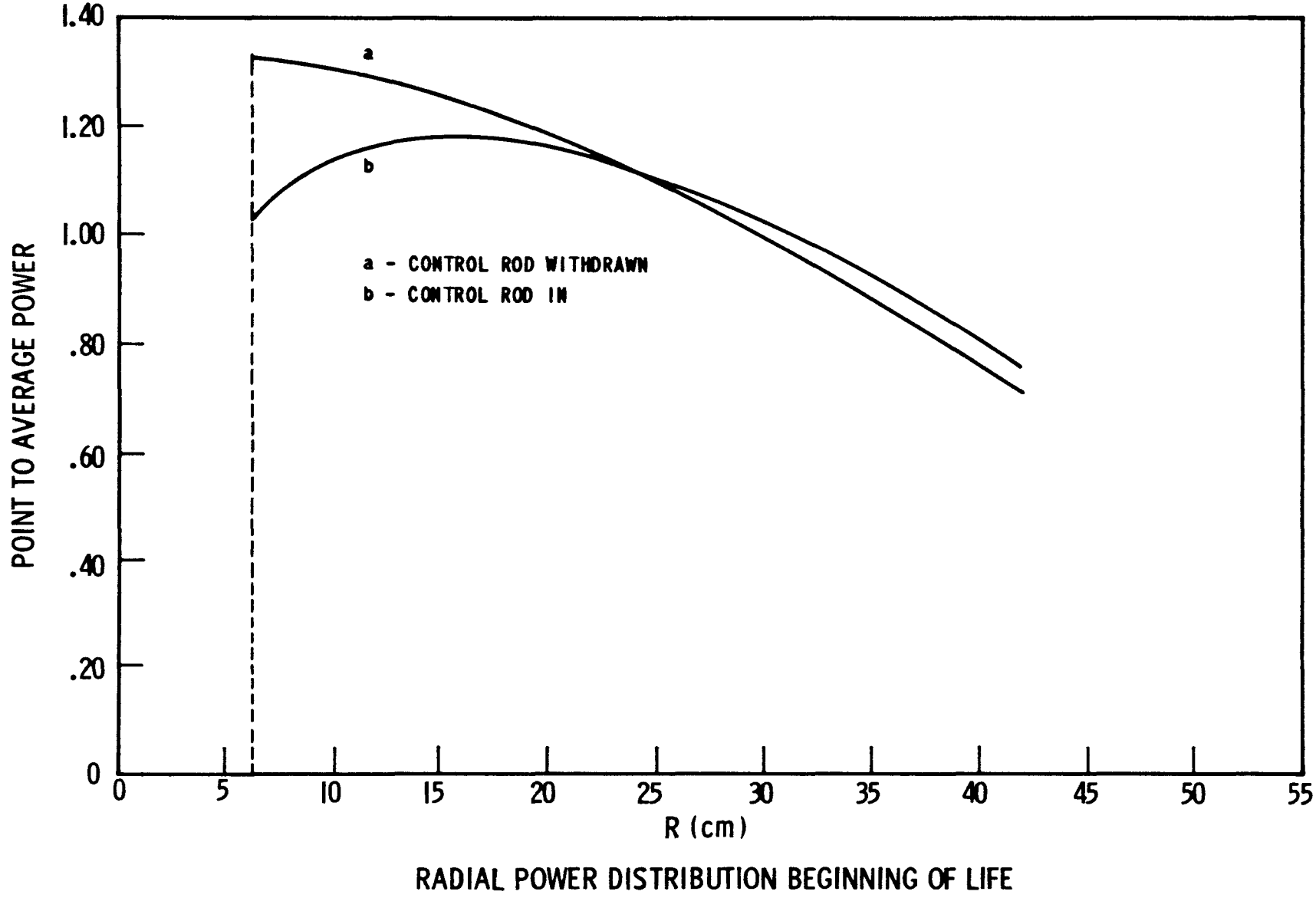

Figure III.6-4

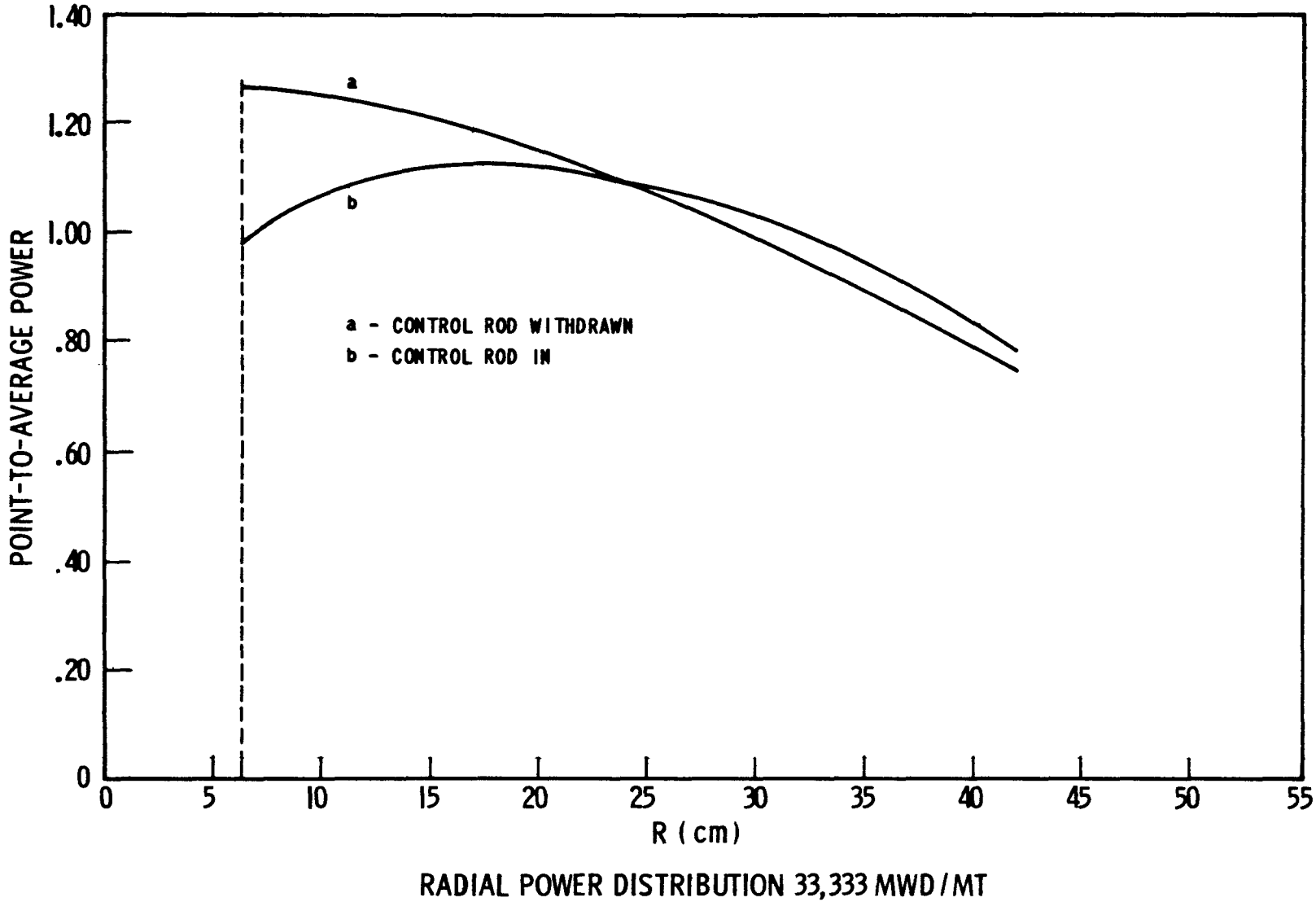

Figure III.6-5

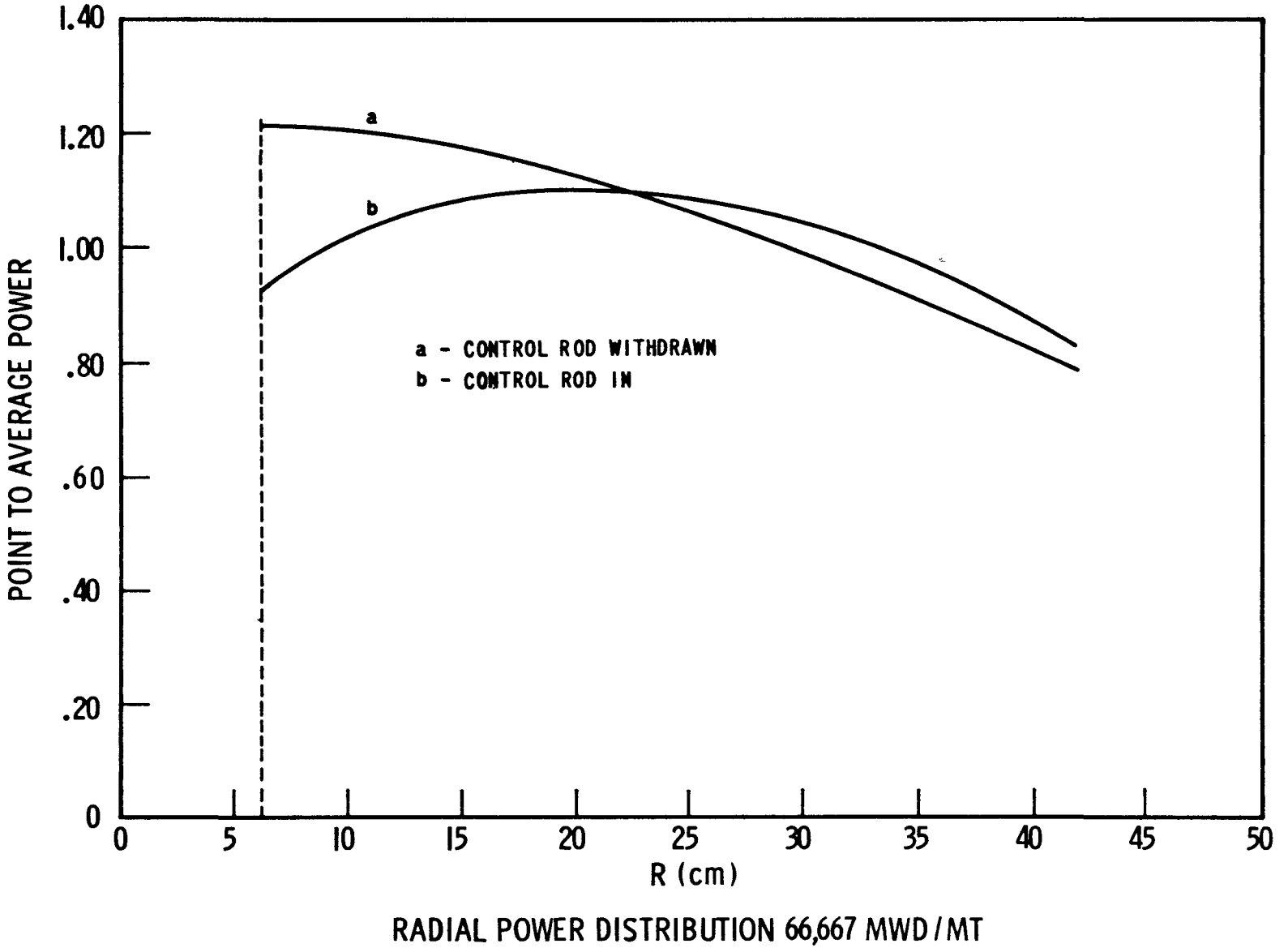

Figure III.6-6

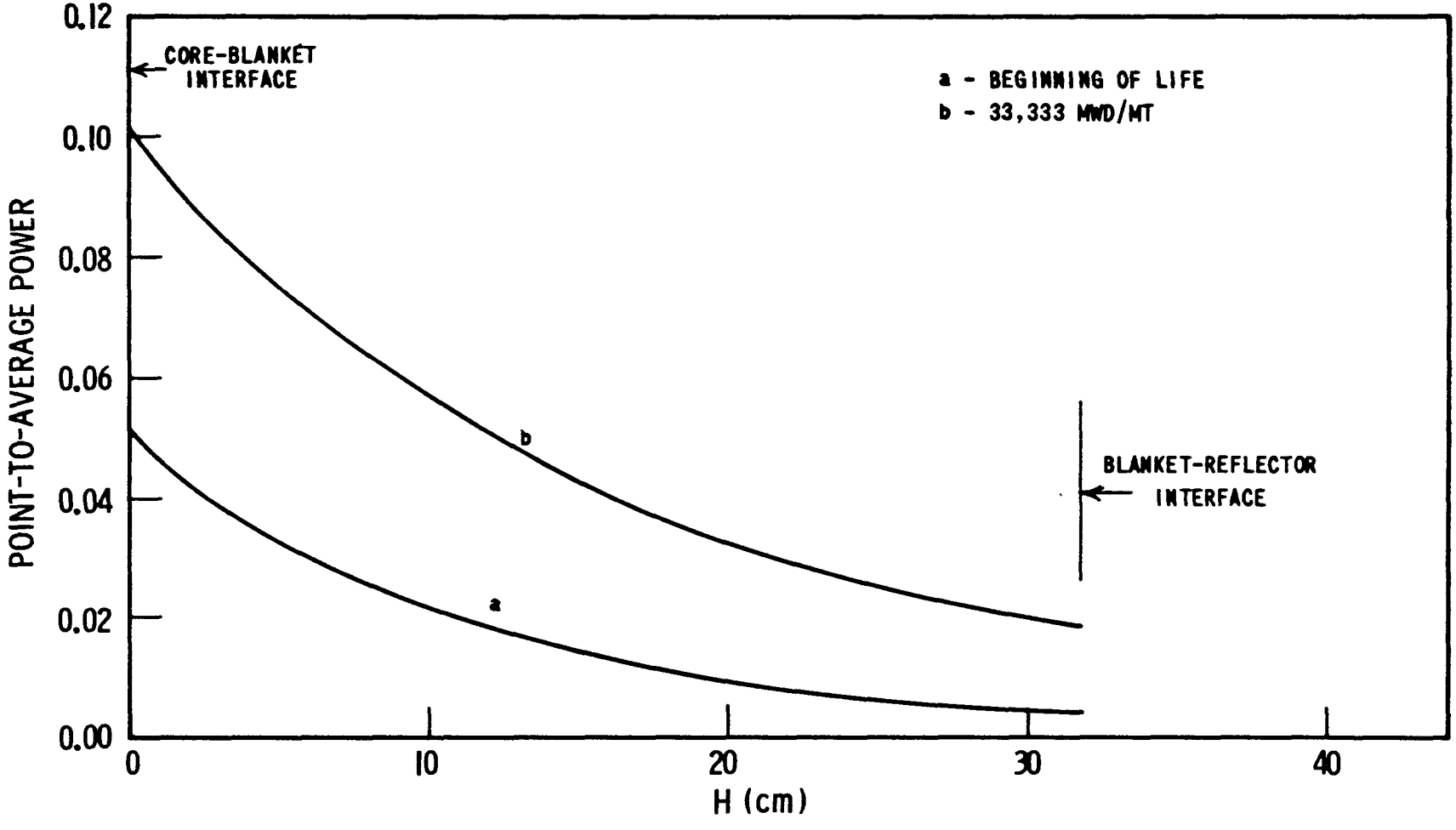

AXIAL BLANKET POWER DISTRIBUTION
(POWER NORMALIZED IN CORE)

Figure III.6-7

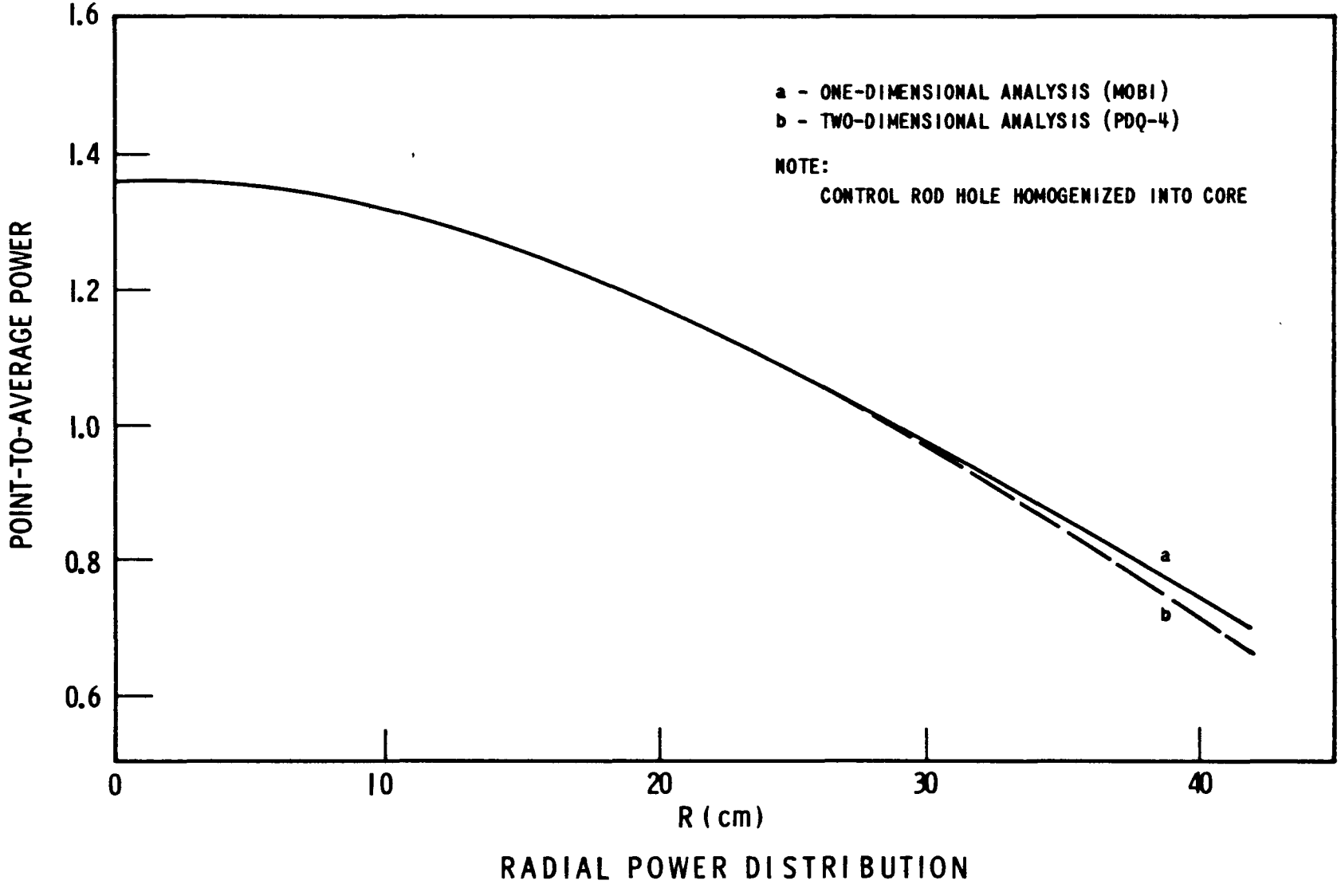

Figure III.6-8

roundelay and for batch loading schemes. The core radial power distribution is presented in Figures III.6-4, III.6-5 and III.6-6. A core peak-to-average radial power of 1.33, 1.27 and 1.215 was obtained for beginning of life, 33,333 MWD/MT, and 66,667 MWD/MT, respectively. The power distribution shown with control material in the central channel (curve b) represents a limiting case of maximum possible poison, not a realistic control rod worth. The axial blanket power distribution (power normalized to core) for two burnups are presented in Figure III.6-7. Figure III.6-8 compares the results of W-MOBI and PDQ-4 analyses. Very close agreement was obtained.

Table III.6-2 presents the reactivity coefficients and other important nuclear data for the reference reactor core. The bowing coefficient indicates that a one mil change in the reactor core radius for the full-core height will change the reactivity by approximately one cent.

Thermal-hydraulic and transient analyses data indicated that high cermet heat rates may be necessary. The easiest way to increase the power in the cermet elements is either to increase the volume fraction of fuel in the stainless steel matrix, or to increase the plutonium content of the fuel in the cermet. In this study, the former was limited to 34 volume percent. The latter presents a problem from a nuclear standpoint, however, because the fuel in the cermet may burn down faster than the ceramic fuel, and hence lead to a strongly changing ratio of cermet to fuel heat generation rates, which effects the transient response of the BCEX concept. The lower breeding ratio inherent with the higher enrichment in the cermet aggrevates the problem. Burnup calculations on a single fuel assembly yield the results shown in Figure III.6-9. Curve "a", a plot of cermet-fuel power ratio versus burnup for equal cermet-fuel enrichments, has been normalized to one at beginning of life. Curve "a" corresponds to a cermet to fuel volumetric heating ratio of 0.244. For the reference core, this corresponds to a cermet fuel having a 0.35 volume fraction of $(PuU)O_2$ with an 85 percent of theoretical

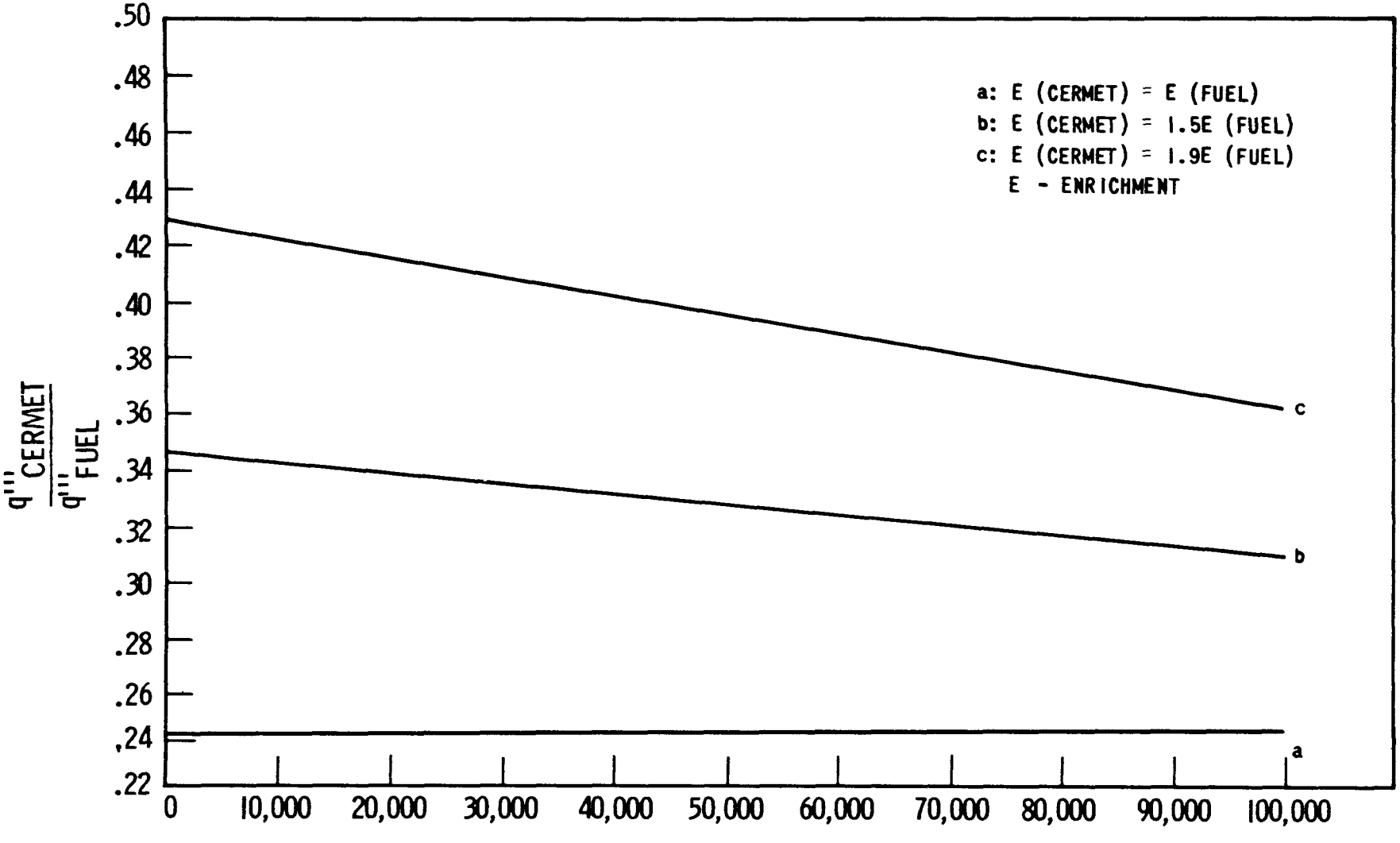

$\frac{q'''_{CERMET}}{q'''_{FUEL}}$ vs. BURNUP

Figure III.6-9

density. Curves "b" and "c" are for cermet to fuel enrichment ratios of 1.5 and 1.9, respectively. Transient analyses must determine if the changes in heat generation rates in the cermet associated with the various enrichments are feasible.

III.6.4 Recommendation and Conclusion

From a nuclear standpoint, the investigation of the CEX concept is straight-forward and amenable to standard Westinghouse Atomic Power Division calculation procedures. Since the nuclear analyses of this concept assumed a supporting role in the study, they served mainly to furnish information for use in the transient analyses. None of the results were very different from either expected or previous values.

The "state-of-the-art" in fast reactor calcualtions is rapidly changing. As design and analysis techniques are improved, more and more confidence can be placed in calculated results. The CEX concept does not present any unique problems in nuclear analysis, hence, the results of this analysis can be accepted confidently. Continued improvement of calculations for Doppler and sodium void effects will be necessary to accurately evaluate the need and relative benefits of safety features such as CEX.

The reactivity effects of either the bundle controlled expansion, BCEX, or the clad controlled expansion, CCEX, can be measured easily by using existing critical facilities (ZPR-III, ZPR-VI). This is an obvious early step in pinning down the coefficients and evaluating the analysis techniques.

In the CEX concept, fissile material is removed from high importance regions of the core (e.g., the core center) and placed in low importance regions (e.g., the core-blanket interface). When this is recognized, it becomes clear that the reactivity worth of various fissile material, as a function of position in the core, is a key quantity. In numerous experiments (notably with ZPR-III) this quantity has been measured and

reported in the literature. An extensive comparison between calculations and experimental determinations of reactivity worths would either increase confidence in present Westinghouse Atomic Power Division calculation methods or indicate that these methods need improvement. This may well be the next logical step before designing a critical experiment test on the CEX concept.

This study was limited to the Westinghouse modular design fast breeder reactor. Analysis of the reactivity effects in pancake reactor cores, right circular cylinder reactor cores (L/D 1), and in reactors using oxide fuels may prove that the CEX concept is the automatic control device that changes a marginal reactor into a safe reactor. This would allow the use of reactors that have superior economic advantages but marginal safety factors.

References Section III.6

1. Heck, F. M. et al, "Liquid Metal Fast Breeder Design Study", WCAP-3251-1, (January 1964).

2. Baller, D. C., "The FAIM Code, A Multigroup, One-Dimensional Diffusion Equation Code", NAA-SR-7137, (April 1962).

III.7 Material Review & Analyses

III.7.1 General

The Westinghouse Large Fast Breeder Modular Reactor core was selected as the reference design for the analyses of the performance characteristics of the bundle controlled expansion (BCEX) fuel assembly concept. This groundrule prescribed the fuel clad and core structual material as 316 L stainless steel; the fuel material as Uranium-plutonium monocarbide; and the cermet material as Uranium-plutonium dioxide particles contained in 316 L stainless steel matrix. These materials were selected based on past Westinghouse sodium-cooled FBR investigations[37, 38, 39, 40, 41, 42, 43].

This section presents the results of the review of these materials for utilization in the bundle controlled expansion (BCEX) fuel assembly concept.

This review included the investigation of the chemical compositions of these materials, the mechanical and physical properties of these materials, known effects of irradiation on these materials, effect of sodium environment on 316 L stainless steel, and design and specification criteria for (U Pu)O2 in 316 L stainless steel cermets.

The materials review and analyses was limited to the information currently available and to the broad requirements of this contact.

III.7.2 Properties of 316 L Stainless Steel

III.7.2.1 Chemical Composition

The chemical composition of 316 L stainless steel is given in Table III-7-1[1].

Table III. 7-1

Chemical Composition of 316 L SS

Element	Percent Concentration
Carbon	0.03 max.
Manganese	2.00 max.
Phosphorus	0.040 max.
Sulphur	0.030 max.
Silicon	1.00 max.
Chromium	16.00 - 18.00
Nickel	10.00 - 14.00
Molybdenum	2.00 - 3.00

III.7.2.2 Mechanical Properties

Tensile Properties[1, 2]

Tensile properties of 316 L are given in Figure III. 7-1. Also given for comparison are the tensile properties of 304 and 347 stainless steels.

Creep Rupture Properties[1, 2]

There appears to be no marked difference in the creep-rupture strength of Types 316 and 316 L stainless steel, and reported values for both steels have been included in the creep-rupture curve as Type 316 L. The creep-rupture behavior of Types 304, 347, and 316 L at 1000, 1200, and 1500°F is given in Figure III. 7-2.

Modulus of Elasticity[3, 4]

The modulus of elasticity of 316 stainless steel is given as a function of temperature in Figure III. 7-3.

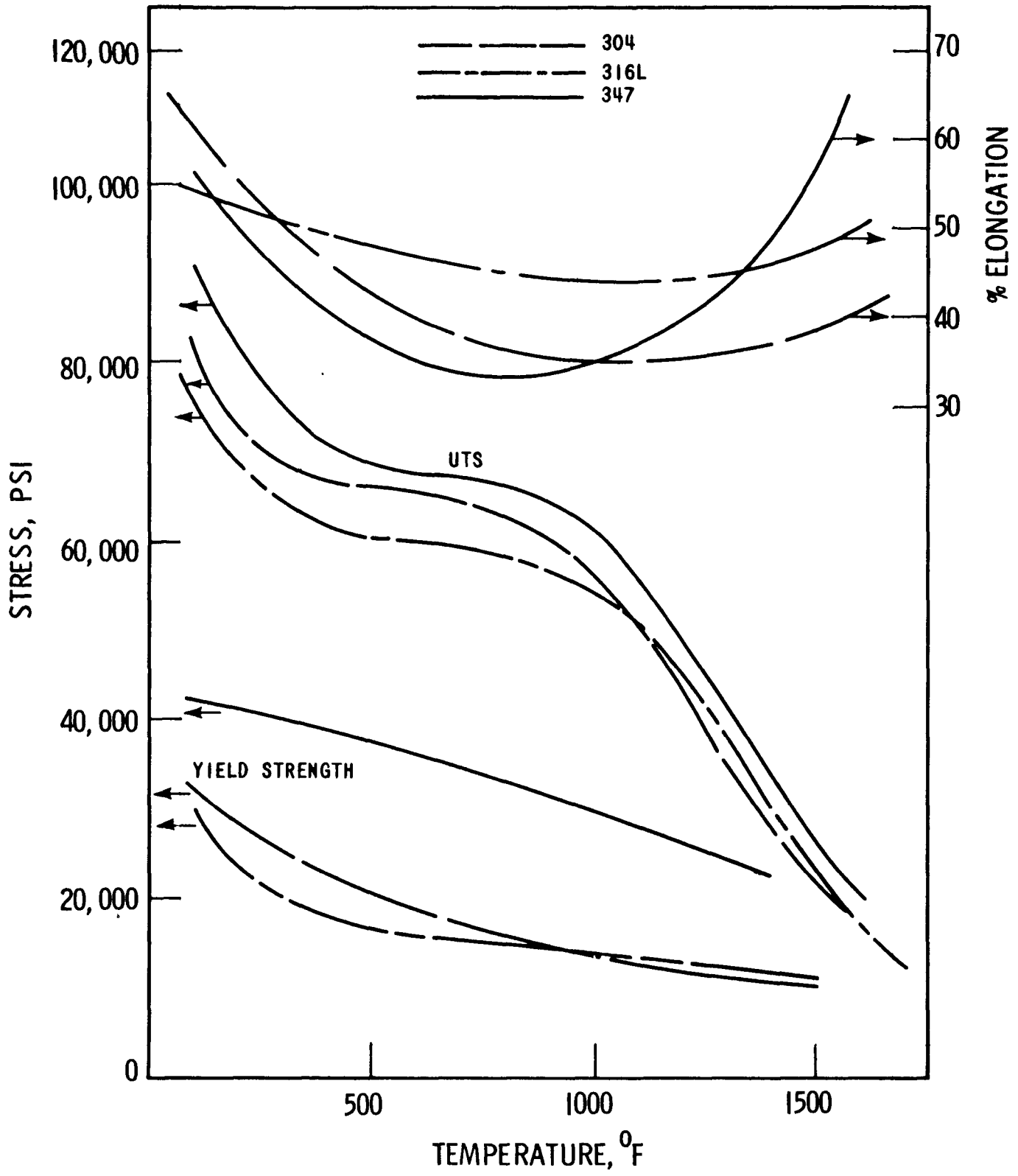

VARIATION IN MECHANICAL PROPERTIES WITH TEMPERATURE

Figure III.7-1

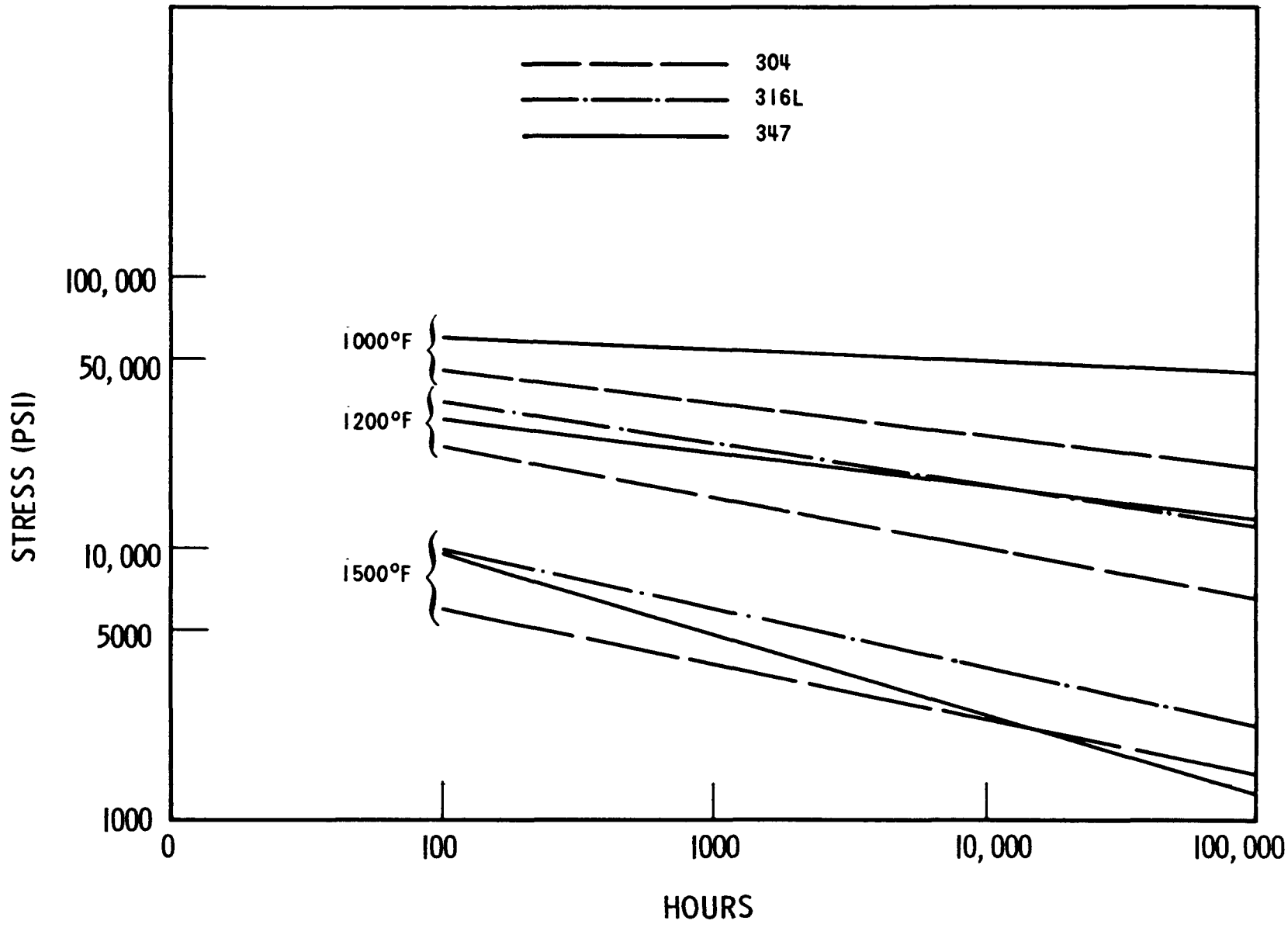

CREEP RUPTURE BEHAVIOR OF SELECTED AUSTENITIC STAINLESS STEEL

Figure III.7-2

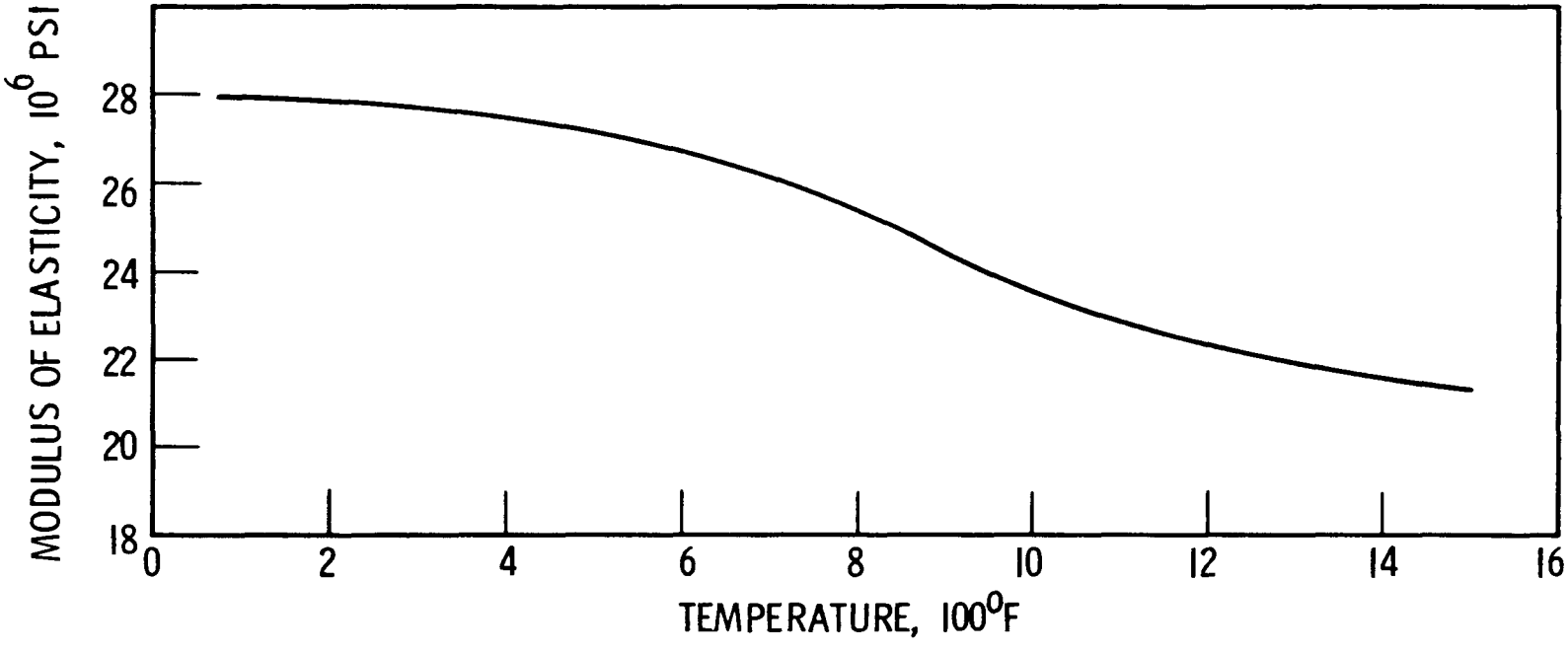

MODULUS OF ELASTICITY OF TYPE 316 STAINLESS STEEL

Figure III.7-3

Poisson's Ratio

No data on Poisson's Ratio was found for Type 316 L. For the austenitic steel in general,[5] Poisson's Ratio varies from about 0.30 at 800°F, to 0.33 at 1300°F.

Impact Strength and Hardness[1]

Values of impact strength and hardness at different temperatures are given in Table III. 7-2.

Table III. 7-2

Impact Strength and Hardness of Type 316 L

	Unexposed	Exposed 1000 hrs. at		
Room Temperature		900 F	1050 F	1200 F
Charpy Keyhole Notch Impact Values (Ft-Lbs.)	79	74	72	51
Brinell Hardness	135	137	135	142

Fatigue Properties

A curve of stress amplitude versus cycles to failure is given for Type 316 stainless steel in Figure III. 7-4. Available data[6] are given for room temperature to 800°F up to 10^6 cycles. Since fatigue life must be estimated for temperatures from 800°F, and up to 10^{11}, cycles the following assumptions were made to extrapolate the available data:

1. The room temperature to 800°F data were linearly extrapolated from 10^6 to 10^{12} cycles
2. A curve of stress amplitude versus cycles to failure at 1300°F was calculated by using the relationship:

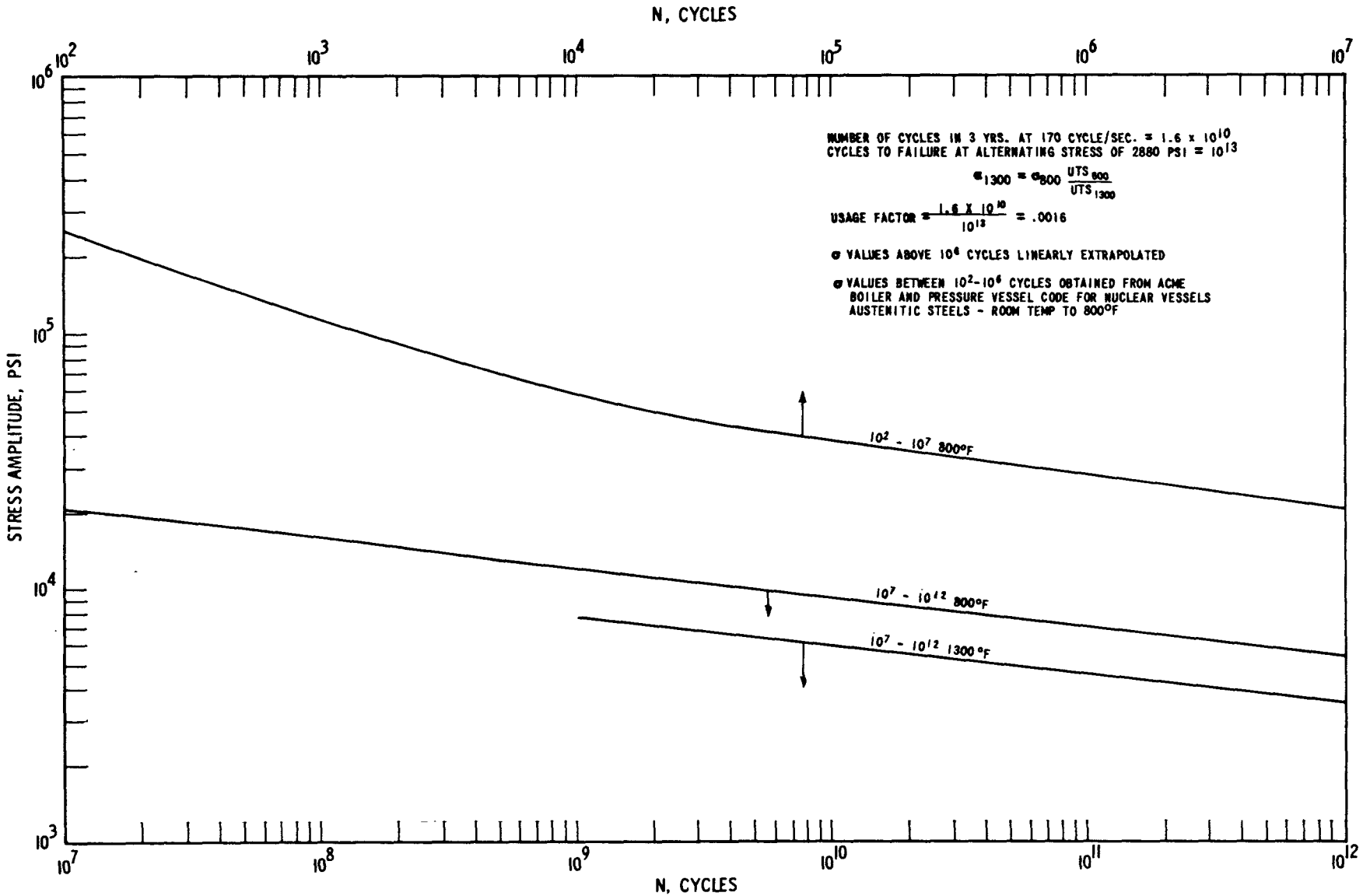

STRESS AMPLITUDE VERSUS CYCLES TO FAILURE FOR 316 SS

Figure III.7-4

$$\sigma_{1300} = 800 \frac{UTS_{800}}{UTS_{1300}}$$

where σ_{1300} = stress at 1300°F

σ_{800} = stress at 800°F

UTS_{800} = ultimate tensile strength of 316 at 800°F

UTS_{1300} = ultimate tensile strength of 316 at 1300°F

III.7.2.3 Physical Properties

The physical properties of Type 316 L stainless steel are assumed to be the same as those of Type 316 stainless steel, for which data are presented.

Thermal Conductivity

The average thermal conductivity of Type 316 as a function of temperature is given in Figure III. 7-5.

Coefficient of Thermal Expansion

The coefficient of thermal expansion as a function of temperature is shown in Figure III. 7-5.

Density

The density of 316 L stainless steel is 8.0 g/cc or 0.29 pounds per cubic inch, at room temperature.(3)

Specific Heat

The specific heat is 0.12 BTU/lb/°F.

Melting Point

The melting point is approximately 2500°F.

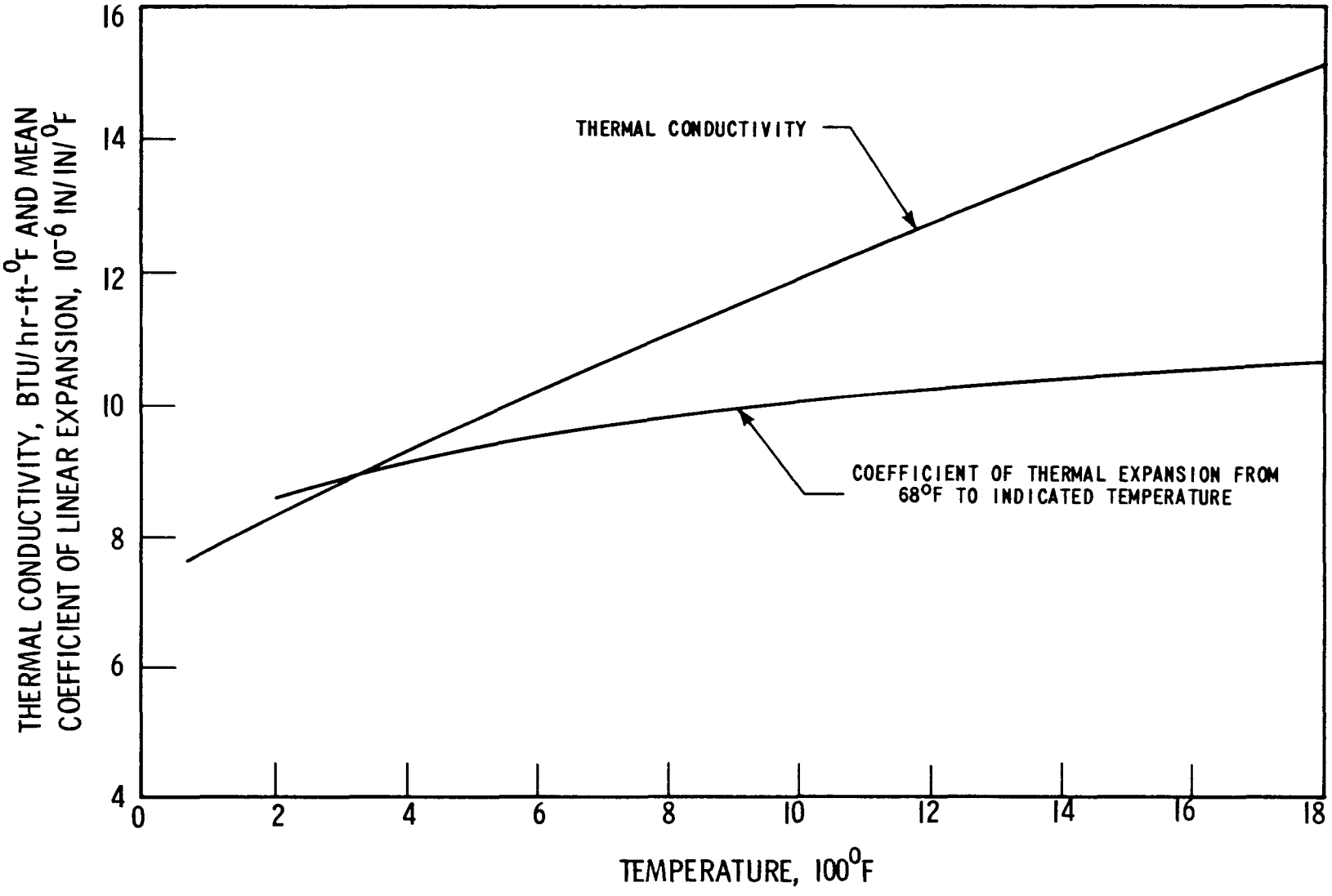

THERMAL CONDUCTIVITY AND MEAN COEFFICIENT OF THERMAL EXPANSION OF TYPE 316 STAINLESS STEEL

Figure III.7-5

III.7.2.4 Effect of Irradiation

Although the effect of neutron irradiation on the tensile properties of Types 316 and 316 L stainless steel has not been investigated as thoroughly as for Types 304 and 347 stainless steel, the results are quite similar. Yield strength is increased much more than tensile strength, while percent elongation is reduced. The effect of irradiation on the ductility of Type 304 stainless steel is shown in Figure III. 7-6.[8] Irradiation has a negligible effect on the thermal conductivity, specific heat, and linear expansion coefficient of stainless steels.

III.7.3 Properties of (U,Pu)C Fuel

III.7.3.1 Chemical Composition

The major element concentration of the reference (U,Pu)C fuels is given in Table III. 7-3.

Table III. 7-3

Major Element Concentration of (U,Pu)C Fuel

Plutonium	23% [a]/o of metal atoms
Plutonium 239 + 241 fraction of total Pu	70.0 w/o min.
Uranium	77% of metal atoms
Equivalent carbon (C+O+N)	4.7 ± 0.1 w/o
Oxygen	1500 ppm max.
Nitrogen	1000 ppm max.
Iron	1.8 w/o

III.7.3.2 Physical Properties of (U,Pu)C Fuel[20]

Thermal Conductivity

The addition of plutonium carbide to uranium carbide to form a solid solution (U,Pu)C reduces the thermal conductivity of the solution

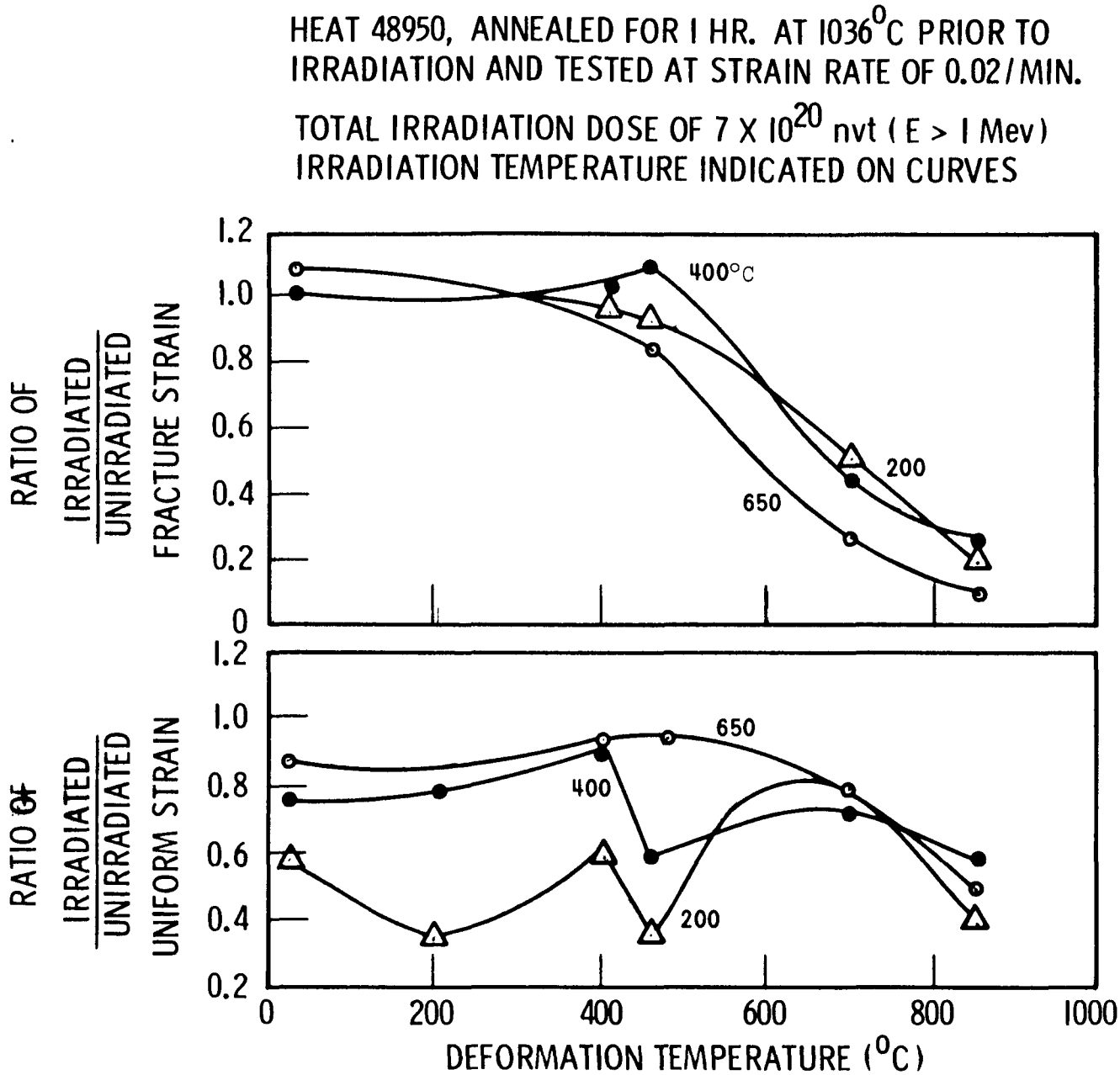

EFFECT OF IRRADIATION ON THE DUCTILITY OF TYPE 304 STAINLESS STEEL

Figure III.7-6

more than would be predicted by a linear interpolation between the respective conductivities of uranium carbide and plutonium carbide.[9] This reduction is most severe with additions of plutonium carbide from zero to about 25 mole percent,[10, 11] the range of interest for fast breeder reactor applications. Further additions of plutonium carbide cause only a gradual reduction in thermal conductivity. These effects are shown for arc-cast material in Figure III. 7-7. In this figure, data generated at Harwell (70°C)[12, 9, 13, 14] and Dounreay (20°C),[11, 15] are compared to LASL data[10] (presumed to be for arc-cast material extrapolated to 20°C. (Using the LASL value for the temperature dependence of the thermal conductivity to adjust the Harwell data to 20°C would only lower the data approximately 0.001 cal/sec-cm-°C).

The Harwell values were measured on material containing 4.55 to 5.23 w/o carbon;[12, 9, 13, 14] the material used at Dounreay was reported to be carbon deficient, but single phase.[11] However, more recent information indicates that 15, 40, 70, and 100% plutonium carbide alloys exhibited a duplex structure,[15] and that the carbon contents ranged from 4.00 w/o to 4.67 w/o. The fact that an alloy with a carbon content of 4.36 w/o (the 10 mole percent plutonium carbide alloy) was reported to be single phase strongly suggests that the materials were far from an equilibrium condition. The material used in the LASL studies was stoichiometric[16] with the exception of the plutonium carbide binary alloy which was carbon deficient ($PuC_{0.86}$)[10].

The temperature dependence of the thermal conductivity of various uranium-plutonium carbides, determined at Los Alamos,[10] is shown in Figure III. 7-8. Although plutonium carbide additions significantly reduce the thermal conductivity at room temperature, the temperature coefficient of the conductivity becomes larger then that for uranium carbides. The net effect is some reduction in the

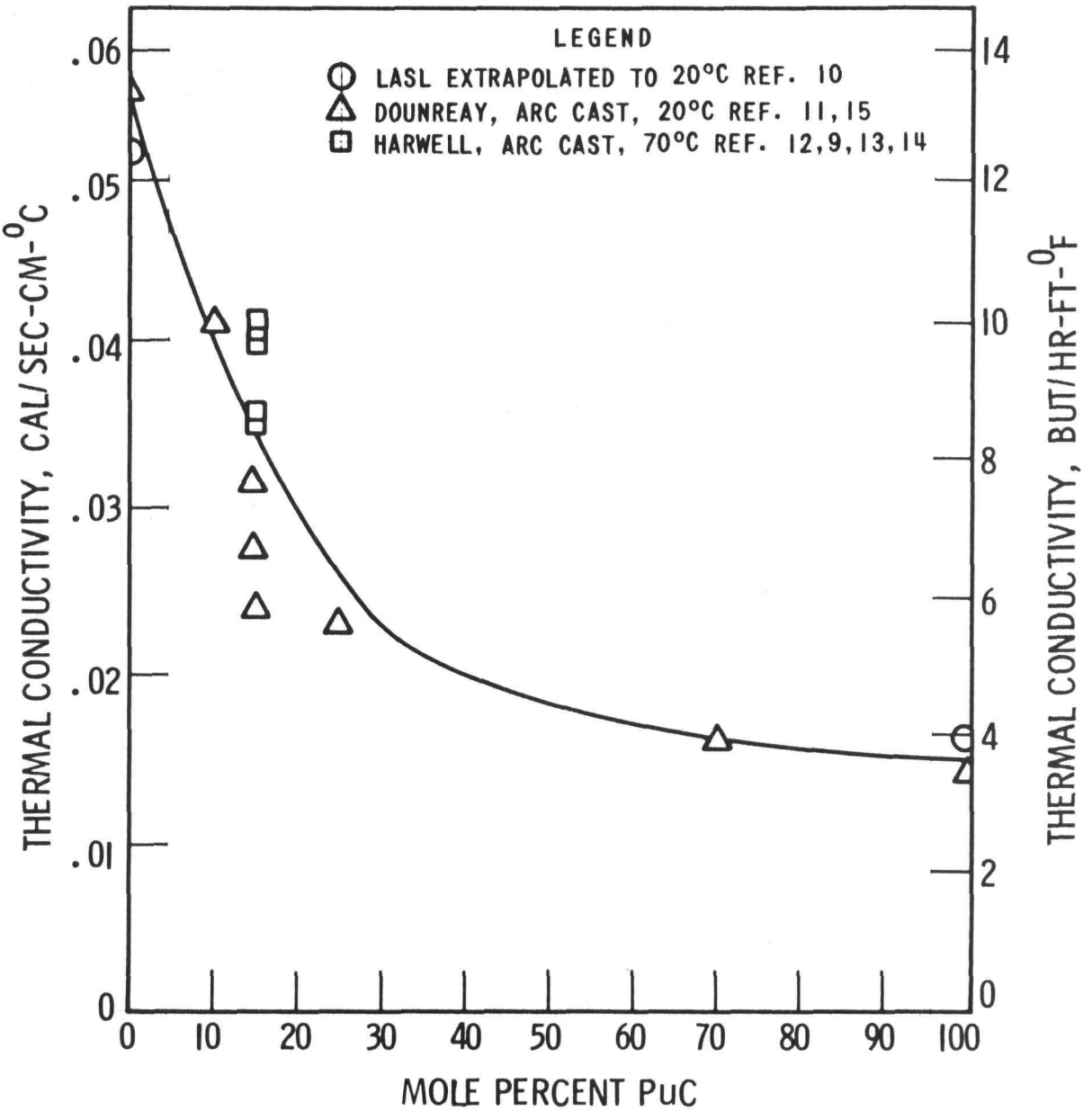

THE EFFECT OF PLUTONIUM CONTENT ON THE THERMAL CONDUCTIVITY OF URANIUM - PLUTONIUM CARBIDES

Figure III.7-7

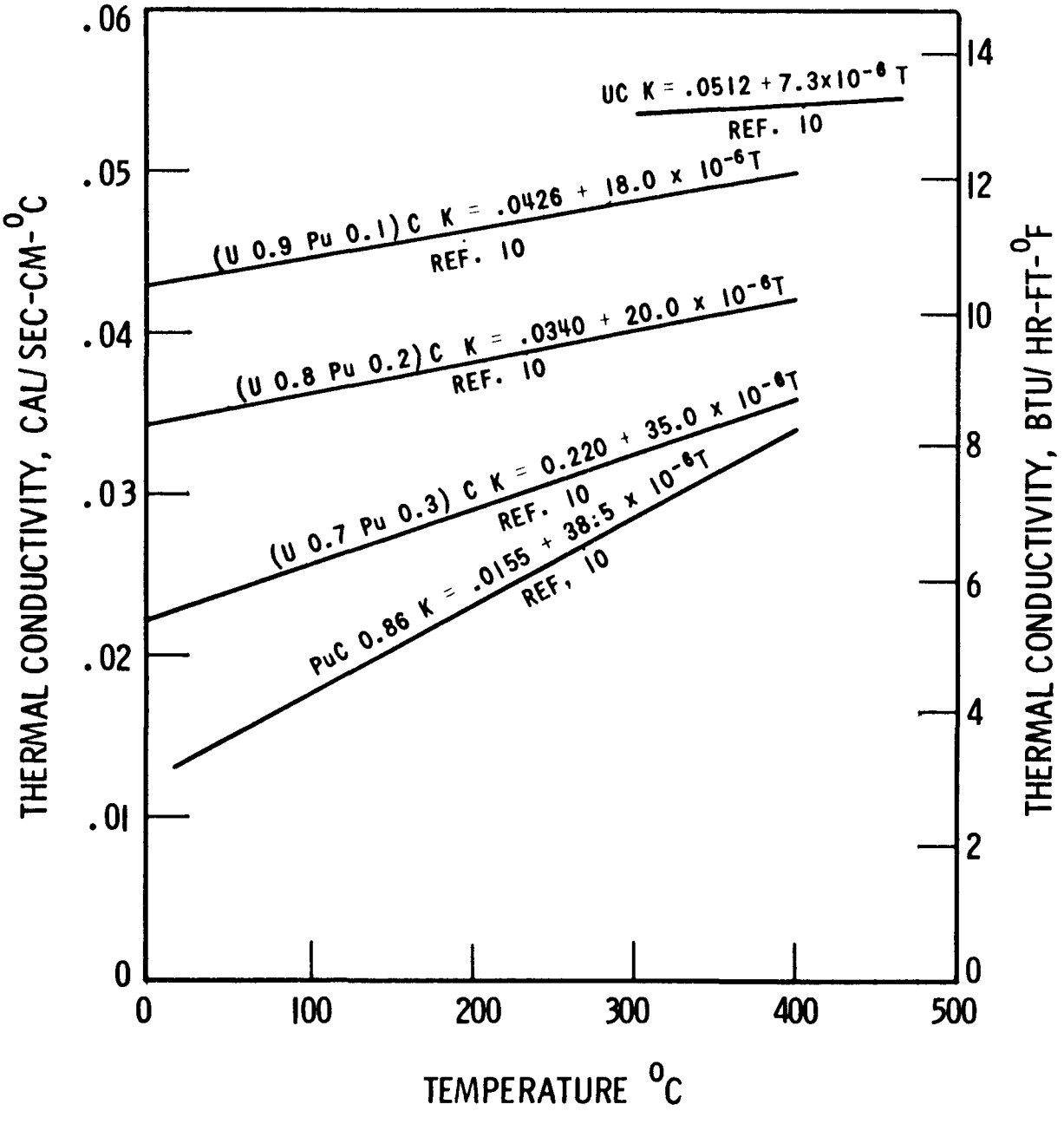

THE INFLUENCE OF TEMPERATURE ON THE THERMAL CONDUCTIVITY OF URANIUM-PLUTONIUM CARBIDES

Figure III.7-8

elevated temperature conductivity, but it is not nearly as great as anticipated from inspection of room temperature values. Extrapolation of these curves to typical average fuel temperatures indicate very little reduction in the thermal conductivity. (Such an extrapolation has not been suggested by the original investigators, and its use is not condoned here. The trend is apparent, but the degree is uncertain, and it is not anticipated that the solid solution carbides have a higher conductivity than uranium carbide - the result implied by continued extrapolation. However, the postulated narrowing of the gap between the thermal conductivities of UC and (U,Pu)C is supported qualitatively by in-pile observations).

The effect of carbon content on the thermal conductivity of $(U_{.85}Pu_{.15})C$ is shown in Figure III. 7-9 for arc-cast and hot-pressed material. The hot-pressed material is all hyperstoichiometric; no marked trend with carbon content is apparent. Corrections for carbon content and porosity appear to more effective, in relating the conductivity of sintered material to that of arc-cast material, than was the case with uranium carbide.

Strasser, et al., have reported the in-pile thermal conductivity of $(U_{0.8}Pu_{0.2})C_{0.95}$ to be equal to, or slightly less than, that observed for uranium carbide.[17, 18, 19] Assuming a helium gap conductance of 2000 BTU/hr-ft^2-°F, they estimate conductivities of approximately 0.037 to 0.053 cal/sec-cm-°C,[17] and 0.47, 0.050, 0.054, and 0.058 cal/sec-cm°C[19] for material of 92% theoretical density.

Specific Heat

Although the available data appear to be restricted to uranium carbide, plutonium carbide or uranium-plutonium carbide will probably have very similar specific heats.

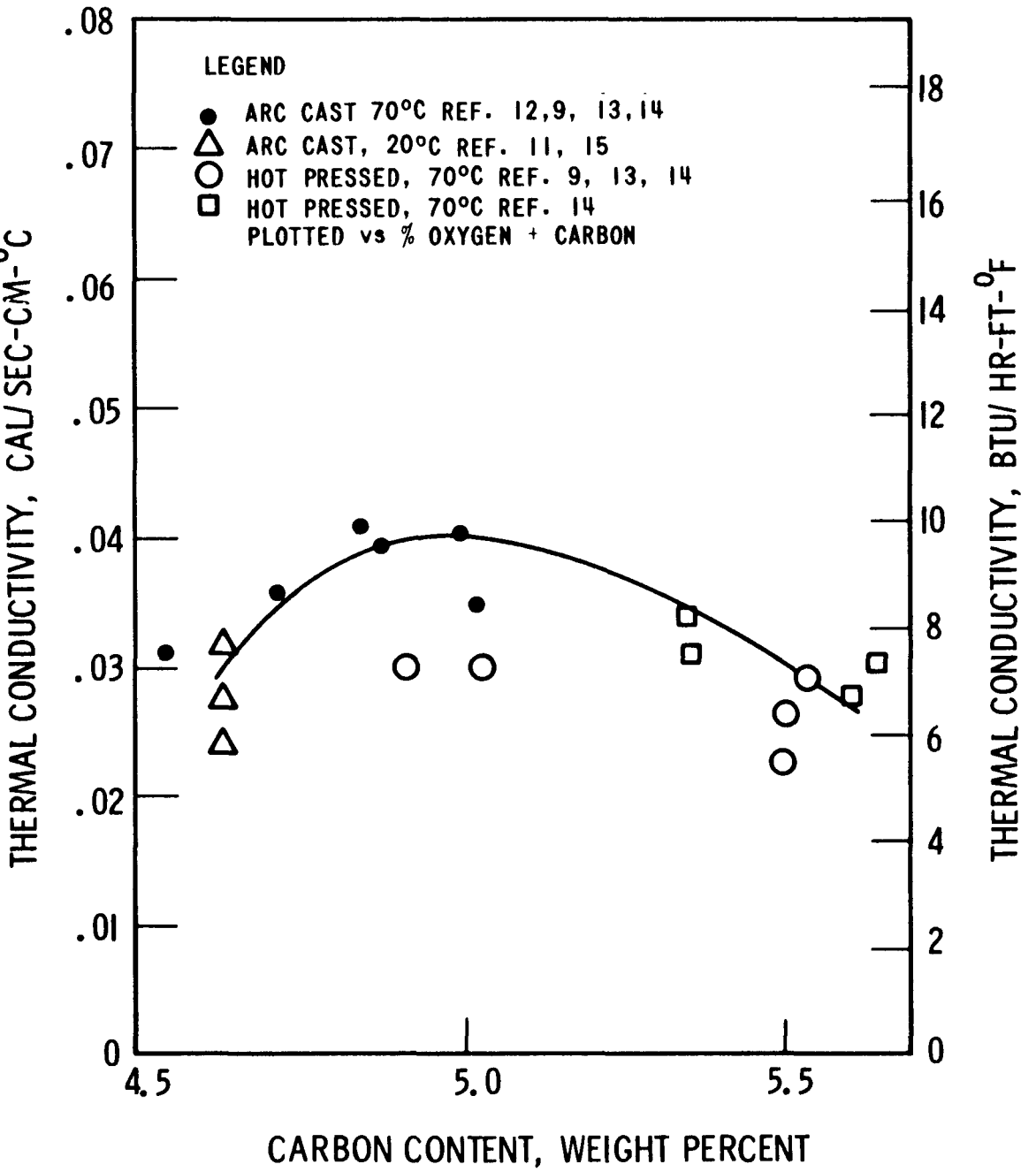

INFLUENCE OF CARBON CONTENT ON THE THERMAL CONDUCTIVITY OF $(U_{0.85}Pu_{0.15})C$

Figure III.7-9

The experimental data, shown in Figure III. 7-10, extend only to 700°K. The data of Mukaibo, et. al.,[21, 22, 23] and Boettcher and Snyder[21, 24] agree fairly well with the more recent data of Westrum[25, 22] and Martin[22] in the region around 350-400°K.

Several investigators have attempted to extrapolate these low temperature results by using various means to estimate the high temperature specific heat. Krikorian[21, 27] has estimated the elevated temperature specific heat of uranium monocarbide from an empirical expression which is a function of S°_{298}, the standard state entropy. The expression resulted in a reasonably good fit at high temperatures for carbides in general; it also fits the intermediate temperature data on uranium carbide fairly well.

A similar expression, suggested by Henney, et. al.,[21] is based on Krikorian's high temperature estimate and the data of Mukaibo. Since this expression does not fit the experimental data points as well as Krikorian's, and follows Krikorian's at higher temperatures, there appears to be little to recommend its use.

Holley[28] has made two estimates of the specific heat of uranium carbide. The first (curve 6 in Figure III. 7-10) is based on Mukaibo's value at 400°K and the work of Levinson on UC_2 at 1750°K. Holley noted that the specific heat of UC_2 can be approximated by that of UC + C, and applied this to Levinson's data. An IAEA panel[22] assessed the thermochemical data on the carbides and concluded that Levinson's data for UC_2 are questionable in view of recent determinations by Mukaibo[22] and Westrum[22]. Therefore, the Holley estimate appears tenuous, and may be seen to be very much higher than other estimates.

A second curve by Holley[28] is a rough estimate based on the "rule" that the specific heat per gram atom is approximately 7.25 cal/°K at the first transition point. In the case of uranium monocarbide,

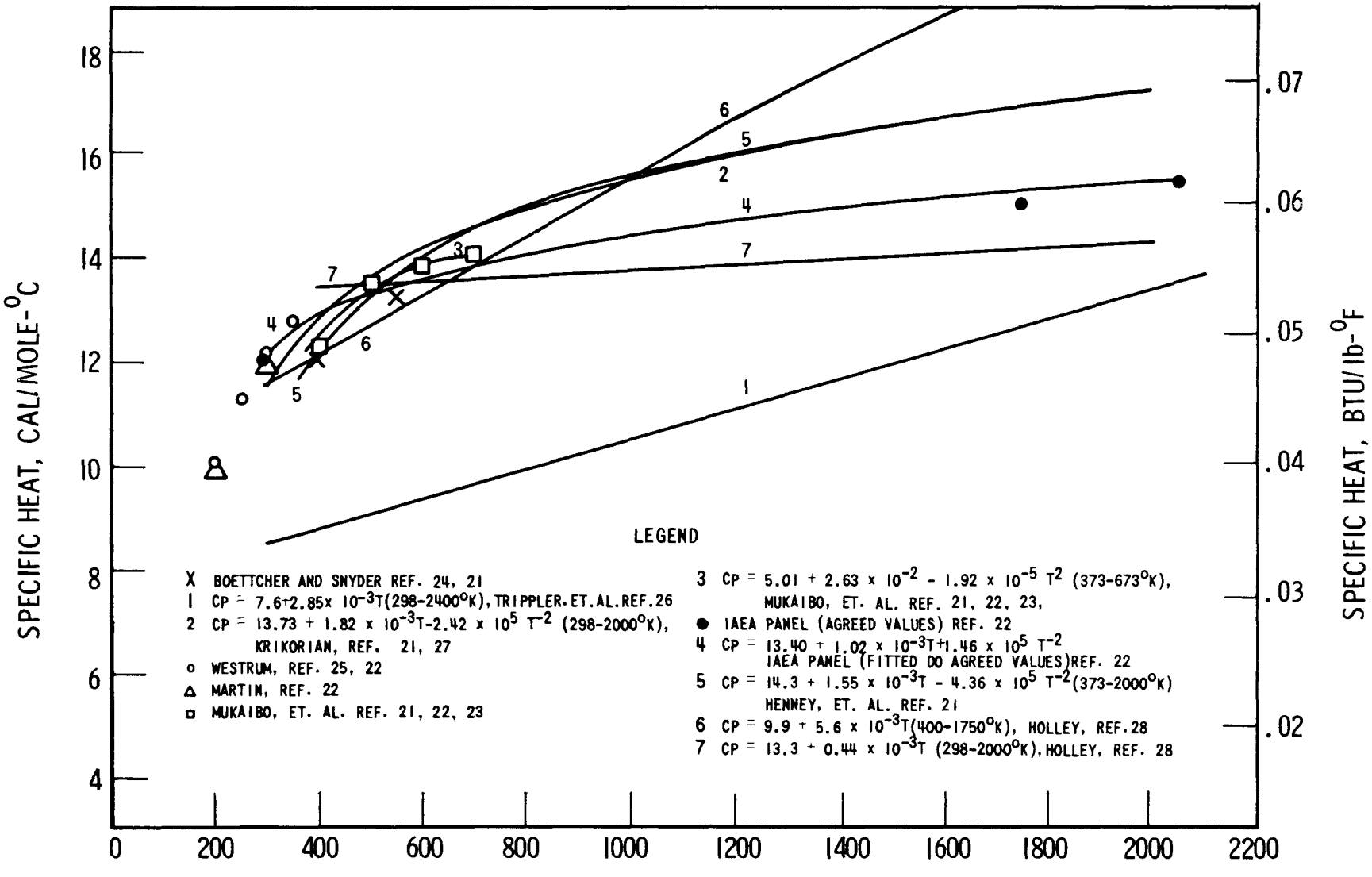

SPECIFIC HEAT OF URANIUM MONOCARBIDE

Figure III.7-10

this results in an estimated specific heat of 14.5 cal/gm-mole-°K at the melting point. This "rule" appears quite crude for many carbides, and the use of this estimate is not recommended.

The IAEA panel assessing the thermochemical data on uranium and plutonium carbides considered the available specific heat data and the need for internal consistency among other thermodynamic values.[22] The panel arrived at suggested values at several temperatures and fitted these by the curve shown in Figure III. 7-10. These values appear to have a better rationale than the estimate proposed by Krikorian, and probably represent the most reasonable estimate of the high temperature specific heat of uranium monocarbide.

Thermal Expansion

The thermal expansion data for uranium-plutonium carbide are more consistent than those for plutonium carbide, and anomalous behavior has not been noted in carbon deficient alloys. Preliminary studies reported by Stahl and Stresser[17] indicated that $(U_{0.95}Pu_{0.05})C_{0.98}$ exhibited an average thermal expansion coefficient of approximately 12.6×10^{-6}/°C from room temperature to 1000°C; this value has been superceded by their later results[18] which are in better agreement with other values reported. Only the latter data are shown in Figure III. 7-11.

The lowest values are those of Ogard, et. al.,[10, 29] for arc-cast single phase $(U_{0.87}\ Pu_{0.13})C$. These results are described by the expression:

$$\frac{\Delta L}{L_o} = 3.8 \times 10^{-4} + 8.7 \times 10^{-6}T + 3.0 \times 10^{-9}T^2$$

This expression is for a temperature range of 25 °C to 900°C. This curve, and one value determined by investigators at Harwell[12, 14], fall outside the data ranges given for uranium carbide. The remain-

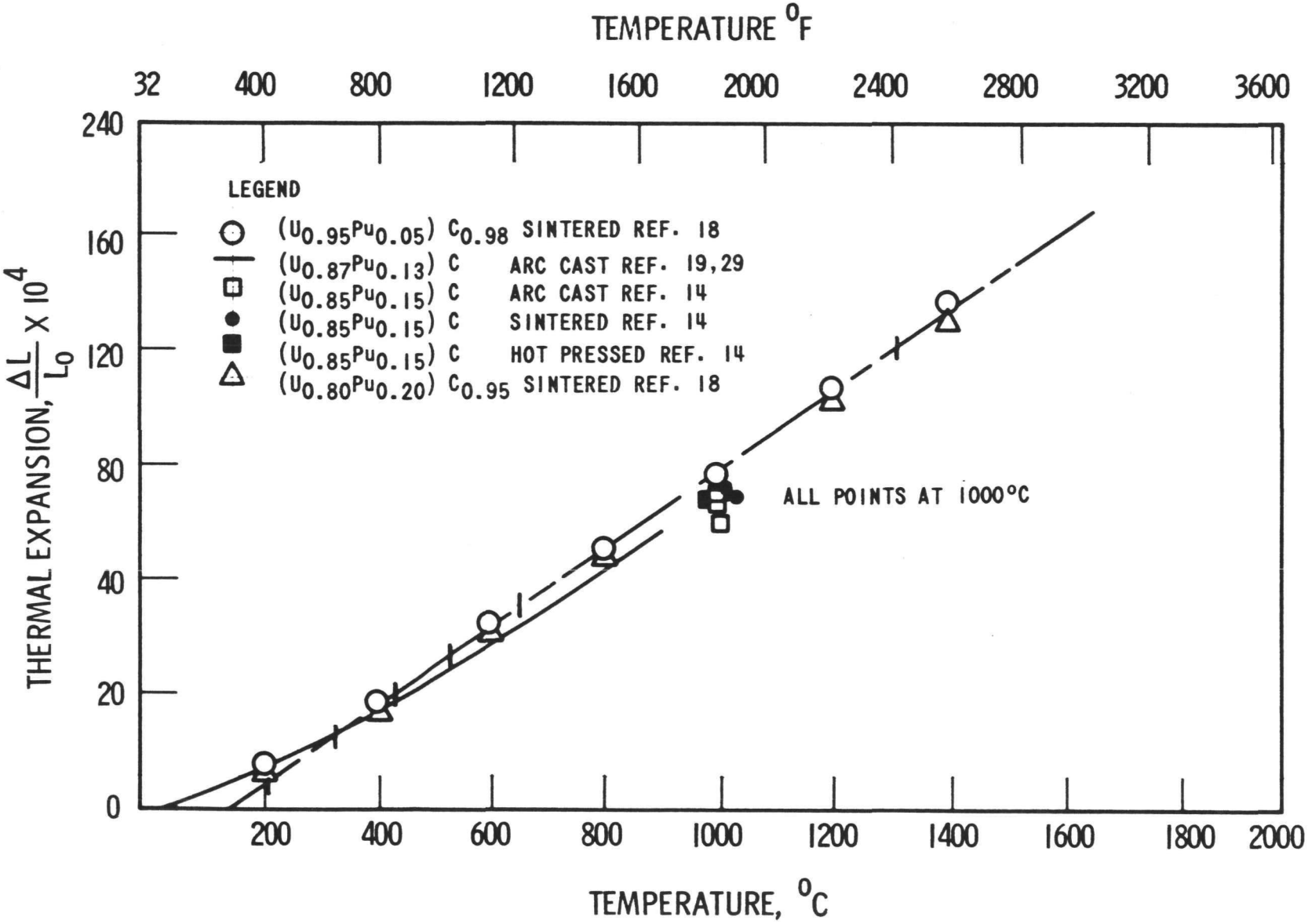

THERMAL EXPANSION OF URANIUM-PLUTONIUM CARBIDE

Figure III.7-11

der of the data[14, 18] fall within the uranium carbide data ranges, although they can best be described as on the low end of these data ranges below 1000°C, and on the high end in the temperature range 1000-1400°C. Therefore, it appears that the coefficient of thermal expansion of uranium-plutonium carbides is more temperature dependent than that of uranium carbide, and that extrapolation above 1400°C would predict greater expansion for the uranium-plutonium carbides.

The thermal expansion does not appear to be very sensitive to plutonium content in the range of 5 to 20%, and neither small carbon deficiencies nor the presence of free metal in small amounts have a marked effect.

Density

The reported density for arc-cast $(U_{0.8}Pu_{0.2})C$ varies from approximately 13.4 to 13.2 g/cc over a carbon composition range of 48 to 52.5 a/o, respectively.[9]

Melting Point

Measured values of the melting points of $(U_{.85}Pu_{.15})C$ and $(U_{.8}Pu_{.2})C$ are 234°C[12] and 2470°C[30], respectively. These results are equal to, or slightly higher than, values estimated by linear interpolation between the melting points of the uranium and plutonium carbides.

Temperature Limitations

The iron modified (U,Pu)C fuel in the region (U,Pu)C + $(U,Pu)Fe_2$ + Fe melts at 1910°F to form a small amount of liquid phase under Westinghouse Large Fast Breeder Reactor conditions.[2] Although no liquid will exist in the fuel below 1910°F, a small portion of the hottest rods will exceed this temperature (maximum fuel line temperature, 2184°F). The portion of the fuel which is at temperatures in the range of 1910 to 2184°F is expected to contain only about 3.5 w/o

of a liquid phase (based on UC-UFe_2 equilibrium data). Although this small amount of liquid should not have a significant effect on fuel performance, the presence of any liquid phase must be regarded as undesirable.

III.7.4 Effect Of Sodium Environment On 316 L Stainless Steel

III.7.4.1 Corrosion of 316 L Cladding

A quantitative expression that is commonly used for average corrosion rates of steels in sodium is given below.[31] Sodium velocity, oxygen concentration, temperature, downstream distance and time enter the expression as follows:

$$\bar{R} = v^{0.884}\, O_x^{1.156} \exp\left(12.845 - \frac{23{,}827}{T + 460} - 0.00676\,\frac{L}{D_i} + \frac{2.26}{t + 1}\right)$$

where:
- v = sodium velocity, ft/sec.
- O_x = oxygen concentration, ppm
- T = temperature, °F
- L/D_i = downstream factor = 0
- t = time, months
- $\bar{R}$ = average corrosion rate, mg/dm^2-mo.

Corrosion rates are given in Table III. 7-4 for a sodium velocity of 36.7 ft/sec. (normal channel average in zone I) for different temperatures and oxygen concentrations at zero downstream distance. Local corrosion rates may be considerably higher than those listed (by a factor of three).[32] A time, t = 4 months, is used in the empirical expression to calculate $\bar{R}$ since corrosion rates are essentially constant for t greater than 4 months.

Table III. 7-4

Coolant Oxygen Level	Average Corrosion Rates for Stainless Steel In Sodium (mils/year)				
	Temperature, °F				
	1100	1150	1200	1250	1300
10	0.3	0.5	0.7	1.1	1.6
25	0.8	1.3	2.0	3.1	4.6
50	1.8	2.9	4.5	6.8	10.1

III.7.4.2 Carburization of 318 Stainless Steel

The level to which 316 stainless steel becomes carburized depends on the amount of carbon available to the sodium. If 2-1/4 Cr is used as the intermediate heat exchanger (IHX) material, carburization to a depth of 5 mils occurs in the 316 stainless steel of the hot zone. Use of 316 stainless steel, or 5 Cr-1/2 Ti in the IHX results in insignificant carbon transfer to the hot zone.[33]

III.7.4.3 Formation of Ferritic Layer

Microprobe analysis of 316 stainless steel samples exposed to sodium shows chromium and nickel depletion and ferritic layer formation to a depth of 5 microns from the surface.[34] This effect is not expected to drastically change the properties of the clad.

III.7.4.4 Corrosion of Unclad Cermet Rod

Experimental evidence indicates that the corrosion mechanism of stainless steels in sodium is diffusion controlled and linearly dependent on the oxygen concentration. A high local oxygen concentration in sodium near the cermet surface (such as would occur with

exposed UO_2) would cause high, if not catastrophic, corrosion rates of the stainless steel matrix. It is recommended that the cermet rod be clad with 316 or 316 L stainless steel.

III.7.4.5 Clad Thickness Required

The required clad thickness depends largely on the maximum local hot spot temperature, oxygen impurity levels, and time of exposure in sodium. For an oxygen level of 10 ppm, 3-year service time, and a maximum cermet surface temperature of 1300°F, 15 mil clad would be required to prevent breakthrough corrosion. For the same oxygen and time limitations, and a maximum surface temperature of 1250°F, 10 mil clad would be adequate. The required clad thickness were calculated from the average corrosion results of Table III. 7-4 using a factor of three multiplier to take into consideration local corrosion effects. For CEX clad temperatures of around 1250°F, a 10 mil clad appears adequate.

III.7.4.6 Effect of Sodium on Mechanical Properties of Steels

Sodium has negligible effect on the mechanical properties of steels.[35] In the hot region where the CEX element would be located, corrosion is the only effect of engineering importance. Integranular attack due to oxygen penetration is apparently not a major factor, although it does occur at downstream locations in an isothermal region and at initial cold locations in a thermal gradient loop.

III.7.4.7 Self-Welding and Galling of Materials in Sodium

Stellite 6, Colmonoy 6, and nitrided steels in sodium at 1000°F give better results than stainless steel with respect to galling.[36] Gross galling occurs with stainless steel against stainless steel.

III.7.5 Calculation of Usage Factor for BCEX Elements

A maximum operating strain of $\pm$ .012% was calculated (see Section III.4) for the BCEX elements in Zone I. This corresponds to a stress amplitude of 2880 psi. From the curve of stress amplitude versus cycles to failure, Figure III.7-4, failure would occur in 10^{13} cycles. The calculated number of cycles for a BCEX element with a core lifetime of three years and subjected to a frequency of 170 cycles/sec. is 1.6×10^{10} cycles. The usage factor, $\frac{N}{Nf}$, = $\frac{1.6 \times 10^{10}}{10^{13}}$ = .0016.

III.7.6 Uranium-Plutonium Dioxide - 316 L Stainless Steel Cermet Fuel

III.7.6.1 Introduction

The Bundle Controlled Expansion fuel assembly (BCEX) consists of upper and lower half-length bundles of ceramic fuel rods which are attached to a central structure of seven full-length cermet fuel rods. During a rapid increase in core power level, the cermet rods heat up and separate the two bundles axially due to differential thermal expansion. This section reviews the feasibility of cermet fuels for BCEX concept utilization.

The reference materials for the BCEX cermet are $(U,Pu)O_2$ fuel particles in a 316 L stainless steel matrix. To design a reactor at the present time using the BCEX concept, it is highly desirable to use materials systems about which a substantial body of data has been accumulated. Further, to minimize corrosion by the sodium coolant, it is desirable to use a single alloy, insofar as possible, for all components in the system. These are some of the considerations which led to the selection of 316 L stainless steel as the cermet cladding and matrix material. For nuclear burnout compatibility of cermet and the (U,Pu)C fuel, $(U,Pu)O_2$ was selected as the cermet fuel; the oxide form was selected for matrix compatibility. Given the reference materials, the literature

was surveyed to obtain cermet design properties and characteristics. Appendix G, "Cermet Materials Literature Search", has been included to cite and categorize some of the many other references encountered during this review which have not been referenced in the following discussions.

III.7.6.2 Cermet Properties

The more easily determined properties of unirradiated uranium dioxide-stainless steel cermet fuels are reported extensively in the literature and, therefore, can be stated accurately. Many properties, such as fatigue and creep, either are not reported, or the data are so sparse as to be virtually meaningless. There are virtually no reports on the properties of irradiated cermets, except for tensile values.

Relatively large uncertainty factors have been applied to several cermet properties - even those which have been extensively reported, because of the wide variety of variables which have significant influence. A large uncertainty factor does not imply an inherent variability, but rather a lack of intensive investigation of specifically defined cermets under well controlled conditions (with the single exception of reference (44)). The development which is necessary to produce process and product specifications for cermet fuel elements to insure reliable core operation; should also insure control of properties near the nominal values.

The properties of cermet after irradiation, particularly physical properties, are much more variable. The precise combination of burnup and temperature exert principal control over the extent of matrix damage. Even for modest burnups, unless burnup and temperature can be well defined, it would be rash to ascribe to a cermet any ability to resist plastic strain.

Miscellaneous Properties

Cermet data are presented in the form of weight percent or volume percent. The conversion from one to the other is given in Figure III.3-3 for a range of enrichment values.

The absolute temperature limitation of a UO_2 - stainless steel cermet is approximately 2450°F, which is 100°F below the melting temperature of stainless steel. A more realistic temperature limitation is imposed by burnup considerations.

The latent heat of fusion of a stainless steel matrix is approximately 125 ± 10 Btu per pound.

The density of stainless steel is 8 g/cc and the theoretical density of UO_2 is approximately 11 g/cc at 68°F. Densities at higher temperature are a function of thermal expansion.

Thermal cycling tests were performed for 1000 cycles on 40 v/o and 50 v/o UO_2 + SS cermets, from 122°F to 1472°F at 90°F/sec, and from 122°F to 1472°F at 392°F/sec. No metallurgical effects were noted in the fuel, matrix or cermet-to-clad bond[45].

The specific heat of a cermet is equal to the weighted average of the specific heats of its constituents. Accepted values of specific heat of stainless steel and UO_2 are shown in Figure III.7-12 with calculated values for various ceramic contents. The only effect of irradiation would be from the exchange of uranium and plutonium for fission products, and from transmutations, both of which are considered negligible. It is not expected that actual values would vary by more than ± 5 percent from the values shown in Figure III.7-12.

Thermal Expansion

The thermal expansion of cermets is controlled by the matrix[44] and is almost independent of ceramic content (at least up to 50 volume percent)*. This observation is reasonable because a hole in a plate

* Up to 65 volume percent UO_2 in stainless steel[46], the alpha correction for ceramic content = $-0.0016 \alpha V$, where α = the coefficient of thermal expansion of stainless steel, and V = the volume percent UO_2.

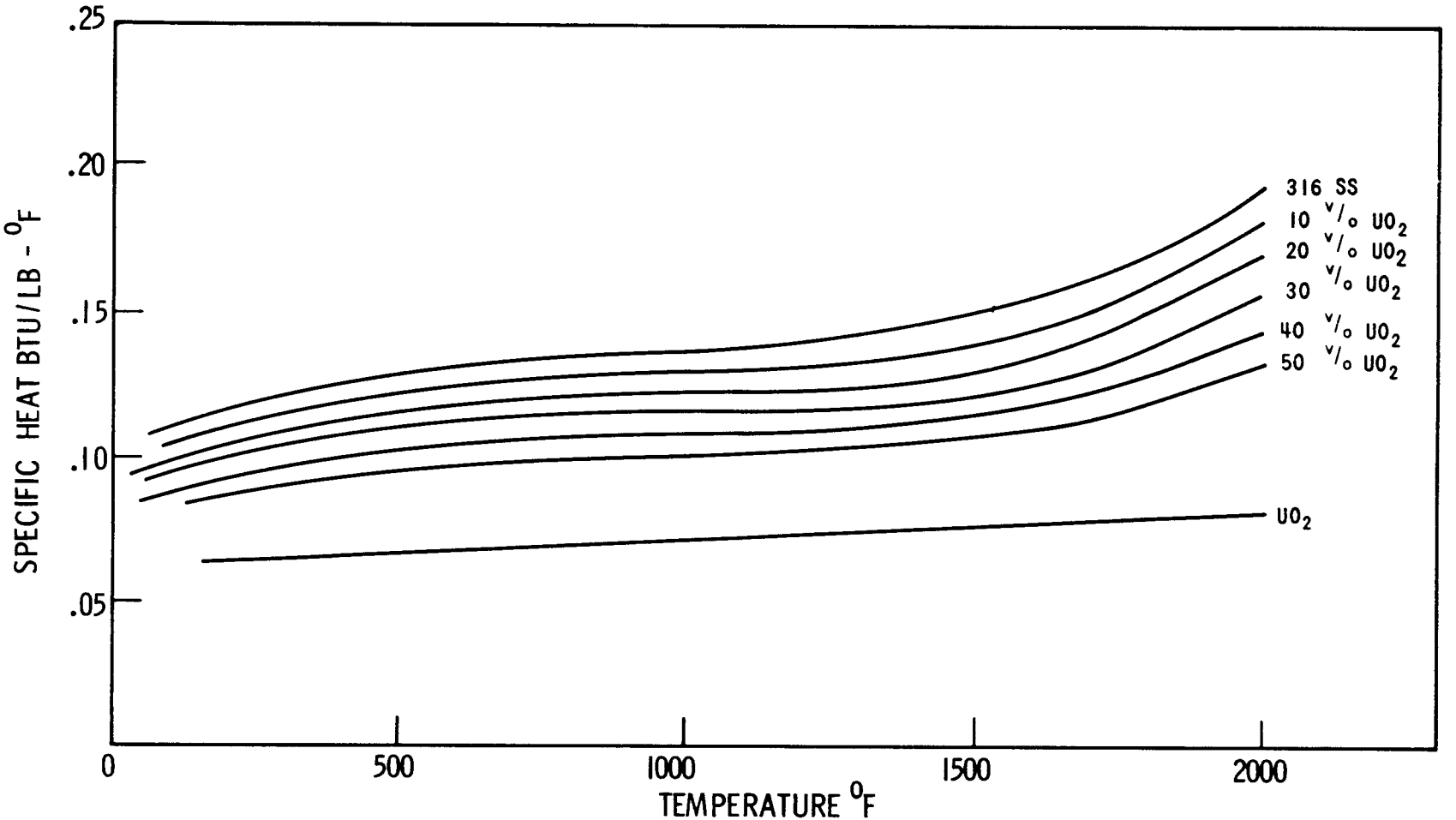

SPECIFIC HEAT ON UO_2 - SS CERMETS AS A FUNCTION OF TEMPERATURE

Figure III.7-12

expands at the same rate as the plate. Also, the expansion of the ceramic particle is less than the expansion of the matrix. One implication is that there is a slightly larger void volume in the fuel particle at elevated temperatures than at lower temperatures.

The effect of irradiation on thermal expansion of stainless steel is reported to be negligible[47]. Thermal cycling is also reported to have negligible effect. Specific data reported[46] are shown in Figure III.7-13. Considering the discrepancy between the reported data as a function of ceramic content, the following design values for the mean coefficient of linear thermal expansion above 68°F are recommended:

Maximum	Per °F	=	$[10.45 + (0.000325 \times °F)] \times 10^{-6}$
Nominal	Per °F	=	$[8.9 + (0.0009 \times °F)] \times 10^{-6}$
Minimum	Per °F	=	$[8.2 + (0.00083 \times °F)] \times 10^{-6}$

It is expected that these values will account for all of the following variables:

Ceramic content from 0 to 50 v/o
Irradiation
Thermal cycling
Normal material variations
Temperature range from 300°F to 2000°F

Thermal Conductivity

The thermal conductivity of cermets is strongly influenced not only by the ceramic content but also by the nature of the matrix, primarily as influenced by the fabrication process. Thermal conductivity is essentially a linear function of ceramic content up to 50 volume percent, especially at higher temperatures.

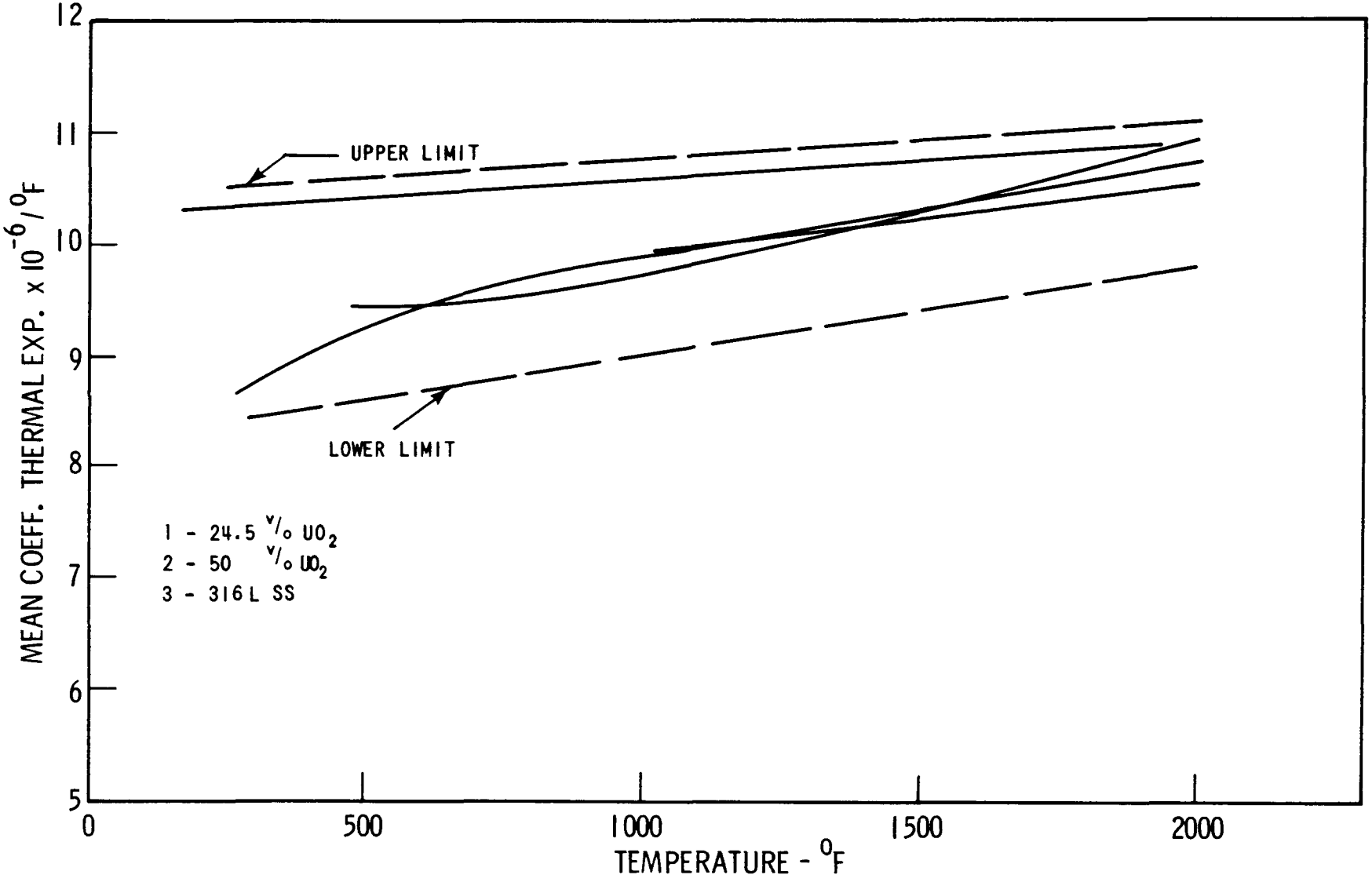

COEFFICIENT OF THERMAL EXPANSION OF UO_2 - 316L - SS AS A FUNCTION OF TEMPERATURE

Figure III.7-13

Data from three independent sources[46,48,49] have been smoothed and plotted as a function of temperature in Figure III.7-14, and as a function of ceramic content in Figure III.7-15. The raw data show consistent trends, and are sufficiently compatible to indicate a representative range of experimental variation.

The influence of irradiation on thermal conductivity of stainless steels, especially at operating temperatures, has been reported[47] to be significant. However, it is known that the recoil zone around fuel particles will become severely damaged with low burnup, and that microcracks and porosity will eventually form in this zone. Assuming a nominal particle size of 300 μ and a recoil zone of 10 μ, the combined volume of the recoil zone and the particle will be 17 percent greater than the volume of the particle alone. If it is assumed that random cracks or pores in the damaged zone reduce the conductivity of the damaged zone by a factor of approximately 2, the remaining conductivity can be approximated as being 3 times that of UO_2. These values permit the effect of irradiation to be estimated as being equal to a 6 percent relative increase in volume percent ceramic*.

The effect of particle size (50-100 μ versus 100-150 μ) was investigated at 54.5 volume percent. A consistent difference of approximately 7 percent conductivity was measured (the smaller particles had the higher conductivity). This effect is considered negligible when compared to observed random variations in the mass of data.

Values shown in Figures III.7-14 and III.7-15 are nominal. The tolerances listed below are expected limits based on observed variations and apply to all ceramic contents:

---

* For example, the conductivity of an irradiated 20 volume percent ceramic cermet would be the same as a 21.2 volume percent ceramic cermet which is unirradiated (20 v/o + 6% of 20 v/o = 21.2 v/o).

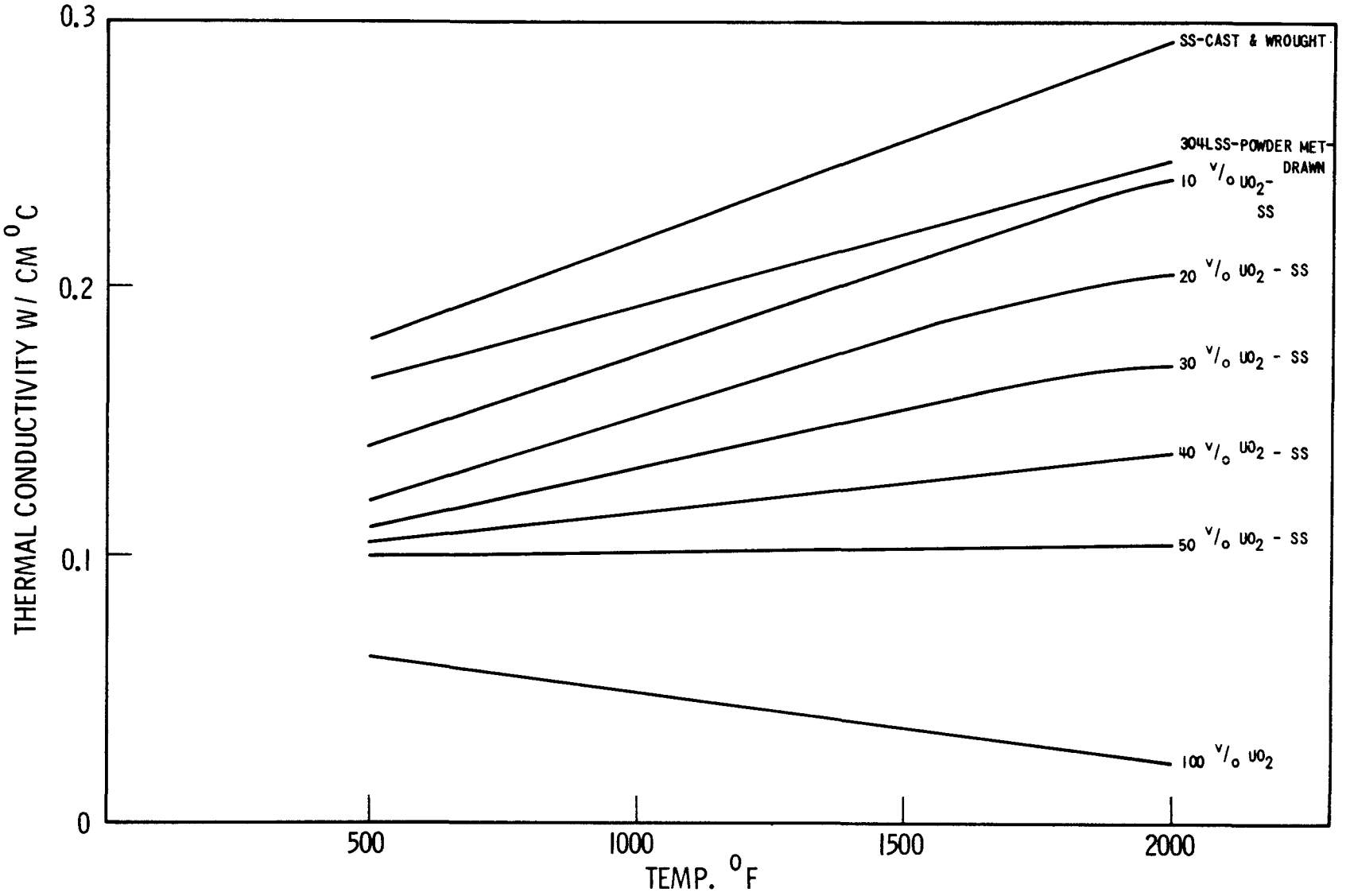

THERMAL CONDUCTIVITY OF UO_2 - SS AS A FUNCTION OF TEMPERATURE

Figure III.7-14

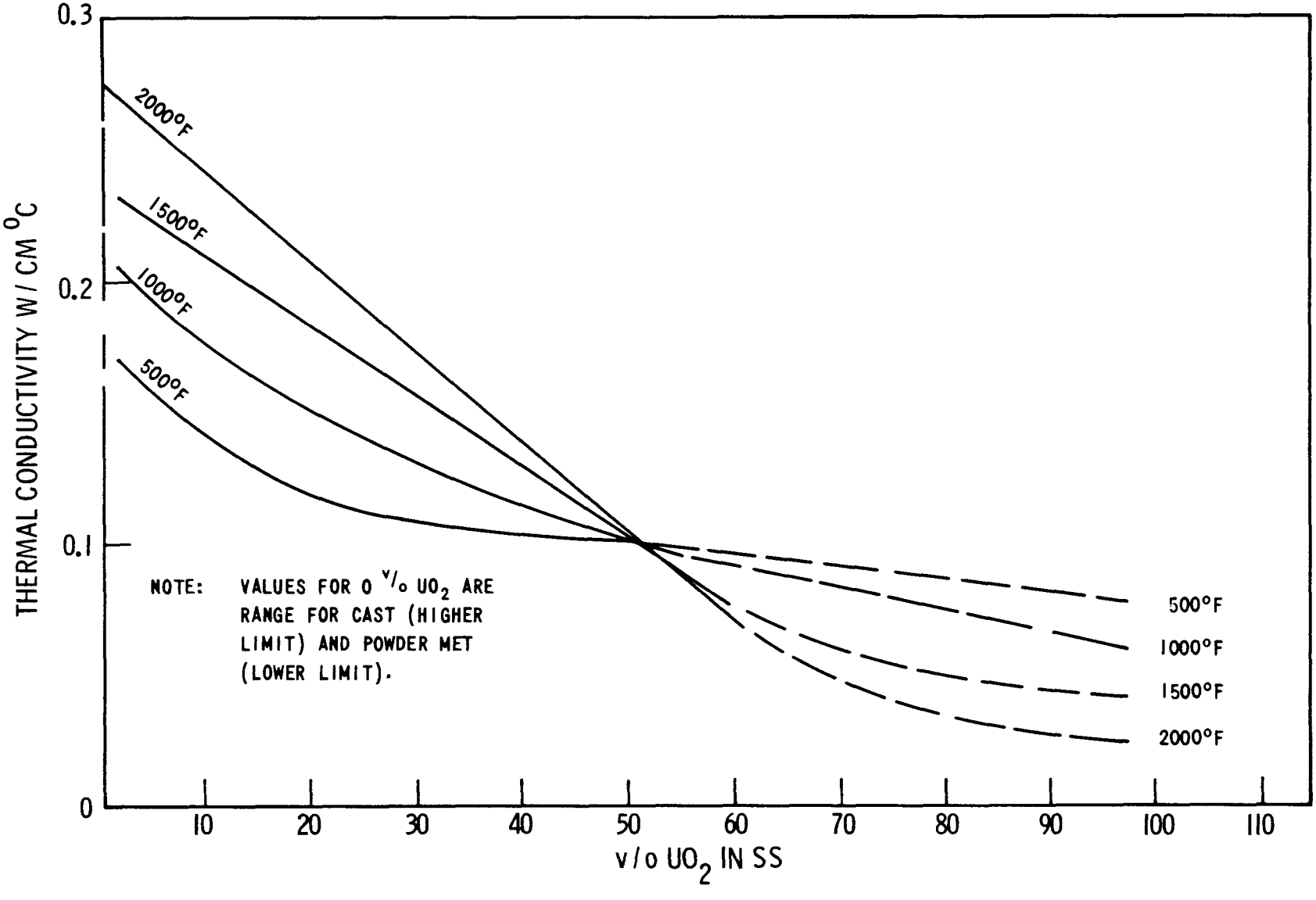

THERMAL CONDUCTIVITY OF UO_2 - SS AS A FUNCTION OF CERAMIC CONTENT

Figure III.7-15

Temperature (°F)	Lower Limit of Conductivity (W/Cm °C)	Upper Limit of Conductivity (W/CM °C)
500	nominal -0.020	nominal +0.020
1000	nominal -0.015	nominal +0.015
1500	nominal -0.015	nominal +0.015
2000	nominal -0.015	nominal +0.015

Ultimate Tensile

The ultimate tensile strength of a cermet of a given composition is far more variable than for a metal, because of the effects of fabrication processes, particle size, particle shape, and burnup.

In addition, irradiation will cause an increase in strength (as predicted for the matrix material) only up to a point. Beyond this point, which should normally occur at low burnup, progressive deterioration takes place until failure occurs due to fuel swelling and fission gas pressure. Therefore, for any reasonable burnup, a cermet will not have a significant, useful, tensile strength. The only post-irradiation tensile tests reported[5] show an increase in tensile strength up to 5 percent burnup of the uranium atoms (25 weight percent UO_2 in 347 SS), and a loss in strength after 10-15 percent burnup. The irradiation temperature, which has an extremely strong effect, was not reported. It is significant that the effect is most pronounced at lower testing temperatures. The results of tensile tests at 10 percent burnup and 1400°F were so variable as to prevent positive conclusions. The most appropriate conclusion may be that under these conditions tensile properties are unreliable.

Particle size effects are not pronounced over a small range. The effect on tensile strength of 50-100 μ versus 100-150 μ particles (50 weight percent in 18-8 SS) averaged 500 psi (2 percent) between 70 and 1300°F[49]; this is far less than the experimental error. A larger effect was noted

when comparing -325 mesh to -65 + 150 mesh (less than 44 μ versus 100-230 μ) particles in a controlled experiment[50]. Tensile strength increased (with finer particles) from 58,000 psi to 66,000 psi.

Reduction from 100% theoretical density has been reported to cause a linear decrease in tensile strength[46] to a value to 50% of the tensile strength at 90% of achievable density.

The ultimate tensile strength of unirradiated UO_2 - SS cermets reported by a number of investigators[44,45,46,49,50,51] has been averaged and smoothed and is shown in Figure III.7-16 as a function of temperature and in Figure III.7-17 as a function of ceramic content as discussed above. Reported variations of data in both controlled and uncontrolled experiments, strongly indicate that a tolerance zone of $\pm$ 50% should be applied to the nominal tensile strengths. It must be repeated that these values apply to unirradiated material. Improvement in tensile strength due to irradiation is quickly lost by subsequent irradiation, especially at elevated temperatures.

Yield Strength

Yield strength, while closely paralleling the characteristics of tensile strength, is a far more interesting property. The yield strength of stainless steel is commonly defined by the 0.2 percent offset method, which is the stress at which 0.2 percent permanent strain is observed. Recent work at WAPD has shown that stainless steel in thermal reactors exposed to a neutron flux approaching 10^{22} nvt cannot sustain 0.2 percent plastic strain. The flux conditions should be even more severe in a fast reactor. Cermets display essentially no uniform elongation as shown by the typical tensile curve[51] in Figure III.7-18. When there is no uniform elongation, the yield strength is commonly reported as the stress at which the strain deviates by 0.2 percent from a line tangent to the stress-strain curve at zero stress. Thus, yield strength of cermets, as reported in the literature, is probably not a valid design

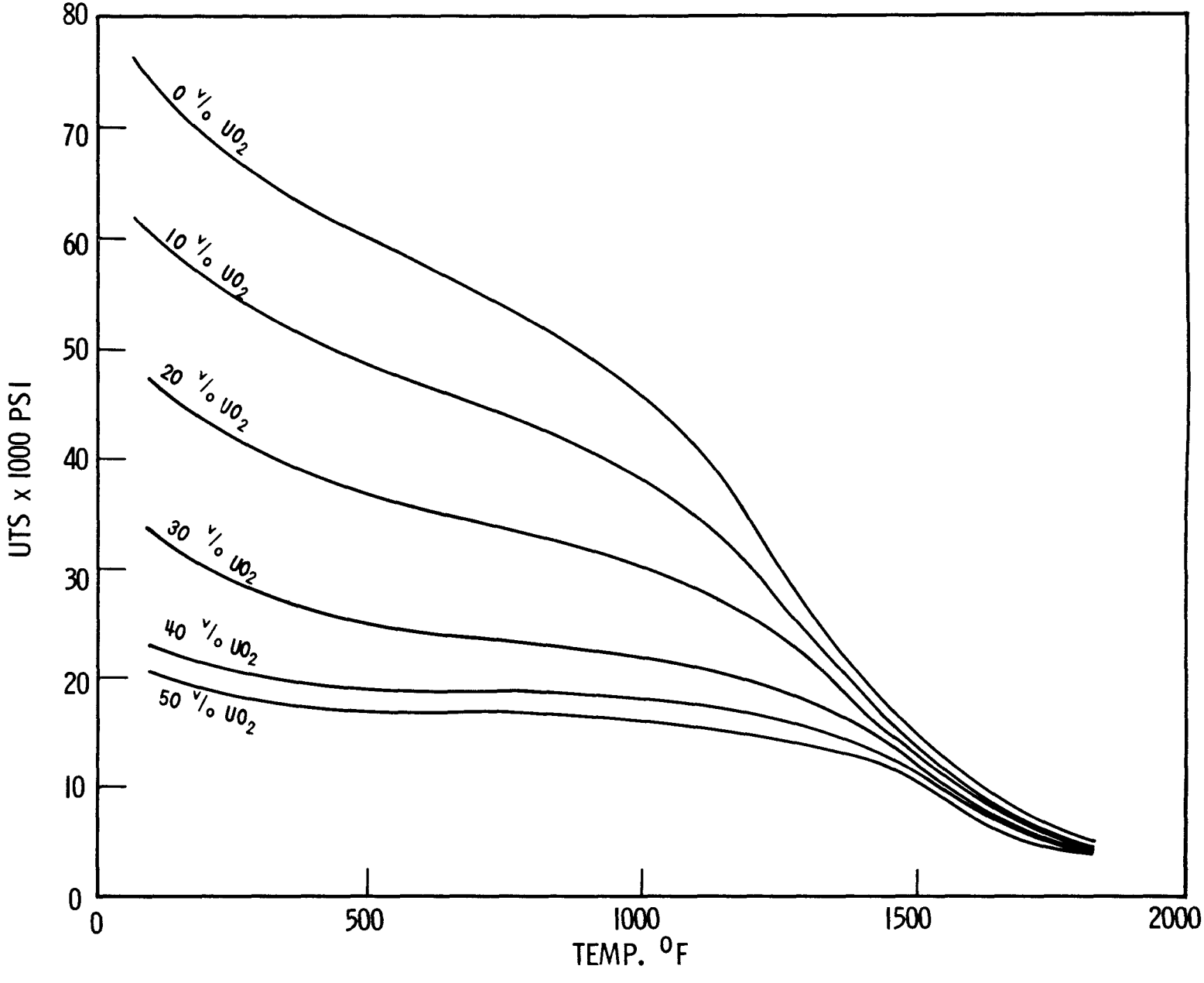

Figure III.7-16 - ULTIMATE TENSILE STRENGTH OF UO_2 - SS CERMETS AS A FUNCTION OF TEMPERATURE

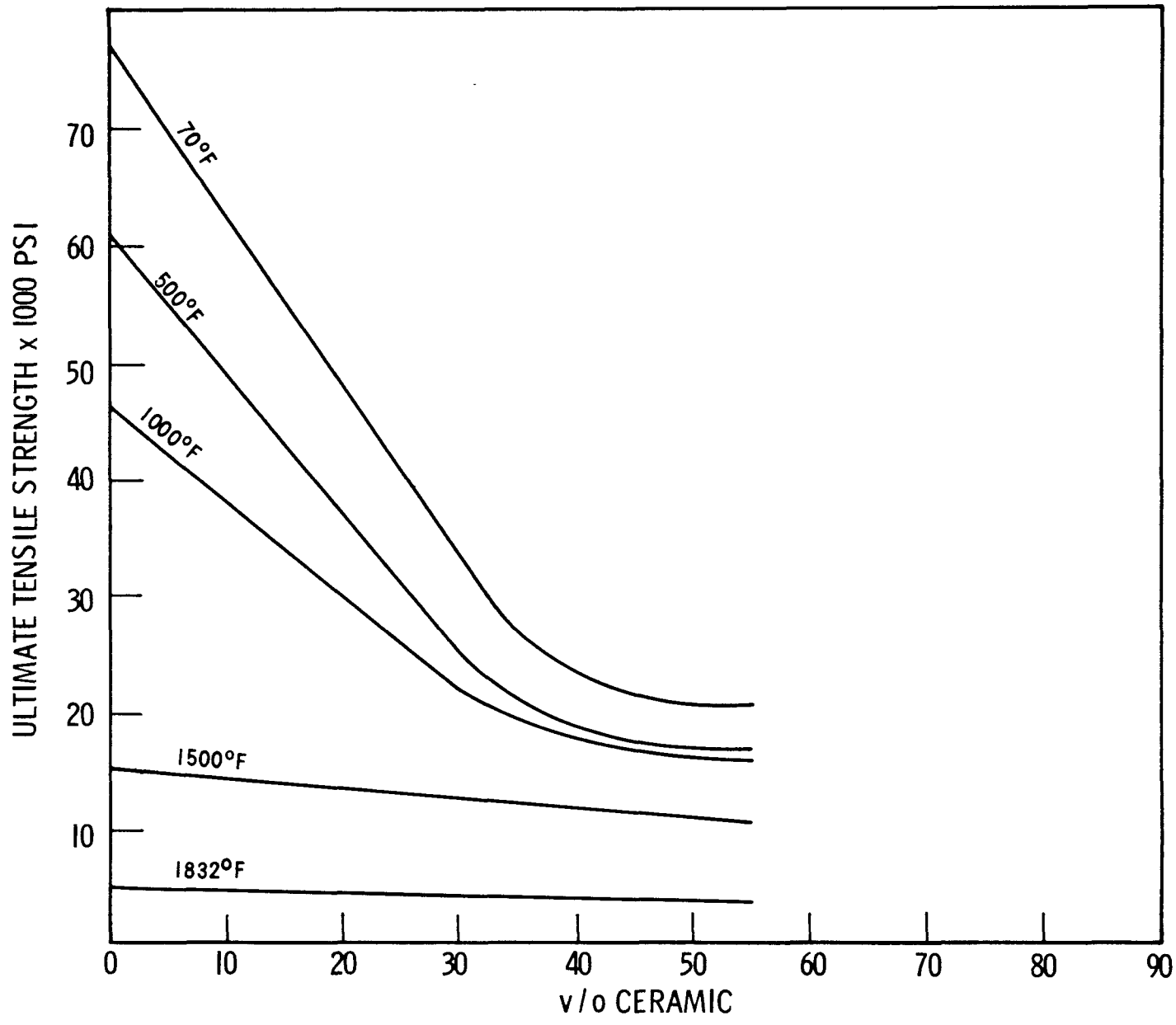

ULTIMATE TENSILE STRENGTH OF UO_2 - SS CERMETS AS A FUNCTION OF CERMET CONTENT

Figure III.7-17

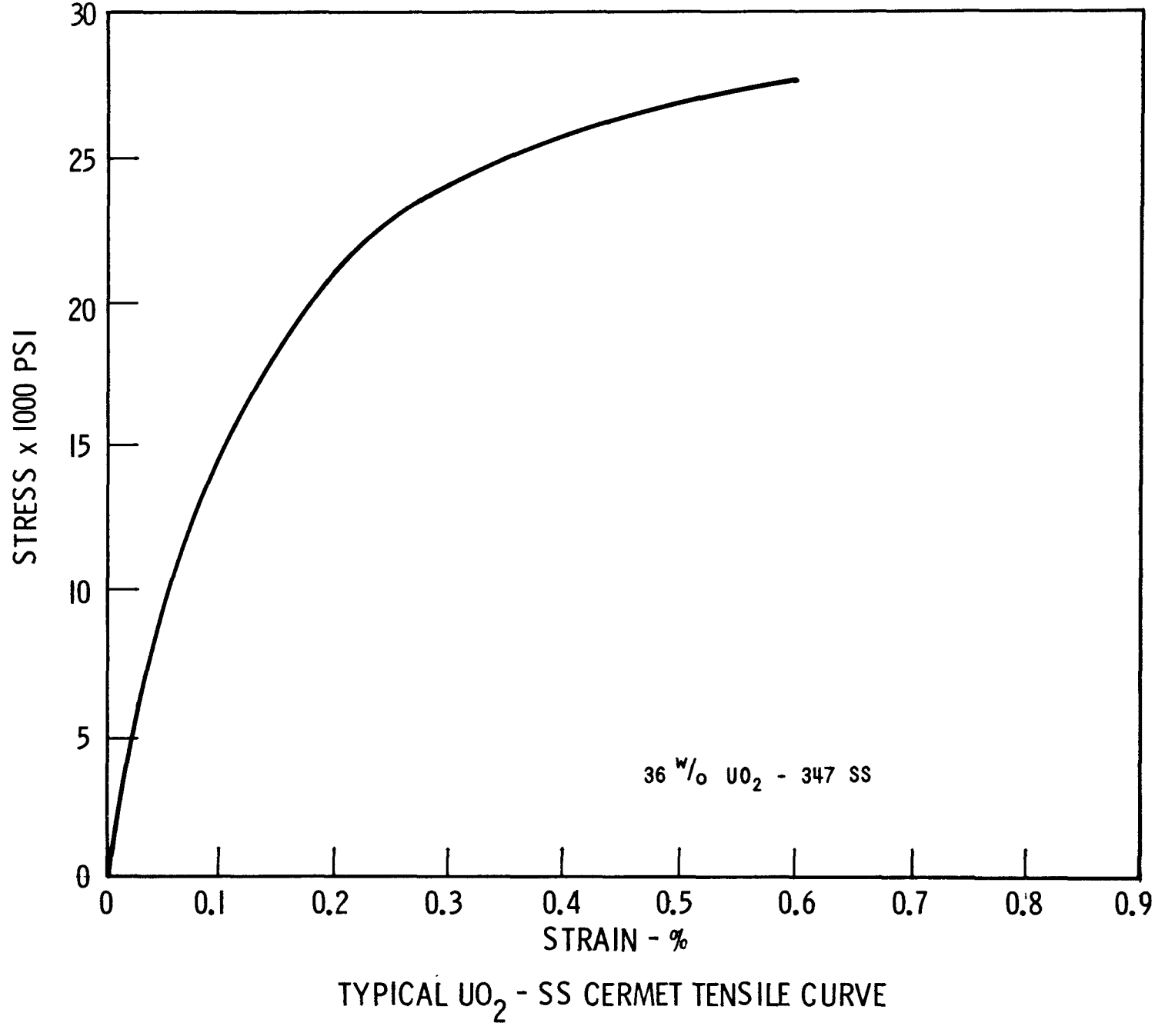

TYPICAL UO_2 - SS CERMET TENSILE CURVE

Figure III.7-18

parameter. There is, however, no recourse if existing data are to be used. However, conclusions from this data must be applied with extreme care.

For the following reasons, yield strength data are evaluated as the ratio $\frac{\text{yield strength}}{\text{tensile strength}}$: (1) the reasons stated above, (2) yield strength data in the literature is more sparse than for tensile strength, and (3) the ratio is more consistent than the absolute values reported. This ratio as a function of temperature and ceramic content is shown in Figure III.7-19.

The discussion of the variables associated with the ultimate strength applies also to yield strength, except that the effect of each variable on yield strength is more pronounced.

It is interesting to note that tests made with clad tubular elements[49] showed that the cladding completely obscured the effect on yield strength of up to 40 weight percent UO_2 additions to the stainless matrix.

Elongation

The elongation of a cermet at failure is considered to be of minor significance, especially as no significant elongation can be expected after irradiation. A 10 volume percent UO_2 addition to stainless steel causes a reduction of elongation of 50 percent (from 50 percent to 25 percent elongation); at 20 volume percent UO_2, elongation is approximately 12 percent with little dependence on temperature. At 50 volume percent UO_2, elongation is approximately 7-8 percent between 158°F and 1292°F[44,45,46].

Modulus of Elasticity

The modulus of elasticity for 347 stainless steel is reported[51] as $[29 - (0.0065 \times °F)] \times 10^6$ psi. The slope is linear to 1000°F, and there is no reason to expect deviation at higher temperatures. The modulus for

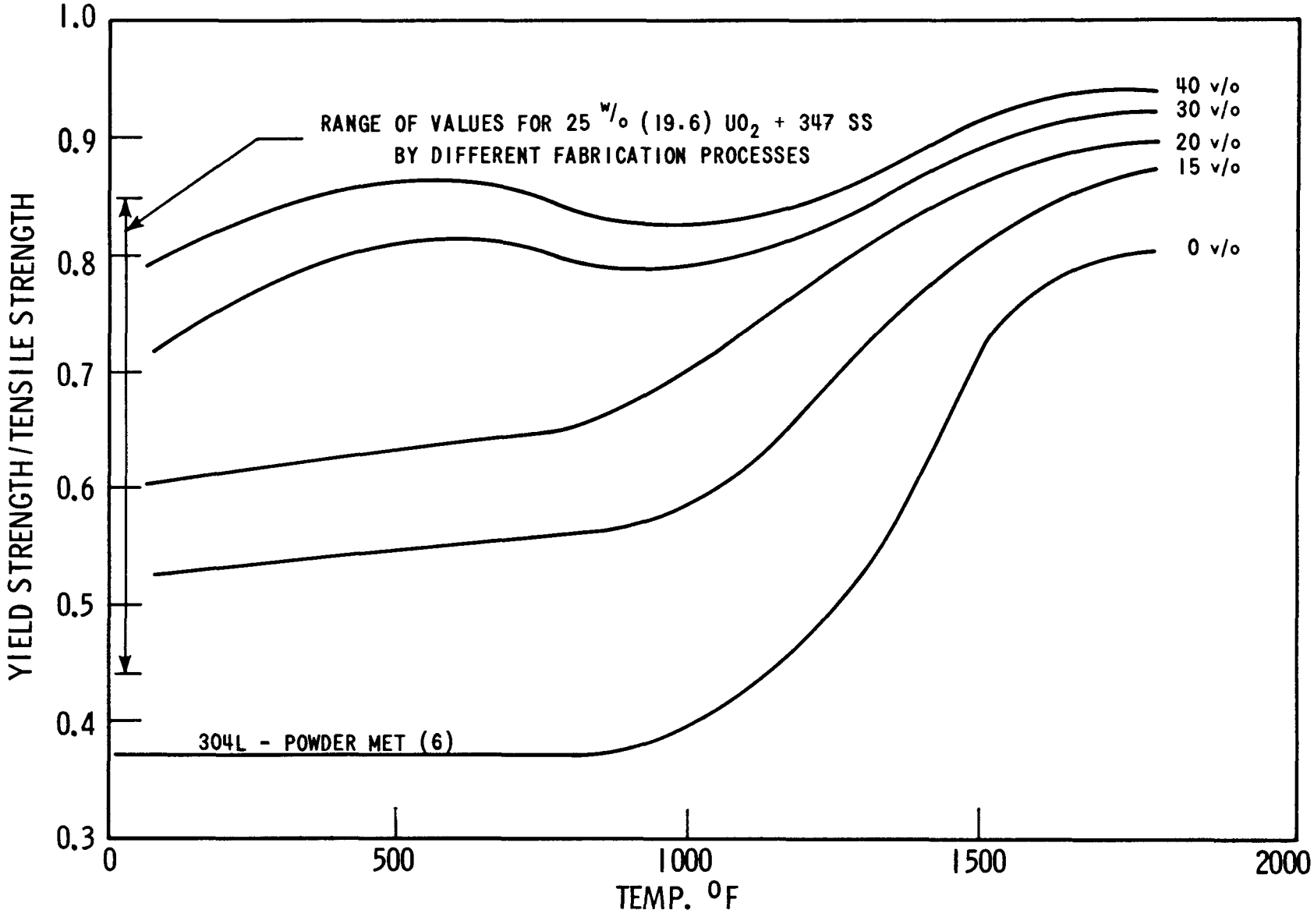

RATIO OF YIELD TO TENSILE STRENGTH FOR UO_2 - SS CERMETS

Figure III.7-19

31 volume percent UO_2 + 374 SS is 80 percent of the modulus for stainless steel. A linear effect of ceramic is probably accurate within ± 5 percent to 50 volume percent UO_2, which provides the following estimated nominal value of Modulus of Elasticity; E:

$$E = [29 - (0.0065 \times {}^{\circ}F)] [1-0.025 \times v/o\ UO_2] \times 10^6 \text{ psi}$$

The dynamic modulus is taken as 20 percent of the static modulus[51]. The effect of irradiation is reported to be small[47].

Fatigue

Fatigue results were reported by only two investigators[50,51], and are presented in Figure III.7-20. It is estimated that a reasonably safe value for stress (or strain) at any number of cycles is 25 percent of the accepted room temperature value for the matrix material.

Bend Test

The only recorded bend testing of stainless steel cermets (25 weight percent ceramic) was performed before and after irradiation on 0.160 inch diameter simple beam specimens centrally located on a 3 inch support span with the results[50] shown in Figure III.7-21.

III.7.6.3 Design and Specification Criteria

The cermet characteristic selection factors which will be discussed and calculated are based upon completely uniform particle distribution and perfectly spherical particles, i.e., a perfect model which obviously can never be a reality. Particle distribution and spheroidicity are statistically distributed, but can be reasonably controlled. In the absence of extensive statistical data and rigorous calculations, the obvious recourse is to apply empirical burnup limit information. This too has limitations, especially in applications of greater than 30 volume percent ceramic. However, application of empirical limits up to 50 volume percent ceramic content may be reasonable if various conservative factors are introduced.

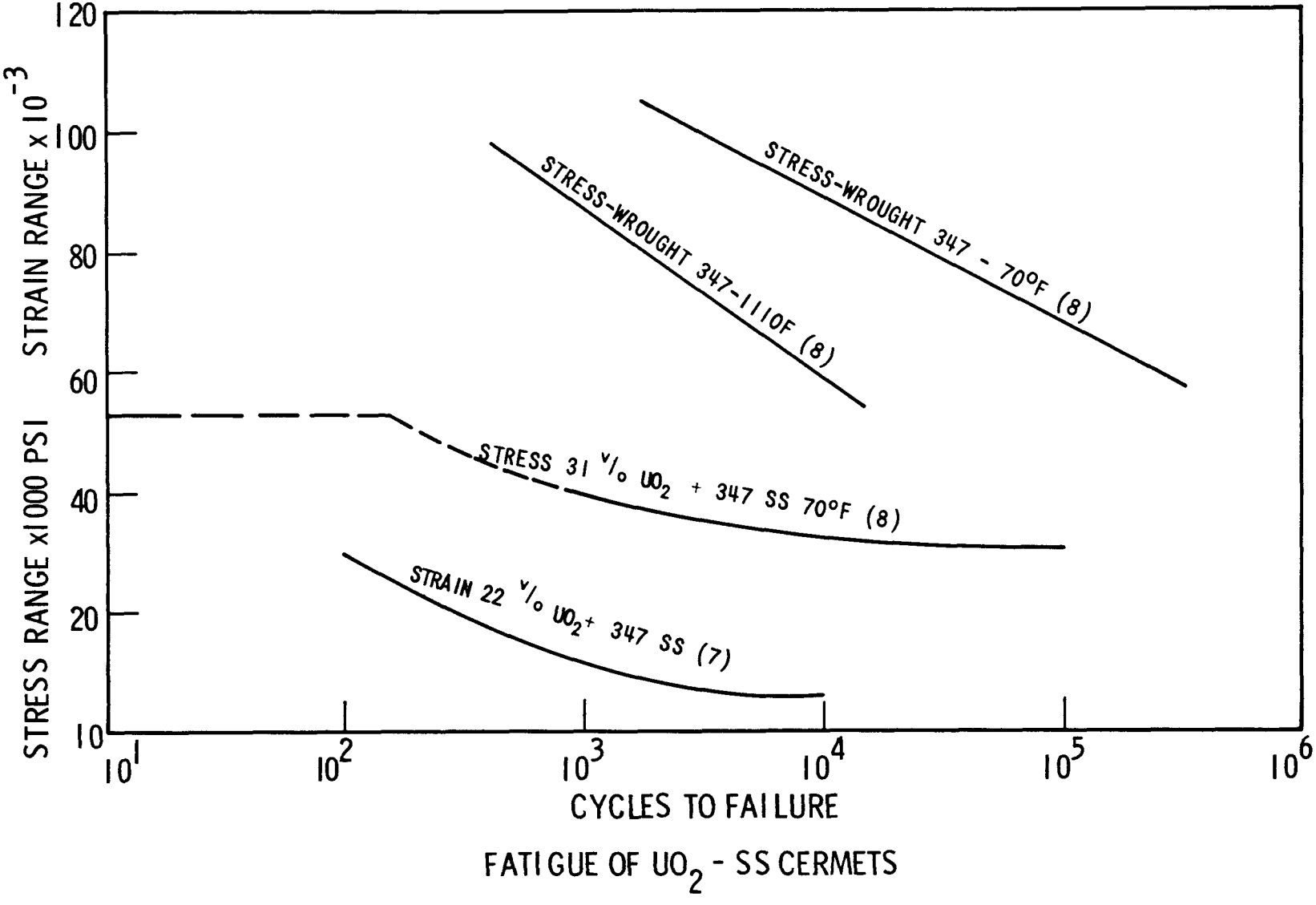

FATIGUE OF UO_2 - SS CERMETS

Figure III.7-20

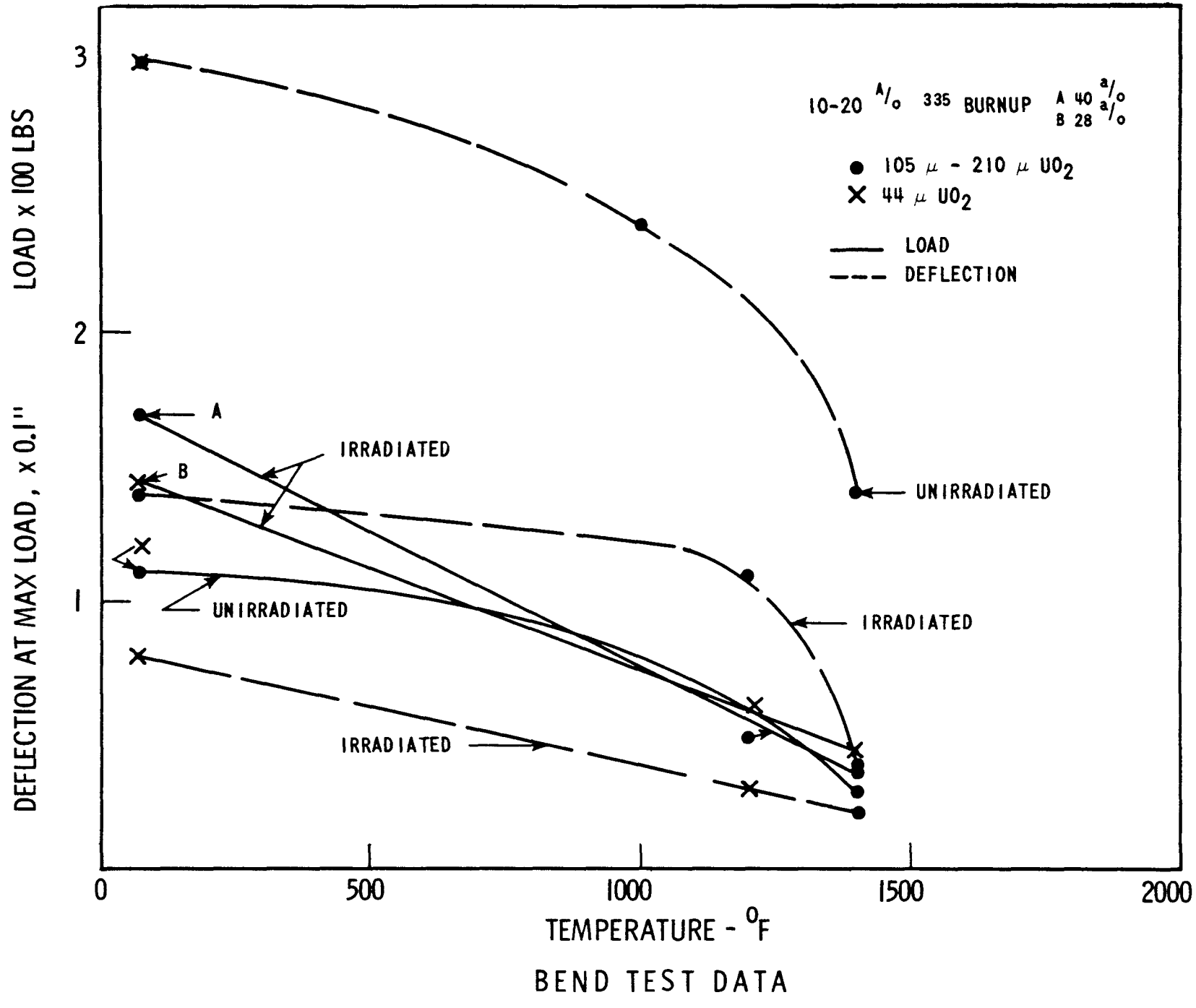

BEND TEST DATA

Figure III.7-21

A better appreciation of the applicability of cermet characteristics and empirical data can be obtained from a knowledge of the design considerations influencing the forces exerted by the fuel particles. A discussion of some of the design considerations for stainless steel cermets is included in this section.

III.7.6.3.1 Cermet Characteristic Selection

The generally accepted operating history and failure mode of a cermet fuel element is as follows:

1. Early in life
   a) The released fission gases fill void spaces in each fuel particle; the other fission products cause slight swelling of the fuel.
   b) Recoil atoms cause severe damage and slight swelling in a 10 μ (maximum) thick matrix shell surrounding each fuel particle (recoil zone).
   c) The rest of the matrix and clad suffer mild irradiation damage.
2. Mid-life
   a) The void volume decreases due to fuel swelling, and the fission gas pressure increases in each fuel particle, causing slight stressing of the surrounding matrix.
   b) The recoil zone material loses all, or nearly all, ductility; it is extensively damaged and swells due to the presence of recoil atoms.
   c) The rest of the matrix and clad suffer progressively greater irradiation damage.
3. End of life
   a) Fission gas pressure (augmented by loss in volume due to fuel swelling) and/or fuel swelling are increased

beyond the limit of restraint by the recoil zone, but are restrained by the surrounding matrix.

b) Fracture occurs, and fission gas pores appear in the recoil zone so that the radius of the shell, which contains the pressure, is effectively increased by 10 μ without a corresponding volume increase.

c) The rest of the matrix and cladding continue to suffer irradiation damage, and effectively loses all room temperature plasticity. The matrix is more highly stressed due to mechanical failure of the recoil zone.

4. Failure

A plate-type fuel element will fail by swelling. Increased fission gas pressure and fuel swelling will rupture the matrix ligaments between the particles; this will cause the plate to swell, with a simultaneous increase in the volume available for gas containment. Consequently, plate elements fail when the swelling rate increases sharply. In rod-type elements, the embrittled cladding has little or no ability to expand without rupturing. Therefore, it can be assumed that complete failure will occur when cracks in the matrix, which are induced by fission gas pressure and swelling, propagate through the clad. Cracks in the matrix are not accompanied by corresponding volume increases; instead, they increase the area over which fission gas pressure is applied. Therefore, it can be assumed that a rod-type cermet fuel element will fail, by rupture of the core and clad, soon after the matrix adjacent to the recoil zone cracks.

It has been shown in practice, that for given materials and operating conditions, the life of a cermet element depends primarily on particle density, particle size, and ceramic content. With given materials and flux conditions, the controlling factors are: 1) the resistance of the

matrix and cladding to stressing at operating conditions (stress rupture, creep), and 2) temperature.

The simplest method of reducing gas pressure is by increasing the void volume available to the gas; this can be accomplished by reducing the density of the fuel particle. Disadvantages associated with low density particles are generally confined to fabricability. The particle density strongly influences particle strength (resistance to fracture and resistance to deformation during fabrication). However, particle density probably does not have a major effect on the overall cermet fuel strength, as the matrix strength is proportional to matrix density, not to particle density. Fabrication processes are designed to achieve 100 percent matrix density and clad-matrix bonding without excessive damage to the fuel particles. Fabrication experience has shown that 100% matrix density can be achieved with conventional 90-95 percent dense fuel particles. The feasibility of fabricating cermets using hollow fuel spheres has been demonstrated but not exploited. Hollow sphere cermets probably can be fabricated (with 100 percent matrix density) at 80 percent, or possibly less than 80 percent, ceramic density. In the absence of more extensive efforts to use hollow spheres, 85 percent as the maximum ceramic density for the cermet fuel can be used as a safe estimate.

For a given ceramic content, as the particle size is increased, the spacing between particles (matrix ligament thickness) increases, and the recoil zone volume becomes a smaller fraction of total matrix volume. The disadvantages of large particle sizes are:

1) The fission gas pressure acts on a larger diameter, and
2) The particles have less resistance to fracture and deformation during fabrication.

Successful fabrication has been reported for particle sizes between 44 μ at 25 volume percent[50] ceramic and 250-350 μ at 50 volume percent ceramic[45]. Therefore, the reference diameter is selected as 250-350 μ. The effect of particle size on fission gas and fuel swelling containment

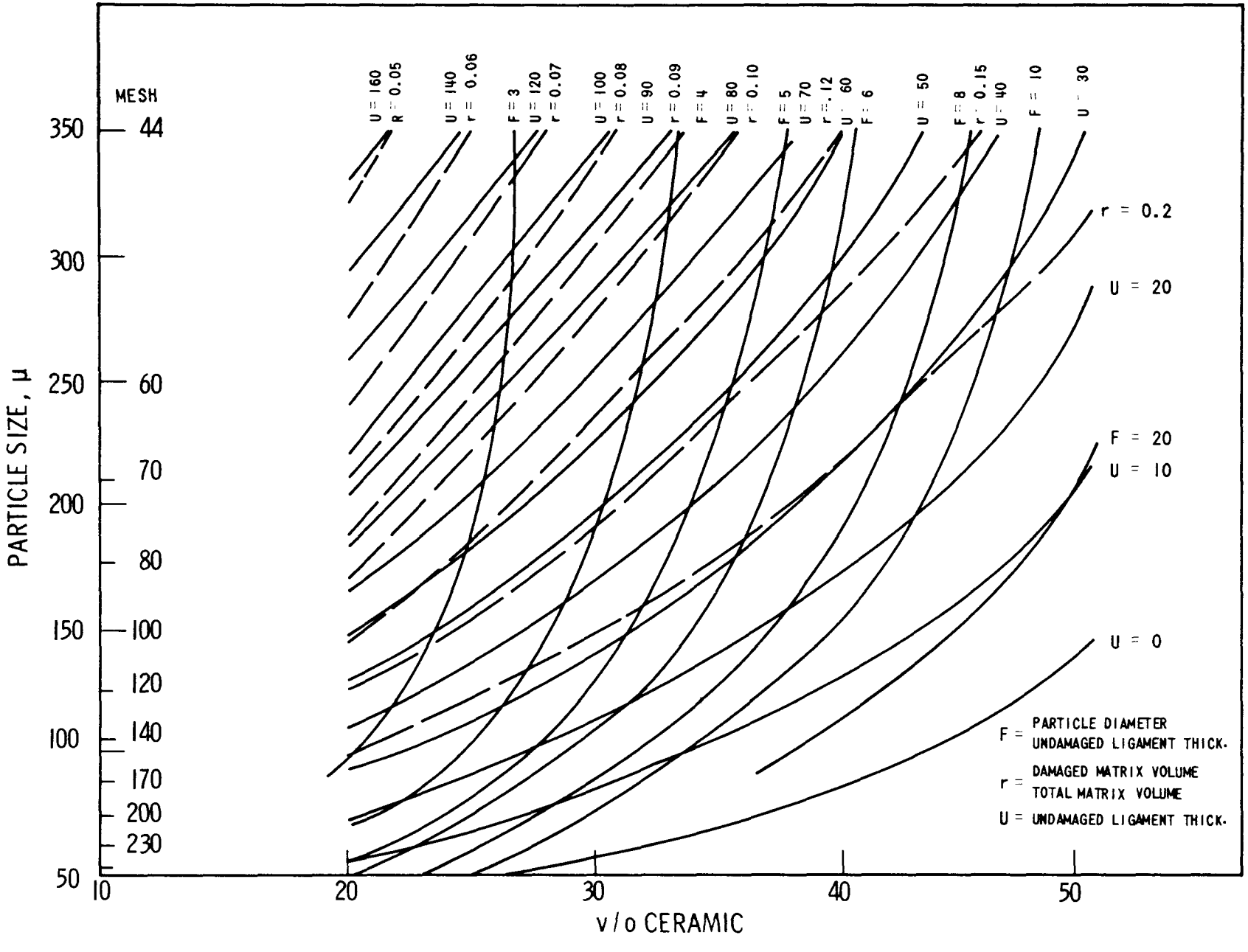

Figure III.7-22 - CALCULATED EFFECT OF DISPERSION FUEL PARTICLE SIZE AND CERAMIC CONTENT ON SELECTION CRITERIA

criteria is shown in Figure III.7-22 for idealized conditions (perfect spheres and uniform distribution). The amount of matrix material that can act as a pressure vessel for a particle is proportional to the thickness of the undamaged matrix area outside of the recoil zone ligament between particles, U. Increases in the ligament thickness are linear with particle size. The effect of the ceramic content is shown in the following equation[52] which was used to calculate the curves in Figure III.7-22:

$$d = D\left[\left(\frac{\pi}{3\sqrt{2V}}\right)^{1/3} - 1\right] - 2\lambda$$

where d = Undamaged Ligament Thickness
D = Particle Diameter
V = Volume Fraction of Ceramic
λ = Recoil Distance (10 μ assumed)

The ratio of damaged (the recoil zone) matrix volume to total matrix volume, γ, indicates that the volume of material contributes to the gross mechanical properties of the cermet. The effect of the particle size on this ratio is greater (and more favorable) for large particle sizes and small ceramic contents. The following equation[52] was also used to calculate the curves in Figure III.7-22:

$$\frac{V_R}{V_T} = \frac{V}{1-V}\left[\left(1 + \frac{1}{D/2}\right)^3 - 1\right]$$

where V_R = Volume of Recoil (damaged) Matrix
V_T = Total Matrix Volume

The stress on a thin-wall spherical pressure vessel is proportional to the ratio of wall thickness to internal diameter. This ratio, F, can serve as a useful approximation of stress in the more complex thick-wall

vessel which represents the undamaged matrix surrounding a fuel particle. The parameter, F, is essentially independent of particle sizes for values greater than 250 μ and for ceramic contents up to 35 volume percent.

The effect of the ceramic content is self-evident; as the ceramic content increases, less matrix material is available to restrain fuel particle pressure. An increase in the particle size is more damaging on each criteria in Figure III.7-22 with greater values of the ceramic content.

Based on the above discussions of failure mode and physical characteristics, the reference design conditions which are recommended to obtain maximum life and maximum feasibility of manufacture of the ceramic fuel are:

85%	-	maximum density
250-350 μ	-	particle size
50 v/o	-	maximum ceramic content

III.7.6.3.2 Empirical Burnup Limits

Several investigators have reported relevant irradiation data for cermets; the most recent report was published in November 1964[53]. The best estimate of usable life is shown in Figure III.7-23 with prior estimates based on 1958 and 1961 data. It is significant that improvements in the technology of both particle manufacture and element fabrication have substantially increased lifetime predictions. It is also significant that the curves were based primarily on plates containing relatively high density fuel particles.

Use of the 1964 ORNL estimate as a basis for present design purposes is basically conservative because of: (1) continuing improvements in the technology, (2) use of rod-type elements, and (3) use of low density fuel particles. Possibly, design life can be extended beyond this limit; this should only be done if justified by theory and ultimately by experi-

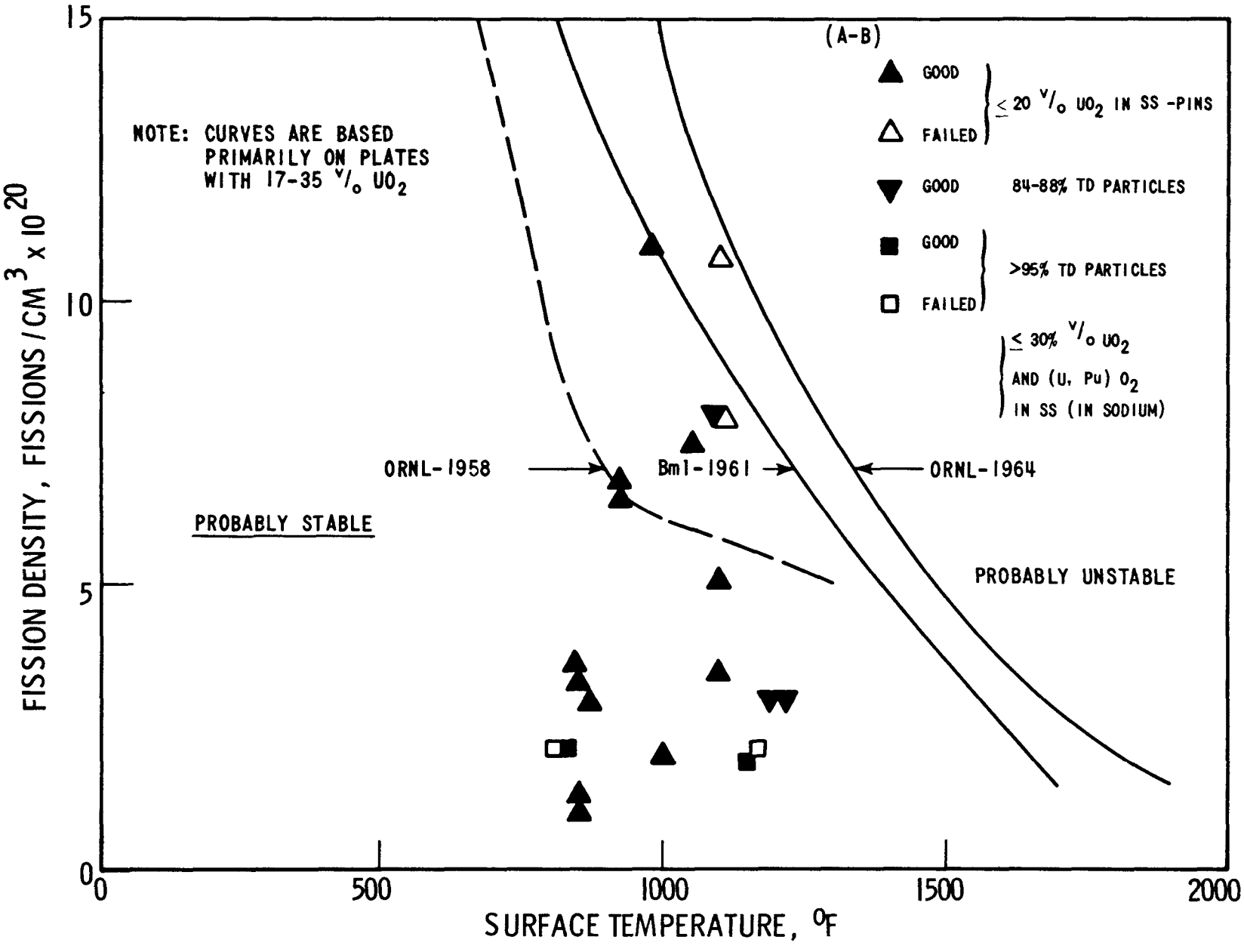

Figure III.7-23 - IRRADIATION BEHAVIOR OF UO_2 - SS CERMETS - ESTIMATES OF USEABLE LIFE AS A FUNCTION OF TEMPERATURE

ment. As the temperature drop across plate type elements (typically 100°F) is generally much less than across the rod-type elements, investigators have attempted to factor this into rod-type element designs. For example, APDA[54] and BNWL[46] have raised the curve 70°F and 100°F[3], respectively and have applied it to centerline temperature. The 1964 ORNL curve shifted 100°F with the revised abscissa is shown in Figure III.7-24.

Other investigators[46] have estimated a substantial reduction in life with a large temperature drop across the fuel rod (50 percent reduction at a ΔT of 600°F) due to thermal stress, residual stress, mechanical restraint and irradiation damage. This reduction is not considered valid, at least not to the extent indicated. Thermal stresses will compress inner fibers (tending to prevent failure), and the stress component, which tends to cause failure in the low temperature (outer) regions, will be lower than at the center. The resultant effect probably negates the temperature drop effect, and makes the mean fuel rod temperature a more valid criterion for pin element life. The 1964 ORNL curve shifted 50°F with the revised coordinate of mean or average fuel rod temperature is shown in Figure III.3-24.

No specific improvement in life has been assumed because of the use of 85% dense fuel; however, a factor of 1.2 has been used[46].

The effect of the preceeding discussion is most easily evaluated by comparing estimates of life from Figure III.7-24 with estimates calculated by a BNWL formula[46]. For a centerline temperature of 1500°F, the estimate of life from Figure III.7-24 is 6.25×10^{20} fissions per cubic centimeter compared to 6.9×10^{20} by BNWL. Agreement within 10% is considered adequate.

Sources[46,54,55] universally agree that no different effect on burnup is anticipated when substituting PuO_2 for UO_2.

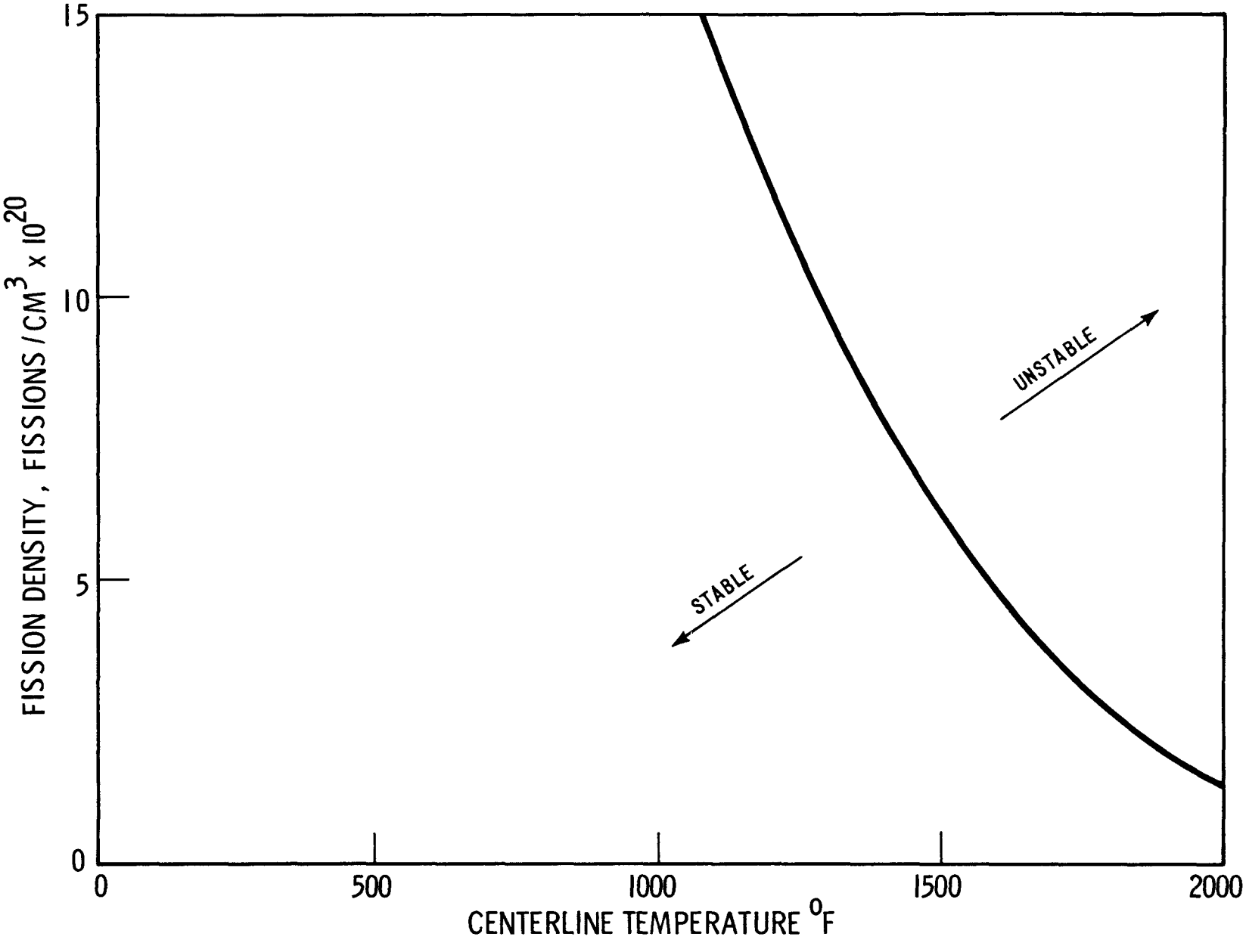

Figure III.7-24 - DESIGN USEABLE LIFE OF UO_2 - SS CERMET AS A FUNCTION OF CENTERLINE TEMPERATURE

III.7.6.3.3 Design Considerations

The subjects discussed in this section are observations of various investigators and are only intended to be a basis for evaluation of theoretical conditions and empirical results. These observations are not expected to supplant the empirical results because of the manifold uncertainties involved in cermet design.

Fuel Swelling

Bulk UO_2 is reported[57] to swell at the rate of 0.7 percent ($\Delta V/V$) per 10^{20} fissions per cc. With an 85 percent dense particle, all void space would be filled at 25.5×10^{20} fissions per cubic centimeter of UO_2. Equating the fractional volume of UO_2 in a cermet, the following equivalents are obtained:

v/o Particles in Cermet	% Swelling per 10^{20} Fissions per cc of Cermet	Fissions per cc of Dispersion to Occupy all Void Space by Fuel Swelling
20	4.12	6.0×10^{20}
30	2.88	9.8×10^{20}
40	2.06	12.0×10^{20}
50	1.65	15.0×10^{20}

Cermet fuels are a highly modified case of bulk UO_2; a substantial fraction of recoil atoms escape into the matrix recoil zone. The quantity is given by[58]:

$$F = \frac{4\lambda}{3a} - \frac{1}{16}\left(\frac{\lambda}{a}\right)^3$$

where: F = fraction of recoil atoms that escape from a sphere

λ = fission fragment range

a = particle radius

F is equal to 8.4 percent for the case where λ = 9.4 μ and a = 150 μ. The above values for fuel swelling probably should be reduced by 8.4 percent. However, as recoil atoms in the matrix cause swelling, the net effect may be approximately equivalent. Apparently, recoil zone swelling and released fission gases compete with fuel swelling for the available void space.

Recoil Zone Swelling

Volume change in the recoil zone is reported[59] to be 1.0 to 1.5 percent per atom percent fission product in the recoil zone. Application of this factor requires the following conversions:

Recoil zone volume = 3.017×10^{-6}	cc. per particle (at 300 μ diameter particle and 10 μ thick recoil zone)
Recoil zone atoms = 25.6×10^{16}	atoms per recoil zone (for 316 L stainless steel)
Particle volume = 14.3×10^{-6}	cc. per particle (at 300 μ diameter particle)
UO_2 volume = 12.0×10^{-6}	cc. per particle (at 85 percent theoretical density)
Particle fissions = 12.0×10^{14}	fissions per particle per 10^{20} fissions per cc. of UO_2
	fissions per particle per 10^{20} fissions per cc. of dispersion* at
70.60×10^{14}	20 v/o particles
47.00×10^{14}	30 v/o particles
35.30×10^{14}	40 v/o particles
28.24×10^{14}	50 v/o particles
Recoil zone fission product = 0.168×10^{14}	atoms entering one recoil zone per 10^{14} fissions per particle (at 8.4 percent of total fission products and 2 fission products per fission)

* $\frac{12 \times 10^{14}}{0.85} \times \frac{100}{\text{v/o particles}}$

Fission product in recoil zone = 0.00656	atom percent per 10^{14} fissions per particle
Recoil zone swelling = 0.0074	percent per 10^{14} fissions per particle

Calculated recoil zone swelling is summarized as follows:

Volume Percent Particles in Dispersion	Recoil Zone Swelling, Percent per 10^{20} Fissions per cc. of Dispersion
20	0.528
30	0.348
40	0.261
50	0.209

Fission Gas Pressure

The fission gas which is released from particles is assumed to result only from diffusion. The use of small, semi-dense particles represents a departure from the bulk case (for which most data is reported), but it should have no particular significance other than loss of a larger percentage of recoil atoms.

The fraction of fission gas released, F, is given by[60]:

$$F = \log^{-1} [0.494(0.602 + \log \alpha)]$$

where $\alpha = \frac{DT}{A^2}$.

D is the diffusion coefficient (cm^2/sec) given by [59]:

$$D = \log^{-1} [-4 - \frac{28,800}{B + 460}]$$

where B = temperature (°F)

T = the time of irradiation in seconds (315,576,000 = 3.16×10^7 sec./yr.)

A = the effective diffusion length in cm. given[59] by $A = \frac{3}{S}$, and

S = the surface area in cm^2/cc, as follows:

% TD	$S(cm^2/cc.)$	$A(cc./cm^2)$	A^2
70	30,000	0.000,100	1.00×10^{-8}
75	25,000	0.000,120	1.44×10^{-8}
80	12,000	0.000,250	6.25×10^{-8}
85	8,000	0.000,375	14.4×10^{-8}
90	2,500	0.001,200	144×10^{-8}
95	300	0.010,000	0.0001

Combining the above equations:

$$F = \log^{-1} \left[0.494 \log \frac{T}{A^2} - 1.678 - \frac{14,210}{B + 460}\right]$$

The calculation of the volume of fission gas generated, from which the above fraction is released, is based on the discussion in the "Recoil Zone Swelling" section and on the information that 0.03857 atoms per fission are krypton and 0.2183 atoms per fission are xenon for a total of 0.247 noble gas atoms per fission[59]. The atoms of gas produced per particle per 10^{20} fissions per cc. of dispersion, which do not enter the recoil zone of the matrix, G, are:

$$G = \left(\frac{12 \times 10^{14}}{.85} \times \frac{100}{\text{v/o particles}}\right) \quad 0.247 \times 0.916 \times 0.85$$

$$G = \frac{2.52 \times 10^{14}}{\text{v/o particles}}$$

Combining the equations for the gas fraction released, F, and the amount produced, G, yields the amount released, R, in atoms per 10^{20} fissions per cc. of dispersion:

$$R = FG$$

Applying the reference conditions of 85 percent theoretical density, operation for approximately 75 percent of total cycle time, and a one year cycle at relatively constant conditions, the gas release reduces to atoms of fission gas released per 10^{20} fissions per cc. of dispersion,

$$R = \frac{2.52 \times 10^{14}}{V} \left[\log^{-1} \left(5.352 - \frac{14,210}{B + 460}\right)\right]$$

From perfect gas considerations, 0.269×10^{20} atoms = 1 cc. at 492°R and 14.7 psia. With 15 percent void in a 300 μ particle, 0.619×10^{14} atoms of fission gas produce a pressure of 14.7 psia at 492°R in the void space in a particle. Stated otherwise, the pressure, P, (psia), produced as a function of temperature, B (°F), is:

$$P = R \left[0.0484 \left(460 + B\right)\right] 10^{-14}$$

Combining

$$P = \frac{1.22 \left(460 + B\right)}{V} \left[\log^{-1} \left(5.352 - \frac{14,210}{B + 460}\right)\right]$$

per 10^{20} fissions per cc. dispersion.

Representative calculations are plotted in Figure III.7-25. It is evident from these results that fission gas pressure is small when the entire particle void volume is available. This fact is not surprising because of the relatively low temperatures considered. However, as the UO_2 swells during use, the void volume available to fission gas is substantially reduced; and, accordingly, pressures are substantially increased.

Failure Calculations

For previously stated reasons, a thorough investigation of theoretical calculations of cermet life is not considered pertinent to this effort. It should suffice to point out that thorough failure analyses have been made for the following cases:

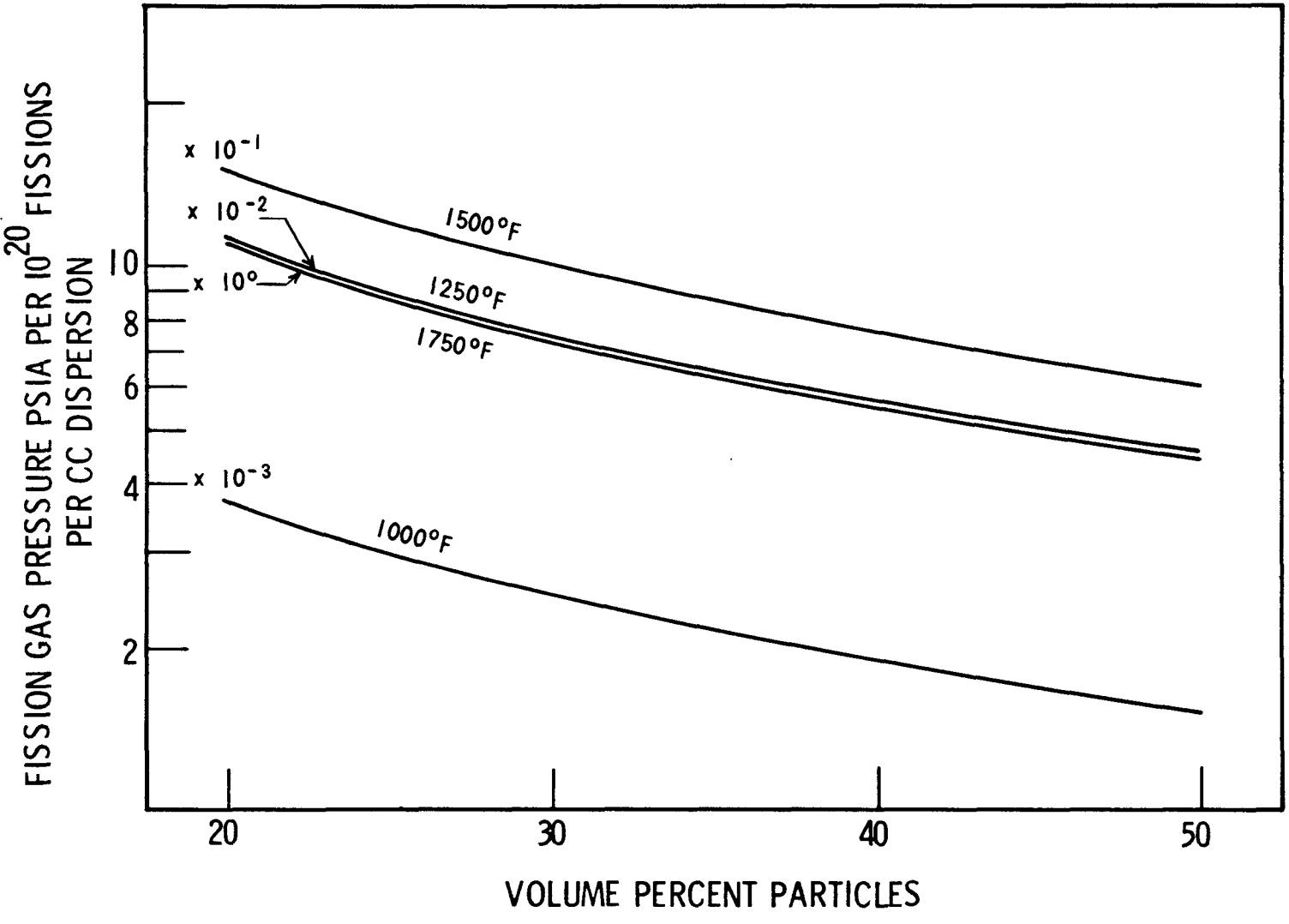

Figure III.7-25 - FISSION GAS PRESSURE IN A PARTICLE AS A FUNCTION OF PARTICLE CONTENT AND TEMPERATURE

1. Low temperature[61] - Failure by fission gas pressure when the matrix yield strength is exceeded.
2. Low temperature[62] - Brittle failure by fission gas pressure and thermal stress in an elastic matrix when the ultimate tensile strength is exceeded.
3. Low temperature[62] - Plastic failure by fission gas pressure and thermal stress in an elastic matrix when the ultimate tensile strength is exceeded.
4. Short term stress peaks[63] - Failure by fission gas pressure during sudden temperature rise when the ultimate tensile strength of the matrix is exceeded.
5. Creep rupture[63] - Failure by creep to rupture due to fission gas pressure at elevated temperatures.

Summary of Design Considerations

It is of interest to select a specific case to examine the relationship of the three considerations contributing to failure, i.e., fuel swelling, recoil zone swelling, and fission gas pressure. Selecting a 40 volume percent dispersion operating at 1500°F, the life curve shows a limit of 6.25×10^{20} fission/cc. Fuel swelling would occupy 71.5 percent of the original void space. Recoil zone swelling would occupy an additional 4.1 percent of the original void space (assuming that 50 percent of the swelling is inward) for a total of 75.6 percent. Fission gas pressure, without volume loss, is shown to be 4.75 psia (assuming, a one year cycle), but is multiplied by a factor of 4.1 to 19.5 psia because of the reduction in the void volume.

At 85 percent particle density, the conversion between fissions per cc. of dispersion and atom percent, U,Pu burnup is:

$$\text{atom percent U,Pu burnup} = \frac{\text{Fissions per cc. dispersion}}{207.74 \times 10^{16} \times \text{volume percent particles}}$$

At 10 atom percent U,Pu burnup, the following table applies:

v/o Particles	Fission per cc. of Dispersion
20	4.1×10^{20}
30	6.2×10^{20}
40	8.3×10^{20}
50	10.4×10^{20}

Therefore, it is apparent that the primary mode of failure is fuel swelling, causing a relatively small volume of gas to exert a high pressure. It is entirely possible that initial fracture of the recoil zone and/or matrix is caused solely by fuel swelling, and that only fracture propagation results from fission gas pressure.

III.7.6.4 Summary and Recommendations

Cermet fuel, consisting of $(U,Pu)O_2$ in a 316 L stainless steel matrix with 316 L stainless steel cladding, has been selected for the control element in a Bundle Controlled Expansion (BCEX) assembly to provide a negative temperature coefficient of reactivity in a sodium cooled fast flux reactor.

Generally, the properties of cermets are linear functions of matrix content; therefore, they are strongly governed by the volume fraction of ceramic particles present. For a given composition, the method of fabrication exerts far more control over properties than any other factor. There is little information available on long term properties such as creep and stress rupture, and even less on post-irradiation properties of the cermet matrix material.

An evaluation of cermet selection characteristics shows that particle size, particle density, and volume percent ceramic are important factors. The reference design particle size was selected as 250-350 μ, because smaller particles give thinner matrix ligaments for restraint of strain. Even larger sizes would be desirable; however, data for larger particle sizes were not reported. The reference particle density was selected as 85 percent maximum, because 1) a low density is desired to obtain more space to accommodate fuel swelling and fission gas, and 2) 85 percent is the lowest density which the literature indicated any confidence of achieving. Volume percent ceramic is limited to 50 percent maximum due to lack of data at higher percentages. The lowest possible volume percent consistent with reactor design requirements is recommended. With a small volume of ceramic, more matrix material is present for restraint of strain.

Empirical burnup limits are defined as a function of operating temperature. Design considerations show the primary mode of failure to be fuel swelling augmented by pressure from fission gas buildup.

An important requirement for further investigation of a cermet fuel for a particular application is the establishment of a reference process and product design including development of optimum size fuel particles. Substantial effort is required in this area of development.

With these reference conditions, typical non-irradiated thermal and mechanical properties can be determined. Long term mechanical properties such as creep, stress rupture, and fatigue must be well established.

Next, irradiation properties must be extensively investigated. The least explored field in cermet technology is irradiation testing. Present data do not permit design of a fuel element with a specific lifetime, based on specific nuclear, thermal, and mechanical conditions. Substantial cost savings may be achieved through a rigorous design study of burnup under given reference conditions with appropriate in-pile verification.

Exploration of alternate matrix materials, which will better resist fuel particle strains at high temperatures, might lead to design improvements. One approach to improving matrix materials to extend the past and current work on materials such as molybdenum, Hasteloys, Inconels, and vanadium alloys. However, these materials would require not only the development described for stainless steel cermets, but substantial additional work to achieve the present stainless steel state-of-the-art.

It is recommended that the development described for a stainless steel matrix cermet be undertaken, and that burnup design studies receive major emphasis. Alternate matrix materials should be used only when absolutely necessary.

Section III.7 - References

1. "Steels for Elevated Temperature Service", United States Steel Corporation, 1961.

2. Heck, F. M., et al, "Liquid Metal Fast Breeder Reactor Design Study", Westinghouse Electric Corporation, Atomic Power Division, WCAP-3251-1, January 1964.

3. "Properties and Selection of Materials", American Society for Metals, Metals Handbook, Vol. 1, 8th Edition, 1961.

4. Reactor Handbook, Vol. 1, Materials, Interscience Publishers, 2nd Edition, 1960.

5. Digest of Steels for High Temperature Service, 6th Edition, 1957, The Timken Roller Bearing Co.

6. ASME Boiler and Pressure Vessel Code for Nuclear Vessels.

7. Lucks, C. F. and Deem, H. W., "Thermal Properties of Thirteen Materials", ASTM Special Technical Publication No. 227, 1958.

8. Martin, W. R. and Weir, J. R., "Effect of Irradiation Temperature on the Post-irradiation Stress-Strain Behavior of Stainless Steel", ORNL-TM-906, October 1964.

9. Murray, P., "Some Aspects of Harwell Research Relating to Dispersed Fuels, Ceramic Matrix Fuels Containing Coated Particles", Proceedings of BMI Symposium, TID 76-4, November 1962.

10. Leary, J. A., Maraman, W. J., Miner, W. N., and Schanfeld, F. W., "Quarterly Status Report on Solid Plutonium Fuels Program for Period up to June 30, 1963", LAMS-2949, July 1963.

11. Brock, P., Cope, L. H., Bagley, K. Q., "Fuel Elements for Fast Reactors", Proceedings - Plutonium as a Power Reactor Fuel, HW-75007, December 1962.

12. Waldron, M. D., "U.K. Research Newsletter - Plutonium Recycling, United Kingdom Atomic Energy Authority", IK-RN-Plut 1.

13. Frost, B. R. T., Mardon, P. G. and Russell, L. E., "Research on the Fabrication, Properties, and Irradiation Behavior of Plutonium Fuels for the U.K. Reactor Program, Proceedings - Plutonium as a Power Reactor Fuel", HW-75007, December 1962.

14. Russell, L. E., "The Structure and Properties of UC and (UPu)C Alloys", AERE-R-4330, May 1963.

15. Cope, L., (Personal Communication to R. J. Allio), "Trip to Dounreay", Trip Report AMS-TR-12, August 14, 1963.

16. Leary, J. A., (Personal Communication to K. R. Jordan), July 1963.

17. Strasser, A., Sheridan, W., Cihi, J., UC-PuC Capsule Irradiation, US/UK Research Newsletter No. 15, Uranium Ceramic Fuels, January 1963.

18. Stahl, D., Strasser, A., Carbide Fuel Development at the United Nuclear Corporation, 4th Uranium Carbide Meeting, East Hartford, Connecticut, May 20-21, 1963.

19. Strasser, A., Stahl, D., Taylor, K., Anderson, J., "Carbide Fuel Development Progress Report", October 1962 to March 1963, UNC 5056, May 1963.

20. Jordan, K. R., "Properties and Performance of Carbide Fuel Materials - A Survey of the Literature", Westinghouse Atomic Power Division, WCAP-2544.

21. Henney, J., Hill, N. A., Livey, D. T., "A Review of Data on Uranium Carbides in the Light of Recent Phase Equilibrium Studies", AERE-R-4175, October 1962.

22. The Uranium - Carbon and Plutonium - Carbon Systems, A Thermochemical Assessment, Technical Report, Series No. 14, Report of Panel in Vienna, October 8-12, 1962.

23. Cunningham, G. W., Ward, J. J., Alexander, C. A., "Thermodynamics for Compatibility Studies of Metal-Clad Uranium Carbide", BMI 1601, October 1962.

24. Boettcher, A. and Schneider, R., "Some Properties of Uranium Monocarbide", Vol. 6A/Conf. 15/P/964, May 1958.

25. Westrum, E. F., "Thermodynamic Properties of Actinide Carbides with Special Reference to the Entropies of Uranium Mono- and Di-carbide", TID 16987, December 1962.

26. Trippler, A. B., Jr., Synder, M. J., Duckworth, W. H., "Further Studies of Sintered Refractory Uranium Compounds", UNC-5056, BMI 1313, January 1959.

27. Krikorian, O. H.,"Estimation of High-Temperature Heat Capacities of Carbides", UCRC 6785, February 1962.

28. Holley, C. E., Jr., "The Thermodynamic Properties of the Uranium and Plutonium Carbide, A Report to the Panel on the Assessment of Thermodynamic Data of Uranium Carbides", LADA-5487, December 1962.

29. Ogard, A. E., Lard, C. C., Leary, J. A., "The Thermal Expansion of PuC and PuC-UC Solid Solution", LA 2766, October 1962.

30. Strasser, A., Stahl, D., (Personal Communication to K. R. Jordan), "Properties of Solid Solution Uranium Plutonium Carbides", Paper to be presented at Harwell Carbide Fuel Conference, November 1963.

31. Lockhart, R. W. and Young, R. S., "Sodium Mass Transfer Program", Paper presented at Information Meeting of Sodium Components Development Program", June 1965, Chicago, Illinois.

32. Mottley, J. D., "A Model for Predicting the Effect of Loop Geometry on the Corrosion Rate of Materials in Sodium", Transactions of the American Nuclear Society, Vol. 8, No. 2., November 1965.

33. Kelman, L. R., Editor, Nuclear Metallurgy, Vol. IX, "Materials for Sodium-Cooled Reactors", 1963 Winter Meeting of the American Nuclear Soceity.

34. Brush, E. G., "Sodium Mass Transfer: XVI, The Selective Corrosion Component of Steel Exposed to Flowing Sodium.

35. Andrews, R. C. and Tepper, F., "The Effect of Sodium on the Mechanical Properties of Austenitic and Ferritic Steels", Paper presented at Information Meeting of Sodium Components Development Program, June 1965, Chicago, Illinois.

36. Kovacic, E. C., McHugh, W. E. and Shoudy, A. A., Jr., Nuclear Metallurgy, Vol. IX, "Materials Problems and Selection in the Enrico Fermi Fast Breeder Reactor", 1963 Winter Meeting of the American Nuclear Society.

37. Heck, F. M., et al, "Liquid Metal Fast Breeder Reactor Design Study", WCAP-3251-1, January 1964.

38. Gunson, W. E., et al, "High Power Density Stainless Steel Reference FBR Core Design", WCAP-2638, July 1964.

39. Gunson, W. E., et al, "The Liquid Metal Fast Breeder Reactor Design Studies", WCAP-2635, July 1964.

40. Keyfitz, I. M., et al, "200 MWe Sodium Fast Reactor Prototype (SFRP) Design Study", WCAP-2628, September 1964.

41. Markley, R. A., et al, "30 MWt Sodium Advanced Fast Experimental Reactor (SAFER) Plant Design and Program", WCAP-2745, February 1965.

42. Heck, F. M., "Neutron Controlled Expansion Fuel for Fast Breeder Reactors", Proceedings of the Conference on Breeding, Economics and Safety in Large Fast Power Reactors", ANL 6792, October 7-10, 1963.

43. Wright, J. H., et al, "Conceptual Design and Preliminary Accident Analysis of a Sodium Cooled, Carbide Fueled, Large Modular Power Reactor", presented in panel discussion on Safety of Large Fast Power Reactors, Fast Reactor Conference, Argonne National Laboratory, Argonne, Illinois, October 11-14, 1965 (to be published).

44. Arthur, G., and Coulson, J., "Physical Properties of Uranium Dioxide-Stainless Steel Cermets", Journal of Nuclear Materials, 13, No. 2, 242-253, 1964.

45. Lloyd, H., "Development of UO_2 Stainless Steel Fuel Plate Containing 30-50 vol. % Oxide" - New Nuclear Materials Including Non-Metallic Fuels, Vol. II, pp. 103-142.

46. BNWL-CC-175, August 1965, Progress Report Conceptual Design Fast-Flux Test Facilities.

47. Bush, S. H., "Irradiation Effects in Structural Materials", (ASM).

48. Brittain, W., et al, "Tubular Core Development Program, PM Core Materials and Processes Status Report", (This report has an excellent presentation of dispersion materials (UO_2) evaluation and fabrication), MND-2706-13, December 1964.

49. Many, L., et al, "Elements Combustibles UO_2-Inox Cylindriques Et Tubulaires - Fabrication Et Properties, New Nuclear Materials Including Non-metallic Fules", Vol. II, pp. 427-465.

50. Valovage, W. D., and Sergiej, R. A., "Mechanical Properties of Stainless Steel-UO_2 Dispersion Fuel Elements", KAPL-1590.

51. Venard, J. T. and Swindemon, R. W., "Mechanical Properties of the UO_2 - Type 347 Stainless Steel Cermet for Core B of the Fermi Reactor", ORNL-TM-655, October 1963.

52. White, D. W., et al, "Irradiation Behavior of Dispersion Fuels", KAPL-P-1849.

53. Thurber, W. C., et al, "Irradiation Testing of Fuel for Core B of the Enrico Fermi Fast Breeder Reactor", ORNL-3709, November 1964.

54. Edwards, J. J., et al, "Fast Reactor Fuel Cycle Costs and Temperature Coefficients of Reactivity for PuO_2 - Stainless Steel and PuO_2-UO_2", APDA-154, April 1963.

55. Frost, B. R. T., "Behavior of Fuels at High Burnup Levels, Part I, Fast Reactor Fuels", Nuclear Engineering, February 1964.

56. Pritchard, W. C., et al, "Compatibility of the Major Elemental of Type 302B Stainless Steel with PuO_2 and UO_2 - New Nuclear Materials Including Non-Metallic Fuels", Vol. II, pp. 155-173.

57. Daniels, R. C., "Effects of High Burnup on Zircaloy Clad Bulk UO_2 Plate Fuel Element Samples", WAPD-263, 1962.

58. Keller, D. L., "Predicting Burnup of Stainless-UO_2 Cermet Fuels", Nucleonics, Vol. 19, No. 6, p. 45, June 1961.

59. Belle, J., "Uranium Dioxide: Properties and Nuclear Applications", USAEC, 1961.

60. Booth, A. H., "A Method of Calculating Fission Gas Diffusion from UO_2 Fuels", CRDC-721, September 1957.

61. Weir, J. R., "A Failure Analysis for the Low Temperature Performance of Dispersion Fuel Elements", ORNL-2902, June 1960.

62. Beck, S. D., "Failure Analysis of Dispersion Fuel Based on Matrix Cracking", APAE-MEMO-298, 1961.

63. Keller, D. L., et al, "A Method of Correlating Irradiation Effects in Dispersion Fuels", BM1-1408, January 1960.

APPENDIX A

BCEX FUEL ASSEMBLY DYNAMICS

1. Introduction

The Bundle Controlled Expansion fuel assembly consists of upper and lower bundles of fuel rods which are attached to a central structure of cermet rods that contain fuel. During a rapid increase in the core power level, the cermet rods heat up faster than the fuel clad, and thus separate the two bundles axially due to differential thermal expansion.

Because of its inertia, the fuel bundle tends to resist this axial movement. This resistance to movement causes compressive stresses in the cermet rods which are proportional to the difference in the unrestrained thermal displacement and the actual or restrained thermal displacement of the fuel bundle. This situation is analogous to a mass (bundle) on a spring (cermet rods), where the spring end opposite to the mass is given a displacement which varies with time.

The detailed analyses of fuel assembly response to changes in cermet temperature are divided into four sections. In the first section, the cermet rods are considered to be an isotropic, elastic, continuum with zero body forces. The assumptions inherent to this model are pointed out. Further similifying assumptions are introduced and discussed. The second section applies appropriate boundary conditions to the continuum, including the reaction forces in the bundle-to-cermet connection. The resulting equation is that of the undamped harmonic oscillator. The third section discusses two types of cermet temperature programs, and the fourth section derives the response of the fuel assembly to these programs. Parameter studies and a discussion complete the work.

2. Nomenclature

A	-	area of cermet rods, $in.^2$
	-	amplitude of bundle vibration, in.
B	-	constant
c	-	sound velocity of cermet, ips
E	-	cermet elastic modulus, psi
F_r	-	total can to bundle force
K	-	cermet/bundle spring rate, lb/in.
L	-	length of cermet assembly, in.
M	-	dynamic mass of bundle/cermet system
n	-	number of cermet rods, also constant
T	-	temperature excess, °F
T_o	-	terminal temperature, °F
t	-	time, sec.
u,v,w	-	components of displacement, in.
x,y,z	-	orthogonal cartesian coordinate system, z axis coincident to cermet ℄
X	-	bundle displacement, in.
Y	-	free cermet thermal expansion, in.
Y_o	-	characteristic expansion, in.
Y_τ	-	terminal or total free expansion, in.
Z	-	cermet compression, in.
α	-	cermet coefficient of thermal expansion, per °F
ξ	-	ramp time, sec.
λ	-	dimensionless distance
μ	-	coefficient of friction
ν	-	Poisson's ratio
ρ	-	cermet density
$\sigma_x,\sigma_y,\sigma_z$	-	normal stresses in x, y, z directions, psi
τ	-	dimensionless time
τ	-	characteristic time, sec.
τ_o	-	characteristic time, sec.
$\tau_{xz},\tau_{xy},\tau_{yz}$	-	shear stresses, psi
ϕ	-	time, sec.
$\omega = \sqrt{K/M}$	-	bundle/cermet natural frequency, rad/sec.

3. Cermet Rod Kinetics

The equilibrium equations for a continuous medium without body forces from reference (1) are:

$$\frac{\partial \sigma_x}{\partial x} + \frac{\partial \tau_{xy}}{\partial y} + \frac{\partial \tau_{xz}}{\partial z} = \rho \frac{\partial^2 u}{\partial t^2}$$

$$\frac{\partial \sigma_y}{\partial y} + \frac{\partial \tau_{xy}}{\partial x} + \frac{\partial \tau_{yz}}{\partial z} = \rho \frac{\partial^2 v}{\partial t^2}$$

$$\frac{\partial \sigma_z}{\partial z} + \frac{\partial \tau_{xz}}{\partial x} + \frac{\partial \tau_{yz}}{\partial y} = \rho \frac{\partial^2 w}{\partial t^2}$$

Stress is related to displacement in an isotropic Hooke solid in reference (1) by:

$$\frac{\partial u}{\partial x} - \alpha T = \frac{1}{E} [\sigma_x - \nu (\sigma_y + \sigma_z)]$$

$$\frac{\partial v}{\partial y} - \alpha T = \frac{1}{E} [\sigma_y - \nu (\sigma_x + \sigma_z)]$$

$$\frac{\partial w}{\partial z} - \alpha T = \frac{1}{E} [\sigma_z - \nu (\sigma_x + \sigma_y)]$$

$$\frac{\partial u}{\partial y} + \frac{\partial v}{\partial x} = \frac{2(1+\nu)}{E} \tau_{xy}$$

$$\frac{\partial u}{\partial z} + \frac{\partial w}{\partial x} = \frac{2(1+\nu)}{E} \tau_{xz}$$

$$\frac{\partial v}{\partial z} + \frac{\partial w}{\partial y} = \frac{2(1+\nu)}{E} \tau_{yz}$$

Assuming that x, y, z are the principle axes with $\tau_{xy} = \tau_{xz} = 0$, and that $\sigma_x = \sigma_y = 0$. The basic equations now are:

$$\frac{\partial \sigma_z}{\partial z} = \rho \frac{\partial^2 w}{\partial t^2}, \quad \frac{\partial^2 u}{\partial t^2} = \frac{\partial^2 v}{\partial t^2} = 0$$

$$\frac{\partial u}{\partial x} - \alpha T = -\nu \sigma_z / E$$

$$\frac{\partial v}{\partial y} - \alpha T = -\nu \sigma_z / E$$

$$\frac{\partial w}{\partial z} - \alpha T = \sigma_z / E$$

$$\frac{\partial^2 w}{\partial z^2} - \alpha \frac{\partial T}{\partial z} = \frac{1}{E} \frac{\partial \sigma_z}{\partial z} = \frac{\rho}{E} \frac{\partial^2 w}{\partial t^2} \qquad \text{(A-1)}$$

$$\frac{\partial u}{\partial y} + \frac{\partial v}{\partial x} = \frac{\partial u}{\partial z} + \frac{\partial w}{\partial x} = \frac{\partial v}{\partial z} + \frac{\partial w}{\partial y} = 0$$

Further simplification would result by setting $\rho/E = 0$. The significance of setting $\rho/E = 0$ will be illustrated in the following problem.

Consider a slender rod of length L, which is fixed at z = 0, and free at z = L. The rod is internally heated so that the rod temperature is uniform throughout the rod volume.

For: $t < 0$, temperature = 0
$0 < t < \xi$, temperature = $(T_o/\xi)t$
$\xi < t$, temperature = T_o

The boundary conditions for equation (A-1) are:

$$w(o,t) = 0 \qquad \frac{\partial^2 w}{\partial t \partial z}(z,0) = 0$$

$$\frac{\partial w}{\partial z}(L,t) = 0 \qquad \frac{\partial T}{\partial z}(z,t) = 0$$

A solution for this system is:

$$\frac{w(z,t)}{\alpha(T_o/\xi)zt} = 1 - \frac{4}{\Pi} \sum_{n=1}^{\infty} \frac{\text{Sin } n\Pi/2}{n} \frac{\text{Sin } n\tau}{n\tau} \frac{\text{Sin } n\lambda}{n\lambda}$$

where, $\tau = \frac{\Pi c}{2L} t$, $\lambda = \frac{\Pi}{2L} z$, $0 < t < \xi$

For z = L:

$$\frac{w(L,t)}{L\alpha T_o t/\xi} = 1 - \frac{8}{\Pi^2}\left[\frac{\text{Sin } \tau}{\tau} + \frac{1}{9}\frac{\text{Sin } 3\tau}{3\tau} + \frac{1}{25}\frac{\text{Sin } 5\tau}{5\tau} + \ldots.\right]$$

The first term within brackets is dominant, thus:

$$\frac{w(L,t)}{L\alpha T_o} = \frac{t}{\xi} - \frac{8}{\Pi^2}\frac{\tau}{\xi\tau}\text{Sin } \tau$$

$$\frac{w(L,t)}{L\alpha T_o} = \frac{t}{\xi} - \frac{8}{\Pi^2}\left(\frac{2L}{\Pi\xi c}\right)\text{Sin}\left(\frac{\Pi\xi c}{2L}\right)\left(\frac{t}{\xi}\right)$$

For $c = \infty$, $\frac{w_\infty(L,t)}{L\alpha T_o} = \frac{\tau}{\xi}$, and the effect of a finite value for c is to superpose an oscillating motion on the steady motion of the rod at z = L. The amplitude of this oscillating motion is $\frac{8}{\Pi^2}\left(\frac{2L^2\alpha T_o}{\Pi\xi c}\right)$. For an acceptable ratio between $\frac{8}{\Pi^2}\left(\frac{2L^2\alpha T_o}{\Pi\xi c}\right)$ and $L\alpha T_o$ of 1%, the following inequality must be observed:

$$\xi \geq \frac{1600}{\Pi^3} \frac{L}{c} \tag{A-2}$$

For $c \sim 160{,}000$ in/sec. and $L \sim 100$ in. $\xi > \sim .03$ sec. Thus, equation (A-2) is satisfied and it is permissible to set $\rho/E = 0$ in equation (A-1).

Equation (A-1) now becomes:

$$\frac{\partial^2 w}{\partial z^2} = \alpha \frac{\partial T}{\partial z} \tag{A-3}$$

Defining the average values for the terms of equation (A-3), averaging over area A:

$$\overline{\frac{\partial^2 w}{\partial z^2}} \equiv \frac{1}{A} \iint_A \frac{\partial^2 w}{\partial z^2} \, dxdy, \text{ and } \overline{\frac{\alpha \partial T}{\partial z}} \equiv \frac{1}{A} \iint_A \alpha \frac{\partial T}{\partial z} \, dxdy$$

Equation (A-3) becomes:

$$\overline{\frac{\partial^2 w}{\partial z^2}} = \overline{\frac{\alpha \partial T}{\partial z}} \tag{A-4}$$

Forming the indefinite integral of equation (A-4) with respect to z and interpreting the arbitrary function of time to be the axial strain in the cermet:

$$\int \overline{\frac{\partial^2 w}{\partial z^2}} \, dz = \int \overline{\frac{\alpha \partial T}{\partial z}} \, dz + \frac{\sigma_{z(t)}}{E} \tag{A-5}$$

Now, integrating equation (A-5) over the cermet length:

$$\int_0^L\int_0^L \overline{\frac{\partial^2 w}{\partial z^2}}\, dzdz = \int_0^L\int_0^L \overline{\frac{\alpha\partial T}{\partial z}}\, dzdz + \frac{\sigma_z L}{E} \qquad \text{(A-6)}$$

Finally, the following definitions are made,

$$X \equiv \int_0^L\int_0^L \overline{\frac{\partial^2 w}{\partial z^2}}\, dzdz, \quad Y \equiv \int_0^L\int_0^L \overline{\frac{\alpha\partial T}{\partial z}}\, dzdz \quad \text{and} \quad Z \equiv \frac{\sigma_z L}{E}, \qquad \text{(A-7a,b,c)}$$

and substituted into equation (A-6) to obtain:

$$X = Y + Z \qquad \text{(A-8)}$$

This expression shows that the displacement of the cermet at z = L equals the free thermal expansion of the cermet plus the elongation due to tensile stress σ_z. The purpose of the preceeding lengthy derivation of this elementary statement was to highlight the inherent assumptions. These assumptions are:

1. The medium is continuous - crystalline structure with a dispersion of fuel has no observable effect on structure dynamics.
2. No body forces exist - considers gravity effects as insignificant.
3. The material is isotropic - no directional variations in structural properties due to fabrication history.
4. A Hooke solid is utilized - linear relation between stress and strain ignores hysteresis and internal damping.
5. Zero shear stress exist on x,y,z axes - this implies no fluid damping.

6. The lateral stresses are zero - no buckling or lateral wave effects.
7. The sound velocity is infinite - no effects from axial stress waves.

4. Cermet/Fuel Bundle Kinetics

The boundary conditions on the cermet surfaces are:

1. Lateral surface stresses are zero.
2. Normal stress on end surfaces is σ_z.

At the cermet/bundle connection, $\sigma_z A = -M\ddot{X}$, where A is the cermet cross sectional area, and M is the sum of the bundle mass plus 1/3 of the cermet rod assembly mass[2] (assuming the fuel bundle as being a rigid body with respect to the cermet rods).

$$\sigma_z = -M\ddot{X}/A$$

Substituting this expression into equation (A-7c)

$$Z = -M\ddot{X}\, L/AE$$

and defining,

$$K \equiv AE/L \text{ and } \omega^2 \equiv K/M$$

the following expression is obtained:

$$\ddot{X} = -Z\omega^2.$$

Equation (A-8) becomes:

$$\begin{aligned} Z &= X - Y \\ \ddot{Z} - \ddot{X} &= -\ddot{Y} \\ \ddot{Z} + \omega^2 Z &= -\ddot{Y} \end{aligned} \qquad \text{(A-9)}$$

Equation (A-9) describes the undamped harmonic oscillator with natural frequency ω consisting of a mass, M, on a spring, spring rate K, with the spring excited in the manner of the shaker table problem by a force proportional to $\ddot{Y}$.

The solution of equation (A-9) is given by reference (3):

$$Z = -\frac{1}{\omega}\int_0^t \ddot{Y}(\xi)\,\sin\,\omega\,(t-\xi)\,d\xi \qquad \text{(A-10)}$$

5. Forcing Functions

In this analysis, both the terminated and unterminated power transient will be examined. For a terminated power transient,

$$Y/Y_\tau = 3(t/\tau)^2 - 2(t/\tau)^3, \quad 0 \leq t \leq \tau \qquad \text{(A-11)}$$

$$Y/Y_\tau = 1, \; t \geq \tau$$

represents the essential features of the free, unrestrained cermet thermal expansion. τ is the characteristic interval of time, from when the cermet starts to expand to when the cermet expansion is essentially complete. Y_τ is the total amount of free cermet expansion.

For an unterminated transient,

$$Y/Y_o = e^{t/\tau_o} - 1 \qquad \text{(A-12)}$$

represents the free cermet thermal expansion. Y_o and τ_o are a characteristic deflection and a characteristic time, respectively.

6. Fuel Bundle Kinematics

Substituting the second derivatives of equations (A-11) and (A-12) into equation (A-10) and carrying out the integration, the solution for the terminated transient is,

$$-Z/Y_\tau = \frac{6}{(\omega\tau)^2}\ (1 - \cos\ \omega\tau) - \frac{12}{(\omega\tau)^3}\ (\omega\tau - \text{Sin}\ \omega\tau) \qquad \text{(A-13)}$$

and the solution for the unterminated transient is,

$$Z/Y_o = \frac{1}{1 + (\omega\tau_o)^2}\ (\cos\ \omega\tau + \frac{1}{\omega\tau_o}\ \text{Sin}\ \omega\tau - e^{t/\tau_o}) \qquad \text{(A-14)}$$

For the terminated case, $Z \equiv Z_\tau$ and $\dot{X} \equiv \dot{X}_\tau$ at $t = \tau$. For $t > \tau$, the bundle oscillates with amplitude A about $X = Y_\tau$. A is found from:

$$(\frac{A}{Y_\tau})^2 = (\frac{Z_\tau}{Y_\tau})^2 + (\frac{\dot{X}_\tau}{\omega Y_\tau})^2 \qquad \text{(A-15)}$$

$X = Y_\tau$ for the first time after $t = \tau$ at $t = \tau + \phi$ where:

$$\phi = \frac{1}{\omega}\ \cos^{-1}\ \frac{\dot{X}_\tau}{A\omega}$$

For the unterminated case, at time t sufficiently large that $e^{t/\tau_o} >> 1$, equations (A-12) and (A-14) become

$$Y/Y_o \doteq e^{t/\tau_o}$$

$$Z/Y_o \doteq -\frac{1}{1 + (\omega\tau_o)^2}\ e^{t/\tau_o}$$

The ratio

$$Z/Y \doteq \frac{1}{1 + (\omega\tau_o)^2} \qquad \text{(A-16)}$$

is a measure of the disparity between bundle displacement and free cermet expansion.

7. Parameters Used in Calculations

Total cermet assembly length	101.07 in.
Total spacer bar length	26.12 in.
Active cermet length	74.95 in.
Spacer bar cross sectional area	1.1 $in.^2$
Cermet O.D.	0.30 in.
Number of cermet rods/bundle	7
Total active cermet cross sectional area	0.50 $in.^2$
Total cermet assembly weight	20 lbs.
Carbide fuel rod length	50.5 in.
Carbide clad O.D.	0.3 in.
Carbide clad wall thickness	0.01 in.
Carbide clad cross sectional area	0.009 $in.^2$
Number of carbide fuel rods/bundle	120
Total fuel clad weight/bundle	15 lbs.
Carbide fuel length	48 in.
Carbide fuel O.D.	.268 in.
Total carbide fuel weight/bundle	160 lbs.
Total carbide fuel + clad weight/bundle	175 lbs.
Cermet Young's Modulus	15×10^6 psi
Clad and spacer bar Young's Modulus	20×10^6 psi
Spacer bar spring rate	0.84×10^6 lbs/in
Active cermet spring rate	0.099×10^6 lbs/in
Cermet assembly spring rate	0.089×10^6 lbs/in
Bundle/cermet assembly natural frequency, ω	430 rad/sec (68 cps)
Cermet density	0.31 lb/cu. in.

8. Effect of Restraining Forces on BCEX Response

For a terminated transient, the previously derived differential equation of motion (equations A-9 and A-11), for the lower rod bundle, when modified by the addition of a term for total can to bundle force is:

$$\ddot{Z} + \omega^2 Z + \frac{\mu F_r}{M} + \frac{6 Y_\tau}{\tau^2} \left(1 - \frac{2t}{\tau}\right) = 0 \qquad \text{(A-17)}$$

Where:

μ = coefficient of friction between fuel rod bundle and can

F_r = total can to bundle force

F_r is defined such that:

at $t = 0$; $F_r = 0$

at $t > 0$; $F_r = F_r$ = constant

The equation of motion is solved and the constants of integration determined from the boundary conditions:

at $t = 0$; $Z = 0$; $\dot{Z} = 0$

The result:

$$Z = \frac{6 Y_\tau}{\omega^2 \tau^2} (\cos \omega t - 1) + \frac{12 Y_\tau}{\omega^3 \tau^3} (\omega t - \sin \omega t) - \frac{\mu F_R}{\omega^2 M} \qquad \text{(A-18)}$$

Since:

$$\omega^2 = \frac{AE}{LM}$$

Thus:

$$Z = \frac{6\,Y_\tau}{\omega^2\,\tau^2}\,(\cos\,\omega t - 1) + \frac{12\,Y_\tau}{\omega^3\,\tau^3}\,(\omega t - \sin\,\omega t) - \frac{\mu\,F_R\,L}{AE} \qquad \text{(A-19)}$$

It is seen that the effect of can to bundle forces is a reduction in response of the lower rod bundle just equal to the elastic compression of the cermet rods by the forces.

For an unterminated transient, a modified differential equation is again written:

$$\ddot{Z} + \omega^2\,Z + \frac{\mu\,F_R}{M} + Bn^2\,e^{nt} = 0 \qquad \text{(A-20)}$$

where B and n are constants.

Which has a solution:

$$Z = \frac{Bn^2}{n^2 + \omega^2}\,(\cos\,\omega t + \frac{n}{\omega}\sin\,\omega t - e^{nt}) - \frac{\mu\,F_R\,L}{AE} \qquad \text{(A-21)}$$

For both terminated and unterminated transients, it is desirable that the effect of can to bundle forces on the response be small. This may be expressed:

$$\frac{\mu\,F_R\,L}{AE} << Y$$

Or:

$$\frac{F_R\,L}{AE} << \alpha\,L\,\Delta\,T$$

Therefore, the limitation on F_R becomes:

$$F_R << \frac{AE\alpha\,\Delta T}{\mu}$$

For the present case:

$A = 0.50 \text{ in.}^2$

$E = 15 \times 10^6 \text{ psi}$

$\alpha = 10.9 \times 10^{-6} \text{ in/in/}^\circ\text{F}$

$\mu = 1.0 \text{ (assumed)}$

Then:

$$F_R << 81.8 \Delta T$$

For a 10° temperature rise:

$$F_R << 818$$

As a result, the limiting value of F_R can be put, somewhat arbitrarily, in the 50-100 lb. range.

References

1. Timoshenko, Theory of Elasticity, McGraw-Hill, 1951.

2. Timoshenko, Vibration Problems in Engineering, Third Edition, pp. 312-14.

3. Thomson, Vibration Theory and Applications, equation (4.4-2), Prentice-Hall, 1965

APPENDIX B

BCEX FUEL ASSEMBLY THERMAL BOWING

1. Introduction

This appendix contains the equations and detailed calculations of the bowing analyses performed under the BCEX project. This appendix is organized as follows:

a. Unrestrained thermal bowing
b. Restrained thermal bowing
c. Effect of transients and clearances on bowing
d. Restraining forces to bowing

The symbols are listed in the nomenclature.

2. Nomenclature

A	-	cross sectional area of cermet bundle, $in.^2$
C	-	constant
D_I	-	inside fuel rod diameter, in.
D_o	-	outside fuel rod diameter, in.
d	-	distance from neutral axis, in.
E	-	modulus of elasticity, psi
F	-	restraining force, lb.
h	-	distance between bundle contact points, in.
I	-	moment of inertia, $in.^4$
L	-	effective cermet rod length, in.
M	-	bending moment, in.-lb
R_o	-	one-half distance across fuel can (outside), in.
R_I	-	one-half distance across fuel can (inside), in.
T	-	temperature, ^oF
V	-	shearing force, lb.

x - distance axially from reactor core plate, in.

y - fuel assembly radial deflection, in.

α - coefficient of thermal expansion, in/in/°F

ρ - radius of curvature, in.

θ - slope, radians

3. Unrestrained Thermal Bowing

In the absence of any radial restraints, under the effect of the radial temperature gradient in a reactor core, a fuel assembly, if restrained at its base only, will bow outward (away from the hot side). If the temperature gradient is linear across the assembly, the radius of curvature at any point on the assembly is:

$$\rho = \frac{1}{T} \qquad \text{(B-1)}$$

Where:

α coefficient of thermal expansion of the assembly - in/in/°F

ΔT = radial thermal gradient - °F/in.

This is related to the deflection, y, by the differential equation:

$$\frac{d^2y}{dx^2} = \frac{1}{\rho} = \alpha\Delta T \qquad \text{(B-2)}$$

In the thermal-hydraulic analyses, the most severe radial temperature gradient in the core was found to exist across the outermost row of core assemblies.

This gradient for beginning life power distribution assuming no transverse coolant mixing, can be expressed as:

$$\Delta T_I = 0 \qquad (0 \leq x \leq 27)$$

$$\Delta T_{II} = 6.6 \left\{ 1 - \cos \frac{\pi\,(x-27)}{75} \right\} \qquad (27 \leq x \leq 102) \qquad \text{(B-3)}$$

$$\Delta T_{III} = 13.2 \qquad (102 \leq x \leq 115)$$

These expressions are plotted in Figure B-1.

Upon substitution and integration of equations (B-3), the following expressions are obtained.

In the core region (II):

$$\frac{d^2 y_{II}}{dx^2} = 6.6\,\alpha \left\{ 1 - \cos \frac{\pi\,(x-27)}{75} \right\}$$

$$\frac{dy_{II}}{dx} = 6.6\,\alpha \left\{ (x-27) - \frac{(75)}{\pi} \sin \pi \frac{(x-27)}{75} \right\} + C_1$$

$$y_{II} = 6.6\,\alpha \left\{ \frac{(x-27)^2}{2} + \frac{(75)^2}{\pi^2} \cos \pi \frac{(x-27)}{75} \right\} + C_1 x + C_2$$

And in the upper blanket (III):

$$\frac{d^2 y_{III}}{dx^2} = 13.2\,\alpha$$

$$\frac{dy_{III}}{dx} = 13.2\,\alpha\, x + C_3$$

$$y_{III} = 6.6\,\alpha\, x^2 + C_3 x + C_4$$

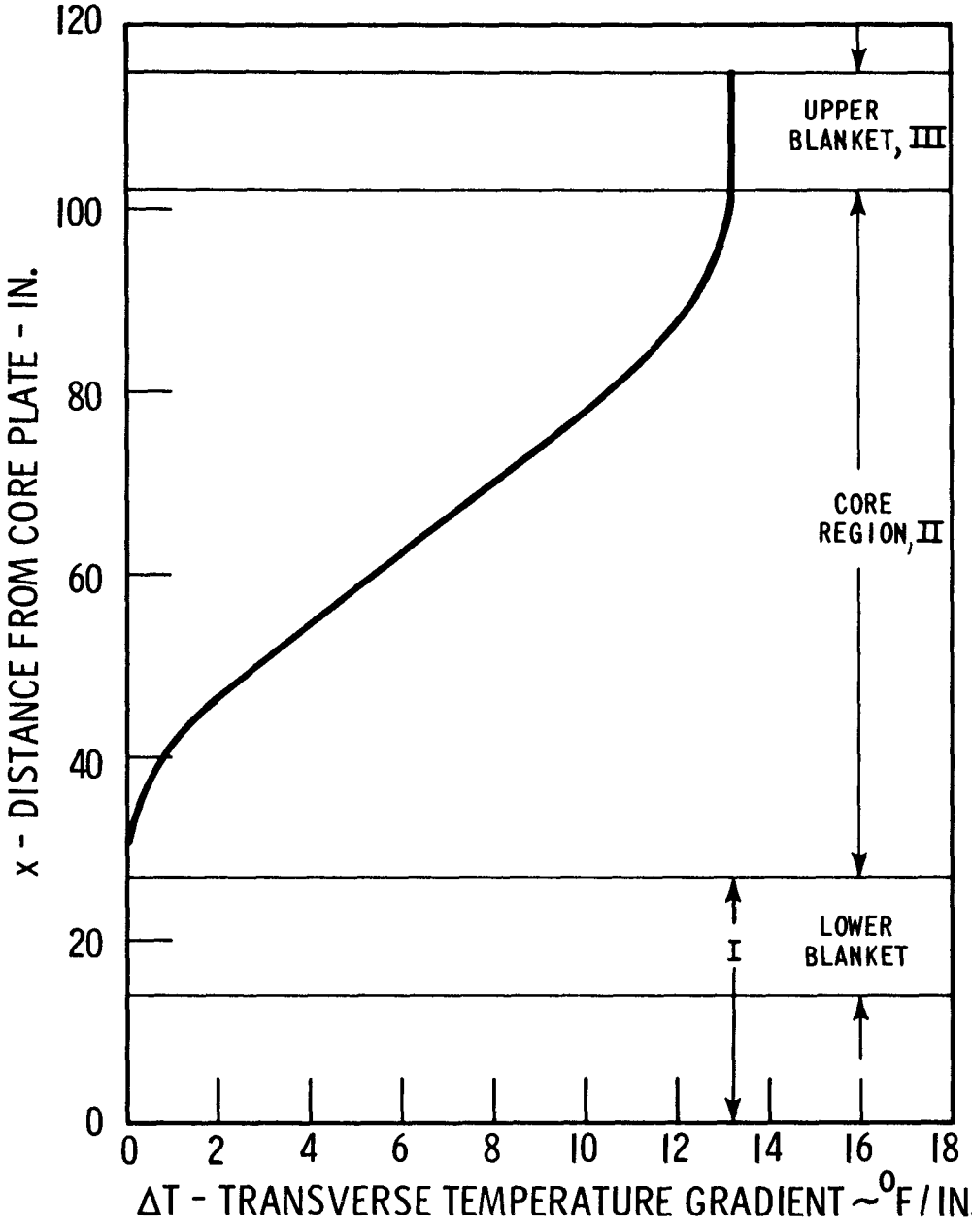

TRANSVERSE TEMPERATURE GRADIENT AS A FUNCTION OF AXIAL POSITION IN OUTERMOST CORE SUBASSEMBLY

Figure B-1

The constants of integration are found from the boundary conditions:

$$x = 27;\ y_{II} = 0;\ \frac{dy_{II}}{dx} = 0$$

Therefore:

$$C_1 = 0;\ C_2 = -6.6\ \alpha\ \frac{(75)^2}{2}$$

Similarly:

$$x = 102;\ y_{II} = y_{III};\ \frac{dy_{II}}{dx} = \frac{dy_{III}}{dx}$$

And:

$$C_3 = -6.6\ \alpha\ (129);\ C_4 = -6.6\ \alpha\left\{(102)^2 + (129)\ (102) - \frac{(75)^2}{2}\right\}$$

Finally:

$$y_I = 0$$

$$y_{II} = 6.6\ \alpha\left\{0.5\ x^2 - 569.9\ (1 - \cos\ \frac{\pi\ (x-27)}{75}\right\}$$

$$y_{III} = 6.6\ \alpha\left\{x^2 - 129\ x - 20749\right\}$$

For austenitic stainless steel at 1000°F, $\alpha = 10.9 \times 10^{-6}$ in/in/°F. Upon substituting this value, the bowing curve presented in Figure III.4-12 is obtained. The maximum deflection of 0.203 inches occurs at the top of the fuel assembly (x = 115). The deflection at the top of the core (x = 102) is 0.120 inches.

4. Restrained Thermal Bowing

A fuel assembly with three upper restraints is shown in Figure B-2. The lower end of the assembly is assumed to be built into the reactor core plate. The restraining forces give rise to the following bending moments in the fuel assembly:

$$M_I = F_1(x_1-x) + F_2(x_2-x) + F_3(x_3-x) \qquad (0 \leq x \leq x_1)$$

$$M_{II} = F_2(x_2-x) + F_3(x_3-x) \qquad (x_1 \leq x \leq x_2)$$

$$M_{III} = F_3(x_3-x) \qquad (x_2 \leq x \leq x_3)$$

The deflection of the fuel assembly is related to the moment by the differential equation:

$$\frac{d^2y}{dx^2} = \frac{M}{EI}$$

If EI is constant, as is approximately the case, the equations can be intergrated to find the slope:

$$\frac{dy_I}{dx} = \frac{F_1}{EI}\left(x_1x - \frac{x^2}{x}\right) + \frac{F_2}{EI}\left(x_2x - \frac{x^2}{2}\right) + \frac{F_3}{EI}\left(x_3x - \frac{x^2}{2}\right) + \theta_0$$

$$\frac{dy_{II}}{dx} = \frac{F_2}{EI}\left(x_2x - \frac{x^2}{2}\right) + \frac{F_3}{EI}\left(x_3x - \frac{x^2}{2}\right) + \theta_1$$

$$\frac{dy_{III}}{dx} = \frac{F_3}{EI}\left(x_3x - \frac{x^2}{2}\right) + \theta_2$$

Where the θ_0, θ_1, and θ_2 are constants of integration. Integrating again to find the deflections:

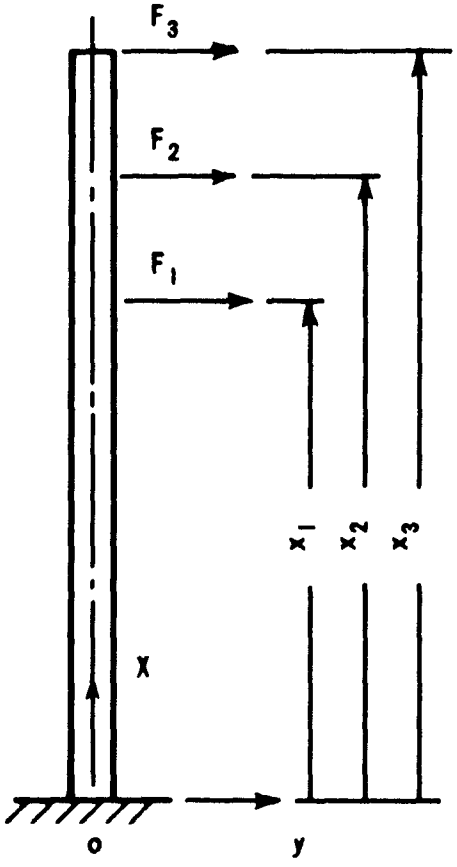

RESTRAINED THERMAL BOWING - ASSUMED GEOMETRY

Figure B-2

$$y_I = \frac{F_1}{2EI}\left(x_1x^2 - \frac{x^2}{3}\right) + \frac{F_2}{2EI}\left(x_2x^2 - \frac{x^3}{3}\right) + \frac{F_3}{2EI}\left(x_3x^2 - \frac{x^3}{3}\right) + \theta_0\, x + y_0$$

$$y_{II} = \frac{F_2}{2EI}\left(x_2x^2 - \frac{x^3}{3}\right) + \frac{F_3}{2EI}\left(x_3x^2 - \frac{x^3}{3}\right) + \theta_1\, x + y_1$$

$$y_{III} = \frac{F_3}{2EI}\left(x_3x^2 - \frac{x^2}{3}\right) + \theta_2\, x + y_2$$

y_0, y_1 and y_2 are also constants of integration. At $x = x_1$:

$$\frac{dy_I}{dx} = \frac{dy_{II}}{dx}$$

$$y_I = y_{II}$$

At $x = x_2$:

$$\frac{dy_{II}}{dx} = \frac{dy_{III}}{dx}$$

$$y_{II} = y_{III}$$

Therefore:

$$\theta_I = \theta_0 + \frac{F_1x_1^2}{2EI}$$

$$y_I = y_0 + \frac{F_1x_1^3}{6EI}$$

$$\theta_{II} = \theta_0 + \frac{F_1x_1^2}{2EI} + \frac{F_2x_2^2}{2EI}$$

$$y_{II} = y_0 + \frac{F_1x_1^3}{6EI} + \frac{F_2x_2^3}{6EI}$$

Since the fuel assembly is assumed to be built into the reactor core plate at x = 0, the slope and deflection at this point are:

$$\theta_0 = y_0 = 0$$

The final equations for the deflection of the fuel assembly under three upper restraints can then be written:

$$y_I = \frac{F_1}{2EI}\left(x_1x^2 - \frac{x^3}{3}\right) + \frac{F_2}{2EI}\left(x_2x^2 - \frac{x^3}{3}\right) + \frac{F_3}{2EI}\left(x_3x^2 - \frac{x^3}{3}\right)$$

$$y_{II} = \frac{F_1}{2EI}\left(x_1^2x - \frac{x_1^3}{3}\right) + \frac{F_2}{2EI}\left(x_2x^2 - \frac{x^3}{3}\right) + \frac{F_3}{2EI}\left(x_3x^2 - \frac{x^3}{3}\right)$$

$$y_{III} = \frac{F_1}{2EI}\left(x^2{}_1x - \frac{x_1^3}{3}\right) + \frac{F_2}{2EI}\left(x_2^2x - \frac{x_2^3}{3}\right) + \frac{F_3}{2EI}\left(x_3x^2 - \frac{x^3}{3}\right)$$

The equations at the points of restraint are:

$$y_1 = \frac{F_1x_1^3}{3EI} + \frac{F_2}{2EI}\left(x_2x_1^2 - \frac{x_1^3}{3}\right) + \frac{F_3}{2EI}\left(x_3x_1^2 - \frac{x_1^3}{3}\right)$$

$$y_2 = \frac{F_1}{2EI}\left(x_1^2x_2 - \frac{x_1^3}{3}\right) + \frac{F_2}{2EI}x_2^3 + \frac{F_3}{2EI}\left(x_3x_2^2 - \frac{x_2^2}{3}\right)$$

$$y_3 = \frac{F_1}{2EI}\left(x_1^2x_3 - \frac{x_1^3}{3}\right) + \frac{F_2}{2EI}\left(x_2^2x_3 - \frac{x_2^3}{3}\right) + \frac{F_3}{3EI}x_3^3$$

In the reference fuel assembly design, restraints are applied to the can at:

x_1 = 65 in.

x_2 = 90 in.

x_3 = 115 in.

If there is to be no net movement at the restraining points, the deflection, due to the restraints, must be equal and opposite to the unrestrained thermal deflections. After substitution:

$$0.9154 \times 10^5 \frac{F_1}{EI} + 1.4435 \times 10^5 \frac{F_2}{EI} + 1.9717 \times 10^5 \frac{F_3}{EI} + 0.010 = 0$$

$$1.4435 \times 10^5 \frac{F_1}{EI} + 2.4300 \times 10^5 \frac{F_2}{EI} + 3.4425 \times 10^5 \frac{F_3}{EI} + 0.065 = 0$$

$$1.9717 \times 10^5 \frac{F_1}{EI} + 3.4425 \times 10^5 \frac{F_2}{EI} + 5.0696 \times 10^5 \frac{F_3}{EI} + 0.203 = 0$$

Solving these equations:

$$F_1 = -4.516 \times 10^{-6} \text{ EI}$$

$$F_2 = 13.006 \times 10^{-6} \text{ EI}$$

$$F_3 = -7.476 \times 10^{-6} \text{ EI}$$

It is then possible to calculate the can deflection at any point. The resulting can deflections for the reference design (three restraints) are plotted in Figures III.4-12 and III.4-14. The bowing of the rod bundles is shown also in Figure III.4-14. The upper bundle is restrained to move with the can. The lower bundle is simply supported from the can at x = 13 in. and from the cermet rods at x = 50. There are no bending moments induced in the lower bundle by this method of support. The bundle curvature is therefore the same as in the unrestrained case.

An alternate fuel assembly design uses two upper restraints at:

$$x_1 = 80 \text{ in.}$$

$$x_2 = 115 \text{ in.}$$

Again the net deflection at the support points is assumed to be equal to zero. Equations are then written:

$$1.7067 \times 10^5 \frac{F_1}{EI} + 2.8267 \times 10^5 \frac{F_2}{EI} + 0.120 = 0$$

$$2.8267 \times 10^5 \frac{F_1}{EI} + 5.0697 \times 10^5 \frac{F_2}{EI} + 0.203 = 0$$

Solving:

$$F_1 = 5.886\ EI \times 10^{-6}$$

$$F_2 = -3.681\ EI \times 10^{-6}$$

The resulting can deflection curve of this alternate approach (two restraints) is plotted in Figures III.4-13 and III.4-15.

For the alternate fuel assembly, each rod bundle is assumed to be simply supported from the can at two points. Each bundle will have the curvature resulting from the unrestrained case but will be translated, as a rigid body by the can movements.

In the same manner, the can bowing curve was determined for one restraint at x = 115 in. This is plotted, for reference purposes, in Figure III.4-13.

5. Effect of Transients and Clearances on Bowing

Previous analyses have considered only bowing under idealized conditions, i.e. steady state power and no movement of fuel assemblies at the points of restraint. To consider the effect of clearances, the equations previously derived are readily modified. If a 0.010 inch movement at the restraint points is assumed, the equations for the reference fuel assembly design become:

$$0.9154 \times 10^5 \frac{F_1}{EI} + 1.4435 \times 10^5 \frac{F_2}{EI} + 1.9717 \times 10^5 \frac{F_3}{EI} + 0 = 0$$

$$1.4435 \times 10^5 \frac{F_1}{EI} + 2.4300 \times 10^5 \frac{F_2}{EI} + 3.4425 \times 10^5 \frac{F_3}{EI} + 0.075 = 0$$

$$1.9717 \times 10^5 \frac{F_1}{EI} + 3.4425 \times 10^5 \frac{F_2}{EI} + 5.0696 \times 10^5 \frac{F_3}{EI} + 0.193 = 0$$

Upon solution, it is found that the direction of F_1 is outward, indicating that the deflection of this point is less than the 0.010 in. clearance. Since F_1 cannot be outward, no restraint can exist at this point, and F_1 must be taken as zero. The problem then reduces to that of an assembly with two upper supports. The deflection curve for this case is plotted in Figure III.4-16.

For 200% power, the equations are again modified. With $F_1 = 0$ for the reference design:

$$2.4300 \times 10^5 \frac{F_2}{EI} + 3.4425 \times 10^5 \frac{F_3}{EI} + 0.140 = 0$$

$$3.4425 \times 10^5 \frac{F_2}{EI} + 5.0696 \times 10^5 \frac{F_3}{EI} + 0.396 = 0$$

The resulting deflection curve is also plotted in Figure III.4-16.

The alternate design was studied in the same manner. The results are plotted in Figure III.4-17.

6. Restraining Forces to Bowing

The cross-section of a fuel assembly is shown in Figure III.4-3. The moment of inertia of the can:

$$I_c = \frac{5\sqrt{3}}{9} (R_o^4 - R_i^4)$$

Where R_o and R_i are 2.552 and 2.459 inches, respectively, then:

$$I_c = 5.632 \text{ in}^4$$

For austenitic stainless steel at 1000°F, the modulus of elasticity:

$$E = 22.9 \times 10^6 \text{ psi}$$

The magnitude of the restraining forces for the case of no-clearances can be calculated using expressions developed in Section B-4. For the reference design:

$$F_1 = -(4.516 \times 10^{-6})(22.9 \times 10^6)(5.632) = -582 \text{ lb.}$$

$$F_2 = (13.006 \times 10^{-6})(22.9 \times 10^6)(5.632) = 1677 \text{ lb.}$$

$$F_3 = -(7.476 \times 10^{-6})(22.9 \times 10^6)(5.632) = -964 \text{ lb.}$$

For the alternate design:

$$F_1 = (0.5886 \times 10^{-5})(22.9 \times 10^6)(5.632) = 758 \text{ lbs.}$$

$$F_2 = (0.3681 \times 10^{-5})(22.9 \times 10^6)(5.632) = -475 \text{ lbs.}$$

The moment and shear distributions, resulting from these forces for the case of no-clearances are shown in Figures III.4-18 and III.4-19. The magnitude of these moments and sheer forces would be reduced for the case where clearances are considered.

The effect of restraining of the lower rod bundle by the can was also studied. If the can and bundle act as a unit, forces will exist between the two. To estimate the magnitude of these forces, the lower bundle is considered to be a free body as shown in Figure B-3. The bending moment in the rod bundle:

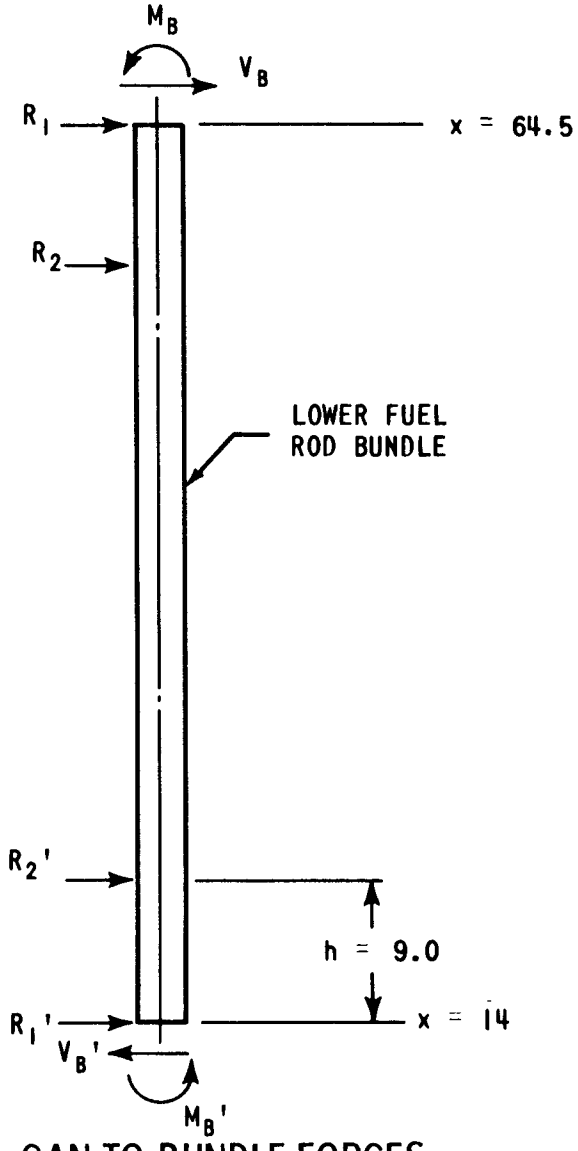
M_B
V_B
R_1
x = 64.5
R_2
LOWER FUEL
ROD BUNDLE
R_2'
h = 9.0
R_1'
x = 14
V_B'
M_B'
CAN TO BUNDLE FORCES

Figure B-3

$$M_B = M_C \frac{I_B}{I_C}$$

where subscript C refers to the assembly can and B to the fuel bundle.

The shear in the bundle:

$$V_B = V_C \frac{I_B}{I_C}$$

At the ends of the bundle, the calculated moments and shears must be reacted by can to bundle forces. With reference to Figure B-3, the reactions at the upper end of the bundle (x = 64.5):

$$R_1 = V_B + \frac{M_B}{h}$$

$$R_2 = - \frac{M_B}{h}$$

Where h = 9.0 inches is assumed to be the distance between rod to bundle contact points. The moment of inertia of the rod bundle is calculated by summing the individual rod moments of inertia. The contribution of each rod to the moment of inertia of the rod bundle:

$$I_{rod,B} = \frac{\pi}{64} (D_o^4 - D_i^4) + \frac{\pi}{4} (D_o^2 - D_i^2) d^2$$

Where:

D_o = outside diameter of cladding of fuel rod

D_i = inside diameter of cladding of fuel rod

d = distance from rod center to neutral axis of subassembly

Using the dimensions of the fuel assembly and fuel rods, the moment of inertia for the bundle is calculated. The procedure is shown in Table B-1. The result:

$$I_B = 1.832 \text{ in.}^4$$

Then:

$$R_1 = 280 \frac{(1.832)}{(5.632)} - \frac{12{,}000\ (1.832)}{(9.0)\ (5.632)} = -343 \text{ lbs.}$$

$$R_2 = \frac{12{,}000\ (1.832)}{(9.0)\ (5.632)} = 434 \text{ lbs.}$$

At the lower end (x = 14):

$$R_1' = V_B' + \frac{M_B'}{h}$$

$$R_2' = -\frac{M_B'}{h}$$

And:

$$R_1' = -280 \frac{(1.832)}{(5.632)} + \frac{2500\ (1.832)}{(9.0)\ (5.632)} = 0$$

$$R_2' = -\frac{2500\ (1.832)}{(9.0)\ (5.632)} = -91 \text{ lbs.}$$

The total restraining force on the lower rod bundle by the can:

$$F_R = |F_1| + |F_2| + |F_1'| + |F_2'| = 343 + 434 + 0 + 91 = 868 \text{ lbs.}$$

Table B-1

Rod Bundle Moment of Inertia

$$I_{rod} = \frac{\pi}{64}(0.300^4 - 0.280^4)$$

$$= 9.589 \times 10^{-5} \text{ in}^4$$

$$A_{rod} = \frac{\pi}{4}(0.300^2 - 0.280^2)$$

$$= 9.032 \times 10^{-3} \text{ in}^2$$

Refering to Figure III.4-3

Row	No. of rods n	d	$9.032 \times 10^{-3} d^2 n$
0	13	0	0
1	24	.369	.0295
2	22	.738	.1033
3	20	1.107	.2214
4	18	1.476	.3542
5	16	1.845	.4919
6	14	2.214	.6198
		Total	1.8201

Total Moment of Inertia

$$I_B = 127(9.589 \times 10^{-5}) + 1.8201 = 1.832 \text{ in}^4$$

APPENDIX C

FUEL CLAD STRESSES AND STRAINS

1. Introduction

The controlled expansion fuel assembly consists of an upper and a lower half-length bundle of fuel rods which are attached to a central full-length assembly of cermet fuel rods. The fuel rods of each bundle are brazed together by intermediate spacer ferrules.

Each fuel rod is vented to the sodium coolant. Venting eliminates clad stresses due to coolant or fission gas pressure. Stresses and strains arise in the fuel cladding from:

a. temperature gradients.
b. static weight.
c. flow drag.
d. flow induced vibration.

The subsequent sections discuss in detail the stresses and strains due to these loadings and relate them to appropriate failure criteria. When appropriate, clad thinning with life time is considered.

In the subsequent discussion:

1. Region 1 refers to the second ring in the core module which consists of six fuel assemblies,
2. Region 2 refers to the third ring in the core module which consists of twelve fuel assemblies, and
3. Region 3 refers to the fourth ring in the core module which consists of eighteen fuel assemblies.

Unless otherwise designated, units of inches, pounds, seconds and Fahrenheit degrees are used in the subsequent analyses.

2. Restraint to Bundle Bowing[1]

The brazed bundle is subject to a core radial variation in coolant temperature. The temperature gradient in the lower bundle is small and the bundle is allowed to bow freely. The upper bundle gradient is much greater, and the bundle must be constrained by the fuel assembly can to remain straight. This constraint results in bending strains across the bundle treated as a beam. Near the bundle ends the bending strain is zero and the ferrules are subjected to shear stresses. The ferrule shear area is four to five times the clad wall area and is therefore stronger than the clad.

Calculations

Axial strain, $\varepsilon_z = \pm \frac{1}{2} \alpha\Delta T$, top bundle, away from bundle ends, outer bundle edge.

α = clad coefficient of thermal expansion; ΔT = maximum bundle temperature gradient in radial direction.

$\varepsilon_z^{\prime}$ = 0, lower bundle - no restraint.

Summary of Results

	Region I				Region II				Region III			
	Top Bundle		Lower Bundle		Top Bundle		Lower Bundle		Top Bundle		Lower Bundle	
	Max.	Min.	Max.	Min.	Max.	Min.	Max.	Min.	Max.	Min.	Max.	Min.
$\alpha \times 10^6$	11.2	9.2	-	-	11.2	9.2	-	-	11.1	9.1	-	-
ΔT	20.8	0	-	-	50.0	0	-	-	67.6	0	-	-
% Mixing in Assembly	0	100	0	100	0	100	0	100	0	100	0	100
$\varepsilon_z \times 10^6$	$\pm$117	0	0	0	$\pm$280	0	0	0	$\pm$375	0	0	0

3. Non-Linear Radial Bundle Temperature Gradient[2]

The core radial coolant temperature across a bundle is not linear but has a quadratic component. This quadratic term in the temperature profile generates stresses and strains equivalent to those in a beam with uniform internal heat generation. Terms α and ε are previously defined.

Calculations

$$\varepsilon = \pm \frac{1}{2} \alpha \Delta T \left(\frac{4}{3} \frac{\Delta T_1}{\Delta T} - \frac{2}{3}\right)$$, away from bundle ends, outer bundle edges.

ΔT_1 - center temperature minus outer temperature in radial direction.

ΔT - temperature difference across bundle in radial direction.

Summary of Results

	Region I				Region II				Region III			
	Top Bundle		Lower Bundle		Top Bundle		Lower Bundle		Top Bundle		Lower Bundle	
	Max.	Min.	Max.	Min.	Max.	Min.	Max.	Min.	Max.	Min.	Min.	Max.
$\alpha \times 10^6$	11.2	9.2	10.9	9.0	11.2	9.2	10.9	9.0	11.1	9.1	10.9	9.0
% Mixing in Assembly	0	100	0	100	0	100	0	100	0	100	0	100
ΔT	20.8	0	10.4	0	50.0	0	25.0	0	67.6	0	33.8	0
$\frac{\Delta T_1}{\Delta T}$	.61	0	.61	0	.55	0	.55	0	.54	0	.54	0
$\pm \varepsilon_z \times 10^6$	17	0	8.3	0	18.8	0	9.1	0	19.9	0	9.8	0

4. Clad Radial Temperature Gradient[1]

The clad heat flux results in a temperature gradient across the clad wall of the fuel and results in clad strain due to internal restraint. ε and α are as previously defined and μ is the clad Poisson's ratio.

Calculations

$$\varepsilon_z = \varepsilon_t = \pm \frac{1}{2} \frac{\alpha \Delta T}{1 - \mu},$$

ΔT = radial temperature drop across carbide fuel clad wall in core mid-plane, where the maximum heat flux exists.

μ = 0.3 min., 0.4 max.

Summary of Results

	Region I				Region II				Region III			
	Top Bundle		Lower Bundle		Top Bundle		Lower Bundle		Top Bundle		Lower Bundle	
	Max.	Min.	Max.	Min.	Max.	Min.	Max.	Min.	Max.	Min.	Max.	Min.
q x 10^6	11.2	9.2	10.9	9.0	11.2	9.2	10.9	9.0	11.1	9.1	10.	9.0
ΔT	115	93	115	93	104	80	104	80	85	62	85	62
$\pm \varepsilon_z = \varepsilon_t$ x 10^6	1073	611	1044	598	971	526	945	514	786	403	772	399

5. Clad Axial Temperature Gradient[3]

The clad temperature varies non-linearly with axial distance. Stresses and strains arise due to the non-linear terms in the axial temperature profile due to internal restraint. ε_z and α are as previously defined; ε_t is the tangential component of clad strain.

Calculations

$\varepsilon_z = \pm 3 \alpha T_1 \bar{R} t/4\iota^2$, where T_1 - axial temperature rise along clad.

ι - length of core.

$\varepsilon_t = \mu\varepsilon_z$

R - mean clad radius

t - clad wall thickness

μ - Poisson's Ratio

Summary of Results (location of ε_z and ε_t is at core-axial blanket interface)

	Region I				Region II				Region III			
	Top Bundle		Lower Bundle		Top Bundle		Lower Bundle		Top Bundle		Lower Bundle	
	Max.	Min.	Max.	Min.	Max.	Min.	Max.	Min.	Max.	Min.	Max.	Min.
$\alpha \times 10^6$	11.2	9.2	10.9	9.0	11.2	9.2	10.9	9.0	11.1	9.1	10.9	9.0
T_1	146	136	146	136	155	133	155	133	135	102	135	102
$\bar{R}$	.145	.145	.145	.145	.145	.145	.145	.145	.145	.145	.145	.145
t	.01	.01	.01	.01	.01	.01	.01	.01	.01	.01	.01	.01
ι	37	37	37	37	37	37	37	37	37	37	37	37
μ	.4	.3	.4	.3	.4	.3	.4	.3	.4	.3	.4	.3
$\pm \varepsilon_z$	Less than 10^{-8} in/in ----------											
$\pm \varepsilon_t$	Less than 10^{-9} in/in ----------											
Actual Temp, °F	1142	1122	850	850	1160	1115	850	850	1120	1054	850	850

6. Static Weight

Each BCEX fuel bundle is supported at its ends by 48 of 120 fuel rods. For completeness of analysis, the stresses and strains in the cladding due to gravity are calculated below:

Calculation

No. of rods	120
Rod length	49.775 in.
Clad vol./in.	.0091 $in.^3$/ in.
Clad density	.29 $lb./in^3$
Clad wt/in.	.0026 $lb./in.^3$
Fuel vol./in.	.0536 $in.^3$/in.
Fuel density	.48 $lb./in.^3$
Fuel wt./in.	.0258 lb./in.
Rod wt./in.	.0283 lb./in.
Bundle wt.	170 lb.
No. Rods supporting bundle	54
Nominal clad wall	.010 in.
Min. clad wall, end of life	.006 in.
Nom. clad support area	.492 $in.^2$
Min. clad support area	.295 $in.^2$
Nom. static wt. stress	345 psi
Max. static wt. stress	575 psi
Young's Modulus Elasticity	20×10^6 psi
Nom. static wt. strain	17×10^{-6}
Max. static wt. strain	29×10^{-6}

7. Flow Drag Less Static Weight

This calculation is similar to C-6, but in this case, it takes into account stresses and strains in the 48 fuel rod clads which support the bundle due to pressure drop across the bundle.

Calculations

Drag Force = No rods x area per rod x ΔP along rod

$= 120 \times \frac{\pi}{4} \times .3^2 \ \Delta P = 8.48 \ \Delta P$

Clad Stress = Drag force/area per clad x no. clads loaded

= 17.2 ΔP, beginning of life

= 28.7 ΔP, end of life

Elastic Modulus = 20×10^6 psi

Summary of Results

	Region I				Region II				Region III			
	Top Bundle		Lower Bundle		Top Bundle		Lower Bundle		Top Bundle		Lower Bundle	
	Max.	Min.	Max.	Min.	Max.	Min.	Max.	Min.	Max.	Min.	Max.	Min.
ΔP	38	38	37	37	30.4	30.4	29.6	29.6	27.8	27.8	27.2	27.2
Drag Stress	-1,090	-655	+1,060	+635	-870	-525	+850	+510	-800	-480	+780	+470
Static Wt.	+575	+345	-575	-345	+575	+345	-575	-345	+575	+345	-575	-345
Net Stress	-515	-310	+485	+290	-295	-180	+275	+165	-225	-135	+205	+125
Net Strain, x 10^{+6}	-26	-16	+24	+15	-15	-9	+14	+8	-12	-7	+10	+7

8. Rod Vibration in Parallel Flow[4]

Flow induced fuel rod vibration between spacer ferrules results in an oscillating component of clad strain at the span natural frequency. The fuel rod span is conservatively taken to be a simply supported beam with a sine function mode shape.

Calculations

B - Burgreen Parameter = $K_1 L^2 \sqrt{\rho}\ V^3 / 10^9 \sqrt{EI}\ \nu\omega$

K_1 - 5, for pinned ends

ρ - sodium density = 750×10^{-7} lb.sec.^{2}/in.^{4}

ν - sodium kinematic viscosity = 440×10^{-6} in.^{2}/sec.

L - Span length between ferrules = 7 in.

ω - Span natural freq., rad/sec = $\Pi^2 \sqrt{gEI/wL^4}$

D_o - rod O.D = .300 in.

w - rod weight/inch = .0283 lb/in.

A - Amplitude of vibration, in.

D_e - Hydraulic dia. = 0.35 in.

ε_z - $\Pi^2 A D_o / 2L^2$; clad strain

V - Coolant flow velocity, in/sec

EI - Rod stiffness, lb-in.^{2}

Summary of Results

	Region I				Region II				Region III			
	Top Bundle		Lower Bundle		Top Bundle		Lower Bundle		Top Bundle		Lower Bundle	
	Min.	Max.	Min.	Max.	Min.	Max.	Min.	Max.	Min.	Max.	Min.	Max.
V	450	440	440	430	396	386	386	377	373	367	367	360
E x 10^{-6}	24	20	24	20	24	20	24	20	24	20	24	20
I x 10^5	9.6	5.5	9.6	5.5	9.6	5.5	9.6	5.5	9.6	5.5	9.6	5.5
ω	1126	780	1126	780	1126	780	1126	780	1126	780	1126	780
B	.0081	.0160	.0076	.0149	.0055	.0108	.0051	.0100	.0046	.0092	.0044	.0087
A/D_e	.0057	.010	.0055	.0090	.0040	.0075	.0040	.0070	.0037	.0063	.0036	.0065
A(max)	.002	.004	.002	.003	.001	.003	.001	.002	.001	.002	.001	.002
$\pm\ \varepsilon_z$ x 10^6	60	120	60	90	30	90	30	60	30	60	30	60

9. Bundle Vibration in Parallel Flow[5]

As the fuel rod vibrates between spacer ferrules because of flow excitation, so does the entire bundle vibrate because of flow excitation. The bundle is conservatively taken to be a beam simply supported at each end.

Calculations

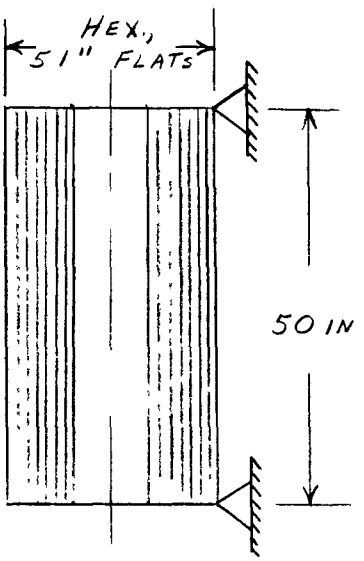

$$A = 2.94\,\alpha^{-4}\left[\frac{M\rho D_h}{EI}\right]^{.8}\frac{L^{3.2}V^{2.4}}{D_r^{.6}}\,\frac{\beta^{2/3}}{1+4\beta}\,\frac{1}{1+2\mu^2}$$

$$\mu^2 = M V^2 L^2/EI, \text{ dimensionless}$$

$$\beta = [1 + m/M]^{-1}$$

Results

A	=	max. bundle amplitude, in.	5×10^{-5}
D_r	=	rod dia., in.	0.30
α^2	=	normal mode eigenvalue	9.87
L	=	bundle length, in.	50
m	=	rod mass per inch of rod, lb-sec^2/in.^{2}	7.3×10^{-5}
M	=	fluid virtual mass per inch of rod, lb-sec^2/in.^{2}	5.3×10^{-6}
V	=	fluid velocity, in./sec	440
EI	=	bundle stiffness, lb-in.^{2}	4×10^{7}
ρ	=	fluid density, lb. sec^2/in.^{4}	7.5×10^{-5}
D_h	=	rod hydraulic diameter, in.	0.35

10. References

1. Roark, "Formulas for Stress and Strain", Third Edition, McGraw-Hill 1954, pg. 335, No. 4.

2. Hankel, "Stress and Temperature Distributions", pg. 168, Nucleonics, Vol. 18, No. 11, November 1960.

3. Kent, "Thermal Stresses in Thin-Walled Cylinders", Trans. ASME APM-53-13.

4. Burgreen, et al, "Vibration of Rods Induced by Water in Parallel Flow", Trans. ASME, Paper No. 57-A-94, Figure 7.

5. Paidoussis, "The Amplitude of Flow-Induced Vibration of Cylinders in Axial Flow", AECL-2225, Chalk River, Ontario, March 1965.

APPENDIX D

CERMET STRESSES AND STRAINS

1. Introduction

The cermet rod design was examined for all possible failure modes. Failure may occur from excessive distortion that would alter the cermet performance characteristics, or from formation of cracks. Distortion may arise from assymetric thermal gradients or forces. Cracks may develop from excessive static, dynamic, or creep strains.

The subsequent sections discuss the cermet stresses and strains due to a variety of causes.

2. Nomenclature

d_{10} - inside diameter of hypothetical fission gas space

d_{20} - outside diameter of hypothetical fission gas space = actual fuel particle diameter

d_{30} - inside diameter of hypothetical spherical shell which contains fission gas

$\dot{N}$ - volumetric fuel swelling rate

P - fission gas pressure

R - fission gas ideal gas constant

S - average fuel particle spacing or pitch; also steady stress

T - temperature

t - wall thickness of hypothetical spherical shell which contains fission gas or minimum ligament thickness

v - secondary creep rate

V - void volume at time τ

V_o - initial fission gas void volume

W - weight of fission gas released to void volume

α - cermet coefficient of thermal expansion

ΔV_1 - change in fission gas volume due to steel matrix creep

ΔV_2 - change in fission gas volume due to fuel swelling

ε - matrix strain

μ - Poisson's ratio = 0.3

ρ - actual fuel density

ρ_τ - theoretical fuel density

σ - stress

σ_c - stress based on original void volume

τ - time

$\xi \equiv V/V_o$

3. Fuel Swelling and Fission Gas Pressure

An analytical model is devised which relates secondary creep strain in the stainless steel matrix to fuel swelling and fission gas pressure. The resulting, first order, non-linear, differential equation is not solved and, therefore, the analysis is not complete. The material is included in this report as a reference for possible future work.

The cermet is idealized to consist of a uniform dispersion of spheroidal fuel particles in an isotropic continuous structure of stainless steel. The porous fuel particle, which just fills a spherical cavity in the stainless steel, is replaced by a smaller particle of 100% theoretical density surrounded by a spherical shell of fission gas space.

A layer of stainless steel bounding the fission gas space is assumed to be damaged by fission product recoil atoms and unable to sustain tangential stresses. The remaining undamaged stainless steel associated with a fuel particle is supposed to be a spherical cell subjected to internal gas pressure only, no other loading being considered in this analysis.

Fission gas release and fuel particle swelling are assumed to be proportional to time. Gas pressure results in tangential stresses in the steel sphere. The steel sphere creeps due to these stresses at the temperatures of interest.

The following sketch illustrates this model.

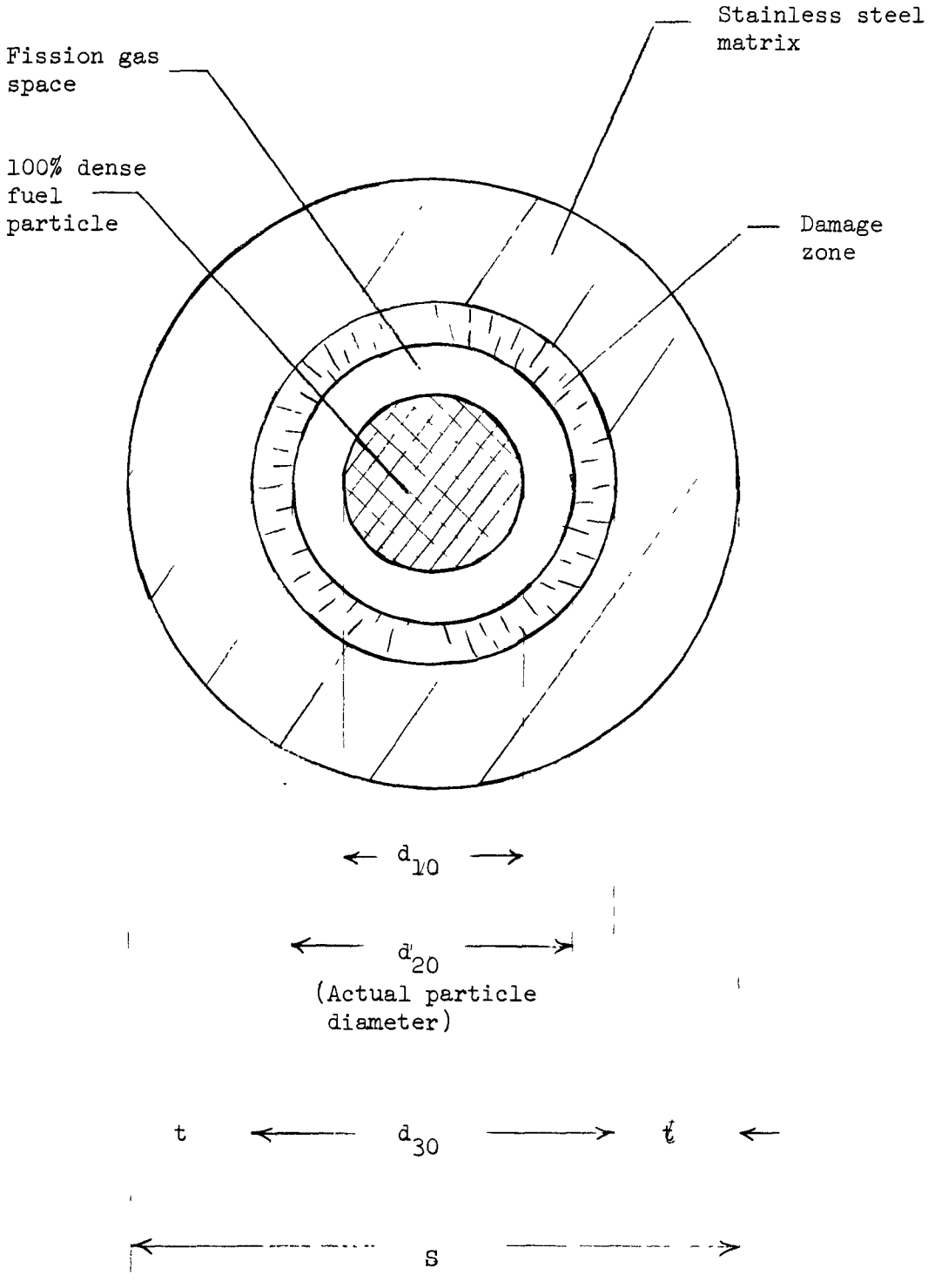

The fission gas volume is given by:

$$V = V_o + \Delta V_1 - \Delta V_2$$

and:

$$\Delta V_1 = 3\varepsilon \frac{\pi}{6} d_{20}^3 = 3\dot{\varepsilon} \frac{\pi}{6} d_{20}^3 \tau$$

$$\Delta V_2 = \dot{N} \frac{\pi}{6} d_{10}^3 \tau$$

Thus:

$$V = V_o + 3\varepsilon \frac{\pi}{6} d_{20}^3 - \dot{N} \frac{\pi}{6} d_{10}^3 \tau \qquad \text{(D-1)}$$

Since by definition

$$V = \frac{V - V_o}{\tau}$$

$$\dot{V} = 3\dot{\varepsilon} \frac{\pi}{6} d_{20}^3 - \dot{N} \frac{\pi}{6} d_{10}^3$$

Since:

$$V_o = \frac{\pi}{6} (d_{20}^3 - d_{10}^3)$$

Then:

$$\frac{\dot{V}}{V_o} = \frac{3\dot{\varepsilon}}{1 - (d_{10}/d_{20})^3} + \frac{\dot{N}}{1 - (d_{20}/d_{10})^3}$$

As idealized:

$$\rho d_{20}^3 = \rho_\tau d_{10}^3$$

Thus:

$$\frac{\dot{V}}{V_o} = \frac{3\dot{\varepsilon}}{1 - \rho/\rho_\tau} + \frac{\dot{N}}{1 - \rho_\tau/\rho} \qquad \text{(D-2)}$$

From Figure III.4-11; the matrix strain in inches per inch is:

$$\dot{\varepsilon} = a\,\sigma^{b} \tag{D-3}$$

where:

$$a = 1.66 \times 10^{23}\,(3.445 \times 10^{-8})^{b}$$

and:

$$b = 14{,}620/T, \text{ where T is in } {}^{\circ}R$$

Substituting (D-3) into (D-2)

$$\frac{\dot{V}}{V_o} = \frac{3a\,\sigma^{b}}{1 - \rho/\rho_\tau} + \frac{\dot{N}}{1 - \rho_\tau/\rho} \tag{D-4}$$

For a thin spherical shell:

$$\sigma = Pd_{30}/4t \tag{D-5}$$

Substituting (D-5) into (D-4):

$$\frac{\dot{V}}{V_o} = \frac{3a\,(d_{30}/4t)^{b}P^{b}}{1 - \rho/\rho_\tau} + \frac{\dot{N}}{1 - \rho_\tau/\rho} \tag{D-6}$$

From Ideal Gas Law:

$$\begin{aligned} P &= WRT/V \\ W &= \dot{W}\tau \\ P &= \dot{W}RT\,\tau/V \end{aligned} \tag{D-7}$$

Substituting (D-7) into (D-6):

$$\frac{\dot{V}}{V_o} = \frac{3a\,(d_{30}/4t)^{b}}{1 - \rho/\rho_\tau}\left(\frac{\dot{W}RT_\tau}{V}\right)^{b} + \frac{\dot{N}}{1 - \rho_\tau/\rho}$$

$$\frac{\dot{V}}{V_o} = \frac{3a\ (d_{30}\dot{W}RT/4t)^b}{1 - \rho/\rho_\tau} \left(\frac{\tau}{V}\right)^b + \frac{\dot{N}}{1 - \rho_\tau/\rho}$$

$$\frac{\dot{V}}{V_o} = \frac{3a\ (d_{30}\dot{W}RT/4tV_o)^b}{1 - \rho/\rho_\tau} \left(\frac{\tau}{V/V_o}\right)^b + \frac{\dot{N}}{1 - \rho_\tau/\rho}$$

Since:

$$\dot{\sigma}_c = d_{30}\dot{W}RT/4tV_o$$

$$\frac{\dot{V}}{V_o} = \frac{3a\ \dot{\sigma}_c^{\ b}}{1 - \rho/\rho_\tau} \left(\frac{\tau}{V/V_o}\right)^b + \frac{\dot{N}}{1 - \rho_\tau/\rho}$$

Define:

$$\xi \equiv V/V_o; \quad \frac{d\varepsilon}{d\tau} \equiv \dot{V}/V_o$$

and

$$A \equiv \frac{3a\ \dot{\sigma}_c^{\ b}}{1 - \rho/\rho_\tau} \quad ; \quad B \equiv - \frac{\dot{N}}{1 - \rho_\tau/\rho}$$

The following differential equation is obtained:

$$\frac{d\xi}{d\tau} = A\ \xi^{-b}\ \tau^b - B$$

or

$$\xi^b \frac{d\xi}{d\tau} + B\xi^b = A\tau^b \qquad \text{(D-8)}$$

The boundary conditions for the non-linear differential equation (D-8) are:

At $\tau = 0$, $\frac{d\xi}{d\tau} = -B$

At $\tau \to \infty$, ξ = const. x τ

The solution to (D-8) can be portrayed as follows:

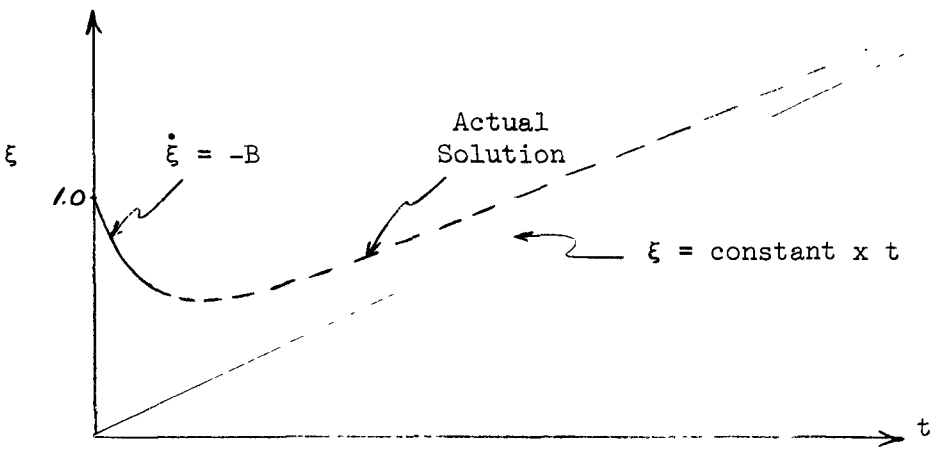

Substituting the solution to (D-8) into (D-1) yields matrix strain versus time. Knowing the maximum allowable strain and desired lifetime enables the designer to select proper cermet design parameters such as ceramic particle size, volume percent and percent of theoretical density.

APPENDIX E

SAMPLE OF WESTINGHOUSE FORE COMPUTER PROGRAM OUTPUT

This appendix presents a partial reproduction of the computer output from the Westinghouse modified FORE code used to study the loss of all electrical power to the primary pumps. This incident is discussed in Section III.5.5.3. This section is limited to a brief discussion of the output listing itself.

The first page of the output lists the power (MW) and integrated energy (BTU/ft^3) as a function of time (sec.). The clad, fuel and/or cermet (BCEX) changes in length (ft.) are also listed as a function of time. Because the fuel bundle is split, the changes in the various lengths were calculated separately for the upper and the lower half-length bundles, and are so tabulated.

The second page of the program output lists all the reactivity feedbacks as a function of time. The worth of the outward expansion of the cermet rod is listed under the heading of Expansion CEX, and the net worth of BCEX is listed under the heading of Axial Total. The sodium density, radial expansion, and Doppler feedbacks are tabulated under their respective headings. All the temperature dependent feedbacks are summed, and the total is listed under the heading of Feedback, which is then added to the input reactivity (under the heading of Programmed) to give the total reactivity (Total) influencing the core as a function of time.

The third page lists the fuel, clad, coolant, and cermet core average temperatures (arithmetic average of all the axial sections) in the average and hot channels as a function of time.

Pages four through twenty-seven list the fuel and cermet temperature data as a function of time in the six axial sections for both the average and hot channels. For each axial section, the fuel and cermet temperatures are printed at five radial node points (centerline to boundary). The radial average of all the calculated node points is also calculated and listed. The fuel clad, cermet clad, coolant, and structure temperatures for the average and hot channels are also listed on these pages.

POWER AND ENERGY FACTORS

TIME	STEP	ENERGY	POWER	LENGTH CLAD	LOWER FUEL	HALF CEX	LENGTH CLAD	UPPER FUEL	HALF CEX
0.	0	0.	4.1546CE 02	0.	0.	0.	0.	0.	0.
0.17750	38	-1.76C56E CC	4.15537E 02	2.8027E-05	0.	2.9575E-06	4.9661E-05	0.	5.3610E-06
0.55875	128	-3.54E69E C1	4.1336CE 02	5.4669E-05	0.	2.6697E-05	1.7178E-C4	0.	6.9855E-05
0.62125	143	-4.764C4E C1	4.13465E 02	1.0718E-04	0.	3.2017E-05	3.1258E-C4	0.	8.6428E-05
0.68375	158	-6.17691E C1	4.12613E 02	8.5610E-05	0.	3.7641E-05	2.6114E-C4	0.	1.0447E-04
0.86875	203	-1.193C1E C2	4.11679E 02	1.5276E-04	0.	5.5060E-05	4.8957E-C4	0.	1.6477E-04
0.93125	218	-1.44C57E C2	4.107C2E 02	1.3661E-04	0.	6.1126E-05	4.2601E-C4	0.	1.8726E-04
0.99375	233	-1.72124E C2	4.10594E 02	1.7218E-04	0.	6.7084E-05	5.6962E-04	0.	2.1042E-04
1.05625	248	-2.02584E C2	4.09663E 02	1.6264E-04	0.	7.3038E-05	5.2052E-C4	0.	2.3433E-04
1.08625	255	-2.19131E C2	4.09827E 02	1.9009E-04	0.	7.5816E-05	6.4626E-C4	0.	2.4594E-04
1.12250	263	-2.39274E C2	4.09119E 02	1.7391E-04	0.	7.9218E-05	5.6395E-04	0.	2.6023E-04
1.49750	355	-5.14729E C2	4.054C9E 02	2.3665E-04	0.	1.1028E-C4	8.3049E-C4	0.	4.1181E-04
1.84250	441	-8.78C97E C2	4.01545E 02	2.9608E-04	0.	1.3628E-04	1.0783E-03	0.	5.5992E-04
2.17250	521	-1.33326E C3	3.98530E 02	3.4929E-04	0.	1.6051E-04	1.3060E-03	0.	7.1485E-04
2.52750	608	-1.94678E C3	3.94857E 02	3.9829E-04	0.	1.8141E-04	1.5551E-03	0.	8.8275E-04
2.91999	702	-2.77449E C3	3.90408E 02	4.4296E-04	0.	1.9819E-04	1.7944E-03	0.	1.0620E-03
3.29749	793	-3.71649E C3	3.86018E 02	4.9068E-04	0.	2.1149E-04	1.9798E-03	0.	1.2301E-03
3.63999	876	-4.65959E C3	3.82227E 02	5.4494E-04	0.	2.2560E-04	2.2742E-03	0.	1.3919E-03
3.70249	891	-4.85184E C3	3.81300E 02	5.4999E-04	0.	2.2788E-04	2.2527E-03	0.	1.4217E-03
3.76499	906	-5.08891E C3	3.80753E 02	5.6042E-04	0.	2.2999E-04	2.3530E-03	0.	1.4512E-03
3.82749	921	-5.29CC0E C3	3.79843E 02	5.6398E-04	0.	2.3185E-04	2.3301E-03	0.	1.4805E-03
3.88999	936	-5.49536E C3	3.79300E 02	5.7321E-04	0.	2.3349E-04	2.4260E-03	0.	1.5093E-03
3.95249	951	-5.7047CE C3	3.78402E 02	5.7694E-04	0.	2.3501E-04	2.4029E-03	0.	1.5378E-03
4.01499	966	-5.91825E C3	3.77863E 02	5.8584E-04	0.	2.3638E-04	2.4964E-03	0.	1.5660E-03
4.07749	981	-6.13574E C3	3.76977E 02	5.8936E-04	0.	2.3763E-04	2.4729E-03	0.	1.5939E-03
4.13999	996	-6.35738E C3	3.76445E 02	5.9783E-04	0.	2.3873E-04	2.5644E-03	0.	1.6215E-03
4.20249	1011	-6.58250E C3	3.75573E 02	6.0108E-04	0.	2.3972E-04	2.5403E-03	0.	1.6487E-03
4.26499	1026	-6.81250E C3	3.75048E 02	6.0894E-04	0.	2.4056E-04	2.6298E-03	0.	1.6756E-03
4.32749	1041	-7.04588E C3	3.74199E 02	6.1046E-04	0.	2.4111E-04	2.6028E-03	0.	1.7019E-03
4.33499	1044	-7.07422E C3	3.74449E 02	6.1235E-04	0.	2.4115E-04	2.6386E-03	0.	1.7050E-03
4.38999	1056	-7.28327E C3	3.73687E 02	6.1750E-04	0.	2.4148E-04	2.6893E-03	0.	1.7276E-03
4.45249	1071	-7.52439E C3	3.72847E 02	6.2026E-04	0.	2.4182E-04	2.6623E-03	0.	1.7530E-03
4.51499	1086	-7.76945E C3	3.72344E 02	6.2808E-04	0.	2.4213E-04	2.7495E-03	0.	1.7782E-03
4.57749	1101	-8.01819E C3	3.71510E 02	6.3156E-04	0.	2.4248E-04	2.7231E-03	0.	1.8032E-03
4.63999	1116	-8.27086E C3	3.71009E 02	6.4001E-04	0.	2.4284E-04	2.8117E-03	0.	1.8281E-03
4.70249	1131	-8.52721E C3	3.70175E 02	6.4420E-04	0.	2.4328E-04	2.7862E-03	0.	1.8530E-03
4.76499	1146	-8.78749E C3	3.69673E 02	6.5335E-04	0.	2.4376E-04	2.8768E-03	0.	1.8779E-03
4.82749	1161	-9.05147E C3	3.68832E 02	6.5853E-04	0.	2.4440E-04	2.8526E-03	0.	1.9030E-03
4.88999	1176	-9.31943E 03	3.68324E 02	6.6849E-04	0.	2.4512E-04	2.9461E-03	0.	1.9283E-03
4.95249	1191	-9.59114E C3	3.67473E 02	6.7418E-04	0.	2.4597E-04	2.9225E-03	0.	1.9538E-03

TIME	REACTIVITY TOTAL	PROGRAMMED	FEEDBACK	DOPPLER	RADIAL EXPANSION	DENSITIES	AXIAL EXPANSION TOTAL	CEX
0.	1.00000E 00	1.00000E 00	0.	0.	0.	0.	0.	0.
0.17750	1.00000E 00	1.00000E 00	1.1748E-08	-2.3937E-07	0.	-3.4567E-06	3.7078E-06	-1.0570E-06
0.55875	9.99995E-01	1.00000E 00	-2.0276E-05	-5.5336E-06	0.	-1.6363E-05	1.6204E-06	-1.2269E-05
0.62125	9.99985E-01	1.00000E 00	-1.3839E-05	-5.3828E-06	0.	-1.9151E-05	1.0695E-05	-1.5050E-05
0.68375	9.99985E-01	1.00000E 00	-2.5450E-05	-7.2520E-06	0.	-2.1407E-05	3.2097E-06	-1.8058E-05
0.86875	9.99966E-01	1.00000E 00	-2.7031E-05	-9.0613E-06	0.	-2.9432E-05	1.1463E-05	-2.7934E-05
0.93125	9.99957E-01	1.00000E 00	-3.9790E-05	-1.1000E-05	0.	-3.1735E-05	2.9458E-06	-3.1561E-05
0.99375	9.99966E-01	1.00000E 00	-3.5350E-05	-1.1019E-05	0.	-3.4566E-05	1.0235E-05	-3.5262E-05
1.05625	9.99956E-01	1.00000E 00	-4.6762E-05	-1.2755E-05	0.	-3.6851E-05	2.8445E-06	-3.9056E-05
1.08625	9.99955E-01	1.00000E 00	-4.0179E-05	-1.2260E-05	0.	-3.8330E-05	1.0411E-05	-4.0884E-05
1.12250	9.99966E-01	1.00000E 00	-5.1090E-05	-1.3715E-05	0.	-3.9504E-05	2.1228E-06	-4.3132E-05
1.49750	9.99935E-01	1.00000E 00	-7.2291E-05	-1.8108E-05	0.	-5.3294E-05	-8.8882E-07	-6.6341E-05
1.84250	9.99915E-01	1.00000E 00	-9.3309E-05	-2.1734E-05	0.	-6.7407E-05	-4.1682E-06	-8.8464E-05
2.17250	9.99895E-01	1.00000E 00	-1.1633E-04	-2.5423E-05	0.	-8.1204E-05	-9.7071E-06	-1.1123E-04
2.52750	9.99866E-01	1.00000E 00	-1.3847E-04	-2.8551E-05	0.	-9.4509E-05	-1.5410E-05	-1.3522E-04
2.91999	9.99844E-01	1.00000E 00	-1.6199E-04	-3.1238E-05	0.	-1.0784E-04	-2.2912E-05	-1.6013E-04
3.29749	9.99824E-01	1.00000E 00	-1.8715E-04	-3.3771E-05	0.	-1.2172E-04	-3.1652E-05	-1.8318E-04
3.63999	9.99794E-01	1.00000E 00	-2.0422E-04	-3.5907E-05	0.	-1.3568E-04	-3.2627E-05	-2.0553E-04
3.70249	9.99795E-01	1.00000E 00	-2.1232E-04	-3.6755E-05	0.	-1.3786E-04	-3.7703E-05	-2.0960E-04
3.76499	9.99786E-01	1.00000E 00	-2.1196E-04	-3.6788E-05	0.	-1.4024E-04	-3.4934E-05	-2.1363E-04
3.82749	9.99786E-01	1.00000E 00	-2.1983E-04	-3.7574E-05	0.	-1.4218E-04	-4.0073E-05	-2.1758E-04
3.88999	9.99786E-01	1.00000E 00	-2.1947E-04	-3.7559E-05	0.	-1.4442E-04	-3.7497E-05	-2.2145E-04
3.95249	9.99786E-01	1.00000E 00	-2.2711E-04	-3.8281E-05	0.	-1.4632E-04	-4.2507E-05	-2.2527E-04
4.01499	9.99776E-01	1.00000E 00	-2.2671E-04	-3.8233E-05	0.	-1.4850E-04	-3.9980E-05	-2.2902E-04
4.07749	9.99776E-01	1.00000E 00	-2.3415E-04	-3.8907E-05	0.	-1.5034E-04	-4.4908E-05	-2.3273E-04
4.13999	9.99766E-01	1.00000E 00	-2.3366E-04	-3.8828E-05	0.	-1.5244E-04	-4.2418E-05	-2.3637E-04
4.20249	9.99766E-01	1.00000E 00	-2.4095E-04	-3.9458E-05	0.	-1.5421E-04	-4.7284E-05	-2.3995E-04
4.26499	9.99766E-01	1.00000E 00	-2.4033E-04	-3.9349E-05	0.	-1.5615E-04	-4.4830E-05	-2.4347E-04
4.32749	9.99766E-01	1.00000E 00	-2.4740E-04	-3.9920E-05	0.	-1.5767E-04	-4.9810E-05	-2.4689E-04
4.33499	9.99756E-01	1.00000E 00	-2.4559E-04	-3.9741E-05	0.	-1.5795E-04	-4.7894E-05	-2.4729E-04
4.38999	9.99756E-01	1.00000E 00	-2.4669E-04	-3.9749E-05	0.	-1.5955E-04	-4.7385E-05	-2.5021E-04
4.45249	9.99756E-01	1.00000E 00	-2.5361E-04	-4.0276E-05	0.	-1.6119E-04	-5.2149E-05	-2.5348E-04
4.51499	9.99746E-01	1.00000E 00	-2.5280E-04	-4.0089E-05	0.	-1.6316E-04	-4.9555E-05	-2.5671E-04
4.57749	9.99746E-01	1.00000E 00	-2.5967E-04	-4.0612E-05	0.	-1.6488E-04	-5.4180E-05	-2.5993E-04
4.63999	9.99746E-01	1.00000E 00	-2.5881E-04	-4.0432E-05	0.	-1.6694E-04	-5.1436E-05	-2.6314E-04
4.70249	9.99746E-01	1.00000E 00	-2.6570E-04	-4.0969E-05	0.	-1.6877E-04	-5.5966E-05	-2.6636E-04
4.76499	9.99736E-01	1.00000E 00	-2.6484E-04	-4.0809E-05	0.	-1.7096E-04	-5.3072E-05	-2.6959E-04
4.82749	9.99736E-01	1.00000E 00	-2.7182E-04	-4.1380E-05	0.	-1.7293E-04	-5.7516E-05	-2.7286E-04
4.88999	9.99736E-01	1.00000E 00	-2.7097E-04	-4.1255E-05	0.	-1.7524E-04	-5.4470E-05	-2.7617E-04
4.95249	9.99736E-01	1.00000E 00	-2.7810E-04	-4.1870E-05	0.	-1.7731E-04	-5.8921E-05	-2.7952E-04

	AVERAGE CHANNEL - AVERAGE TEMPERATURE				HOT CHANNEL - AVERAGE TEMPERATURE			
TIME	FUEL	CLAD	COOLANT	CERMET	FUEL	CLAD	COOLANT	CERMET
0.	1.2846E 03	1.0535E 03	9.8454E 02	1.1629E 03	1.3768E 03	1.0849E 03	9.9870E 02	1.2234E 03
0.17750	1.2847E 03	1.0541E 03	9.8575E 02	1.1630E 03	1.3768E 03	1.0862E 03	1.0000E 03	1.2234E 03
0.55875	1.2874E 03	1.0564E 03	9.9053E 02	1.1645E 03	1.3794E 03	1.0883E 03	1.0053E 03	1.2245E 03
0.62125	1.2874E 03	1.0593E 03	9.9134E 02	1.1649E 03	1.3793E 03	1.0919E 03	1.0062E 03	1.2249E 03
0.68375	1.2883E 03	1.0582E 03	9.9232E 02	1.1653E 03	1.3802E 03	1.0903E 03	1.0073E 03	1.2252E 03
0.86875	1.2894E 03	1.0627E 03	9.9502E 02	1.1660E 03	1.3812E 03	1.0955E 03	1.0103E 03	1.2264E 03
0.93125	1.2904E 03	1.0615E 03	9.9602E 02	1.1670E 03	1.3823E 03	1.0939E 03	1.0114E 03	1.2269E 03
0.99375	1.2905E 03	1.0642E 03	9.9688E 02	1.1675E 03	1.3823E 03	1.0972E 03	1.0123E 03	1.2273E 03
1.05625	1.2914E 03	1.0633E 03	9.9784E 02	1.1680E 03	1.3832E 03	1.0959E 03	1.0134E 03	1.2276E 03
1.08625	1.2912E 03	1.0656E 03	9.9820E 02	1.1683E 03	1.3830E 03	1.0988E 03	1.0138E 03	1.2281E 03
1.12250	1.2919E 03	1.0641E 03	9.9879E 02	1.1686E 03	1.3838E 03	1.0968E 03	1.0145E 03	1.2283E 03
1.49750	1.2946E 03	1.0691E 03	1.0037E 03	1.1716E 03	1.3864E 03	1.1023E 03	1.0199E 03	1.2314E 03
1.84250	1.2969E 03	1.0738E 03	1.0087E 03	1.1745E 03	1.3885E 03	1.1074E 03	1.0254E 03	1.2343E 03
2.17250	1.2992E 03	1.0780E 03	1.0137E 03	1.1775E 03	1.3907E 03	1.1120E 03	1.0309E 03	1.2373E 03
2.52750	1.3013E 03	1.0825E 03	1.0184E 03	1.1806E 03	1.3926E 03	1.1170E 03	1.0361E 03	1.2405E 03
2.91999	1.3033E 03	1.0868E 03	1.0231E 03	1.1839E 03	1.3944E 03	1.1216E 03	1.0414E 03	1.2439E 03
3.29749	1.3052E 03	1.0904E 03	1.0282E 03	1.1869E 03	1.3960E 03	1.1253E 03	1.0469E 03	1.2469E 03
3.63999	1.3068E 03	1.0957E 03	1.0331E 03	1.1899E 03	1.3972E 03	1.1312E 03	1.0524E 03	1.2499E 03
3.70249	1.3073E 03	1.0954E 03	1.0340E 03	1.1904E 03	1.3978E 03	1.1308E 03	1.0533E 03	1.2504E 03
3.76499	1.3075E 03	1.0971E 03	1.0347E 03	1.1909E 03	1.3978E 03	1.1328E 03	1.0542E 03	1.2510E 03
3.82749	1.3080E 03	1.0968E 03	1.0355E 03	1.1914E 03	1.3983E 03	1.1323E 03	1.0550E 03	1.2515E 03
3.88999	1.3080E 03	1.0984E 03	1.0362E 03	1.1919E 03	1.3983E 03	1.1342E 03	1.0558E 03	1.2520E 03
3.95249	1.3085E 03	1.0981E 03	1.0370E 03	1.1924E 03	1.3988E 03	1.1337E 03	1.0567E 03	1.2525E 03
4.01499	1.3086E 03	1.0997E 03	1.0377E 03	1.1929E 03	1.3988E 03	1.1355E 03	1.0574E 03	1.2531E 03
4.07749	1.3090E 03	1.0993E 03	1.0384E 03	1.1934E 03	1.3992E 03	1.1350E 03	1.0582E 03	1.2536E 03
4.13999	1.3091E 03	1.1009E 03	1.0391E 03	1.1939E 03	1.3992E 03	1.1368E 03	1.0590E 03	1.2541E 03
4.20249	1.3095E 03	1.1005E 03	1.0398E 03	1.1944E 03	1.3996E 03	1.1363E 03	1.0598E 03	1.2545E 03
4.26499	1.3096E 03	1.1020E 03	1.0404E 03	1.1948E 03	1.3996E 03	1.1381E 03	1.0604E 03	1.2550E 03
4.32749	1.3100E 03	1.1016E 03	1.0410E 03	1.1953E 03	1.4000E 03	1.1375E 03	1.0611E 03	1.2555E 03
4.33499	1.3099E 03	1.1022E 03	1.0411E 03	1.1953E 03	1.3999E 03	1.1382E 03	1.0612E 03	1.2555E 03
4.38999	1.3100E 03	1.1031E 03	1.0416E 03	1.1957E 03	1.3999E 03	1.1392E 03	1.0618E 03	1.2559E 03
4.45249	1.3103E 03	1.1027E 03	1.0423E 03	1.1961E 03	1.4003E 03	1.1386E 03	1.0625E 03	1.2564E 03
4.51499	1.3103E 03	1.1041E 03	1.0429E 03	1.1966E 03	1.4002E 03	1.1404E 03	1.0632E 03	1.2568E 03
4.57749	1.3107E 03	1.1036E 03	1.0436E 03	1.1970E 03	1.4005E 03	1.1398E 03	1.0640E 03	1.2572E 03
4.63999	1.3107E 03	1.1053E 03	1.0443E 03	1.1974E 03	1.4004E 03	1.1416E 03	1.0647E 03	1.2577E 03
4.70249	1.3111E 03	1.1049E 03	1.0450E 03	1.1978E 03	1.4008E 03	1.1410E 03	1.0655E 03	1.2581E 03
4.76499	1.3111E 03	1.1064E 03	1.0457E 03	1.1983E 03	1.4007E 03	1.1428E 03	1.0663E 03	1.2585E 03
4.82749	1.3115E 03	1.1061E 03	1.0465E 03	1.1987E 03	1.4011E 03	1.1423E 03	1.0672E 03	1.2589E 03
4.88999	1.3115E 03	1.1077E 03	1.0472E 03	1.1991E 03	1.4010E 03	1.1442E 03	1.0680E 03	1.2594E 03
4.95249	1.3119E 03	1.1074E 03	1.0481E 03	1.1996E 03	1.4014E 03	1.1437E 03	1.0689E 03	1.2598E 03

AVERAGE CHANNEL TEMPERATURES - FUEL
AXIAL POSITION 1

TIME	FUEL RADIUS NUMBER CENTER	2	4	6	BOUNDARY	CLAD	COOLANT	AVERAGE
0.	1.1929E 03	1.1292E 03	1.0643E 03	9.9804E 02	9.3037E 02	9.0768E 02	8.6424E 02	1.0634E 03
0.17750	1.2025E 03	1.1262E 03	1.0638E 03	9.9782E 02	9.2938E 02	9.0795E 02	8.6448E 02	1.0634E 03
0.55875	1.2051E 03	1.1286E 03	1.0639E 03	9.9807E 02	9.3155E 02	9.0810E 02	8.6511E 02	1.0640E 03
0.62125	1.2051E 03	1.1286E 03	1.0639E 03	9.9806E 02	9.3026E 02	9.0842E 02	8.6521E 02	1.0639E 03
0.68375	1.2052E 03	1.1286E 03	1.0640E 03	9.9816E 02	9.3139E 02	9.0833E 02	8.6533E 02	1.0640E 03
0.86875	1.2051E 03	1.1286E 03	1.0640E 03	9.9820E 02	9.3075E 02	9.0872E 02	8.6565E 02	1.0640E 03
0.93125	1.2050E 03	1.1285E 03	1.0639E 03	9.9825E 02	9.3152E 02	9.0868E 02	8.6576E 02	1.0640E 03
0.99375	1.2049E 03	1.1284E 03	1.0639E 03	9.9822E 02	9.3097E 02	9.0885E 02	8.6585E 02	1.0639E 03
1.05625	1.2047E 03	1.1283E 03	1.0638E 03	9.9824E 02	9.3153E 02	9.0883E 02	8.6596E 02	1.0639E 03
1.08625	1.2047E 03	1.1283E 03	1.0638E 03	9.9821E 02	9.3100E 02	9.0895E 02	8.6600E 02	1.0639E 03
1.12250	1.2046E 03	1.1282E 03	1.0638E 03	9.9822E 02	9.3159E 02	9.0889E 02	8.6606E 02	1.0638E 03
1.49750	1.2032E 03	1.1272E 03	1.0631E 03	9.9793E 02	9.3153E 02	9.0917E 02	8.6656E 02	1.0632E 03
1.84250	1.2016E 03	1.1260E 03	1.0623E 03	9.9753E 02	9.3157E 02	9.0945E 02	8.6717E 02	1.0624E 03
2.17250	1.1997E 03	1.1246E 03	1.0613E 03	9.9707E 02	9.3164E 02	9.0966E 02	8.6770E 02	1.0615E 03
2.52750	1.1974E 03	1.1229E 03	1.0602E 03	9.9642E 02	9.3151E 02	9.0979E 02	8.6819E 02	1.0603E 03
2.91999	1.1947E 03	1.1209E 03	1.0587E 03	9.9560E 02	9.3132E 02	9.0985E 02	8.6868E 02	1.0589E 03
3.29749	1.1919E 03	1.1188E 03	1.0573E 03	9.9483E 02	9.3134E 02	9.0997E 02	8.6928E 02	1.0575E 03
3.63999	1.1894E 03	1.1170E 03	1.0560E 03	9.9414E 02	9.3111E 02	9.1014E 02	8.6981E 02	1.0562E 03
3.70249	1.1890E 03	1.1166E 03	1.0558E 03	9.9402E 02	9.3125E 02	9.1013E 02	8.6990E 02	1.0559E 03
3.76499	1.1885E 03	1.1163E 03	1.0555E 03	9.9387E 02	9.3106E 02	9.1017E 02	8.6996E 02	1.0557E 03
3.82749	1.1880E 03	1.1159E 03	1.0553E 03	9.9373E 02	9.3118E 02	9.1014E 02	8.7004E 02	1.0555E 03
3.88999	1.1875E 03	1.1156E 03	1.0550E 03	9.9358E 02	9.3099E 02	9.1017E 02	8.7011E 02	1.0552E 03
3.95249	1.1871E 03	1.1152E 03	1.0548E 03	9.9344E 02	9.3111E 02	9.1014E 02	8.7019E 02	1.0549E 03
4.01499	1.1866E 03	1.1149E 03	1.0545E 03	9.9328E 02	9.3092E 02	9.1017E 02	8.7026E 02	1.0547E 03
4.07749	1.1861E 03	1.1145E 03	1.0543E 03	9.9314E 02	9.3103E 02	9.1014E 02	8.7033E 02	1.0544E 03
4.13999	1.1856E 03	1.1141E 03	1.0540E 03	9.9298E 02	9.3084E 02	9.1016E 02	8.7040E 02	1.0542E 03
4.20249	1.1851E 03	1.1138E 03	1.0537E 03	9.9284E 02	9.3095E 02	9.1013E 02	8.7047E 02	1.0539E 03
4.26499	1.1847E 03	1.1134E 03	1.0535E 03	9.9268E 02	9.3076E 02	9.1015E 02	8.7052E 02	1.0537E 03
4.32749	1.1842E 03	1.1131E 03	1.0532E 03	9.9253E 02	9.3084E 02	9.1011E 02	8.7057E 02	1.0534E 03
4.33499	1.1841E 03	1.1130E 03	1.0532E 03	9.9250E 02	9.3076E 02	9.1012E 02	8.7058E 02	1.0534E 03
4.38999	1.1837E 03	1.1127E 03	1.0530E 03	9.9236E 02	9.3065E 02	9.1012E 02	8.7064E 02	1.0531E 03
4.45249	1.1832E 03	1.1123E 03	1.0527E 03	9.9221E 02	9.3075E 02	9.1009E 02	8.7071E 02	1.0529E 03
4.51499	1.1827E 03	1.1120E 03	1.0524E 03	9.9205E 02	9.3057E 02	9.1011E 02	8.7078E 02	1.0526E 03
4.57749	1.1823E 03	1.1116E 03	1.0522E 03	9.9191E 02	9.3067E 02	9.1009E 02	8.7086E 02	1.0524E 03
4.63999	1.1818E 03	1.1113E 03	1.0519E 03	9.9176E 02	9.3050E 02	9.1012E 02	8.7094E 02	1.0521E 03
4.70249	1.1813E 03	1.1109E 03	1.0517E 03	9.9162E 02	9.3061E 02	9.1010E 02	8.7102E 02	1.0519E 03
4.76499	1.1808E 03	1.1105E 03	1.0514E 03	9.9147E 02	9.3044E 02	9.1014E 02	8.7111E 02	1.0516E 03
4.82749	1.1804E 03	1.1102E 03	1.0512E 03	9.9134E 02	9.3056E 02	9.1013E 02	8.7120E 02	1.0514E 03
4.88999	1.1799E 03	1.1098E 03	1.0509E 03	9.9120E 02	9.3040E 02	9.1018E 02	8.7129E 02	1.0511E 03
4.95249	1.1794E 03	1.1095E 03	1.0507E 03	9.9108E 02	9.3052E 02	9.1017E 02	8.7139E 02	1.0509E 03

AVERAGE CHANNEL TEMPERATURES - FUEL
AXIAL POSITION 2

TIME	CENTER	FUEL RADIUS NUMBER 2	4	6	BOUNDARY	CLAD	COOLANT	AVERAGE
0.	1.4319E 03	1.3321E 03	1.2292E 03	1.1231E 03	1.0133E 03	9.7522E 02	9.0236E 02	1.2269E 03
0.17750	1.4472E 03	1.3365E 03	1.2284E 03	1.1227E 03	1.0111E 03	9.7603E 02	9.0314E 02	1.2271E 03
0.55875	1.4514E 03	1.3316E 03	1.2292E 03	1.1240E 03	1.0179E 03	9.7693E 02	9.0538E 02	1.2286E 03
0.62125	1.4515E 03	1.3317E 03	1.2294E 03	1.1240E 03	1.0132E 03	9.7814E 02	9.0574E 02	1.2286E 03
0.68375	1.4517E 03	1.3318E 03	1.2296E 03	1.1245E 03	1.0176E 03	9.7779E 02	9.0616E 02	1.2289E 03
0.86875	1.4518E 03	1.3321E 03	1.2300E 03	1.1250E 03	1.0151E 03	9.7938E 02	9.0731E 02	1.2293E 03
0.93125	1.4517E 03	1.3321E 03	1.2301E 03	1.1253E 03	1.0183E 03	9.7922E 02	9.0771E 02	1.2295E 03
0.99375	1.4517E 03	1.3322E 03	1.2302E 03	1.1254E 03	1.0162E 03	9.7994E 02	9.0807E 02	1.2295E 03
1.05625	1.4516E 03	1.3322E 03	1.2303E 03	1.1256E 03	1.0184E 03	9.7990E 02	9.0844E 02	1.2297E 03
1.08625	1.4516E 03	1.3321E 03	1.2303E 03	1.1256E 03	1.0165E 03	9.8040E 02	9.0860E 02	1.2296E 03
1.12250	1.4515E 03	1.3321E 03	1.2304E 03	1.1258E 03	1.0187E 03	9.8021E 02	9.0883E 02	1.2297E 03
1.49750	1.4503E 03	1.3315E 03	1.2303E 03	1.1263E 03	1.0193E 03	9.8181E 02	9.1074E 02	1.2297E 03
1.84250	1.4485E 03	1.3304E 03	1.2299E 03	1.1267E 03	1.0203E 03	9.8338E 02	9.1286E 02	1.2293E 03
2.17250	1.4464E 03	1.3291E 03	1.2294E 03	1.1270E 03	1.0215E 03	9.8478E 02	9.1482E 02	1.2288E 03
2.52750	1.4437E 03	1.3274E 03	1.2285E 03	1.1269E 03	1.0223E 03	9.8603E 02	9.1662E 02	1.2279E 03
2.91999	1.4405E 03	1.3252E 03	1.2272E 03	1.1266E 03	1.0230E 03	9.8715E 02	9.1842E 02	1.2267E 03
3.29749	1.4371E 03	1.3229E 03	1.2259E 03	1.1264E 03	1.0242E 03	9.8841E 02	9.2057E 02	1.2254E 03
3.63999	1.4340E 03	1.3209E 03	1.2248E 03	1.1263E 03	1.0247E 03	9.8981E 02	9.2253E 02	1.2244E 03
3.70249	1.4335E 03	1.3205E 03	1.2246E 03	1.1263E 03	1.0253E 03	9.8995E 02	9.2285E 02	1.2242E 03
3.76499	1.4329E 03	1.3202E 03	1.2244E 03	1.1262E 03	1.0250E 03	9.9020E 02	9.2313E 02	1.2240E 03
3.82749	1.4323E 03	1.3198E 03	1.2242E 03	1.1261E 03	1.0255E 03	9.9029E 02	9.2340E 02	1.2237E 03
3.88999	1.4317E 03	1.3194E 03	1.2239E 03	1.1260E 03	1.0252E 03	9.9051E 02	9.2367E 02	1.2235E 03
3.95249	1.4312E 03	1.3190E 03	1.2237E 03	1.1260E 03	1.0257E 03	9.9060E 02	9.2395E 02	1.2233E 03
4.01499	1.4306E 03	1.3186E 03	1.2234E 03	1.1259E 03	1.0254E 03	9.9082E 02	9.2421E 02	1.2230E 03
4.07749	1.4300E 03	1.3182E 03	1.2232E 03	1.1258E 03	1.0259E 03	9.9091E 02	9.2448E 02	1.2228E 03
4.13999	1.4294E 03	1.3178E 03	1.2229E 03	1.1257E 03	1.0256E 03	9.9111E 02	9.2474E 02	1.2225E 03
4.20249	1.4288E 03	1.3173E 03	1.2226E 03	1.1256E 03	1.0260E 03	9.9119E 02	9.2499E 02	1.2223E 03
4.26499	1.4282E 03	1.3169E 03	1.2224E 03	1.1255E 03	1.0257E 03	9.9138E 02	9.2520E 02	1.2220E 03
4.32749	1.4276E 03	1.3165E 03	1.2221E 03	1.1254E 03	1.0261E 03	9.9140E 02	9.2540E 02	1.2217E 03
4.38999	1.4270E 03	1.3161E 03	1.2218E 03	1.1253E 03	1.0258E 03	9.9157E 02	9.2564E 02	1.2214E 03
4.45249	1.4264E 03	1.3156E 03	1.2215E 03	1.1252E 03	1.0262E 03	9.9164E 02	9.2589E 02	1.2212E 03
4.51499	1.4258E 03	1.3152E 03	1.2213E 03	1.1250E 03	1.0260E 03	9.9183E 02	9.2615E 02	1.2209E 03
4.57749	1.4251E 03	1.3148E 03	1.2210E 03	1.1249E 03	1.0264E 03	9.9192E 02	9.2643E 02	1.2206E 03
4.63999	1.4245E 03	1.3143E 03	1.2207E 03	1.1248E 03	1.0261E 03	9.9213E 02	9.2671E 02	1.2203E 03
4.70249	1.4239E 03	1.3139E 03	1.2204E 03	1.1248E 03	1.0266E 03	9.9224E 02	9.2701E 02	1.2201E 03
4.76499	1.4233E 03	1.3135E 03	1.2202E 03	1.1247E 03	1.0263E 03	9.9246E 02	9.2732E 02	1.2198E 03
4.82749	1.4227E 03	1.3130E 03	1.2199E 03	1.1246E 03	1.0266E 03	9.9262E 02	9.2765E 02	1.2196E 03
4.88999	1.4221E 03	1.3126E 03	1.2197E 03	1.1245E 03	1.0266E 03	9.9287E 02	9.2798E 02	1.2193E 03
4.95249	1.4215E 03	1.3122E 03	1.2195E 03	1.1245E 03	1.0271E 03	9.9303E 02	9.2833E 02	1.2191E 03

AVERAGE CHANNEL TEMPERATURES - FUEL
AXIAL POSITION 3

TIME	CENTER	FUEL RADIUS NUMBER 2	4	6	BOUNDARY	CLAD	COOLANT	AVERAGE
0.	1.5845E 03	1.4675E 03	1.3466E 03	1.2212E 03	1.0908E 03	1.0443E 03	9.5539E 02	1.3435E 03
0.17750	1.5826E 03	1.4657E 03	1.3457E 03	1.2207E 03	1.0869E 03	1.0458E 03	9.5671E 02	1.3436E 03
0.55875	1.5876E 03	1.4674E 03	1.3473E 03	1.2236E 03	1.1025E 03	1.0472E 03	9.6101E 02	1.3464E 03
0.62125	1.5879E 03	1.4677E 03	1.3477E 03	1.2233E 03	1.0882E 03	1.0504E 03	9.6167E 02	1.3462E 03
0.68375	1.5881E 03	1.4680E 03	1.3481E 03	1.2245E 03	1.1016E 03	1.0489E 03	9.6252E 02	1.3471E 03
0.86875	1.5886E 03	1.4688E 03	1.3492E 03	1.2254E 03	1.0916E 03	1.0530E 03	9.6476E 02	1.3478E 03
0.93125	1.5887E 03	1.4691E 03	1.3496E 03	1.2264E 03	1.1035E 03	1.0518E 03	9.6559E 02	1.3486E 03
0.99375	1.5888E 03	1.4693E 03	1.3499E 03	1.2264E 03	1.0944E 03	1.0541E 03	9.6626E 02	1.3486E 03
1.05625	1.5889E 03	1.4695E 03	1.3502E 03	1.2273E 03	1.1034E 03	1.0533E 03	9.6705E 02	1.3493E 03
1.08625	1.5889E 03	1.4696E 03	1.3504E 03	1.2271E 03	1.0946E 03	1.0552E 03	9.6733E 02	1.3491E 03
1.12250	1.5890E 03	1.4697E 03	1.3506E 03	1.2278E 03	1.1042E 03	1.0539E 03	9.6781E 02	1.3496E 03
1.49750	1.5898E 03	1.4703E 03	1.3519E 03	1.2298E 03	1.1043E 03	1.0578E 03	9.7165E 02	1.3509E 03
1.84250	1.5906E 03	1.4708E 03	1.3528E 03	1.2316E 03	1.1064E 03	1.0613E 03	9.7581E 02	1.3518E 03
2.17250	1.5914E 03	1.4713E 03	1.3535E 03	1.2334E 03	1.1095E 03	1.0645E 03	9.7974E 02	1.3526E 03
2.52750	1.5924E 03	1.4719E 03	1.3540E 03	1.2349E 03	1.1116E 03	1.0676E 03	9.8340E 02	1.3530E 03
2.91999	1.5935E 03	1.4725E 03	1.3540E 03	1.2360E 03	1.1139E 03	1.0705E 03	9.8706E 02	1.3531E 03
3.29749	1.5944E 03	1.4731E 03	1.3536E 03	1.2372E 03	1.1172E 03	1.0734E 03	9.9121E 02	1.3530E 03
3.63999	1.5952E 03	1.4736E 03	1.3539E 03	1.2386E 03	1.1189E 03	1.0768E 03	9.9517E 02	1.3531E 03
3.70249	1.5953E 03	1.4739E 03	1.3539E 03	1.2388E 03	1.1203E 03	1.0772E 03	9.9582E 02	1.3532E 03
3.76499	1.5954E 03	1.4737E 03	1.3539E 03	1.2390E 03	1.1198E 03	1.0778E 03	9.9642E 02	1.3531E 03
3.82749	1.5956E 03	1.4740E 03	1.3539E 03	1.2392E 03	1.1211E 03	1.0781E 03	9.9697E 02	1.3532E 03
3.88999	1.5958E 03	1.4743E 03	1.3539E 03	1.2393E 03	1.1205E 03	1.0787E 03	9.9753E 02	1.3531E 03
3.95249	1.5954E 03	1.4745E 03	1.3538E 03	1.2395E 03	1.1218E 03	1.0789E 03	9.9809E 02	1.3531E 03
4.01499	1.5949E 03	1.4748E 03	1.3538E 03	1.2396E 03	1.1213E 03	1.0795E 03	9.9864E 02	1.3530E 03
4.07749	1.5945E 03	1.4745E 03	1.3537E 03	1.2398E 03	1.1225E 03	1.0798E 03	9.9918E 02	1.3530E 03
4.13999	1.5940E 03	1.4743E 03	1.3536E 03	1.2398E 03	1.1219E 03	1.0803E 03	9.9971E 02	1.3529E 03
4.20249	1.5935E 03	1.4740E 03	1.3536E 03	1.2400E 03	1.1231E 03	1.0805E 03	1.0002E 03	1.3528E 03
4.26499	1.5931E 03	1.4737E 03	1.3535E 03	1.2400E 03	1.1226E 03	1.0811E 03	1.0007E 03	1.3527E 03
4.32749	1.5926E 03	1.4735E 03	1.3534E 03	1.2402E 03	1.1236E 03	1.0812E 03	1.0011E 03	1.3526E 03
4.33499	1.5925E 03	1.4734E 03	1.3533E 03	1.2401E 03	1.1232E 03	1.0813E 03	1.0012E 03	1.3526E 03
4.38999	1.5921E 03	1.4732E 03	1.3532E 03	1.2402E 03	1.1231E 03	1.0817E 03	1.0016E 03	1.3525E 03
4.45249	1.5916E 03	1.4729E 03	1.3531E 03	1.2403E 03	1.1241E 03	1.0819E 03	1.0021E 03	1.3524E 03
4.51499	1.5911E 03	1.4726E 03	1.3530E 03	1.2403E 03	1.1236E 03	1.0824E 03	1.0026E 03	1.3522E 03
4.57749	1.5906E 03	1.4722E 03	1.3529E 03	1.2404E 03	1.1247E 03	1.0826E 03	1.0031E 03	1.3521E 03
4.63999	1.5901E 03	1.4719E 03	1.3527E 03	1.2405E 03	1.1243E 03	1.0832E 03	1.0037E 03	1.3520E 03
4.70249	1.5895E 03	1.4716E 03	1.3526E 03	1.2406E 03	1.1253E 03	1.0834E 03	1.0043E 03	1.3519E 03
4.76499	1.5890E 03	1.4713E 03	1.3525E 03	1.2407E 03	1.1250E 03	1.0840E 03	1.0049E 03	1.3518E 03
4.82749	1.5885E 03	1.4710E 03	1.3524E 03	1.2408E 03	1.1261E 03	1.0843E 03	1.0055E 03	1.3518E 03
4.88999	1.5880E 03	1.4707E 03	1.3523E 03	1.2410E 03	1.1257E 03	1.0849E 03	1.0062E 03	1.3517E 03
4.95249	1.5875E 03	1.4705E 03	1.3523E 03	1.2412E 03	1.1269E 03	1.0853E 03	1.0068E 03	1.3516E 03

AVERAGE CHANNEL TEMPERATURES - FUEL
AXIAL POSITION 4

TIME	CENTER	FUEL RADIUS NUMBER 2	4	6	BOUNDARY	CLAD	COOLANT	AVERAGE
0.	1.6351E 03	1.5197E 03	1.4006E 03	1.2772E 03	1.1491E 03	1.1026E 03	1.0137E 03	1.3977E 03
0.17750	1.6530E 03	1.5186E 03	1.3997E 03	1.2768E 03	1.1446E 03	1.1044E 03	1.0154E 03	1.3978E 03
0.55875	1.6561E 03	1.5201E 03	1.4021E 03	1.2810E 03	1.1671E 03	1.1065E 03	1.0216E 03	1.4015E 03
0.62125	1.6585E 03	1.5206E 03	1.4027E 03	1.2806E 03	1.1437E 03	1.1117E 03	1.0226E 03	1.4013E 03
0.68375	1.6586E 03	1.5211E 03	1.4033E 03	1.2825E 03	1.1669E 03	1.1089E 03	1.0239E 03	1.4027E 03
0.86875	1.6596E 03	1.5225E 03	1.4052E 03	1.2837E 03	1.1464E 03	1.1161E 03	1.0272E 03	1.4036E 03
0.93125	1.6601E 03	1.5230E 03	1.4059E 03	1.2858E 03	1.1721E 03	1.1129E 03	1.0285E 03	1.4053E 03
0.99375	1.6604E 03	1.5235E 03	1.4065E 03	1.2854E 03	1.1505E 03	1.1178E 03	1.0295E 03	1.4051E 03
1.05625	1.6607E 03	1.5240E 03	1.4072E 03	1.2873E 03	1.1722E 03	1.1155E 03	1.0308E 03	1.4065E 03
1.08625	1.6608E 03	1.5242E 03	1.4074E 03	1.2865E 03	1.1493E 03	1.1196E 03	1.0311E 03	1.4060E 03
1.12250	1.6610E 03	1.5244E 03	1.4076E 03	1.2882E 03	1.1737E 03	1.1163E 03	1.0319E 03	1.4072E 03
1.49750	1.6624E 03	1.5259E 03	1.4111E 03	1.2920E 03	1.1726E 03	1.1226E 03	1.0379E 03	1.4103E 03
1.86250	1.6632E 03	1.5266E 03	1.4136E 03	1.2956E 03	1.1745E 03	1.1288E 03	1.0441E 03	1.4130E 03
2.17250	1.6636E 03	1.5302E 03	1.4164E 03	1.2995E 03	1.1809E 03	1.1339E 03	1.0502E 03	1.4157E 03
2.52750	1.6638E 03	1.5317E 03	1.4189E 03	1.3029E 03	1.1827E 03	1.1395E 03	1.0559E 03	1.4181E 03
2.91999	1.6636E 03	1.5327E 03	1.4211E 03	1.3062E 03	1.1862E 03	1.1447E 03	1.0617E 03	1.4203E 03
3.29749	1.6630E 03	1.5334E 03	1.4229E 03	1.3096E 03	1.1960E 03	1.1489E 03	1.0679E 03	1.4223E 03
3.63999	1.6623E 03	1.5341E 03	1.4249E 03	1.3126E 03	1.1940E 03	1.1554E 03	1.0740E 03	1.4242E 03
3.70249	1.6622E 03	1.5343E 03	1.4253E 03	1.3136E 03	1.2011E 03	1.1552E 03	1.0750E 03	1.4248E 03
3.76499	1.6621E 03	1.5344E 03	1.4257E 03	1.3136E 03	1.1958E 03	1.1571E 03	1.0760E 03	1.4249E 03
3.82749	1.6620E 03	1.5346E 03	1.4260E 03	1.3140E 03	1.2024E 03	1.1569E 03	1.0769E 03	1.4255E 03
3.88999	1.6619E 03	1.5347E 03	1.4263E 03	1.3149E 03	1.1975E 03	1.1586E 03	1.0778E 03	1.4256E 03
3.95249	1.6618E 03	1.5348E 03	1.4266E 03	1.3156E 03	1.2036E 03	1.1584E 03	1.0787E 03	1.4261E 03
4.01499	1.6617E 03	1.5349E 03	1.4269E 03	1.3158E 03	1.1990E 03	1.1601E 03	1.0795E 03	1.4262E 03
4.07749	1.6616E 03	1.5350E 03	1.4272E 03	1.3165E 03	1.2048E 03	1.1599E 03	1.0804E 03	1.4266E 03
4.13999	1.6615E 03	1.5350E 03	1.4274E 03	1.3167E 03	1.2005E 03	1.1615E 03	1.0812E 03	1.4267E 03
4.20249	1.6613E 03	1.5351E 03	1.4276E 03	1.3174E 03	1.2059E 03	1.1614E 03	1.0821E 03	1.4271E 03
4.26499	1.6612E 03	1.5352E 03	1.4279E 03	1.3176E 03	1.2019E 03	1.1628E 03	1.0828E 03	1.4272E 03
4.32749	1.6611E 03	1.5352E 03	1.4281E 03	1.3182E 03	1.2069E 03	1.1627E 03	1.0835E 03	1.4275E 03
4.38999	1.6611E 03	1.5352E 03	1.4281E 03	1.3181E 03	1.2045E 03	1.1632E 03	1.0836E 03	1.4275E 03
4.45249	1.6608E 03	1.5352E 03	1.4283E 03	1.3183E 03	1.2031E 03	1.1640E 03	1.0842E 03	1.4276E 03
4.51499	1.6607E 03	1.5352E 03	1.4284E 03	1.3189E 03	1.2079E 03	1.1639E 03	1.0850E 03	1.4279E 03
4.57749	1.6605E 03	1.5352E 03	1.4286E 03	1.3190E 03	1.2043E 03	1.1653E 03	1.0858E 03	1.4279E 03
4.63999	1.6603E 03	1.5352E 03	1.4288E 03	1.3196E 03	1.2089E 03	1.1652E 03	1.0866E 03	1.4283E 03
4.70249	1.6600E 03	1.5352E 03	1.4289E 03	1.3198E 03	1.2056E 03	1.1666E 03	1.0874E 03	1.4283E 03
4.76499	1.6598E 03	1.5352E 03	1.4291E 03	1.3204E 03	1.2101E 03	1.1666E 03	1.0883E 03	1.4286E 03
4.82749	1.6596E 03	1.5352E 03	1.4293E 03	1.3206E 03	1.2069E 03	1.1680E 03	1.0892E 03	1.4287E 03
4.88999	1.6594E 03	1.5352E 03	1.4295E 03	1.3212E 03	1.2113E 03	1.1681E 03	1.0902E 03	1.4290E 03
4.95249	1.6591E 03	1.5352E 03	1.4297E 03	1.3215E 03	1.2084E 03	1.1696E 03	1.0911E 03	1.4291E 03
4.95249	1.6589E 03	1.5352E 03	1.4299E 03	1.3221E 03	1.2127E 03	1.1698E 03	1.0921E 03	1.4295E 03

AVERAGE CHANNEL TEMPERATURES - FUEL
AXIAL POSITION 5

TIME	CENTER	FUEL RADIUS NUMBER 2	4	6	BOUNDARY	CLAD	COOLANT	AVERAGE
0.	1.5775E 03	1.4816E 03	1.3834E 03	1.2821E 03	1.1776E 03	1.1396E 03	1.0667E 03	1.3814E 03
0.17750	1.5924E 03	1.4803E 03	1.3827E 03	1.2819E 03	1.1749E 03	1.1412E 03	1.0685E 03	1.3816E 03
0.55875	1.5968E 03	1.4826E 03	1.3855E 03	1.2866E 03	1.1943E 03	1.1450E 03	1.0760E 03	1.3855E 03
0.62125	1.5972E 03	1.4831E 03	1.3862E 03	1.2865E 03	1.1755E 03	1.1496E 03	1.0773E 03	1.3855E 03
0.68375	1.5977E 03	1.4838E 03	1.3871E 03	1.2865E 03	1.1954E 03	1.1477E 03	1.0788E 03	1.3870E 03
0.86875	1.5990E 03	1.4857E 03	1.3896E 03	1.2906E 03	1.1784E 03	1.1553E 03	1.0831E 03	1.3889E 03
0.93125	1.5995E 03	1.4865E 03	1.3905E 03	1.2929E 03	1.2026E 03	1.1528E 03	1.0848E 03	1.3906E 03
0.99375	1.6000E 03	1.4872E 03	1.3914E 03	1.2929E 03	1.1824E 03	1.1578E 03	1.0861E 03	1.3908E 03
1.05625	1.6006E 03	1.4880E 03	1.3924E 03	1.2951E 03	1.2040E 03	1.1557E 03	1.0877E 03	1.3924E 03
1.08625	1.6008E 03	1.4883E 03	1.3928E 03	1.2944E 03	1.1814E 03	1.1604E 03	1.0882E 03	1.3920E 03
1.12250	1.6012E 03	1.4888E 03	1.3934E 03	1.2963E 03	1.2059E 03	1.1571E 03	1.0892E 03	1.3934E 03
1.49750	1.6046E 03	1.4933E 03	1.3986E 03	1.3023E 03	1.2076E 03	1.1655E 03	1.0971E 03	1.3986E 03
1.84250	1.6075E 03	1.4971E 03	1.4035E 03	1.3079E 03	1.2110E 03	1.1733E 03	1.1051E 03	1.4033E 03
2.17250	1.6102E 03	1.5009E 03	1.4084E 03	1.3139E 03	1.2205E 03	1.1802E 03	1.1131E 03	1.4083E 03
2.52750	1.6131E 03	1.5049E 03	1.4133E 03	1.3195E 03	1.2225E 03	1.1882E 03	1.1207E 03	1.4130E 03
2.91999	1.6159E 03	1.5089E 03	1.4181E 03	1.3252E 03	1.2268E 03	1.1958E 03	1.1284E 03	1.4178E 03
3.29749	1.6181E 03	1.5121E 03	1.4224E 03	1.3313E 03	1.2470E 03	1.2005E 03	1.1364E 03	1.4226E 03
3.63999	1.6200E 03	1.5153E 03	1.4267E 03	1.3358E 03	1.2331E 03	1.2113E 03	1.1442E 03	1.4262E 03
3.70249	1.6204E 03	1.5159E 03	1.4275E 03	1.3379E 03	1.2556E 03	1.2089E 03	1.1457E 03	1.4278E 03
3.76499	1.6207E 03	1.5165E 03	1.4283E 03	1.3377E 03	1.2356E 03	1.2137E 03	1.1469E 03	1.4278E 03
3.82749	1.6211E 03	1.5171E 03	1.4291E 03	1.3396E 03	1.2577E 03	1.2113E 03	1.1482E 03	1.4293E 03
3.88999	1.6215E 03	1.5177E 03	1.4298E 03	1.3396E 03	1.2379E 03	1.2160E 03	1.1493E 03	1.4293E 03
3.95249	1.6219E 03	1.5183E 03	1.4306E 03	1.3416E 03	1.2597E 03	1.2136E 03	1.1506E 03	1.4308E 03
4.01499	1.6223E 03	1.5188E 03	1.4313E 03	1.3413E 03	1.2400E 03	1.2182E 03	1.1517E 03	1.4308E 03
4.07749	1.6226E 03	1.5194E 03	1.4320E 03	1.3433E 03	1.2618E 03	1.2157E 03	1.1530E 03	1.4322E 03
4.13999	1.6230E 03	1.5199E 03	1.4326E 03	1.3430E 03	1.2420E 03	1.2203E 03	1.1540E 03	1.4321E 03
4.20249	1.6233E 03	1.5204E 03	1.4333E 03	1.3450E 03	1.2637E 03	1.2178E 03	1.1552E 03	1.4336E 03
4.26499	1.6236E 03	1.5209E 03	1.4339E 03	1.3446E 03	1.2439E 03	1.2223E 03	1.1561E 03	1.4335E 03
4.32749	1.6240E 03	1.5214E 03	1.4346E 03	1.3465E 03	1.2656E 03	1.2197E 03	1.1572E 03	1.4348E 03
4.33499	1.6240E 03	1.5214E 03	1.4346E 03	1.3460E 03	1.2539E 03	1.2218E 03	1.1573E 03	1.4345E 03
4.38999	1.6243E 03	1.5219E 03	1.4352E 03	1.3461E 03	1.2456E 03	1.2241E 03	1.1581E 03	1.4347E 03
4.45249	1.6246E 03	1.5223E 03	1.4358E 03	1.3480E 03	1.2674E 03	1.2215E 03	1.1593E 03	1.4360E 03
4.51499	1.6248E 03	1.5227E 03	1.4363E 03	1.3475E 03	1.2472E 03	1.2260E 03	1.1602E 03	1.4358E 03
4.57749	1.6251E 03	1.5231E 03	1.4369E 03	1.3494E 03	1.2693E 03	1.2233E 03	1.1614E 03	1.4371E 03
4.63999	1.6253E 03	1.5235E 03	1.4374E 03	1.3489E 03	1.2488E 03	1.2279E 03	1.1623E 03	1.4369E 03
4.70249	1.6256E 03	1.5240E 03	1.4380E 03	1.3506E 03	1.2714E 03	1.2252E 03	1.1636E 03	1.4383E 03
4.76499	1.6258E 03	1.5243E 03	1.4385E 03	1.3504E 03	1.2505E 03	1.2300E 03	1.1646E 03	1.4381E 03
4.82749	1.6260E 03	1.5248E 03	1.4391E 03	1.3524E 03	1.2735E 03	1.2273E 03	1.1659E 03	1.4394E 03
4.88999	1.6262E 03	1.5252E 03	1.4397E 03	1.3519E 03	1.2522E 03	1.2322E 03	1.1670E 03	1.4392E 03
4.95249	1.6264E 03	1.5256E 03	1.4403E 03	1.3540E 03	1.2758E 03	1.2294E 03	1.1684E 03	1.4407E 03

AVERAGE CHANNEL TEMPERATURES - FUEL
AXIAL POSITION 6

TIME	CENTER	FUEL RADIUS NUMBER 2	4	6	BOUNDARY	CLAD	COOLANT	AVERAGE
0.	1.4155E 03	1.3560E 03	1.2954E 03	1.2337E 03	1.1710E 03	1.1483E 03	1.1048E 03	1.2946E 03
0.17750	1.4246E 03	1.3550E 03	1.2950E 03	1.2338E 03	1.1698E 03	1.1494E 03	1.1064E 03	1.2948E 03
0.55875	1.4277E 03	1.3571E 03	1.2979E 03	1.2383E 03	1.1822E 03	1.1547E 03	1.1141E 03	1.2984E 03
0.62125	1.4281E 03	1.3577E 03	1.2987E 03	1.2388E 03	1.1743E 03	1.1576E 03	1.1156E 03	1.2989E 03
0.68375	1.4285E 03	1.3583E 03	1.2996E 03	1.2404E 03	1.1840E 03	1.1576E 03	1.1172E 03	1.3001E 03
0.86875	1.4301E 03	1.3607E 03	1.3025E 03	1.2435E 03	1.1793E 03	1.1636E 03	1.1221E 03	1.3027E 03
0.93125	1.4306E 03	1.3616E 03	1.3036E 03	1.2453E 03	1.1904E 03	1.1635E 03	1.1238E 03	1.3041E 03
0.99375	1.4314E 03	1.3625E 03	1.3048E 03	1.2462E 03	1.1831E 03	1.1666E 03	1.1254E 03	1.3050E 03
1.05625	1.4322E 03	1.3635E 03	1.3059E 03	1.2480E 03	1.1927E 03	1.1668E 03	1.1272E 03	1.3064E 03
1.08625	1.4326E 03	1.3640E 03	1.3065E 03	1.2481E 03	1.1843E 03	1.1691E 03	1.1279E 03	1.3066E 03
1.12250	1.4330E 03	1.3646E 03	1.3072E 03	1.2494E 03	1.1946E 03	1.1684E 03	1.1289E 03	1.3077E 03
1.49750	1.4384E 03	1.3710E 03	1.3144E 03	1.2573E 03	1.2009E 03	1.1777E 03	1.1381E 03	1.3148E 03
1.84250	1.4437E 03	1.3770E 03	1.3211E 03	1.2646E 03	1.2078E 03	1.1864E 03	1.1472E 03	1.3214E 03
2.17250	1.4488E 03	1.3831E 03	1.3280E 03	1.2724E 03	1.2171E 03	1.1951E 03	1.1564E 03	1.3284E 03
2.52750	1.4547E 03	1.3898E 03	1.3354E 03	1.2803E 03	1.2242E 03	1.2041E 03	1.1654E 03	1.3356E 03
2.91999	1.4611E 03	1.3969E 03	1.3430E 03	1.2885E 03	1.2323E 03	1.2131E 03	1.1746E 03	1.3432E 03
3.29749	1.4667E 03	1.4032E 03	1.3499E 03	1.2962E 03	1.2442E 03	1.2210E 03	1.1837E 03	1.3503E 03
3.63999	1.4717E 03	1.4090E 03	1.3565E 03	1.3034E 03	1.2472E 03	1.2305E 03	1.1920E 03	1.3567E 03
3.70249	1.4726E 03	1.4101E 03	1.3577E 03	1.3050E 03	1.2540E 03	1.2312E 03	1.1944E 03	1.3582E 03
3.76499	1.4736E 03	1.4112E 03	1.3590E 03	1.3061E 03	1.2502E 03	1.2336E 03	1.1959E 03	1.3592E 03
3.82749	1.4745E 03	1.4123E 03	1.3602E 03	1.3077E 03	1.2509E 03	1.2341E 03	1.1974E 03	1.3606E 03
3.88999	1.4755E 03	1.4134E 03	1.3614E 03	1.3087E 03	1.2531E 03	1.2364E 03	1.1986E 03	1.3616E 03
3.95249	1.4764E 03	1.4145E 03	1.3626E 03	1.3103E 03	1.2596E 03	1.2370E 03	1.2003E 03	1.3630E 03
4.01499	1.4774E 03	1.4155E 03	1.3637E 03	1.3113E 03	1.2550E 03	1.2392E 03	1.2017E 03	1.3639E 03
4.07749	1.4783E 03	1.4166E 03	1.3649E 03	1.3126E 03	1.2622E 03	1.2397E 03	1.2031E 03	1.3653E 03
4.13999	1.4792E 03	1.4176E 03	1.3660E 03	1.3137E 03	1.2585E 03	1.2419E 03	1.2044E 03	1.3662E 03
4.20249	1.4802E 03	1.4187E 03	1.3671E 03	1.3152E 03	1.2648E 03	1.2423E 03	1.2058E 03	1.3675E 03
4.26499	1.4811E 03	1.4197E 03	1.3682E 03	1.3161E 03	1.2610E 03	1.2444E 03	1.2070E 03	1.3684E 03
4.32749	1.4820E 03	1.4207E 03	1.3693E 03	1.3175E 03	1.2672E 03	1.2448E 03	1.2083E 03	1.3697E 03
4.33499	1.4821E 03	1.4208E 03	1.3694E 03	1.3175E 03	1.2645E 03	1.2454E 03	1.2084E 03	1.3697E 03
4.38999	1.4829E 03	1.4216E 03	1.3703E 03	1.3183E 03	1.2633E 03	1.2468E 03	1.2095E 03	1.3705E 03
4.45249	1.4837E 03	1.4226E 03	1.3714E 03	1.3197E 03	1.2696E 03	1.2471E 03	1.2107E 03	1.3717E 03
4.51499	1.4846E 03	1.4235E 03	1.3723E 03	1.3205E 03	1.2656E 03	1.2492E 03	1.2119E 03	1.3725E 03
4.57749	1.4854E 03	1.4244E 03	1.3733E 03	1.3218E 03	1.2719E 03	1.2495E 03	1.2132E 03	1.3737E 03
4.63999	1.4862E 03	1.4253E 03	1.3743E 03	1.3226E 03	1.2679E 03	1.2516E 03	1.2144E 03	1.3745E 03
4.70249	1.4870E 03	1.4262E 03	1.3753E 03	1.3240E 03	1.2743E 03	1.2519E 03	1.2157E 03	1.3757E 03
4.76499	1.4878E 03	1.4271E 03	1.3763E 03	1.3248E 03	1.2702E 03	1.2540E 03	1.2170E 03	1.3765E 03
4.82749	1.4886E 03	1.4280E 03	1.3772E 03	1.3261E 03	1.2768E 03	1.2544E 03	1.2184E 03	1.3777E 03
4.88999	1.4894E 03	1.4289E 03	1.3782E 03	1.3270E 03	1.2726E 03	1.2566E 03	1.2198E 03	1.3785E 03
4.95249	1.4901E 03	1.4298E 03	1.3792E 03	1.3284E 03	1.2794E 03	1.2570E 03	1.2212E 03	1.3797E 03

AVERAGE CHANNEL TEMPERATURES - CEX
AXIAL POSITION 1

	CEX REGION							
TIME	CENTER 1	2	4	6	BOUNDARY	CLAD	STRUCTURE	AVERAGE
0.	1.0725E 03	1.0277E 03	9.8240E 02	9.3640E 02	8.8981E 02	8.8186E 02	8.6589E 02	9.8197E 02
0.17750	1.0767E 03	1.0272E 03	9.8227E 02	9.3643E 02	8.8993E 02	8.8201E 02	8.6599E 02	9.8200E 02
0.55075	1.0798E 03	1.0270E 03	9.8210E 02	9.3654E 02	8.9038E 02	8.8251E 02	8.6651E 02	9.8221E 02
0.62125	1.0800E 03	1.0270E 03	9.8211E 02	9.3658E 02	8.9046E 02	8.8260E 02	8.6661E 02	9.8225E 02
0.68375	1.0801E 03	1.0271E 03	9.8212E 02	9.3662E 02	8.9055E 02	8.8269E 02	8.6671E 02	9.8230E 02
0.86875	1.0805E 03	1.0271E 03	9.8218E 02	9.3677E 02	8.9080E 02	8.8297E 02	8.6703E 02	9.8241E 02
0.93125	1.0806E 03	1.0271E 03	9.8220E 02	9.3682E 02	8.9089E 02	8.8306E 02	8.6713E 02	9.8245E 02
0.99375	1.0806E 03	1.0271E 03	9.8222E 02	9.3686E 02	8.9097E 02	8.8315E 02	8.6724E 02	9.8248E 02
1.05625	1.0807E 03	1.0271E 03	9.8223E 02	9.3691E 02	8.9105E 02	8.8324E 02	8.6734E 02	9.8251E 02
1.08625	1.0808E 03	1.0271E 03	9.8224E 02	9.3693E 02	8.9109E 02	8.8328E 02	8.6739E 02	9.8252E 02
1.12250	1.0808E 03	1.0271E 03	9.8225E 02	9.3695E 02	8.9114E 02	8.8333E 02	8.6745E 02	9.8253E 02
1.49750	1.0814E 03	1.0270E 03	9.8225E 02	9.3714E 02	8.9153E 02	8.8376E 02	8.6798E 02	9.8256E 02
1.84250	1.0819E 03	1.0267E 03	9.8214E 02	9.3720E 02	8.9195E 02	8.8423E 02	8.6851E 02	9.8248E 02
2.17250	1.0823E 03	1.0262E 03	9.8190E 02	9.3736E 02	8.9233E 02	8.8466E 02	8.6905E 02	9.8232E 02
2.52750	1.0824E 03	1.0257E 03	9.8166E 02	9.3730E 02	8.9265E 02	8.8503E 02	8.6956E 02	9.8203E 02
2.91999	1.0773E 03	1.0249E 03	9.8122E 02	9.3726E 02	8.9292E 02	8.8538E 02	8.7005E 02	9.8160E 02
3.29749	1.0726E 03	1.0240E 03	9.8071E 02	9.3715E 02	8.9326E 02	8.8579E 02	8.7056E 02	9.8111E 02
3.63999	1.0748E 03	1.0232E 03	9.8025E 02	9.3708E 02	8.9359E 02	8.8619E 02	8.7111E 02	9.8066E 02
3.70249	1.0745E 03	1.0230E 03	9.8016E 02	9.3706E 02	8.9364E 02	8.8625E 02	8.7120E 02	9.8058E 02
3.76499	1.0743E 03	1.0229E 03	9.8007E 02	9.3704E 02	8.9368E 02	8.8630E 02	8.7128E 02	9.8048E 02
3.82749	1.0741E 03	1.0227E 03	9.7998E 02	9.3701E 02	8.9372E 02	8.8634E 02	8.7136E 02	9.8039E 02
3.88999	1.0738E 03	1.0226E 03	9.7988E 02	9.3698E 02	8.9375E 02	8.8639E 02	8.7144E 02	9.8029E 02
3.95249	1.0736E 03	1.0224E 03	9.7978E 02	9.3695E 02	8.9379E 02	8.8644E 02	8.7151E 02	9.8019E 02
4.01499	1.0733E 03	1.0222E 03	9.7968E 02	9.3691E 02	8.9382E 02	8.8649E 02	8.7158E 02	9.8009E 02
4.07749	1.0731E 03	1.0221E 03	9.7958E 02	9.3688E 02	8.9386E 02	8.8653E 02	8.7166E 02	9.7999E 02
4.13999	1.0726E 03	1.0219E 03	9.7947E 02	9.3684E 02	8.9389E 02	8.8658E 02	8.7173E 02	9.7988E 02
4.20249	1.0726E 03	1.0217E 03	9.7937E 02	9.3680E 02	8.9392E 02	8.8662E 02	8.7180E 02	9.7976E 02
4.26499	1.0723E 03	1.0215E 03	9.7926E 02	9.3676E 02	8.9395E 02	8.8666E 02	8.7186E 02	9.7967E 02
4.32749	1.0721E 03	1.0214E 03	9.7915E 02	9.3672E 02	8.9396E 02	8.8668E 02	8.7192E 02	9.7956E 02
4.33499	1.0721E 03	1.0214E 03	9.7914E 02	9.3671E 02	8.9396E 02	8.8669E 02	8.7193E 02	9.7955E 02
4.38999	1.0718E 03	1.0212E 03	9.7904E 02	9.3667E 02	8.9398E 02	8.8672E 02	8.7198E 02	9.7945E 02
4.45249	1.0716E 03	1.0210E 03	9.7893E 02	9.3662E 02	8.9401E 02	8.8676E 02	8.7204E 02	9.7934E 02
4.51499	1.0713E 03	1.0208E 03	9.7881E 02	9.3658E 02	8.9404E 02	8.8680E 02	8.7210E 02	9.7923E 02
4.57749	1.0711E 03	1.0207E 03	9.7870E 02	9.3653E 02	8.9407E 02	8.8685E 02	8.7217E 02	9.7911E 02
4.63999	1.0708E 03	1.0205E 03	9.7859E 02	9.3649E 02	8.9411E 02	8.8689E 02	8.7224E 02	9.7900E 02
4.70249	1.0706E 03	1.0203E 03	9.7848E 02	9.3645E 02	8.9415E 02	8.8695E 02	8.7231E 02	9.7889E 02
4.76499	1.0703E 03	1.0201E 03	9.7836E 02	9.3642E 02	8.9419E 02	8.8700E 02	8.7239E 02	9.7876E 02
4.82749	1.0700E 03	1.0199E 03	9.7825E 02	9.3638E 02	8.9423E 02	8.8706E 02	8.7247E 02	9.7868E 02
4.88999	1.0698E 03	1.0198E 03	9.7814E 02	9.3635E 02	8.9428E 02	8.8712E 02	8.7255E 02	9.7857E 02
4.95249	1.0695E 03	1.0196E 03	9.7804E 02	9.3632E 02	8.9433E 02	8.8719E 02	8.7264E 02	9.7846E 02

AVERAGE CHANNEL TEMPERATURES - CEX
AXIAL POSITION 2

	CEX REGION							
TIME	CENTER	2	4	6	BOUNDARY	CLAD	STRUCTURE	AVERAGE
0.	1.2418E 03	1.1699E 03	1.0966E 03	1.0218E 03	9.4524E 02	9.3190E 02	9.0513E 02	1.0950E 03
0.17750	1.2468E 03	1.1691E 03	1.0964E 03	1.0218E 03	9.4505E 02	9.3241E 02	9.0543E 02	1.0957E 03
0.35875	1.2537E 03	1.1690E 03	1.0965E 03	1.0226E 03	9.4736E 02	9.3426E 02	9.0725E 02	1.0964E 03
0.62125	1.2546E 03	1.1691E 03	1.0966E 03	1.0229E 03	9.4768E 02	9.3461E 02	9.0762E 02	1.0966E 03
0.88375	1.2543E 03	1.1691E 03	1.0967E 03	1.0231E 03	9.4802E 02	9.3495E 02	9.0799E 02	1.0968E 03
0.88875	1.2545E 03	1.1694E 03	1.0972E 03	1.0238E 03	9.4902E 02	9.3602E 02	9.0913E 02	1.0973E 03
0.93125	1.2550E 03	1.1695E 03	1.0973E 03	1.0240E 03	9.4936E 02	9.3636E 02	9.0951E 02	1.0975E 03
0.99375	1.2551E 03	1.1696E 03	1.0975E 03	1.0243E 03	9.4969E 02	9.3671E 02	9.0990E 02	1.0977E 03
1.05625	1.2552E 03	1.1697E 03	1.0977E 03	1.0245E 03	9.5002E 02	9.3705E 02	9.1027E 02	1.0978E 03
1.06625	1.2552E 03	1.1698E 03	1.0978E 03	1.0246E 03	9.5016E 02	9.3721E 02	9.1045E 02	1.0979E 03
1.12250	1.2553E 03	1.1698E 03	1.0978E 03	1.0248E 03	9.5036E 02	9.3740E 02	9.1066E 02	1.0980E 03
1.49750	1.2554E 03	1.1703E 03	1.0987E 03	1.0260E 03	9.5205E 02	9.3916E 02	9.1265E 02	1.0989E 03
1.84250	1.2552E 03	1.1705E 03	1.0993E 03	1.0271E 03	9.5380E 02	9.4103E 02	9.1460E 02	1.0996E 03
2.17250	1.2548E 03	1.1706E 03	1.0999E 03	1.0283E 03	9.5548E 02	9.4280E 02	9.1660E 02	1.1002E 03
2.52750	1.2541E 03	1.1706E 03	1.1004E 03	1.0293E 03	9.5702E 02	9.4442E 02	9.1850E 02	1.1007E 03
2.91999	1.2532E 03	1.1703E 03	1.1007E 03	1.0301E 03	9.5849E 02	9.4600E 02	9.2035E 02	1.1009E 03
3.29749	1.2521E 03	1.1696E 03	1.1008E 03	1.0309E 03	9.6011E 02	9.4777E 02	9.2223E 02	1.1011E 03
3.63999	1.2509E 03	1.1693E 03	1.1010E 03	1.0319E 03	9.6174E 02	9.4952E 02	9.2425E 02	1.1013E 03
3.70249	1.2507E 03	1.1693E 03	1.1010E 03	1.0320E 03	9.6200E 02	9.4979E 02	9.2459E 02	1.1014E 03
3.76499	1.2505E 03	1.1692E 03	1.1010E 03	1.0321E 03	9.6225E 02	9.5006E 02	9.2492E 02	1.1014E 03
3.82749	1.2503E 03	1.1691E 03	1.1011E 03	1.0323E 03	9.6247E 02	9.5029E 02	9.2522E 02	1.1014E 03
3.88999	1.2500E 03	1.1690E 03	1.1011E 03	1.0324E 03	9.6268E 02	9.5052E 02	9.2551E 02	1.1014E 03
3.95249	1.2498E 03	1.1689E 03	1.1011E 03	1.0325E 03	9.6290E 02	9.5076E 02	9.2579E 02	1.1014E 03
4.01499	1.2496E 03	1.1688E 03	1.1011E 03	1.0326E 03	9.6311E 02	9.5099E 02	9.2607E 02	1.1014E 03
4.07749	1.2493E 03	1.1687E 03	1.1011E 03	1.0327E 03	9.6332E 02	9.5121E 02	9.2634E 02	1.1014E 03
4.13999	1.2491E 03	1.1686E 03	1.1011E 03	1.0328E 03	9.6352E 02	9.5144E 02	9.2661E 02	1.1014E 03
4.20249	1.2489E 03	1.1684E 03	1.1011E 03	1.0329E 03	9.6372E 02	9.5165E 02	9.2687E 02	1.1014E 03
4.26499	1.2486E 03	1.1683E 03	1.1010E 03	1.0330E 03	9.6391E 02	9.5186E 02	9.2713E 02	1.1014E 03
4.32749	1.2484E 03	1.1682E 03	1.1010E 03	1.0330E 03	9.6406E 02	9.5201E 02	9.2736E 02	1.1013E 03
4.38999	1.2483E 03	1.1682E 03	1.1010E 03	1.0330E 03	9.6407E 02	9.5203E 02	9.2736E 02	1.1013E 03
4.38999	1.2481E 03	1.1681E 03	1.1010E 03	1.0331E 03	9.6422E 02	9.5220E 02	9.2758E 02	1.1013E 03
4.45249	1.2479E 03	1.1679E 03	1.1009E 03	1.0332E 03	9.6440E 02	9.5240E 02	9.2781E 02	1.1013E 03
4.51499	1.2476E 03	1.1678E 03	1.1009E 03	1.0332E 03	9.6459E 02	9.5261E 02	9.2805E 02	1.1012E 03
4.57749	1.2474E 03	1.1677E 03	1.1009E 03	1.0333E 03	9.6479E 02	9.5283E 02	9.2829E 02	1.1012E 03
4.63999	1.2471E 03	1.1675E 03	1.1008E 03	1.0334E 03	9.6499E 02	9.5306E 02	9.2855E 02	1.1012E 03
4.70249	1.2469E 03	1.1674E 03	1.1008E 03	1.0335E 03	9.6521E 02	9.5330E 02	9.2882E 02	1.1012E 03
4.76499	1.2466E 03	1.1672E 03	1.1008E 03	1.0336E 03	9.6543E 02	9.5355E 02	9.2910E 02	1.1011E 03
4.82749	1.2463E 03	1.1671E 03	1.1007E 03	1.0336E 03	9.6568E 02	9.5382E 02	9.2939E 02	1.1011E 03
4.88999	1.2461E 03	1.1669E 03	1.1007E 03	1.0338E 03	9.6593E 02	9.5410E 02	9.2969E 02	1.1011E 03
4.95249	1.2458E 03	1.1668E 03	1.1007E 03	1.0339E 03	9.6618E 02	9.5438E 02	9.3001E 02	1.1011E 03

AVERAGE CHANNEL TEMPERATURES - CEX
AXIAL POSITION 3

TIME	CENTER	2	4	6	BOUNDARY	CLAD	STRUCTURE	AVERAGE
	C E X	R E G I O N						
0.	1.3610E 03	1.2757E 03	1.1885E 03	1.0993E 03	1.0077E 03	9.9145E 02	9.5877E 02	1.1871E 03
0.17750	1.3693E 03	1.2747E 03	1.1883E 03	1.0994E 03	1.0084E 03	9.9231E 02	9.5925E 02	1.1872E 03
0.55875	1.3751E 03	1.2747E 03	1.1888E 03	1.1012E 03	1.0117E 03	9.9586E 02	9.6205E 02	1.1886E 03
0.62125	1.3755E 03	1.2749E 03	1.1890E 03	1.1016E 03	1.0124E 03	9.9655E 02	9.6336E 02	1.1890E 03
0.66375	1.3759E 03	1.2750E 03	1.1893E 03	1.1020E 03	1.0130E 03	9.9723E 02	9.6408E 02	1.1893E 03
0.86875	1.3766E 03	1.2757E 03	1.1903E 03	1.1035E 03	1.0150E 03	9.9935E 02	9.6630E 02	1.1904E 03
0.93125	1.3768E 03	1.2759E 03	1.1907E 03	1.1040E 03	1.0157E 03	1.0000E 03	9.6707E 02	1.1908E 03
0.99375	1.3770E 03	1.2761E 03	1.1910E 03	1.1046E 03	1.0164E 03	1.0007E 03	9.6782E 02	1.1912E 03
1.05625	1.3772E 03	1.2764E 03	1.1914E 03	1.1051E 03	1.0171E 03	1.0014E 03	9.6857E 02	1.1916E 03
1.08625	1.3772E 03	1.2765E 03	1.1916E 03	1.1053E 03	1.0174E 03	1.0018E 03	9.6893E 02	1.1918E 03
1.12250	1.3773E 03	1.2767E 03	1.1918E 03	1.1056E 03	1.0178E 03	1.0021E 03	9.6935E 02	1.1920E 03
1.49750	1.3781E 03	1.2782E 03	1.1940E 03	1.1085E 03	1.0213E 03	1.0058E 03	9.7337E 02	1.1942E 03
1.84250	1.3787E 03	1.2795E 03	1.1960E 03	1.1112E 03	1.0249E 03	1.0096E 03	9.7722E 02	1.1962E 03
2.17250	1.3791E 03	1.2807E 03	1.1979E 03	1.1139E 03	1.0285E 03	1.0132E 03	9.8123E 02	1.1982E 03
2.52750	1.3794E 03	1.2819E 03	1.1998E 03	1.1166E 03	1.0318E 03	1.0167E 03	9.8508E 02	1.2001E 03
2.91999	1.3797E 03	1.2830E 03	1.2017E 03	1.1192E 03	1.0351E 03	1.0201E 03	9.8886E 02	1.2019E 03
3.29749	1.3797E 03	1.2838E 03	1.2032E 03	1.1216E 03	1.0386E 03	1.0237E 03	9.9260E 02	1.2035E 03
3.63999	1.3795E 03	1.2845E 03	1.2048E 03	1.1241E 03	1.0421E 03	1.0274E 03	9.9661E 02	1.2052E 03
3.70249	1.3795E 03	1.2847E 03	1.2051E 03	1.1246E 03	1.0427E 03	1.0280E 03	9.9730E 02	1.2054E 03
3.76499	1.3794E 03	1.2848E 03	1.2054E 03	1.1250E 03	1.0432E 03	1.0286E 03	9.9796E 02	1.2057E 03
3.82749	1.3794E 03	1.2849E 03	1.2057E 03	1.1254E 03	1.0437E 03	1.0291E 03	9.9859E 02	1.2060E 03
3.88999	1.3793E 03	1.2851E 03	1.2059E 03	1.1258E 03	1.0442E 03	1.0297E 03	9.9919E 02	1.2062E 03
3.95249	1.3793E 03	1.2852E 03	1.2062E 03	1.1262E 03	1.0447E 03	1.0302E 03	9.9978E 02	1.2065E 03
4.01499	1.3793E 03	1.2853E 03	1.2064E 03	1.1265E 03	1.0452E 03	1.0307E 03	1.0004E 03	1.2067E 03
4.07749	1.3792E 03	1.2854E 03	1.2067E 03	1.1269E 03	1.0457E 03	1.0312E 03	1.0009E 03	1.2070E 03
4.13999	1.3792E 03	1.2855E 03	1.2069E 03	1.1272E 03	1.0462E 03	1.0317E 03	1.0015E 03	1.2072E 03
4.20249	1.3791E 03	1.2856E 03	1.2071E 03	1.1276E 03	1.0466E 03	1.0322E 03	1.0020E 03	1.2074E 03
4.26499	1.3791E 03	1.2857E 03	1.2073E 03	1.1279E 03	1.0471E 03	1.0326E 03	1.0025E 03	1.2076E 03
4.32749	1.3790E 03	1.2858E 03	1.2075E 03	1.1282E 03	1.0475E 03	1.0330E 03	1.0030E 03	1.2078E 03
4.33499	1.3790E 03	1.2858E 03	1.2076E 03	1.1282E 03	1.0475E 03	1.0331E 03	1.0031E 03	1.2078E 03
4.38999	1.3789E 03	1.2859E 03	1.2077E 03	1.1285E 03	1.0479E 03	1.0334E 03	1.0035E 03	1.2080E 03
4.45249	1.3789E 03	1.2860E 03	1.2079E 03	1.1288E 03	1.0483E 03	1.0339E 03	1.0040E 03	1.2082E 03
4.51499	1.3788E 03	1.2860E 03	1.2081E 03	1.1291E 03	1.0487E 03	1.0343E 03	1.0044E 03	1.2084E 03
4.57749	1.3787E 03	1.2861E 03	1.2083E 03	1.1294E 03	1.0491E 03	1.0348E 03	1.0049E 03	1.2085E 03
4.63999	1.3787E 03	1.2861E 03	1.2084E 03	1.1297E 03	1.0496E 03	1.0353E 03	1.0055E 03	1.2087E 03
4.70249	1.3786E 03	1.2862E 03	1.2086E 03	1.1300E 03	1.0501E 03	1.0358E 03	1.0060E 03	1.2089E 03
4.76499	1.3785E 03	1.2862E 03	1.2088E 03	1.1303E 03	1.0506E 03	1.0363E 03	1.0065E 03	1.2091E 03
4.82749	1.3784E 03	1.2863E 03	1.2090E 03	1.1306E 03	1.0511E 03	1.0369E 03	1.0071E 03	1.2093E 03
4.88999	1.3783E 03	1.2863E 03	1.2091E 03	1.1310E 03	1.0516E 03	1.0374E 03	1.0077E 03	1.2095E 03
4.95249	1.3782E 03	1.2864E 03	1.2093E 03	1.1313E 03	1.0522E 03	1.0380E 03	1.0083E 03	1.2097E 03

AVERAGE CHANNEL TEMPERATURES - CEX
AXIAL POSITION 4

	CEX REGION							
TIME	CENTER	2	4	6	BOUNDARY	CLAD	STRUCTURE	AVERAGE
0.	1.4141E 03	1.3300E 03	1.2440E 03	1.1501E 03	1.0660E 03	1.0498E 03	1.0171E 03	1.2427E 03
0.17750	1.4223E 03	1.3290E 03	1.2438E 03	1.1563E 03	1.0609E 03	1.0508E 03	1.0177E 03	1.2429E 03
0.35675	1.4281E 03	1.3294E 03	1.2448E 03	1.1589E 03	1.0717E 03	1.0560E 03	1.0225E 03	1.2448E 03
0.62125	1.4285E 03	1.3294E 03	1.2452E 03	1.1596E 03	1.0726E 03	1.0570E 03	1.0235E 03	1.2453E 03
0.66375	1.4289E 03	1.3297E 03	1.2456E 03	1.1603E 03	1.0736E 03	1.0580E 03	1.0246E 03	1.2458E 03
0.86875	1.4296E 03	1.3306E 03	1.2471E 03	1.1626E 03	1.0767E 03	1.0612E 03	1.0279E 03	1.2475E 03
0.93125	1.4300E 03	1.3310E 03	1.2477E 03	1.1634E 03	1.0777E 03	1.0623E 03	1.0290E 03	1.2481E 03
0.99375	1.4303E 03	1.3314E 03	1.2483E 03	1.1642E 03	1.0788E 03	1.0634E 03	1.0302E 03	1.2487E 03
1.05625	1.4305E 03	1.3318E 03	1.2489E 03	1.1650E 03	1.0796E 03	1.0644E 03	1.0313E 03	1.2493E 03
1.08625	1.4307E 03	1.3320E 03	1.2492E 03	1.1654E 03	1.0803E 03	1.0649E 03	1.0319E 03	1.2496E 03
1.12250	1.4308E 03	1.3323E 03	1.2495E 03	1.1659E 03	1.0809E 03	1.0655E 03	1.0325E 03	1.2500E 03
1.49750	1.4324E 03	1.3351E 03	1.2534E 03	1.1706E 03	1.0865E 03	1.0713E 03	1.0387E 03	1.2537E 03
1.84250	1.4341E 03	1.3377E 03	1.2569E 03	1.1751E 03	1.0921E 03	1.0770E 03	1.0446E 03	1.2573E 03
2.17250	1.4357E 03	1.3404E 03	1.2603E 03	1.1797E 03	1.0977E 03	1.0828E 03	1.0507E 03	1.2609E 03
2.52750	1.4375E 03	1.3433E 03	1.2643E 03	1.1844E 03	1.1031E 03	1.0883E 03	1.0568E 03	1.2647E 03
2.91999	1.4395E 03	1.3464E 03	1.2682E 03	1.1890E 03	1.1085E 03	1.0939E 03	1.0627E 03	1.2685E 03
3.29749	1.4414E 03	1.3491E 03	1.2717E 03	1.1934E 03	1.1140E 03	1.0995E 03	1.0684E 03	1.2721E 03
3.63999	1.4430E 03	1.3516E 03	1.2752E 03	1.1979E 03	1.1196E 03	1.1053E 03	1.0745E 03	1.2756E 03
3.70249	1.4432E 03	1.3521E 03	1.2758E 03	1.1987E 03	1.1206E 03	1.1063E 03	1.0756E 03	1.2763E 03
3.76499	1.4435E 03	1.3526E 03	1.2765E 03	1.1995E 03	1.1215E 03	1.1072E 03	1.0766E 03	1.2769E 03
3.82749	1.4436E 03	1.3530E 03	1.2771E 03	1.2003E 03	1.1224E 03	1.1081E 03	1.0776E 03	1.2775E 03
3.88999	1.4441E 03	1.3535E 03	1.2777E 03	1.2010E 03	1.1232E 03	1.1090E 03	1.0785E 03	1.2781E 03
3.95249	1.4443E 03	1.3540E 03	1.2783E 03	1.2017E 03	1.1240E 03	1.1098E 03	1.0795E 03	1.2787E 03
4.01499	1.4446E 03	1.3544E 03	1.2789E 03	1.2024E 03	1.1248E 03	1.1107E 03	1.0804E 03	1.2793E 03
4.07749	1.4449E 03	1.3549E 03	1.2795E 03	1.2031E 03	1.1257E 03	1.1115E 03	1.0813E 03	1.2798E 03
4.13999	1.4452E 03	1.3553E 03	1.2800E 03	1.2038E 03	1.1264E 03	1.1123E 03	1.0822E 03	1.2804E 03
4.20249	1.4455E 03	1.3557E 03	1.2806E 03	1.2045E 03	1.1272E 03	1.1131E 03	1.0831E 03	1.2809E 03
4.26499	1.4457E 03	1.3562E 03	1.2811E 03	1.2051E 03	1.1280E 03	1.1138E 03	1.0839E 03	1.2815E 03
4.32749	1.4460E 03	1.3566E 03	1.2816E 03	1.2058E 03	1.1287E 03	1.1145E 03	1.0847E 03	1.2820E 03
4.33499	1.4460E 03	1.3566E 03	1.2817E 03	1.2058E 03	1.1287E 03	1.1146E 03	1.0848E 03	1.2820E 03
4.38999	1.4463E 03	1.3570E 03	1.2822E 03	1.2064E 03	1.1293E 03	1.1152E 03	1.0854E 03	1.2825E 03
4.45249	1.4465E 03	1.3574E 03	1.2827E 03	1.2069E 03	1.1300E 03	1.1159E 03	1.0862E 03	1.2830E 03
4.51499	1.4468E 03	1.3578E 03	1.2831E 03	1.2075E 03	1.1307E 03	1.1167E 03	1.0870E 03	1.2835E 03
4.57749	1.4470E 03	1.3582E 03	1.2836E 03	1.2081E 03	1.1315E 03	1.1174E 03	1.0877E 03	1.2839E 03
4.63999	1.4473E 03	1.3585E 03	1.2841E 03	1.2087E 03	1.1322E 03	1.1182E 03	1.0885E 03	1.2844E 03
4.70249	1.4475E 03	1.3589E 03	1.2846E 03	1.2093E 03	1.1330E 03	1.1190E 03	1.0893E 03	1.2849E 03
4.76499	1.4478E 03	1.3593E 03	1.2850E 03	1.2099E 03	1.1338E 03	1.1198E 03	1.0902F 03	1.2854E 03
4.82749	1.4480E 03	1.3596E 03	1.2855E 03	1.2106E 03	1.1346E 03	1.1207E 03	1.0910E 03	1.2859E 03
4.88999	1.4482E 03	1.3600E 03	1.2860E 03	1.2112E 03	1.1354E 03	1.1216E 03	1.0919E 03	1.2864E 03
4.95249	1.4484E 03	1.3603E 03	1.2865E 03	1.2119E 03	1.1363E 03	1.1225E 03	1.0929E 03	1.2869E 03

AVERAGE CHANNEL TEMPERATURES - CEX
AXIAL POSITION 5

	CEX REGION							
TIME	CENTER	2	4	6	BOUNDARY	CLAD	STRUCTURE	AVERAGE
0.	1.3939E 03	1.3247E 03	1.2544E 03	1.1827E 03	1.1096E 03	1.0963E 03	1.0695E 03	1.2535E 03
0.17750	1.4006E 03	1.3239E 03	1.2542E 03	1.1829E 03	1.1105E 03	1.0974E 03	1.0701E 03	1.2537E 03
0.55675	1.4054E 03	1.3243E 03	1.2555E 03	1.1861E 03	1.1162E 03	1.1036E 03	1.0757E 03	1.2559E 03
0.62125	1.4058E 03	1.3245E 03	1.2560E 03	1.1870E 03	1.1174E 03	1.1048E 03	1.0770E 03	1.2565E 03
0.68375	1.4061E 03	1.3249E 03	1.2566E 03	1.1878E 03	1.1187E 03	1.1061E 03	1.0783E 03	1.2571E 03
0.86075	1.4070E 03	1.3261E 03	1.2585E 03	1.1907E 03	1.1225E 03	1.1102E 03	1.0824E 03	1.2592E 03
0.93125	1.4073E 03	1.3265E 03	1.2593E 03	1.1916E 03	1.1239E 03	1.1115E 03	1.0839E 03	1.2600E 03
0.99375	1.4076E 03	1.3271E 03	1.2601E 03	1.1929E 03	1.1252E 03	1.1129E 03	1.0854E 03	1.2608E 03
1.05625	1.4079E 03	1.3276E 03	1.2609E 03	1.1940E 03	1.1266E 03	1.1143E 03	1.0868E 03	1.2616E 03
1.08625	1.4080E 03	1.3279E 03	1.2613E 03	1.1945E 03	1.1272E 03	1.1150E 03	1.0875E 03	1.2620E 03
1.12250	1.4082E 03	1.3282E 03	1.2618E 03	1.1951E 03	1.1280E 03	1.1158E 03	1.0884E 03	1.2625E 03
1.49750	1.4106E 03	1.3322E 03	1.2671E 03	1.2016E 03	1.1355E 03	1.1234E 03	1.0960E 03	1.2677E 03
1.86250	1.4134E 03	1.3365E 03	1.2721E 03	1.2077E 03	1.1427E 03	1.1309E 03	1.1042E 03	1.2728E 03
2.17250	1.4164E 03	1.3405E 03	1.2774E 03	1.2141E 03	1.1502E 03	1.1385E 03	1.1121E 03	1.2780E 03
2.52750	1.4199E 03	1.3453E 03	1.2832E 03	1.2207E 03	1.1576E 03	1.1460E 03	1.1201E 03	1.2837E 03
2.91999	1.4241E 03	1.3506E 03	1.2893E 03	1.2275E 03	1.1650E 03	1.1535E 03	1.1281E 03	1.2898E 03
3.29749	1.4283E 03	1.3556E 03	1.2950E 03	1.2339E 03	1.1723E 03	1.1610E 03	1.1356E 03	1.2955E 03
3.63999	1.4319E 03	1.3601E 03	1.3004E 03	1.2403E 03	1.1798E 03	1.1686E 03	1.1434E 03	1.3010E 03
3.70249	1.4326E 03	1.3610E 03	1.3014E 03	1.2415E 03	1.1811E 03	1.1699E 03	1.1449E 03	1.3020E 03
3.76499	1.4333E 03	1.3618E 03	1.3024E 03	1.2426E 03	1.1824E 03	1.1712E 03	1.1462E 03	1.3030E 03
3.82749	1.4340E 03	1.3627E 03	1.3034E 03	1.2436E 03	1.1836E 03	1.1724E 03	1.1476E 03	1.3039E 03
3.88999	1.4346E 03	1.3635E 03	1.3044E 03	1.2449E 03	1.1848E 03	1.1737E 03	1.1489E 03	1.3049E 03
3.95249	1.4353E 03	1.3644E 03	1.3054E 03	1.2459E 03	1.1859E 03	1.1748E 03	1.1501E 03	1.3059E 03
4.01499	1.4360E 03	1.3652E 03	1.3063E 03	1.2470E 03	1.1871E 03	1.1760E 03	1.1513E 03	1.3068E 03
4.07749	1.4367E 03	1.3661E 03	1.3073E 03	1.2480E 03	1.1882E 03	1.1771E 03	1.1526E 03	1.3078E 03
4.13999	1.4374E 03	1.3669E 03	1.3082E 03	1.2491E 03	1.1893E 03	1.1782E 03	1.1537E 03	1.3087E 03
4.20249	1.4380E 03	1.3677E 03	1.3091E 03	1.2501E 03	1.1904E 03	1.1793E 03	1.1549E 03	1.3096E 03
4.26499	1.4387E 03	1.3686E 03	1.3101E 03	1.2511E 03	1.1915E 03	1.1804E 03	1.1560E 03	1.3105E 03
4.32749	1.4394E 03	1.3694E 03	1.3110E 03	1.2520E 03	1.1925E 03	1.1814E 03	1.1571E 03	1.3114E 03
4.38999	1.4395E 03	1.3695E 03	1.3111E 03	1.2522E 03	1.1926E 03	1.1815E 03	1.1572E 03	1.3115E 03
4.38999	1.4401E 03	1.3702E 03	1.3118E 03	1.2530E 03	1.1934E 03	1.1824E 03	1.1582E 03	1.3123E 03
4.45249	1.4408E 03	1.3710E 03	1.3127E 03	1.2539E 03	1.1944E 03	1.1833E 03	1.1592E 03	1.3131E 03
4.51499	1.4414E 03	1.3718E 03	1.3135E 03	1.2548E 03	1.1954E 03	1.1844E 03	1.1602E 03	1.3139E 03
4.57749	1.4421E 03	1.3725E 03	1.3144E 03	1.2557E 03	1.1964E 03	1.1854E 03	1.1613E 03	1.3148E 03
4.63999	1.4428E 03	1.3733E 03	1.3152E 03	1.2566E 03	1.1974E 03	1.1864E 03	1.1623E 03	1.3156E 03
4.70249	1.4434E 03	1.3740E 03	1.3160E 03	1.2575E 03	1.1985E 03	1.1875E 03	1.1634E 03	1.3165E 03
4.76499	1.4441E 03	1.3748E 03	1.3168E 03	1.2585E 03	1.1995E 03	1.1886E 03	1.1645E 03	1.3173E 03
4.82749	1.4447E 03	1.3755E 03	1.3177E 03	1.2594E 03	1.2006E 03	1.1897E 03	1.1656E 03	1.3181E 03
4.88999	1.4453E 03	1.3762E 03	1.3185E 03	1.2604E 03	1.2017E 03	1.1909E 03	1.1668E 03	1.3190E 03
4.95249	1.4460E 03	1.3770E 03	1.3193E 03	1.2614E 03	1.2029E 03	1.1920E 03	1.1679E 03	1.3198E 03

AVERAGE CHANNEL TEMPERATURES - CEX
AXIAL POSITION 0

TIME	CENTER	2	4	6	BOUNDARY	CLAD	STRUCTURE	AVERAGE
	CEX REGION							
0.	1.3015E 03	1.2595E 03	1.2169E 03	1.1739E 03	1.1304E 03	1.1225E 03	1.1065E 03	1.2166E 03
0.17750	1.3056E 03	1.2598E 03	1.2168E 03	1.1741E 03	1.1312E 03	1.1234E 03	1.1070E 03	1.2168E 03
0.55875	1.3086E 03	1.2594E 03	1.2183E 03	1.1775E 03	1.1371E 03	1.1298E 03	1.1126E 03	1.2190E 03
0.62125	1.3088E 03	1.2597E 03	1.2188E 03	1.1784E 03	1.1383E 03	1.1311E 03	1.1139E 03	1.2196E 03
0.68375	1.3090E 03	1.2600E 03	1.2194E 03	1.1793E 03	1.1397E 03	1.1325E 03	1.1153E 03	1.2203E 03
0.86675	1.3098E 03	1.2613E 03	1.2216E 03	1.1825E 03	1.1440E 03	1.1370E 03	1.1199E 03	1.2225E 03
0.93125	1.3100E 03	1.2618E 03	1.2225E 03	1.1837E 03	1.1455E 03	1.1386E 03	1.1215E 03	1.2234E 03
0.99375	1.3103E 03	1.2624E 03	1.2234E 03	1.1849E 03	1.1470E 03	1.1401E 03	1.1231E 03	1.2243E 03
1.05625	1.3107E 03	1.2631E 03	1.2243E 03	1.1862E 03	1.1485E 03	1.1417E 03	1.1248E 03	1.2253E 03
1.08625	1.3108E 03	1.2634E 03	1.2248E 03	1.1868E 03	1.1493E 03	1.1425E 03	1.1256E 03	1.2257E 03
1.12250	1.3110E 03	1.2636E 03	1.2254E 03	1.1875E 03	1.1502E 03	1.1434E 03	1.1265E 03	1.2263E 03
1.49750	1.3140E 03	1.2686E 03	1.2317E 03	1.1952E 03	1.1589E 03	1.1523E 03	1.1361E 03	1.2325E 03
1.84250	1.3177E 03	1.2738E 03	1.2380E 03	1.2025E 03	1.1673E 03	1.1609E 03	1.1448E 03	1.2387E 03
2.17250	1.3219E 03	1.2793E 03	1.2446E 03	1.2102E 03	1.1760E 03	1.1697E 03	1.1539E 03	1.2453E 03
2.52750	1.3271E 03	1.2858E 03	1.2520E 03	1.2184E 03	1.1848E 03	1.1786E 03	1.1632E 03	1.2526E 03
2.91999	1.3335E 03	1.2933E 03	1.2601E 03	1.2270E 03	1.1938E 03	1.1877E 03	1.1727E 03	1.2606E 03
3.29749	1.3399E 03	1.3004E 03	1.2677E 03	1.2350E 03	1.2025E 03	1.1964E 03	1.1815E 03	1.2682E 03
3.33999	1.3456E 03	1.3069E 03	1.2748E 03	1.2429E 03	1.2112E 03	1.2053E 03	1.1904E 03	1.2754E 03
3.70249	1.3469E 03	1.3081E 03	1.2762E 03	1.2444E 03	1.2127E 03	1.2068E 03	1.1920E 03	1.2767E 03
3.76499	1.3480E 03	1.3093E 03	1.2775E 03	1.2458E 03	1.2143E 03	1.2084E 03	1.1936E 03	1.2780E 03
3.82749	1.3496E 03	1.3105E 03	1.2786E 03	1.2473E 03	1.2157E 03	1.2099E 03	1.1952E 03	1.2794E 03
3.88999	1.3501E 03	1.3118E 03	1.2802E 03	1.2487E 03	1.2172E 03	1.2113E 03	1.1967E 03	1.2807E 03
3.95249	1.3512E 03	1.3130E 03	1.2815E 03	1.2501E 03	1.2186E 03	1.2128E 03	1.1982E 03	1.2820E 03
4.01499	1.3523E 03	1.3142E 03	1.2828E 03	1.2514E 03	1.2200E 03	1.2142E 03	1.1997E 03	1.2833E 03
4.07749	1.3535E 03	1.3154E 03	1.2841E 03	1.2528E 03	1.2214E 03	1.2156E 03	1.2011E 03	1.2845E 03
4.13999	1.3546E 03	1.3167E 03	1.2854E 03	1.2541E 03	1.2228E 03	1.2169E 03	1.2026E 03	1.2858E 03
4.20249	1.3557E 03	1.3179E 03	1.2867E 03	1.2554E 03	1.2241E 03	1.2183E 03	1.2039E 03	1.2871E 03
4.26499	1.3568E 03	1.3191E 03	1.2879E 03	1.2567E 03	1.2254E 03	1.2196E 03	1.2053E 03	1.2883E 03
4.32749	1.3579E 03	1.3203E 03	1.2892E 03	1.2580E 03	1.2267E 03	1.2208E 03	1.2066E 03	1.2896E 03
4.38999	1.3590E 03	1.3216E 03	1.2905E 03	1.2593E 03	1.2281E 03	1.2221E 03	1.2079E 03	1.2909E 03
4.45249	1.3601E 03	1.3227E 03	1.2916E 03	1.2605E 03	1.2291E 03	1.2233E 03	1.2092E 03	1.2920E 03
4.51499	1.3613E 03	1.3238E 03	1.2928E 03	1.2617E 03	1.2304E 03	1.2245E 03	1.2104E 03	1.2932E 03
4.57749	1.3624E 03	1.3250E 03	1.2940E 03	1.2629E 03	1.2316E 03	1.2257E 03	1.2117E 03	1.2943E 03
4.63999	1.3635E 03	1.3262E 03	1.2952E 03	1.2641E 03	1.2328E 03	1.2270E 03	1.2129E 03	1.2955E 03
4.70249	1.3646E 03	1.3273E 03	1.2963E 03	1.2653E 03	1.2341E 03	1.2282E 03	1.2142E 03	1.2967E 03
4.76499	1.3658E 03	1.3284E 03	1.2975E 03	1.2665E 03	1.2353E 03	1.2295E 03	1.2154E 03	1.2978E 03
4.82749	1.3667E 03	1.3295E 03	1.2986E 03	1.2677E 03	1.2366E 03	1.2308E 03	1.2167E 03	1.2990E 03
4.88999	1.3678E 03	1.3306E 03	1.2998E 03	1.2689E 03	1.2379E 03	1.2322E 03	1.2181E 03	1.3002E 03
4.95249	1.3689E 03	1.3318E 03	1.3010E 03	1.2701E 03	1.2393E 03	1.2335E 03	1.2194E 03	1.3014E 03

HOT CHANNEL TEMPERATURES - FUEL
AXIAL POSITION 1

TIME	FUEL RADIUS NUMBER CENTER	2	4	6	BOUNDARY	CLAD	COOLANT	AVERAGE
0.	1.2799E 03	1.1990E 03	1.1178E 03	1.0343E 03	9.4907E 02	9.2048E 02	8.6574E 02	1.1167E 03
0.17750	1.2919E 03	1.1983E 03	1.1172E 03	1.0340E 03	9.4778E 02	9.2078E 02	8.6601E 02	1.1167E 03
0.55875	1.2951E 03	1.1987E 03	1.1172E 03	1.0342E 03	9.5042E 02	9.2087E 02	8.6671E 02	1.1172E 03
0.82125	1.2951E 03	1.1987E 03	1.1172E 03	1.0342E 03	9.4878E 02	9.2126E 02	8.6681E 02	1.1172E 03
0.88375	1.2951E 03	1.1987E 03	1.1172E 03	1.0343E 03	9.5018E 02	9.2112E 02	8.6694E 02	1.1173E 03
0.86875	1.2950E 03	1.1986E 03	1.1172E 03	1.0343E 03	9.4933E 02	9.2157E 02	8.6730E 02	1.1172E 03
0.93125	1.2946E 03	1.1985E 03	1.1171E 03	1.0344E 03	9.5027E 02	9.2149E 02	8.6742E 02	1.1172E 03
0.99375	1.2947E 03	1.1984E 03	1.1171E 03	1.0343E 03	9.4957E 02	9.2170E 02	8.6752E 02	1.1171E 03
1.05625	1.2945E 03	1.1982E 03	1.1170E 03	1.0343E 03	9.5026E 02	9.2165E 02	8.6764E 02	1.1171E 03
1.08625	1.2944E 03	1.1982E 03	1.1169E 03	1.0343E 03	9.4959E 02	9.2180E 02	8.6768E 02	1.1170E 03
1.12250	1.2943E 03	1.1981E 03	1.1169E 03	1.0343E 03	9.5032E 02	9.2171E 02	8.6775E 02	1.1170E 03
1.49750	1.2925E 03	1.1967E 03	1.1160E 03	1.0338E 03	9.5017E 02	9.2199E 02	8.6833E 02	1.1161E 03
1.84250	1.2903E 03	1.1951E 03	1.1148E 03	1.0332E 03	9.5012E 02	9.2225E 02	8.6898E 02	1.1150E 03
2.17250	1.2879E 03	1.1933E 03	1.1136E 03	1.0326E 03	9.5013E 02	9.2243E 02	8.6957E 02	1.1137E 03
2.52750	1.2849E 03	1.1910E 03	1.1120E 03	1.0317E 03	9.4988E 02	9.2252E 02	8.7010E 02	1.1122E 03
2.91999	1.2814E 03	1.1884E 03	1.1101E 03	1.0306E 03	9.4957E 02	9.2252E 02	8.7064E 02	1.1103E 03
3.29749	1.2779E 03	1.1857E 03	1.1082E 03	1.0295E 03	9.4951E 02	9.2256E 02	8.7131E 02	1.1084E 03
3.63999	1.2746E 03	1.1833E 03	1.1065E 03	1.0286E 03	9.4913E 02	9.2272E 02	8.7189E 02	1.1067E 03
3.70249	1.2740E 03	1.1829E 03	1.1062E 03	1.0284E 03	9.4930E 02	9.2268E 02	8.7199E 02	1.1064E 03
3.76499	1.2734E 03	1.1824E 03	1.1059E 03	1.0282E 03	9.4905E 02	9.2272E 02	8.7207E 02	1.1061E 03
3.82749	1.2728E 03	1.1820E 03	1.1056E 03	1.0280E 03	9.4919E 02	9.2267E 02	8.7215E 02	1.1058E 03
3.88999	1.2722E 03	1.1815E 03	1.1052E 03	1.0278E 03	9.4893E 02	9.2270E 02	8.7223E 02	1.1054E 03
3.95249	1.2716E 03	1.1811E 03	1.1049E 03	1.0276E 03	9.4907E 02	9.2265E 02	8.7231E 02	1.1051E 03
4.01499	1.2710E 03	1.1806E 03	1.1046E 03	1.0274E 03	9.4882E 02	9.2268E 02	8.7239E 02	1.1048E 03
4.07749	1.2703E 03	1.1801E 03	1.1042E 03	1.0272E 03	9.4895E 02	9.2263E 02	8.7247E 02	1.1044E 03
4.13999	1.2697E 03	1.1797E 03	1.1039E 03	1.0270E 03	9.4870E 02	9.2265E 02	8.7255E 02	1.1041E 03
4.20249	1.2691E 03	1.1792E 03	1.1036E 03	1.0268E 03	9.4882E 02	9.2260E 02	8.7262E 02	1.1038E 03
4.26499	1.2685E 03	1.1787E 03	1.1032E 03	1.0266E 03	9.4858E 02	9.2262E 02	8.7268E 02	1.1034E 03
4.32749	1.2679E 03	1.1783E 03	1.1029E 03	1.0264E 03	9.4868E 02	9.2255E 02	8.7274E 02	1.1031E 03
4.38999	1.2673E 03	1.1778E 03	1.1025E 03	1.0262E 03	9.4857E 02	9.2256E 02	8.7281E 02	1.1028E 03
4.45249	1.2667E 03	1.1773E 03	1.1022E 03	1.0260E 03	9.4854E 02	9.2251E 02	8.7289E 02	1.1024E 03
4.51499	1.2660E 03	1.1769E 03	1.1019E 03	1.0258E 03	9.4830E 02	9.2253E 02	8.7297E 02	1.1021E 03
4.57749	1.2654E 03	1.1764E 03	1.1015E 03	1.0256E 03	9.4842E 02	9.2249E 02	8.7305E 02	1.1018E 03
4.63999	1.2648E 03	1.1759E 03	1.1012E 03	1.0254E 03	9.4819E 02	9.2251E 02	8.7314E 02	1.1014E 03
4.70249	1.2642E 03	1.1755E 03	1.1009E 03	1.0252E 03	9.4832E 02	9.2248E 02	8.7323E 02	1.1011E 03
4.76499	1.2636E 03	1.1750E 03	1.1005E 03	1.0250E 03	9.4809E 02	9.2251E 02	8.7333E 02	1.1008E 03
4.82749	1.2630E 03	1.1746E 03	1.1002E 03	1.0248E 03	9.4823E 02	9.2249E 02	8.7343E 02	1.1005E 03
4.88999	1.2624E 03	1.1741E 03	1.0999E 03	1.0246E 03	9.4801E 02	9.2253E 02	8.7353E 02	1.1001E 03
4.95249	1.2618E 03	1.1737E 03	1.0996E 03	1.0244E 03	9.4815E 02	9.2251E 02	8.7364E 02	1.0998E 03

HOT CHANNEL TEMPERATURES - FUEL
AXIAL POSITION 2

TIME	CENTER	FUEL RADIUS NUMBER 2	4	6	BOUNDARY	CLAD	COOLANT	AVERAGE
0.	1.5751E 03	1.4493E 03	1.3198E 03	1.1859E 03	1.0476E 03	9.9967E 02	9.0787E 02	1.3169E 03
0.17750	1.5943E 03	1.4472E 03	1.3186E 03	1.1854E 03	1.0448E 03	1.0006E 03	9.0873E 02	1.3169E 03
0.55875	1.5992E 03	1.4482E 03	1.3192E 03	1.1867E 03	1.0530E 03	1.0014E 03	9.1121E 02	1.3184E 03
0.62125	1.5993E 03	1.4483E 03	1.3194E 03	1.1866E 03	1.0470E 03	1.0028E 03	9.1161E 02	1.3184E 03
0.68375	1.5994E 03	1.4484E 03	1.3196E 03	1.1871E 03	1.0524E 03	1.0023E 03	9.1207E 02	1.3187E 03
0.86875	1.5994E 03	1.4486E 03	1.3199E 03	1.1876E 03	1.0492E 03	1.0042E 03	9.1335E 02	1.3190E 03
0.93125	1.5993E 03	1.4486E 03	1.3200E 03	1.1879E 03	1.0531E 03	1.0039E 03	9.1379E 02	1.3192E 03
0.99375	1.5991E 03	1.4485E 03	1.3201E 03	1.1880E 03	1.0504E 03	1.0047E 03	9.1418E 02	1.3192E 03
1.05625	1.5990E 03	1.4485E 03	1.3201E 03	1.1882E 03	1.0532E 03	1.0046E 03	9.1460E 02	1.3193E 03
1.08625	1.5989E 03	1.4484E 03	1.3201E 03	1.1882E 03	1.0507E 03	1.0052E 03	9.1477E 02	1.3192E 03
1.12250	1.5988E 03	1.4484E 03	1.3202E 03	1.1884E 03	1.0535E 03	1.0050E 03	9.1502E 02	1.3194E 03
1.49750	1.5970E 03	1.4473E 03	1.3198E 03	1.1886E 03	1.0539E 03	1.0067E 03	9.1713E 02	1.3190E 03
1.86250	1.5944E 03	1.4456E 03	1.3189E 03	1.1889E 03	1.0549E 03	1.0083E 03	9.1948E 02	1.3182E 03
2.17250	1.5914E 03	1.4437E 03	1.3180E 03	1.1889E 03	1.0561E 03	1.0098E 03	9.2164E 02	1.3173E 03
2.52750	1.5878E 03	1.4413E 03	1.3166E 03	1.1886E 03	1.0568E 03	1.0111E 03	9.2363E 02	1.3159E 03
2.91999	1.5834E 03	1.4382E 03	1.3147E 03	1.1879E 03	1.0574E 03	1.0122E 03	9.2563E 02	1.3140E 03
3.29749	1.5789E 03	1.4350E 03	1.3127E 03	1.1873E 03	1.0585E 03	1.0135E 03	9.2800E 02	1.3121E 03
3.63999	1.5746E 03	1.4321E 03	1.3110E 03	1.1869E 03	1.0589E 03	1.0149E 03	9.3017E 02	1.3105E 03
3.70249	1.5739E 03	1.4316E 03	1.3107E 03	1.1866E 03	1.0596E 03	1.0151E 03	9.3052E 02	1.3102E 03
3.76499	1.5731E 03	1.4311E 03	1.3104E 03	1.1867E 03	1.0592E 03	1.0153E 03	9.3083E 02	1.3099E 03
3.82749	1.5724E 03	1.4306E 03	1.3101E 03	1.1866E 03	1.0598E 03	1.0154E 03	9.3112E 02	1.3096E 03
3.88999	1.5716E 03	1.4300E 03	1.3097E 03	1.1864E 03	1.0594E 03	1.0156E 03	9.3142E 02	1.3092E 03
3.95249	1.5708E 03	1.4295E 03	1.3094E 03	1.1863E 03	1.0599E 03	1.0157E 03	9.3173E 02	1.3089E 03
4.01499	1.5700E 03	1.4289E 03	1.3090E 03	1.1861E 03	1.0595E 03	1.0160E 03	9.3203E 02	1.3085E 03
4.07749	1.5692E 03	1.4284E 03	1.3087E 03	1.1860E 03	1.0601E 03	1.0160E 03	9.3232E 02	1.3082E 03
4.13999	1.5685E 03	1.4278E 03	1.3083E 03	1.1858E 03	1.0597E 03	1.0162E 03	9.3260E 02	1.3078E 03
4.20249	1.5677E 03	1.4272E 03	1.3079E 03	1.1857E 03	1.0602E 03	1.0163E 03	9.3289E 02	1.3074E 03
4.26499	1.5669E 03	1.4267E 03	1.3076E 03	1.1855E 03	1.0598E 03	1.0165E 03	9.3312E 02	1.3071E 03
4.32749	1.5661E 03	1.4261E 03	1.3072E 03	1.1853E 03	1.0602E 03	1.0165E 03	9.3334E 02	1.3067E 03
4.33499	1.5660E 03	1.4260E 03	1.3071E 03	1.1853E 03	1.0600E 03	1.0166E 03	9.3336E 02	1.3066E 03
4.38999	1.5653E 03	1.4255E 03	1.3068E 03	1.1851E 03	1.0598E 03	1.0167E 03	9.3360E 02	1.3063E 03
4.45249	1.5645E 03	1.4249E 03	1.3064E 03	1.1850E 03	1.0603E 03	1.0167E 03	9.3388E 02	1.3059E 03
4.51499	1.5637E 03	1.4243E 03	1.3060E 03	1.1847E 03	1.0599E 03	1.0169E 03	9.3417E 02	1.3055E 03
4.57749	1.5629E 03	1.4238E 03	1.3056E 03	1.1846E 03	1.0604E 03	1.0170E 03	9.3447E 02	1.3052E 03
4.63999	1.5622E 03	1.4232E 03	1.3052E 03	1.1844E 03	1.0601E 03	1.0172E 03	9.3479E 02	1.3048E 03
4.70249	1.5612E 03	1.4226E 03	1.3048E 03	1.1843E 03	1.0605E 03	1.0173E 03	9.3512E 02	1.3044E 03
4.76499	1.5604E 03	1.4220E 03	1.3045E 03	1.1841E 03	1.0602E 03	1.0176E 03	9.3546E 02	1.3040E 03
4.82749	1.5596E 03	1.4214E 03	1.3041E 03	1.1840E 03	1.0607E 03	1.0177E 03	9.3583E 02	1.3037E 03
4.88999	1.5588E 03	1.4208E 03	1.3037E 03	1.1838E 03	1.0604E 03	1.0180E 03	9.3619E 02	1.3033E 03
4.95249	1.5580E 03	1.4203E 03	1.3034E 03	1.1837E 03	1.0610E 03	1.0181E 03	9.3657E 02	1.3030E 03

HOT CHANNEL TEMPERATURES - FUEL
AXIAL POSITION 3

TIME	CENTER	FUEL RADIUS NUMBER 2	4	6	BOUNDARY	CLAD	COOLANT	AVERAGE
0.	1.7592E 03	1.6116E 03	1.4594E 03	1.3014E 03	1.1371E 03	1.0785E 03	9.6648E 02	1.4555E 03
0.17750	1.7616E 03	1.6093E 03	1.4580E 03	1.3006E 03	1.1320E 03	1.0802E 03	9.6794E 02	1.4555E 03
0.55675	1.7874E 03	1.6106E 03	1.4594E 03	1.3035E 03	1.1509E 03	1.0813E 03	9.7269E 02	1.4582E 03
0.62125	1.7877E 03	1.6111E 03	1.4598E 03	1.3031E 03	1.1328E 03	1.0852E 03	9.7342E 02	1.4580E 03
0.66375	1.7876E 03	1.6113E 03	1.4602E 03	1.3044E 03	1.1496E 03	1.0832E 03	9.7436E 02	1.4589E 03
0.68875	1.7881E 03	1.6120E 03	1.4612E 03	1.3052E 03	1.1307E 03	1.0880E 03	9.7684E 02	1.4595E 03
0.93125	1.7881E 03	1.6122E 03	1.4616E 03	1.3064E 03	1.1515E 03	1.0863E 03	9.7775E 02	1.4604E 03
0.99375	1.7881E 03	1.6123E 03	1.4619E 03	1.3063E 03	1.1399E 03	1.0892E 03	9.7850E 02	1.4602E 03
1.05625	1.7881E 03	1.6125E 03	1.4622E 03	1.3073E 03	1.1512E 03	1.0880E 03	9.7937E 02	1.4609E 03
1.08625	1.7881E 03	1.6126E 03	1.4623E 03	1.3070E 03	1.1400E 03	1.0903E 03	9.7968E 02	1.4607E 03
1.12250	1.7881E 03	1.6126E 03	1.4625E 03	1.3076E 03	1.1520E 03	1.0887E 03	9.8021E 02	1.4613E 03
1.49750	1.7872E 03	1.6120E 03	1.4636E 03	1.3097E 03	1.1517E 03	1.0930E 03	9.8445E 02	1.4625E 03
1.84250	1.7854E 03	1.6121E 03	1.4640E 03	1.3115E 03	1.1536E 03	1.0968E 03	9.8905E 02	1.4628E 03
2.17250	1.7832E 03	1.6113E 03	1.4644E 03	1.3130E 03	1.1569E 03	1.1002E 03	9.9340E 02	1.4632E 03
2.52750	1.7805E 03	1.6100E 03	1.4643E 03	1.3143E 03	1.1590E 03	1.1036E 03	9.9745E 02	1.4632E 03
2.91999	1.7770E 03	1.6081E 03	1.4636E 03	1.3152E 03	1.1613E 03	1.1066E 03	1.0015E 03	1.4626E 03
3.29749	1.7731E 03	1.6057E 03	1.4629E 03	1.3160E 03	1.1649E 03	1.1097E 03	1.0061E 03	1.4619E 03
3.63999	1.7695E 03	1.6038E 03	1.4625E 03	1.3171E 03	1.1664E 03	1.1133E 03	1.0105E 03	1.4615E 03
3.76249	1.7682E 03	1.6034E 03	1.4624E 03	1.3174E 03	1.1681E 03	1.1136E 03	1.0112E 03	1.4614E 03
3.76499	1.7682E 03	1.6031E 03	1.4623E 03	1.3175E 03	1.1673E 03	1.1144E 03	1.0118E 03	1.4613E 03
3.82749	1.7675E 03	1.6026E 03	1.4622E 03	1.3177E 03	1.1669E 03	1.1146E 03	1.0124E 03	1.4612E 03
3.88999	1.7669E 03	1.6024E 03	1.4621E 03	1.3177E 03	1.1681E 03	1.1153E 03	1.0131E 03	1.4611E 03
3.95249	1.7663E 03	1.6020E 03	1.4619E 03	1.3179E 03	1.1695E 03	1.1165E 03	1.0137E 03	1.4610E 03
4.01499	1.7656E 03	1.6016E 03	1.4618E 03	1.3179E 03	1.1688E 03	1.1162E 03	1.0143E 03	1.4608E 03
4.07749	1.7650E 03	1.6012E 03	1.4616E 03	1.3180E 03	1.1702E 03	1.1164E 03	1.0149E 03	1.4606E 03
4.13999	1.7643E 03	1.6008E 03	1.4614E 03	1.3180E 03	1.1695E 03	1.1170E 03	1.0155E 03	1.4604E 03
4.20249	1.7636E 03	1.6004E 03	1.4612E 03	1.3181E 03	1.1708E 03	1.1172E 03	1.0160E 03	1.4603E 03
4.26499	1.7629E 03	1.6000E 03	1.4610E 03	1.3181E 03	1.1701E 03	1.1178E 03	1.0166E 03	1.4601E 03
4.32749	1.7623E 03	1.5996E 03	1.4609E 03	1.3182E 03	1.1714E 03	1.1179E 03	1.0170E 03	1.4599E 03
4.38999	1.7622E 03	1.5995E 03	1.4608E 03	1.3182E 03	1.1708E 03	1.1181E 03	1.0171E 03	1.4599E 03
4.39999	1.7616E 03	1.5991E 03	1.4606E 03	1.3182E 03	1.1706E 03	1.1185E 03	1.0175E 03	1.4597E 03
4.45249	1.7609E 03	1.5987E 03	1.4604E 03	1.3182E 03	1.1719E 03	1.1186E 03	1.0181E 03	1.4595E 03
4.51499	1.7601E 03	1.5982E 03	1.4601E 03	1.3182E 03	1.1712E 03	1.1192E 03	1.0187E 03	1.4592E 03
4.57749	1.7594E 03	1.5977E 03	1.4599E 03	1.3182E 03	1.1724E 03	1.1194E 03	1.0193E 03	1.4590E 03
4.63999	1.7587E 03	1.5973E 03	1.4597E 03	1.3182E 03	1.1718E 03	1.1200E 03	1.0199E 03	1.4587E 03
4.70249	1.7579E 03	1.5968E 03	1.4594E 03	1.3183E 03	1.1731E 03	1.1203E 03	1.0205E 03	1.4586E 03
4.76499	1.7572E 03	1.5963E 03	1.4592E 03	1.3183E 03	1.1725E 03	1.1209E 03	1.0212E 03	1.4583E 03
4.82749	1.7564E 03	1.5958E 03	1.4590E 03	1.3184E 03	1.1738E 03	1.1212E 03	1.0219E 03	1.4582E 03
4.88999	1.7557E 03	1.5954E 03	1.4588E 03	1.3184E 03	1.1733E 03	1.1219E 03	1.0226E 03	1.4579E 03
4.95249	1.7550E 03	1.5949E 03	1.4586E 03	1.3186E 03	1.1746E 03	1.1222E 03	1.0233E 03	1.4578E 03

HOT CHANNEL TEMPERATURES - FUEL
AXIAL POSITION 4

TIME	CENTER	FUEL RADIUS NUMBER 2	4	6	BOUNDARY	CLAD	COOLANT	AVERAGE
0.	1.8139E 03	1.8686E 03	1.5184E 03	1.3630E 03	1.2015E 03	1.1430E 03	1.0309E 03	1.5147E 03
0.17750	1.8362E 03	1.8660E 03	1.5171E 03	1.3622E 03	1.1958E 03	1.1450E 03	1.0328E 03	1.5147E 03
0.55875	1.8417E 03	1.8670E 03	1.5191E 03	1.3666E 03	1.2230E 03	1.1466E 03	1.0397E 03	1.5184E 03
0.82125	1.8426E 03	1.8683E 03	1.5197E 03	1.3658E 03	1.1934E 03	1.1530E 03	1.0408E 03	1.5179E 03
0.88375	1.8422E 03	1.8687E 03	1.5203E 03	1.3680E 03	1.2224E 03	1.1493E 03	1.0422E 03	1.5195E 03
0.88875	1.8429E 03	1.8695E 03	1.5221E 03	1.3690E 03	1.1960E 03	1.1578E 03	1.0459E 03	1.5203E 03
0.93125	1.8431E 03	1.8703E 03	1.5228E 03	1.3715E 03	1.2252E 03	1.1536E 03	1.0473E 03	1.5221E 03
0.99375	1.8435E 03	1.8708E 03	1.5234E 03	1.3709E 03	1.2008E 03	1.1597E 03	1.0484E 03	1.5217E 03
1.05625	1.8435E 03	1.8712E 03	1.5240E 03	1.3730E 03	1.2280E 03	1.1563E 03	1.0498E 03	1.5233E 03
1.06625	1.8436E 03	1.8714E 03	1.5243E 03	1.3719E 03	1.1991E 03	1.1619E 03	1.0502E 03	1.5225E 03
1.12250	1.8437E 03	1.8717E 03	1.5247E 03	1.3739E 03	1.2297E 03	1.1573E 03	1.0511E 03	1.5239E 03
1.49750	1.8440E 03	1.8730E 03	1.5279E 03	1.3779E 03	1.2274E 03	1.1647E 03	1.0577E 03	1.5269E 03
1.8425E	1.8440E 03	1.8750E 03	1.5303E 03	1.3814E 03	1.2288E 03	1.1712E 03	1.0546E 03	1.5293E 03
2.17250	1.8441E 03	1.8761E 03	1.5327E 03	1.3854E 03	1.2306E 03	1.1767E 03	1.0713E 03	1.5318E 03
2.52750	1.8436E 03	1.8770E 03	1.5350E 03	1.3888E 03	1.2373E 03	1.1829E 03	1.0776E 03	1.5340E 03
2.91999	1.8424E 03	1.8775E 03	1.5368E 03	1.3921E 03	1.2409E 03	1.1885E 03	1.0840E 03	1.5358E 03
3.26749	1.8407E 03	1.8773E 03	1.5381E 03	1.3954E 03	1.2522E 03	1.1929E 03	1.0909E 03	1.5374E 03
3.63999	1.8369E 03	1.8773E 03	1.5396E 03	1.3983E 03	1.2488E 03	1.2001E 03	1.0976E 03	1.5388E 03
3.70249	1.8360E 03	1.8774E 03	1.5401E 03	1.3995E 03	1.2576E 03	1.1997E 03	1.0987E 03	1.5394E 03
3.76499	1.8365E 03	1.8774E 03	1.5404E 03	1.3994E 03	1.2508E 03	1.2019E 03	1.0998E 03	1.5394E 03
3.82749	1.8361E 03	1.8774E 03	1.5406E 03	1.4003E 03	1.2589E 03	1.2015E 03	1.1008E 03	1.5400E 03
3.88999	1.8370E 03	1.8775E 03	1.5409E 03	1.4005E 03	1.2526E 03	1.2036E 03	1.1017E 03	1.5400E 03
3.95249	1.8375E 03	1.8775E 03	1.5411E 03	1.4013E 03	1.2601E 03	1.2032E 03	1.1027E 03	1.5405E 03
4.01499	1.8373E 03	1.8774E 03	1.5414E 03	1.4014E 03	1.2543E 03	1.2052E 03	1.1037E 03	1.5404E 03
4.07749	1.8370E 03	1.8774E 03	1.5416E 03	1.4022E 03	1.2613E 03	1.2049E 03	1.1046E 03	1.5409E 03
4.13999	1.8367E 03	1.8774E 03	1.5417E 03	1.4023E 03	1.2559E 03	1.2067E 03	1.1055E 03	1.5409E 03
4.20249	1.8364E 03	1.8773E 03	1.5419E 03	1.4030E 03	1.2625E 03	1.2064E 03	1.1065E 03	1.5413E 03
4.26499	1.8361E 03	1.8773E 03	1.5421E 03	1.4031E 03	1.2574E 03	1.2081E 03	1.1073E 03	1.5412E 03
4.32749	1.8357E 03	1.8772E 03	1.5423E 03	1.4036E 03	1.2636E 03	1.2078E 03	1.1081E 03	1.5416E 03
4.38999	1.8357E 03	1.8772E 03	1.5423E 03	1.4037E 03	1.2605E 03	1.2084E 03	1.1082E 03	1.5415E 03
4.45249	1.8354E 03	1.8771E 03	1.5424E 03	1.4039E 03	1.2587E 03	1.2094E 03	1.1089E 03	1.5415E 03
4.51499	1.8351E 03	1.8770E 03	1.5425E 03	1.4045E 03	1.2646E 03	1.2092E 03	1.1097E 03	1.5418E 03
4.57749	1.8347E 03	1.8769E 03	1.5426E 03	1.4045E 03	1.2600E 03	1.2107E 03	1.1106E 03	1.5417E 03
4.63999	1.8343E 03	1.8768E 03	1.5426E 03	1.4051E 03	1.2656E 03	1.2106E 03	1.1115E 03	1.5420E 03
4.70249	1.8339E 03	1.8766E 03	1.5427E 03	1.4052E 03	1.2613E 03	1.2122E 03	1.1124E 03	1.5419E 03
4.76499	1.8335E 03	1.8765E 03	1.5428E 03	1.4056E 03	1.2668E 03	1.2121E 03	1.1134E 03	1.5422E 03
4.82749	1.8331E 03	1.8763E 03	1.5429E 03	1.4059E 03	1.2627E 03	1.2137E 03	1.1144E 03	1.5421E 03
4.88999	1.8326E 03	1.8761E 03	1.5430E 03	1.4060E 03	1.2681E 03	1.2137E 03	1.1155E 03	1.5424E 03
4.95249	1.8322E 03	1.8760E 03	1.5431E 03	1.4067E 03	1.2643E 03	1.2153E 03	1.1165E 03	1.5424E 03
4.99249	1.8317E 03	1.8758E 03	1.5433E 03	1.4074E 03	1.2695E 03	1.2154E 03	1.1176E 03	1.5427E 03

HOT CHANNEL TEMPERATURES - FUEL
AXIAL POSITION 5

TIME	CENTER	FUEL RADIUS NUMBER 2	4	6	BOUNDARY	CLAD	COOLANT	AVERAGE
0.	1.7331E 03	1.6125E 03	1.4885E 03	1.3609E 03	1.2293E 03	1.1813E 03	1.0895E 03	1.4860E 03
0.17750	1.7516E 03	1.6103E 03	1.4874E 03	1.3603E 03	1.2255E 03	1.1830E 03	1.0915E 03	1.4860E 03
0.55875	1.7560E 03	1.6121E 03	1.4898E 03	1.3652E 03	1.2488E 03	1.1867E 03	1.0998E 03	1.4898E 03
0.62125	1.7564E 03	1.6126E 03	1.4905E 03	1.3649E 03	1.2250E 03	1.1924E 03	1.1012E 03	1.4896E 03
0.68375	1.7567E 03	1.6131E 03	1.4913E 03	1.3671E 03	1.2498E 03	1.1897E 03	1.1029E 03	1.4913E 03
0.86875	1.7577E 03	1.6150E 03	1.4938E 03	1.3691E 03	1.2277E 03	1.1986E 03	1.1077E 03	1.4929E 03
0.93125	1.7581E 03	1.6156E 03	1.4947E 03	1.3718E 03	1.2580E 03	1.1952E 03	1.1095E 03	1.4948E 03
0.99375	1.7585E 03	1.6163E 03	1.4957E 03	1.3715E 03	1.2323E 03	1.2013E 03	1.1110E 03	1.4948E 03
1.05625	1.7590E 03	1.6170E 03	1.4966E 03	1.3740E 03	1.2592E 03	1.1984E 03	1.1127E 03	1.4967E 03
1.08625	1.7592E 03	1.6174E 03	1.4971E 03	1.3731E 03	1.2306E 03	1.2042E 03	1.1133E 03	1.4961E 03
1.12250	1.7595E 03	1.6178E 03	1.4977E 03	1.3753E 03	1.2615E 03	1.1999E 03	1.1144E 03	1.4977E 03
1.49750	1.7626E 03	1.6223E 03	1.5032E 03	1.3817E 03	1.2624E 03	1.2092E 03	1.1231E 03	1.5030E 03
1.84250	1.7650E 03	1.6259E 03	1.5079E 03	1.3874E 03	1.2654E 03	1.2179E 03	1.1319E 03	1.5077E 03
2.17250	1.7671E 03	1.6295E 03	1.5128E 03	1.3938E 03	1.2762E 03	1.2254E 03	1.1408E 03	1.5127E 03
2.52750	1.7696E 03	1.6333E 03	1.5178E 03	1.3997E 03	1.2775E 03	1.2343E 03	1.1492E 03	1.5175E 03
2.91999	1.7719E 03	1.6371E 03	1.5228E 03	1.4057E 03	1.2817E 03	1.2426E 03	1.1577E 03	1.5223E 03
3.29749	1.7735E 03	1.6400E 03	1.5269E 03	1.4121E 03	1.3059E 03	1.2474E 03	1.1665E 03	1.5272E 03
3.63999	1.7747E 03	1.6428E 03	1.5311E 03	1.4165E 03	1.2872E 03	1.2597E 03	1.1752E 03	1.5305E 03
3.70249	1.7749E 03	1.6433E 03	1.5319E 03	1.4190E 03	1.3153E 03	1.2565E 03	1.1768E 03	1.5323E 03
3.76499	1.7752E 03	1.6439E 03	1.5327E 03	1.4186E 03	1.2899E 03	1.2624E 03	1.1781E 03	1.5321E 03
3.82749	1.7755E 03	1.6444E 03	1.5335E 03	1.4210E 03	1.3176E 03	1.2591E 03	1.1796E 03	1.5338E 03
3.88999	1.7758E 03	1.6450E 03	1.5343E 03	1.4206E 03	1.2924E 03	1.2648E 03	1.1808E 03	1.5336E 03
3.95249	1.7761E 03	1.6455E 03	1.5350E 03	1.4229E 03	1.3198E 03	1.2616E 03	1.1823E 03	1.5353E 03
4.01499	1.7764E 03	1.6460E 03	1.5357E 03	1.4224E 03	1.2947E 03	1.2672E 03	1.1834E 03	1.5351E 03
4.07749	1.7766E 03	1.6465E 03	1.5364E 03	1.4247E 03	1.3219E 03	1.2639E 03	1.1849E 03	1.5367E 03
4.13999	1.7769E 03	1.6470E 03	1.5371E 03	1.4242E 03	1.2969E 03	1.2695E 03	1.1860E 03	1.5365E 03
4.20249	1.7771E 03	1.6475E 03	1.5378E 03	1.4264E 03	1.3241E 03	1.2662E 03	1.1873E 03	1.5381E 03
4.26499	1.7774E 03	1.6480E 03	1.5384E 03	1.4259E 03	1.2990E 03	1.2717E 03	1.1884E 03	1.5378E 03
4.32749	1.7776E 03	1.6484E 03	1.5390E 03	1.4281E 03	1.3261E 03	1.2682E 03	1.1896E 03	1.5393E 03
4.33499	1.7777E 03	1.6485E 03	1.5391E 03	1.4274E 03	1.3114E 03	1.2709E 03	1.1896E 03	1.5389E 03
4.38999	1.7779E 03	1.6489E 03	1.5396E 03	1.4274E 03	1.3008E 03	1.2737E 03	1.1905E 03	1.5390E 03
4.45249	1.7781E 03	1.6492E 03	1.5402E 03	1.4296E 03	1.3281E 03	1.2702E 03	1.1918E 03	1.5405E 03
4.51499	1.7783E 03	1.6496E 03	1.5407E 03	1.4289E 03	1.3025E 03	1.2758E 03	1.1928E 03	1.5401E 03
4.57749	1.7784E 03	1.6500E 03	1.5413E 03	1.4310E 03	1.3302E 03	1.2722E 03	1.1941E 03	1.5416E 03
4.63999	1.7786E 03	1.6503E 03	1.5418E 03	1.4303E 03	1.3042E 03	1.2779E 03	1.1952E 03	1.5412E 03
4.70249	1.7787E 03	1.6507E 03	1.5423E 03	1.4325E 03	1.3324E 03	1.2743E 03	1.1966E 03	1.5427E 03
4.76499	1.7788E 03	1.6510E 03	1.5429E 03	1.4318E 03	1.3060E 03	1.2801E 03	1.1977E 03	1.5423E 03
4.82749	1.7789E 03	1.6513E 03	1.5434E 03	1.4341E 03	1.3347E 03	1.2765E 03	1.1992E 03	1.5438E 03
4.88999	1.7790E 03	1.6516E 03	1.5439E 03	1.4334E 03	1.3078E 03	1.2825E 03	1.2004E 03	1.5434E 03
4.95249	1.7790E 03	1.6519E 03	1.5445E 03	1.4357E 03	1.3373E 03	1.2788E 03	1.2020E 03	1.5450E 03

HOT CHANNEL TEMPERATURES - FUEL
AXIAL POSITION 6

TIME	CENTER	FUEL RADIUS NUMBER 2	4	6	BOUNDARY	CLAD	COOLANT	AVERAGE
0.	1.5231E 03	1.4481E 03	1.3718E 03	1.2941E 03	1.2150E 03	1.1864E 03	1.1317E 03	1.3708E 03
0.17750	1.5343E 03	1.4466E 03	1.3710E 03	1.2939E 03	1.2133E 03	1.1876E 03	1.1333E 03	1.3708E 03
0.55875	1.5376E 03	1.4486E 03	1.3735E 03	1.2984E 03	1.2277E 03	1.1930E 03	1.1419E 03	1.3741E 03
0.62125	1.5373E 03	1.4486E 03	1.3742E 03	1.2989E 03	1.2175E 03	1.1965E 03	1.1435E 03	1.3745E 03
0.68375	1.5376E 03	1.4492E 03	1.3751E 03	1.3006E 03	1.2295E 03	1.1962E 03	1.1453E 03	1.3757E 03
0.86875	1.5388E 03	1.4513E 03	1.3781E 03	1.3036E 03	1.2228E 03	1.2030E 03	1.1507E 03	1.3763E 03
0.93125	1.5394E 03	1.4522E 03	1.3792E 03	1.3058E 03	1.2365E 03	1.2027E 03	1.1526E 03	1.3799E 03
0.99375	1.5400E 03	1.4531E 03	1.3804E 03	1.3066E 03	1.2270E 03	1.2063E 03	1.1544E 03	1.3806E 03
1.05625	1.5407E 03	1.4541E 03	1.3816E 03	1.3066E 03	1.2390E 03	1.2063E 03	1.1563E 03	1.3822E 03
1.08625	1.5410E 03	1.4546E 03	1.3822E 03	1.3087E 03	1.2262E 03	1.2091E 03	1.1572E 03	1.3824E 03
1.12250	1.5415E 03	1.4552E 03	1.3829E 03	1.3101E 03	1.2410E 03	1.2080E 03	1.1583E 03	1.3835E 03
1.49750	1.5468E 03	1.4618E 03	1.3906E 03	1.3186E 03	1.2475E 03	1.2183E 03	1.1685E 03	1.3910E 03
1.84250	1.5520E 03	1.4680E 03	1.3976E 03	1.3265E 03	1.2549E 03	1.2279E 03	1.1785E 03	1.3980E 03
2.17250	1.5571E 03	1.4743E 03	1.4049E 03	1.3348E 03	1.2651E 03	1.2374E 03	1.1886E 03	1.4053E 03
2.52750	1.5631E 03	1.4813E 03	1.4127E 03	1.3434E 03	1.2727E 03	1.2474E 03	1.1987E 03	1.4131E 03
2.91999	1.5697E 03	1.4888E 03	1.4209E 03	1.3522E 03	1.2815E 03	1.2573E 03	1.2088E 03	1.4212E 03
3.29749	1.5755E 03	1.4953E 03	1.4282E 03	1.3606E 03	1.2950E 03	1.2659E 03	1.2188E 03	1.4287E 03
3.63999	1.5803E 03	1.5013E 03	1.4351E 03	1.3682E 03	1.2974E 03	1.2765E 03	1.2288E 03	1.4355E 03
3.70249	1.5812E 03	1.5024E 03	1.4365E 03	1.3700E 03	1.3058E 03	1.2770E 03	1.2306E 03	1.4370E 03
3.76499	1.5822E 03	1.5036E 03	1.4378E 03	1.3712E 03	1.3007E 03	1.2798E 03	1.2323E 03	1.4381E 03
3.82749	1.5831E 03	1.5047E 03	1.4391E 03	1.3729E 03	1.3089E 03	1.2803E 03	1.2340E 03	1.4396E 03
3.88999	1.5841E 03	1.5059E 03	1.4404E 03	1.3740E 03	1.3039E 03	1.2829E 03	1.2356E 03	1.4406E 03
3.95249	1.5851E 03	1.5070E 03	1.4416E 03	1.3757E 03	1.3119E 03	1.2834E 03	1.2372E 03	1.4421E 03
4.01499	1.5860E 03	1.5081E 03	1.4429E 03	1.3766E 03	1.3069E 03	1.2860E 03	1.2387E 03	1.4431E 03
4.07749	1.5870E 03	1.5093E 03	1.4441E 03	1.3784E 03	1.3148E 03	1.2863E 03	1.2402E 03	1.4446E 03
4.13999	1.5880E 03	1.5104E 03	1.4453E 03	1.3794E 03	1.3098E 03	1.2889E 03	1.2417E 03	1.4456E 03
4.20249	1.5889E 03	1.5115E 03	1.4465E 03	1.3811E 03	1.3176E 03	1.2892E 03	1.2432E 03	1.4470E 03
4.26499	1.5899E 03	1.5125E 03	1.4477E 03	1.3820E 03	1.3126E 03	1.2917E 03	1.2446E 03	1.4480E 03
4.32749	1.5908E 03	1.5136E 03	1.4489E 03	1.3836E 03	1.3203E 03	1.2920E 03	1.2460E 03	1.4493E 03
4.33499	1.5910E 03	1.5137E 03	1.4490E 03	1.3835E 03	1.3168E 03	1.2927E 03	1.2461E 03	1.4493E 03
4.38999	1.5916E 03	1.5146E 03	1.4500E 03	1.3845E 03	1.3152E 03	1.2944E 03	1.2473E 03	1.4502E 03
4.45249	1.5927E 03	1.5157E 03	1.4511E 03	1.3860E 03	1.3229E 03	1.2946E 03	1.2487E 03	1.4516E 03
4.51499	1.5936E 03	1.5166E 03	1.4522E 03	1.3868E 03	1.3177E 03	1.2970E 03	1.2500E 03	1.4524E 03
4.57749	1.5944E 03	1.5176E 03	1.4532E 03	1.3883E 03	1.3254E 03	1.2972E 03	1.2514E 03	1.4537E 03
4.63999	1.5953E 03	1.5185E 03	1.4542E 03	1.3891E 03	1.3202E 03	1.2996E 03	1.2528E 03	1.4545E 03
4.70249	1.5961E 03	1.5195E 03	1.4553E 03	1.3906E 03	1.3280E 03	1.2998E 03	1.2542E 03	1.4558E 03
4.76499	1.5969E 03	1.5204E 03	1.4563E 03	1.3914E 03	1.3227E 03	1.3023E 03	1.2557E 03	1.4566E 03
4.82749	1.5976E 03	1.5213E 03	1.4573E 03	1.3929E 03	1.3308E 03	1.3025E 03	1.2572E 03	1.4578E 03
4.88999	1.5984E 03	1.5222E 03	1.4583E 03	1.3937E 03	1.3253E 03	1.3051E 03	1.2587E 03	1.4586E 03
4.95249	1.5991E 03	1.5231E 03	1.4594E 03	1.3953E 03	1.3336E 03	1.3054E 03	1.2603E 03	1.4599E 03

HOT CHANNEL TEMPERATURES - CEX
AXIAL POSITION 1

TIME	CEX REGION CENTER	2	4	6	BOUNDARY	CLAD	STRUCTURE	AVERAGE
0.	1.1281E 03	1.0717E 03	1.0146E 03	9.5673E 02	8.9795E 02	8.8793E 02	8.6782E 02	1.0141E 03
0.17750	1.1334E 03	1.0711E 03	1.0144E 03	9.5666E 02	8.9808E 02	8.8810E 02	8.6790E 02	1.0141E 03
0.55875	1.1372E 03	1.0707E 03	1.0141E 03	9.5670E 02	8.9854E 02	8.8862E 02	8.6846E 02	1.0142E 03
0.62125	1.1374E 03	1.0707E 03	1.0141E 03	9.5674E 02	8.9862E 02	8.8872E 02	8.6858E 02	1.0143E 03
0.68375	1.1376E 03	1.0707E 03	1.0141E 03	9.5677E 02	8.9872E 02	8.8882E 02	8.6869E 02	1.0143E 03
0.86875	1.1380E 03	1.0707E 03	1.0141E 03	9.5690E 02	8.9899E 02	8.8912E 02	8.6903E 02	1.0144E 03
0.93125	1.1380E 03	1.0707E 03	1.0141E 03	9.5695E 02	8.9908E 02	8.8922E 02	8.6915E 02	1.0144E 03
0.99375	1.1380E 03	1.0707E 03	1.0141E 03	9.5699E 02	8.9917E 02	8.8932E 02	8.6927E 02	1.0145E 03
1.05625	1.1381E 03	1.0707E 03	1.0141E 03	9.5704E 02	8.9926E 02	8.8941E 02	8.6938E 02	1.0145E 03
1.08625	1.1381E 03	1.0707E 03	1.0141E 03	9.5706E 02	8.9929E 02	8.8946E 02	8.6943E 02	1.0145E 03
1.12250	1.1381E 03	1.0707E 03	1.0141E 03	9.5708E 02	8.9935E 02	8.8951E 02	8.6950E 02	1.0145E 03
1.49750	1.1377E 03	1.0704E 03	1.0141E 03	9.5723E 02	8.9977E 02	8.8998E 02	8.7009E 02	1.0145E 03
1.84250	1.1371E 03	1.0699E 03	1.0138E 03	9.5729E 02	9.0020E 02	8.9048E 02	8.7067E 02	1.0143E 03
2.17250	1.1362E 03	1.0693E 03	1.0135E 03	9.5733E 02	9.0060E 02	8.9093E 02	8.7127E 02	1.0140E 03
2.52750	1.1350E 03	1.0685E 03	1.0131E 03	9.5725E 02	9.0092E 02	8.9133E 02	8.7183E 02	1.0135E 03
2.91999	1.1334E 03	1.0675E 03	1.0124E 03	9.5706E 02	9.0119E 02	8.9168E 02	8.7237E 02	1.0129E 03
3.29749	1.1316E 03	1.0663E 03	1.0117E 03	9.5682E 02	9.0152E 02	8.9211E 02	8.7292E 02	1.0122E 03
3.63999	1.1301E 03	1.0652E 03	1.0111E 03	9.5666E 02	9.0185E 02	8.9253E 02	8.7353E 02	1.0116E 03
3.70249	1.1298E 03	1.0650E 03	1.0109E 03	9.5662E 02	9.0190E 02	8.9259E 02	8.7363E 02	1.0114E 03
3.76499	1.1295E 03	1.0647E 03	1.0108E 03	9.5658E 02	9.0195E 02	8.9265E 02	8.7373E 02	1.0113E 03
3.82749	1.1292E 03	1.0645E 03	1.0107E 03	9.5653E 02	9.0198E 02	8.9269E 02	8.7381E 02	1.0112E 03
3.88999	1.1289E 03	1.0643E 03	1.0105E 03	9.5648E 02	9.0201E 02	8.9274E 02	8.7390E 02	1.0111E 03
3.95249	1.1286E 03	1.0641E 03	1.0104E 03	9.5643E 02	9.0205E 02	8.9279E 02	8.7396E 02	1.0109E 03
4.01499	1.1283E 03	1.0639E 03	1.0103E 03	9.5637E 02	9.0208E 02	8.9284E 02	8.7406E 02	1.0108E 03
4.07749	1.1279E 03	1.0637E 03	1.0101E 03	9.5632E 02	9.0211E 02	8.9289E 02	8.7414E 02	1.0106E 03
4.13999	1.1276E 03	1.0634E 03	1.0100E 03	9.5626E 02	9.0214E 02	8.9293E 02	8.7422E 02	1.0105E 03
4.20249	1.1273E 03	1.0632E 03	1.0098E 03	9.5620E 02	9.0217E 02	8.9297E 02	8.7429E 02	1.0104E 03
4.26499	1.1270E 03	1.0630E 03	1.0097E 03	9.5614E 02	9.0220E 02	8.9301E 02	8.7437E 02	1.0102E 03
4.32749	1.1267E 03	1.0627E 03	1.0095E 03	9.5608E 02	9.0221E 02	8.9303E 02	8.7444E 02	1.0101E 03
4.33499	1.1266E 03	1.0627E 03	1.0095E 03	9.5607E 02	9.0221E 02	8.9304E 02	8.7444E 02	1.0100E 03
4.38999	1.1263E 03	1.0625E 03	1.0094E 03	9.5601E 02	9.0222E 02	8.9307E 02	8.7450E 02	1.0099E 03
4.45249	1.1260E 03	1.0623E 03	1.0092E 03	9.5594E 02	9.0225E 02	8.9311E 02	8.7456E 02	1.0098E 03
4.51499	1.1257E 03	1.0621E 03	1.0091E 03	9.5587E 02	9.0227E 02	8.9315E 02	8.7463E 02	1.0096E 03
4.57749	1.1253E 03	1.0618E 03	1.0089E 03	9.5581E 02	9.0230E 02	8.9320E 02	8.7470E 02	1.0095E 03
4.63999	1.1250E 03	1.0616E 03	1.0088E 03	9.5574E 02	9.0233E 02	8.9325E 02	8.7478E 02	1.0093E 03
4.70249	1.1247E 03	1.0613E 03	1.0086E 03	9.5568E 02	9.0237E 02	8.9330E 02	8.7486E 02	1.0092E 03
4.76499	1.1243E 03	1.0611E 03	1.0085E 03	9.5562E 02	9.0241E 02	8.9336E 02	8.7494E 02	1.0090E 03
4.82749	1.1240E 03	1.0608E 03	1.0083E 03	9.5556E 02	9.0245E 02	8.9342E 02	8.7503E 02	1.0089E 03
4.88999	1.1236E 03	1.0606E 03	1.0082E 03	9.5550E 02	9.0250E 02	8.9348E 02	8.7512E 02	1.0087E 03
4.95249	1.1233E 03	1.0604E 03	1.0080E 03	9.5545E 02	9.0255E 02	8.9355E 02	8.7521E 02	1.0086E 03

HOT CHANNEL TEMPERATURES - CEX
AXIAL POSITION 2

TIME	CENTER	CEX REGION 2	4	6	BOUNDARY	CLAD	STRUCTURE	AVERAGE
0.	1.3356E 03	1.2450E 03	1.1526E 03	1.0583E 03	9.6190E 02	9.4510E 02	9.1136E 02	1.1513E 03
0.17750	1.3442E 03	1.2439E 03	1.1523E 03	1.0583E 03	9.6230E 02	9.4561E 02	9.1161E 02	1.1513E 03
0.55875	1.3501E 03	1.2433E 03	1.1520E 03	1.0590E 03	9.6411E 02	9.4760E 02	9.1357E 02	1.1519E 03
0.62125	1.3505E 03	1.2434E 03	1.1521E 03	1.0592E 03	9.6445E 02	9.4798E 02	9.1397E 02	1.1521E 03
0.68375	1.3508E 03	1.2434E 03	1.1522E 03	1.0594E 03	9.6481E 02	9.4835E 02	9.1438E 02	1.1522E 03
0.86875	1.3513E 03	1.2436E 03	1.1526E 03	1.0601E 03	9.6589E 02	9.4951E 02	9.1563E 02	1.1527E 03
0.93125	1.3514E 03	1.2437E 03	1.1527E 03	1.0603E 03	9.6627E 02	9.4989E 02	9.1606E 02	1.1529E 03
0.99375	1.3515E 03	1.2438E 03	1.1529E 03	1.0606E 03	9.6662E 02	9.5027E 02	9.1648E 02	1.1531E 03
1.05625	1.3515E 03	1.2438E 03	1.1530E 03	1.0606E 03	9.6698E 02	9.5063E 02	9.1690E 02	1.1532E 03
1.08625	1.3515E 03	1.2439E 03	1.1531E 03	1.0610E 03	9.6714E 02	9.5082E 02	9.1710E 02	1.1533E 03
1.12250	1.3515E 03	1.2439E 03	1.1532E 03	1.0611E 03	9.6735E 02	9.5102E 02	9.1733E 02	1.1534E 03
1.49750	1.3514E 03	1.2442E 03	1.1540E 03	1.0624E 03	9.6918E 02	9.5295E 02	9.1954E 02	1.1542E 03
1.84250	1.3509E 03	1.2441E 03	1.1544E 03	1.0635E 03	9.7106E 02	9.5497E 02	9.2167E 02	1.1547E 03
2.17250	1.3500E 03	1.2439E 03	1.1549E 03	1.0646E 03	9.7288E 02	9.5689E 02	9.2389E 02	1.1552E 03
2.52750	1.3489E 03	1.2436E 03	1.1552E 03	1.0656E 03	9.7453E 02	9.5867E 02	9.2600E 02	1.1555E 03
2.91999	1.3475E 03	1.2430E 03	1.1552E 03	1.0664E 03	9.7611E 02	9.6037E 02	9.2805E 02	1.1556E 03
3.29749	1.3457E 03	1.2420E 03	1.1551E 03	1.0671E 03	9.7782E 02	9.6227E 02	9.3009E 02	1.1555E 03
3.63999	1.3440E 03	1.2411E 03	1.1550E 03	1.0679E 03	9.7957E 02	9.6417E 02	9.3233E 02	1.1555E 03
3.70249	1.3436E 03	1.2410E 03	1.1550E 03	1.0681E 03	9.7985E 02	9.6447E 02	9.3271E 02	1.1555E 03
3.76499	1.3433E 03	1.2408E 03	1.1550E 03	1.0682E 03	9.8012E 02	9.6476E 02	9.3308E 02	1.1554E 03
3.82749	1.3430E 03	1.2407E 03	1.1550E 03	1.0683E 03	9.8035E 02	9.6500E 02	9.3342E 02	1.1554E 03
3.88999	1.3427E 03	1.2405E 03	1.1550E 03	1.0684E 03	9.8058E 02	9.6526E 02	9.3374E 02	1.1554E 03
3.95249	1.3423E 03	1.2403E 03	1.1549E 03	1.0685E 03	9.8081E 02	9.6551E 02	9.3405E 02	1.1554E 03
4.01499	1.3420E 03	1.2402E 03	1.1549E 03	1.0686E 03	9.8104E 02	9.6576E 02	9.3436E 02	1.1553E 03
4.07749	1.3416E 03	1.2400E 03	1.1548E 03	1.0687E 03	9.8126E 02	9.6601E 02	9.3467E 02	1.1553E 03
4.13999	1.3413E 03	1.2398E 03	1.1548E 03	1.0688E 03	9.8147E 02	9.6624E 02	9.3496E 02	1.1552E 03
4.20249	1.3410E 03	1.2396E 03	1.1547E 03	1.0688E 03	9.8168E 02	9.6648E 02	9.3525E 02	1.1552E 03
4.26499	1.3406E 03	1.2394E 03	1.1547E 03	1.0689E 03	9.8189E 02	9.6670E 02	9.3554E 02	1.1551E 03
4.32749	1.3403E 03	1.2393E 03	1.1546E 03	1.0690E 03	9.8204E 02	9.6687E 02	9.3580E 02	1.1550E 03
4.33499	1.3402E 03	1.2392E 03	1.1546E 03	1.0690E 03	9.8206E 02	9.6689E 02	9.3583E 02	1.1550E 03
4.38999	1.3399E 03	1.2391E 03	1.1545E 03	1.0690E 03	9.8221E 02	9.6707E 02	9.3605E 02	1.1550E 03
4.45249	1.3396E 03	1.2389E 03	1.1544E 03	1.0690E 03	9.8240E 02	9.6728E 02	9.3630E 02	1.1549E 03
4.51499	1.3392E 03	1.2386E 03	1.1544E 03	1.0691E 03	9.8260E 02	9.6751E 02	9.3656E 02	1.1548E 03
4.57749	1.3389E 03	1.2384E 03	1.1543E 03	1.0691E 03	9.8281E 02	9.6774E 02	9.3683E 02	1.1547E 03
4.63999	1.3385E 03	1.2382E 03	1.1542E 03	1.0692E 03	9.8302E 02	9.6799E 02	9.3710E 02	1.1546E 03
4.70249	1.3381E 03	1.2380E 03	1.1541E 03	1.0692E 03	9.8325E 02	9.6824E 02	9.3739E 02	1.1545E 03
4.76499	1.3377E 03	1.2377E 03	1.1540E 03	1.0693E 03	9.8348E 02	9.6851E 02	9.3770E 02	1.1545E 03
4.82749	1.3373E 03	1.2375E 03	1.1539E 03	1.0694E 03	9.8374E 02	9.6880E 02	9.3801E 02	1.1544E 03
4.88999	1.3370E 03	1.2373E 03	1.1538E 03	1.0695E 03	9.8400E 02	9.6909E 02	9.3835E 02	1.1543E 03
4.95249	1.3366E 03	1.2370E 03	1.1537E 03	1.0695E 03	9.8427E 02	9.6939E 02	9.3869E 02	1.1542E 03

HOT CHANNEL TEMPERATURES – CEX
AXIAL POSITION 3

TIME	CEX REGION CENTER	2	4	6	BOUNDARY	CLAD	STRUCTURE	AVERAGE
0.	1.4775E 03	1.3701E 03	1.2602E 03	1.1478E 03	1.0324E 03	1.0119E 03	9.7074E 02	1.2584E 03
0.17750	1.4677E 03	1.3686E 03	1.2597E 03	1.1477E 03	1.0331E 03	1.0128E 03	9.7115E 02	1.2584E 03
0.35875	1.4544E 03	1.3680E 03	1.2597E 03	1.1493E 03	1.0366E 03	1.0160E 03	9.7477E 02	1.2595E 03
0.62125	1.4549E 03	1.3681E 03	1.2599E 03	1.1497E 03	1.0373E 03	1.0174E 03	9.7555E 02	1.2598E 03
0.80375	1.4552E 03	1.3681E 03	1.2602E 03	1.1502E 03	1.0380E 03	1.0181E 03	9.7633E 02	1.2601E 03
0.98875	1.4556E 03	1.3686E 03	1.2610E 03	1.1517E 03	1.0402E 03	1.0204E 03	9.7879E 02	1.2612E 03
0.99125	1.4559E 03	1.3688E 03	1.2614E 03	1.1522E 03	1.0409E 03	1.0212E 03	9.7962E 02	1.2615E 03
0.99375	1.4560E 03	1.3690E 03	1.2617E 03	1.1528E 03	1.0417E 03	1.0220E 03	9.8047E 02	1.2619E 03
1.05625	1.4561E 03	1.3692E 03	1.2621E 03	1.1533E 03	1.0424E 03	1.0227E 03	9.8129E 02	1.2623E 03
1.08625	1.4562E 03	1.3693E 03	1.2623E 03	1.1536E 03	1.0427E 03	1.0231E 03	9.8169E 02	1.2625E 03
1.12250	1.4562E 03	1.3694E 03	1.2625E 03	1.1539E 03	1.0432E 03	1.0235E 03	9.8216E 02	1.2627E 03
1.49750	1.4560E 03	1.3707E 03	1.2647E 03	1.1569E 03	1.0470E 03	1.0275E 03	9.8663E 02	1.2649E 03
1.84250	1.4567E 03	1.3717E 03	1.2665E 03	1.1596E 03	1.0509E 03	1.0316E 03	9.9083E 02	1.2667E 03
2.17250	1.4566E 03	1.3726E 03	1.2683E 03	1.1625E 03	1.0548E 03	1.0356E 03	9.9527E 02	1.2686E 03
2.52750	1.4564E 03	1.3735E 03	1.2702E 03	1.1653E 03	1.0585E 03	1.0394E 03	9.9955E 02	1.2704E 03
2.91999	1.4562E 03	1.3743E 03	1.2719E 03	1.1679E 03	1.0620E 03	1.0431E 03	1.0038E 03	1.2722E 03
3.29749	1.4559E 03	1.3747E 03	1.2732E 03	1.1703E 03	1.0657E 03	1.0471E 03	1.0078E 03	1.2736E 03
3.63999	1.4547E 03	1.3750E 03	1.2740E 03	1.1729E 03	1.0696E 03	1.0511E 03	1.0123E 03	1.2750E 03
3.76249	1.4546E 03	1.3751E 03	1.2749E 03	1.1734E 03	1.0702E 03	1.0518E 03	1.0130E 03	1.2753E 03
3.76499	1.4544E 03	1.3752E 03	1.2752E 03	1.1738E 03	1.0708E 03	1.0524E 03	1.0138E 03	1.2756E 03
3.82749	1.4543E 03	1.3753E 03	1.2754E 03	1.1742E 03	1.0714E 03	1.0530E 03	1.0145E 03	1.2758E 03
3.88999	1.4541E 03	1.3753E 03	1.2757E 03	1.1747E 03	1.0719E 03	1.0535E 03	1.0152E 03	1.2760E 03
3.95249	1.4540E 03	1.3754E 03	1.2759E 03	1.1750E 03	1.0725E 03	1.0541E 03	1.0158E 03	1.2763E 03
4.01499	1.4539E 03	1.3755E 03	1.2761E 03	1.1754E 03	1.0730E 03	1.0547E 03	1.0164E 03	1.2765E 03
4.07749	1.4537E 03	1.3755E 03	1.2763E 03	1.1758E 03	1.0735E 03	1.0552E 03	1.0171E 03	1.2767E 03
4.13999	1.4536E 03	1.3756E 03	1.2765E 03	1.1761E 03	1.0740E 03	1.0557E 03	1.0177E 03	1.2769E 03
4.20249	1.4534E 03	1.3756E 03	1.2767E 03	1.1765E 03	1.0745E 03	1.0563E 03	1.0183E 03	1.2771E 03
4.26499	1.4533E 03	1.3757E 03	1.2769E 03	1.1768E 03	1.0750E 03	1.0568E 03	1.0189E 03	1.2773E 03
4.32749	1.4532E 03	1.3757E 03	1.2771E 03	1.1772E 03	1.0754E 03	1.0572E 03	1.0194E 03	1.2775E 03
4.33499	1.4531E 03	1.3757E 03	1.2771E 03	1.1772E 03	1.0755E 03	1.0573E 03	1.0195E 03	1.2775E 03
4.38999	1.4530E 03	1.3757E 03	1.2773E 03	1.1774E 03	1.0758E 03	1.0577E 03	1.0199E 03	1.2776E 03
4.45249	1.4528E 03	1.3758E 03	1.2774E 03	1.1777E 03	1.0763E 03	1.0581E 03	1.0205E 03	1.2778E 03
4.51499	1.4527E 03	1.3758E 03	1.2776E 03	1.1780E 03	1.0768E 03	1.0586E 03	1.0210E 03	1.2779E 03
4.57749	1.4525E 03	1.3758E 03	1.2777E 03	1.1783E 03	1.0772E 03	1.0591E 03	1.0215E 03	1.2781E 03
4.63999	1.4523E 03	1.3757E 03	1.2778E 03	1.1786E 03	1.0777E 03	1.0597E 03	1.0221E 03	1.2782E 03
4.70249	1.4521E 03	1.3757E 03	1.2780E 03	1.1789E 03	1.0782E 03	1.0602E 03	1.0227E 03	1.2783E 03
4.76499	1.4519E 03	1.3757E 03	1.2781E 03	1.1792E 03	1.0788E 03	1.0608E 03	1.0233E 03	1.2785E 03
4.82749	1.4517E 03	1.3756E 03	1.2782E 03	1.1795E 03	1.0793E 03	1.0614E 03	1.0239E 03	1.2786E 03
4.88999	1.4515E 03	1.3756E 03	1.2783E 03	1.1799E 03	1.0799E 03	1.0620E 03	1.0245E 03	1.2788E 03
4.95249	1.4513E 03	1.3756E 03	1.2785E 03	1.1802E 03	1.0805E 03	1.0626E 03	1.0252E 03	1.2789E 03

HOT CHANNEL TEMPERATURES - CEX
AXIAL POSITION 4

TIME	CENTER	2	4	6	BOUNDARY	CLAD	STRUCTURE	AVERAGE
	C E X	R E G I O N						
0.	1.5355E 03	1.4294E 03	1.3211E 03	1.2104E 03	1.0969E 03	1.0764E 03	1.0352E 03	1.3194E 03
0.17750	1.5455E 03	1.4286E 03	1.3206E 03	1.2103E 03	1.0977E 03	1.0774E 03	1.0357E 03	1.3194E 03
0.53875	1.5519E 03	1.4272E 03	1.3208E 03	1.2127E 03	1.1028E 03	1.0830E 03	1.0407E 03	1.3209E 03
0.62125	1.5522E 03	1.4273E 03	1.3212E 03	1.2134E 03	1.1038E 03	1.0841E 03	1.0419E 03	1.3214E 03
0.66375	1.5525E 03	1.4275E 03	1.3216E 03	1.2141E 03	1.1049E 03	1.0852E 03	1.0430E 03	1.3218E 03
0.86875	1.5531E 03	1.4282E 03	1.3230E 03	1.2164E 03	1.1082E 03	1.0887E 03	1.0467E 03	1.3234E 03
0.93125	1.5532E 03	1.4284E 03	1.3235E 03	1.2172E 03	1.1093E 03	1.0898E 03	1.0479E 03	1.3239E 03
0.99375	1.5534E 03	1.4286E 03	1.3241E 03	1.2181E 03	1.1105E 03	1.0911E 03	1.0492E 03	1.3245E 03
1.05625	1.5535E 03	1.4291E 03	1.3247E 03	1.2189E 03	1.1116E 03	1.0922E 03	1.0505E 03	1.3251E 03
1.08625	1.5536E 03	1.4293E 03	1.3250E 03	1.2194E 03	1.1121E 03	1.0928E 03	1.0511E 03	1.3255E 03
1.12250	1.5537E 03	1.4295E 03	1.3253E 03	1.2199E 03	1.1128E 03	1.0934E 03	1.0518E 03	1.3258E 03
1.49750	1.5548E 03	1.4321E 03	1.3292E 03	1.2249E 03	1.1189E 03	1.0997E 03	1.0587E 03	1.3296E 03
1.84250	1.5559E 03	1.4345E 03	1.3326E 03	1.2296E 03	1.1249E 03	1.1060E 03	1.0652E 03	1.3331E 03
2.17250	1.5570E 03	1.4369E 03	1.3363E 03	1.2345E 03	1.1311E 03	1.1123E 03	1.0719E 03	1.3368E 03
2.52750	1.5584E 03	1.4397E 03	1.3402E 03	1.2394E 03	1.1371E 03	1.1185E 03	1.0786E 03	1.3406E 03
2.91999	1.5601E 03	1.4427E 03	1.3442E 03	1.2444E 03	1.1430E 03	1.1245E 03	1.0853E 03	1.3446E 03
3.29749	1.5615E 03	1.4452E 03	1.3477E 03	1.2490E 03	1.1489E 03	1.1307E 03	1.0915E 03	1.3481E 03
3.63999	1.5625E 03	1.4474E 03	1.3511E 03	1.2537E 03	1.1550E 03	1.1370E 03	1.0982E 03	1.3516E 03
3.76249	1.5627E 03	1.4478E 03	1.3517E 03	1.2546E 03	1.1561E 03	1.1381E 03	1.0994E 03	1.3523E 03
3.76499	1.5629E 03	1.4483E 03	1.3524E 03	1.2554E 03	1.1571E 03	1.1392E 03	1.1006E 03	1.3529E 03
3.82749	1.5631E 03	1.4487E 03	1.3530E 03	1.2563E 03	1.1581E 03	1.1401E 03	1.1017E 03	1.3535E 03
3.88999	1.5633E 03	1.4492E 03	1.3537E 03	1.2570E 03	1.1590E 03	1.1411E 03	1.1028E 03	1.3542E 03
3.95249	1.5635E 03	1.4496E 03	1.3543E 03	1.2578E 03	1.1599E 03	1.1420E 03	1.1038E 03	1.3548E 03
4.01499	1.5637E 03	1.4501E 03	1.3549E 03	1.2586E 03	1.1608E 03	1.1429E 03	1.1048E 03	1.3554E 03
4.07749	1.5639E 03	1.4505E 03	1.3555E 03	1.2593E 03	1.1617E 03	1.1438E 03	1.1058E 03	1.3559E 03
4.13999	1.5642E 03	1.4509E 03	1.3561E 03	1.2600E 03	1.1625E 03	1.1447E 03	1.1068E 03	1.3565E 03
4.20249	1.5644E 03	1.4513E 03	1.3566E 03	1.2607E 03	1.1634E 03	1.1456E 03	1.1077E 03	1.3571E 03
4.26499	1.5646E 03	1.4518E 03	1.3572E 03	1.2614E 03	1.1642E 03	1.1464E 03	1.1087E 03	1.3576E 03
4.32749	1.5648E 03	1.4522E 03	1.3577E 03	1.2621E 03	1.1650E 03	1.1472E 03	1.1096E 03	1.3582E 03
4.33499	1.5649E 03	1.4522E 03	1.3578E 03	1.2622E 03	1.1651E 03	1.1473E 03	1.1097E 03	1.3582E 03
4.38999	1.5651E 03	1.4526E 03	1.3583E 03	1.2628E 03	1.1657E 03	1.1479E 03	1.1104E 03	1.3587E 03
4.45249	1.5653E 03	1.4530E 03	1.3588E 03	1.2634E 03	1.1665E 03	1.1487E 03	1.1113E 03	1.3592E 03
4.51499	1.5655E 03	1.4533E 03	1.3593E 03	1.2640E 03	1.1672E 03	1.1495E 03	1.1121E 03	1.3597E 03
4.57749	1.5657E 03	1.4537E 03	1.3597E 03	1.2646E 03	1.1680E 03	1.1503E 03	1.1129E 03	1.3602E 03
4.63999	1.5659E 03	1.4540E 03	1.3602E 03	1.2652E 03	1.1688E 03	1.1512E 03	1.1138E 03	1.3606E 03
4.70249	1.5660E 03	1.4543E 03	1.3607E 03	1.2659E 03	1.1697E 03	1.1521E 03	1.1147E 03	1.3611E 03
4.76499	1.5662E 03	1.4547E 03	1.3611E 03	1.2665E 03	1.1705E 03	1.1530E 03	1.1156E 03	1.3616E 03
4.82749	1.5663E 03	1.4550E 03	1.3616E 03	1.2672E 03	1.1714E 03	1.1539E 03	1.1166E 03	1.3621E 03
4.88999	1.5664E 03	1.4553E 03	1.3621E 03	1.2678E 03	1.1723E 03	1.1549E 03	1.1175E 03	1.3626E 03
4.95249	1.5666E 03	1.4555E 03	1.3625E 03	1.2685E 03	1.1733E 03	1.1558E 03	1.1185E 03	1.3631E 03

HOT CHANNEL TEMPERATURES - CEX
AXIAL POSITION 5

	CEX REGION							
TIME	CENTER	2	4	6	BOUNDARY	CLAD	STRUCTURE	AVERAGE
0.	1.5018E 03	1.4146E 03	1.3260E 03	1.2356E 03	1.1436E 03	1.1268E 03	1.0930E 03	1.3248E 03
0.17750	1.5100E 03	1.4134E 03	1.3255E 03	1.2356E 03	1.1444E 03	1.1279E 03	1.0935E 03	1.3248E 03
0.55875	1.5149E 03	1.4126E 03	1.3260E 03	1.2386E 03	1.1505E 03	1.1345E 03	1.0994E 03	1.3265E 03
0.62125	1.5151E 03	1.4127E 03	1.3264E 03	1.2394E 03	1.1518E 03	1.1359E 03	1.1008E 03	1.3270E 03
0.68375	1.5153E 03	1.4129E 03	1.3269E 03	1.2403E 03	1.1531E 03	1.1373E 03	1.1022E 03	1.3276E 03
0.86875	1.5157E 03	1.4138E 03	1.3287E 03	1.2433E 03	1.1573E 03	1.1417E 03	1.1068E 03	1.3295E 03
0.93125	1.5158E 03	1.4141E 03	1.3294E 03	1.2443E 03	1.1588E 03	1.1432E 03	1.1084E 03	1.3303E 03
0.99375	1.5160E 03	1.4146E 03	1.3302E 03	1.2455E 03	1.1602E 03	1.1448E 03	1.1100E 03	1.3311E 03
1.05625	1.5162E 03	1.4150E 03	1.3310E 03	1.2466E 03	1.1617E 03	1.1462E 03	1.1116E 03	1.3319E 03
1.08625	1.5163E 03	1.4153E 03	1.3314E 03	1.2472E 03	1.1624E 03	1.1470E 03	1.1124E 03	1.3323E 03
1.12250	1.5164E 03	1.4156E 03	1.3319E 03	1.2478E 03	1.1633E 03	1.1478E 03	1.1133E 03	1.3328E 03
1.49750	1.5181E 03	1.4194E 03	1.3373E 03	1.2548E 03	1.1715E 03	1.1562E 03	1.1225E 03	1.3381E 03
1.84250	1.5204E 03	1.4232E 03	1.3424E 03	1.2612E 03	1.1794E 03	1.1644E 03	1.1308E 03	1.3432E 03
2.17250	1.5229E 03	1.4273E 03	1.3478E 03	1.2680E 03	1.1875E 03	1.1728E 03	1.1396E 03	1.3486E 03
2.52750	1.5262E 03	1.4322E 03	1.3539E 03	1.2752E 03	1.1957E 03	1.1810E 03	1.1485E 03	1.3546E 03
2.91999	1.5303E 03	1.4377E 03	1.3605E 03	1.2826E 03	1.2039E 03	1.1894E 03	1.1573E 03	1.3611E 03
3.29749	1.5343E 03	1.4427E 03	1.3663E 03	1.2894E 03	1.2118E 03	1.1975E 03	1.1656E 03	1.3670E 03
3.63999	1.5377E 03	1.4472E 03	1.3719E 03	1.2963E 03	1.2200E 03	1.2059E 03	1.1742E 03	1.3727E 03
3.70249	1.5383E 03	1.4481E 03	1.3730E 03	1.2975E 03	1.2214E 03	1.2073E 03	1.1758E 03	1.3737E 03
3.76499	1.5390E 03	1.4490E 03	1.3741E 03	1.2988E 03	1.2228E 03	1.2088E 03	1.1773E 03	1.3748E 03
3.82749	1.5396E 03	1.4498E 03	1.3751E 03	1.3000E 03	1.2242E 03	1.2101E 03	1.1788E 03	1.3758E 03
3.88999	1.5403E 03	1.4507E 03	1.3762E 03	1.3012E 03	1.2255E 03	1.2115E 03	1.1802E 03	1.3769E 03
3.95249	1.5410E 03	1.4516E 03	1.3772E 03	1.3024E 03	1.2268E 03	1.2127E 03	1.1816E 03	1.3779E 03
4.01499	1.5417E 03	1.4525E 03	1.3783E 03	1.3035E 03	1.2280E 03	1.2141E 03	1.1830E 03	1.3789E 03
4.07749	1.5423E 03	1.4534E 03	1.3793E 03	1.3047E 03	1.2293E 03	1.2153E 03	1.1843E 03	1.3799E 03
4.13999	1.5430E 03	1.4543E 03	1.3803E 03	1.3058E 03	1.2305E 03	1.2165E 03	1.1857E 03	1.3809E 03
4.20249	1.5437E 03	1.4551E 03	1.3813E 03	1.3069E 03	1.2317E 03	1.2177E 03	1.1869E 03	1.3819E 03
4.26499	1.5444E 03	1.4560E 03	1.3823E 03	1.3080E 03	1.2329E 03	1.2189E 03	1.1882E 03	1.3829E 03
4.32749	1.5451E 03	1.4569E 03	1.3833E 03	1.3090E 03	1.2340E 03	1.2200E 03	1.1894E 03	1.3838E 03
4.33499	1.5452E 03	1.4570E 03	1.3834E 03	1.3092E 03	1.2341E 03	1.2201E 03	1.1896E 03	1.3839E 03
4.38999	1.5456E 03	1.4576E 03	1.3842E 03	1.3101E 03	1.2350E 03	1.2211E 03	1.1906E 03	1.3848E 03
4.45249	1.5465E 03	1.4586E 03	1.3851E 03	1.3111E 03	1.2361E 03	1.2222E 03	1.1917E 03	1.3857E 03
4.51499	1.5472E 03	1.4594E 03	1.3861E 03	1.3121E 03	1.2372E 03	1.2233E 03	1.1929E 03	1.3866E 03
4.57749	1.5479E 03	1.4602E 03	1.3869E 03	1.3130E 03	1.2383E 03	1.2244E 03	1.1940E 03	1.3874E 03
4.63999	1.5486E 03	1.4610E 03	1.3878E 03	1.3140E 03	1.2394E 03	1.2256E 03	1.1952E 03	1.3884E 03
4.70249	1.5492E 03	1.4617E 03	1.3887E 03	1.3150E 03	1.2405E 03	1.2267E 03	1.1963E 03	1.3892E 03
4.76499	1.5499E 03	1.4625E 03	1.3895E 03	1.3160E 03	1.2417E 03	1.2279E 03	1.1976E 03	1.3901E 03
4.82749	1.5505E 03	1.4632E 03	1.3904E 03	1.3170E 03	1.2429E 03	1.2291E 03	1.1988E 03	1.3910E 03
4.88999	1.5511E 03	1.4640E 03	1.3913E 03	1.3180E 03	1.2441E 03	1.2304E 03	1.2001E 03	1.3919E 03
4.95249	1.5517E 03	1.4647E 03	1.3921E 03	1.3190E 03	1.2454E 03	1.2317E 03	1.2013E 03	1.3927E 03

HOT CHANNEL TEMPERATURES - CEX
AXIAL POSITION 6

TIME	CENTER	2	4	6	BOUNDARY	CLAD	STRUCTURE	AVERAGE
	C E X	R E G I O N						
0.	1.3795E 03	1.3265E 03	1.2729E 03	1.2187E 03	1.1639E 03	1.1539E 03	1.1337E 03	1.2725E 03
0.17750	1.3844E 03	1.3257E 03	1.2726E 03	1.2187E 03	1.1646E 03	1.1548E 03	1.1341E 03	1.2725E 03
0.55875	1.3869E 03	1.3250E 03	1.2732E 03	1.2217E 03	1.1708E 03	1.1616E 03	1.1400E 03	1.2741E 03
0.62125	1.3870E 03	1.3251E 03	1.2736E 03	1.2226E 03	1.1722E 03	1.1631E 03	1.1414E 03	1.2746E 03
0.68375	1.3871E 03	1.3252E 03	1.2742E 03	1.2236E 03	1.1737E 03	1.1646E 03	1.1430E 03	1.2752E 03
0.80875	1.3872E 03	1.3261E 03	1.2762E 03	1.2269E 03	1.1783E 03	1.1695E 03	1.1480E 03	1.2773E 03
0.93125	1.3873E 03	1.3265E 03	1.2770E 03	1.2281E 03	1.1799E 03	1.1712E 03	1.1497E 03	1.2781E 03
0.99375	1.3874E 03	1.3270E 03	1.2778E 03	1.2294E 03	1.1816E 03	1.1730E 03	1.1515E 03	1.2790E 03
1.05625	1.3875E 03	1.3276E 03	1.2788E 03	1.2307E 03	1.1833E 03	1.1747E 03	1.1534E 03	1.2799E 03
1.08625	1.3876E 03	1.3279E 03	1.2792E 03	1.2314E 03	1.1841E 03	1.1755E 03	1.1542E 03	1.2804E 03
1.12250	1.3877E 03	1.3282E 03	1.2798E 03	1.2321E 03	1.1850E 03	1.1765E 03	1.1553E 03	1.2810E 03
1.49750	1.3900E 03	1.3329E 03	1.2864E 03	1.2404E 03	1.1946E 03	1.1863E 03	1.1659E 03	1.2874E 03
1.84250	1.3933E 03	1.3366E 03	1.2929E 03	1.2481E 03	1.2038E 03	1.1957E 03	1.1754E 03	1.2938E 03
2.17250	1.3972E 03	1.3436E 03	1.2998E 03	1.2564E 03	1.2133E 03	1.2054E 03	1.1854E 03	1.3007E 03
2.52750	1.4024E 03	1.3503E 03	1.3077E 03	1.2653E 03	1.2230E 03	1.2153E 03	1.1959E 03	1.3085E 03
2.61999	1.4036E 03	1.3518E 03	1.3105E 03	1.2748E 03	1.2330E 03	1.2255E 03	1.2064E 03	1.3171E 03
3.29749	1.4157E 03	1.3636E 03	1.3246E 03	1.2835E 03	1.2425E 03	1.2349E 03	1.2160E 03	1.3253E 03
3.63999	1.4217E 03	1.3726E 03	1.3322E 03	1.2921E 03	1.2520E 03	1.2446E 03	1.2253E 03	1.3329E 03
3.76249	1.4226E 03	1.3739E 03	1.3337E 03	1.2936E 03	1.2537E 03	1.2463E 03	1.2270E 03	1.3343E 03
3.76499	1.4239E 03	1.3752E 03	1.3351E 03	1.2952E 03	1.2554E 03	1.2480E 03	1.2294E 03	1.3358E 03
3.82749	1.4256E 03	1.3769E 03	1.3366E 03	1.2968E 03	1.2571E 03	1.2497E 03	1.2312E 03	1.3372E 03
3.88999	1.4266E 03	1.3778E 03	1.3380E 03	1.2984E 03	1.2587E 03	1.2513E 03	1.2329E 03	1.3387E 03
3.95249	1.4274E 03	1.3792E 03	1.3395E 03	1.2999E 03	1.2603E 03	1.2529E 03	1.2346E 03	1.3401E 03
4.01499	1.4285E 03	1.3805E 03	1.3409E 03	1.3014E 03	1.2618E 03	1.2544E 03	1.2362E 03	1.3415E 03
4.07749	1.4297E 03	1.3818E 03	1.3423E 03	1.3029E 03	1.2633E 03	1.2560E 03	1.2378E 03	1.3429E 03
4.13999	1.4309E 03	1.3832E 03	1.3437E 03	1.3044E 03	1.2649E 03	1.2575E 03	1.2394E 03	1.3443E 03
4.20249	1.4321E 03	1.3845E 03	1.3451E 03	1.3058E 03	1.2663E 03	1.2590E 03	1.2409E 03	1.3457E 03
4.26499	1.4333E 03	1.3858E 03	1.3465E 03	1.3072E 03	1.2678E 03	1.2604E 03	1.2425E 03	1.3470E 03
4.32749	1.4345E 03	1.3871E 03	1.3479E 03	1.3087E 03	1.2692E 03	1.2618E 03	1.2439E 03	1.3484E 03
4.38999	1.4357E 03	1.3883E 03	1.3493E 03	1.3100E 03	1.2706E 03	1.2632E 03	1.2454E 03	1.3497E 03
4.45249	1.4370E 03	1.3896E 03	1.3506E 03	1.3114E 03	1.2719E 03	1.2645E 03	1.2468E 03	1.3511E 03
4.51499	1.4382E 03	1.3910E 03	1.3519E 03	1.3127E 03	1.2732E 03	1.2659E 03	1.2481E 03	1.3524E 03
4.57749	1.4394E 03	1.3923E 03	1.3532E 03	1.3140E 03	1.2746E 03	1.2672E 03	1.2495E 03	1.3537E 03
4.63999	1.4406E 03	1.3936E 03	1.3545E 03	1.3153E 03	1.2760E 03	1.2686E 03	1.2509E 03	1.3549E 03
4.70249	1.4417E 03	1.3948E 03	1.3558E 03	1.3166E 03	1.2773E 03	1.2700E 03	1.2523E 03	1.3562E 03
4.76499	1.4429E 03	1.3960E 03	1.3570E 03	1.3180E 03	1.2787E 03	1.2714E 03	1.2537E 03	1.3575E 03
4.82749	1.4441E 03	1.3972E 03	1.3583E 03	1.3193E 03	1.2801E 03	1.2728E 03	1.2551E 03	1.3587E 03
4.88999	1.4452E 03	1.3984E 03	1.3595E 03	1.3206E 03	1.2816E 03	1.2743E 03	1.2565E 03	1.3600E 03
4.95249	1.4463E 03	1.3996E 03	1.3608E 03	1.3219E 03	1.2831E 03	1.2758E 03	1.2580E 03	1.3613E 03

APPENDIX F

NEUTRON ENERGY GROUP STRUCTURE OF STANDARD WAPD 18 GROUP LIBRARY

Group	Lower Energy (ev)	Lethargy Width
0	9.9700×10^{6}	
1	3.6678×10^{6}	1.00000
2	2.2246×10^{6}	0.50000
3	1.3493×10^{6}	0.50000
4	8.1839×10^{5}	0.50000
5	4.9638×10^{5}	0.50000
6	3.0107×10^{5}	0.50000
7	1.8261×10^{5}	0.50000
8	1.1076×10^{5}	0.50000
9	6.7177×10^{4}	0.50000
10	4.0745×10^{4}	0.50000
11	2.4713×10^{4}	0.50000
12	1.4989×10^{4}	0.50000
13	0.0915×10^{3}	0.50000
14	4.0000×10^{3}	0.82104
15	1.0000×10^{3}	1.38629
16	3.0000×10^{2}	1.20397
17	1.0000×10^{2}	1.09861
18	3.0000×10^{1}	1.20397

APPENDIX G

CERMET MATERIALS LITERATURE SEARCH

The following documents were reviewed as reference sources only as part of the Cermet Fuel Review, Section III.7.6.

Reactor Core Materials

Nuclear Science Abstracts
May 1963 through 1965

The following documents are sources of matrix material data:

Bush, S. H., Irradiation Effects in Structural Materials (ASM)

Bush, S. H., Nuclear Metallurgy, Vol. IX, AIME, 1963

APED-4542, Radiation Effects on 304 Stainless Steel

ASTM-STP-341, Symposium on Radiation Effects on Metals and Neutron Dosimetry, (page 311, M. B. Reynolds, Radiation Effects in Reactor Structural Materials)

ASTM-STP-233, 1953 Radiation Effects on Materials

ASTM-STP-364, 1962 Reactor Structural Materials

A/Conf. 15/1878, H. M. Bartz, Performance of Materials, June 1958

APED-4542, Radiation Effects on 304 Stainless Steel

The following documents were reviewed and found to contain no pertinent information:

BMI-1294	BMI-1442	BMI-1529
BMI-1034	BMI-1464	BMI-APDA-647
BMI-1307	BMI-1469	ORNL-2988
BMI-1315	BMI-1473	ORNL-3077
BMI-1325	BMI-1480	ORNL-3386
BMI-1330	BMI-1527	ORNL-3470
	BMI-1528	

Weber, C. E., Progress on Dispersion Elements, Progress in Nuclear Energy, Series V, Vol. 2, 1959.

Kittel, J. H., et al, "Metallic Fuel Elements for Fast Reactors", Fast Reactor Technology ANS-100, pp. 157-169, April 1965.

Zebroski, C. P., et al, "Radiation Damage in Fast Reactor Components", Fast Reactor Technology ANS-100, pp. 110-125, April 1965.

CF-58-2-71 V. D. Hayes, Summary of UO_2 - SS Dispersion Element Irradiation Experiments, 1958.

Goslee, D. E., Improving Performance of Stainless Steel UO_2 Cermet Fuels, Nucleonics, Vol. 21, No. 7, p. 48-52.

A/Conf. 28/P/239, J. H. Kittel, et al, Irradiation Behavior of Metallic Fuels, May 1954.